**RADIONUCLIDE MIGRATION**

SANTA FE, NM. U.S.A.

SEPTEMBER 13-18, 2015
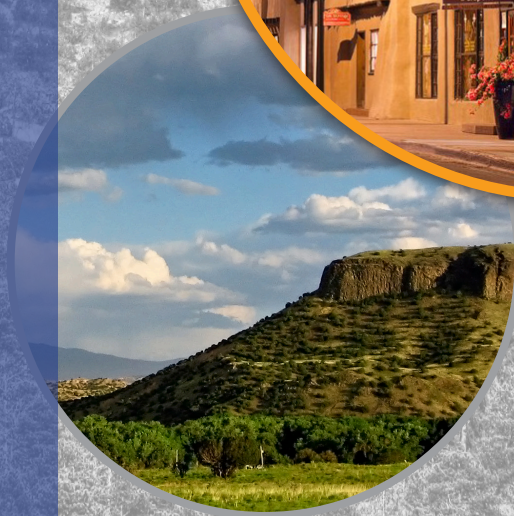
MIGRATION 2015

15th International Conference on the Chemistry and Migration Behaviour of Actinides and Fission Products in the Geosphere

Migration 2015 Abstracts

Santa Fe Community Convention Center
Santa Fe, USA
September 13 – 18, 2015

Abstracts Book

This Page Intentionally Blank

Background

The MIGRATION conferences provide an international forum for the timely exchange of scientific information on chemical processes controlling the migration behaviour of actinides and fission products in natural aquifer systems. Experimental investigations and predictive modelling of these processes are the main topics of the conferences. The information generated from the MIGRATION conferences is the basis for the mechanistic understanding of the migration behaviour of long-lived radionuclides in the geosphere, which is essential for the long-term performance assessment of nuclear waste disposal.

The first MIGRATION conference was held in 1987 in Munich, Germany. It was followed by MIGRATION '89 in Monterey, California, USA; MIGRATION '91 in Jerez de la Frontera, Spain; MIGRATION '93 in Charleston, South Carolina, USA; MIGRATION '95 in Saint-Malo, France; MIGRATION '97 in Sendai, Japan, MIGRATION '99 at Lake Tahoe, Nevada, USA, MIGRATION '01 in Bregenz, Austria, MIGRATION '03 in Gyeongju, Korea, MIGRATION '05 in Avignon, France, MIGRATION '07 in Munich, MIGRATION '09 in Kennewick, Washington, USA, Migration 2011 in Beijing, China and Migration 2013 in Brighton, UK.

Scope

The MIGRATION conferences focus on recent developments in the fundamental chemistry of actinides, fission and activation products in natural aquifer systems, their interactions and migration in the geosphere, and the processes involved in modelling their geochemical behaviour.

The sessions in MIGRATION'15 cover the following areas:

A   Aquatic chemistry of actinides and fission products

1) Solubility and dissolution
2) Solid solution and secondary phase formation
3) Complexation with inorganic and organic ligands
4) Redox reactions and radiolysis effects
5) Solid-water interface reactions
6) Colloid formation
7) Experimental methods
8) Computational chemistry

B   Migration behaviour of radionuclides

1) Sorption/desorption phenomena in dynamic systems
2) Diffusion and other migration processes
3) Colloid migration
4) Effects of biological and organic materials
5) Field and large scale experiments
6) Natural analogues

C   Geochemical and transport modelling

1) Data selection and evaluation
2) Coupling chemistry and transport
3) Development and application of models
4) Model validation
5) Safety assessment and repository concepts

Repository and Remediation Programmes in the US

International Programmes

Conference Committees

International Steering Committee:

H. Geckeis (Chairman) (Germany)   P. Toulhoat (France)
D.L. Clark (USA)   V. Vallet (France)
S.B. Clark (USA)   L. Van Loon (Switzerland)
B. Grambow (France)   J.-I. Yun (Korea)

International Scientific Committee:

M.H. Baik (Korea)   Liu Chunli (China)
U. Berner (Switzerland)   T. Ohnuki (Japan)
D. Bosbach (Germany)   T. Payne (Australia)
V. Brendler (Germany)   Ch. Poinssot (France)
J. Bruno (Spain)   D. Reed (USA)
N.D. Bryan (UK)   T. Sasaki (Japan)
P. de Canniere (Belgium)   K. Spahiu (Sweden)
N. Evans (UK)   B.S. Tomar (India)
A. Felmy (USA)   Wang Xiangke (China)

Scientific Secretary:

Th. Rabung (Germany)   D. Reed (USA)

Local Committees:

Los Alamos, USA: *National Labs/ Universities, USA:*

P. Dixon   N. Hess (PNNL)
B. Robinson   D. Kaplan (SRNL)
R. Roback   A. Kersting (LLNL)
W. Runde   B. Powell (Clemson University)
K. Birdsell

Carlsbad/Wipp, USA:

R. Hardy (NMSU)
R. Patterson (DOE-CBFO)
A. Van Luik (DOE-CBFO)

Contacts

Technical and programmatic content/issues

Don Reed (Los Alamos National Laboratory)

Phone: +1 575 234 5559

Email: dreed@lanl.gov

Thomas Rabung (KIT-INE)

Phone: +49 721 608 2546

Email: thomas.rabung@kit.edu

Conference logistics and operation

Shannan Yeager (New Mexico Consortium)

Phone: +1 505-412-4200

Email: migration2015@newmexicoconsortium.org

Organization and Support

Migration 2015 is being organized by Los Alamos National Laboratory, New Mexico Consortium and KIT/INE

Los Alamos NATIONAL LABORATORY EST.1943   New Mexico CONSORTIUM   KIT Karlsruhe Institute of Technology

Support for conference activities is provided by the German Federal Ministry for Economic Affairs and Energy, the Carlsbad Environmental Monitoring and Research Center, Los Alamos National Laboratory, and the US Department of Energy:

Federal Ministry for Economic Affairs and Energy   **Provisions for the opening day reception and poster sessions**

Carlsbad Environmental Monitoring & Research Center   **Carlsbad Environmental Monitoring and Research Center**
Provisions for the poster sessions

NWP Nuclear Waste Partnership   **Nuclear Waste Partnership, M&O for the WIPP Project**
Provisions for the poster sessions

Los Alamos NATIONAL LABORATORY EST.1943   **Student registration subsidy, poster boards and program printing**

Department of Energy United States of America   **Overall meeting sponsorship and support**

This Page Intentionally Blank

List of Abstracts

(UK)

THURSDAY SESSIONS (September 16)

MIGRATION 2015
ABSTRACTS

This Page Intentionally Blank

OVERVIEW AND UPDATE OF EM/ER NUCLEAR SITE REMEDIATION AND NUCLEAR WASTE MANAGEMENT

Dr. Monica Regalbuto
Associate Principal Deputy Assistant Secretary

The Office of Environmental Management (EM) program was established in 1989 and is responsible for the cleanup of millions of gallons of liquid radioactive waste, thousands of tons of spent (used) nuclear fuel and special nuclear material, disposition of large volumes of transuranic and mixed/low-level waste, huge quantities of contaminated soil and water, and deactivation and decommissioning of thousands of excess facilities. This environmental cleanup program results from five decades of nuclear weapons development and production and government-sponsored nuclear energy research. EM has completed cleanup activities at 91 sites in 30 states; EM is responsible for the remaining cleanup at 16 sites in 11 states. Sites like Fernald in Ohio and Rocky Flats in Colorado, both of which once housed large industrial complexes, are now wildlife preserves that are also available for recreational use. At the Idaho National Laboratory, we have decommissioned and demolished more than two million square feet of excess facilities, and removed all EM special nuclear material (e.g., enriched uranium) from the state. At Savannah River Site, South Carolina, we have produced almost 4,000 canisters of vitrified high-level waste and closed six of the site's underground storage tanks. At our Portsmouth, Ohio, and Paducah, Kentucky, sites, we have designed, constructed and now operate two facilities to convert depleted uranium hexafluoride into a more stable form suitable for beneficial reuse or disposal. Across the EM complex, our progress in footprint reduction is significant, approximately 90 percent, with now less than 250 square miles remaining, and the progress continues. EM continues to pursue its cleanup objectives safely within a framework of regulatory compliance commitments and best business practices. Most importantly, EM will continue to discharge its responsibilities by conducting cleanup within a "Safety First" culture that integrates environmental, safety, and health requirements and controls into all work activities. This ensures protection for the workers, public, and the environment.

PROGRESS AND CHALLENGES IN REPOSITORY PROJECTS: AN INTERNATIONAL PERSPECTIVE

L.H. Johnson

Independent consultant, Winnipeg, Manitoba, Canada

Programs for the development of repositories for spent fuel/high-level waste and long-lived intermediate level waste are underway in many countries, with some programs being at an advanced stage in the licensing process, while others are still at an early stage in siting or have deferred siting for various reasons. Different repository host rocks are under study, including argillaceous rocks, crystalline rocks and salt. Repository projects that are nationally driven are able to develop a strongly focused program of studies, but the recognized benefits of collaboration and resource limitations lead to the search for fruitful international collaboration. Nonetheless, with the significant differences in repository schedules and rock types, there are special challenges in establishing and executing cooperative RD&D (research, development and demonstration) for those projects that are in an advanced stage. Worldwide, these challenges have been addressed through conferences that have brought experts together to collaborate informally, through international organisations such as the NEA and IAEA that have initiated projects or working groups on topics of common interest, and in Europe through international research coordinated and co-funded by the EU. In the past few years, through an initiative supported by the EU, a group of organisations having responsibility for implementing repositories in various European countries began to develop a more intensive level of cooperation through the IGD-TP (technology platform of the EC for implementing geological repositories) with an increased focus on RD&D that supports repository implementation.

The IGD-TP grew out of the need to enhance collaboration among implementing organisations and to use the Technology Platform mechanism (a funding structure of the EU research program), in which industry takes a strong role in defining the required RD&D. The IGD-TP was launched in 2009 and issued a Strategic Research Agenda (SRA) [1] in 2011 and a Deployment Plan [2] in 2012. Together these define a broad common research agenda and a rough schedule for initiating projects (and other types of collaborations, such as Working Groups or Information Exchange Platforms). The IGD-TP Executive Group has met twice a year since this time to review topics in the SRA that might be pursued through development of project proposals to the EU or to establish Working Groups. The proposals themselves are developed by a consortium of research organizations, universities and waste management organizations.

The range of projects initiated since 2011 illustrates the inevitable shift from R&D to D&D that takes place with the increased focus on implementation. The spectrum of collaborative projects that have been pursued over recent years will be briefly reviewed, including some highlights and the linkages to some on-going repository projects that drove the initiation of the projects.

[1] http://www.igdtp.eu/index.php/key-documents/doc_download/14-strategic-research-agenda
[2] http://www.igdtp.eu/index.php/key-documents/doc_download/65-deployment-plan-2011-2016

STATUS OF THE WASTTE ISOLATION PILOT PLAN AND ITS RECOVERY

Abraham Van Luik

U.S. Department of Energy, Carlsbad Field Office, 4021 S. National Parks Highway, Carlsbad, New Mexico, 88220 abraham.vanluik@cbfo.doe.gov

The Waste Isolation Pilot Plant (WIPP) experienced two unrelated events in February of 2014 that closed the facility for the first time, after almost 15 years of successful operation. The two events were (1) a salt haul truck fire on February 5, and (2) an underground release of radioactive waste from one drum that underwent a runaway chemical reaction on February 14.

An Accident Investigation Board was convened that thoroughly examined the cultural and physical causes of both events and determined both events to have been preventable. The AIB, in its reports prescribed changes in the oversight processes and in the safety cultures of participant organizations, as well as changes in the processes and the physical plant necessary to prevent recurrence.

Cultural and structural changes are being made as suggested. The surface contamination levels in the underground are being lowered to a degree that will allow minimal use of personal protective equipment (Figure 1). Suspect waste locations have been sealed off from underground air ventilation (Figure 2). Preparations are being made to resume limited operations until a new ventilation system is in place, after which full operations can resume.

A systematic program of recovery was planned and is being worked step by step to assure that when the repository resumes operations it will have a firmer safety basis and will have improved in every aspect related to assuring continued safety from culture changes, process and procedure changes, to upgrades of safety-relevant equipment.

Mine habitability restoration was a high priority requiring soot removal to allow electrical equipment to function underground, rock bolting in both clean and contaminated areas, the removal and control of combustibles, and fixing the removable alpha contamination using a water spray to either remove it to the floor, or seal it into the salt. In higher traffic areas contamination washed down onto the floor is being covered with yellow brattice cloth and 5-6 inches of run of mine salt to allow traffic without remobilizing contamination. In lesser traffic areas, such as where waste is moved into disposal rooms, there will be a water spray application to fix any potentially contaminated salt dust prior to every operation.

Another high priority was the isolation of suspect waste drums, meaning drums with some of the same content as the failed drum that experience a runaway chemical reaction and caused the release. Isolating these waste locations from the working areas and its ventilation air provided an important assurance of safety. This was done using run-of mine salt and a steel bulkhead (Figure 2).

This preliminary waste panel isolation system is to be followed by a permanent waste panel isolation system consisting of two steel bulkheads with 100 feet of run of mine salt piled as high as practicable, without compaction, between them (Figure 3). As the surrounding salt creeps to fill any open spaces, it will crush both the waste and the run of mine salt at these seal locations and over time effectively isolate the waste panels from each other. Each waste Panel will be sealed in this manner, as will the main entry drifts at three locations (see Figure 4).

In order to enhance the number of workers that can be allowed underground, plus allow them to operate their bolting and other equipment, the ventilation system is being enhanced in a stepwise manner. The final step is adding a permanent new ventilation system to allow full operations to resume in several more years. To allow limited operations to resume much earlier, however, interim and supplemental ventilation system enhancements are currently being installed to increase the underground flow rate and thus allow recovery operations to accelerate so that limited waste disposal operations can resume as early as 2016, and full operations, after a new exhaust shaft, connecting drift, and ventilation system are completed, will resume in 2019.

Fig. 1. Underground process for mitigating worker radiological risk using water spray.
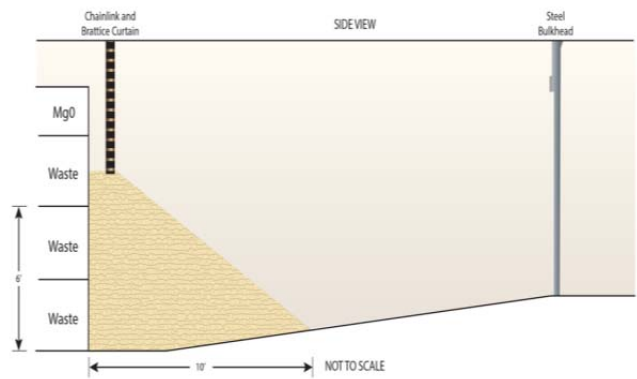
Fig. 2. Brattice-cloth curtain, run of mine salt, and steel bulkhead used to preliminarily seal off areas with suspect waste stream content from underground ventilation.
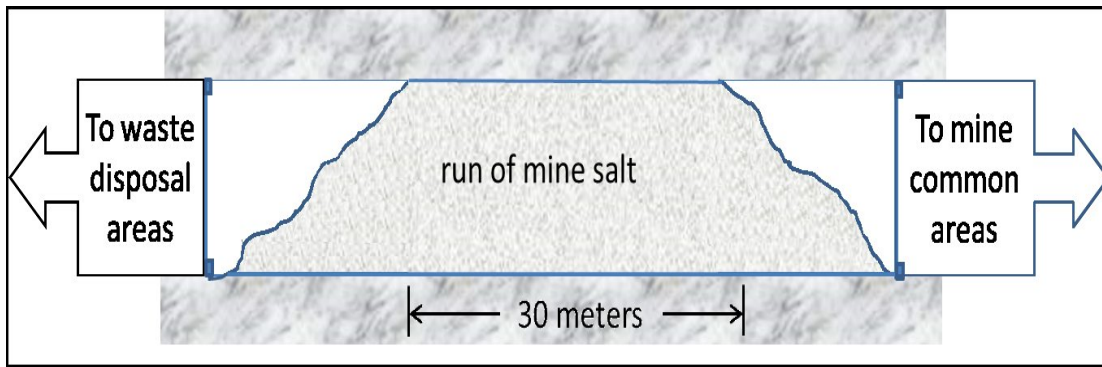
Fig. 3. Proposed final disposal panel closure system, two steel bulkheads with run-of-mine-salt between (not to scale).
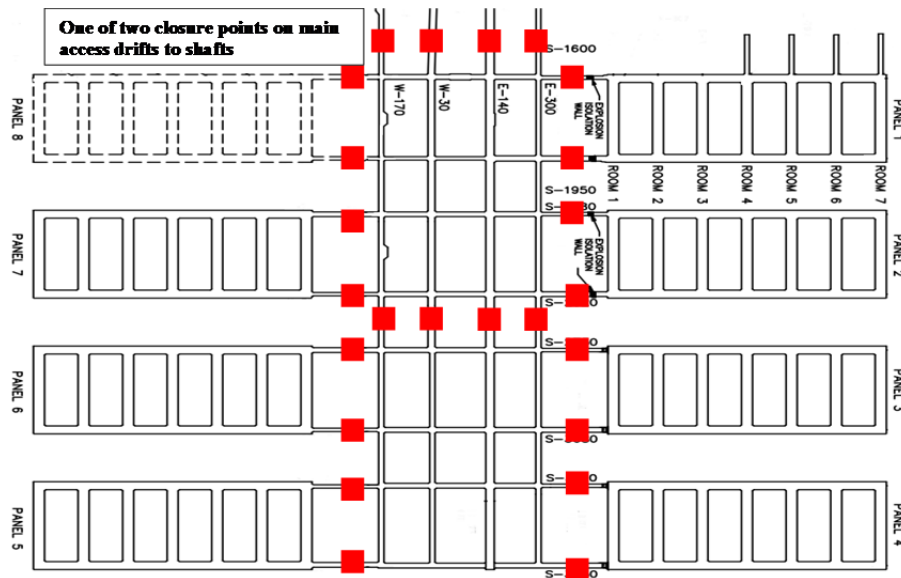
Fig. 4. Planned locations of panel closures illustrated in Figure 3.

RADIOACTIVE WASTE DISPOSAL: THE SCIENCE AND THE PUBLIC

B. Grambow[1]

[1]*Subatech (Mines-Nantes, Université de Nantes, CNRS-IN2P3),4 rue Alfred Kastler, 44307 Nantes, France*

Disposal of radioactive waste on land was proposed in 1957 by the US National Research Council, and corresponding research is ongoing since then. There is a broad technical consensus that geologic disposal of highly-radioactive waste will provide for the safety of humankind and the environment, now, and far into the future. Still, no disposal site for high level waste is available. First repositories are expected to become operating in the following 10 years, but many disposal programs have experienced very large delays. Long term safety predictions have demonstrated that the risk, as measured by exposure to radiation, will be of little consequence until eternity. Many scientific teams worldwide work hard since 30 or more years to gather the geophysical, hydrological, geochemical, radiochemical or materials science data sustaining these analyses but the "overall picture" on safety is typically established by agencies responsible for constructing or for reviewing/licensing repository projects. Important parts of the public do not share the confidence in these calculations.

In the paper we argue for a stronger connection between the scientific data and their meaning for the determination of the long-term safety, considering credibility of the assessments in the context of a much broader historical, epistemological and societal context. In contrast to the belief of many scientists, there is certainly no direct link between increased scientific understanding and a public position for or against different strategies of nuclear waste disposal. This is not due to the public being poorly informed or irrational, but rather due to cultural cognition of expertise and historical and cultural perception of hazards to regions selected to host a geologic repository. The societal and cultural dimension does not diminish the role of science, as scientific results become even more important in distinguishing between the conflicting views of the risk of geologic disposal of radioactive waste. The conference of citizen held in 2013/14 at the occasion of the public debate on the French CIGEO project is a good example. The citizens were arbitrarily selected by a company specialized in public polls and were formed for three weeks in antagonist manner by experts (scientists, administrators, politicians, or representatives of WMO, TSO) on issues like energy policy, waste inventories and definitions of what is considered waste, risks during construction, operation and long term closure of repository, ethics and the role of the media. The results show that complicated scientific issues can be dealt with if opposing views are respected in a balanced democratic and open context. A prototype disposal was proposed and integrated in the French concept.

THE CURRENT STATUS OF TWO UNIQUE IN-SITU RADIONUCLIDE MIGRATION TESTS AT THE GRIMSEL TEST SITE

A. Martin[(1)], I. Blechschmidt [(1)]

[(1)]*Nagra (National Cooperative for the Disposal of Radioactive Waste), Hardstrasse 73, 5430 Wettingen, Switzerland*

The current status of two very unique in-situ radionuclide migration tests [1] at the Grimsel Test Site (GTS) (www.grimsel.com) designed to simulate the long-term behavior of radionuclides in the repository near-field and the surrounding host rock are presented: (1) the Colloid Formation and Migration ([*]CFM) project, which focuses on colloid generation and migration from a bentonite source spiked with radionuclides and, (2) the Long-Term Diffusion ([**]LTD) project, which focuses on in-situ verification and understanding of the processes that control the long-term diffusion of radionuclides.

The CFM project was set-up to study colloid facilitated transport of radionuclides in a well characterised shear zone under realistic boundary conditions. In order to control the flow velocity in the selected shear zone, a state-of-the-art tunnel packer system (Figure 1) was first specially designed and constructed. This was followed by numerous tracer migration tests, two with radionuclides, in order to help understand the hydraulic properties and flow pathways of the selected shear zone. Many of the tests were repeated in the same geometry but with reduced extraction rates.
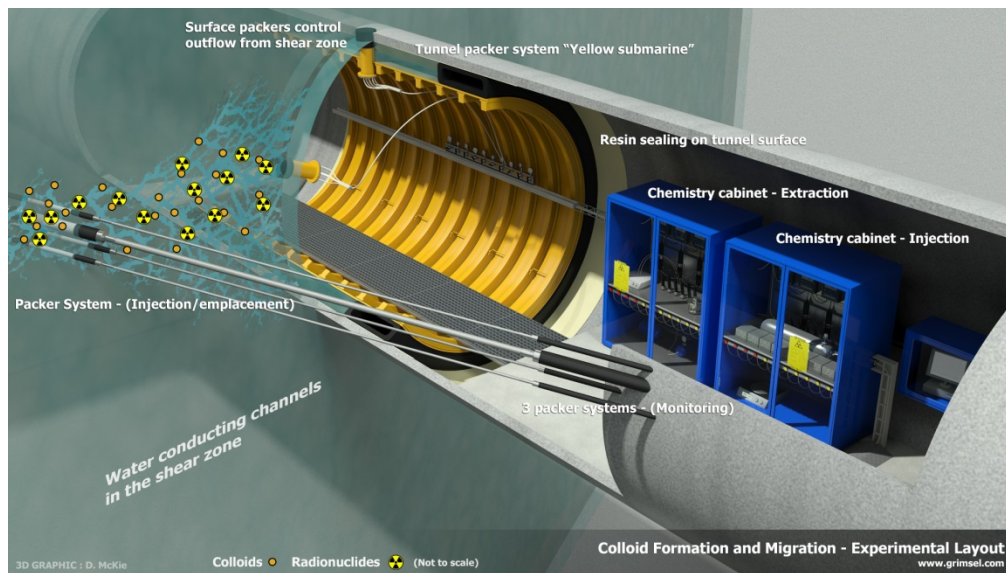
Figure 1. Experimental layout of the CFM field test.

On 11th May 2014, a specially designed bentonite emplacement packer system made up of bentonite rings inserted with 16 glass 1 mL ampoules containing radionuclide (Ca-45, Se-75, Tc-99, Cs-137, U-233, Am-241, Pu-242 and Np-237) labelled bentonite paste was successfully emplaced in the shear zone and has since been continuously monitored via near-field boreholes and sampling of an outflow point on the tunnel wall (far field monitoring). The bentonite source will remain in place for at least 3 – 5 years under steady flow conditions with the option to increase flow around the source depending on the monitored bentonite and tracer loss. Eventually the whole source term and parts of the shear zone will be overcored after stabilization by resin injection for detailed lab based studies on the source term by the CFM partner organisations.

One key target of the ongoing LTD project is to derive diffusion coefficients in-situ, and to determine and assess any differences in the values derived from laboratory tests on rock samples; the standard method for deriving diffusion coefficients (i.e. upscaling from lab scale to field scale). As part of the field study program of the LTD

project, a second in-situ field test (Figure 2) was set up to study the in-situ diffusion of HTO, Cl-36, Na-22, Ba-133 (Sr-90 analogue) and Cs-124 as well as stable Se(VI) (Se-79 analogue).
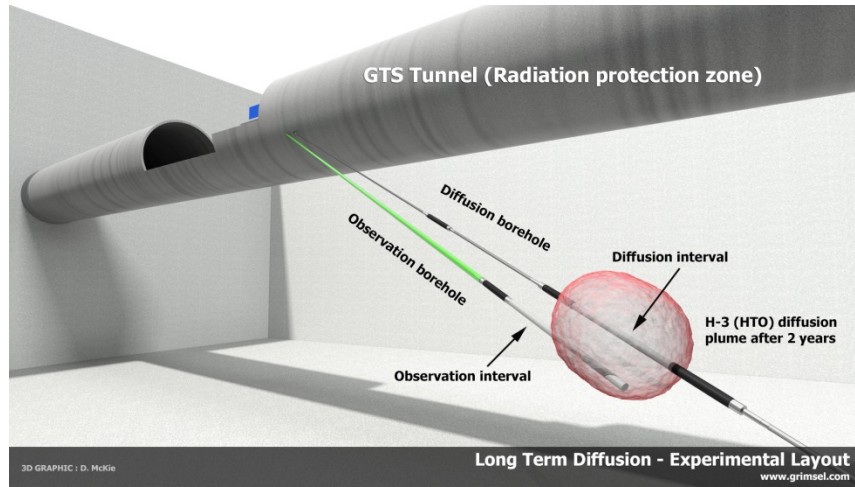
Figure 2. Illustration of the LTD field test consisting of surface equipment in the GTS radiation controlled zone, injection borehole (17 m) and observation borehole (15 m).

Circulation of the radionuclide cocktail was started on 5th March 2014 and will be monitored for at least three years before being overcored and analysed. Monitoring of radionuclide concentration decrease with time due to diffusion and sorption is ongoing. The HTO diffusion plume breakthrough was detected in the observation borehole six months after the start of circulation.

[*]CFM project partners: BMWi/KIT-INE (Germany), JAEA (Japan), POSIVA (Finland), KAERI (South Korea), DOE/Los Alamos (United States of America), RWM (United Kingdom) and NAGRA (Switzerland).
[**]LTD project partners: JAEA (Japan), SURAO/UJV (Czech Republic), HYRL (Finland) and NAGRA (Switzerland).

[1] Martin, A. J. and I. Blechschmidt (2009). "Studies on radionuclide transport behaviour – The next generation of in-situ experiments at the Grimsel Test Site." Mater. Res. Soc. 1193: 159 – 167.

MIGRATION MECHANISMS OF PLUTONIUM, OTHER ACTINIDES AND FISSION PRODUCTS AT THE LITTLE FOREST LEGACY SITE

T.E. Payne, M.J. Comarmond, J.J. Harrison, M.A.C. Hotchkis, C.E. Hughes, M.P. Johansen

Australian Nuclear Science and Technology Organisation, Locked Bag 2001, Kirrawee DC, Sydney, New South Wales 2232, Australia

The Little Forest Legacy Site (LFLS), located on the urban fringes of the major city of Sydney, Australia, was used by the Australian Atomic Energy Commission (AAEC) to dispose of low level radioactive waste in shallow trenches during the 1960s. According to operational records, various radionuclides were disposed, including both plutonium and uranium. The total amount of Pu disposed was a few grams, with [239]Pu being the isotope most commonly mentioned in available disposal records. The uranium waste included the man-made isotope [233]U and uranium enriched in [235]U. Environmental samples from LFLS and its environs often contain [241]Am in association with Pu and U isotopes, as well as the fission products ^{137}Cs and [90]Sr. The presence of readily measurable tritium in many groundwater samples (and some surface water samples) from the site has enabled the pathways of water movement to be identified [1]. A major project is underway to study the movement of radioactivity at the site with the primary objective of assessing the most suitable long-term management options [2]. The project includes a range of sampling, analysis and field experiments.

One of the main findings from the project has been the identification of a mechanism known as "bathtubbing" which has caused significant quantities of radionuclides (particularly Pu and Am) to be present in surface soils near the trenches [3]. Bathtubbing is a process by which the former trenches, which are located in a low-permeability clay-rich surface layer, fill with water during major rainfall episodes and overflow at the ground surface. As a result, it appears that the plutonium primarily moves in surface pathways rather than through groundwater. Due to the importance of the bathtub mechanism for actinide dispersal at LFLS, the chemical form and oxidation state of Pu in the LFLS trench-waters has been subject to detailed study and the formation of a colloidal Pu phase has been described [4]. Studies of several other issues relevant to the site are in progress, including the uptake of radionuclides in vegetation, the isotopic composition of plutonium in LFLS samples (as compared with local fallout), and the adsorption of radionuclides on local soils.

The present paper synthesises the available information on the distribution of radionuclides at the site, and contrasts the behaviour of the various radionuclides, particularly the relative importance of different pathways and mechanisms. While the subsurface clays have been effective in retarding the migration of actinides, it is the low-permeability of these clays which is largely responsible (together with infiltration from episodic rainfall) for the the contamination of the actinides in the surface soils. The behaviour of the fission products (^{90}Sr and ^{137}Cs) is more complex, and these radionuclides may move by both surface and sub-surface pathways. Adsorption experiments have shown that the mobility of Sr is dependent on groundwater pH, which is variable across the site. Tritium is a useful marker of subsurface water movement. However, as tritium and plutonium move by different pathways, tritium cannot be relied on as an advance indicator of the migration of plutonium. Similar conclusions have been reported for the Mortandad Canyon near Los Alamos National Laboratory in the USA [5]. Further away from the LFLS, the isotopic content of traces of Pu in environmental samples enables the signature derived from the LFLS to be differentiated from local fallout.

[1] C.E. Hughes, et al. J. Environmental Radioactivity, 102, 943 (2011).
[2] T.E. Payne. Background Report on the Little Forest Burial Ground Legacy Waste site. ANSTO E-780. Australian Nuclear Science and Technology Organisation (2012).
[3] T.E. Payne, et al. Environmental Science & Technology, 47, 13284 (2013).
[4] A. Ikeda-Ohno, et al. Environmental Science & Technology, 48, 10045 (2014).
[5] W.R. Penrose, et al. Environmental Science & Technology, 24, 228 (1990).

SPECTROSCOPY AND SPECIATION OF ACTINIDES IN NATURAL SEAWATER

M. Maloubier[1], C. Moulin[2], M. Monfort[2], P. L. Solari[3], P. Moisy[4], <u>C. Den Auwer[1]</u>

[1]*Université Nice Sophia Antipolis, Institut de Chimie de Nice UMR7272, 06108 Nice, France*
[2]*Commissariat à l'Energie Atomique, DAM/DIF/DASE 91297 Arpajon, France*
[3]*Synchrotron SOLEIL, MARS beam line, 91192 Gif sur Yevette, France*
[4]*Commissariat à l'Energie Atomique, DEN/DRCP 30207 Bagnols sur Cèze, France*

In the framework of research on the environmental and biological impact of radionuclides, it is of crucial importance to attempt to perform direct determinations of the physico-chemical species or speciation of these elements in the various compartments of the biosphere [1]. Among the different environmental matrices, seawater has not been extensively studied although it contains traces of radionuclides from previous atmospheric nuclear tests or accidental releases. It is also the ultimate receptacle of rivers containing radionuclides at trace levels. The latest event of the Fukushima accident has dramatically demonstrated that seawater might be of first major concern [2-3] due to the potential impact of numerous radionuclides present within the reactors. We address here the speciation of uranium (under the $\{UO_2^{2+}\}$ form), neptunium (under the $\{NpO_2^+\}$ form) and americium (under the Am^{3+} form) with a combination of Extended X-ray Absorption Fine Structure (EXAFS), Time-Resolved Laser-Induced Fluorescence (TRLIF) and speciation modeling using the JCHESS code [4]. Given the available sensitivities of both TRLIF and EXAFS spectroscopic probes we have decided to work at a doping concentration of [U, Np, Am] = $5 \ 10^{-5}$ M (10^{-5} M was also performed). This value is most probably not representative of the amount, which can be released, in accidental cases but it is a compromise between our lowest workable concentration for EXAFS acquisition and the less intrusive doping concentration. Indeed, at $5 \ 10^{-5}$ M actinide concentrations are still below the main ion concentrations (in particular carbonates).

Figure 1 shows the adjusted EXAFS spectra at the L_{III} and L_{II} edges of uranium and neptunium respectively (for Np, the presence of bromine in seawater precludes the use of L_{III} edge). For uranium(VI), comparison between the theoretical speciation using JCHESS and the spectroscopic data (TRLIF and EXAFS) lead to unambiguously identify the $Ca_2UO_2(CO_3)_3$ complex as the main uranium species in doped seawater at [U(VI)] = $5 \ 10^{-5}$ M. Interestingly, the spectroscopic data on doped seawater obtained in this work are in very good agreement with previous work on natural water from a different matrix (source water [5]) for which the predominant species was determined to be the $Ca_2UO_2(CO_3)_3$ complex, although the presence of the ternary $Mg-UO_2-CO_3$ complex has also been reported lately [6]. For neptunium(V), EXAFS data indicate the presence of at least one carbonate ligand but a mixing cannot be precluded. Indeed according to the speciation calculation, neptunium should be present in two forms in approximately equal amounts : the Np(V) aquo ion and the monocarbonato complex. Using a specific design for diluted samples, EXAFS data have been obtained at 10^{-5} M (which is only three order of magnitude higher than uranium natural concentration) and similar results have been obtained. For americium, the theoretical speciation predicts a monocarbonato species and the analysis of the EXAFS data confirms this speciation with a monodentate carbonate ligand. Similar work has been performed on neptunyl and uranyl cations at the same doping concentration ($5 \ 10^{-5}$ M) but also at a lower concentration (10^{-5} M). These data bellow $5 \ 10^{-5}$ M have been recorded with a new design used for radioactive dilute samples. An attempt at concentration 10^{-6} M for a doped neptunium seawater solution has also been performed and a XANES spectrum has been obtained.

These data confirm the role of carbonates in seawater and the importance of the speciation to understand the behavior of radionuclides in complex natural media, in particular seawater. For instance in the case of uranium, the $Ca_2UO_2(CO_3)_3$ complex is not bioavailable.
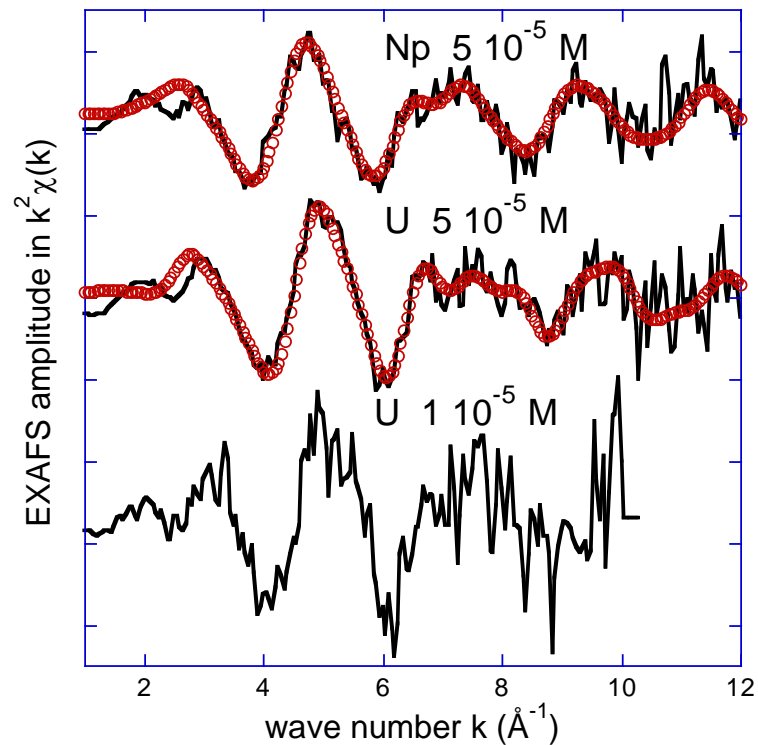
Figure 1 : Experimental and adjusted EXAFS spectra at the L_{III} and L_{II} edges of uranium and neptunium respectively in doped seawater.

[1] G. Choppin, B. Allard, A. Freeman, C. Keller, Handbook on the Physics and Chemistry of the Actinides. A J Freeman and C. Keller Ed (1985).
[2] P. C. Burns, R. C. Ewing, A. Navrotsky, Science(Washington) 335, 1184 (2012).
[3] S. Maxwell, B. Culligan, J. Hutchison, R. Utsey, D. McAlister, J Radioanal Nucl Chem., 300, 1175 (2014).
[4] J. Van der Lee, JCHESS version 2.0. École des Mines de Paris, Centre d'information géologique, 2000–2001 (2010).
[5] O. Prat, T. Vercouter, E. Ansoborlo, P. Fichet, P. Perret, P. Kurttio, L. Salonen, Environmental Science & Technology, 43, 3941 (2009).
[6] F. Endrizzi, L. Rao, Chemistry, a European Journal, 20, 14499 (2014)

MODELLING OF IN-SITU DIFFUSION EXPERIMENTS PERFORMED IN ONKALO UNDERGROUND FACILITY

M. Voutilainen[(1)], P. Kekäläinen[(1)], M. Siitari-Kauppi[(1)], K. Helariutta[(1)], J. Ikonen[(1)], J. Sammaljärvi[(1)], A. Poteri[(2)], P. Andersson[(3)], K. Nilsson[(3)], J. Byegård[(3)], M. Skålberg[(3)], J. Kuva[(4)], P. Pitkänen[(5)], K. Kemppainen[(5)], J. Liimatainen[(5)], I. Aaltonen[(5)], L. Koskinen[(5)]

[(1)]Department of Chemistry, University of Helsinki, P.O.Box 55, 00014 University of Helsinki, Finland [(2)]VTT, P.O.Box 1000, 02044 VTT, Finland
[(3)]Geosigma AB, P.O.Box 894, 75108 Uppsala, Sweden
[(4)]Department of Physics, University of Jyväskylä, P.O.Box 35, 40014 University of Jyväskylä, Finland
[(5)]Posiva Oy, Olkiluoto, 27160 Eurajoki, Finland

Spent nuclear fuel from nuclear power plants, owned by TVO (Teollisuuden Voima Oy) and Fortum, is planned to be disposed in a repository at a depth of more than 400 meters in the bedrock of Olkiluoto (Eurajoki, Finland). The repository system of multiple release barriers consists of both manmade and natural barriers. The surrounding rock acts as the last barrier if other barriers fail during passage of the millennia. Therefore, safe disposal of spent nuclear fuel requires information on the radionuclide transport and retention properties within the porous and water saturated rock matrix along the water conducting flow paths.

It is assumed that the main retention mechanisms are diffusion from the fractures into the rock and sorption on mineral surfaces both on the fracture walls and in the rock. Numerical parameters for diffusion and sorption phenomena (effective diffusion coefficient D_e and distribution coefficient K_d) used in the current safety case calculations are determined by laboratory experiments. However, recent studies imply that values determined in laboratory may overestimate these parameters and thus retention caused by them. The aim is to study diffusion and sorption of radionuclides in the rock matrix in real in-situ conditions and compare the results with parallel laboratory results. These in-situ experiments are being performed and planned in ONKALO, the underground rock characterization facility in Olkiluoto, as a part of a project "rock matrix REtention PROperties" (REPRO) [1]. The REPRO research niche is located at a depth of 420 meters close to the planned repository site.

The first two in-situ experiments using radioactive tracers were performed during 2012-2014. In these in-situ water phase matrix diffusion experiments (WPDE1 and WPDE2) a short concentrated pulse of selected radionuclides was injected to a water flow through an artificial fracture and their breakthrough was measured after passing the fracture. The 1 mm thick artificial fracture was formed by a 2 meter long packed-off section of a drill hole and a flow guide placed on center of the drill hole. Breakthrough of radionuclides was determined as a function of time with an online gamma detector and by collecting laboratory water samples from the outflow. In WPDE1 constant flow rate of 20 μl/min and a mixture of HTO, ^{22}Na, ^{36}Cl and ^{125}I were used. As for WPDE2, constant flow rate of 10 μl/min and a mixture of HTO, ^{22}Na, ^{36}Cl, ^{85}Sr and ^{133}Ba were used. Otherwise the experiments were identical.

The measured breakthrough curves of HTO, ^{22}Na and ^{36}Cl were analyzed using analytical solution of partial differential equation group describing the system [2] (see Figure 1). The model takes into account advection, diffusion and dispersion in flow channel, diffusion and sorption in rock matrix and simple heterogeneity of the flow field and the rock matrix. In the breakthrough curves the early time behavior was explained by advection and the effect of heterogeneities whereas properties of intact rock come visible at late times. The solution for tracer breakthrough curve couples rock porosity (ε), effective diffusion coefficient (D_e) and distribution coefficient (K_d) in one fitting parameter. Thus, this analysis is based on the porosity value from laboratory experiments [3]. Table 1 presents the results; note that D_e has been converted to apparent diffusion coefficient (D_a) using ε and K_d. Using ε from laboratory experiments we were able to determine D_e for HTO from the fitting parameter (K_d was assumed to be zero). Furthermore, these ε and D_e were used to determine K_d for ^{22}Na. Behavior of ^{36}Cl could not be explained thoroughly using the same values of D_e and ε as for HTO. Since it is unrealistic to decrease only D_e or ε, both were decreased following Archie's law kind of relation. As ^{36}Cl is an anion, it is plausible that it is repelled by the negatively charged mineral surfaces and thus it can diffuse only in part of the pore space. Results from both experiments are in good agreement and the same parameters were used to explain early time behavior

which builds confidence on the analysis performed. Analyses for ^{125}I, [85]Sr and [133]Ba, for which the results have shown sorption onto the minerals surfaces, are still in progress.
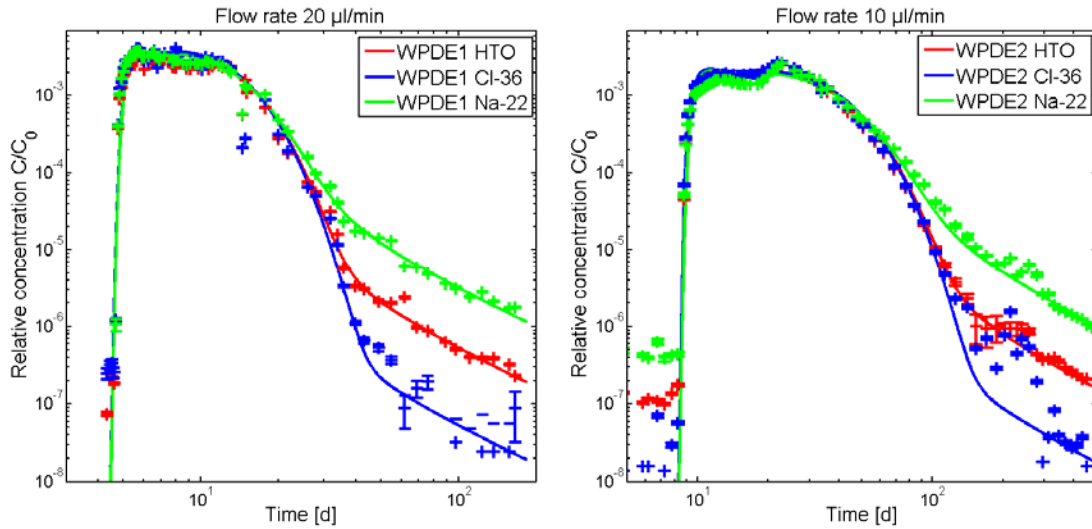
Figure 1. Breakthrough curves of HTO (red), [36]Cl (blue) and [22]Na (green) from first (left) and second (right) water phase matrix diffusion experiments. Effect of retardation by matrix diffusion and sorption is seen in the late time behavior.

Table 1. Rock matrix porosities (ε), apparent diffusion coefficients (D_a) and distribution coefficients (K_d) determined from measured breakthrough curves of HTO, [36]Cl and [22]Na from both experiments.

	WPDE1, 20 µl/min			WPDE2, 10 µl/min		
	ε [%]	D_a [m^2/s] $\times 10^{-11}$	K_d [m^3/kg] $\times 10^{-4}$	ε [%]	D_a [m^2/s] $\times 10^{-11}$	K_d [m^3/kg] $\times 10^{-4}$
HTO	0.6 ± 0.1	1.6 ± 0.8	-	0.6 ± 0.1	1.7 ± 0.9	-
[36]Cl	0.10 ± 0.05	0.6 ± 0.4	-	0.11 ± 0.05	0.6 ± 0.4	-
[22]Na	0.6 ± 0.1	0.016 ± 0.011	1.3 ± 0.7	0.6 ± 0.1	0.015 ± 0.010	1.5 ± 0.8

[1] Voutilainen, M., Poteri, A., Helariutta, K., Siitari-Kauppi, M., Nilsson, K., Andersson, P., Byegård, J., Skålberg, M., Kekäläinen, P., Timonen, J., Lindberg, A., Pitkänen, P., Kemppainen, K., Liimatainen, J., Hautojärvi, A. and Koskinen, L. (2014). "In-situ experiments for investigating the retention properties of rock matrix in ONKALO, Olkiluoto, Finland." Waste Management 2014 Conference Proceedings 40, 14258.
[2] Kekäläinen, P., (2014). "Analytical solutions to matrix diffusion problems", AIP Conference Proceedings 1618(1), 513-516.
[3] Sammaljärvi, J., Ikonen, J., Voutilainen, M., Kuva, J., Lindberg, A., Siitari-Kauppi, M., Timonen, J., (2014). "Investigation of rock matrix retention properties. Supporting laboratory studies I: Mineralogy, porosity and pore structure." Posiva working report 2014-68.

POROSITY IMPAIRMENT INDUCED BY DIFFUSION OF REACTIVE FLUIDS IN POROUS MATERIALS: EXPERIMENT APPROACH AND MODELING

I. Fatnassi[1,2], S. Savoye[1], P. Arnoux[1], O. Bildstein[3], V. Detilleux[4], C. Wittebroodt[5], P. Gouze[2]

[1] CEA, DEN, DPC, Laboratory of Radionuclides Migration Measurements and Modeling, F-91191 Gif-sur-Yvette, France. (*ikram.fatnassi@cea.fr*; *sebastien.savoye@cea.fr*; *patrick.arnoux@cea.fr*)

[2] Géosciences Montpellier, CNRS UMR 5243, Université de Montpellier, F-34095 Montpellier Cedex 5, France. (*philippe.gouze@univ-montp2.fr*)

[3] CEA, DEN, DTN, Laboratory for modeling of transfers in the Environment, F-13108 Saint Paul lez Durance, France. (*olivier.bildstein@cea.fr*)

[4] Bel V, 148 Walcourtstraat, B-1070 Brussels, Belgium. (*valery.detilleux@belv.be*)

[5] IRSN, PRP-DGE, SRTG, LETIS F-92260 Fontenay-aux-Roses, France. (*charles.wittebroodt@irsn.fr*)

Disposal in geological clay formations is one of the solutions envisaged for managing the fate of high / intermediate level as well as long-lived nuclear wastes. The long-term evolution of these repositories is expected to be largely governed by a.o. geochemical processes that can irreversibly modify the containment properties of the materials used in the multi-barrier system. For instance, mineral dissolution and precipitation can significantly change their transport properties by enlarging or clogging the pore space. However, addressing the feedback of porosity changes in the long-term simulations coupling chemistry and diffusive transport is still an issue, especially because of the lack of dedicated experiments required for calibrating the numerical models. The objective of this study is to assess the ability of numerical codes (two reactive transport tools, HYTEC and CRUNCH) to reproduce experimental results obtained from reactive diffusion experiments carried out through porous media with an increasing complexity (from glass frit, to sandstone, chalk, and argillite). For that purpose, a large data set was acquired from experiments for which inert and reactive tracers diffuse through the porous media while precipitation and/or dissolution reactions take place. The solution chemistry and the tracer fluxes were monitored by regular sampling into the reservoirs. At the end of the experiments, complementary experimental techniques such as SEM-EDS or gamma-autoradiography were used, allowing the quantification of the mineralogy/porosity changes within the aged materials.

The results showed that the tracer diffusion into most of the reacting porous media was affected by precipitation, the impact intensity being roughly related to the pore size distribution and the precipitate type. For instance, the cells with chalk in which barite was expected to precipitate, displayed a clear impact of the clogging process from the experiment start, with a continued decrease of the HTO flux that became 40 times lower than the flux measured in the sound chalk sample (Figure 1). Conversely, the clogging effect on HTO fluxes induced by gypsum precipitation was observed (i) much later (i.e. 70 days after the beginning of the experiment) and (ii) with a weaker intensity, the HTO flux decreasing by a factor of 3 compared to the sound chalk sample. These results suggest that the clogging efficiency would be more related to the nature of the mineral than the amount of precipitated matter.

Finally, most of the simulations performed with CRUNCH and HYTEC were, at this stage, unable to properly reproduce the experimental results, especially those obtained in the diffusion/precipitation barite experiments (Figures 1 and 2). This issue will be discussed regarding the kinetic laws considered in the two codes and the empirical formulation of Archie's law used to relate the diffusion coefficient with the porosity change.
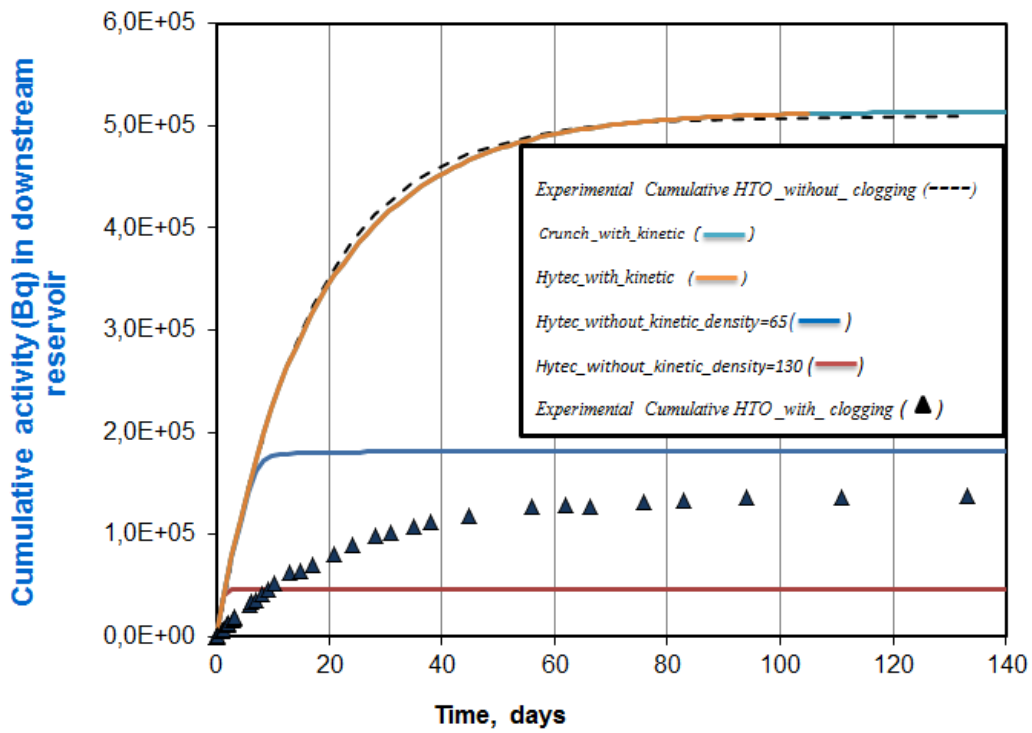
Figure 1: Cumulative activity in downstream reservoir in the chalk/barite experiment
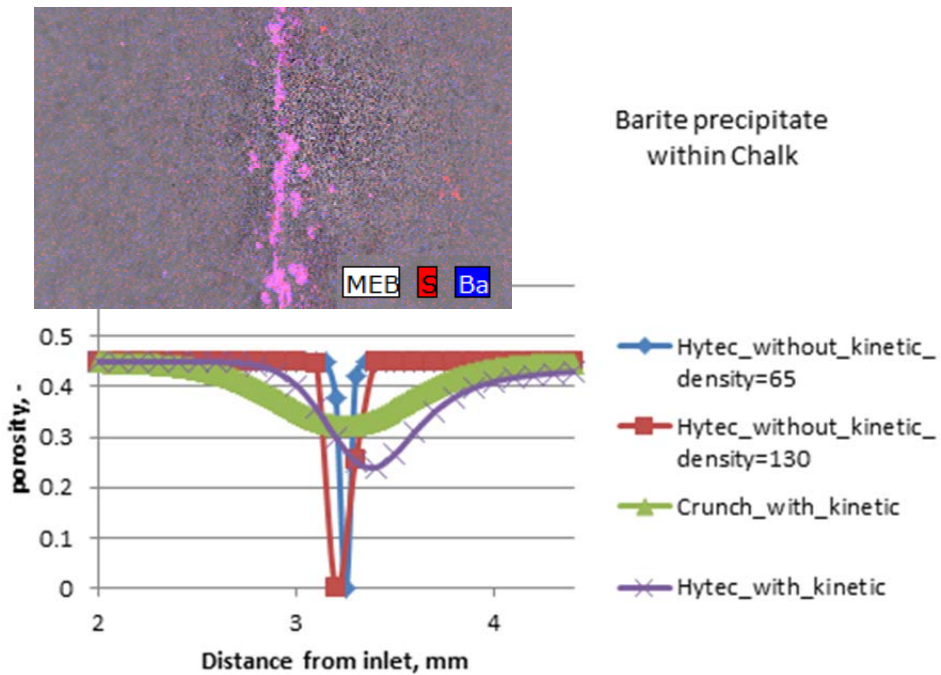
Figure 2: Comparison between the barite precipitate location in the experiment and the calculated porosity in reactive transport simulations

COUPLED GROUNDWATER FLOW AND REACTIVE TRANSPORT REGIONAL-SCALE SIMULATIONS OF THE EVOLUTION OF GROUNDWATER CHEMISTRY FOR

A GEOLOGICAL SPENT NUCLEAR FUEL REPOSITORY

S. Joyce [(1)], L. Hartley [(1)], H. Woollard [(1)], N. Marsic [(2)], M. Sidborn [(2)], B. Gylling [(3)], I. Puigdomenech [(3)], L. Koskinen [(4)]

[(1)]Amec Foster Wheeler, Building 150, Harwell Oxford, Didcot, Oxfordshire, OX11 0QB, United Kingdom

[(2)] Kemakta Konsult AB, Box 1265, 112 93 Stockholm, Sweden

[(3)] SKB, Box 25, SE-101 24, Stockholm, Sweden

[(4)] Posiva Oy, Olkiluoto, FI-27160 Eurajoki, Finland

SKB has submitted a license application for a spent nuclear fuel repository at Forsmark sited in crystalline rocks of the Fennoscandian shield [1]. In support of this application various quantitative assessments were made to demonstrate the long-term safety of the proposed repository. One such assessment involved simulation of groundwater chemical evolution to quantify impacts on safety functions for the disposal system related to the geochemical conditions, particularly salinity, pH and redox conditions. In the reference case the current temperate period lasts until 12,000 AD. A case of prolonged meteoric infiltration to 60,000 AD is also considered resulting from e.g. global warming [2]. This is to fulfil a regulatory request to assess whether extended dilute water infiltration might lead to a rise in redox potential and also to an increase in erosion of the bentonite barrier due to formation of colloids. In order to perform long transient simulations of groundwater flow and solute transport with water-solute-rock interactions, new tools have been developed to closely couple geochemical, groundwater flow and transport calculations, and perform these efficiently using parallel computing techniques [3]. In assessing this case, sensitivities are tested to the geochemical reaction schemes appropriate to the site. The results of this work predict the chemical environment at repository depth stabilises at around 20,000 AD and shows little change beyond that (Figure 1). The salinity of the groundwater is governed by the low permeability (ca. 10^{-19} m^2) of the bedrock and rock matrix diffusion, resulting in relatively shallow and slow circulation of groundwater (Figure 2). The chemical reactions influence concentrations of reactive species, the calculated pH and redox potential. In particular, the redox reactions thought to be relevant for the Forsmark site maintain reducing conditions at repository depth, even with infiltration at the ground surface of meteoric water with relatively high redox potential.
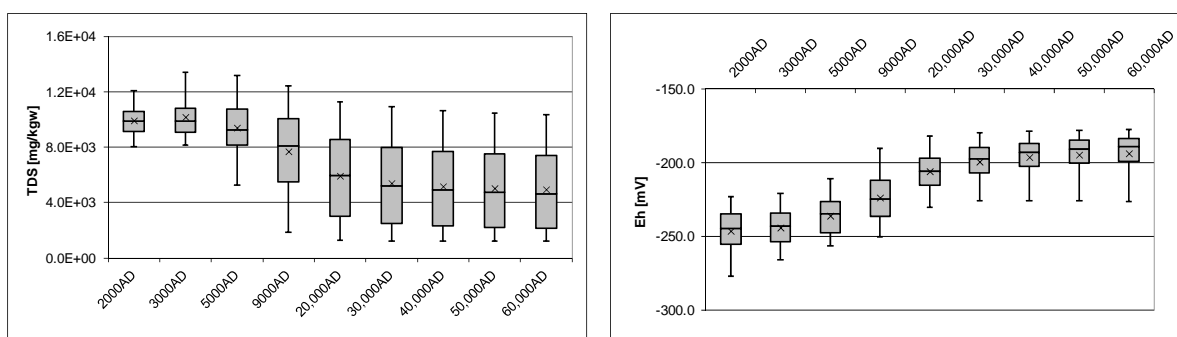
Figure1. Box and whisker plot showing the statistical distribution of total dissolve solids, TDS, (left) and redox potential, Eh, (right) for the Forsmark repository volume. The statistical measures are the median, the 25th and 75th percentiles (box), the mean (cross) and the 5th and 95th percentiles (whiskers). The reactions included are equilibration of groundwater with calcite, quartz and amorphous iron (II) sulphide.
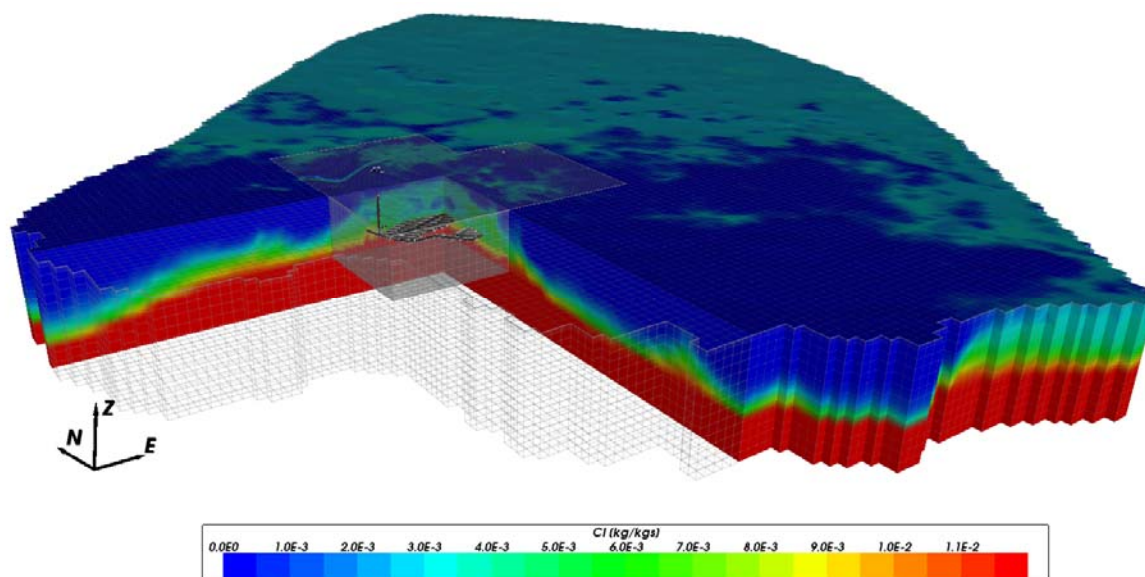
Figure 2. Forsmark regional-scale model coloured by the chloride mass fraction at 2000 AD. The repository is shown in the centre in black for context, but is not explicitly represented in the far-field in the model. Part of the model has been removed to reveal the interior.

[1] SKB. Long-term safety for the final repository for spent nuclear fuel at Forsmark. SKB TR-11-01, Svensk Kärnbränslehantering AB. (2011).

[2] S. Joyce, H. Woollard, N. Marsic, M. Sidborn. Future evolution of groundwater composition at Forsmark during an extended temperate period. SKB R-14-26, Svensk Kärnbränslehantering AB (2014).

[3] S. Joyce, D. Applegate, P. Appleyard, A. Gordon, T. Heath, F. Hunter, J. Hoek, P. Jackson, D. Swan, H. Woollard. Groundwater flow and reactive transport modelling in ConnectFlow. SKB R-14-19, Svensk Kärnbränslehantering AB (2014).

ROCK FRACTURE CLOSURE MEDIATED BY PRESSURE SOLUTION IN A COUPLED FLOWING CHANNEL–ROCK MATRIX–STAGNANT ZONE SYSTEM

B. Mahmoudzadeh, L. Liu, L. Moreno, I. Neretnieks

Department of Chemical Engineering and Technology,
Royal Institute of Technology, KTH,
S-10044 Stockholm, Sweden

Fracture apertures in crystalline rocks may decrease or increase by different mechanical and chemical mechanisms. In fractured rocks, the two surfaces of a fracture are in contact with each other in some asperities but are open in other locations. At the contact asperities, the local stress is higher than the average stress on the whole fracture since stress is concentrated in a small part of entire fracture surface. When fractured rocks contain water, the minerals dissolve if the water is not saturated. At contacting asperities with high concentrated stress the solubility of minerals is higher than at fracture voids. The minerals tend to dissolve there and precipitate where the stress is lower. This, so-called pressure dissolution process may lead to closure of the fracture. In contrast, free-face dissolution at fracture voids with unsaturated fluid may result in local fracture widening [1].

In addition, any advective flow through the fracture that can carry in or away dissolved minerals and even colloidal mineral fragments complicates the situation. Matrix diffusion has been found to be an important process that retards contaminant transport in fractured crystalline rocks [2]. It is recently shown that matrix diffusion is also very important for chemically mediated closing of fractures in crystalline rocks [3]. The effect of stagnant water zones in a fracture plane on solute retardation has been recently studied [4]. In the present study, it will show that stagnant water zones in the fracture plane can also affect fracture closure in crystalline rocks.

A model is developed to study closure rate of a fracture in fractured rocks. It accounts for advection through the fracture, diffusion into the rock matrix as well as into the stagnant water existing in the fracture plane, pressure dissolution and free-face dissolution/precipitation of stressed and unstressed minerals in the fracture. Analytical expressions for the Laplace-transformed concentrations in the flowing channel, the stagnant water zone and the rock matrix are derived. In the analytical solution the rates of different competing processes is summarized in a limited number of characteristic terms. A pseudo-steady-state approach is used to get closure/opening rate of fracture due to stress or the conditions that may cause growing of the fracture aperture.

The developed model has been applied to examine the concentration of dissolved minerals in a flow-through test on a natural fracture [5]. As seen in Figure 1, the model shows a fair agreement with the experimental observations at high temperatures although at low temperatures there is a difference of about three orders of magnitude with the results of our model. It results from the possibility that there may be a contribution of released colloidal particles in the experiments at low temperatures which has not been accounted for in the present model.

A multitude of simulations are performed to illustrate contribution of different processes/mechanisms to the closure rate of fracture under different circumstances. The results, as exemplified in Figure 2 for concentration in the stagnant water zone, show that the times involved for any changes in aperture are very much larger than the times needed for concentrations of dissolved minerals to reach steady state in the rock matrix, the stagnant water zone and the flowing channel. This suggests that the steady state model can be used to assess the evolution of concentration in the rock fracture. Moreover, simulations present that diffusion into the rock matrix, which acts as a sink/source for dissolved minerals, clearly dominates the rate of concentration change and consequently the rate of evolution of the fracture aperture.

[1] Liu, J., J. Sheng, A. Polak, D. Elsworth, H. Yasuhara, and A. Grader (2006), A fully-coupled hydrological–mechanical–chemical model for fracture sealing and preferential opening, *Int. J. Rock Mech. Min. Sci.*, 43: 23–36
[2] Neuman, S. P. (2005), Trends, prospects and challenges in quantifying flow and transport through fractured rocks, *Hydrogeol. J.*, 13: 124–147
[3] Neretnieks, I. (2014), Stress-mediated closing of fractures—Impact of matrix diffusion, J. Geophys. Res. Solid Earth, 119, doi:10.1002/2013JB010645
[4] Mahmoudzadeh, B., L. Liu, L. Moreno, and I. Neretnieks (2013), Solute transport in fractured rocks with stagnant water zone and rock matrix composed of different geological layers—Model development and simulations. *Water Resources. Res.* 49: 1709–1727

[5] Yasuhara, H., A. Polak, Y. Mitani, A. Grader, P. Halleck, and D. Elsworth (2006), Evolution of fracture permeability through fluid-rock reaction under hydrothermal conditions. *Earth Planet Sci. Lett.* 244:186–200
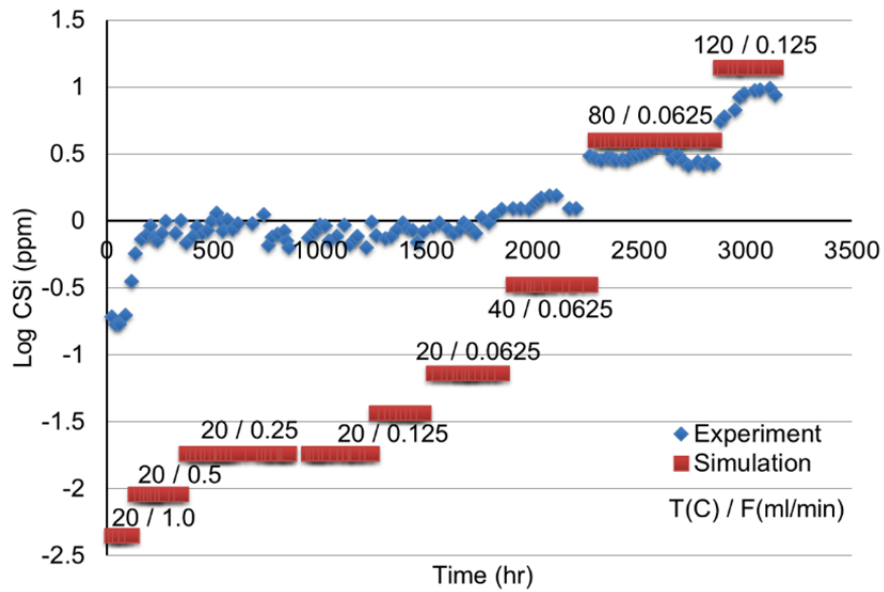
Figure 1. Comparison of Si concentration between experimental results [5] and model predictions
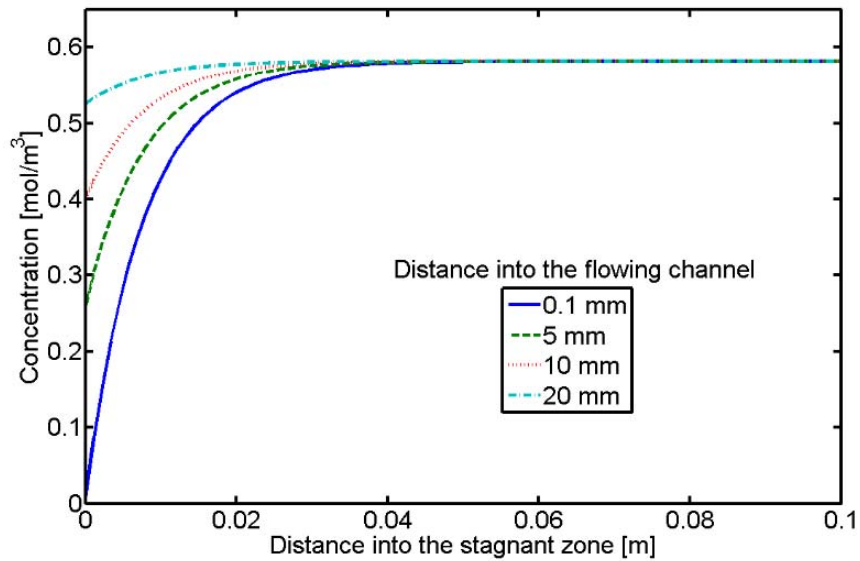
Figure 2. Concentration of dissolved minerals in the stagnant water zone

"RESET" OF UNITED STATES NUCLEAR WASTE MANAGEMENT STRATEGY AND POLICY

R.C. Ewing[1]

[1]Center for International Security and Cooperation, Stanford University Stanford, CA 94305-6165

In February of this year, the *Freeman Spogli Institute for International Studies* and the *Precourt Institute for Energy* sponsored the first of a series of meetings on U.S. nuclear waste management strategy and policy. This presentation is a report on the first meeting.

The motivation for these meetings is that the U.S. nuclear waste management program is stymied on multiple fronts – from the disposal of HLW and transuranic waste of defense programs, to spent nuclear fuel from commercial nuclear power plants, and even, the disposition of fissile material from dismantled nuclear weapons. At Hanford, Washington, the vitrification plant for the solidification of high-level, radioactive waste has been plagued by design problems, escalating cost and continued delays. The disposal of transuranic waste at the WIPP in New Mexico, has been interrupted by the accidental release of radioactivity on Valentine's day of 2014. WIPP may remain closed for several years for clean-up and until a new ventilation system is installed. Commercial spent fuel is stranded on sites at nuclear power plants. Interim storage has become a forced solution in the absence of a clear path forward for a geologic repository. The Mixed Oxide Fuel Fabrication Facility, under construction at Savannah River in South Carolina, continues to suffer from rising life-cycle costs, prompting a reconsideration of alternatives that were last considered 20 years ago.

In 2002, Congress approved President George W. Bush's decision that a site at Yucca Mountain in Nevada be selected for the nation's repository for high-activity radioactive waste. In 2008, the DOE submitted an application to the Nuclear Regulatory Commission to construct that facility. Two years later, the Administration concluded that developing a repository at Yucca Mountain was "unworkable." It established the *Blue Ribbon Commission on America's Nuclear Future* (BRC) to make recommendations on what steps should be taken next. The BRC issued its final report in January, 2012. DOE responded favorably to the report in January, 2013. Bi-partisan legislation to implement at least some of the BRC's recommendations has been introduced in the Senate, and hearings were held. But the measure never came to a vote. Today a stalemate prevails between those who continue to maintain that the Yucca Mountain project is "unworkable" and those who believe that the choice of the site is the "law". The stalemate shows no sign of being broken soon.

Against this background, the first meeting (http://fsi.stanford.edu/events/"reset"-us-nuclear-waste-management) assembled a steering committee whose members had extensive experience with the U.S. program or an international nuclear waste management program. The first charge of the committee was to identify the critical issues that must be addressed in ordert to move the U.S. program forward. The audience consisted of a mix of Stanford faculty, fellows and students, but also members of affected communities and scientists and engineers from national laboratories. Many in the audience had no previous exposure to the U.S. nuclear waste program. After two days of presentations and discussion, a third day was devoted to identifing the most important issues to be addressed at subsequent meetings.

The issues identified in order of priority were:
- Structure, properties, and characteristics of a new nuclear waste management organization
- Definition of a consent-based process
- Integration of the entire waste system - from production to disposal of waste
- Review and revision of regulations and risk methodology
- Risk assessment of the *status quo* of the U.S. system over the next several hundred years

Very clearly, the discussion and selection of these topics drew heavily on the recommendations of the Blue Ribbon Commission, but there were subtle and important insights that developed at this meeting – particularly from students. I will try to convey the essense of the discussion of these issues.

WIPP, DE-COMMINGLING, AND THE US REPOSITORY PATH FORWARD

Bruce A. Robinson[1]

[1]*Los Alamos National Laboratory, Los Alamos, New Mexico, USA*

This study considers the benefits of de-commingling of defense and civilian high-level waste through the development a defense waste repository (DWR) in salt. The talk explores the possibility of achieving greater cost efficiency in upstream waste management costs, including waste processing and transportation, in addition to disposal costs, and compares these potential savings to the added cost of developing a separate repository for defense wastes. A systems-level assessment is taken, considering all significant aspects of the management of EM wastes: from waste storage and processing, to packaging, to transportation, to disposal.

A basic premise of the study is that a repository geologic medium that does not require the same level of durability of waste form, disposal package, and engineered barriers may enable cost efficiencies in waste processing, such that the total system cost is favorably impacted by the availability of a DWR in that medium. A salt repository is selected to perform the analysis because of the experience gained from the Waste Isolation Pilot Plant (WIPP), which provides a positive example of the efficacy of bedded salt for the disposal of nuclear waste. Studies have also shown that salt is likely to be among the least expensive geologic media in which to dispose waste.

The principle conclusion is that a DWR in salt could provide cost savings in upstream waste processing that are greater than the expected added cost associated with the development of a separate repository for defense wastes. Cost avoidances are identified for the Hanford tank waste, for which a salt DWR would enable a relaxation of the requirements for waste form durability, and would also provide an earlier disposal end point, thereby reducing storage costs. Direct disposal of cesium and strontium capsules in a DWR is another potential cost avoidance at Hanford, when compared with the introduction of these radionuclides into the glass waste forms at the end of the tank waste treatment mission. Direct disposal of calcine waste at Idaho National Laboratory is a third major cost avoidance, when compared to the current plan to employ hot isostatic pressing as the waste processing technology. Finally, if a DWR in salt could be developed in advance of the expected repository availability date for a repository for both commercial and defense wastes, storage cost savings would be achieved for vitrified high level waste at the Savannah River Site, as well as for defense-related spent nuclear fuel being managed by DOE EM.

Regarding the safety case for disposal of defense wastes in a separate DWR, the WIPP repository provides a strong foundation for building the case for the safety of disposal of high-level waste in salt. The principle gap for defense wastes is that our understanding of salt repository behavior for heat-generating wastes needs to be demonstrated at the field scale by conducting thermal testing in an underground research laboratory. Because the heat generated by defense waste is, in general, lower than for commercial spent nuclear fuel, the technical uncertainties for this waste are modest. By conducting a thermal test at the heat loads of defense waste, the safety case for a salt DWR is enhanced, and public acceptability is more likely to follow. Additionally, a test at modest heat loads would be an important steppingstone for future high-heat load tests to understand the strengths or limitations of salt as a disposal medium for commercial waste.

ACTINIDE SOLUBILITY AND SPECIATION IN A SALT REPOSITORY: CURRENT STATUS

[1]D. T. Reed and [2]M. Altmaier

[1]*Los Alamos National Laboratory, 1400 University Drive, Carlsbad NM, USA.*
[2]*Karlsruhe Institute of Technology, Institute for Nuclear Waste Disposal, Karlsruhe, Germany.*

The salt repository concept is a viable, implementable and cost-effective option for the permanent disposal of nuclear waste, including spent fuel, high-level, and transuranic nuclear waste. This remains true even though there have been some recent operational setbacks in the implementation of this repository concept. This viability is based on the very favorable geology and relative ease of mining bedded and domed salt formations. Salt creep will lead to rapid (< 200 y) self-sealing that can permanently isolate the emplaced waste once repository operations are completed. In this context, the expected and most likely scenario is that little/no brine will be introduced to the waste horizon and the repository will remain unsaturated for the regulatory period of repository performance.

This very favorable geology does not preclude the need for a strong scientific basis and understanding of wasteform behavior and actinide chemistry in a salt repository setting. The importance of this actinide brine chemistry is driven by the regulatory process for the licensing of a nuclear repository which also requires an accounting of the low-probability scenario of brine intrusion. This is in fact the experience of the Waste Isolation Pilot Plant (WIPP) transuranic repository which was licensed in 1999 and has since successful completed two 5-year recertifications. The low-probability brine intrusion scenarios will solubilize and potentially mobilize the actinides present. In this context, it is critical to show that a salt repository will meet the regulatory requirements for actinide containment even in the unexpected (worse-case) scenarios of brine inundation and subsequent release.

A significant amount of research has been completed over the past decade to improve our understanding of actinide/brine chemistry and it is a key goal of this presentation to provide an overview and status of this progress. This scientific progress has also been the subject of a series of international workshops entitled "Actinide and Brine Chemistry in a Salt Repository (ABC-Salt)" [1-3] co-organized by LANL and KIT-INE. Additionally there are a number of ongoing Nuclear Energy Agency (NEA) activities that link to the salt repository concept that address actinide chemistry most notably a detailed assessment of the Pitzer interaction parameters within the NEA Thermodynamic Database Project.

A key observation in these workshops has been the existence of data gaps and the lack of a full understanding of the brine chemistry that defines the mobile actinide concentration when brine interacts with the emplaced waste in addition to remaining unresolved issues regarding the specific radionuclide chemistry itself. This has led to the use of a high degree of conservatism in the performance assessment modeling of actinide solubility and potential release. A key driver of the continued research in this field is the need to remove or minimize these conservatisms to move toward a more realistic but defensible descriptions of the likely actinide speciation and solubility.

The total concentration of actinides in a brine-intrusion scenario is defined by the oxidation state distribution, its solubility, its sorption behavior, and the accounting for colloidal species. The inundated brines are Na-Mg-Cl dominated brines with lesser amounts of sulfate, borate, potassium and bromide that are relatively high in ionic strength (*I* typically > 5 m). This requires the use of the Pitzer approach with a self-consistent set of ion interaction parameters for the key actinide species. There are relatively few data for the transuranic actinides leading to a high reliance on oxidation-state-invariant analogs (e.g., Th(IV) for An(IV), Nd(III) and Cm(III) for An(III)) for solubility measurements [4-7].

Significant progress has been made in understanding some of the key factors that affect oxidation state distribution of multivalent actinides, specifically U, Np, Pu and Am. The presence of reduced iron in anoxic brine systems can lead to the reduction of higher-valent plutonium to Pu(III/IV) and establishes a highly reducing brine chemistry (see Figure 1). There have also been some key correlations with ionic strength and pH in some brine systems. The overall interpretation of the likely oxidation state distribution is however relatively complex and attempts to provide a consistent measurement and quantitative approach have not been completely successful. For this reason there remains a reliance on expert opinion where all redox- impacting factors can be more fully considered.
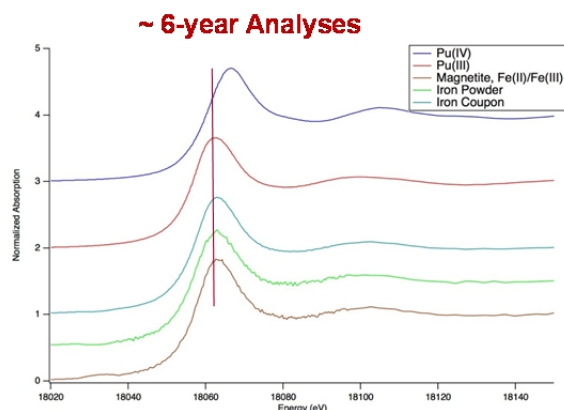
Figure 1.   XANES of precipitated/ associated Pu in Pu-Fe long-term brine experiments showing a predominance of Pu(III) when reduced iron and magnetite were present (analysis performed by J. Terry and D. Olive, IIT at the Argonne Advanced Photons Source synchrotron).

Lastly, there also remain questions on the impacts of radiolysis, microbial activity, sorption, and colloid formation on the actinide source term. These are all the subject of ongoing studies. Overall, although these can have readily measurable impacts on the actinide source term, the effects tend to be relatively small from the perspective of performance assessment (always less than an order of magnitude and typically less than a factor of 2-3). A brief summary of progress in these areas will be given.

References:
1. D. T. Reed and M. Altmaier (Eds.). Proceedings of the International Workshop on Actinide and Brine Chemistry in a Salt-Based Repository (ABC-Salt). Los Alamos National Laboratory report LA-UR-14-28463, Los Alamos, NM, USA, 2014.
2. M. Altmaier, C. Bube, B. Kienzler, V. Metz and D. T. Reed (Eds.). Proceedings of the International Workshops ABC-Salt (II) and HiTAC 2011. Karlrsruhe Institute of Technology, KIT Scientific report 7625. Karlsruhe Germany, 2012.
3. D. T. Reed and M. Altmaier (Eds.). Proceedings of the Third International Workshop on Actinide and Brine Chemistry in a Salt-Based Repository (ABC-Salt III). Los Alamos National Laboratory report LA-UR-15-21114, Los Alamos, NM, USA, 2015.
4. Altmaier, M., V. Neck, and Th. Fanghänel. 2004. *Solubility and Colloid formation of Th(IV) in concentrated NaCl and MgCl₂ Solutions*. Radiochimica Acta, vol. 92: 537–43.
5. Altmaier M., V. Neck, and Th. Fanghänel. 2008. *Solubility of Zr(IV), Th(IV) and Pu(IV) hydrous oxides in CaCl₂ solutions and the formation of ternary Ca-M(IV)-OH complexes*. Radiochimica Acta 96, (9-11) 541-550.
6. Borkowski, M. J-F. Lucchini, M.K. Richmann, and D.T. Reed. 2010a. *Actinide (III) Solubility in WIPP Brine: Data Summary and Recommendations*. Report LA-14360. Los Alamos, NM: Los Alamos National Laboratory.
7. Borkowski, M., M.K. Richmann, and J-F. Lucchini. 2012. *Solubility of An(IV) in WIPP Brine: Thorium Analog Studies in WIPP Simulated Brine*. Los Alamos Report LCO-ACP-17, LA-UR 12-24417. Carlsbad, NM: Los Alamos National Laboratory.

INDEPENDENT MONITORING OF THE 2014 RADIATION RELEASE FROM THE WASTE ISOLATION PILOT PLANT IN NEW MEXICO, USA-AN OVERVIEW.

P. Thakur, B.G. Lemons, S. Ballard and R. Hardy

Carlsbad Environmental Monitoring & Research Center, 1400 University Drive, Carlsbad, New Mexico-88220, USA.

The Waste Isolation Pilot Plant, also known as WIPP, is a transuranic (TRU) waste repository operated by the U.S. Department of Energy (DOE). The repository is emplacing defense-related transuranic (TRU) wastes in the Salado Formation, a bedded salt formation approximately 655 m (2150 ft.) below the surface of the Earth. Located in the Chihuahuan desert of southeastern New Mexico near Carlsbad, the WIPP facility is the world's first underground repository licensed to accept TRU waste, with activity concentrations of alpha-emitting isotopes >3700 Bq/g (> 100 nCi/g) and half-life >20 years. The repository, which became operational in March 1999, has since disposed of more than 86,000 m^3 of TRU waste in more than 165,000 containers, cleaning up 22 waste-generator sites nationwide.

After almost 15 years of operations, the WIPP had one of its waste drums breach underground as a result of a runaway chemical reaction in the waste it contained [1]. This incident occurred February, 14, 2014. Moderate levels of radioactivity were released into the underground air. A small amount of radioactivity also escaped to the surface through the ventilation system and was detected approximately 0.6 miles away from the facility. It was the first unambiguous release from the WIPP repository. The dominant radionuclides released were americium and plutonium, in a ratio that matches the content of the breached drum. The release was detected by an underground CAM located near panel 7 where waste was being emplaced. As soon as CAM alarmed on the night of February 14 went off, the WIPP's ventilation system automatically switched to the filtration mode, reduced the flow, and directed the exhaust air stream through HEPA filter banks. This is intended to prevent any discharge into the atmosphere in the event of an accident involving waste underground. The ventilation system appeared, at the time, to be functioning as designed, so there was no reason to suspect any substantial release to the environment. Since this incident occurred during the night, only a few employees were at the WIPP site and no employees were in the underground. Personnel were frisked and none were reported to have external contamination; however, 21 personnel were found to have positive bioassay results for [241]Am. Follow-up testing results were below the detectable limits of the laboratory analysis, indicating that the radioactive isotopes were excreted from the body. No long-term adverse health effects are expected for these employees.

Following the announcement of the underground radiation detection event by DOE, an independent oversight organization, the Carlsbad Environmental Monitoring & Research Center (CEMRC) used its fixed ambient air radiation monitors located at (1) Onsite, which is about 0.1 km northwest of the WIPP exhaust shaft, (2) Near Field, about 1 km northwest of the facility; and (3) Cactus Flats, about 19 km southeast of the WIPP site to ascertain whether or not there were releases to the ground surface [2]. An accelerated analysis of the underground air both before and after the HEPA filters, called Station A and Station B, respectively was also performed in order to determine the amount and type of radionuclides that were ultimately released into the environment.

Independent analytical results of air filters from sampling stations on and near the WIPP facility released by CEMRC on February 19, 2014 confirmed brief detection of trace amounts of [241]Am and [239+240] Pu at two sampling locations (Onsite and Near Field). The filters that were analyzed had been installed at these stations prior to the event, on February 11, 2014 and were removed on February 16, 2014. The Onsite filter was removed on February 18, 2014 because the site was not accessible until then. A third ambient air- filter station at Cactus Flats showed no detectable americium or plutonium. The highest activity detected was 115.2 µBq/m^3 for [241]Am and 10.2 µBq/m^3 for [239+240] Pu at a sampling station located 91 meters away from the underground air exhaust point and 81.4 µBq/m^3 of [241]Am and 5.8 µBq/m^3 of [239+240]Pu at a monitoring station located approximately one kilometer (0.6 miles) northwest of the WIPP facility. The levels detected were very low, well below any level of public health or environmental contamination concern.

This paper presents the data collected in the aftermath of this incident by an independent oversight organization, the Carlsbad Environmental Monitoring & Research Center (CEMRC). Results to date have been both low and localized, and in many instances, are not even detectable, demonstrating no long-term radiation-related health effects among local workers or the public are expected.
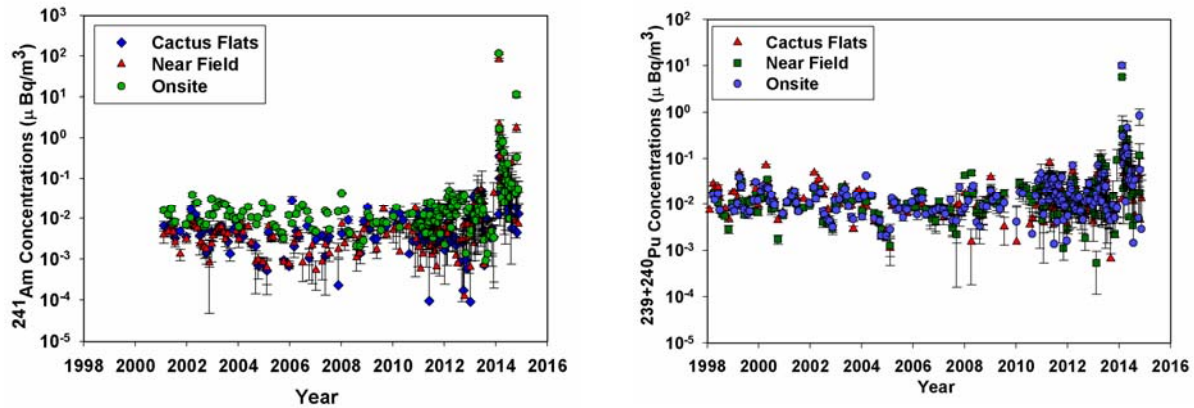
Figure 1. The Pre- and post-release event ^{241}Am (left) and $^{239+240}$Pu (right) and concentrations in ambient air at three stations in the vicinity of the WIPP site.

[1] Waste Isolation Pilot Plant (WIPP). www.wipp.energy.gov.
[2] Carlsbad Environmental Monitoring & Research Center (CEMRC). www.cemrc.org.
http://www.cemrc.org/2014/02/19/cemrc-detects-trace-amounts-radioactive-particles-air-sampling-station-near-wipp-facility/

MINERALOGY OF PLUTONIUM AT THE HANFORD SITE

E. C. Buck,[*] D. D. Reilly, A. R. Felmy, Kirk J. Cantrell

Pacific Northwest National Laboratory, 902 Battelle Blvd., Richland, WA, 99353, USA

Many sophisticated technologies are available that provide nano-scale information, including; speciation, morphology, trace element, and isotopic distribution in plutonium contaminated sediments and soils. Such information can be used to develop environmental risk assessments and for potential remediation strategies.

We will discuss different disposal locations near the Plutonium Finishing Plant at the Hanford site. All of these disposal sites received high concentrations of Pu, as high as 150 kg at the Z-9 trench. However, the types of waste disposed at each location are quite different. This difference in waste chemistry resulted in dramatic differences in subsurface migration behavior. It also resulted in different chemical forms of the disposed Pu and Am. Recent studies designed to determine this chemical form, including X-Ray absorption spectroscopy (XAS), transmission electron microscopy (TEM) and NanoSIMS analysis will be discussed. Briefly, the XAS results clearly demonstrate that the chemical form of the Pu is quite different between the different sites, being primarily monomeric Pu at the Z-12 site and present as PuO_2 like or Pu phosphate particles at the Z-9 trench. More detailed TEM analysis of the Z-9 sediments also strongly support the presence of Pu-phosphate or Pu-phosphate-silicate phases at the Z-9 trench. The phosphate required to precipitate the Pu compounds apparently originated from the co-disposal of organics at the site (Figure 1).

Phosphates are known to play an important role in the disposition of several heavy metals, including lead and uranium. This study has demonstrated the possible role of phosphate in Pu environmental chemistry. By using the advanced analytical tools available, we have provided evidence for the formation of Pu phosphate in the Z9 crib sediments. At this time, the environmental importance of this phase is unknown. It is unclear whether the phase will undergo extensive migration or will contribute to the attenuation of Pu in the environment. It is possible that this phase has little or no impact on the long-term behavior of Pu. The presence of phosphate phases is significant since past research efforts into the environmental behavior of Pu particles have focused on the formation of PuO_2 or PuO_{2+x} owing to the stability of these phase in environmental systems.

The complexity in the natural environment may lead to the formation of phases that may not be predicted in simple laboratory set-ups. Increasingly, new studies point to the complexity of Pu chemistry in complex media and the need to probe these environments with tools that can distinguish the micro-environments.
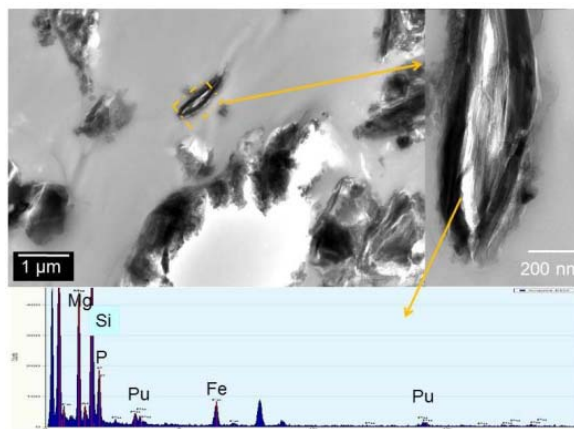
Figure 1. Thin-Sectioned 216-Z-9 Crib Sediment Showing the Occurrence of a Pu-Phosphate Region Within a Clay-Like Phase. The higher magnification image shows the strands of clay fibers. The composition is consistent with mica with Mg, Si, and Fe as the major components (Buck et al. 2014).

ACTINIDE ENVIRONMENTAL SITES AT LANL: CHALLENGES AND OPPORTUNITIES

Robert C. Roback[1], Hakim Boukhalfa[1], Kay Birdsell[1], and Danny Katzman[2]

[1]*Earth and Environmental Sciences Division, Alamos National Laboratory, P.O. Box 1663, Mail Stop J966, Los Alamos, NM 87545*
[2]*Environmental Remediation Program, Alamos National Laboratory, P.O. Box 1663, Mail Stop M992, Los Alamos, NM 87545*

Since the initiation of the Manhattan Project in 1943, LANL has performed diverse applied and exploratory research activities involving actinides. The legacy of more than 70 years of actinide research includes numerous large and small environmental sites scattered through the roughly 110 km^2 of the National Laboratory. These sites comprise a spectrum of environmental settings and initial waste depositional forms, which can be generally grouped as: solid waste disposal sites; facility drain lines, septic tanks and sumps; wastewater outfalls and adsorption beds; firing ranges; areas contaminated by leaks from storage tanks; and spills. Most of these sites represent small contaminant occurrences, however a few large sites contain significant actinide inventory. Environmental investigation and remediation efforts at LANL conducted by the Environmental Programs Directorate are ongoing and have successfully reduced the number of environmental sites requiring further action from the original total by more than 60 percent. As remediation progresses, scientific opportunities to characterize some of the oldest occurrences of actinides in the environment and evaluate their migration have and will continue to materialize.

One such example of combined remediation and scientific investigations was recently performed at LANL's TA-21, formerly known as Delta Prime Site, which was used from 1945 to 1978 as a plutonium processing and research site. Recent accelerated remediation efforts at TA-21 have resulted in the decontamination and demolition of over 24 buildings throughout the site and the removal of more than 45,000 cubic yards of soil and debris from a shallow solid waste disposal trenches at Material Disposal Area (MDA) -B. We collected solid samples containing micro-curie/g levels of mixed Pu+Am during this remediation effort. Highlights of our work that include particle fractionation, sequential leaching, microscopy and synchrotron-based spectroscopy studies on select samples from this site will be presented. Another recent remediation investigation was conducted at the General's Tanks, which comprise two, 50,000-gallon cylindrical steel storage tanks that were used initially in 1945 for underground storage of plutonium-bearing sludge from waste solutions. We conducted plutonium mobilization experiments on tank sludge to evaluate potential remediation strategies. We tested solutions of 1.0 M nitric acid, synthetic chelators (EDTA and NTA), and carbonate+H_2O_2. These results show efficient removal of the actinides from the sludge and demonstrate a potential remediation option that involves simple chemistry and the utilization of common reagents.

MDA-T represents one of the largest actinide environmental sites at LANL and within the DOE complex. The remediation strategy and long-term stewardship plans for this site are still to be finalized. The site contains four adsorption beds into which untreated acidic nuclear waste was discharged between 1945 and 1952, resulting in the accumulation of 10s of Ci of plutonium, 100s of Ci of americium, along with numerous fission products and process chemicals, including complexing agents. Concentration profiles of Am and Pu are from solid and liquid-phase samples collected beneath the adsorption beds demonstrate migration through porous and fractured tuff to depths of ~10 meters with low concentrations of plutonium in unsaturated zone water to depths of >90 meters. In addition to the adsorption beds, MDA-T contains 64 concrete shafts which received sludge derived from mixed-waste water treatment process ($FeSO_2$ precipitation process) that was mixed with Portland cement. These shafts contain an estimated inventory of >4000 Ci actinides most of which is americium-241 and present a potential opportunity to study some of the oldest cementitious waste forms in existence.

USING ADVANCED MODELING TECHNIQUESTO SEE BEANEATH THE EARTH'S SURFACE AND IMPROVE ENVIRONMENTALCLEANUP EFFORTS

Paul Dixon[1], Mark Freshley[2], Vicky Freedman[2], David Moulton[1], Haruko Wainwright[3], Stefan Finsterle[3], Carl Steefel[3], Roger Seitz[4] and Justin Marble[5]

[1] *Los Alamos National Laboratory, P.O. Box 1663, Los Alamos New Mexico, 87545*
[2] *Pacific Northwest National Laboratory, 902 Battelle Boulevard, P.O. Box 999, MSIN K9-36, Richland, WA 99352 USA*
[3] *Lawrence Berkeley National Laboratory, 1 Cyclotron Road, MS 74R-316C, Berkeley, CA 94720*
[4] *Savannah River National Laboratory, Aiken, SC 29808*
[5] *U.S. Department of Energy Department of Environmental Management, Office of Soil and Groundwater Remediation, Washington DC 20005*

Nuclear weapon production during the Cold War has resulted in groundwater contaminations at many locations in the United Sates. This groundwater contamination poses one of the most technically challenging and complex cleanup efforts in the world. The US Department of Energy (DOE) Office of Environmental Management (EM) challenged a multi-National Laboratory team to develop the next generation numerical tools and modeling workflow to allow accurate prediction of the long-term behavior of subsurface radioactive contamination plumes and the engineered materials used for waste disposal. In response, computer and environmental scientists from four DOE laboratories created the Advanced Simulation Capability for Environmental Management (ASCEM). ASCEM is a modular set of tools and approach that support standardized assessments of performance and risk for DOE-EM cleanup and closure. This computational framework is being used to create simulations that are a proven approach for accelerating innovation, significantly reducing development times, and lowering costs for new approaches focused on complex systems.

Examples of deployment of the ASCEM modeling work flow at several different DOE cleanup sites will be highlighted in this presentation. At these cleanup sites, ASCEM is being used to provide the technical underpinnings to currently unaddressed regulator concerns. Both new forward modeling predictions as well as informative 2D and 3D visualizations of information will be highlighted. Examples will be from the Savannah River H tank farm, groundwater plume evolution in complex geologic terrain from the Pahute Mesa area of the Nevada National Security Site, modeling to support regulator questions at Hanford C Tank farm, and modeling of U and H^3 ground water plumes from the Savannah River F-Basin site.
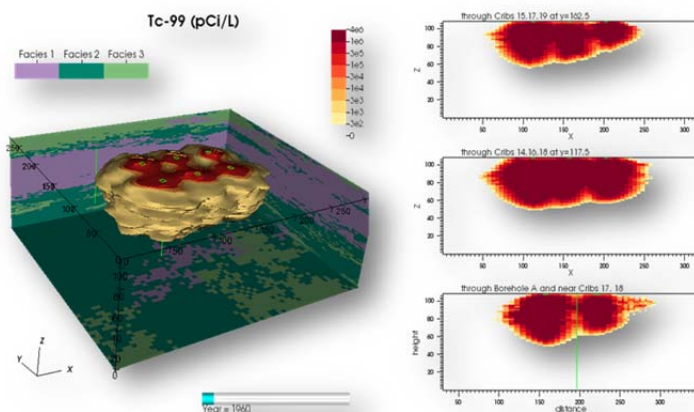
Figure1. Example of modelling results illustrating the evolution of technetium plume at Hanford's B-C Cribs

SCIENCE-BASED CLEANUP OF ROCKY FLATS.
TEN YEARS LATER, WHAT HAVE WE LEARNED?

David L. Clark

National Security Education Center, Los Alamos National Laboratory, Los Alamos, NM, 87544 USA

The Rocky Flats Environmental Technology Site (RFETS) was a U.S. Department of Energy (DOE) environmental cleanup site for a previous manufacturing plant that made components for the U.S. nuclear weapons arsenal. The facility was shut down in 1989 to address environmental and safety concerns, and left behind a legacy of contaminated facilities, soils, surface and ground water. The extent of long-term adverse health effects will depend on the mobility of plutonium and other actinides in the environment and on our ability to develop cost-effective scientific methods of removing or isolating actinides from the environment. Studying the complex chemistry of plutonium and other actinides in the environment is one of the most important technological challenges, and one of the greatest scientific challenges in actinide science today.[1]

In 1995, the Site contractor established the Actinide Migration Evaluation (AME) advisory group to provide advice and technical expertise on issues of actinide behavior and mobility in the air, surface water, groundwater, and soil. Through a combination of expert judgment supported by state-of-the-art scientific measurements and geostatistical models, it was shown that under environmental conditions at Rocky Flats, plutonium and americium form insoluble oxides that adhere to small soil, organic, and mineral particles and colloids, or are colloidal materials themselves. The scientific understanding gained from such studies was used to guide stakeholder interactions, and cleanup decisions on the Site.

I will summarize how that understanding was developed into a science-based decision-making tool that saved billions of dollars by focusing Site-directed efforts in the correct areas, and aided the most extensive cleanup in the history of Superfund legislation to finish one year ahead of schedule, ultimately resulting in billions of dollars in taxpayer savings.[2]

Under the Rocky Flats National Wildlife Refuge Act of 2001, most of the 6,240-acre (25.3 km^2) Rocky Flats site became a wildlife refuge in 2007, following certification from the US Environmental Protection Agency (EPA) that the cleanup and closure had been completed. 2015 marks the ten-year anniversary of the closure of the Site. I will discuss my perspectives on how well the cleanup and closure has worked, and lessons learned for future cleanup activities.

Figure. (Left), A 1995 Aerial photograph of the Rocky Flats Site showing the Industrial Area.
(Right), A 2011 Aerial photo of the remediated Rocky Flats Site.

1. Clark, D. L., Hecker, S. S. Jarvinen, G. D., Neu, M. P., "Chapter 7, Plutonium" in *The Chemistry of the Actinides and Transactinides*, 3rd Edition, Lester R. Morss, Norman M. Edelstein, Jean Fuger, Eds. **2006**, Springer, New York, 813-1264.
2. Clark, D. L., Janecky, D. R. and Lane, L. J. *Phys. Today*, **2006**. 59(9): p. 34-40.

RETENTION OF TRIVALENT ACTINIDES BY STRUCTURAL INCORPORATION

M. Schmidt[1)*], S. Peschel[1)], S. Hofmann[2)], C. Walther[3)], D. Bosbach[4)], T. Stumpf[1)]

[1)]Helmholtz-Zentrum Dresden-Rossendorf, Institute of Resource Ecology, Dresden, Germany.
[2)]Karlsruhe Institute of Technology, Institute for Nuclear Waste Disposal, Karlsruhe, Germany.
[3)]Leibniz University Hanover, Institute for Radioecology and Radiation Protection, Hanover, Germany.
[4)]Forschungszentrum Jülich, Institute of Energy and Climate Research, Nuclear Waste Management and Reactor Safety (IEK-6), 52425 Jülich, Germany.

The incorporation of radionuclides into a host mineral's crystal structure is a particularly efficient means of retention, due to the fact that the incorporated radionuclide is removed from the water path. The process is relevant, both, naturally occurring under repository conditions[1], and as a technical means for the sequestration of actinide waste streams. Consequently, it is of utmost importance to understand the processes leading up to the incorporation, as well as the structural properties of the formed solid solution at the molecular level[2].

We will give an overview on the incorporation of trivalent actinides and lanthanides into Ca- and Ln-bearing mineral phases of technical and geochemical relevance. The minor actinides dominate the radiotoxicity in a nuclear waste storage site over hundreds of thousands of years. For Am and Cm the trivalent oxidation states is the only relevant oxidation in aqueous solutions, and even Pu may be present as Pu(III) under reducing repository conditions. The trivalent actinides have ionic radii closely matched to their lanthanides homologues as well as calcium, making mineral phases with these host cations ideal matrices for the incorporation of the trivalent minor actinides.

To identify and characterize actinides in solid solutions at the trace concentration level, we make use of time-resolved laser fluorescence spectroscopy (TRLFS). TRLFS allows for speciation of Cm(III) at concentrations below 10^{-9} mol/L, or 1 ppm in the solid state. Cm TRLFS can be complemented by experiments with Eu(III), which, while less sensitive, are more sensitive to changes in the local coordination geometry of the fluorescent probe.

An overview will be given on the characterization of solid solutions of secondary phases relevant under repository conditions. We will compare a phase formed close to equilibrium (calcite) with a metastable phase undergoing a phase transition (vaterite[3]), as well as a phase from high-temperature synthesis (powellite[4]). The effect of various reaction parameters on the reactions, and their implications for the stability of the formed solid solutions, and hence the retention of the radionuclides will be discussed.

Figure 1. ($^7F_0 \rightarrow {}^5D_0$) excitation spectra of Eu$^{(III)}$ in calcite, vaterite, and powellite. Integrated intensity of the ($^5D_0 \rightarrow {}^7F_{1,2}$)-transitions (585-630 nm) is plotted as a function of the excitation wavelength.
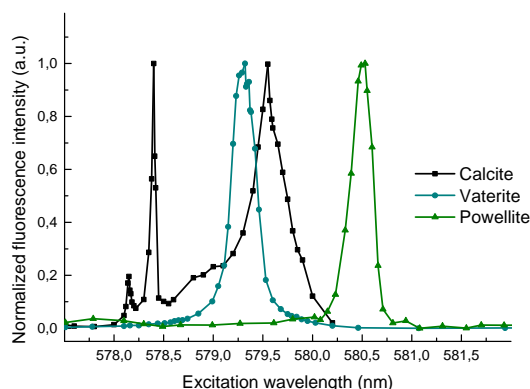
[1] T. Stumpf and Th. Fanghänel, J. Colloid Interf. Sci. 249, 119 (2002).
[2] H. Geckeis, et al., Chem. Rev. 113, 1016 (2013).
[3] M. Schmidt, et al., J. Colloid Interf. Sci. 351, 50 (2010).
[4] M. Schmidt, et al., Dalton Trans. 42, 8387 (2013).

MINERALOGY AND URANIUM-BINDING ENVIRONMENT IN THE RHIZOSPHERE OF WETLAND SOILS

D. I. Kaplan[1]*, P. Jaffe[2], D. Li[1], M. Bowden[3], J. Seaman[4], R. Kukkadapu[3], B. Arey[3], A. Dohnalkova[3], T. Varga[3]

[1]*Savannah River National Laboratory, Aiken, South Carolina 29808, United States*
[2] *Princeton University, Princeton, New Jersey 08540, United States*
[3] *Environmental Molecular Sciences Laboratory, Pacific Northwest National Laboratory, Richland, Washington 29803, United States*
[4]*University of Georgia, Aiken, South Carolina 29802, United States*

Wetlands mitigate the migration of groundwater contaminants through the creation of biogeochemical gradients that enhance multiple contaminant-binding processes. Previous work showed that U was 15X more concentrated in the rhizosphere (zone chemically and biologically impacted by roots) than in bulk wetland soils [1, 2]. Our hypothesis was that wetland plants not only contribute organic carbon, produce strong redox gradients, and elevate microbial populations to soils, but together these conditions also promote the formation of Fe oxyhydroxides that may also contribute to contaminant immobilization. Mineralogy and U binding environments of the rhizosphere were evaluated in samples collected from contaminated and non-contaminated areas of a wetland (pH ~6.0) on the Savannah River Site in South Carolina. Based on Mössbauer spectroscopy, rhizosphere soil collected from the field study site was greatly enriched with nano-goethite (<15-nm) and poorly crystalline nanoparticulate Fe-oxide/ferrihydrite-like materials. X-ray computed tomography, HAADF-STEM, HIM and TEM showed that root plaques, tens-of-microns thick, consisted of highly oriented nanoparticles in an orientation suggestive that the roots were involved in the Fe-nanoparticle formation. Based on SEM/EDS, U in the root plaques was always found in association with P and frequently with Fe [3]. Based on U L_3-edge X-ray absorption spectroscopy, U in the wetland sediments existed primarily as U(VI) bonded as a bidentate to carboxylic sites (U–C bond distance at ~2.88 Å), rather than phenolic or other sites of natural organic matter (NOM) [4]. Uranium existed on the roots as both U(IV) and U(VI), but primarily as U(VI) bidentate bonds to carbon. The U(VI) also formed U phosphate bonds. The predominance of the oxidized form of U, U(VI), in these otherwise generally reducing sediments, may be attributed to the release by roots of dissolved O_2 into the rhizosphere. After 140 days of air exposure, all U(IV) was reoxidized to U(VI) but remained as bidentate bonds to carbon. These results have significant implication on the remediation and long-term stewardship of U-contaminated wetlands.

[1] H.-S. Chang, et al., Environ. Sci. Technol. 48(16), 9270 (2014).

[2] P. Jaffe, et al., Terrestrial Ecosystem Science – Subsurface Biogeochemistry Research PI's Meeting. Washington, DC. May 6 – 7, 2014.

[3] D. I. Kaplan, et al., Environ. Sci. Technol. (submitted) (2015)

[4] D. Li, et al., Environ. Sci. Technol. (In Press; 10.1021/es505369g) (2015)

EXPERIMENTAL AND SIMULATION STUDY OF PHASE EQUILIBRIUM IN THE SYSTEM (Ba,Sr,Ra)SO$_4$ + H$_2$O

M. Klinkenberg[1], F. Brandt[1], J. Weber[1], V.L. Vinograd[1], K. Rozov[1], D. Kulik[2], B. Winkler[3], D. Bosbach[1],

[1]*Institute of Energy and Climate Research (IEK–6), Forschungszentrum Jülich, Germany*
[2]*Laboratory for Waste Management, Nuclear Energy and Safety Research Department, Paul Scherrer Institute, Villigen, Switzerland*
[3]*Institute of Geosciences, Goethe University, Frankfurt, Germany*

An important role of barite, BaSO$_4$, in the retention of Ra is widely appreciated in assessments of the safety of long-term disposal of high-level nuclear waste in deep geological formations. This retention is determined by two factors: 1) the ease of formation of a solid solution between BaSO$_4$ and RaSO$_4$ and 2) a high Ba/Ra ratio in the system [1]. These two factors lead to the formation of a very dilute solid solution of RaSO$_4$ in BaSO$_4$, which dictates a correspondingly low activity of Ra^{2+} in the aqueous phase. However, in some clay formations that are considered as prospective hosts, barite is not detected, while celestine, SrSO$_4$, is relatively abundant [2]. It is thus important to assess the effectiveness of the retention of Ra in systems with high Sr/Ba and Sr/Ra ratios. In this study we report on: 1) the experimental results on the phase equilibrium in the system (Ba,Sr,Ra)SO$_4$ + H$_2$O, 2) the results of atomistic simulation of the excess properties of mixing in the ternary solid solution, and 3) the results of thermodynamic modelling of the solid – aqueous equilibrium, which use the theoretically predicted parameters of the ternary mixed phase.

The effect of Sr on the effectiveness of Ra retention was investigated experimentally at 90 ºC in batch experiments of two different types: 1) the re-crystallization of pure barite in the presence of a trace amount of Ra and of an elevated concentration of Sr in the aqueous solution and 2) the re-crystallization of pure SrSO$_4$ in the presence of a trace amount of Ra.

Pure barite purchased from Sachtleben was put in contact with an aqueous solution with the initial concentration of 5.0·10^{-6} mol/L of RaBr$_2$ and 0.1 mol/L of NaCl. The concentration of Sr was either 0.05 or 0.005 mol/L. These concentrations were chosen such that the activity product {Sr^{2+}}{SO$_4^{2-}$}, as calculated with the GEM-Selector code [3], was either above or below the solubility product of SrSO$_4$. In the latter case, in the experiments with the solid/liquid ratio (S/L) of 5 g/L, a plateau in the Ra concentration was reached, indicating an approach to the thermodynamic equilibrium with a ternary (Ba,Sr,Ra)SO$_4$ solid solution. These experiments have shown that the uptake of Ra by the Ba-rich and Sr-poor ternary phase is almost as effective as in the case of a binary (Ba,Ra)SO$_4$ solution [4]. When the Sr concentration was higher than the solubility product, the uptake of Ra was significantly slower. In the case of S/L = 0.5 g/L, no significant uptake was observed.

A high purity celestine (99.99+ %), as purchased from Chempur, was put in contact with an aqueous solution containing 5.0·10^{-6} mol/L of RaBr$_2$ and 0.1 mol/L of NaCl. The solid/liquid ratios were 5 g/L or 0.5 g/L. In these experiments, a significant Ra uptake was not expected, because the formation of a solid solution between celestine and Ra-barite should be disfavoured by the large difference in the radii of Sr^{2+} and Ra^{2+} ions. Contrary to expectations, in the experiments at 0.5 and 5 g/L, an uptake of 92 % and 80 % of the initial Ra was observed (Fig.1 a). The SEM investigation showed the formation of a tiny amount of idiomorphic Ba- and Ra-rich crystals on the surface of the celestine, which remained stable for more than 200 days (Fig. 1 b). The formation of these crystals suggested that traces of Ba were still present in the celestine. Interestingly, no Ba-rich crystals were formed in the reference experiments without Ra, while the addition of Ra into the system has caused the release of Ba from the celestine. The formation of the Ba- and Ra-rich crystals was coincident with a significant increase in Ba(aq). The concentration of Ba in the aqueous phase was thus controlled by the presence or absence of the Ra-rich phase.

In support of these observations, atomistic simulations of the mixing properties in the ternary solid solution were performed. The regular mixing parameters in the binary mixtures have been computed from first principles in our earlier study [5]. Our results suggested that the interaction parameters increase in the row: W_{BaRa} = 2.4, W_{BaSr} = 8.4 and W_{SrRa} = 20.0 kJ/mol. The present study was concerned with deviations from the regular mixing in the binaries and in the (Ba,Sr,Ra)SO$_4$ ternary system. The energies of the exchange reactions AA + BB = 2AB,

where A/B = {Ba, Ra, Sr}, were computed for all pairs, which fall within a 2×2×2 supercell of barite, with the DFT-based package CASTEP [6]. Effects of mixing and ordering were investigated with the Monte Carlo method. No stable intermediate compounds were predicted. Deviations from the regular model

$$\Delta H_{mix} = x_{Ba} x_{Ra} W_{BaRa} + x_{Ba} x_{Sr} W_{BaSr} + x_{Sr} x_{Ra} W_{SrRa} \quad (1)$$

were investigated with the aid of ternary quasi-random structures. These calculations showed slightly negative deviations from Eqn. 1. However, these deviations affect predominantly the intermediate compositions that fall into a miscibility gap. Therefore, the phase relations are relatively insensitive to the ternary parameter. Due to the large values of W_{SrRa} and W_{BaSr}, the ternary solution must decompose at ~90 °C into a nearly pure celestine and a $(Ba,Ra)SO_4$ phase of variable composition (Fig 1c).

Both, our experimental and theoretical results appear consistent in the following aspects: 1) $RaSO_4$ mixes very favourably with $BaSO_4$, 2) $RaSO_4$ can still mix (but less favourably) with a dilute solid solution of $SrSO_4$ in $BaSO_4$, 3) the mixing of $RaSO_4$ with $SrSO_4$ is totally unfavourable, 4) the mixing between $BaSO_4$ and $SrSO_4$ is more favourable than between $RaSO_4$ and $SrSO_4$.

Our thermodynamic calculations with the GEM-Selector code showed that the mole fraction of $RaSO_4$ in this phase could increase dramatically at high Sr/Ba ratios, even when the total amount of Ra in the system is small. This prediction is entirely consistent with our experimental data on re-crystallization of celestine and with the predicted change in the slope of the tie lines within the ternary gap (Fig. 1c). As the activity of Ra^{2+} in the aqueous phase is linked to the large mole fraction of $RaSO_4$ in the solid, it remains relatively high in a Sr-rich system. This negative effect on Ra retention is compensated, however, by a higher activity of the SO_4^{2-} ion caused by a larger mole fraction of celestine in solid solution.
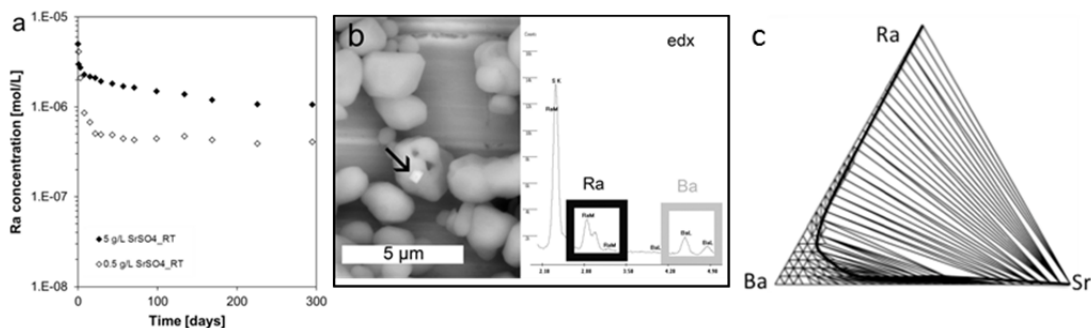
Fig. 1. a) Temporal evolution of the Ra(aq) concentration in contact with celestine. b) BSE-image of celestine after 226 days in contact with a Ra containing solution. The Ra- and Ba-rich phase (white crystal) is marked with an arrow. It's EDS spectrum is shown to the right. c) Phase relations in the ternary $(Ba,Sr,Ra)SO_4$ system at 75 °C based on the results of Monte Carlo simulations. The thick solid line shows the miscibility gap.

[1] J. Bruno, et al., *in* Chemical Thermodynamics Series 10, Paris, OECD (2007).
[2] E. Gaucher, et al., Physics and Chemistry of the Earth, 29, 55 (2004).
[3] D. A. Kulik, et al., Computat. Geosci., 17, 1 (2013); T. Wagner, et al., Canad. Mineral. 50, 1173 (2012); http://gems.web.psi.ch
[4] F. Brandt, et al., Geochim. et Cosmochim. Acta, *in print* (2015).
[5] V. L. Vinograd et al., Geochim. et Cosmochim. Acta, 122, 398 (2013).
[6] S. J. Clark, et al., Z. Kristallogr., 220, 567 (2005).

TRIVALENT ACTINIDES RETENTION BY IRON (HYDR)OXIDES

N. Finck[1], S. Nedel[2], K. Didereksen[3], M. L. Schlegel[4]

[1]*Institute for Nuclear Waste Disposal (INE), Karlsruhe Institute of Technology (KIT), Hermann-von-Helmholtz-Platz 1, D-76344 Eggenstein-Leopoldshafen (Germany).*
[2]*Haldor Topsoe A/S, Nymøllevej 55, DK-2800 Kgs. Lyngby (Denmark).*
[3]*Nano-Science Centre, Department of Chemistry, University of Copenhagen, Universitetsparken 5, DK-2100 Copenhagen (Denmark).*
[4]*CEA Saclay, DEN / DPC / SEARS / LISL, Building 391, F-91191 Gif-sur-Yvette (France).*

The disposal of high-level nuclear waste in deep repositories is considered a prime solution in most countries producing nuclear energy. In such deep facilities, the waste will be surrounded by man-made barriers (metallic canister, backfill material) to delay the intrusion of ground water up to the waste matrix, and by the natural (host rock) barriers. However, during the long term evolution of the repository system, water may move through the barriers and come in contact with the canister. Under the anoxic conditions and the high temperatures expected to prevail in the repository, the presence of water will lead to anaerobic corrosion of the canister. Long term corrosion experiments performed in the laboratory under conditions relevant for a clay based repository have been reported [e.g., 1]. It has been shown that the corrosion layer at the iron-clay interface is made of a magnetite-containing internal sublayer and an external clay transformation sublayer. Magnetite is a mixed $Fe^{(II/III)}$ oxide ($Fe^{II}Fe^{III}_2O_4$) that may likely have formed from green rust (e.g., $[Fe^{II}_3Fe^{III}(OH)_8]\cdot[Cl,\sim2H_2O]$) precursors that underwent oxidation in aqueous environment. Such Fe (hydr)oxides can have a considerable uptake capacity for radionuclides (RN), thus delaying the migration of these species. One uptake mechanism is the RN incorporation in the bulk structure of Fe (hydr)oxides. However, almost no information on trivalent actinides incorporation in these phases is available in the literature. Therefore, our goal was to investigate the uptake of $Am^{(III)}$ by GR and magnetite and to decipher the actual binding mode by EXAFS spectroscopy.

Magnetite and chloride green rust (GR) were synthesized by direct precipitation in the presence of $Am^{(III)}$. Subsequently, part of the green rust suspension was centrifuged, suspended in water and the pH increased to initiate the conversion to magnetite. Separately, $Am^{(III)}$ was adsorbed on pre-formed magnetite and used as reference sample. The solid phases were characterized by XRD and SEM, and the $Am^{(III)}$ local environment probed by EXAFS spectroscopy. In the magnetite co-precipitation experiment, XRD and SEM data indicate the presence of fine-grained magnetite and the absence of any separate Am-containing phase. The data are similar to that of the pre-formed material used for the adsorption, pointing to the absence of any Am influence on the synthesis protocol. The SEM data further showed that GR preparation was made of hexagonal platelets, as expected for this mineral. In the GR conversion sample, XRD data indicate the presence of magnetite and $Fe(OH)_2$. This is also clear on the SEM micrographs where large platelets covered by-fine grained Fe_3O_4 can be seen. The observed conversion is consistent with reported studies [2].

In the GR sample, Am is 6-fold coordinated by oxygen atoms and Fe atoms are detected at ~3.40 Å, consistent with $Am^{(III)}$ incorporation in a Fe octahedral site of the GR structure. This chemical environment changed only slightly upon pH increase of the GR suspension to initiate the conversion to magnetite. According to the sample structural characterization Am can be associated with $Fe(OH)_2$ and/or Fe_3O_4 in this transformation sample, and based on EXAFS data the largest part of Am is certainly associated with the octahedral sheet of ferrous hydroxide. The Am local environment differs substantially in the Fe_3O_4 co-precipitation experiment. The actinide is very likely located in a distorted magnetite-like environment, being bound to 6-7 O atoms and having Fe neighbors located at ~3.40 and ~3.60 Å. The data are consistent with an accommodation of magnetite for the large Am, with the next Fe octahedral shell split in two subshells. For the magnetite adsorption sample, Am is surrounded by ~9 O atoms at 2.47 Å and an Fe shell at ~3.50 Å. The first ligand shell is similar to that of the aqua ions and differs significantly from that of the co-precipitation samples, meaning that the actinide is located at structurally different sites in both samples. Finally, EXAFS data were collected for Am-containing magnetite aged for about two years. In contrast to the freshly prepared sample, the Am first coordination sphere is split in two O subshells, with a total of ~6 O atoms, and the nearest Fe shell is located at ~3.40 Å. This shows that the local chemical environment evolved slightly with ageing time, however the data may still be compatible with bulk

retention. With time, the structure could slightly re-organize around Am$^{(III)}$, consolidating the binding site. The hypothesis of a release and subsequent surface sorption of Am can be dismissed as the first shell data significantly differ from that of the sorption sample. This is the first time where such a co-precipitated sample has been investigated and the results provide valuable information with regard to the long term evolution of this potential retention mode.

[1] M. L. Schlegel *et al.*, Appl. Geochem., 23, 2619-2633 (2008).
[2] J.-P. Jolivet *et al.*, Chem. Comm., 2004, 481-487 (2004).

RETENTION OF CESIUM AND STRONTIUM BY SORPTION ON URANOPHANE

A. Espriu[1], J. de Pablo[1,2], J. Giménez[1], I. Casas[1]

[1] *Department of Chemical Engineering, Universitat Politècnica de Catalunya (UPC), Avda. Diagonal 647, E-08028 Barcelona, Spain*
[2] *Fundació CTM Centre Tecnològic, Plaça de la Ciència 2, E-08243 Manresa, Spain*

Different spent nuclear fuel (SF) leaching studies show that some U(VI) secondary solid phases might precipitate on the surface of the fuel depending on the chemical conditions of the groundwater, e.g. uranophane, $Ca(UO_2)_2(SiO_3OH)_2 \cdot 5H_2O$. In addition, this is known to be the most abundant secondary phase for uranium found in nature. The net release of radionuclides from the fuel matrix to the waters might be affected by the formation of such secondary solid phases, because of their possible incorporation to the solids through different mechanisms such as ionic exchange and sorption, as it was shown for caesium, strontium and selenium, which were found to be retained on studtite [1-3].

In this work, the sorption capacity of uranophane for cesium and strontium was studied through a series of experiments with the aim of determining the rate of sorption, the maximum sorption capacity as well as the effect of on the sorption capacity. Cesium and strontium, formed in the SF as the products of fission reactions, were studied because they have a relatively high mobility in water and their migration would not be retarded by precipitation, so sorption or ionic exchange would be the main processes for they retention.

Uranophane was synthesized according to the literature and characterized using Raman and X-ray diffraction techniques. The point of zero charge of the solid was determined by the immersion methodology (pH_{pzc}=7.93±0.01 at 0.01 mol·dm^{-3} ionic strength) and the surface area of the solid by the BET method (33.42±0.06 m^2·g^{-1}).

Sorption was very fast for both metals, with equilibrium reached in less than 1 hour; this indicates that the sorption or incorporation of the radionuclides to the solids would not be kinetically controlled.

The variation of the metal sorbed as a function of metal concentration in solution (sorption isotherms) was determined in the range of initial concentrations between $5 \cdot 10^{-6}$ mol·dm^{-3} and $5 \cdot 10^{-3}$ mol·dm^{-3}. The results obtained showed that both metals were sorbed onto the solids following a Langmuir behaviour, indicating that the sorption followed a monolayer coverage.

The variation of the sorption with pH was carried out in the pH range between 7 and 12 (at more acidic pH values, the uranophane dissolution was relatively high). The results obtained showed that sorption increased with pH, pointing to a sorption depending on electrostatic interactions, because at pH values higher than the pH_{pzc}, the surface of the solid would be negatively charged and the interaction with cations in solution would increase, as it was already observed for cesium and strontium sorption onto uranyl peroxide [1,2]

Considering cesium and strontium concentrations expected to be released in the High-Level Nuclear Waste Repository, and the results obtained in this work, uranophane may have an important role on the retardation of such radionuclides released from the SF.

[1] J. Giménez, X. Martínez-Lladó, M. Rovira, J. de Pablo, I. Casas, Radiochim. Acta. 98, 479 (2010).
[2] R. Sureda, X. Martínez-Lladó, M. Rovira, J. de Pablo, I. Casas, J. Giménez, J. Hazard. Mater. 181, 881 (2010).
[3] A. Martínez-Torrents, J. Giménez, X. Martínez-Lladó, J. de Pablo, I. Casas, J. Radioanal. Nucl. Chem. 303, 153 (2015)

REMOVAL OF U(VI) USING GRAPHENE NANOMATERIALS STUDIED BY BATCH AND SPECTROSCOPY TECHNIQUES

X.K. Wang[*]

School of Environment and Chemical Engineering, North China Electric Power University, Beijing 102206, P.R. China

Email: *xkwang@ipp.ac.cn* or *xkwang@ncepu.edu.cn*

The adsorption and desorption of U(VI) on graphene oxides (GOs), carboxylated GOs (HOOC-GOs) and reduced GOs (rGOs) were investigated by batch experiments, EXAFS technique and theoretical calculations. Isothermal adsorptions showed that the adsorption capacities of U(VI) were GOs > HOOC-GOs > rGOs, whereas the desorbed amounts of U(VI) were rGOs > GOs > HOOC-GOs by desorption kinetics. According to EXAFS analysis, inner-sphere surface complexation dominated the adsorption of U(VI) on GOs and HOOC-GOs at pH 4.0, whereas outer-sphere surface complexation of U(VI) on rGO was observed at pH 4.0, which was consistent with surface complexation modeling. Based on the theoretical calculations, the binding energy of $[G^{...}UO_2]^{2+}$ (8.1 kcal/mol) was significantly lower than those of $[HOOC\text{-}GOs^{...}UO_2]^{2+}$ (12.1 kcal/mol) and $[GOs\text{-}O^{...}UO_2]^{2+}$ (10.2 kcal/mol), suggesting the physisorption of UO_2^{2+} on rGOs.

Graphene oxide/polypyrrole (GO/PPy) composites were synthesized via dielectric barrier discharge (DBD) plasma technique in nitrogen conditions and applied to remove U(VI) from aqueous solutions. The sorption capacity of U(VI) on GO/PPy composites was much higher than those of U(VI) on GO, PPy and many other today's materials. The sorption of U(VI) on GO/PPy composites obeyed the Langmuir model, and was mainly attributed to surface complexation via the coordination of U(VI) ions with oxygen- and nitrogen-containing functional groups. The selectivity sorption of U(VI) ions on GO/PPy compositesin the presence of other metal ions (i.e., Co(II), Ni(II), Cd(II), Sr(II), Zn(II)) indicated an overall preference for U(VI) ions. Moreover, the GO/PPy composites could be regenerated through the desorption of adsorbed U(VI) ions by using 1.0 M HCl solution, and cycling reused without obvious decrease of sorption capacity. The results play an important role in designing GOs for the preconcentration and removal of radionuclides in environmental pollution cleanup applications.

THERMODINAMIC STUDIES ON EUROPIUM(III) BEHAVIOUR ON THERMALLY AGED CALLOVIAN-OXFORDIAN ARGILLITE

P. Parant[1], <u>M.V. Di Giandomenico</u>[1], L. Mercier[1], X. Crozes[1]

[1] *EDF R&D, Chemistry and Materials of Energetic Efficienty, Materials and Mechanics of Components Department, Les Renardières, 77818 Moret-sur-Loing, France*

In France, the intermediate and high level long lived wastes will be stored in a deep geological disposal. The geological composition of this storage, chosen by the french national radioactive waste management agency (ANDRA), is the Callovo-Oxfordian (COx) argillaceous structure [1]. This rock is mainly made up of:

- clay that confers chemical retention properties, some deformability and ability to creep

- carbonates that are involved in pH regulation

- tectosilicates (quartz) that explain the rock's strength and its capacity to evacuate the wastes thermal decrease.

Thanks to all these properties a strong radionuclides confinement is ensured.

Europium(III) is usually considered as an analogous of actinide(III) elements. A previous work [2] studied the influence of natural organic matter on europium(III) retention on the callovian-oxfordian argillite. The aim of this study was to understand and quantify the radionuclides retention as a function of argillite thermal treatment. Two samples were used:

- natural argillite, that was crushed and sieved in a glove box to obtain a powder with grains smaller than 63 μm, checked by laser granulometry [2];

- argillite previously aged 9 months at 90 °C that was just filed. The obtained powder could not be sieved as before, thus leading to differences in grain sizes with respect to the natural argillite.

Sorption isotherms were studied for europium(III) – argillite system. Kinetics studies were performed in a previous work [2] and it has proven that about 20 days are necessary to achieve steady state. Sorption batchs with clay stone were prepared under chemical COx conditions. In each batch, argillite was put in suspension in representative COx pore water. Experiments were carried out in glove box filled with a gas mixture: N_2/CO_2 with 1% of CO_2.

Eu(III) sorption, a physical chemistry mechanism, is partially function of argillite nature (natural argillite or aged one). This is confirmed by the scanning electron microscopy analysis (SEM) that showed a difference in calcite grains size. Therefore, chemical analysis prove that Eu(III) precipitation, a thermodynamic mechanism, is not affected by argillite nature. Then, a mineralogical analysis is in progress in order to know the chemical differences between the two samples.

[1] ANDRA, Dossier 2005 Argile, (2005).
[2] Vu-Do L., PhD Thesis « Influence de la matière organique naturelle mobile sur la rétention de l'europium sur l'argilite de Bure », Paris South University (2013).

URANIUM BEHAVIOUR IN HIGH pH CEMENTITIOUS SYSTEMS

Ryan Telchadder[(1)], Rosemary Hibberd[(1),(2)], Pieter Bots[(2)], Gareth Law[(1)], Katherine Morris[(2)], Nick Bryan[(3)], Kurt Smith[(3)], Adam Swinbourne[(1)], Anna Taylor[(1)], Louise Natrajan[(1)], Rebecca Beard[(4)], Steve Williams[(4)]

[1]*Centre for Radiochemistry Research, School of Chemistry, University of Manchester, U.K.*
[2]*Research Centre for Radwaste & Decommissioning, School of Earth, Atmospheric & Environmental Sciences, University of Manchester, U.K.*
[3]*National Nuclear Laboratory, Chadwick House, Risley WA3 6AE, U.K.*
[4]*RWM, B587 Curie Avenue, Harwell Oxford, OX11 0RH, U.K.*

In the multiple barrier concept, the waste containers will be placed in underground vaults, which will be 'backfilled' with material designed to reduce the mobility of any radionuclides escaping from the containers. One backfill that has been suggested is very high pH cement, which should promote hydrolysis, precipitation and sorption. We have studied the sorption behaviour of the uranyl ion in systems of a potential high pH backfill material (NRVB), which is a mixture of Ordinary Portland Cement, hydrated lime and limestone flour (ratio = 265:291:100; with 1.8:1 solid mixture: water) [1]. We have also studied the interaction of uranyl with other solids: calcium silicate hydrate (CSH) and Portlandite.

For the NRVB systems, ethylenediaminetetraacetic acid (EDTA), humic acid and isosaccharinic acid (ISA) were used as competing ligands. At trace concentrations (2×10^{-10} mol dm^{-3}), NRVB is an effective sorber of UO_2^{2+}, with less than 4 % remaining in solution after 48 hours. Sorption by CSH depends upon the Ca:Si ratio, but is less than that of NRVB, despite higher specific surface areas. Sequential ultrafiltration showed that nearly all of the ^{232}U (79 %) remaining in solution was present in the $1 – 2$ nm size range, which is consistent with some previous observations of nanometre sized colloid formation in cementitious systems [2, 3]. Under similar conditions, in calcite systems, sorption is retarded by colloid formation [3].

Experiments were performed where ligands (EDTA, ISA) were introduced to the radionuclides before the NRVB ('sorption') and after ('desorption'). In sorption experiments, high concentrations of EDTA (> 0.01 M) and ISA (≥ 0.01 M) reduced the extent of uptake at apparent equilibrium. The addition of these competing ligands to a pre-equilibrated system of $^{232}UO_2^{+2}$ and NRVB, resulted in a temporary suspension of some uranium, but this very quickly reduced. Hence, there is considerable irreversibility in these systems. At equilibrium, humic acid (up to 100 ppm) had very little effect upon sorption. Figure 1 shows sorption and desorption data for EDTA and ISA systems. The behaviour in the absence of ligands is also shown.
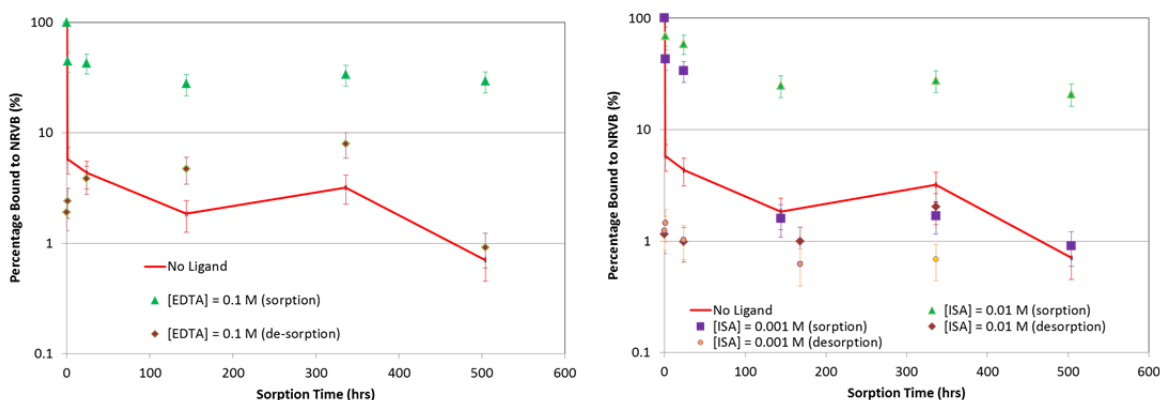
Figure1. Uranyl sorption and desorption in the absence of ligand, and in in the presence of ligands (EDTA, left; ISA, right).

Luminescence spectroscopy was used to analyse the mechanism of sorption to NRVB and CSH (^{238}U; 1 ppm). For the CSH samples, the uranyl appeared to be largely incorporated, with some evidence of surface complexation

too. As hydrated lime is a component of the NRVB, uranyl/calcium hydroxide systems were also studied: the spectrum showed the presence of a calcium uranate-like species. The spectrum for NRVB was complex, with broad features, which probably resulted from its heterogeneous nature. The main feature was in the region for incorporated and surface complexed uranyl species, but there was also a low energy tail, which appeared to be due to a calcium uranate-like phase. Therefore, it seems that uranyl may interact with NRVB via more than one mechanism.

[1] McCarter, W., Crossland, I., Chrisp, I., 2004. Hydration and drying of Nirex Reference Vault Backfill. *Building and Environment*, **39**, 211_221.
[2] Smith, K., Bryan, D., Swinburne, A., Pieter, B., Shaw, S., Natrajan, L., Mosselmans, F., Morris, K., 2015, U(VI) behaviour in hyperalkaline calcite systems. *Geochim. Cosmochim. Acta*. 148**,** 343-359.
[3] Bots, P., Morris, K., Rosemary, H., Law, G., Mosselmans, F., Brown, A., Doutch, J., Smith, A., Shaw, S., 2014, Formation of stable uranium(VI) colloidal nanoparticles in conditions relevant to radioactive waste disposal, *Langmuir*. **30**, 14396-14405.

U(VI) AND Eu(III) DISSOCIATION FROM BULK AND COLLOIDAL BENTONITE, A KINETIC INVESTIGATION

N. Sherriff[1],[3], R. Issa[1], F.R. Livens[1],[2], S. Heath[1], K. Morris[2], K. Smith[3] and N. Bryan[3]

[1]Centre for Radiochemistry Research, School of Chemistry, University of Manchester, U.K.
[2]Research Centre for Radwaste and Decommissioning, School of Earth, Atmospheric and Environmental Sciences, University of Manchester, U.K.
[3]National Nuclear Laboratory, 5th Floor, Chadwick House, Birchwood, Warrington, WA3 6AE, U.K.

The interactions of radionuclides with bulk and colloidal bentonite clay are important, because it is a potential repository backfill material [1]. For colloids to have a significant role in the transport of radionuclides in the geosphere, they have to be present, stable, mobile and their interactions with radionuclides must not be instantaneously reversible [1, 2]. Specifically, the time taken for dissociation must be comparable with, or longer than, the residence time of the colloids in the groundwater [2]. Therefore, the dissociation kinetics of U(VI) and Eu(III), from bulk and colloidal bentonite have been studied.

Ternary systems of ^{152}Eu(III), bulk bentonite and ethylenediaminetetraacetic acid (EDTA) ([Eu] = 7.9 x 10^{-10} M; pH = 6.0 – 7.0) have been studied. Without EDTA, there was slow uptake in a two stage process, with initial rapid sorption of Eu(III) (96%), followed by slower uptake of a much smaller fraction (3.0 % over a period of 1 month). The reversibility of Eu(III) binding was tested by allowing Eu(III) to sorb to bentonite for 1 – 322 days. EDTA was added to the pre-equilibrated Eu bentonite systems at 0.01 M, a concentration that was sufficient to suppress sorption in a system where EDTA was present prior to the contact of Eu(III) with bentonite. A fraction of the Eu was released instantaneously (30 - 50 %), but a significant amount remained bound. With time, the amount of Eu(III) retained by the bentonite reduced, with a slow fraction dissociation rate constant of approximately 4.3 x 10^{-8} s^{-1} (values in the range 2.2 x 10^{-8} – 1.0 x 10^{-7} s^{-1}) for pre-equilibration times ≥ 7 days. Eventually, the amount of Eu(III) remaining bound to the bentonite was within error of that when EDTA was present prior to contact (4.5 % ± 0.6), although in systems with pre-equilibration times > 100 days, full release took up to 500 days.

Europium interactions with colloidal bentonite were also studied, and the dissociation rate constant measured by a resin competition method [3]. For the colloids, more Eu was found in the slowly dissociating fraction (60 – 70 %), but the first order dissociation rate constant was faster, with an average rate constant of 8.8 x 10^{-7} s^{-1} and a range of 7.7 x 10^{-7} – 9.5 x 10^{-7} s^{-1}. Figure 1 shows the dissociation of Eu(III) from the bentonite colloids as a function of Eu/colloid pre-equilibration time. In this system, when the Eu was added to the resin before the addition of colloids, 1.4 ± 0.34 % remained in solution: this represents the equilibrium position for these experiments (horizontal line, Figure 1). The colloid dissociation rate constants are consistent with values estimated by Wold [4] and those of Huber et al [5] for Am(III) from competition experiments using fracture filling material.

The dissociation of ^{232}U(VI), from bentonite colloids ([U] = 5.43 x 10^{-10} M; pH = 8.8 ± 0.2) has also been studied using an resin ion exchange competition technique. It was found that only approximately 50% of the uranium was associated with the colloids. The reversibility of the interaction was studied by allowing U(VI) to sorb to bentonite colloids for periods between 1 – 35 days. A fraction of the U(VI) was available for release instantaneously, which was consistent with the amount of U that was not colloid associated. With time, the amount of U(VI) retained by the bentonite colloid reduced further, with a first order dissociation rate constant of 5.6 x 10^{-7} s^{-1} (values in the range of 3.1 x 10^{-7} – 7.3 x 10^{-7} s^{-1}). The pre-equilibration time of the ^{232}U(VI) with the colloids (1 – 35 days) did not affect the rate of dissociation in these experiments. The U(VI) rate constants are close to those estimated by Wold [4].

Although slow dissociation was observed for Eu(III) and U(VI) from bulk and colloidal bentonite, in no case was there convincing evidence for 'irreversible binding' of the radionuclides by the clay.
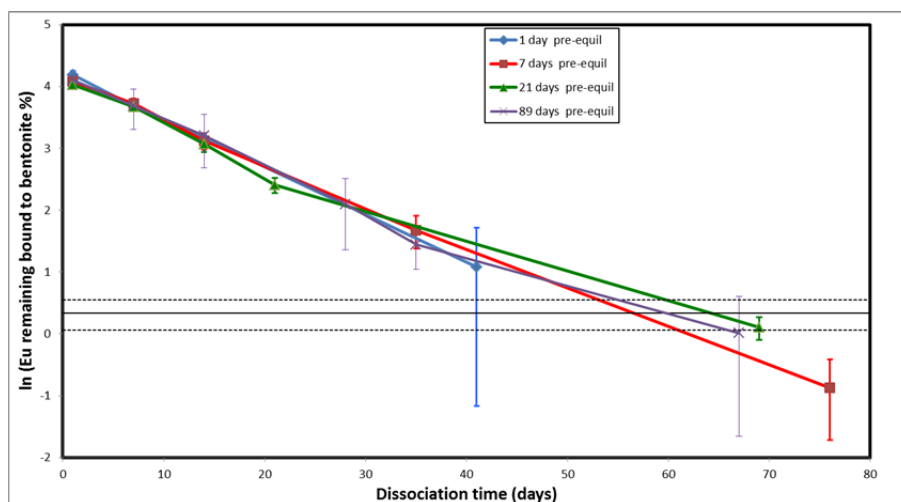
Figure1. Natural log plot of the colloid dissociation experiment: ln(percentage bound to bentonite) vs Dowex resin contact times, as a function of pre-equilibration time (pH = 8.8 ± 0.1).

[1] A. Möri, W.R. Alexander, H. Geckeis, W. Hauser, T. Schäfer, J. Eikenberg, T. Fierz, C. Degueldre, T. Missana, Colloids and Surfaces A: Physicochemical and Engineering Aspects, 217, 33-47, 2003.
[2] N.D. Bryan, D.L.M. Jones, R.E. Keepax, D.H. Farrelly, L.G. Abrahamsen, P. Warwick, N. Evans, Journal of Environmental Monitoring, 9, 329-347, 2007.
[3] J.M. Monsallier, W. Schuessler, G. Buckau, T. Rabung, J.I. Kim, D. Jones, R. Keepax, N. Bryan, *Analytical Chemistry,* **75**, 13, 3168-3174, 2003.
[4] S. Wold, 2010, Sorption of prioritized elements on montmorillonite colloids and their potential to transport radionuclides, SKB Technical Report, TR-10-20.
[5] F. Huber, P. Kunze, H. Geckeis, T. Schäfer, 2011, Applied Geochemistry, 26, 2226–2237.

INFLUENCE OF BACKGROUND ELECTROLYTE ON THORIUM[IV] SORPTION BEHAVIOR

S. Hellebrandt[1)], M. Schmidt[1)], K. E. Knope[2,a], S. S. Lee[2], J. E. Stubbs[3], P. J. Eng[3], L. Soderholm[2], P. Fenter[2]

[1)]*Helmholtz-Zentrum Dresden-Rossendorf, Institute of Resource Ecology, Dresden, Germany.*
[2)]*Chemical Science and Engineering Division, Argonne National Laboratory, Argonne, IL, USA.*
[3)]*Center for Advanced Radiation Sources, University of Chicago, Chicago, IL, USA.*
[a)]*Current address: Department of Chemistry, Georgetown University, Washington, DC, USA.*

The study of actinides in their low oxidation states is of high importance for the safety assessment of nuclear waste disposal sites due to the predominance of these valences in deep geological formations. In particular, studying the mineral-water interface chemistry of these radionuclides is fundamental for better understanding their interactions with mineral phases in a repository. Clay minerals are relevant for nuclear waste disposal sites, due to their retardation properties, and are indeed considered as host rock formations, e.g. in Switzerland and France. Muscovite, a phyllosilicate material, is similar to clay minerals but forms large single crystals with high quality surfaces (nearly flat, hard, no defects). These are required for X-ray measurements as performed for this study. As complementary techniques resonant anomalous x-ray reflectivity (RAXR) and crystal truncation rods (CTR) deliver structural information on the distribution of the actinides at a mineral's surface, on a molecular level. Understanding sorption and associated processes at this level are essential for reliable safety assessments.

In a series of experiments we demonstrate that the background electrolyte has a significant influence on the sorption behavior of actinides, specifically thorium(IV). We study the sorption of Th(IV) ($c_{TH} = 1 \times 10^{-4}$ mol/L), the softest of the tetravalent actinides, at the muscovite basal plane with several background electrolytes ($NaClO_4$, $KClO_4$, $LiClO_4$). Previous investigations [1], with sodium chloride (NaCl, 1×10^{-1} mol/L) as background electrolyte, act as reference for these experiments. We find that the sorption behavior of thorium is substantially affected by both, changes in the electrolyte cation (Li^+, K^+) and anion (Cl^-, ClO_4^-).

RAXR data of the NaCl reference system show an occupancy of 0.4 thorium per area of the unit cell (Th/A_{UC}, A_{UC} = 46.72 Å^2), consistent with simple adsorption. In contrast, strongly enhanced sorption (~4.9 Th/A_{UC}) can be observed with $LiClO_4$ (1×10^{-1} mol/L) as background electrolyte. The opposite happens with $NaClO_4$ (hiNaClO$_4$, 1×10^{-1} mol/L), where sorption is almost completely suppressed. By decreasing the ionic strength of $NaClO_4$ (loNaClO$_4$, 1×10^{-2} mol/L) the sorption was increased moderately (~0.04 Th/A_{UC}), which is comparable to that observed with potassium ($KClO_4$, 1×10^{-1} mol/L, ~0.07 Th/A_{UC}) as cation (Table 1), but still significantly (6 – 10-fold) lower than sorption from NaCl solution. These results are corroborated by α-spectrometry.

Table 1. Overview of ionic strength and thorium coverage

	NaCl	hiNaClO$_4$	loNaClO$_4$	KClO$_4$	LiClO$_4$
c (mol/L)	1×10^{-1}	1×10^{-1}	1×10^{-2}	1×10^{-1}	1×10^{-1}
(Th/A$_{UC}$)	0.4	0	0.04	0.07	4.90

The huge increase of sorption in the system with $LiClO_4$ cannot be explained by sorption of (partly) hydrated metal ions. CTR/RAXR measurements show that the thorium distribution consists of similarly occupied, broad peaks at ~4.1 Å and ~29 Å over the mineral surface (Figure 1). The first species can be interpreted as a mixture of different sorption species [2], its increased occupancy in combination with the second broad distribution is similar to that observed with plutonium on the basal plane of muscovite [3]. This suggests that the unusually strong sorption is due to the adsorption of Th-nanoparticles, presumably *via* the initial formation of oligomers. Whether these oligomers are formed in the solution or due to high concentrations directly on the surface will require further investigation.
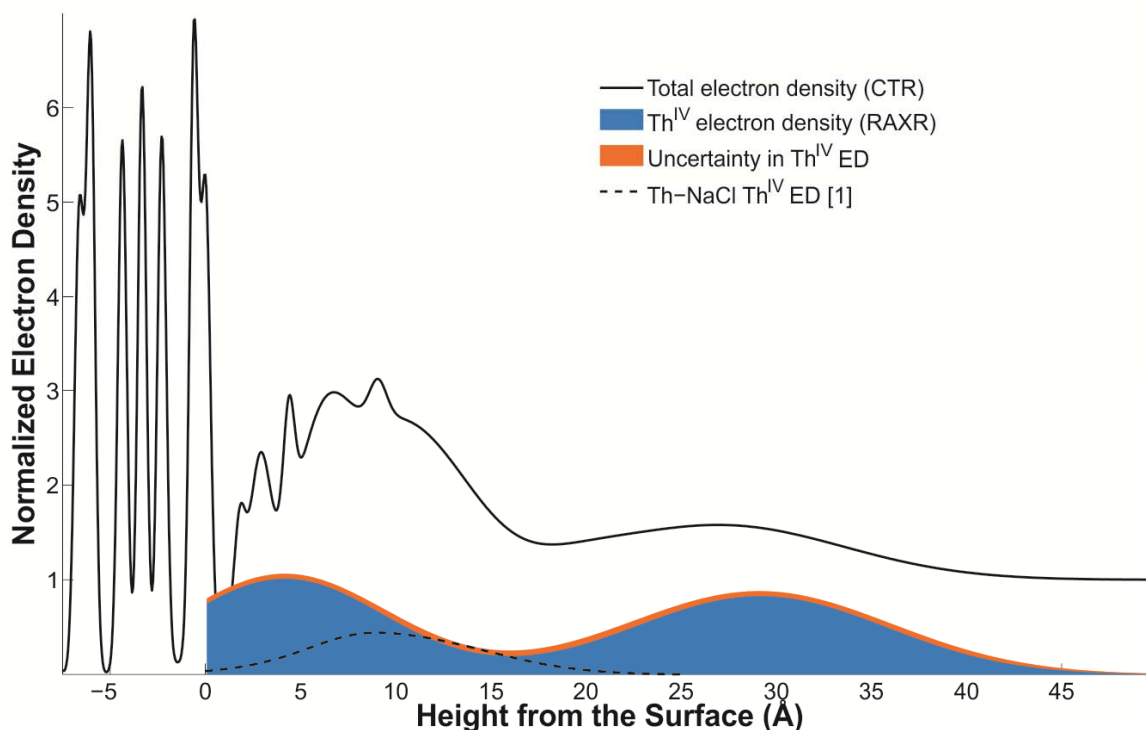
Figure 1. Total electron density (black) measured by CTR and electron density (blue, uncertainty orange) of Th^{IV} measured by RAXR in the Th-LiClO$_4$ system. Dashed black is the electron density of Th^{IV} in the Th-NaCl system of the reference sample [1]. Th^{IV} and total electron densities are normalized to the electron density of bulk water ($\rho(H_2O) = 0{,}33 e^-/ Å^3$) which is normalized to 1.

[1] M. Schmidt, et al., Geochim. Cosmochim. Acta 88, 66-76 (2012).
[2] M. Schmidt, et al., submitted to Geochim. Cosmochim. Acta.
[3] M. Schmidt, et al., Environ. Sci. Technol. 47, 14178-14184 (2013).

AM ASSOCIATION WITH MAGNESIUM HYDROXIDE COLLOIDS

Z. Maher[1], M. Randall[1], P. Ivanov[2], L. O'Brien[3], H. Sims[4], R.J. Taylor[1], S.L. Heath[5], F.R. Livens [5], D. Goddard[6], S. Kellet[7], P. Rand[7], N.D. Bryan[3]

[1] National Nuclear Laboratory, Sellafield, Cumbria, CA20 1PG, U.K.
[2] The National Physical Laboratory, Hampton Road, Teddington, Middlesex, TW11 0LW, U.K.
[3] National Nuclear Laboratory, Chadwick House, Birchwood, Warrington, WA3 6AE, U.K.
[4] National Nuclear Laboratory, Harwell Business Centre, Didcot OX11 0QJ, U.K.
[5] The Centre for Radiochemistry Research, School of Chemistry, The University of Manchester, Oxford Road, Manchester, M13 9PL, U.K.
[6] National Nuclear Laboratory, Preston, Lancashire, PR4 0XJ, U.K.
[7] Sellafield Ltd, Seascale, Cumbria CA20 1PG, U.K.

The Brucite ($MgO/Mg(OH)_2$) system has been suggested as a potential backfill for a radioactive waste repository [1]. Further, in the U.K. there are some wastes that contain significant amounts of brucite mixed with actinides and fission products [2]. Therefore, there is an interest in studying radionuclide interactions with bulk and colloidal brucite. Previously, it has been shown that both bulk [1, 3] and colloidal [4] brucite are able to bind radionuclides relatively strongly. Further, there is evidence that Pu(IV) is incorporated into the brucite subsurface at substantial concentrations and to a depth of at least 50 nm [1, 3].

In this study, the distribution of ^{241}Am(III) on brucite (magnesium hydroxide) colloids of different sizes was studied under alkaline conditions (pH = 10.4). All experiments were performed under an argon atmosphere to limit CO_2 dissolution. The association of ^{241}Am(III) with the brucite colloids was studied by sequential ultrafiltration coupled with gamma ray-spectrometry. The brucite colloids were generated by equilibrating a solid brucite sample with a solution of pH = 10.4; I = 0.1 ($NaClO_4$), according to the method of Pitois et al [4]. The concentration of Mg present as colloids (> 1 nm) was 2.8 ± 0.8 ppm. The brucite colloid size distributions by mass, total surface area and number are shown in Figure 1.
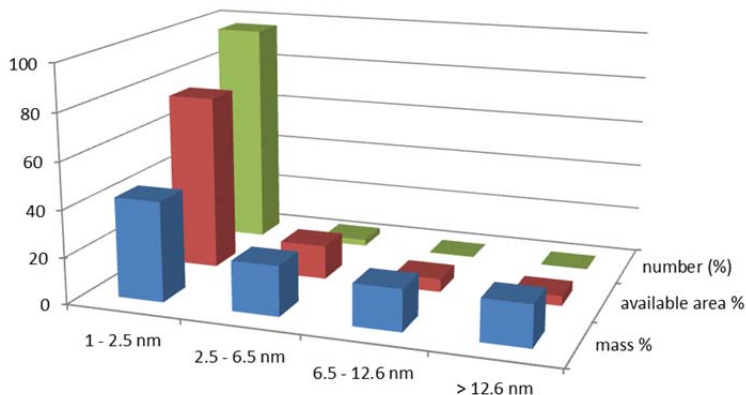
Figure1. Size fraction data for brucite colloids expressed as mass, surface area and number

In the absence of carbonate, the ^{241}Am(III) was mainly associated with larger colloids. Further, there was a shift from the smaller size fractions to the larger over a period of 6 months. Figure 2A shows the shift in distribution with time. The americium has a disproportionately low association with the small colloids, and it is clear that the larger colloids represent a more stable host, even at short contact times, and over time there is further transfer to the larger fractions. The behaviour is consistent with ^{241}Am(III) incorporation within the brucite structure, as has been observed previously for Pu(IV) [1, 3]. For carbonate concentrations up to 10^{-3} M, the Am remains associated with the larger colloidal fractions. However, at higher carbonate concentrations (10^{-2} M), the Am was

predominantly found in the true solution (Figure 2B), which was attributed to the formation of Am(III) carbonate complexes that competed effectively with the brucite for Am.
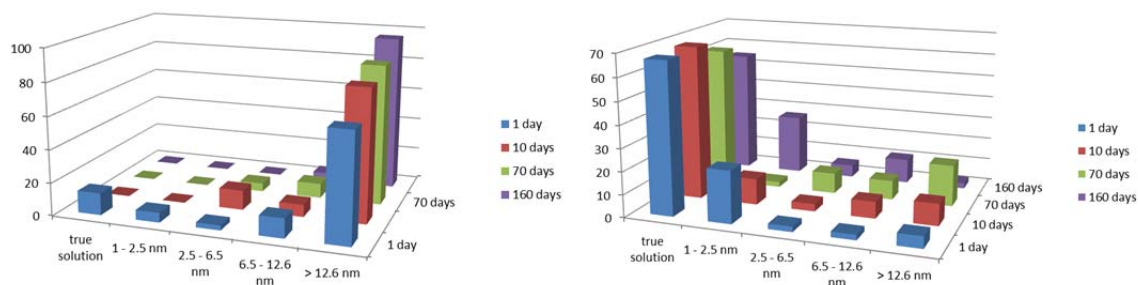
Figure 2. (A, left) Distribution of Am between true solution (< 1 nm) and different size fractions for carbonate free system; (B, right) Am distributions in the presence of 10^{-2} M carbonate.

References
[1] J.D. Farr, M.P. Neu, P.K. Schulze, B.D. Honeyman, J. Alloys Compd. 444 (2006) 533-539.
[2] S.A. Parry, L. O'Brien, A.S. Fellerman, C.J. Eaves, N.B. Milestone, N.D. Bryan, F.R. Livens, Energy Environ. Sci. 4 (2011) 1457-1464.
[3] J.D. Farr, P.K. Schulze, B.D. Honeyman, Radiochim. Acta 88(9-11) (2000) 675-679.
[4] A. Pitois, P.I. Ivanov, L.G. Abrahamsen, N.D. Bryan, R.J. Taylor, H.E. Sims, J. Environ. Monit. 10 (2008) 315-324.

CAESIUM SORPTION ON MAIN MINERALS OF CRYSTALLINE ROCK; OLKILUOTO CASE STUDY

E. Muuri[1], L. Qian [1], M. Siitari-Kauppi [1], M. Matara-aho[1], J. Ikonen[1], A. Lindberg[2], S. Holgersson[3], L. Koskinen[4]

[1]*Department of Chemistry, University of Helsinki, P.O. Box 55, 00014 University of Helsinki, Finland*
[2]*Geological Survey of Finland, Betonimiehenkuja 4, 02151 Espoo, Finland*
[3] *Department of Chemical and Biological Engineering, Nuclear Chemistry, Chalmers University of Technology, Kemivägen 4, SE-41296 Göteborg, Sweden*
[4]*Posiva Oy, Finland*

The final disposal of high-level nuclear waste has been considered to take place in crystalline granitic rock in Finland and the transport of radionuclides in the rock matrix has been subject to extensive research in the safety assessment of the deep geological repositories [1]. However, one of the most important parameters regarding the research of radionuclide transport is the distribution coefficient which describes the sorption of radionuclides onto the mineral surfaces. It is thus crucial to investigate the sorption behaviour of the high priority nuclear waste nuclides in the conditions of the deep geological repositories because the sorption is the main mechanism by which the radionuclides are retarded along the way from the repository to the biosphere. In this study the sorption behaviour of caesium was investigated in two crystalline rocks obtained from the Onkalo underground in situ diffusion test site in Olkiluoto and their main minerals. The tests were carried out in the presence of the groundwater simulant made to resemble the saline groundwater in the Onkalo test site.

The distribution coefficients of caesium in the Olkiluoto pegmatite, veined gneiss and their main minerals (quartz, plagioclase, potassium feldspar and biotite) were obtained by batch sorption experiments carried out as a function of both pH and concentration in room temperature. The compositions of the rocks and minerals were monitored with the XRD method and the specific surface areas were measured with the BET method. The effect of the specific surface area to the sorption results was also studied. The sorption results were also modelled with the PHREEQC calculation code. In addition, the results of different rocks and minerals were compared with each other and the sorption mechanisms onto different mineral surfaces were evaluated. The sorption results of caesium on the main minerals were also compared with sorption results obtained from a previous study in a low salinity groundwater simulant to assess the effect of competing ions.

The results showed that the distribution coefficients of caesium were largest in biotite and the sorption of caesium on potassium feldspar and plagioclase was approximately linear with changing concentration. In addition, the sorption of caesium on quartz was negligibly small in all investigated concentrations. The sorption results of veined gneiss and pegmatite followed their mineralogical composition. Veined gneiss has a high percentage of biotite and the sorption of caesium on it was relatively high. On the other hand, in pegmatite there is practically no biotite and the sorption of caesium on it was considerably lower than on veined gneiss. In addition, the distribution coefficient results followed the trend of the specific surface areas which provides proof that the specific surface area is an important tool in assessing the magnitude of sorption on mineral surfaces. It was also discovered that the distribution coefficients in saline water were considerably smaller than the results obtained from previous studies in low salinity water. This suggests that competing ions play a significant role in the sorption of caesium. Fig. 1 presents the distribution coefficients of caesium in veined gneiss, pegmatite, biotite and plagioclase as a function of concentration in pH 7.0.

Experiments regarding the transport of caesium in the Olkiluoto rock will continue. In future in situ diffusion tests will be started in the in situ test site. Also laboratory diffusion and sorption tests for rock blocks will be carried out.
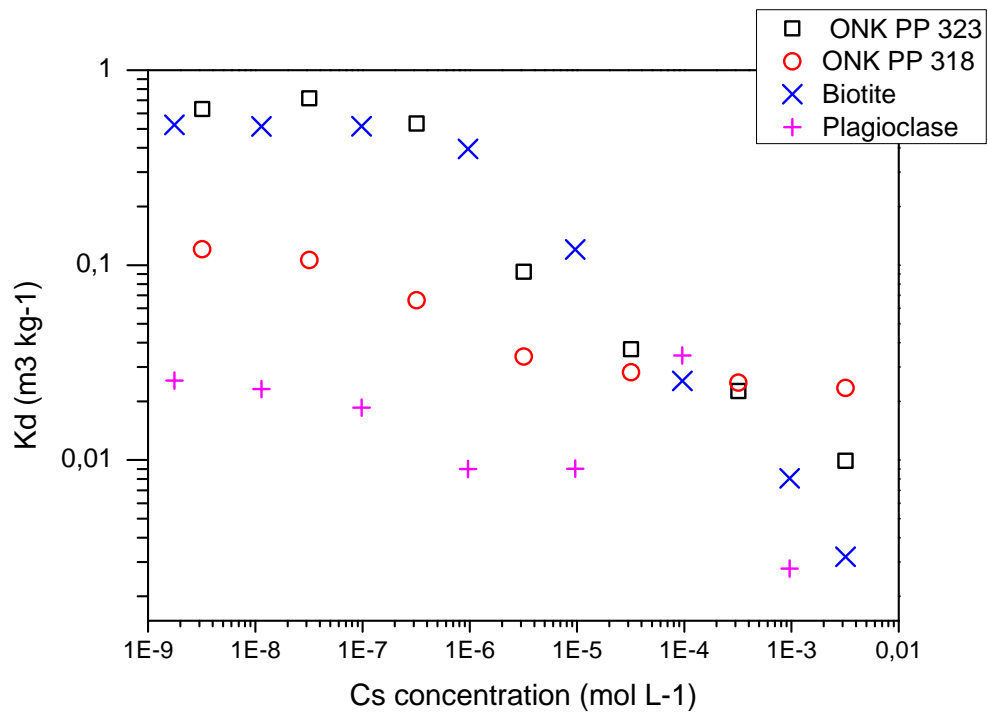
Fig 1. The distribution coefficients of veined gneiss (ONK PP 323), pegmatite (ONK PP 318), biotie and plagioclase as a function of concentration in pH 7.0.

[1] Radionuclide Transport in the Repository Near-Field and Far-Field. A. Poteri, H. Nordman, V-M. Pulkkanen. POSIVA 2014-02 (2014).

INVESTIGATING UO$_2^{2+}$ MONTMORILLONITE SPECIATION USING FLUORESCENCE AND PHOSPHORESCENCE LIFETIME IMAGE MAPPING

M. Williams[1)], L. Natrajan[1)], S. Shaw[2)], Andy Ward[3)] and Stanley Botchway[3)]

[1)] *Centre for Radiochemistry Research, School of Chemistry, The University of Manchester, Manchester, UK, M13 9PL*
[2)] *Research Centre for Radwaste and Decommissioning and Williamson Research Centre, School of Earth, Atmospheric and Environmental Sciences, The University of Manchester, M13 9PL, UK.*
[3)] *Central Laser Facility, Rutherford Appleton Laboratory, Harwell Oxford, Didcot, Oxfordshire, OX11 0QX, UK.*

The sorption of uranium(VI) to minerals control its mobility, reactivity and bioavailability in the many subsurface environments. Elucidating U(VI) speciation in environmental materials, is key to understanding the retardation of uranium through a geological barrier system and the geosphere. This work demonstrates the use of steady-state and time resolved emission spectroscopy in combination with fluorescence and phosphorescence microscopy to probe changes in the electronic structure of uranium, associated with mineral particles, on the sub-micrometre scale.

The luminescence profile of uranyl(VI) sorbed to montmorillonite clay suspended within an aqueous solution under controlled carbonate conditions has been studied by fluorescence and phosphorescence lifetime image mapping over a range of pH values. Spectra collected of the imaged clay aggregates provide a new level of detail. The sorption of uranyl(VI) onto the aluminosilicate minerals, montmorillonite and muscovite and the simpler 'building-block minerals' silica and alumina will also be presented. Sorption isotherms, elemental characterisation and batch sorption experiments were performed to determine the uptake and kinetics of uranyl(VI)-clay interactions in salt solution (0.1 M, NaNO$_3$) within natural groundwater pH ranges. Geochemical modelling in PHREEQC has been used to aid speciation analysis, as well as highlighting the effect of carbonate, pH and ionic strength.
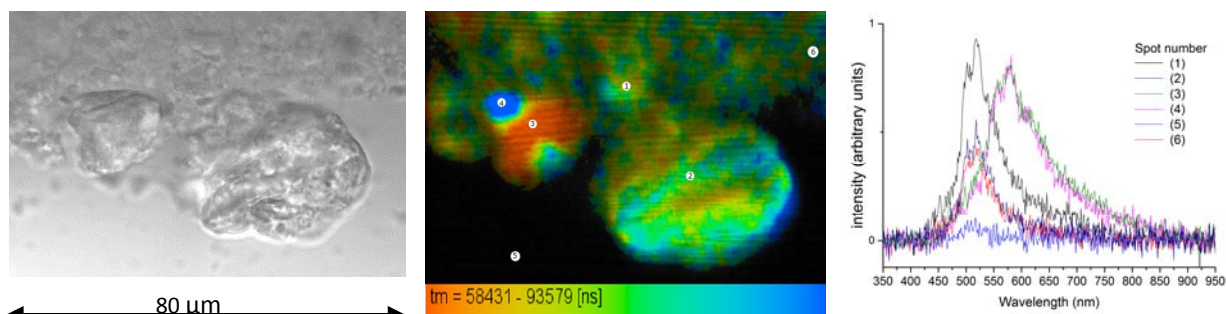
From left to right: brightfield confocal optical image of wet montmorillonite clay at pH 6.78 loaded with 1000 ppm uranyl(VI) under carbonate free conditions; phosphorescence lifetime image map of the same image; steady state uranyl(VI) emission spectra collected at different locations, corresponding to numbered spots on the centre image.

This investigation highlights the variation in speciation across simple uranium-mineral systems and that a combination of steady-state luminescence spectroscopy, confocal microscopy and lifetime image mapping greatly aids in the assignment of uranyl(VI) speciation on these mineral surfaces. It is anticipated that work in this field could expand our understanding of radionuclide-mineral interactions at the sub-micron scale and at low, geologically relevant, uranium concentrations.

[1] D. D. Cohen, J. Inorg. Nucl. Chem. 32, 3525 (1970).
[2] T. I. Docrat, et al., Inorg. Chem. 38, 1879 (1999).
[3] C. Madic, D. E. Hobard, G. M. Begun, Inorg. Chem. 22, 1494 (1983).

[4] L. Gagliardi, I. Grenthe, B. O. Roos, Inorg. Chem. 40, 2976 (2001).
[5] K. Mizuoka, I. Grenthe, Y. Ikeda, Inorg. Chem. 44, 4472 (2005).

[1] OECD NEA (2013), "TDB-0–TDB-6, TDB project guidelines", http://www.oecd-nea.org/dbtdb/guidelines/

[1] OECD NEA (2013), "Thermochemical Database (TDB) Project Publications - Chemical Thermodynamics Series",

www.oecd-nea.org/dbtdb/info/publications/

EFFECTS OF pH, TEMPERATURE, AND ORGANIC MATTERS ON THE SORPTION-DESORPTION BEHAVIORS OF U(VI) ON SILICON OXIDE NANOPARTICLES

H. Wu, P. Li, Q. Fan[*], W. Wu[*]

Radiochemistry Laboratory, Lanzhou University, Lanzhou, 730000, Gansu, China.

Nanomaterials are being increasingly utilized in many different fields, i.e., medical, pharmaceutical, food, energy and engineering, to improve pro duct performance. In spite of these promising applications, they also bear a potential risk because they can also be released unintentionally either inside the human body or into the environment [1, 2]. Silicon dioxide nanoparticles (SONPs) are one of the common industrial additives and have various applications, the toxicities of which have been studied for antimicrobial activity and soil microbial communities [3, 4]. In consideration of the unpredictable biotoxicity, the exploitation of SONPs as a treatment of radionuclides is economical and cost-effective.

Natural organic matters (NOM) like humic and fulvic acids could possibly negate the toxic effects of SONPs through various mechanisms [4]. And NOM owing high negative charge density on their molecules can induce a strong complex constant with metal ions and radionuclides in environment. Therefore, organic matters will affect the mobility, migration, bioavailability and toxicity of radionuclides and metal ions in the environment [5].

The present study is aimed to identify the immobilization of U(VI) on SONPs under various physicochemical conditions using batch approach, which includes the effect of pH, ionic strength on U(VI) sorption, the kinetic and thermodynamic estimation, and the influence of the humic acid (HA) on the stability of SONPs and the sorption-desorption process. U(VI) sorption on SONPs was a chemical process and the rate limitation was not only due to intraparticle diffusion. Generally, the sorption of U(VI) on SONPs was strongly dependent on pH and ionic strength. In the presence of HA, U(VI) sorption was obviously improved at pH < 5.0, whilst U(VI) sorption was restrained at high pH range. Sorption–desorption showed the reversible sorption of U(VI) on SONPs, which might indicated a weak sorption species formed, for example, outer-sphere complexes. However, the presence of HA can change the reversible process into an irreversible one. It suggested a strong species of U(VI) sorption, i.e., inner-sphere complexes in the ternary system. Besides, the thermodynamic estimation indicated that the sorption process was endothermic and spontaneous and high temperature favored the sorption procedure.
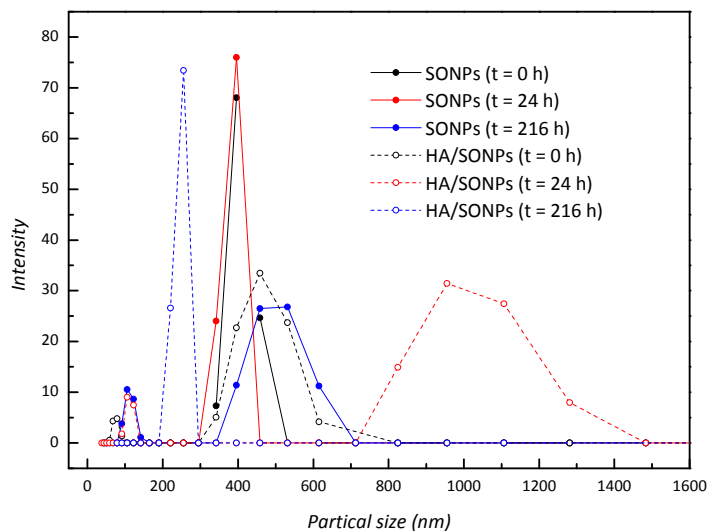
Figure1. Particle size distribution for SONPs in the absence and presence of HA ($C_{[HA]}$ = 15 mg/L)
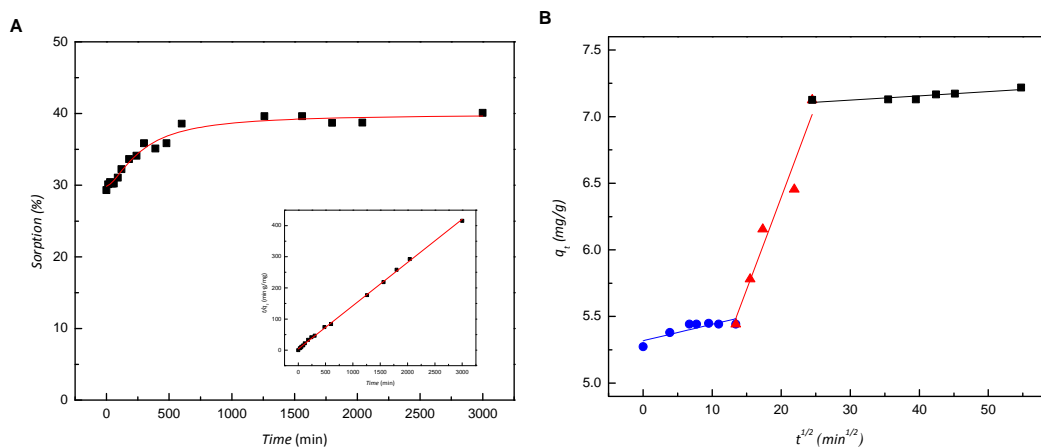
Figure 2 (A) The influence of contact time on U(VI) sorption to SONPs. Bottom right: the fitting plot of the pseudo-second-order equation; (B) Weber-Morris model (T = 298±1 K, S/L = 0.6 g/L, I = 0.01 mol/L NaClO$_4$, C$_{[U(VI)]}$ = 2.0×10-5 mol/L, pH = 5.0±0.1)
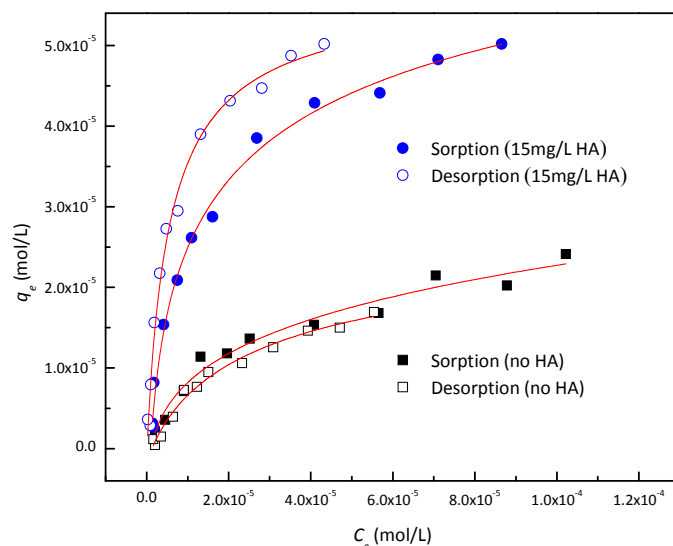
Figure 3   Sorption-desorption isotherm of HA on SONPs (T = 298±1 K, S/L = 0.6 g/L, I = 0.01 mol/L NaClO$_4$, pH = 4.5±0.1)

[1] Rivera-Gil P. The challenge to relate the physicochemical properties of colloidal nanoparticles to their cytotoxicity. Acc Chem Res, 2013, 46: 743-749.

[2] Okoturo-Evans O. Elucidation of toxicity pathways in lung epithelial cells induced by silicon dioxide nanoparticles. PLOS One, 2013, 8: e72363.

[3] Campos B. Adsorption of uranyl ions on kaolinite, montmorillonite, humic acid and composite clay material. Applied Clay Science, 2013, 85: 53-63.

[4] Dinesh R. Engineered nanoparticles in the soil and their potential implications to microbial activity. Geoderma, 2012, 173-174: 19-27.

[5] Fan Q. The adsorption behavior of U (VI) on granite. Environ Sci: Processes Impacts, 2013, 16, 534–541.

EFFECTS OF pH, IONIC STRENTH AND HUMIC ACID ON THE SOPRTION OF NEPTUNIUM(V) TO Na-BENTONITE

LI Ping[1], LIU Zhi[1], MA Feng[2], SHI Quan-lin[2], GUO Zhi-jun[1*], WU Wang-suo[1*]

[1]Radiochemistry Laboratory, Lanzhou University, Lanzhou 730000, China
[2]Northwest Institute of Nuclear Technology, Xi'an 710024, China

A method was developed for the determination of [237]Np with liquid scintillation counting (LSC) in the batch experiment of neptunium sorption onto bentonite. Before we use the pulse shape analysis (PSA) technique to discriminate α/β emission, an effective approach was developed to set the optimum PSA by measuring a mixed α/β emitters sample and a background sample. The mathematic treatment of neptunium spectrum indicated that at the selected PSA-level of 38 approximately 86% of the total α emission is detected, which is suitable for the determination of samples in the batch sorption experiments. Moreover, we confirmed that, at mass to volume radio 0~10 g/L the bentonite suspension in samples does not influence LSC determination obviously. Thus, sorption percentage can be easily obtained by counting equivalent amount of suspension and supernatant from the same sample.

By applying the method mentioned above, effects of ionic strength, pH, temperature, humic acid (HA) and adsorbate concentration on Np(V) sorption to Na–bentonite were investigated in detail. The sorption of Np(V) to Na–bentonite was significantly dependent on pH and independent of temperature. In the presence of HA, Np(V) sorption was enhanced significantly at low pH; whilst obvious negative effect was observed in higher pH range. Np(V) sorption followed the Freundlich isotherm indicating a heterogeneous sorption of Np(V) on the surface of Na–bentonite. The surface complexation model (SCM) suggests sorption of Np(V) on Na–bentonite was mainly dominated by ion exchange at low pH values, and two dominant monodentate inner-sphere complexes of $\equiv SiONpO_2^0$ (logK = -4.55) and $\equiv AlO(NpO_2OH)^-$ (logK = -13.80) contributed to Np(V) sorption on Na–bentonite over high pH range.
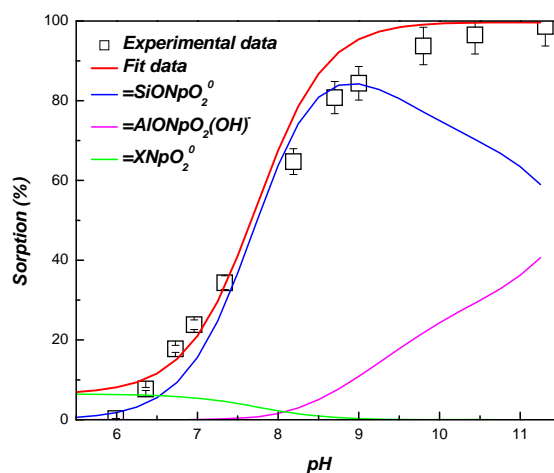
Fig. 1 The sorption species of Np(V) on Na-bentonite as a function of pH. C(Np(V)) = 4.0×10^{-7} mol/L; I = 0.1 mol/L NaCl; s/l = 10 g/L; T = 25±1 ^{0}C.

AGING EFFECT OF SORPTION OF 32-YEAR-OLD PLUTONIUM COMPLEXES ON SAVANNAH RIVER SITE SEDIMENTS

Hilary P. Emerson and Brian A. Powell

Department of Environmental Engineering and Earth Science, Clemson University, 342 Computer Court, Anderson, SC 29625

It has been previously noted that the reversibility of actinide sorption decreases over time even though the specific mechanisms responsible for this process are unknown [1-3]. Further studies have suggested that groundwater constituents may play a role in mobilizing actinide elements, especially natural organic matter [4, 5]. In this study sorption/desorption experiments were used to investigate the desorption processes and aging effects of plutonium sorption in the presence of a subsurface clayey sediment from an 11 year lysimeter experiment completed at the Savannah River Site 21 years ago (soils have now aged in the presence of $^{239/240}$Pu for a total of 32 years) [6].

Desorption experiments were completed for 3, 7, 28 and 168 days on source materials amended with ~2 µg/g of $^{239/240}$Pu at a pH of 6.4±0.4. The 3 and 168 day data also added ~3.7 µg/L of ^{242}Pu in order to consider sorption K_d's in addition to the desorption K_d's. A variety of inorganic and organic ligands were added to the solutions including:

- NaCl, CaCl$_2$, Na$_2$PO$_4$, or NaF from 0.1 to 10 mM
- Citric Acid, Suwanee River Fulvic Acid, or DFOB from 0.05 to 5 mg$_{carbon}$/L
- Or H$_2$O$_2$ from 0.01 to 1% (3 to 300 mM) or NH$_2$OH·HCl at 1 mM

However, the 3 and 168 day data was collected only at the highest ligand and ionic strength conditions. The results showed that desorption of $^{239/240}$Pu was independent of the chosen ionic strengths and ligands with average desorption log K_d values ranging from 3.7-4.2 as shown in Table 1 below for each time period. These values are averaged because the variable ionic strength and ligand concentrations did not produce statistically different results as compared by Tukey and Dunnett's method. This result was verified using a redox-coupled generalized composite surface complexation model. However, the comparison of the ^{242}Pu and $^{239/240}$Pu values appears to be statistically different. It must be noted that this represents a sorption of 99% versus 99.9% and more than half of the ^{242}Pu values were within three times the minimum detectable concentrations. Therefore, it is likely that this statistical difference is an experimental artefact. The distribution coefficients obtained from Pu(IV) and Pu(V) sorption to uncontaminated SRS soil by Powell et al., [7] and Pu desorption from a soil contaminated for 30+ years from the current work are within an order of magnitude of each other (for similar pH values). This is rather remarkable behavior given the wide range of chemical reactants used in the current work to facilitate desorption. Overall the amount of desorbed Pu was very small and there were no significant differences between the Pu desorption over time.

Previous work by Kaplan, et al. [8] showed that desorption data on this soil with respect to pH exhibits a similar trend to Pu(V)/PuO$_2$(am) solubility data published by Rai et al. [9] but with ~3.4 orders of magnitude lower aqueous Pu values due to sorption. Thus, it appeared that Pu partitioning to the aqueous phase was controlled by solubility. Figure 1 below compares the data measured in these experiments with those in Kaplan et al. [8]. Similar aqueous Pu concentrations were reached in the desorption experiments described above. To further examine this potential for solubility control, experiments were performed with varying concentrations of contaminated soil (i.e. effectively changing the total amount of Pu in the system). Preliminary data indicate that they system does indeed reach a constant aqueous Pu concentration despite a 100x change in total Pu in the system.

References

[1] Tinnacher, R.M., Zavarin, M., Powell, B.A., Kersting, A.B. (2011) "Kinetics of neptunium (V) sorption and desorption on goethite: An experimental and modeling study." *Geochimica et Cosmochimica Acta*, 75, 6584-6599.
[2] Missana, T., Garcia-Gutierrez, M., and Alonso, U. (2004) "Kinetics and irreversibility of cesium and uranium sorption onto bentonite colloids in a deep granitic environment." *Applied Clay Science*, 26, 137-150.
[3] Kaplan, D.I., Powell, B.A., Demirkanli, D.I., Fjeld, R.A., Molz, F.J., Serkiz, S.M., and Coates, J.T. (2004) "Influence of oxidation states on plutonium mobility during long-term transport through an unsaturated subsurface environment." *Environmental Science and Technology*, **38**, 5053-5058.

[4] McCarthy, J.F., Sanford, W.E., Stafford, P.L. (1998) "Lanthanide field tracers demonstrate enhanced transport of transuranic radionuclides by natural organic matter." *Environmental Science and Technology*, 32 (24), 3901-3906.

[5]McCarthy, J.F., Czerwinski, K.R., Sanford, W.E., Jardine, P.M., and Marsh, J.D. (1998) "Mobilization of transuranic radionuclides from disposal trenches by natural organic matter." *Journal of Contaminant Hydrology*, 30, 49-77.

[6] Kaplan, D.I., Demirkanli, D.I., Gumapas, L., Powell, B.A., Fjeld, R.A., Molz, F.J., and Serkiz, S.M. (2006) "Eleven-year field study of Pu migration from Pu III, IV, and VI sources." *Environmental Science and Technology*, 40 (2), 443-448.

[7] Powell, B.A., Fjeld, R.A., Coates, J.T., Kaplan, D.I., and Serkiz, S.M. (2003) "Plutonium Oxidation State Geochemistry in the SRS Subsurface Environment (U)." Savannah River Site Report# WSRC-TR-2003-00035.

[8] Kaplan, D.I., Powell, B.A., Gumapas, L., Coates, J.T., Fjeld, R.A. and Diprete, D.P. (2006) "Influence of pH on Plutonium Desorption/Solubilization from Sediment." *Environmental Science and Technology*, 40, 5937-5942.

[9] Rai, D. (1984) "Solubility of Pu(IV) hydrous oxide and equilibrium constants of Pu(IV)/Pu(V), Pu(IV)/Pu(VI), and Pu(V)/Pu(VI) couples." *Radiochimica Acta*, 35, 95-106.

Table 1: Summary of average and standard deviation of all measurements in the presence of variable ligands and ionic strengths for batch sorption (^{242}Pu) and batch desorption ($^{239/240}$Pu)

Parameter	3 days		7 days	28 days	168 days	
	$^{239/240}$Pu	^{242}Pu	$^{239/240}$Pu	$^{239/240}$Pu	$^{239/240}$Pu	^{242}Pu
LogK$_d$ (mL/g)	3.69±0.25	3.22±0.38	4.16±0.34	4.24±0.35	4.17±0.24	3.41±0.29
Fraction Sorbed (%)	99.6±0.3	98.6±1.6	99.4±0.6	99.7±0.3	99.6±0.2	98.7±1.6
Aqueous Pu x10^{-10} (mol/L)	3.8±3.8	45.9±40.3	6.5±6.2	11.7±10.5	7.3±5.1	1.6±1.9
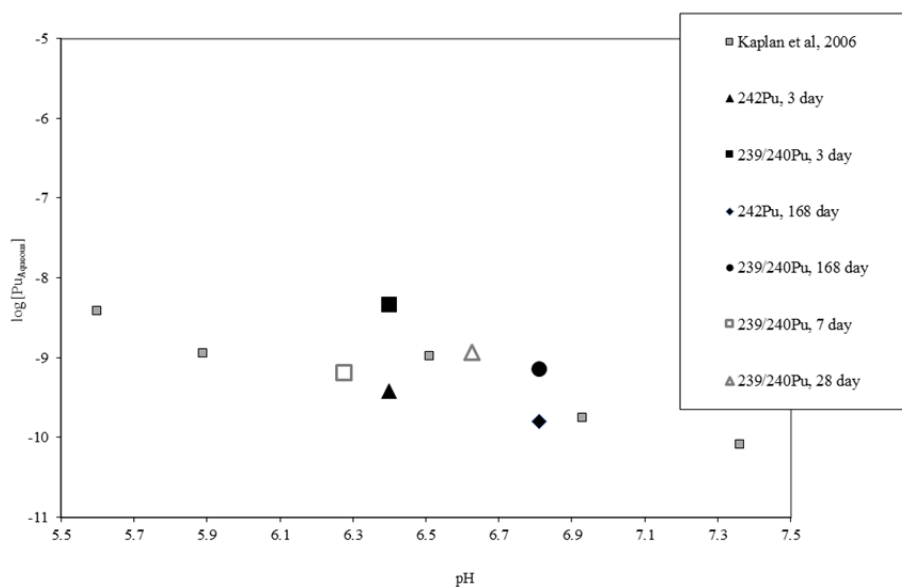
Figure 1: Comparison of Aqueous Pu (mol/L) concentrations measured in desorption experiments in this study at soil concentrations of ~50 (*gray, unfilled*) and ~70 g$_{soil}$/L (*black, filled)* versus desorption experiments by Kaplan et al. [8] at ~50 g$_{soil}$/L (*gray, filled*).

RETARDATION AND RELEASE OF URANIUM ON PHLOGOPITE MICA AT THE ABSENCE AND PRESENCE OF HUMIC ACID: A BATCH AND TRLFS STUDY

D. Pan [(1)], Z. Wang [(2)], W. Wu[*] [(1)]

[(1)] *School of Nuclear Science and Technology, Lanzhou University, Lanzhou, Gansu 730000, China*
[(2)] *Pacific Northwest National Laboratory, Richland, WA 99352, United States*

Hexavalent Uranium, which is fertile in mining tailings and wastewater from nuclear production activities, is a prominent radioactive contaminant and has dispersed into both sediments and water around the uranium-related processing sites, posing a potential health and environmental risk to the biosphere [1,2]. The mobility of uranium in natural medium is significantly controlled by the sorption/desorption behavior which is influenced by uranium speciation, sorbent properties and coexisted organic/inorganic ligands [3,4]. As the sorption mechanism can vary due to changes in sorption conditions, such as ligand complexation and change of pH or temperature, uranium retardation and release rate in environmental media can be perturbed by altering these parameters. Understanding the sorption mechanism and sorption reversibility of uranium is imperative to predict the future retention/migration behavior of uranium and to remediate contaminated soils and subsurface sediments.

In this work, the batch sorption experiments and cryogenic time-resolved laser-induced fluorescence spectroscopy (TRLFS) technique were applied to investigate uranium(VI) sorption and desorption on phlogopite at the absence and presence of humic acid (HA). The results showed that at the absence of HA, the uranium(VI) sorption on phlogopite was strongly dependent on pH while minimally affected by the ionic strength, multiple inner-sphere surface species (including $\equiv SOUO_2^+$, $\equiv SO(UO_2)_2(OH)_2CO_3^-$ and $\equiv SOUO_2(CO_3)_x^{1-2x}$) were formed with their abundance varying as a function of pH, and a portion of uranium precipitated as uranyl oxyhydroxides at high pH (> 9).

The presence of HA made little difference below pH 4 while inhibited uranium(VI) sorption above pH 4, and such effect became much more pronounced by increasing HA concentration from 20 mg/L to 50 mg/L. Time-resolved uranium fluorescence spectra indicated the formation of ternary surface complex at low pH, uranium-humate complex preferred binding directly on surface rather than via HA. Multiple aqueous uranium-humate complexes were responsible for the suppression of uranium sorption at high pH.

The uranium(VI) sorption on phlogopite increased with an increase of temperature, however, the enhancement of sorption at high temperature could be reversed by lowering the temperature. The spectral evidence indicated that the uranium speciation remained the same at high temperature. The presence of HA enhanced uranium mobility without altering dominant surface species before and after desorption treatment.

[1] Chakraborty, S. et al. (2010). "U(VI) Sorption and Reduction by Fe(II) Sorbed on Montmorillonite." *Environ. Sci. Technol*. 44(10): 3779-3785.

[2] Zhao, G. et al. (2012). "Preconcentration of U(vi) ions on few-layered graphene oxide nanosheets from aqueous solutions." *Dalton T*. 41(20): 6182-6188.

[3] Chang, H.S. et al. (2006). "Adsorption of Uranyl on Gibbsite: A Time-Resolved Laser-Induced Fluorescence Spectroscopy Study." *Environ. Sci. Technol*. 40(4): 1244-1249.

[4] Chisholm-Brause, C.J. et al. (2001). "Uranium(VI) Sorption Complexes on Montmorillonite as a Function of Solution Chemistry." *J. Colloid Interf. Sci*. 233(1): 38-49.

ORGANIC MODIFICATION OF GMZ BENTONITE AND ITS APPLICATION FOR PERRHENATE UPTAKE FROM AQUEOUS SOLUTION [*]

K. L. Shi , Y. M. Li, M.L. Bi, R. Li, W.S. Wu

Radiochemistry Lab, School of Nuclear Science and Technology, Lanzhou University, 730000, Lanzhou, P. R. China

In the geologic disposal of high-level nuclear waste, sorption is treated as an effective way to evaluate the migration of radionuclide in the environment. The investigation on the sorption behavior of interesting ions (such as $^{99}TcO_4^-$) on natural or modified mineral is therefore significant and many authors have focused on it [1-3]. In this work, the sorption of ReO_4^- (a nonradioactive surrogate for $^{99}TcO_4^-$) by hexadecyl trimethyl ammonium bromide (HDTMA) modified bentonite in aqueous solution was investigated in details. The experiment results show that Na-bentonite sample is successfully modified and a certain amount of HDTMA has been connected with bentonite. The XRD spectrum indicates that beside on surface, some amount of HDTMA molecules also enter into the interlayer of two silicon-oxygen tetrahedron layers of bentonite sample. The stability of HDTMA in sample (see figure 1) is favorable and there is no loss of HDTMA happening with the increasing of calcination temperature (<200 ^0C). The uptake ratio of ReO_4^- is relatively rapid and the sorption kinetics of ReO_4^- can be successfully described by the pseudo-second-order model. The thermodynamic study reveals that the sorption process is more favorable at lower temperature. The negative ΔG values confirm the feasibility of the process for sorption of ReO_4^- onto modified bentonite and spontaneous nature of sorption. The uptake ratio of ReO_4^- on HDTMA modified bentonite enhances significantly compared with unmodified one, besides the ion exchange reaction, surface precipitate between HDTMA and ReO_4^- would be the main mechanism for ReO_4^- uptake by HDTMA modified bentonite.
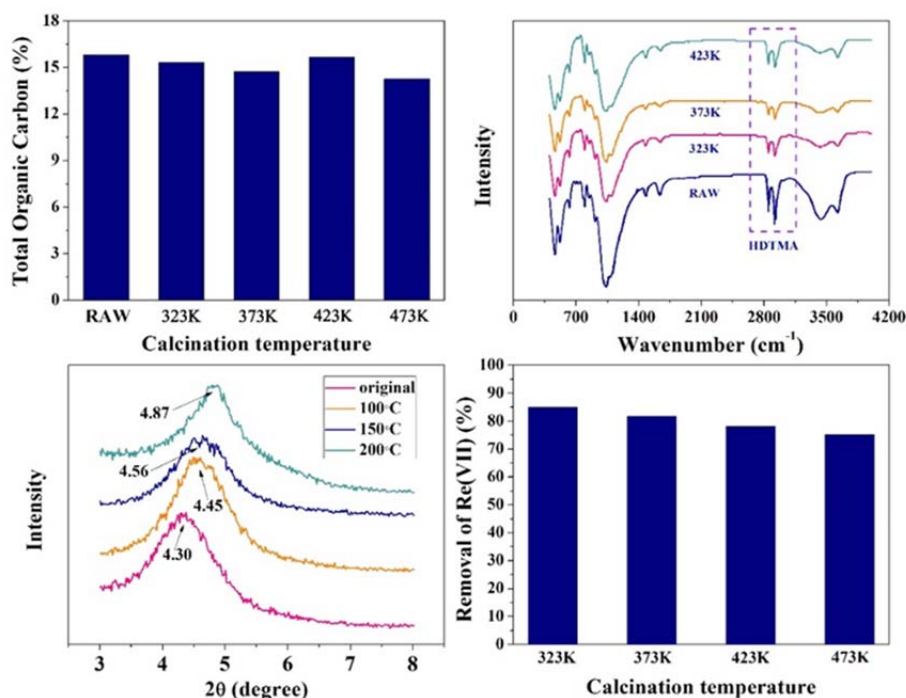
Figure 1. The stability and sorption ability of HDTMA modified bentonite at different calcination temperature

[1] K.L. Shi, et al., J. Radioanal. Nucl. Chem. 299, 583 (2014).
[2] Y. H. Su, et al., J. Hazard. Mater. 173, 47 (2010).
[3] B. Wakoff, K. L. Nagy, Environ. Sci. Technol. 38, 1765 (2004).

EFFECTS OF HUMIC ACIDS IN DIFFERENT STATES ON
Eu(III) ADSORPTION ON BAYERITE

Z. Niu, Z. Guo[*], C. Gao, W. Wu

School of Nuclear Science and Technology, Lanzhou University, Lanzhou 730000, China

There have been numerous studies on the adsorption of radionuclides on various minerals in the presence of purified humic substances (HSs) which were actually in different states as compared to HSs in the environment. To evaluate the effect of this difference, we compared the adsorption of Eu(III) on bayerite (BT) in the presence of humic acid (HA) in different states, i.e., purified HA and HS assembled in BT (HA@BT). For this purpose, both naked BT and HA@BT (C_{HA}= 5%wt.) were synthesized by using the same precipitation method, except that HA (5%) was involved in HA@BT synthesis. The synthesized samples were characterized in detail by using XRD, SEM, N2-BET and potentiometric titration. Eu(III) adsorption was carried out using a batch method. The adsorption systems, Eu(III)/BT, Eu(III)/HA/BT and Eu(III)/HA@BT, were characterized by time-resolved laser fluorescence spectroscopy (TRLFS).

It was found that the peak intensities of XRD pattern for HA@BT were lower than those for naked BT, whereas the average size of HA@BT aggregation particles and HA@BT specific surface area were larger than those for naked BT, respectively, indicating that more crystal defects were formed in HA@BT. As found in previous studies[1-3], the adsorption of Eu(III) in Eu(III)/HA/BT system was higher than that in Eu(III)/BT system in the low pH range, whereas it was lower in the high pH range, due to the binding of HA on BT at low pH values and the complexation of HA with Eu(III) in aqueous phase at high pH values. In contrast, the adsorption of Eu(III) in Eu(III)/HA@BT system was always higher than that in Eu(III)/BT system before reaching adsorption plateau. Eu fluorescence emission spectra indicated that the ratios of the $^5D_0{\rightarrow}^7F_2$ transition (616 nm) to the $^5D_0{\rightarrow}^7F_1$ (592 nm) transition increased with pH in all three adsorption systems, but the ratios at the same pH value were different from one another, especially for Eu(III)/HA/BT system and Eu(III)/HA@BT system. This may indicate that different adsorption mechanisms were involved when HA was in different states. The adsorption systems were also characterized by EXAFS.

[1] Th. Rabung, Th. Stumpf, H. Geckeis, R. Klenze, J. Kim, Radiochim. Acta. 88, 711(2000).

[2] N. Janot, M. F. Benedetti, P.E. Reiller, Geochim Cosmochim. Acta 123, 35(2013).

[3] X. Wang, D. Xu, L. Chen, X. Zhou, A. Ren, C. Chen, Appl. Radiat. Isot. 64, 414(2006).

REDOX-COUPLED SURFACE COMPLEXATION MODELING (SCM) FOR PLUTONIUM (IV) SORPTION ONTO GOETHITE AND KAOLINITE

Y. Xie, B. A. Powell

Department of Environmental Engineering and Earth Sciences,
Clemson University, Anderson, South Carolina, USA, 29625

The inherent sensitivity of Pu to redox transformations is one of the major factors that hinders the understanding of Pu transport in the subsurface due to the varying mobility of each oxidation state. The coexistence of multiple Pu oxidation states and variance with respect to pH and redox potential pose a significant challenge for predicting the fate and transport of Pu in the environment. Generally speaking, Pu(III) can occur under acidic/anoxic conditions. As the pH and redox potential increase, the more oxidized oxidation states of Pu(IV), Pu(V), and Pu(VI) become stable and dominant species in the aqueous phase. As these oxidation states are stabilized in different systems, Pu sorption as a function of oxidation state will follow the trend: Pu(IV) > Pu(VI) ≈ Pu(III) > Pu(V) [1]. In order to simulate Pu speciation in natural systems, coupled speciation models that account for both redox and sorption reactions are necessary.

Here we developed a sorption model that coupled Pu redox speciation and considered surface complexation via a diffuse-layer model and ion exchange based on a Vanselow convention. The potentials for Pu redox reactions were converted to stability constants (log K) using the Nernst Equation and coupled to Pu aqueous and surface reactions within the model database. Goethite (α-FeOOH) and kaolinite ($Al_2Si_2O_5$) were used as model minerals for Pu sorption. For kaolinite, batch sorption of Pu(IV) onto kaolinite at pH 2 – 8 was conducted under both aerobic and anaerobic condition. The pH and E_H was monitored and the oxidation state of Pu in the aqueous and sorbed phases were analyzed using solvent extraction. Experiments were initially spiked with Pu(IV), but was partially oxidized to Pu(V/VI) under aerobic conditions and partially reduced to Pu(III) under anaerobic conditions. Pu(IV) was the predominant sorbed species on kaolinite under both aerobic and anaerobic conditions. These changes in the distribution of Pu oxidation states have observable effects on the sorption behavior. Under aerobic conditions, a zone of decreased of sorption was seen between pH 4 and 6 due to the ingrowth of aqueous Pu(V) with increasing pH. Conversely, under anaerobic conditions, the presence of Pu(III) in the aqueous phase lead to a notable shift in the pH sorption edge to higher pH values due to the lower affinity of Pu(III) for kaolinite relative to Pu(IV). A redox coupled surface complexation model was developed to approximate the changing Pu redox speciation and the sorption behavior of each oxidation state. The model suggested that under aerobic conditions, the cation exchange sites on kaolinite dominate Pu sorption at pH < 4.5 and aluminol and silanol kaolinite edge sites contribute to Pu sorption at pH 4.5 – 8. Interestingly, under anaerobic conditions, Pu(III) is found as the dominant aqueous oxidation state but Pu(IV) was observed as the dominant sorbed species. This apparent redox disequilibrium is somewhat analogous to previous observations under aerobic conditions where Pu(V) was observed as the dominant aqueous phase oxidation state and Pu(IV) was the dominant sorbed species [2] [3].

A similar redox coupled sorption model, though without the need for an ion exchange reaction, was used to describe Pu sorption to goethite. To further examine Pu redox speciation, initially Pu(IV) sorption to goethite was monitored at pH 1 – 6 and from 15 °C to 65 °C. Similar experiments were also performed using Th(IV) as a stable tetravalent analog. The pH and E_H were monitored, and the oxidation state of Pu both aqueous and solid phases were analyzed. The oxidation of Pu(IV) to Pu(V/VI) in the aqueous phase had a resulting decrease in Pu sorption to goethite relative to that of Th(IV). In all cases sorption of Pu and Th increased with increasing temperature and van't Hoff plots of the distribution coefficients indicated that sorption was driven by a positive entropy. A fully redox coupled sorption model could not be developed at higher temperatures due to the lack of Pu hydrolysis constants at those temperatures. A redox-coupled model at 25 °C is presented.

[1] Choppin, G. R.; Bond, A. H.; Hromadka, P. M., Redox speciation of plutonium. *Journal of radioanalytical and nuclear chemistry* **1997,** *219*, (2), 203-210.
[2] Powell, B. A.; Fjeld, R. A.; Kaplan, D. I.; Coates, J. T.; Serkiz, S. M., Pu (V) O_2^+ adsorption and reduction by synthetic hematite and goethite. *Environmental science & technology* **2005,** *39*, (7), 2107-2114.
[3] Powell, B. A.; Fjeld, R. A.; Kaplan, D. I.; Coates, J. T.; Serkiz, S. M., Pu (V) O_2^+ adsorption and reduction by synthetic magnetite (Fe_3O_4). *Environmental science & technology* **2004,** *38*, (22), 6016-6024.

RETENTION OF RADIOCARBON BY ISOTOPE EXCHANGE BETWEEN GROUNDWATER AND CALCITE

J. Lempinen, D. Apter, J. Lehto

Laboratory of Radiochemistry, Department of Chemistry,
P.O. Box 55, 00014 University of Helsinki, Finland

Radiocarbon (^{14}C) is one of the key radionuclides considering the radiation doses to humans and biota due to the final disposal of spent nuclear fuel. The main uncertainty in assessing its behaviour in geosphere is its speciation. In groundwater, the prevailing species of carbon are dissolved carbon dioxide and methane, which is why the radiocarbon released from the repository is expected to be present as methane or dissolved inorganic carbon species as well. The radiocarbon as methane is not retained by the bedrock and will thus migrate along the groundwater flow. For radiocarbon in groundwater as dissolved carbon dioxide sorption mechanisms such as the isotope exchange between groundwater and calcite can be considered.

The carbon isotope exchange between fracture calcite ($CaCO_3$) and groundwater is a process in systems where calcite is at solubility equilibrium with the groundwater. This process occurs in nature [1] and has been investigated in laboratory using both stable ^{13}C [2] and radioactive ^{14}C [3] as tracer isotopes. At solubility equilibrium the dissolution and precipitation of calcite occur at equal rates, and therefore no changes in concentrations of the calcium or carbonate ions are observed. However, if radiocarbon as dissolved carbon dioxide is present in the groundwaters, it can also be precipitated as calcite and become part of the solid phase. Due to the isotope exchange, the activity of radiocarbon in solution decreases as a function of time until the carbon isotope composition is equal in groundwater and on the surface of calcite. The reaction equation for the isotope exchange can be written as

$$CaCO_3 \text{ (calcite)} + H^{14}CO_3^- \text{ (aq)} \Leftrightarrow Ca^{14}CO_3 \text{ (calcite)} + HCO_3^- \text{ (aq)}$$
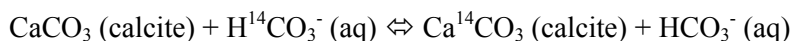
The rate of the isotope exchange was investigated in various solutions with different concentrations of calcium and bicarbonate ions using batch experiments. After allowing synthetic calcite to attain solubility equilibrium with the solution, the solution was radiolabelled with $H^{14}CO_3^-$ tracer. The calcium concentration, pH and activity of radiocarbon in solution were then measured as a function of time. Figure 1 shows the solution activity of radiocarbon as a function of time in selected solutions. The activity decreased exponentially as a function of time in all of the solutions, although the calcium concentration and pH did not change. An exponential fit on the activity data in each solution as a function of time was done to quantify the rate of the isotope exchange. The fitting function was

$$A(t) = A_0 e^{-kt} + y_0$$

where k is the rate constant of the isotope exchange in that particular solution. The half-life of the isotope exchange was then calculated from the equation

$$t_{1/2} = \frac{\ln 2}{k}$$

Figure 2 shows the half-life of the isotope exchange as a function of the calcium concentration of the solution. As can be seen the half-life of the isotope exchange decreases as the calcium concentration increases, but is practically constant, at 4.7 days, at calcium concentrations higher than 10 mM.

The isotope exchange half-lives ranging from a few to hundreds of days are very short time periods compared to the half-life of radiocarbon (5730 y) and the time scale of the groundwater movements. Therefore the isotope exchange between groundwater and calcite can significantly slow down the transport of radiocarbon through the bedrock especially in saline groundwaters with high calcium ion concentrations. Typical calcium concentration of the final disposal depth in Olkiluoto is 17 mM in brackish and 100 mM in saline groundwaters. [4]
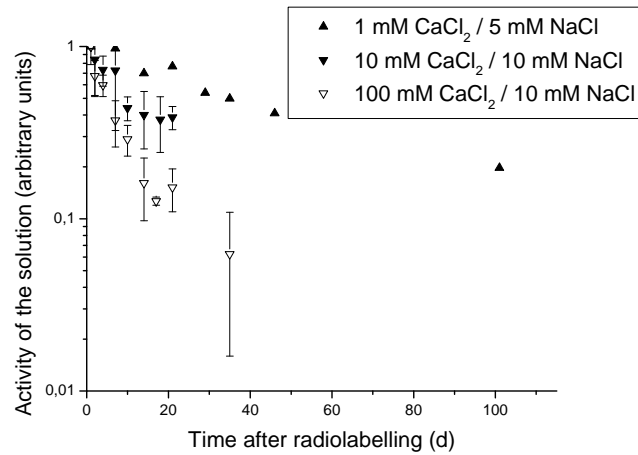
Figure1. The activity of radiocarbon in solution as a function of time after labelling of calcite and CaCl$_2$/NaCl mixtures with H^{14}CO$_3^-$.
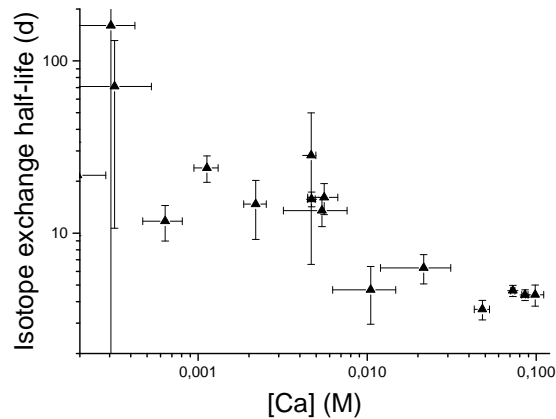
Figure 2. The half-life of the carbon isotope exchange between groundwater and calcite as a function of the equilibrium calcium concentration of the solution.

[1] Gonfiantini, R. and Zuppi, G. (2003) "Carbon isotope exchange rate of DIC in karst groundwater" Chemical Geology 197(1-4): 319-336

[2] Avramahov, N., Sivan, O., Yechieli, Y. and Lazar, B. (2013) "Carbon isotope exchange during calcite interaction with brine: implication for C-14 dating of hypersaline groundwater" Radiocarbon 55(1): 81-107

[3] Sheppard, S., Ticknor, K. and Evenden, W. (1998) "Sorption of inorganic ^{14}C on to calcite, montmorillonite and soil" Applied Geochemistry 13: 43-47

[4] Vuorinen, U. and Snellman, M. (1998) "Finnish reference waters for solubility, sorption and diffusion studies", Posiva Working Report 98-61

SORPTION OF PLUTONIUM(IV) ONTO SANDSTONE AND GRANITE IN CARBONATE SOLUTIONS

K. Hemmi, Y. Iida, T. Yamaguchi, T. Tanaka

Nuclear Safety Research Center, Japan Atomic Energy Agency, Tokai, Ibaraki, 319-1195, Japan

Migration of dissolved radionuclide from radioactive wastes to biosphere is expected to be retarded by sorption onto host rocks in safety assessments of geological disposal systems. Plutonium-242 is one of the important elements in safety assessments for geological disposal of high-level wastes and trans-uranium radioactive wastes in Japan [1, 2]. The oxidation state of Pu varies from +III to +VI, and Pu is likely to be stable as Pu(IV) under reducing conditions in deep subsurface environments [3]. Although not a few data associated with Pu sorption onto rocks and minerals have been reported [4], information on the experimental conditions is often not sufficient for sorption modeling. In addition, some distribution coefficients (K_d) of Pu are likely to be over-estimated due to Pu precipitation. In this study, sorption of Pu(IV) on sandstone, granite and quartz in carbonate solutions were experimentally investigated. Carbonate ions are ubiquitous in natural groundwaters and are likely to form Pu(IV) hydroxide–carbonate complexes in a reference groundwater [5].

The sorption of Pu(IV) onto sandstone and granite, representative rocks in Japan, and their major constituent mineral, quartz, were investigated by batch sorption experiments in an Ar atmosphere glovebox. XRD indicated that the sandstone contained plagioclase, calcite and clay minerals. Plutonium-238 stock solution was prepared as a 1×10^{-7} mol dm^{-3} (1.5×10^7 Bq dm^{-3}) solution in 1 mol dm^{-3} HNO$_3$. Experimental solutions were prepared by adding 0.01 cm^3 of the Pu(IV) stock solution into 25 cm^3 of NaHCO$_3$/ Na$_2$CO$_3$ / NaCl mixed solutions in polypropylene test tubes. The initial concentration of Pu, pH, total carbonate concentration and ionic strength of the mixed solutions were 4.0×10^{-11} mol dm^{-3} (6.0×10^3 Bq dm^{-3}), 8.0-11.2, 0.01-0.3 mol dm^{-3} and 0.5 mol kg^{-1}, respectively. Sorption experiments were conducted referring to the procedure by Yamaguchi *et al*. [6]. A 0.4 cm^3 portion of the solution was removed and filtered through a 0.45 μm filter to pretreat the filter and the filter container with the experimental solutions. After the first filtrate was discarded, a new 1.3 cm^3 portion of the solution was filtered using the same filter and containers. One cm^3 portion of the second filtrates was sampled for concentration determination. Concentrations of ^{238}Pu were determined by liquid scintillation counter. After 24 h and after 48 h, concentrations of ^{238}Pu were determined in the same sampling and filtering manners. After confirming that ^{238}Pu was stable in dissolved state in the starting solutions, the rock and mineral samples (0.5 g) were immersed in a 19.91 cm^3 volume of the starting solutions in polypropylene test tubes and agitated manually for 1 minute. Aliquots of the solutions were sampled and filtered to determine the concentration of ^{238}Pu 1 h after adding rock, after 24 h and after 48 h. After each sampling, the suspensions were agitated again.

Sorption equilibrium deemed to be attained within 24 h because the concentrations of ^{238}Pu 48 h after adding the rocks and the mineral were almost identical to those after 24 h. The K_d values decreased with increasing carbonate concentrations for all the rocks and the mineral. The obtained K_d (m^3 kg^{-1}) values at total carbonate concentration (C_{tot}) 0.11-0.3 mol dm^{-3} are shown in figure 1. The K_d values for sandstone decreased with increasing pH at pH < 9.7, and increased with increasing pH at pH > 9.7. The K_d values of granite and quartz were almost constant in the region of pH 8.0-9.7, and increased with increasing pH at pH > 9.7. It appears that granite and quartz have similar sorption capacities for Pu under the condition of high carbonate concentration. The results of sorption onto granite suggest that the quartz would be the main Pu sorber in the granite. The obtained sorption data will be used for sorption modeling of Pu(IV) onto rocks.
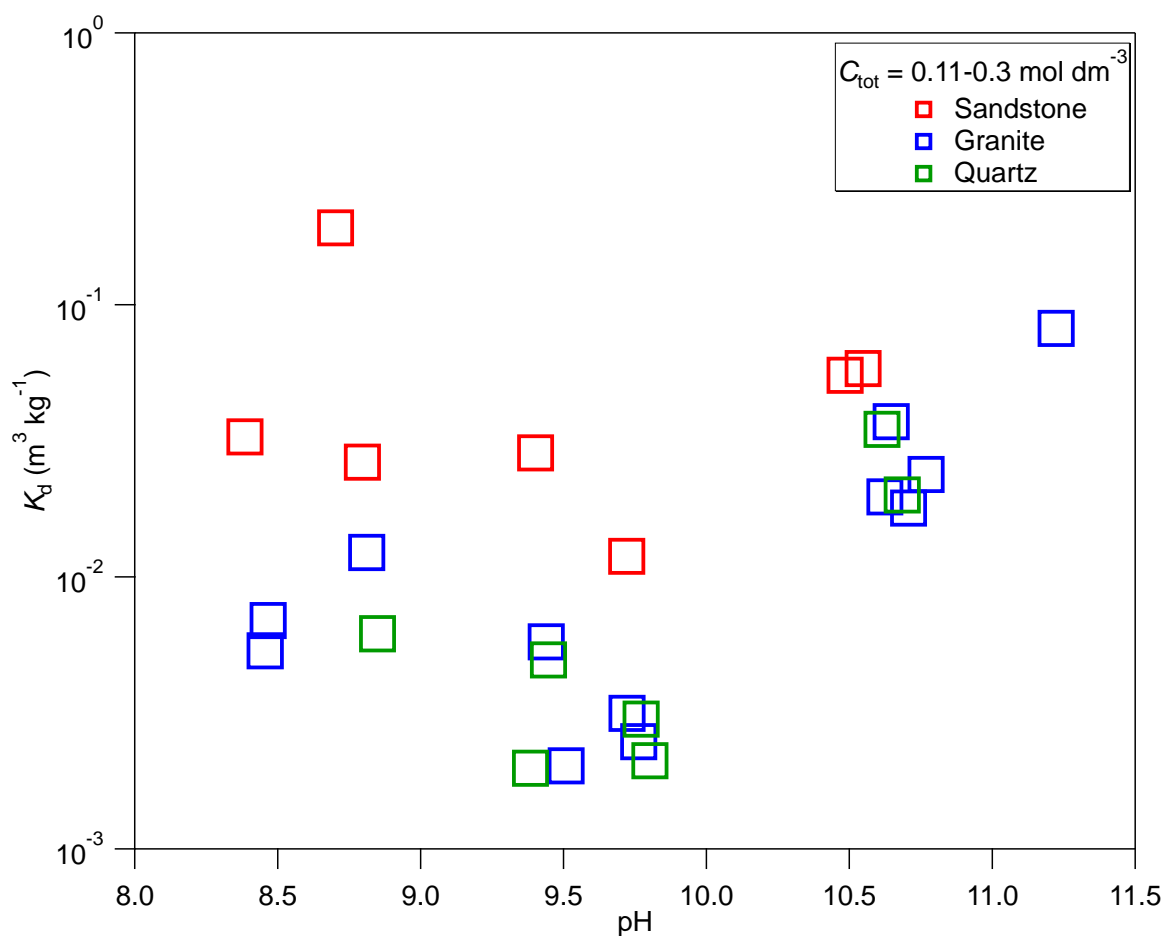
Figure1. Distribution coefficients (K_d) of Pu onto sandstone granite and quartz *vs*. pH. The red, blue and green-colored points represent sandstone, granite and quartz respectively. The squares represent the data obtained at total carbonate concentration (C_{tot}) 0.11-0.3 mol dm^{-3}.

[1] H12 Project to Establish the Scientific and Technical Basis for HLW Disposal in Japan – Supporting Report 3, Safety Assessment of the Geological Disposal System, Japan Nuclear Cycle Development Institute, JNC TN1400 99-023, 1999.
[2] Progress Report on Disposal Concept for TRU Waste in Japan – 2nd Report, Japan Nuclear Cycle Development Institute and The Federation of Electric Power Companies, JNC TY1400 2005-013/TRU TR-2005-02, 2005.
[3] W. Runde, The Chemical Interactions of Actinides in the Environment. Los Alamos Sci. 26, 392 (2000).
[4] T. Suyama et al., Development of Sorption Database (JAEA-SDB): Update of Sorption Data Including Soil and Cement Systems, Japan Atomic Energy Agency, JAEA-Data/Code 2011-022, 2011.
[5] T. Yamaguchi et al., Radiochim. Acta, 102(11): 999-1008 (2014).
[6] T. Yamaguchi et al., Radiochim. Acta, 92, 677-682 (2004).

MACROSCOPIC INTERACTION OF RADIONUCLIDES WITH MONTMORILLONITE AND BENTONITE COLLOIDS

P. Hölttä[1], V. Suorsa[1], O. Elo[1], J. Lehto[1]

[1]*University of Helsinki, Department of Chemistry, Laboratory of Radiochemistry, P. O. Box 55, FI-00014 University of Helsinki, Finland.*

In Finland, the repository for spent nuclear fuel (SNF) will be excavated at a depth of about 500 meters in the fractured crystalline bedrock in Olkiluoto at Eurajoki, the site proposed by Posiva Oy. The bentonite erosion resulting in the formation of colloids may have a direct impact on the overall performance of the bentonite buffer used in the Engineered Barrier System (EBS). Radionuclides diffused and retarded in the buffer could be released directly into the groundwater flow attached with generated colloids. The potential relevance of colloids for radionuclide transport is highly dependent on the formation and presence of stable and mobile colloids and their interaction with radionuclides. The objective of this work was to study the adsorption of radionuclides onto montmorillonite and bentonite colloid surfaces in different groundwater conditions by the means of the batch sorption experiments.

The materials were Nanocor PGN Montmorillonite (98 %), MX-80 Volclay type bentonite and colloid dispersion solution made from MX-80 bentonite powder. The stability of colloids was determined by analyzing particle size distribution and Zeta potential applying the photon correlation spectroscopy (PCS) method (Malvern Zetasizer Nano ZS). Colloid concentration was estimated using a standard series made from bentonite colloids and a count rate obtained PCS measurements or by analyzing the aluminum content of montmorillonite using ICP-MS. Solutions of different ionic strength and pH were low salinity granitic Allard ($I = 4.2 \cdot 10^{-3}$ M) and diluted OLSO, saline Olkiluoto ($I = 0.517$ M) reference groundwater and NaCl and $CaCl_2$ electrolytes ($I = 1$ M – $1 \cdot 10^{-7}$ M).

The interaction of the radionuclides (Sr-85, Cs-134 and Eu-152) with montmorillonite, bentonite and bentonite colloids was investigated as a function of ionic strength, pH (3 to 11) and radionuclide concentration ($10^{-9} – 10^{-6}$ M). The sorption parameters were determined by conducting batch experiments in a clove box under CO_2 free conditions. The solid liquid–ratio was studied to obtain an optimum mineral concentration needed to conduct batch experiments, in which the amount of mineral or colloid is not the limiting the radionuclide sorption. The kinetic experiments were conducted to optimize the equilibration time for the batch experiments. The Zeta potential of the system was determined as a function of pH with and without a studied radionuclide in order to provide information about the adsorption mechanisms, whether outer-sphere or inner-sphere complexation occurs on the mineral surface. In the sorption experiments, mineral or colloid suspension was added to the solution spiked with a tracer, 4.7 mL aliquot were taken after 2 h, 1, 2 and 7 days and solid colloid fraction was separated by ultracentrifugation (90000 rpm/60 min). Particle size distribution and concentration in the separated liquid phase are determined in order to check the number and size of remaining particles. The radioactivity of Sr-85, Cs-134 and Eu-152 was detected using an automatic gamma counter (Perkin Elmer, 1480 Wizard 3). Sorption was quantified by the determination of the distribution ratio of radionuclide activity between solid and liquid phase.

Radionuclide adsorption onto the bentonite colloids and montmorillonite was highly pH dependent, adsorption increasing with increasing pH. Strontium sorption onto bentonite colloids in 1 mM and 100 mM OLSO is shown as a function of pH in Figure 1. Zeta potential of montmorillonite or colloid dispersion determined as a function of pH was negative from the beginning and decreased with increasing pH due to deprotonation and that the mineral surfaces were negatively charged across the pH range. Zeta potential was less negative with europium suggesting europium adsorption mechanism appeared not to be purely electrostatic but also via inner-sphere complex due to the aluminol sites present on clay minerals. In the case of strontium and cesium, no change in the Zeta potential curve was found meaning the sorption is based on electrostatic ion-ion interactions.

Ionic strength and pH have a great influence on the chemical form of the radionuclides, especially actinides, thus the batch results are an important source of data for further studies using specific methods. The results from batch sorption experiments are given, and the importance of bentonite colloids to the migration of radionuclides in environmentally relevant conditions for SNF repository is discussed.
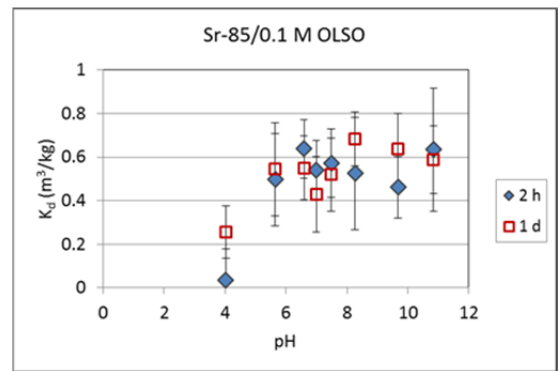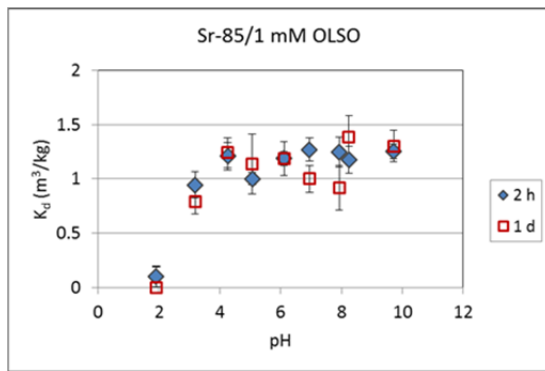
Figure 1. The distribution coefficient K_d-values of Sr-85 for bentonite colloids in 1 mM (left) and 100 mM (right) OLSO reference water as a function of pH.

THE SPECIFIC SORPTION OF Np(V) ON CORUNDUM IN THE PRESENCE AND ABSENCE OF TRIVALENT LANTHANIDES

S. Virtanen[1], A. Ikeda-Ohno[2], A. Rossberg[2] T. Rabung[3] J. Lehto[1] and N. Huittinen[2]

[1]) *Laboratory of Radiochemistry, Department of Chemistry, University of Helsinki, P.O. Box 55, 00014 University of Helsinki, Finland*
[2]) *Helmholtz-Zentrum Dresden-Rossendorf, Institute of Resource Ecology, Bautzner Landstrasse 400, 01328 Dresden, Germany*
[3]) *Institut für Nukleare Entsorgung, Karlsruhe Institute of Technology, P.O. Box 3640, 76021 Karlsruhe, Germany*

The uptake of metal ions present in spent nuclear fuel (SNF) by various solid phases is, in most studies, investigated in very simplified environments, considering one radionuclide and its sorption behavior at a time. In reality, however, there is a wide variety of other dissolved radioactive and stable elements in different concentrations present in the near- or far-field of the SNF repository that could compete for mineral surface binding sites and, thus, affect the extent of sorption of radionuclides released from the SNF over time. In competitive sorption studies by Bradbury and Baeyens [1], metal ion competition for sorption sites on montmorillonite was only observed when two elements with the same oxidation states were present simultaneously. Introducing metals with different oxidation states, however, showed no competitive behavior for the montmorillonite surface, suggesting that sorption competition is selective and that different surface sites are responsible for the uptake of metal ions with different chemistries. In a recent study by Soltermann et al. [2] on competitive uptake of Fe(II)-Zn(II) by montmorillonite, the authors showed that Fe(II) influenced the sorption of Zn(II) in the trace concentration range, while Zn(II) had no influence on Fe(II) despite their identical oxidation states. This process was explained by the oxidation of Fe(II) to Fe(III), that had a higher affinity towards the surface sorption sites on montmorillonite compared to Zn(II). Based on these studies, it is clear that the uptake behavior of radionuclides in the presence of multiple solutes is rather intricate and in general not a very well understood process.

In this study, the sorption of pentavalent neptunium (NpO_2^+) on corundum (α-Al_2O_3) was investigated in the absence and presence of trivalent europium or gadolinium as competing element under CO_2-free conditions. Corundum is used as a model mineral for the reactive surface aluminol groups Al-OH in more complex aluminosilicates, such as montmorillonite. Montmorillonite is the major constituent of bentonite, which is considered as buffer material for a number of spent nuclear fuel repository concepts. The objective of this study was to investigate how a trivalent metal ion with a greater complexation strength and a higher charge than that of the neptunyl ion would affect the sorption of Np(V) when allowed to adsorb on the mineral surface before the addition of Np(V). Batch sorption experiments were conducted as a function of pH in the absence and presence of 10^{-5} M Eu(III) for two Np(V) concentrations of 10^{-9} M and 10^{-6} M. To investigate the influence of the number of available surface groups for metal ion attachment, two different corundum concentrations of 0.5 g/l and 5 g/l were used, while keeping the background electrolyte ($NaClO_4$) concentration constant at 10 mM. To account for potential changes occurring in the coordination environment of the neptunium ion in the presence of a trivalent lanthanide, X-ray absorption spectroscopic (XAS) studies of samples containing only Np(V) or Np(V) with Gd(III) were conducted. The metal ion and solid concentrations in the samples were kept constant at 40 μM and 5 g/l, respectively.

In the batch sorption studies the uptake of Np(V) as a function of pH can be seen to shift to higher pH values when increasing the initial Np concentration from 10^{-9} M to 10^{-5} M, Figure 1. This shift is often attributed to either saturation of available sorption sites or the multiplicity of the sites [3]. A similar shift on the Np(V) pH-edge is expected if the competing metal ion introduced to the system is retained on the same surface sites on the mineral or if surface sites are blocked by electrostatic effects. However, in Figure 2 we see that 10^{-5} M Eu(III) introduced to the sample before 10^{-9} M Np(V) addition does not affect the sorption of Np(V) in neither of the two mineral concentrations. Thus, our results indicate that the sorption of these two metals takes place at different corundum surface sites. In addition, as the trivalent metal adsorbed on the corundum surface should exert a stronger repelling force on the neptunyl cations in solution, our results indicate that electrostatic effects as a reason for the observed shift of the pH-edge towards higher pH-values (Figure 1) is an insufficient explanation for the observed phenomenon.

The collected Np-XAS data is currently being analyzed, in order to gain an insight into the coordination environment and speciation of Np(V) sorbed on the corundum surface in the presence and absence of Gd(III).
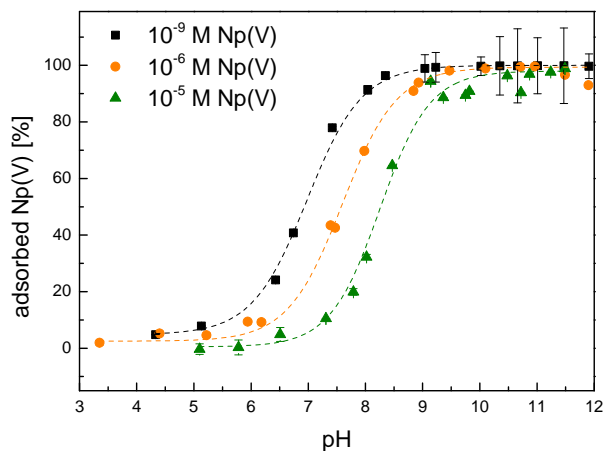
Figure 1 The sorption of 10^{-9} M, 10^{-6} M and 10^{-5} M Np(V) on corundum (5.0 g/l) as a function of pH.
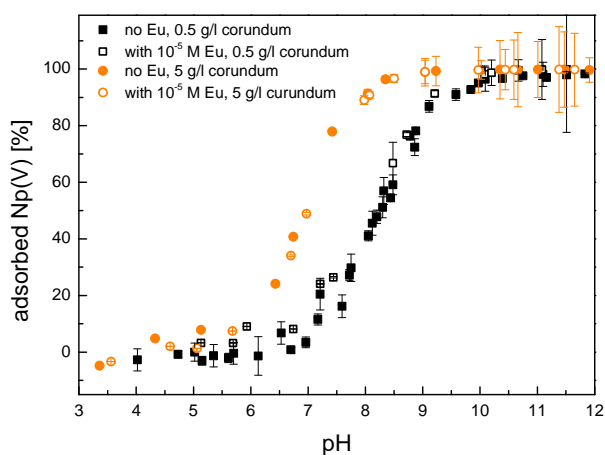
Figure 2 The sorption of 10^{-9} M Np(V) on corundum (0.5 g/l or 5.0 g/l) as a function of pH in the presence and absence of 10^{-5} M Eu(III) added prior to Np(V) sorption.

[1] Bradbury M. H. and Baeyens B. (2005) Experimental measurements and modelling of sorption competition on montmorillonite. Geochimica et Cosmochimica Acta, 69, 4187-4197

[2] Soltermann D., Marques M. F., Baeyens B., Brendlé J. M., and Dähn R. (2014) Competitive Fe(II)–Zn(II) uptake on a synthetic montmorillonite. Environmental Science & Technology 48(1), 190-198.

[3] Dzombak D. and Morel F. (1990) Surface Complexation Modeling: Hydrous Ferric Oxide, Wiley, USA

LUMINESCENCE STUDIES ON THE SORPTION AND SPECIATION OF EUROPIUM ONTO KAOLINITE IN THE PRESENCE OF HUMIC ACID

P. K.Verma*, M. Mohapatra, P. K. Mohapatra

*Radiochemistry Division, Bhabha Atomic Research Centre, Mumbai, INDIA,*parveen@barc.gov.in*

The migration of radionuclides in the ecosphere is of main concern for the safe disposal of nuclear waste in deep geological repositories. Under the conditions prevailing there, variety of factors influence the migration of radionuclides in the aquatic environment such as pH of media, presence of complexing anions, temperature, nature of surrounding clay minerals etc., to name a few. Humic substances are invariably present in most of the natural aquatic system as they are mainly originating from the degradation and decomposition of plant and animals, either directly or from their by products. The humic substances mainly comprising humic acid (HA) are heterogeneous and can easily bind the radionuclides and can alter their migration behaviour. The radionuclides in the presence of clay minerals present in their near vicinity can form a surface complex (inner or outer sphere) which is one of the important factors in deciding the fate of the radionuclides. The interactions with HA and clay minerals can influence the migration of the radionuclides. The sorption of Eu(III) onto the clay minerals were investigated by several researchers under variety of conditions. The formation of inner-sphere/outer-sphere surface complexes, where the ions directly coordinate/ electrostatically adsorb to surface sites was investigated by TRLFS studies [1-3].

In the present study we have investigated the sorption o ^{152}Eu(III) ($\sim 10^{-5}$ M) onto kaolinite with and without HA(10mg/L). The interaction between Eu(III), kaolinite and HA was also studied by luminescence spectroscopy to get an insight into the nature of complex (inner or outer sphere) of Eu(III) with kaolinite in the presence/absence of HA. The sorption experiments were performed with varying pH (pH 3 - 8). The luminescence studies for speciation were carried out at pH $\sim$ 5.30 (close to environmental pH) using 10^{-4} M Eu(III) for better signal to noise ratio.

The sorption of Eu(III) was quantitative even at low pH, and was found to be increasing with increasing pH (**Fig.1**). It was of interest to see the effect of the addition sequence of Eu(III), HA and kaolinite to the sorption profile of Eu(III) onto kaolinite. For this two sets of experiment were done viz HA was added after Eu(III) and kaolinite were equilibrated (set 1) and Eu(III) was added after HA and kaolinite was equilibrated (set 2). In both the cases the equilibration was done for 16 h followed by centrifugation. Assaying of ^{152}Eu was done radio metrically using gamma ray counting.

Fig.1 shows the Eu(III) sorption profile onto kaolinite with varying order of addition of HA and Eu(III). For Set 1, the Eu(III) sorption profile looks like an desorption phenomenon in which the Eu(III) sorbed onto kaolinite was desorbed in the presence of complexing HA to the aqueous phase, whereas in Set 2, the sorption of Eu(III) onto HA equilibrated kaolinite shows sharp decrease after   pH 4. This can be explained as the pH of the medium is increasing the sorption of HA onto the kaolinite was decreased but at the same time the HA become more deprotonated and can complex with the Eu(III), this will make the majority of Eu(III) complex with HA into the aqueous phase.

To get an insight into the nature of the complex (inner/outer sphere or ternary) formed in the sorption process, luminescence studies were done using sanples containing different Eu(III)(mg/L):HA(mg/L) ratio, viz Eu(III):HA::1.5:1 and Eu(III):HA::0.15:1. At Eu(III):HA::1.5:1 and fixed kaolinite concentration (1g/L), the luminescence was recorded with varying order of addition of Eu(III), kaolinite and HA. **Table 1** shows the lifetime and peak ratio data of various samples. The lifetime data suggests species of similar nature in all the samples probably coordinated with 9-10 nearest -OH groups, whereas the peak ratio varies slightly in various samples. As compared to Eu(III)$_{aq}$ the peak ratio for Eu(III) sorbed onto kaolinite was a little higher, this could be due to the distortion in Eu(III)$_{aq}$ structure due to interaction with the surface of kaolinite, however the nature of the interaction is not very strong and is of outer-sphere in nature **[4].** The addition of the HA to Eu(III) increase the overall intensity in emission spectra of Eu(III) but the lifetime remains approximately same. This is in line with earlier studies **[5, 6]** but the changes in the peak ratio (617/591) suggests the distortion in the Eu(III) structure upon HA complexation. In the presence of both kaolinite and HA the intensity in emission spectra enhanced as in the case of pure HA complexation with Eu(III). To confirm this, the suspension was centrifuged at 12000 rpm for 20 min and the supernatant was used for luminescence measurements. The emission spectra of the supernatant were similar to the suspension but with slightly lower intensity of emission lines. The lifetime of the

supernatant and suspension were approximately same suggesting similar emitting species present in both the suspension and the supernatant.

Table 1: Lifetime and intensity ratio of various samples			**Fig.1:** Effect of order of addition onto sorption of Eu(III) onto kaolinite with varying pH

Sample	Life Time	Intensity Ratio (617/591)
Eu(III): 10^{-4} M, KA: 1 g/L, **HA : 10 mg/L**		
Eu$_{aq}$	114-115 µs	0.56 or 0.65
Eu + HA	108 µs	0.76
[a]Eu + KA	104 -113 µs	0.68 or 0.69
[b]Eu + KA	114 µs	0.54
[a] (Eu + KA) + HA	107 µs	0.92
[b] (Eu + KA) + HA	112 µs	0.67
[a] (Eu + HA) + KA	103 µs	0.83
[b] (Eu + HA) + KA	110 µs	0.65
[a] (KA + HA) + Eu	104 µs	0.74
[b] (KA + HA) + Eu	110 µs	0.62
Eu(III): 10^{-4} M, KA: 1 g/L, **HA : 100 mg/L**		
Eu + HA	115 µs	1.24
[a] (Eu + HA) + KA	87 µs	1.66
[a] (Eu + KA) + HA	75 µs	1.41

[a]suspension; [b] supernatant
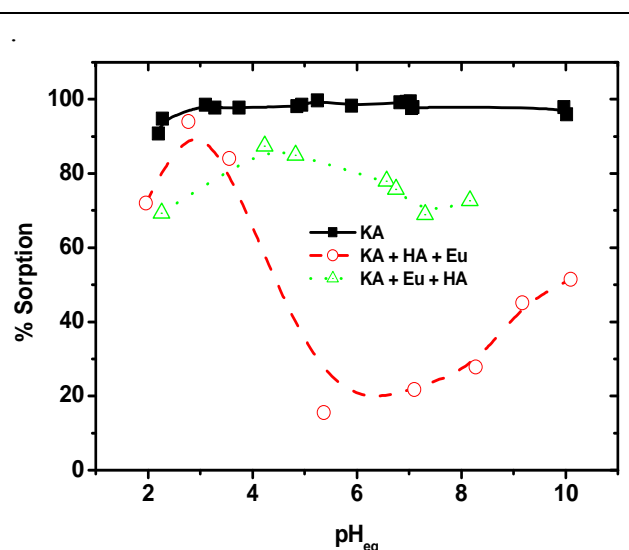
Note: KA+HA/Eu+Eu/HA means KA and HA/Eu were shaken for 16 h then Eu(III)/HA was added and again shaken for 16 h before calculation of % sorption.

The luminescence spectra was also recorded at lower Eu:HA under similar condition. With increasing concentration of HA, the peak ratio increases showing more distortion of complex structure but the lifetime value suggests similar nature of emitting Eu(III) species as in Eu$_{aq}$. The luminescence spectra of suspension at higher HA concentration was also showing similar lifetime but higher intensity of emission lines compared to Eu:HA of 1.5. This suggests that although the HA comlexation with Eu(III) is strong enough to keep it in aqueous phase, the primary coordination sphere of Eu(III) appeared unchanged as reflected in similar value of lifetime in all samples, on the other hand the enhancement in peak ratio suggests perturbation of local symmetry on HA complexation as suggested by higher intensities of Eu(III) emission lines.

[1] Tertre, E. Berger, G. Simoni, E. Castet, S. Giffaut, E. Loubet, M. Catalette, H. (2006) "Europium retention onto clay minerals from 25 to 150 C: Experimental measurements, spectroscopic features and sorption modelling" Geochimica et Cosmochimica Acta 70 :4563–4578.
[2] Ishida, K. Saito, T. Aoyagi, N. Kimura, T. Nagaishi, R. Nagasaki, S.Tanaka, S. (2012) "Surface speciation of Eu3+ adsorbed on kaolinite by time-resolved laser fluorescence spectroscopy (TRLFS) and parallel factor analysis (PARAFAC)" Journal of Colloid and Interface Science 374: 258–266.
[3] Stumpf, Th., Bauer, A., Coppin, F., Fanghänel, Th., Kim, J.I. (2002) "Inner-sphere, outer-sphere and ternary surface complexes: A TRLFS study of the sorption process of Eu(III) onto smectite and kaolinite" Radiochimica Acta 90(6): 345-349.
[4] Rabung, Th. Pierret, M. C. Bauer, Geckeis, A. H. Bradbury, M. H. Baeyens, B. (2005) "Sorption of Eu(III)/Cm(III) on Ca-montmorillonite and Na-illite. Part 1: Batch sorption and time-resolved laser fluorescence spectroscopy experiments" Geochimica et Cosmochimica Acta, 69(23):5393–5402.
[5] Plancque, G. Moulin, V. Toulhoat, P. Moulin, C. (2003) "Europium speciation by time-resolved laser-induced fluorescence" Analytica Chimica Acta 478:11–22.
[6] Lukman S., Saito, T. Aoyagi, N. Kimura, T. Nagasaki, S. (2012) "Speciation of Eu3+ bound to humic substances by time-resolved laser fluorescence spectroscopy (TRLFS) and parallel factor analysis (PARAFAC)" Geochimica et Cosmochimica Acta 88:199–215.

THE EFFECT OF SURFACE SITE ACIDITY ON ACTINIDE SORPTION TO ALUMINUM (HYDR)OXIDE MINERAL PHASES

Teresa Baumer, Patricia Kay, Alexander Ko, Amy E. Hixon

Department of Civil & Environmental Engineering & Earth Sciences,
University of Notre Dame, Notre Dame, IN, USA

Actinide contamination is a worldwide problem due to nuclear weapons production and testing and several aspects of the nuclear fuel cycle. The presence of these elements in the geosphere poses a long-term environmental concern due to their toxicity and the long half-lives of several isotopes. Therefore, understanding the mechanisms responsible for enhancing or retarding the mobility of actinides in the environment is important for risk management.

Actinide mobility is partially controlled by surface interactions, such as sorption and desorption. Previous studies investigating actinide behavior at the mineral-water interface relied on empirical approaches, such as K_d measurements, to describe metal-mineral interactions. These approaches are insufficient because they lack specificity and are only valid for the particular conditions of the experiments. Most notably, a K_d approach is unable to predict metal sorption under the changing conditions of solution concentration, ionic strength, or pH. Conversely, mechanistic approaches can differentiate between interaction mechanisms and predict metal sorption as a function of solution chemistry. Thus, mechanistic approaches provide a structured and consistent method of examining experimental data. When they are coupled with spectroscopic data describing the bonding environment of metals associated with a solid phase, the resulting surface-complexation model is based on both micro- and macro-scale observations.

The surface acidities of corundum (α-Al_2O_3), γ-alumina (γ-Al_2O_3), and gibbsite (γ-$Al(OH)_3$) were previously determined though evaluation of their acid-base properties and hydration-dehydration mechanisms[1]. The surface acidities of these minerals were established to follow the trend corundum > gibbsite > γ-alumina, which is presumably related to the amount of aluminum exposed to the surface. Actinides behave as Lewis acids and should therefore bind preferentially to γ-alumina, but the relationship between surface acidity and sorption affinity has not been explicitly established. Therefore, the objective of this work was to examine the relationship between sorption affinity and surface acidity within the framework of a mechanistically-accurate surface complexation model.

Batch sorption experiments were conducted to determine sorption of Eu(III), Th(IV), Np(V) and U(VI) to corundum, gibbsite, and γ-alumina. These metal ions were chosen for investigation as stable oxidation state analogs of plutonium, which may exist in several oxidation states simultaneously. Sorption was monitored as a function of time (days to months), pH (3-8), ionic strength (0.01 - 1 M NaCl), and mineral and metal concentrations (0.8-10 m^2/L and $10^{-5} – 10^{-8}$ M, respectively). Inductively coupled plasma optical emission spectrometry (ICP-OES) and/or inductively coupled plasma mass spectrometry (ICP-MS) were used to quantify sorption. High-resolution transmission electron microscopy (HRTEM) imaging was used to monitor for surface precipitation, colloid formation, and morphological changes in the solid phases.

Experimental results do not indicate a dependence of surface acidity on sorption and instead suggest that all three aluminum mineral phases analyzed will account for the same amount of actinide removal from solution. Similar sorption tendencies were observed for each actinide regardless of the mineral phase present. This suggests that surface site acidity is not a major factor controlling sorption in these systems. The reason(s) for this are unclear, but are a topic of current and future research.

Batch sorption experiments will be supported by time-resolved laser induced fluorescence spectroscopy (TRLFS) and speciation modeling to develop a mechanistically accurate surface complexation model for these systems.

This research supports the eventual investigation of plutonium sorption to aluminum (hydr)oxide minerals where, based on previous research, surface-mediated reduction and strong inner-sphere surface complexation is expected.[2,3]

[1] X. Yang, et al., J. Colloid Interface Sci. 308, 395-404 (2007)
[2] B. A. Powell, et al., Environ. Sci. Technol. 39, 2107-2114 (2005)
[3] A. E. Hixon, et al., J. Colloid Interface Sci. 403, 105-112 (2013)

SORPTION PROPERTIES OF GRANITOID AND MAFIC ROCKS FROM THE "ENISEYSKY" AREA OF NIZHNEKANSKY MASSIF TOWARDS Cs(I), Ra(II), Am(III), Pu(III,IV), Np(IV) AND Se(II)

V.G. Petrov[1], N.V. Kuzmenkova[1,2], I.E. Vlasova[1], A.A. Kashtanov[1], V.A. Petrov[3], V.V. Poluektov[3], J. Hammer[4], S.N. Kalmykov[1]

[1]*Lomonosov Moscow State University, Chemistry Department, 119991, Leninskie gory 1/3, Moscow, Russia*
[2]*Vernadsky Institute of Geochemistry and Analytical Chemistry of RAS (GEOHI RAS), Department of Chemistry, 119991, Kosygina 19, Moscow, Russia*
[3]*Institute of Geology of Ore Deposits, Petrography, Mineralogy and Geochemistry of RAS (IGEM RAS), 119017, Staromonetnyy per. 35, Moscow, Russia*
[4]*BGR, Geozentrum Hannover, 30655 Stilleweg 2, Hannover, Germany*

A granitoid gneiss formation near the Krasnoyarsk city is proposed as a potential place for the deep final disposal of high-level radioactive waste in Russia. The first steps in evaluation of possibilities to build the repository are the examination of properties of the host rocks in lab scale and further construction of underground laboratory. Earlier, the sorption properties of rock samples of Nizhnekansky granitoid massif were investigated towards Cs, Eu, U, Pu and Am [1-4]. Values of the distribution coefficient were about $10^2 - 10^3$ ml/g for Eu, U, Pu and Am and about $0 - 2$ ml/g for Np. But these experiments were carried out under aerobic oxidative conditions. The Eh values for groundwaters in the level of planned repository are around -200 mV and pH values are about 7-8, that means reducing properties. Under these conditions redox sensitive radionuclides like Np, Pu and U have predominantly low valence state and should be characterized by higher sorption.

The aim of present work is to study the sorption properties of rock samples from "Eniseysky" area in the exocontact of Nizhnekansky granitoid massif under anaerobic conditions. The simulated natural water was preequilibrated with bentonite, ultrafiltrated to exclude the influence of bentonite colloids. Final Eh value was ca. -200 mV, pH = 7.6. The initial concentrations of radionuclides (^{135,137}Cs, ^{226}Ra, ^{79}Se, ^{237,239}Np, ^{239,240}Pu, ^{241,243}Am) were 10^{-9} M. Solid to liquid ratio was 1:4. The aliquots of investigated suspensions were periodically centrifuged (30,000 g) to remove solid particles, and then aliquots of liquid phase were analyzed by liquid-scintillation counting. Six rock samples, taken from various depths, were analyzed.

The radionuclide sorption reaches the steady state in 1-4 hours of experiment in the case of Cs, Ra, Np, Pu and Am. Distribution coefficients were 20-100 ml/g for Cs and Ra and 50-300 ml/g for Np, Pu and Am depending on rock samples. The sorption of Se, which is stable in the form of selenide-ion under reducing conditions, was insignificant within the whole period of the experiment (2 weeks).

Uneven distribution of the radionuclides on the investigated granitoid samples surface was revealed by method of digital radiography. The radionuclide distribution is related to content and distribution of different mineral phases within the rocks. Thus, sorption of radionuclides onto quartz and unaltered feldspars (plagioclase, potassium feldspar) was negligible, while other minerals (smectite, sericite, biotite etc.) demonstrated medium and high sorption ability.

It was shown that rock samples from the "Eniseysky" area in the exocontact of Nizhnekansky granitoid massif demonstrate fast and quantitative sorption behavior towards cesium, radium, neptunium, plutonium and americium.

[1] Anderson E.B., et al. MRS'2000, Sydney, Australia, (2000).
[2] Anderson E.B., et al. Sim. on HLW, LLW, Mixed Wastes and Environmental Restoration (WM'02), Tucson, USA, (2002).
[3] Petrov V.G., et al. KIT scientific reports, 7629, 37 (2012).
[4] Petrov V., et al. ICRER'14, Barcelona, Spain, (2014).

BISMUTH-BASED INORGANIC SORBENTS FOR THE REMOVAL OF IODINE FROM SUBSURFACE PLUMES

M.E. Leonard [1], T.G. Levitskaia [1], J. Romero [1], S. Chatterjee [1], J.M. Peterson [1], T. Varga [2], V. Shutthanandan [2], B. Schwenzer [2], T. Kaspar [2]

[1] *Radiochemical Processing Laboratory, Pacific Northwest National Laboratory, Richland, WA, 99352*
[2] *Environmental Molecular Sciences Laboratory, Pacific Northwest National Laboratory, Richland, WA, 99352*

Iodine-129 (^{129}I) is one of the most persistent radioactive isotopes present in subsurface plumes at the U.S. Department of Energy Hanford site. It is of particular concern due to its long half-life ($t_{1/2} = 1.6 \times 10^7$ y), its ability to move rapidly in the environment, and its distribution over a large area. Removal of ^{129}I from the subsurface will substantially reduce environmental and health risks. Remediation efforts face serious technical challenges, however. In Hanford groundwater and vadose zone, ^{129}I exists in various chemical forms including iodate IO_3^-, iodide I^-, and organoiodine. Removal of ^{129}I by simple ion exchange is often impeded by its occurrence in multiple chemical forms, regional variations in pH and the presence of competing ions in high concentrations. These obstacles make iodine removal exceedingly difficult.

Recent work at PNNL has focused on bismuth-based inorganic materials having high affinity for iodine in its various forms, with the aim of directly removing it from groundwater without requiring preconditioning steps such as reduction of IO_3^- to I^- [1]. A library of sorbents based on bismuth (III) has been synthesized and screened for iodine removal from deionized water and Hanford groundwater. Raman spectroscopy is used to monitor and quantify IO_3^- uptake, while inductively coupled plasma mass spectrometry (ICP/MS) is used to measure total iodine uptake in batch tests using Hanford groundwater. Several materials prepared at PNNL have demonstrated virtually quantitative uptake of iodine.

A typical synthesis involves suspending a bismuth inorganic salt in ethylene glycol or water, then subjecting the mixture to solvothermal treatment. In addition to yielding sorbents with consistent iodine uptake behavior, the solvothermal method can be used to control the size and morphology of reaction products at the nanometer or micrometer scale [2, 3]. The ability to tune materials to desired morphology is interesting, because it may enhance a sorbent's performance for a specific configuration (i.e. column) currently used for pump and treat anion removal.

The molecular, structural, and electronic properties of these materials have been determined prior to and after iodine uptake in deionized water. Characterization has been performed by Raman and FTIR spectroscopy, x-ray diffraction analysis, scanning electron microscopy, x-ray photoelectron scattering spectroscopy, ICP-optical emission spectrometry, UV-visible reflectance spectroscopy, and helium ion microscopy. The batch contact testing using actual Hanford groundwater has been conducted to evaluate efficiency of total iodine removal in presence of interfering ions.

[1] T. Levitskaia, D. Chatterjee, J. Peterson, E. Campbell, *Inorganic Sorbents for Iodine Removal from Subsurface Plumes: FY 2013 Status Report (PNNL-22865)*, Pacific Northwest National Laboratory (2013).
[2] X. Zhang, Y. Zheng, D. McCulloch, L. Yeo, J. Friend, D. MacFarlane, J. Mater. Chem. A 38, 16491 (2012).
[3] F. Qin, G. Li, R. Wang, J. Wu, H. Sun, R. Chen, Chem.—Eur. J. 2, 2275 (2014).

THE EFFECT OF NATURAL ORGANIC MATTER ON PLUTONIUM SORPTION TO GOETHITE

Nathan Conroy[1], Mavrik Zavarin[2], Annie B. Kersting[2], and Brian A. Powell[1]

1. *Environmental Engineering and Earth Sciences, Clemson University*
2. *Physical and Life Sciences Directorate, Glenn T. Seaborg Institute, Lawrence Livermore National Laboratory*

The effect of several natural organic matter (NOM) components (citric acid (CA), Deferoxamine B (DFOB), Suwannee River fulvic acid (FA), and Leonardite humic acid (HA)) on plutonium sorption to goethite was studied using batch sorption experiments at 5 $mg_C \cdot L^{-1}$ and 50 $mg_C \cdot L^{-1}$ NOM, 10^{-10} M plutonium, and 0.1 $g \cdot L^{-1}$ goethite. Aqueous concentrations of both plutonium and NOM in the bulk solution were monitored by liquid scintillation counting (LSC) in order to understand the extent of NOM and plutonium sorption to goethite and possible ternary complex formation. This was made possible through the utilization of radiolabeled NOM where possible. Commercially available ^{14}C-citric acid was purchased, while FA and HA were labeled with tritium as a part of this study using tritiated $NaBH_4$ to reduce NOM ketones to secondary alcohols while minimally affecting structure or reactivity. DFOB could not be labeled by the same mechanism, as it lacks ketones, and no radiolabeled DFOB is commercially available. Therefore DFOB sorption was determined by total organic carbon analysis in a separate plutonium free experiment.

These data indicate that NOM type, NOM concentration, and system pH significantly impact plutonium sorption affinity, as well as the underlying sorption mechanisms. All the NOM components studied reduced plutonium sorption from near pH 4 to the point of zero charge of goethite (~ pH 8). CA, FA, and HA decreased aqueous plutonium concentrations below pH 4 presumably through ternary complex formation with the goethite surface or, in the case of HA, by incorporation into coagulating NOM complexes. In systems above pH 8, Pu sorption relative to an NOM free system was decreased. However, competition between NOM complexes and hydrolysis products leads to less significant reduction in sorption.

Mechanisms for ternary complex formation were characterized by Fourier transform infrared (FTIR) spectroscopy in the absence of plutonium. For this study, high concentrations of NOM (2.5 $g_C \cdot L^{-1}$) were mixed for several days with goethite and the pH regularly adjusted to ~ 4.5. The solid fraction of these suspensions were lyophilized and the powder was analyzed by attenuated total reflectance FTIR spectroscopy. CA and FA demonstrated clear surface interactions with goethite whereas no DFOB interactions were observed. The observation of no/limited DFOB interactions with goethite is consistent with batch sorption data at all the pH values studied. Spectra indicate significant homoaggregation of HA and little goethite surface interaction near pH 4.5. These data augment that of the batch sorption experiments in determining the mechanisms of plutonium removal from the bulk aqueous solutions either by 1) binary sorption to the goethite surface 2) NOM assisted sorption to the goethite surface 3) incorporation into an NOM aggregate. Plutonium sorption to goethite can be either enhanced by formation of ternary surface complexes at low pH or reduced via formation of soluble plutonium-NOM complexes at intermediate pH. The former has implications for colloid facilitated transport of plutonium where certain NOM components (i.e. CA and FA) may stabilize iron mineral colloids and also provide strong association of plutonium with the colloids.

Extended x-ray absorption fine structure (EXAFS) spectroscopy was used to study the coordinating environment of plutonium sorbed to goethite under conditions suggested by batch sorption and FTIR spectroscopic data to result in ternary complex formation. EXAFS data support the formation of a ternary, goethite-plutonium-citrate, complex near pH 4.

NOVEL INORGANIC SORBENTS FOR IODINE REMOVAL FROM GROUNDWATER

T.G. Levitskaia, S. Chatterjee, J.M. Peterson, N. Pence, M. Leonard, J. Romero, T. Varga,
B.W. Arey, L. Kovarik, Y. Hong, V. Shutthanandan, B. Schwenzer

Pacific Northwest National Laboratory

The radioactive contaminant iodine-129 (^{129}I) is one of the top risk drivers at radiological waste disposal and contaminated groundwater sites where nuclear material fabrication or reprocessing has occurred. The risk stems largely from ^{129}I having a high radiotoxicity, a high bioaccumulation factor, a high inventory at source terms (due to its high fission yield), an extremely long half-life (16 million years), and rapid mobility in the subsurface environment. However, currently there are very few approaches that effectively manage the risk that ^{129}I presents to human health and the environment.

In the subsurface aquatic environment, ^{129}I mainly exists as iodate (IO_3^-), iodide (I^-), elemental iodine (I_2), and organic derivatives of iodine. It has been previously established that Hanford groundwater contains predominantly IO_3^-. Its separation from groundwater via commercial ion exchange resins is ineffective. The objective of this study is to design engineered inorganic composite sorbents that will effectively separate all species of iodine present in Hanford groundwater; specifically targeting the development of composite materials with high affinity for IO_3^- to enable direct removal of this contaminant from the groundwater in the pump and treat system without introducing the preconditioning steps such as reduction of IO_3^- to I^-.

The structures of the inorganic composite materials investigated in this study are similar to layered double hydroxide (LDH), a class of materials that can be thought of as anionic clays consisting of ordered, positively charged sheets intercalated with interchangeable hydrated anions. LDH sorbents have been previously demonstrated as promising materials for the removal of harmful oxyanions such as arsenate, chromate, perchlorate, pertechnetate, iodate, and others from contaminated and waste waters [1 and references therein]. These materials typically consist of two-dimensional nano-structured divalent cations, octahedrally coordinated by hydroxide ions, where some of the divalent cations are isomorphously replaced by tri- or tetravalent cations. Such a replacement results in the charged sheets, where the net positive charge is compensated by anions in the interlayer region.

A large library of the composite materials was obtained and tested for the IO_3^- affinity. It was demonstrated that the materials containing Cr(III), Ag(I), or Bi(III) exhibited nearly quantitative uptake of IO_3^-. The most promising candidate materials were characterized by several techniques including x-ray powder diffraction, x-ray photoelectron spectroscopy, scanning electron microscopy/ energy-dispersive spectroscopy, and optical spectroscopy of various types. The structural changes observed upon IO_3^- uptake of at high loading helped in elucidation of the sorption mechanism.

The IO_3^- and I^- sorption performance of the selected composite materials was further evaluated using Hanford groundwater from well 299-W19-36 in the systematic batch contact testing. In these tests, the IO_3^- or I^- concentration in the groundwater was adjusted to 15 to 130,000 μg/L. The inductively coupled plasma-mass spectrometry method was used to quantify iodine uptake. The Ag(I)-based composite was very effective for I-uptake, with the $K_d(I^-)$ values approaching 900,000 mL/g. This composite also displayed superior performance removing iodine from the unmodified Hanford groundwater, with the $K_d(iodine)$ values of ~1,800 mL/g. The Bi(III)-based composites exhibited superior IO_3^- sorption in the entire concentration range tested, with the $K_d(IO_3^-)$ values of ~4,000 mL/g at the low loading regime. This confirms effective IO_3^- uptake in presence of excess chloride and nitrate, which occur in the groundwater at 181,000 and 317,000 μg/L, respectively. The $K_d(IO_3^-)$ values observed for the Cr(III) composites were in the 1,000 to 2,000 mL/g range at low sorbent loading. A separate study demonstrated that the unmodified groundwater containing 8.6 μg/L total iodine can be successfully treated by the most promising candidate materials.

[1] K-H. Goh, T. T. Lim, Z. Dong. Water Res. 42, 1343 (2008).

POTENTIAL DIFFERENCES IN URANIUM(VI) SORPTION TO SODIUM-MONTMORILLONITE, AND UNTREATED AND HEAT-TREATED BENTONITE

R. M. Tinnacher[1], J. A. Davis[1], M. C. Cheshire[2,3], F. A. Caporuscio[2]

[1]*Earth Sciences Division, Lawrence Berkeley National Laboratory, Berkeley, CA 94720, USA*
[2]*Earth and Environmental Science Division, Los Alamos National Laboratory,*
Los Alamos, NM 87545, USA
[3]*Chemical Sciences Division, Oak Ridge National Laboratory, Oak Ridge, TN 37831, USA*

Clay media have been proposed as engineered barrier materials or host rocks for high-level radioactive waste repositories in several countries. The selection of compacted bentonite as a backfill material in engineered barrier systems is largely driven by its low permeability and strong sorptive properties. The limited permeability of bentonite is at least partially the result of its low porosity and the swelling of sodium-montmorillonite (its major component) in water. Due to these characteristics, the transport of contaminants through bentonite layers is expected to be limited and dominated by diffusion. However, there are large differences in diffusion behavior between various radionuclides, e.g. between halides (^{36}Cl, ^{129}I) and actinides ($^{238,235}U$, ^{237}Np, ^{232}Th) as a result of the two major processes controlling macroscopic diffusive transport, i.e. molecular diffusion and sorption. Hence, laboratory sorption studies are an essential component for the design of waste containment barriers, and the calibration of diffusion-based transport models.

Furthermore, given the close proximity to the source term, environmental risk assessments need to take into account potential mineral alterations in the bentonite barrier, such as smectite illitization, due to the heat generation of nuclear waste. This is particularly relevant for disposal scenarios involving high-capactity metal canisters with the aim to reduce the repository footprint. Mineral transformations over time and space may have further impacts on the system's solution composition and the sorption affinities of radioactive contaminants for these solid phases. In particular, the fate of uranium, which, as the basis of nuclear fuel will be present at high abundances, must be understood under these varying conditions.

In this study, we investigate uranium(VI) sorption characteristics onto three, different types of solids: 'pure' Na-montmorillonite, and untreated and heat-treated bentonite. Sodium-montmorillonite was obtained from the Clay Minerals Society (SWy-2), and pretreated to remove known impurities of quartz (8%), feldspars (16%) and calcite. Untreated bentonite, primarily containing montmorillonite with minor amounts of clinoptilolite, silicates, and remnant glass, was mined from a reducing horizon in Colony, Wyoming. Heat-treated bentonite was a pulverized bentonite sample, which had been exposed to 300 °C and 150 – 160 bar in contact with a K-Ca-Na-Cl-bearing synthetic groundwater solution (pH 6.74) over six-weeks. Extracted reaction liquids were analyzed for major cations and trace metals by inductively coupled plasma-optical emission spectroscopy (Perkin Elmer Optima 2100 DV) and inductively coupled plasma-mass spectroscopy (Elan 6100). Before and after the hydrothermal experiment, the mineral compositions of bentonite samples were characterized by X-ray diffraction, X-ray fluorescence and electron microprobe analyses, as well as scanning electron microscopy coupled with energy dispersive X-ray spectroscopy. Based on analytical results, montmorillonite possibly underwent a partial dissolution developing fibrous illite. Furthermore, a phase change of clinoptilolite yielded a Si-rich analcime in addition to authigenic silica phases.

Batch sorption experiments will be used to characterize U(VI) sorption behavior to these various solid phases at fixed ionic strength and over a wide range of pH conditions (0.5 g L^{-1} solid, I = 0.1 M NaCl, pH of 4 – 9). Changes in the solution composition due to solution-mineral interactions during sorption experiments will be monitored by analyzing for a suite of elements (e.g., Si, Al, Mg, K, Ca).

We will present experimental results regarding the potential differences in uranium(VI) sorption behavior between the solids described above. Experimental results will allow us to discuss the influence of mineral impurities in bentonite based on a comparison of sorption data between pretreated sodium-montmorillonite and untreated bentonite. Furthermore, the potential impacts of mineral transformations in bentonite due to the exposure to heat will be evaluated using results from untreated and heat-treated bentonite samples.

SORPTION OF U(VI) ONTO MUSCOVITE

Zhuoxin Yin, Duoqiang Pan, Ping Li, Wangsuo Wu*

Radiochemistry Laboratory, School of Nuclear Science and Technology, Lanzhou University, Lanzhou 730000, Ganshu, P.R. China

On account of the increasing development of nuclear industries,many factories and laboratories investigate and apply the nuclear technology for the extraction, separation and beneficiation of radioelement. A large amount of radioactive waste is produced in the working process.

Uranium is the main reactant of the nuclear reactors, and it is one of the primary components of spent fuel.For the sake of the demands of nuclear power plant fuel,more mining of uranium mine is necessary. In nature,uranium exists as the form of U(VI) ion easily dissolved in water, and it can facility transport with the flowing open and underground water,endanger the safety of the biosphere.

Granite is one of common mineral rocks in the nature,it is selected for the surrounding rock of the China's high-level radioactive waste repository. Muscovite is one of the major component of granite,a widespread group of minerals.The structure of muscovite is one silicon oxygen octahedral sheet sandwiched by two silicon oxygen tetrahedral sheets. There are active hydroxyl groups and some permanent negative charge.So, the investigation of the sorption onto muscovite has the important significance for exploring the migration/retardation of uranium.The further research for the migration mechanism of uranium in the surrounding rock granite can provide theoretical basis for security evaluation of high-level radioactive waste repository.

The sorption of U(VI) onto muscovite was studied by batch technique. The effects of contact time, pH, background electrolyte, ionic strength, temperature and the presence of humic acid (HA) were investigated in detail. The results demonstrated that the sorption tended to equilibrium after about 12 hours, and sorption data could be fitted well by psedo-second-order kinetic reaction. The sorption strongly depended on pH, but slightly relied on ionic strength and background electrolyte types, showing that the inner-sphere complexation was the predominant mechanism in the sorption process. High temperature was favorable for U(VI) sorption, and the isotherms could be described better by Langmuir model than Freundlich and D-R model. Humic acid had positive impact on sorption under acid ambient condition, and the sorption of U(VI) increased with the increasing HA concentration.

The ambient condition affects the species of U(VI) in aqueous solution, further lead to the sorption of U(VI) on solid-liquid interface. When pH less than 4, the UO_2^{2+} is the main specie;allowing pH increases, the content of hydrolysate $(UO_2)_3(OH)_5^+$,UO_2OH^+ and $(UO_2)_2(OH)_2^{2+}$ rise; pH = 6.5, the major specie is $(UO_2)_2CO_3(OH)_3^-$ (~70%)；pH > 8, $UO_2(CO_3)_3^{4-}$ content rise gradually, and become main species. With the rise of pH,the deprotonation of function sites on muscovite surface increases. Under the effect of static electricity, the adsorbance grow with pH increase. When pH > 7, electrostatic repulsion result of the weak sorption of anions, $UO_2(CO_3)_2^{2-}$ and $UO_2(CO_3)_3^{4-}$. By the way, muscovite structure contains a small amount of Ca^{2+}. When pH > 8, calcium ion and U(VI) form coordination compound $Ca_2UO_2(CO_3)$ that is hard to be adsorbed, and result in the decrease of U(VI) adsorbance.The sorption onto muscovite affected greatly by pH, it shows the main control mechanism of adsorption is surface complexation.

The different anions have disparate impact on sorption of U(VI）at the same ionic strength. Under the condition of different background electrolyte, the U(VI) adsorption percentage is highest in $NaClO_4$ solution, the lowest in NaCl solution. Because U(VI) can coordinate with Cl^- and NO_3^-, and form soluble ligand compounds. Ionic radius order: $r(Cl^-) < r(NO_3^-) < r(ClO_4^-)$. Chloridion with smaller radius can form with U(VI) easier. Most uranium ions exist as the form of soluble content in aqueous phase, the form of the ions results in the decrease of adsorption percentage. On the other hand, contrast to nitrate ions, chloride ions are more likely to adsorption on solid surface, their adsorption change the property of the surface of the solid, reduce the ratio of adsorption sites of U(VI) ions.

Generally speaking, when the adsorbate and adsorbent form inner-space complexes, adsorption percentage is almost not influenced by ionic strength changes.If the adsorbate adsorbed as the form of surface complexation,the adsorbate and adsorbent form the outer-space complexes,the ionic strength has a greater effect on adsorption.In this context，the adsorption percentage of U(VI) onto muscovite remain stable at different ionic strength. In

terms of the adsorption percentage of U(VI) onto muscovite almost not affected by the change of background electrolyte ion intensity,the main form of the the U(VI）sorption onto muscovite is inner-space complexes.
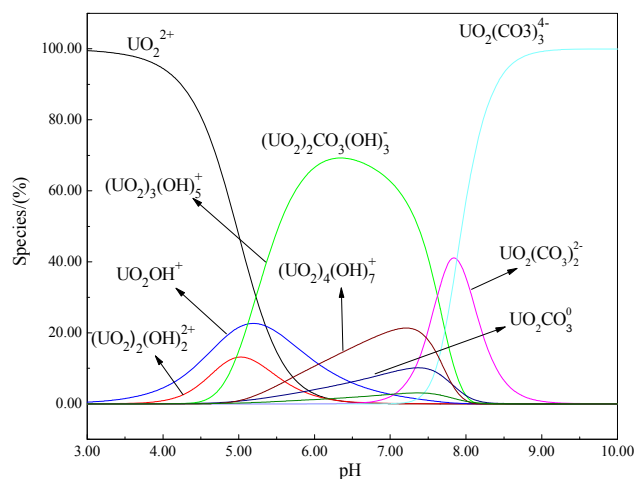
Figure. 1 Uranium speciation in 0.01 mol/L $NaClO_4$ solution in equilibrium with air ($P_{CO2}=10^{-3.58}$atm)

Species	Reaction	logK[a]
$(UO_2)_3(OH)_5^+$	$5H_2O + UO_2^{2+} \leftrightarrow 5H^+ + (UO_2)_3(OH)_5^+$	-15.55
UO_2OH^+	$H_2O + UO_2^{2+} \leftrightarrow H^+ + UO_2OH^+$	-5.25
$(UO_2)_2(OH)_2^{2+}$	$2H_2O + UO_2^{2+} \leftrightarrow 2H^+ + (UO_2)_2(OH)_2^{2+}$	-5.62
$(UO_2)_4(OH)_7^+$	$7H_2O + 4UO_2^{2+} \leftrightarrow 7H^+ + (UO_2)_4(OH)_7^+$	-21.9
$UO_2(CO_3)_2^{2-}$	$UO_2^{2+} + 2H_2CO_3 \leftrightarrow UO_2(CO_3)_2^{2-} + 4H^+$	16.61
$UO_2CO_3^0$	$UO_2^{2+} + H_2CO_3 \leftrightarrow UO_2CO_3^0 + 2H^+$	9.94
H_2CO_3	$2H^+ + CO_3^{2-} \leftrightarrow H_2CO_3$	16.681

Table 1 Reaction and parameters used in the model calculations(from Minteq database)

IONOSILICAS FOR ION EXCHANGE REACTIONS: Tc(VII) SEPARATION

M. Gigue[1], L. Venault[1], P. Hesemann[2], P. Moisy[1]

[1]*CEA Marcoule DEN/DRCP, 30207 Bagnols-sur-Cèze, France*
[2]*Institut Charles Gerhardt, 34095 Montpellier Cedex 05, France*

Ion exchange reactions are among the most powerful separation techniques and found numerous applications in various separation, purification and decontamination processes in particular in the nuclear fuel cycle.

One of the major fission products formed during the irradiation of nuclear fuel is [99]Tc. It occurs as a high yield (6.06% from thermal neutron fission of [235]U) with a long half-life (2.1×10^5 yr). During the reprocessing of nuclear fuel, the irradiated fuel is first dissolved in nitric acid: under such non-reducing process conditions, Tc is oxidized to the +7 oxidation state, which is the most stable oxidation state of Tc in solution, and forms strong pertechnetic acid $HTcO_4$. This acid is easily dissociated to form H^+ and the oxo-anion TcO_4^-.

Ionosilicas are defined as silica based materials containing covalently tethered ionic groups. These materials, situated at the interface of silica hybrid materials and ionic liquids, have large potential in separation. Ionosilicas are usually obtained *via* template directed hydrolysis-polycondensation reactions using ionic trialkoxysilylated precursors. Due to their ionic nature, these precursors often display very particular behavior in these bottom-up approaches, especially in the presence of ionic structure directing agents. Nanostructured phases can particularly be obtained *via* the formation of special precursor-surfactant assemblies, thus ensuring high accessibility of the immobilized ionic species.

This talk will focus on applications of ionosilicas as Tc(VII) anion exchange materials[1]. We will firstly show that imidazolium containing ionosilicas[2] (scheme 1) are highly efficient anion exchange materials displaying high distribution coefficients for a large range of soft anionic species (fig. 1). The distribution coefficient of Tc(VII) (D) is calculated considering the quantity of Tc(VII) in the solution (before and after contacting) and the number of ion exchanging groups in the solid, obtained from the mass of the solid *m*, the molar mass of the solid *M*, and the degree of functionalization of the anion exchanging material *n* calculated from solid state [29]Si OP-MAS spectroscopy*:*

$$D = \frac{([Tc]_{init} - [Tc]_{eq})}{[Tc]_{eq}} \times \frac{V}{m} \times \frac{M}{n}$$

Furthermore, we observed that these materials display Hofmeister selectivity (fig. 2). The distribution coefficients D differ according to the nature of the anion: for soft anions such as pertechnetate (TcO_4^-), considerably higher D-values were observed than for harder anions (chloride, bromide). This behavior enabled us to use the TcO_4^--anion as a probe revealing the hardness/softness of anionic species.

In conclusion, our results show that ionosilicas are highly efficient anion exchange materials. Besides the high potential of these materials for applications in nuclear waste treatment in the nuclear fuel cycle, this study gives interesting results concerning the accessibility of functional groups in silica based anion exchange materials.
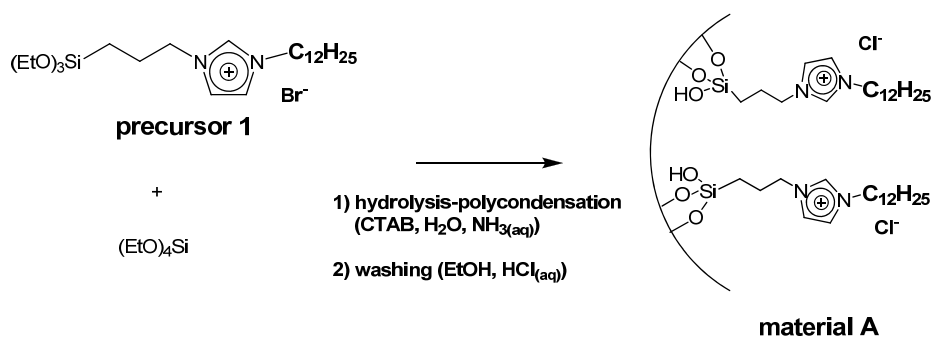
Scheme 1 Synthesis of mesostructured surface functionalized ionosilica containing covalently bound dodecyl imidazolium groups
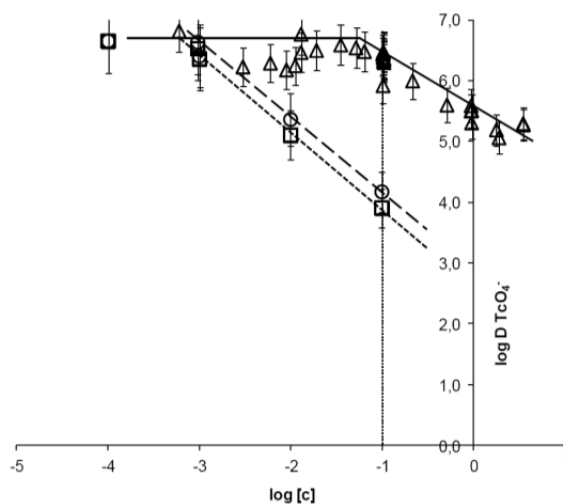
Figure 1 Distribution curves of TcO$_4^-$ in the presence of material **A** in the presence of chloride ($\triangle$), perchlorate ($\circ$) and perrhenate ($\square$) ions
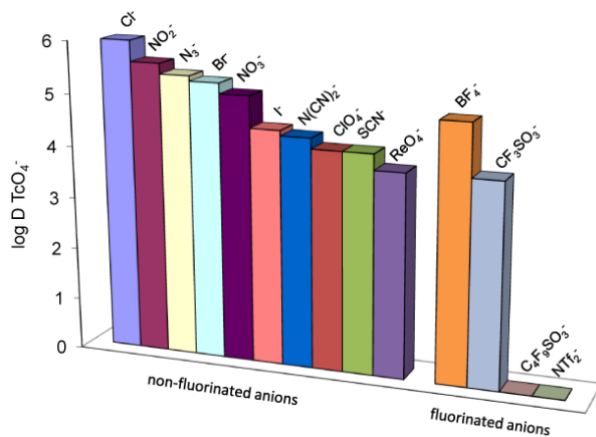
Figure 2 Distribution coefficients of TcO$_4^-$ in the presence of different competing ions (c = 0.1 mol L^{-1})

References
1. . Petrova, M. Guigue, L. Venault, Ph. Moisy, P. Hesemann, *PCCP*, **2015**, in press
2. B. Gadenne, P. Hesemann, J.J.E. Moreau, *Chem. Commun*. **2004**, 1768-1769

A THERMODYNAMIC ANALYSIS ON THE SWELLING STRESS OF NA-BENTONITE AS AN ENGINEERED BARRIER MATERIAL COMPOSING MULTI-BARRIER SYSTEM FOR RADIOACTIVE WASTE DISPOSAL UNDER VARIOUS SOLUTION CONDITIONS

H. Sato [1] and M. Fukazawa [2]

[1] *Graduate School of Natural Science and Technol., Okayama Univ., Tsushima-naka 3-1-1, Kita-ku, Okayama-shi, Okayama 700-8530, Japan*
[2] *Faculty of Eng., Okayama Univ., Tsushima-naka 3-1-1, Kita-ku, Okayama-shi, Okayama 700-8530, Japan*

Na-bentonite will be used as a buffer material composing engineered barrier system not only for a high-level radioactive waste (HLW) disposal (waste is disposed of in deep geological formation which is 300m or deeper, namely geological disposal), but also for a low-level radioactive waste (LLW) disposal (waste is disposed in shallow land within several meters in depth or subsurface with 50-100m in depth). Na-bentonite will be also mixed with surplus rock (muck) as a backfill material for disposal tunnel and access tunnels, etc. In addition, Na-bentonite will be mixed as a backfill material for impermeable layer in the LLW disposal. Since the major clay mineral constituent of Na-bentonite is Na-montmorillonite having the nature of swelling by coming in contact with groundwater and restricts the groundwater flow. Swelling stress (pressure) develops by hydration of the interlayer of montmorillonite. Whilst, the swelling property of bentonite is strongly dependent on water condition, such as saline water [1-3]. Moreover, a large amount of nitrate is contained in part of the TRU (Trans-uranium) waste which is one of the LLWs, and it is fear that nitrate is dissolved by contacting with groundwater after being disposed, and has an influence on engineered barriers and the surrounding environment. Therefore, understanding the thermodynamic properties of interlayer water in montmorillonite is important.

The authors have constructed a thermodynamic model for calculating the swelling stress of bentonite, based on the thermodynamic data of interlayer water in Na-montmorillonite in earlier studies [4, 5]. The activity of interlayer water in Na-montmorillonite was measured as a function of water content (0-83%) and temperature (15-40°C) by a vapour pressure method, and the relative partial molar Gibbs free energy (dG_{H2O}) was determined from the activities. In addition, an empirical correlation between dG_{H2O} and water content was derived. In this work, based on the thermodynamic model for swelling stress, the empirical correlation between dG_{H2O} and water content [4, 5] and basic data for electrolyte solutions, the swelling stress of water-saturated Na-bentonite was calculated for various bentonite dry densities and solution conditions such as salinity and nitrate concentration, etc.

Swelling stress versus montmorillonite partial density [6] was estimated for solutions of various salinities ([NaCl] = 0-3.4m, m: molality) [5] and nitrate concentrations ([$NaNO_3$] = 0-6m) by using the developed model and compared to data measured for bentonites with various montmorillonite contents and silica sand contents. Figure 1 shows the calculated and measured [7-9] results of swelling stress for nitrate as a function of montmorillonite partial density. The calculated swelling stresses commonly decreased with an increase of salinity and nitrate concentration at the same dry density of montmorillonite. The trend of swelling stress versus salinity was in good agreement with the measured results. The trend versus nitrate concentration was also similar to that versus salinity, but the quantitative calculated results were much different from the measured data ([$NaNO_3$] = 3, 5M, montmorillonite partial density = 0.76-0.87 Mg/m^3) [7-9]. As shown in Fig. 1, even though those measurements were carried out under the condition of high ionic strength ([$NaNO_3$] = 3, 5M), the obtained swelling stresses were almost the same as in the condition of distilled water. Since the measurement periods were quite short to be several tens of hours [7, 8], a possibility that those measured data have not reached equilibrium is high. This cause will be carried out as one of the future works. In this paper, not only NaCl and $NaNO_3$, but also the calculated results for other various solution conditions such as NaOH and KOH will be reported.
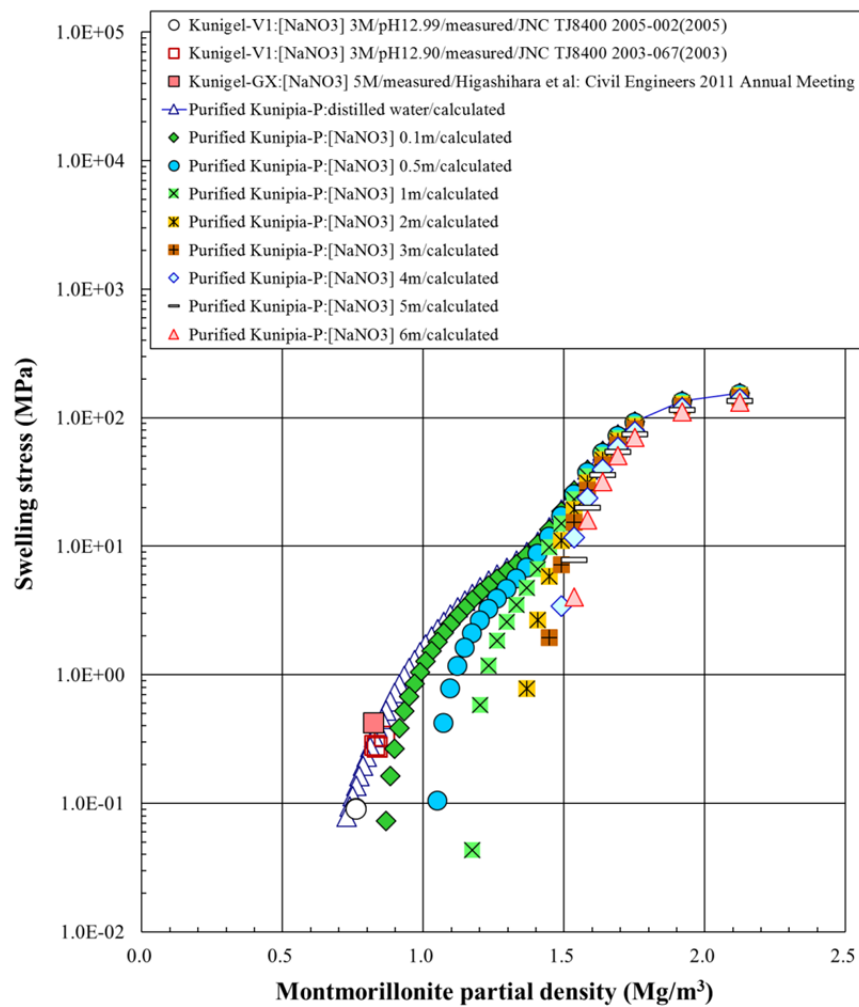
Figure 1.   The calculated and measured [7-9] results of swelling stress for nitrate (NaNO₃) as a function of montmorillonite partial density

[1] Suzuki, H. and Fujita, T. (1999). "Swelling characteristics of buffer materials." JNC Tech. Rep. JNC TN8410 99-038.

[2] Kikuchi, H. and Tanai, K. (2004). "Basic characteristic test of buffer / backfill material under Horonobe groundwater condition." JNC Tech. Rep. JNC TN8430 2004-005.

[3] Tanaka, Y., Hasegawa, T. and Nakamura, K. (2007). "Modeling hydraulic conductivity and swelling pressure of several kinds of bentonites affected by concentration of saline water." Civil Eng. Res. Lab. Rep., Central Res. Inst. of Electric Power Industry No.N07008.

[4] Sato, H. (2008). "Thermodynamic model on swelling of bentonite buffer and backfill materials." Physics and Chemistry of the Earth **33**: S538-S543.

[5] Sato, H. (2009). "A thermodynamic approach on the effect of salt concentration on swelling pressure of water-saturated bentonite." Mater. Res. Soc. Symp. Proc. Vol.**1124**: 6 pages (in pdf format).

[6] Sato, H. and Miyamoto, S. (2004). "Diffusion behaviour of selenite and hydroselenide in compacted bentonite." Appl. Clay Sci. **26**: 47-55.

[7] Iriya, K., Fujii, K. and Kubo, H. (2003). "Evolution of hydraulic conductivities of bentonite and rock under hyper alkaline and nitrate conditions (II)." JNC Tech. Rep. JNC TJ8400 2003-067.

[8] Iriya, K. and Kubo, H. (2004). "Evolution of hydraulic conductivities of bentonite and rock under hyper alkaline and nitrate conditions (III)." JNC Tech. Rep. JNC TJ8400 2005-002.

[9] Higashihara, T., Shimomura, M., Fujiwara, N., Masuoka, K. and Aoki, T. (2011). "Effect of degradation factor for low permeable layer of subsurface disposal facility (2)." Japan Society of Civil Engineers 2011 Annual Meeting: 47-48.

ANTIMONY(III, V) ADSORPTION ON ZIRCONIUM HYDROXIDE AT ELEVATED TEMPERATURES

L. Qiu[1], S. Rousseau[1]

[1]*Canadian Nuclear Laboratories, Chalk River, Ontario, Canada K0J 1J0*

Release of radionuclides from nuclear reactor accidents, terrorist attacks and radioactive waste facilities may give rise to severe environmental pollution and threats to human health. Typically, radionuclides can migrate as aerosols, dissolved species or adsorbed on other materials. Sorption data for radionuclides are required to predict adsorption uptake, reduce activity transport, mitigate economic losses from radionuclide contamination and remediate the contaminated environment during and following nuclear incidents.

Antimony is produced in nuclear reactor cores by activation of trace impurities in materials of construction released by corrosion and wear and transported to the core, and is also a fission product. Although antimony is found in natural water and has been studied in some minerals around room temperature, adsorption of Sb(III) and Sb(V) on zirconium oxide has not been investigated thoroughly. This paper reports the results of adsorption and desorption studies of antimony (III, V) on $Zr(OH)_4$. $Zr(OH)_4$ is a model for the hydrated outermost layer of the ZrO_2 corrosion films found on zirconium alloys in nuclear reactor cores, as well as being a good adsorbent. Data on antimony adsorption on zirconium hydroxide have not previously been reported in the literature. This paper presents the results of experimental studies of the effects of temperature, pH and concentration on the antimony adsorption mechanism on $Zr(OH)_4$. The data show that adsorption of Sb(III) and Sb(V) follows second order reaction kinetics, with adsorption equilibrium being reached within 2 days and 8 days, respectively. Sb(III) and Sb(V) strongly adsorb onto the surface of $Zr(OH)_4$ and the amount adsorbed is almost independent of pH, with adsorption percentages above 98.8%. Overall, the effect of temperature on Sb(III) adsorption is not significant; however, increasing the temperature increases Sb(V) adsorption. The adsorption data obtained can be described by the Freundlich isotherm and show that the adsorption process is mainly by chemisorption.
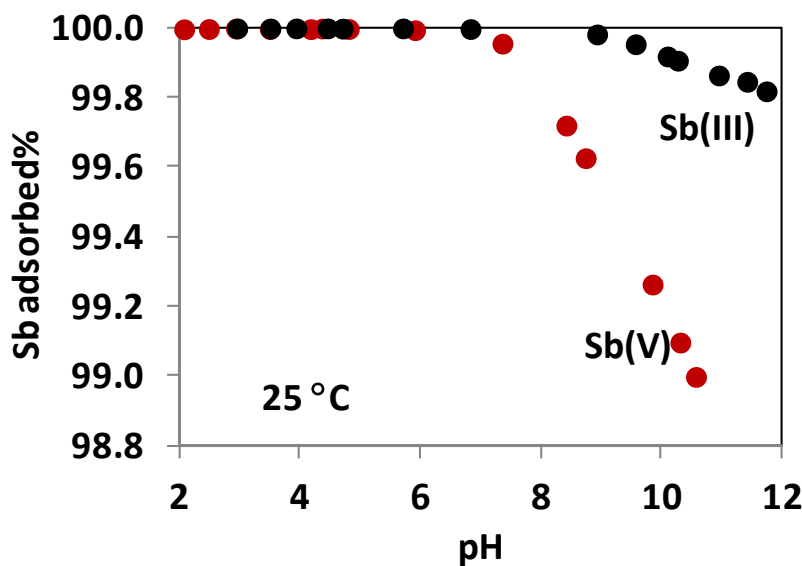
Figure 1. Antimony (III, V) adsorption on $Zr(OH)_4$ as a function of pH.

THE PHOSPHORESCENCE OF URANYL CARBONATES – ONLY A RESULT OF DYNAMIC QUENCHING?

G. Geipel, B. Drobot, T. Stumpf

Helmholtz-Zentrum Dresden – Rossendorf, Institute of Resource Ecology, Bautzener Landstr. 400, 01328 Dresden, Germany

It is well known, that uranyl carbonates emits at room temperature only phosphorescence with very short lifetimes $\{Ca_2UO_2(CO_3)_3 \sim 50$ ns$\}$[1, 2]. The lifetime of $UO_2(CO_3)_3^{4+}$ in aqueous solution at room temperature was determined to be 9.2 ± 0.05 ns. Freezing these solutions results normally in a strong increase of the luminescence lifetime as well as in a strong increase in the measured intensity. This effect is usually explained by the dynamic quench effect of the carbonate ion as well as the dynamic quench effect of the water molecules in the solvation shell. In addition all spectra of the uranyl carbonates show a hypsochromic shift.

The emission of the uranyl ion is assigned to a triplet state. It is also known that the non-complexed uranyl ion has two phosphorescence emitting levels (20500 and 21270 cm^{-1})[3,4]. The first one is assigned to the direct transition to the lowest vibronic level in the ground state, the second is assigned to the transition of a exited vibronic level to the ground state. The emission peaks at lower wavenumbers correspond to vibronic levels in the ground state and are usually assigned to the transition from the lowest triplet state[5]. Complexes formed with sulfate and phosphate do not show the higher emitting level. The higher emitting level is too close to the lower lever, that it is assumed as emitting level from the T_2 state.

Assuming that the emission of the higher level of the uranyl ion is from the triplet manifold it might be obvious that also higher levels in the manifold are able to emit phosphorescence if they are populated and if the lowest level may be not accessible. Under these assumptions we can at first deconvolute the emission spectrum of the uranyl ion including transition from the 21060 cm^{-1} (and the next higher, third) vibronic triplet level to the several vibronic levels in the ground state. In addition to this it is also possible to explain the luminescence spectra of the carbonate complexes as emissions mainly from the third vibronic triplet level.

In the table are summarized the transitions of the uranyl ion in an aquatic environment as well as of the uranyl tricarbonato complex.

	UO_2^{2+}			$UO_2(CO_3)_3^{4-}$		
	T_0^2	T_0^1	T_0^0	T_0^2	T_0^1	T_0^0
S_0^0	21940 (456)	21060 (474)	20480 (488)	21270 (470)	20580 (486)	
S_0^1		20360 (491)	19590 (510)		19780 (506)	
S_0^2		19520 (512)	18710 (534)		19000 (526)	
S_0^3		18340 (545)	17840 (560)		18190 (549)	
S_0^4		17450 (573)	17000 (588)		17360 (576)	

Values in wavenumbers cm^{-1}, in brackets (wavelength in nm); S_0: Ground state with vibronic levels; T_0: lowest triplet state

As it is commonly accepted that emission of photons are usually occur from the lowest level in the triplet state (or in case of fluorescence from the lowest singlet state), therefore there must be some reason that the lowest triplet state cannot not populated in the carbonate system.

[1] G. Bernhard, G. Geipel, et al., Radiochim. Acta 74, 87-91(1996).
[2] G. Bernhard, G. Geipel, et al., J.Alloys & Comp. 271-273, 201-205 (1998).
[3] S. Formosinho, H.D. Burrows, et al., Photochem. Photobiol. Sci., 2, 569-575 (2003).
[4] M. da Graca, M. Miguel, et al., J. Chem. Soc., Faraday Trans. 1, 80, 1735-1744 (1984).
[5] G. Meinrath, Aquatic Chemistry of Uranium, 1998, Freiberg On-line Geoscience Vol.1.

DEVELOPMENT OF AN EXPERIMENTAL METHOD DEDICATED TO THE DETERMINATION OF VERY LOW SOLUBILITY: ZIRCONIUM OXYDE

A. Astorg[1], V. Zinovyeva[2], C. Cannes[2], L. Mercier[1], M. Mahe[1], X. Crozes[1], M. V. Di Giandomenico[1]

[1]*EDF R&D, Chemistry and Materials of Energetic Efficiency, Materials and Mechanics of Components Department, Les Renardières, 77818 Moret-sur-Loing, France*
[2]*Université Paris-Sud 11, Institut de Physique Nucléaire, CNRS UMR 8608 – 15, Rue Georges Clémenceau, 91406 Orsay, France*

The fuel claddings used in pressurized water reactors are made of zirconium alloy. In reactor, the oxidation of this material leads to the formation of zirconium oxide (ZrO_2) which contains activation products, including carbon 14. Claddings are compacted to form intermediate level – long lived waste. These wastes are intended to be put in cement package and then in deep geological disposal chosen by the french national radioactive waste management agency (ANDRA). To determine a model of release of these radionuclides in geological storage conditions, we have to know:

- diffusion rate of radionuclides in zirconium oxide,
- dissolution rate of zirconium oxide in cement environment.

This work focuses on the dissolution rate of zirconium oxide in cement (figure 1) [1], in order to develop an experimental method dedicated to low solubility determination. Two experimental techniques are coupled: the Quartz Crystal Microbalance (QCM) and the Inductively Coupled Plasma Mass Spectrometry (ICP-MS).
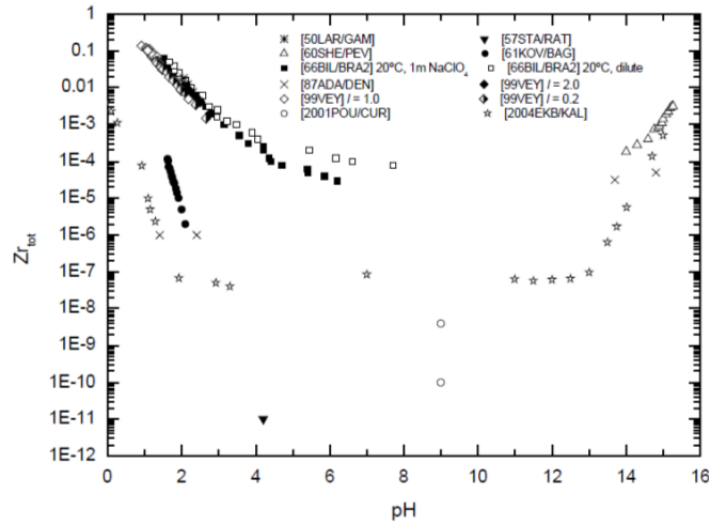
Figure1: Solubility of $ZrO_{2(cr)}$ and $Zr(OH)_4$ from various sources at 25°C [1]

The samples are synthesized by an electrochemical method; the deposition of a thin layer of zirconium oxide is performed on the working electrode. This deposition is optimized to form a layer chemically similar to the oxide formed in reactor.

After about three months of sample lixiviation, zirconium concentration in cement solution is still very low, around 10^{-8} M. This result is in good agreement with literature. Therefore, between 25 to 70°C, no influence of temperatures has been observed on layer solubility.

In the field of low solubility determination, the present work shows the relevance of coupling QCM/ICP-MS.

[1] Chemical Thermodynamics of Zirconium (OECD Nuclear Energy Agency, ed.) - Vol. 8., Paul L. Brown et al., Elsevier, 2005.

DETERMINATION OF PLUTONIUM AND AMERICIUM IN SNOW AND RAIN

K. Gückel[1)], T. Shinonaga[1)], K. Hain[2)], G. Korschinek[2)]

1) Helmholtz Zentrum München, German Research Center for Environmental Health, Institute of Radiation Protection, Ingolstädter Landstr. 1, 85764 Neuherberg, Germany
2) Technische Universität München, Physics Department, James-Franck-Str.1, 85748 Garching, Germany

For the forecast of long-term radiological consequences of an accidental release of actinides into the environment, it is important to know the long-term behaviour of those elements. Since the first explosion of a nuclear weapon (Trinity test) in 1945, plutonium (Pu) and americium (Am) are being released into the environment through various events, e.g. weapon tests, accidents of nuclear facilities, crashes of satellites and planes, and discharging of effluents from reprocessing factories and it is assumed that around $1.4 \cdot 10^{16}$ Bq of $^{239+240}$Pu were released into the environment ([1] and references therein). Americium-241 ($T_{1/2}$= 432.2 years), is the beta-decay product of ^{241}Pu ($T_{1/2}$= 14.325 years), and its concentration in the environment is increasing. It was estimated that ^{241}Am will reach its maximum activity in the middle of 21st century [2]. Such Pu and Am are considered as hazardous radionuclides to the biosphere.

Limited data of the Pu and Am amount wet-deposited in the alpine area exists [3-6] and details on the transport of the actinides from snow area into hydrosphere are still not well known. However, a recent study relating the transport of airborne Pu up to 120 km distance from the Fukushima Daiichi nuclear power plants within a few days [7] suggests an importance to study the mechanisms of the transport of actinides in the atmosphere.

Our project "plutonium and americium in snow-hydrosphere" focuses on studying the pathway, quantity and atomic ratios of Pu and Am isotopes in snow and rain. For the fg (10^6~10^9 atoms) level of Pu and Am analysis, the chemical separation procedure and measurement technique are improving considering sample material treatment, pre-concentration, and isolation from matrix.

In literature numerous methods for the sample preparation are described and the chemical separation with extraction chromatographic resins is widely used [8, 9]. Because of a possible interference of ^{238}U tails with ^{239}Pu when using mass spectrometry, U is required to be extracted from Am/Pu fractions. For this purpose, the extraction chromatographic resin UTEVA$^{®}$ (Eichrom Technologies, LLC) was used in this study. The extractant in the UTEVA-resin, diamyl, amylphosphonate (DAAP), forms nitrato complexes with the actinide elements, but Am(III) and Pu(III) are not retained under any nitric acid concentrations. The chemical separation of these actinides with a TRU-resin$^{®}$ (Eichrom Technologies, LLC) column was improved in this study and was performed in tandem with the UTEVA-resin column. The TRU-resin extracts nitrato complexes of tri-, tetra-, and hexavalent actinides with a strong selectivity. The actinides can be recovered individually or in groups with acidic solutions, complexing agents, or redox reagents.

In this study, accelerator mass spectrometry (AMS), which is one of the most selective and sensitive techniques for the analysis of the atomic ratio of long-lived actinides, was used for the isotopic ratio measurements. Using this method, a low detection limit can be achieved by dissociation of molecules during the stripping process in the accelerator, and the use of highly sensitive detectors for the final determination of the ions. The AMS measurements were performed at the Maier-Leibnitz-Laboratory, Technische Universität München [10, 11]. Both Pu and Am were injected into the tandem accelerator as the negatively charged oxygen compounds using a terminal voltage of 10 MV. The ions were identified by a 2.9 m long time of flight (TOF) path, with a micro channel plate detector and a silicon surface barrier detector serving as start and stop signal, respectively.

As a first step of environmental sample analysis, Pu and Am in snow from Mt Zugspitze, German alpine region and rain from Neuherberg, Bavaria, Germany were analysed with AMS after chemical separation for each nuclide, using the current analytical conditions. The results provide us with an idea of the amount of Pu and Am wet-deposited on Mt Zugspitze and in Neuherberg, and might help to understand the behaviour of those actinides in snow-hydrosphere and rain. Additionally, using the variations of the atomic ratios of the Pu isotopes, it may be possible to consider the Pu origin. First results of Pu and Am amounts in the rain collected in Neuherberg starting in July 2014 and the snow collected on Mt. Zugspitze in the winter 2014/2015 will be presented and discussed.

1.   Bisinger, T., *Bestimmung von Plutonium-Isotopen in der Umwelt: Analyse mittels Alphaspektrometrie und Beschleunigermassenspektrometrie* 2010: Südwestdeutscher Verlag fuer Hochschulschriften.

2.   Lehto, J., *Americium in the Finnish environment.* Boreal Environment Research, 2009. **14**(3): p. 427-437.

3.   Gabrieli, J., et al., *Contamination of Alpine snow and ice at Colle Gnifetti, Swiss/Italian Alps, from nuclear weapons tests.* Atmospheric Environment, 2011. **45**(3): p. 587-593.

4.   Rosner, G., H. Hötzl, and R. Winkler, *Long-term behaviour of plutonium in air and deposition and the role of resuspension in a semi-rural environment in Germany.* Science of the Total Environment, 1997. **196**(3): p. 255-261.

5.   Rosner, G. and R. Winkler, *Long-term variation (1986-1998) of post-Chernobyl Sr-90, Cs-137, Pu-238 and Pu-239,Pu-240 concentrations in air, depositions to ground, resuspension factors and resuspension rates in south Germany.* Science of the Total Environment, 2001. **273**(1-3): p. 11-25.

6.   Warneke, T., et al., *A new ground-level fallout record of uranium and plutonium isotopes for northern temperate latitudes.* Earth and Planetary Science Letters, 2002. **203**(3-4): p. 1047-1057.

7.   Shinonaga, T., et al., *Airborne Plutonium and Non-Natural Uranium from the Fukushima DNPP Found at 120 km Distance a Few Days after Reactor Hydrogen Explosions.* Environmental Science & Technology, 2014. **48**(7): p. 3808-3814.

8.   Macsik, Z., et al., *Improved radioanalytical method for the simultaneous determination of Th, U, Np, Pu and Am(Cm) on a single TRU column by alpha spectrometry and ICP-MS.* Radiochimica Acta, 2013. **101**(4): p. 241-251.

9.   Lee, M.H., et al., *Radiochemical separation of Pu, U, Am and Sr isotopes in environmental samples using extraction chromatographic resins.* Journal of Radioanalytical and Nuclear Chemistry, 2013. **295**(2): p. 1419-1422.

10.   Wallner, C., et al., *Development of a very sensitive AMS method for the detection of supernova-produced longliving actinide nuclei in terrestrial archives.* Nuclear Instruments & Methods in Physics Research Section B-Beam Interactions with Materials and Atoms, 2000. **172**: p. 333-337.

11.   Knie, K., et al., *High-sensitivity AMS for heavy nuclides at the Munich Tandem accelerator.* Nuclear Instruments & Methods in Physics Research Section B-Beam Interactions with Materials and Atoms, 2000. **172**: p. 717-720.

APPLICATIONS OF TIME RESOLVED LUMINESCENCE/CHEMILUMINESCENCE LASER SPECROSCOPY FOR DETECTION OF ACTINIDES AND LANTHANIDES IN SOLUTIONS

I.N. Izosimov

Joint Institute for Nuclear Research, 141980 Dubna, Russia

Development of laser spectroscopy with tunable lasers gives rise to new procedures for detection of trace amounts of various substances in various media. A possibility to tune a wavelength of laser radiation allows selective action on certain atoms and molecules and, hence, selective detection of these [1-3] species. Using short laser pulses for excitation of molecules and ions in liquids and time resolution for registration of luminescence and chemiluminescence produced by actinide and lanthanide ions we can efficiently separate target signals from short-lived background luminescence. The limit of detection (*LOD*) of some lanthanides and actinides in solutions by the time-resolved laser luminescence spectroscopy is up to 10^{-13} mole/liter. An analysis requires about 1 ml of solution. Thus, *LOD* for a sample can reach 10^{-16} moles per 1 ml. The time-resolved laser luminescence spectroscopy technique features selectivity in four parameters: the laser radiation wavelength, measured radiation wavelength, measurement delay with respect to the pulse laser, and measurement time. Unfortunately, Pu, Np, and some U compounds do not produce direct luminescence in solutions, but when excited by laser radiation, they can induce chemiluminescence of some chemiluminogen (luminol in our experiments) [1-3]. Currently, chemiluminescence methods are used for detection of various substances with *LOD* of 10^{-6}M -10^{-13}M [4]. We demonstrated a possibility of using the chemiluminescence method for detection and determination of valence states of Pu, Np, and U. A key problem of chemiluminescence application to detection of lanthanides and actinides in solutions is an increase in the selectivity of detection. Appropriate selectivity of lanthanide or actinide molecules excitation can be reached by initiation of transitions within 4f- or 5f-electron shell, which correspond to visible spectral range of absorbed laser radiation. Since the energy of one-quantum excitation in visible range may be insufficient for initiation of chemiluminescence it was proposed to excite lanthanide or actinide ion by multi-quantum absorption of visible light [1-3].

The use of laser radiation with tunable wavelength allows selective excitation of actinide or lanthanide species with subsequent registration of direct actinide/lanthanide luminescence or chemiluminescence of chemiluminogen initiated by excited actinide/lanthanide molecules [1-3].

The details of multi-step luminescence/chemiluminescence excitation in solutions containing Sm, U, and Pu species are considered. It is shown that a multi-step schemes of luminescence/chemiluminescence excitation increase both the sensitivity and selectivity of lanthanide and actinide detection.

[1] I.N. Izosimov, Phys. Part. Nucl. 38, 177 (2007). DOI: 10.1134/s1063779607020025

[2] I.N. Izosimov, N.G. Firsin, N.G. Gorshkov, et al., Hyperfine Interact. 227, 271 (2014).

DOI: 10.1007/s10751-013-0990-7

[3] I.N. Izosimov, Journal of Radioanalytical and Nucl. Chem. (2015). DOI: 10.1007/s10967-014-3601-4

[4] C. Dodeigne, L. Thunus, R. Lejeune, Talanta, 51, 415 (2000).

THE SPECIATION ANALYSIS OF INORGANIC SELENIUM AND IODINE IN GROUNDWATER FROM BEISHAN AREA, CHINA

Zhe Nie[a], Weiyue Feng[b], Xiaoyu Yang[a], Chunli Liu[a*]

[a] *Beijing National Laboratory for Molecular Sciences, Radiochemistry & Radiation Chemistry Key Laboratory for Fundamental Science, College of Chemistry and Molecular Engineering, Peking University, Beijing 100871,China*
[b] *CAS Key Laboratory of Nuclear Radiation and Nuclear Energy Technology, Key Laboratory for Biomedical Effects of Nanomaterials and Nanosafety, Institute of High Energy Physics, Chinese Academy of Sciences, Beijing 100049, China*
Author for correspondence liucl@pku.edu.cn

[79]Se and [129]I are both fission products of [235]U. Because of the long half-lives (2.95×10^5 y for [79]Se and 1.57×10^7 y for [129]I), high solubilities, and weak sorptivities, their potential migration behavior from a waste containment site into the geosphere, with a subsequent impact on the environmental system, is critical in both the design and the assessment of a high-level radioactive waste repository. It is reported that the predominant pathway for radionuclide migration is solute transport in groundwater[1]. During their migration, the chemical form of the radionuclides is one of the important factors that govern their geochemical behavior, such as their sorption, diffusion and precipitation. Therefore, insight into the speciation of selenium and iodine in groundwater will help elucidate their biogeochemical behavior in the environment and will provide reliable data for assessment of the geological disposal of high-level radioactive wastes.

Therefore, this study aimed at developing a method for speciation analysis of selenium and iodine in groundwater and acquiring background data of selenium and iodine species in Beishan groundwater samples (these samples were collected, transported and stored under anoxic conditions). Considering the high sensitivity and accuracy of HPLC-ICP-MS method (High-Performance Liquid Chromatography-Inductively Coupled Plasma Mass Spectrometry), it is applicable to apply this method in the quantitative determination of inorganic selenium and iodine species, including selenite, selenate, iodide and iodate, in groundwater. This study was based on a PRP-X100 (250 mm × 4.6 mm, 5 μm) anion-exchange column (Hamilton, Reno, NV, USA), a Waters Acquity UPLC system (Waters, Milford, MA, USA), and a Perkin-Elmer NexIon 300D ICP-MS (Perkin Elmer, Branford, CT, USA). The effects of the mobile phase composition, pH and organic modifier content on the separation, as well as the matrix effects on the measurement, were investigated and optimized. Baseline separation of selenite, selenate, iodide and iodate within a single chromatographic run of 10 min was achieved with the optimized mobile phase of 3 mM ammonium citrate, 25 mM ammonium perchlorate and 2% (v/v) methanol at pH 8.5. The mass spectrometric operating conditions, including the reaction cell gas, cell gas flow rate, and rejection parameter q (RPq) were optimized to detect selenium and iodine simultaneously. A typical chromatogram of a mixture containing selenium and iodine is shown in Fig. 1.

ANALYSIS OF URANIUM, NEPTUNIUM, PLUTONIUM, AMERICIUM AND CURIUM ISOTOPES BELOW PPQ LEVELS IN GROUNDWATER SAMPLES FROM AN UNDERGROUND RESEARCH FACILITY IN SWITZERLAND

F. Quinto[1], R. Golser[2], M. Lagos[1], M. Plaschke[1], P. Steier[2], T. Schäfer[1] and H. Geckeis[1]

[1] *Institute for Nuclear Waste Disposal (INE), Karlsruhe Institute of Technology, Hermann-von-Helmholtz-Platz 1 76344 Eggenstein Leopoldshafen*
[2] *VERA Laboratory, Faculty of Physics, University of Vienna, Währinger Straße 17, A-1090 Vienna, Austria*

Accelerator Mass Spectrometry (AMS) is presently one of the most sensitive analytical techniques for the determination of actinides; that is due to the stripping process and acceleration of the ions to MeV energies providing both the destruction of molecular isobaric background and a strong reduction of tailing interferences. The Vienna Environmental Research Accelerator (VERA) has developed abundance sensitivities (AS) for ^{236}U, ^{237}Np and ^{239}Pu relative to ^{238}U at levels $\leq 10^{-15}$ [1] and detection limits (DL) at the value of 10^4 atoms per sample [2]. These features allow accurate measurements of actinide concentrations below ppq levels, particularly advantageous when a limited sample size is available. Such an analytical challenge is encountered, e.g., when investigating environmental samples affected by low levels nuclear contamination, like the global fallout, or in the frame of field experiments employing actinide tracers, like the international Colloid Formation and Migration Project (CFM) at the Grimsel Test Site in Switzerland [3].

A further challenge in the determination of ^{237}Np and of ^{243}Am lies in the non-availability of pure enough isotopic tracers for mass spectrometric measurements when investigating concentrations of 10^5 to 10^8 atoms in a sample. To overcome this limitation, we have investigated the use of non-isotopic tracers, developing a new method in which different actinide nuclides can be measured sequentially without previous chemical separation from each other exploiting the exceptional AS of AMS. The chemical treatment consists principally in the purification of the group of actinides from the matrix elements with a $Fe(OH)_3$ co-precipitation.

Multi-isotope tracer solutions with known amounts of ^{233}U, ^{237}Np, ^{239}Pu, ^{243}Am and ^{248}Cm added to groundwater samples were treated by the same sample and target preparation procedure like the "real" samples originating from the migration experiment. Such "calibration samples" were repeatedly measured together with the "real samples", both providing the same groundwater matrix, in order to compensate for the different chemical and ionization yields of the several actinides in the Cs negative ions sputtering source of AMS.

This procedure, allowing for the first time the simultaneous mass spectrometric determination of ultra-trace levels of several actinide nuclides in presence of naturally occurring U, is especially suited for groundwater and seawater samples. At the Grimsel Test Site, in the frame of the CFM Project, a first radionuclide tracer test under low-flow conditions has been performed in 2012 (run 12-02). In this experiment ^{237}Np, ^{242}Pu and ^{243}Am have been injected in a water conducting shear zone fracture in order to investigate the colloid mediated transport of actinides.

In the present study we have investigated six groundwater background (BG) samples, which were collected in the tailing of the tracer pulse experiment breakthrough curve from 60 up to 210 days after the start of the experiment. The concentration of the injected tracers in these samples was supposed to be below the detection limits of sector field (SF) ICP-MS (equal to 10 ppq), employed for the measurements of the preceding samples.

The size of the BG samples was limited to a mass of 500 g or to 250 g, in which the concentrations of ^{237}Np and ^{242}Pu have been determined by using ^{239}Pu as yield tracer, while that of ^{243}Am by using ^{248}Cm.
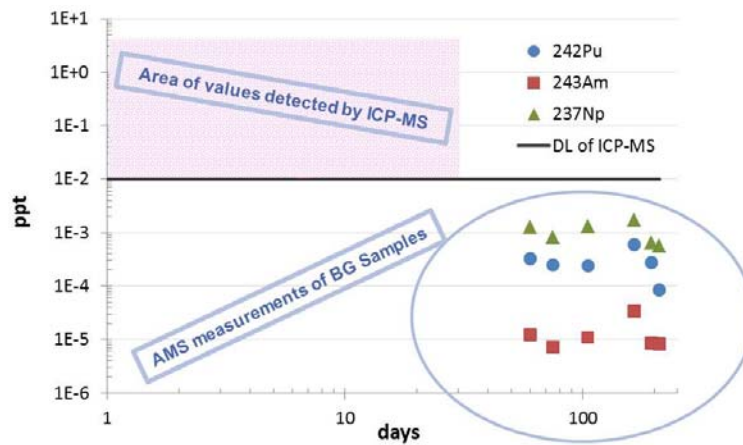
Figure 1: ^{242}Pu (blue circles), ^{237}Np (green triangles) and ^{243}Am (red squares) concentrations in the eluent fractions of the experiment run 12-02 in the frame of the CFM Project. Above and below the black line indicating the DL of SF-ICP-MS, the area of data detectable with the first technique and the data obtained with AMS, respectively, are depicted.

The detection of ^{237}Np, ^{242}Pu and ^{243}Am down to the levels of fg/g and ag/g was successful in the investigated samples, as shown in Fig. 1. The use of non-isotopic tracers has led to a higher uncertainty in the determination of ^{237}Np and ^{243}Am than of ^{242}Pu. In fact, while, the maximum relative uncertainty on the measured values of ^{239}Pu, due solely to the counting error, is equal to ~ 5%, the relative uncertainties of the measured values of ^{237}Np and ^{243}Am reach ~ 16% and ~ 24%, respectively. However, it is possible to detect even the initially colloid associated actinides (Pu and Am) in the tailing, as shown in Fig 1. These findings prove that the long term release and retention of actinide tracers can still be studied in samples collected up to 6 months after the starting of the experiment.

The extraordinary sensitivity of AMS, allowing the detection of ultra-trace levels of actinides, provides the capability to observe their behaviour in a variety of environmental systems. We exploit this feature in field studies whose results are complementary to those of the fundamental research on the speciation of actinides.

[1] P. Steier et al. "The AMS isotope Uranium-236 at VERA" Presentation at the 13th International Conference on Accelerator Mass Spectrometry, 37, 24-29 August 2014, Aix en Provence, France.

[2] P. Steier et al., (2010) "Analysis and application of heavy isotopes in the environment" Nucl. Instr. Meth. Phys. Res. Sect. B 268: 104-109.

[3] http://www.grimsel.com/gts-phase-vi/cfm-section .

RAD EMSL, AN INTERNATIONAL USER FACILITY FOR THE STUDY OF RADIOLOGICAL ENVIRONMENTAL SAMPLES

Nancy J. Hess[1]

[1]EMSL, Pacific Northwest National Laboratory, Richland WA 99352 USA

Rad EMSL, a new state-of-the-art laboratory to facilitate application of advanced analytical methods to environmental samples containing radionuclides, has been operational for two years at EMSL, a U.S. DOE Office of Biological and Environmental Research user facility located at Pacific Northwest National Laboratory in Richland, Washington. It supports world-class research in the biological, energy and environmental sciences through integration of computational and experimental capabilities, as well as collaborating among disciplines to yield a strong synergistic scientific environment.

Critical determinants of radionuclide chemical reactivity and mobility are oxidation state, chemical speciation, and formation of surface and solution complexes. Accurate representation of how environmental biogeochemical conditions impact these determinants is key to predictive modelling of radionuclide fate and transport in terrestrial and subsurface ecosystems. Molecular-level characterization of radionuclide containing materials can also be used to trace point of origin in forensic applications. These determinants also impact the chemical behaviour of radionuclides in the nuclear fuel cycle from separations processing to the creation of waste forms and aging under repository conditions. Unfortunately, the application of advanced molecular characterization techniques to radiological samples has often lagged because of the need for dedicated equipment and specialized facilities. Additionally there are fundamental difficulties of observing molecular level processes for radionuclides that are often present in very minor amounts in environmentally contaminated soils and sediments.

Rad EMSL provides scientific support and specialized environment where scientists are using advanced imaging and spectroscopic approaches together with NWChem, EMSL's premier computational modelling code, to study radionuclide speciation in environmental samples, nuclear fuel simulants, and in high level nuclear waste storage tanks. The radiological facility consists of approximately 6000 sq ft of contiguous lab space for NMR, EPR, XPS, and fluorescence spectroscopies and EMP, FIB/SEM, SEM, and aberration-corrected TEM imaging to enable investigation of radionuclide systems using multiple experimental and computational vantage points.

Access to Rad EMSL is granted through a competitve, peer review process in response to call for proposals. Typcial access is free. The results of several research projects conducted at Rad EMSL that highlight the integration of multiple experimental and computational approaches will be presented.

Figure 1. Left panel, Rad EMSL layout showing advanced spectroscopy and imaging laboratories. Right panel, cyrogenic EPR of Tc complexes in Hanford waste simulants
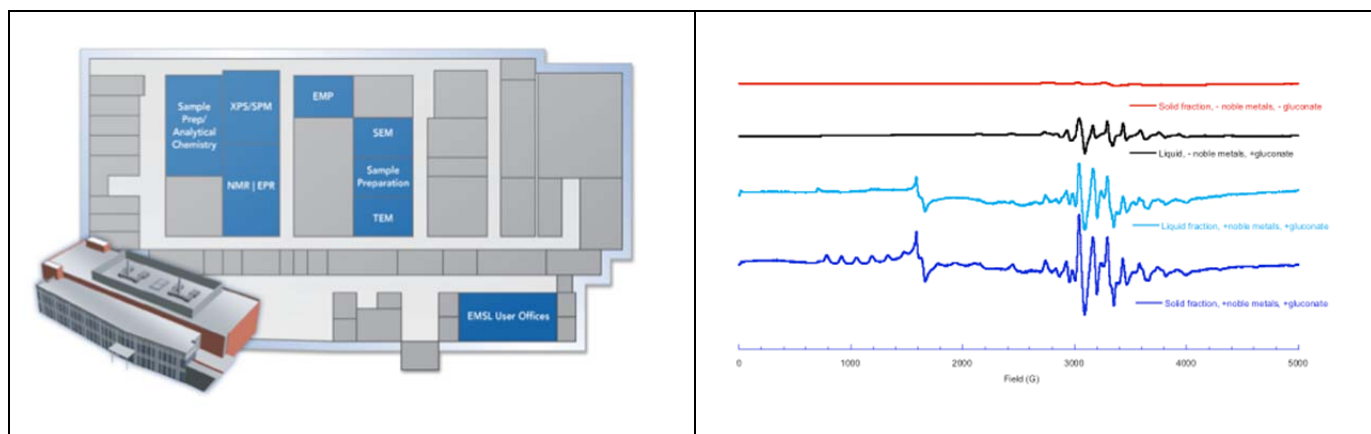
NOVEL INORGANIC COMPOSITES FOR TECHNETIUM MANAGEMENT

Sayandev Chatterjee, Tatiana G Levitskaia, Jesus Romero, James Peterson, Natasha Pence, Tamas Varga, Mark Bowden, Mark Engelhard, Bruce Arey, Libor Kovarik

Technetium (Tc) is one of the most problematic long-lived contaminants to be addressed at the U.S. DOE Hanford Site because of its complex chemical behavior in the tank waste, limited incorporation during LAW vitrification, and high mobility in subsurface environments. Significant concentrations of ^{99}Tc is observed in the multicomponent liquid matrices such as those related to the contaminated groundwater found in the Hanford area vadose zone, liquid nuclear tank waste, and solution generated during used nuclear fuel reprocessing. Tc transport and discharge from waste sites/sources to ground- and surface water resources creates potential for ecological exposure and significant health risks due to the possibility of its accumulation in several plants and animals resulting in biomagnification of ^{99}Tc in the food chain. This has necessitated an imminent need for ^{99}Tc sequestration and removal from tank waste, soil, watersheds and ground water and long term storage. However, the designing of novel sorbent materials for efficient ^{99}Tc removal is complicated by its ability to exist in a variety of oxidation states and chemical forms with varying mobilities depending upon the environment. In the strongly alkaline oxidative environments it exists mostly as Tc(VII) in the form of pertechnetate TcO_4^-. Reducing conditions, presence of organics and noble metal catalysts promote low oxidation states of Tc, such as Tc(I) tricarbonyl species derived from $[Tc(CO)_3]^+$. Presence of a non-pertechnetate species significantly complicates Tc removal from LAW and its immobilization in the low temperature waste forms. To address this, we have developed novel transition metal based inorganic ion exchange materials that can be applied to tank waste solutions to separate and immobilize all chemical forms of Tc in a one-step process. These materials can be represented by the general formulae $[M_{1-x}^{2+}M_x^{m+}(OH)_2]^{x+}(A^{n-})_{x/n} \cdot yH_2O$ where M^{2+} is a divalent transition metal cation and M^{m+} is a trivalent or tetravalent cation; and A is the interlayer anion (e.g. hydroxide, phosphate, molybdate, tungstate).We have tailored the composition of these materials for the quantitative uptake of TcO_4^- or non-TcO_4^- species from the high nitrate alkaline solutions present in tank waste supernatants and convert them to Tc(IV). Introduction of redox active centers in the composite structure allowed us to maintain the desired +4 oxidation state of Tc and to suppress back oxidation to the highly mobile Tc(VII) upon exposure to the alkaline environments typical for tank waste conditions, preventing its release. This suggests that these materials have potential for both capture as well as a storage medium for Tc. This presentation will focus molecular, structural and electronic properties of these composites, with an effort to identify the Tc-solid matrix interactions which result in uptake. Subsequent distribution and speciation of Tc within the solid matrices will also be discussed using a range of spectroscopic and microscopic techniques FTIR and Raman spectroscopies, X-ray diffraction analysis, scanning and transmission electron microscopies, X-ray photoelectron scattering spectroscopy and UV-visible reflectance spectroscopy.

COMPUTATIONAL MODELING OF ACTINIDES ADSORPTION ON EDGE SURFACES OF MONTMORILLONITE

Alena Kremleva, Sven Krüger, Notker Rösch

Department Chemie, Technische Universität München, 85747 Garching, Germany

Adsorption at mineral surfaces is regarded as efficient retardation mechanism against transport of radioactive elements in the environment. A mechanistic understanding of actinide adsorption at the atomic level is thus an important prerequisite for modeling transport and distribution of these elements in the environment or in geological formations chosen as sites for radioactive waste long-term repositories. Basic fundamental questions in this respect are the nature of the adsorbed species and the sites they occupy. A view on the atomic scale is partly reachable by spectroscopic methods, like EXAFS, TRLFS, FTIR, RAXR, etc. [iii] Quantum chemistry (QC) calculations are a worthwhile complementary approach in this respect.

We study the adsorption of uranyl(VI) and neptunyl(V) on edge surfaces of montmorillonite with the density functional method using the plane-wave based projector augmented wave (PAW) approach as implemented in the program VASP [iv] and periodic supercell models.

One of the major problems when modeling adsorption on mineral surfaces is the proper treatment of surface solvation. In our QC models we include a water layer to account for surface solvation. The optimized structure and the total energy of adsorption complexes depends on the initial structure of this solvation monolayer, which also influences relative energies. More reliable energies of adsorption complexes are achieved by careful equilibrating the water overlayer. To circumvent a computationally very costly fully dynamical approach, a simulated annealing (SA) procedure was developed to equilibrate the structures of various adsorption complexes and to calculate adsorption energies. This procedure is efficient enough to still allow a systematic study of various adsorption complexes at many sites of mineral surfaces. With our advanced approach to surface solvation we determined for the first time the preferred sites of uranyl(VI) and neptunyl(V) adsorption on edge surfaces of 2:1 dioctahedral clay minerals. We were able to suggest most likely adsorption complexes using a charge analysis [v] and surface deprotonation energies. With the help of our new optimization procedure we have shown that the (010) surface is more reactive compared to (110). While a single preferred site for uranyl (and neptunyl) adsorption was found at the (110) surface, the (010) surface offers a set of sites with similar formation energies for uranyl (neptunyl calculations are in progress). Besides the typical five-coordinated uranyl adsorbate, also uranyl hydroxide and a lowering of the coordination number to 4 was calculated for some sites. In contrast to uranyl(VI), NpO_2^+ prefers monodentate adsorption and coordination number 4 is mostly preferred. No hydrolysis on the surface was observed in this case.
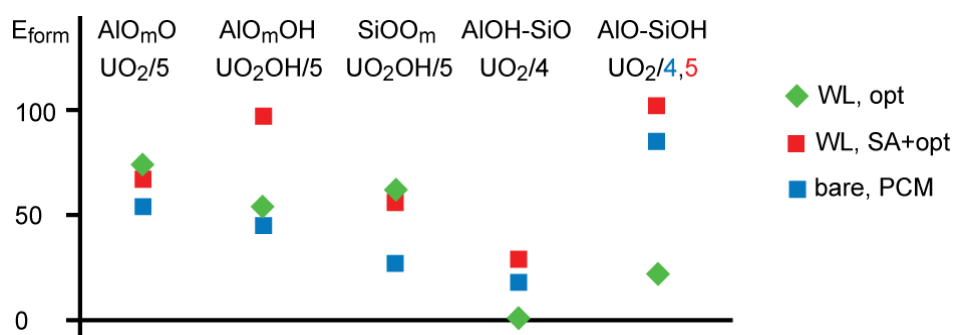
Figure 1. Relative formation energies of uranyl adsorption complexes on various sites of the (110) montmorillonite edge surface with inner substitution. Computational approaches: model with water layer (WL) as surface solvation, optimized (green diamonds); model with water layer as surface solvation, simulated annealing for pre-equilibration and subsequent optimization (red squares); model without explicit water layer (bare), solvation treated by PCM (blue squares).

Another efficient approach to account for surface solvation is to model the solvent by a polarizable continuum model. A pertinent method has recently been implemented in VASP [vi]. In order to validate this new method, we

have optimized uranyl adsorption complexes on the (110) edge surface of montmorillonite. PCM energies are similar to formation energies as determined with the SA approach for UO_2^{2+} as adsorbate, but lower for UO_2OH^+. Comparison of various adsorbed species at the same site with the PCM approach lead to the same preferred species as obtained by SA. Also relative energies of adsorbed uranyl complexes between various sites agree with the results of SA calculations. The polarizable continuum model is also was successfully used for modeling adsorption of Np(V) on edge surfaces of montmorillonite.

ARTIFICIAL NEURAL NETWORKS - ANOTHER VIEW
ON ACTINIDE CHEMISTRY

A. Rossberg[1)*], A. C. Scheinost[1)]

[1)] *Helmholtz-Zentrum Dresden-Rossendorf, Institute of Resource Ecology, Bautzner Landstrasse 400, 01328 Dresden, Germany*

Driven by the enormous increase of computing power in the last few years, several theoretical models for biological neural networks have been developed and new modelling concepts are coming up. Close to their biological counterpart, artificial neural networks (ANNs) have been developed, which can be trained by presenting input data along with the desired output [1]. ANNs are used for example to recognize hand-written text, human faces, natural speech or personal interests, all features now commonly used by web-based social networks like Facebook or by search engines like Google. Another step forward was the development of spiking neural networks, a third generation ANN, which counts at the moment as the closest approximation of biological neural networks [2] and is strongly discussed in the community [3]. In general, ANNs can be considered as a method to infer functional relationships between a cause and the resulting effect. Note that these functional relationships are not inferred from mathematical models; first, the mathematical treatment would be too complex, and second, the required mathematical simplifications by using justified assumptions and constraints would most probably lead to a poor description of the problem. Therefore ANNs are seen as a more efficient and more accurate method to describe complex functional relationships. Here we demonstrate using two examples, that self-organizing maps (SOM) [4,5], a special kind of ANN, are well suited for analysing the complex chemistry of actinides.

The first example shows the relationships between the structure of aliphatic ((di-)hydroxy-)carboxylic acids and their complexation mode towards uranyl (U^{VI}). For this, U L_{III}-edge EXAFS spectra from 13 aliphatic carboxylic acids (acetic, succinic, tartaric, lactic, 3-hydroxybutyric, citric, formic, malic, maleic, malonic, oxalic, propionic, and tricarballylic acid) at a range of pH, uranium and ligand concentrations were measured, resulting in 60 EXAFS spectra [6]. Based on the known structures of the ligands, SOM was used to determine the dependencies between the structure of the U^{VI} carboxylate complexes and the structure of the interacting ligands, and to derive a predictive classification of the former. SOM revealed, for instance, that acids with an OH-group in α-position cause the formation of monomeric chelates and dimeric and trimeric U^{VI} complexes, while an OH-group in β-position leads only to monomers, where uranyl is bidentately coordinated to the carboxylic group. In the second example, we apply SOM to the U L_{III}-edge EXAFS spectra of U^{VI} sorption complexes with Al(hydr)oxides in order to determine the dependency of the structure of the formed sorption complexes on relevant physicochemical parameters like pH, pCO_2, surface area, and surface loading. SOM here clearly reveals, for example, that polynuclear sorption complexes become predominant the higher the pH and the surface loading, while at low pH mononuclear complexes are present either as binary complexes or – in the presence of carbonate - as ternary complexes.

A properly trained SOM can also be used for the prediction of the spectra and the fractions of the complexes for a given ligand and a set of physicochemical parameters, hence SOM can replace thermodynamic speciation calculations, in case complex formation constants are not available. In turn, for a given spectrum, the corresponding physicochemical parameter can be predicted. SOM is not only restricted to EXAFS, but can use input from any other spectroscopy like NMR, UV-vis, infrared and Raman, or from diffraction/scattering patterns -together with chemical information- in order to derive a reliable multiscale speciation of actinides.

[1] D. E. Rummelhart, G. E. Hinton, R. J. Williams, Nature 323, 533 (1986).
[2] W. Maass, Neural Networks 10, 1659 (1997).
[3] A. Grüning, S. M. Bohte, Proceedings of ESANN (2014).
[4] T. Kohonen, Proc. of the IEEE. 78, 1464 (1990).
[5] K. Domaschke, André Rossberg, T. Villmann, Proceedings of ESANN (2014).
[6] C. Lucks, doctoral thesis, Dresden (2013).

WHY IS URANYL FORMOHYDROXAMATE RED?

Silver, Mark A. [1]; Dorfner, Walter, L. [2]; Cary, Samantha K. [1]; Cross, Justin N. [1]; Lin, Jian[1]; Schelter, Eric J.*[2]; Albrecht-Schmitt, Thomas E.*[1]

[1] Department of Chemistry and Biochemistry, Florida State University, 102 Varsity Way, Tallahassee, Florida 32306, United States
[2] P. Roy and Diana T. Vagelos Laboratories, Department of Chemistry, University of Pennsylvania, 231 South 34th Street, Philadelphia, Pennsylvania 19104, United States

Fuel separations was the main topic of discussion in nuclear chemistry in the second half of the twentieth century, and driving research still occurs today. The 1980s and 1990s saw the birth and refinement of the UREx and PUREx processes, separations techniques in which organic ligands are used to coordinate actinide ions in an acid/organic solvent mixture. One such ligand, formohydroxamic acid (FHA), was thought to be an excellent candidate, due to its very unique structural chemistry. Its coordination effects on actinide cations presented in this research leads to its classification as a strong π-donor. The chelating agent features a formaldehyde species with hydroxylamine bound in place of a hydrogen. When FHA coordinates with f-elements, typical oxygen-metal bonds are formed by the bidentate ligand. What is interesting is that a π-bond develops between the nitrogen and neighboring carbon atom upon coordination. This property allows the hydroxamate group to behave aggressively with $5f$-orbitals. In the lanthanide systems, no unique behavior was observed. Crystallization occurs via slow evaporation with elements La, Nd-Gd, and Dy-Lu. It is believed that the reducing ability of FHA may have a negative effect on crystallization with the omitted lanthanides, who are known to have +3 and +4 oxidation states. Typical electronic phenomenon were observed in the UV-Vis spectra of the crystallized $Ln(FHA)_n$. Actinide-FHA complexes, however, exhibited peculiar properties, like red uranyl(VI) and Pu(IV) molecular dimers. In $UO_2(FHA)_2$, distorted hexagonal bipyramids twist in one-dimensional chains in a primitive orthorhombic lattice. These geometric distortions are the result of the strong π-donation of the FHA ligand. In each unit, the uranyl bond bends by 6.5°, as determined from x-ray diffraction data. In addition, large equatorial distortions occur throughout the six "orthogonal" oxygen atoms, whose planarity is offset by 46° at most. This deviation from planarity results in the twist mentioned for the $UO_2(FHA)_2$ system. DFT calculations were performed on the $UO_2(FHA)_2(H_2O)_2$ unit, yielding theoretical results in support of the delocalization of $5f_z^3/6d$ orbital density towards the hydroxylamine μ_3-oxonium, while $2p$ orbital density is donated from the aldehyde oxygen. This exchange of orbital character between ligand and metal offers a complete understanding of the interactions occurring in the structure. Resulting theoretical absorption data for the affected unit matches well with experimental IR, Raman, and solution and solid-state UV-Vis spectra. Typical O≡U≡O peaks in IR and Raman are found near 900 cm^{-1}, whereas in $UO_2(FHA)_2$, the same peak is found 827 cm^{-1}. The hypsochromic shift of the first peak in the solution UV-Vis spectrum is corroborated by the calculated spectra, which attributes the shift of ~50 nm as a result of LMCT. The existence of the second peak is indicative of an unusual electronic structure distortion created by the FHA$^-$-environment. Photoluminescence is also absent in this system which is atypical of uranyl(VI), an effect associated with the π-orbital donation of the ligand. Pu(IV)-FHA displays peculiar geometries and properties as well. Nine-coordinate molecular muffin dimers of $Pu(FHA)_4$ provide a unique environment for the $5f^4$ ion. Notable features in the UV-Vis absorption spectrum of $Pu(FHA)_4$ includes a large charge transfer band which spans nearly the entire visible region, among other typical peaks for Pu(IV). Magnetometric analysis of $Pu(FHA)_4$ displayed nonmagnetic traits, typical of $5f^4$-systems. Complexation with additional actinides Np(VI), Am(III), Cm(III), and Cf(III) is speculated to coordinate mid-$5f$ elements in unseen geometries. Extending from these coordinations will be the effect on electronic and magnetic structure for the transuranic elements.

HYDROLYSIS OF Tc(IV) AND FORMATION OF TERNARY Na/Ca-Tc^{IV}-OH SPECIES IN NaCl/CaCl$_2$ SYSTEMS: A QUANTUM CHEMICAL STUDY

Robert Polly[(1)], Bernd Schimmelpfennig[(1)], Ezgi Yalcintas[(1)], Xavier Gaona[(1)], Marcus Altmaier[(1))]

[(1)] Institut für nukleare Entsorgung, Karlsruher Institut für Technologie, Campus Nord, Postfach 3640, D-76021 Karlsruhe

Technetium–99 is a β–emitting fission product highly relevant for the safety assessment of nuclear waste repositories due to its significant inventory in radioactive waste, long half-life (t½ ~211.000 a) and redox sensitive character. Due to the very reducing conditions expected under repository conditions, an appropriate knowledge of the Tc(IV) aqueous chemistry in NaCl, MgCl$_2$ and CaCl$_2$ systems is required in the context of nuclear waste disposal. Tc(IV) shows a very strong tendency to hydrolyze, which results in an amphoteric behavior and consequent formation of anionic hydrolysis species under hyperalkaline pH conditions. TcO(OH)$_3^-$ is defined as the limiting hydrolysis species forming in dilute to concentrated NaCl and KCl solutions with pH$_m \geq 11$ [1-4]. In concentrated alkaline MgCl$_2$ and CaCl$_2$ solutions, recent solubility studies conducted at KIT–INE hint towards the formation of higher hydrolysis species of the type Mg/Ca$_x$[TcO(OH)$_5$]$^{2x-3}$ (see Fig. 1) [2,4]. Analogous species have been previously reported for An(III), An(IV) and An(V) in concentrated CaCl$_2$ brines [5-7]. In contrast to actinides and because of the very low solubility of Tc(IV), no spectroscopic confirmation of the newly proposed species can be obtained for technetium.

Quantum chemical calculations are well suited to analyze Tc(IV) solvation processes in aqueous solution and to assist in the interpretation of experimental results. At the core of all species investigated in this work is TcO^{2+}. However, so far there are no accurate high level multireference ab initio calculations on TcO^{2+}, allowing a theoretical sound characterization of the lowest electronic states, but only on TcO [8] and density functional theory (DFT) calculations on TcO^{2+} [9].

Fig. 1. Experimental solubility data of Tc(IV) in dilute to concentrated NaCl and CaCl$_2$ systems as reported in [2,4]. Dashed lines corresponding to calculated Tc(IV) solubility in NaCl and CaCl$_2$ media using thermodynamic data reported in [2,4]
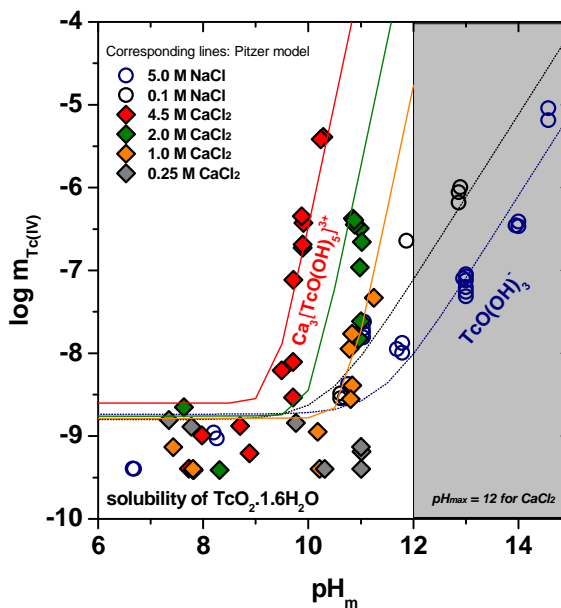
Therefore we performed pilot studies on the TcO^{2+} species with high level multireference Complete Active Space Self Consistent Field (CASSCF) and Multi Reference Configuration Interaction (MRCI) calculations to identify the electronic configuration of the ground states of these species. This is a very important prerequisite for the theoretical sound application of DFT since the application of DFT is restricted to single reference states only!

We used the Stuttgart-type pseudopotentials and the corresponding Gaussian basis set on Tc. For oxygen we applied the cc-pVTZ basis set.

As a result of our multireference calculations we found that the lowest doublet and quartet state of TcO^{2+} are single reference states, respectively (see Fig. 2). We assigned the $^2\Delta$ and the $^4\prod$ quantum numbers to these states.

Hence the ground states of the hydrolysis species $[TcO(OH)_y]^{2-y}$, $Ca_x[TcO(OH)_y]^{2+2x-y}$ and $Na_x[TcO(OH)_y]^{2+x-y}$ are single reference states as well and therefore the application of large-scale DFT calculations is permitted to determine the structure of relevant Tc(IV) species in alkaline NaCl and CaCl$_2$ solutions involving a large number of water molecules and solvated ions in more detail (see Fig. 3).

With this realistic model system we probed the species $[TcO(OH)_5]^{3-}$, $Na_x[TcO(OH)_5]^{x-3}$ and $Ca_3[TcO(OH)_5]^{3+}$. Only for the $Ca_3[TcO(OH)_5]^{3+}$ species enwrapped by one hundred water molecules a stable structure could be found. This was not possible neither for the $[TcO(OH)_5]^{3-}$ species nor for the $Na_x[TcO(OH)_5]^{x-3}$ species. This is a very strong theoretical hint for the existence of the $Ca_3[TcO(OH)_5]^{3+}$ species in alkaline CaCl$_2$ solutions and in agreement with the experimental observation [2,4] that in NaCl solutions no $Na_x[TcO(OH)_5]^{x-3}$ species could be found.

This work highlights the application of quantum chemistry for the study of repository-relevant systems. Further investigations combining solution chemistry and quantum chemical calculations on the systems Tc(IV)–CO$_3$–H$_2$O, Tc(IV)–NO$_3$–H$_2$O and Tc(IV)–S(–II)–H$_2$O are currently on-going at KIT–INE.

The calculations were carried out with MOLPRO and TURBOMOLE.
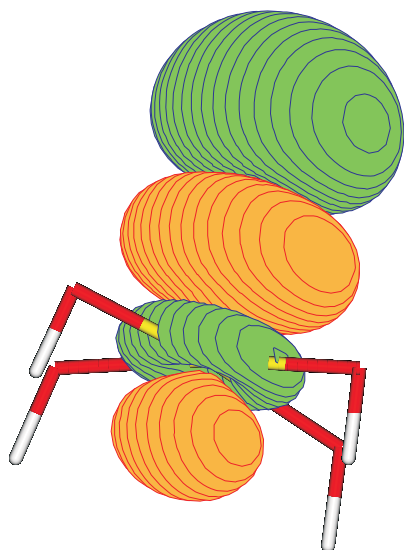
Fig. 2: Bonding d orbital of TcO^{2+}
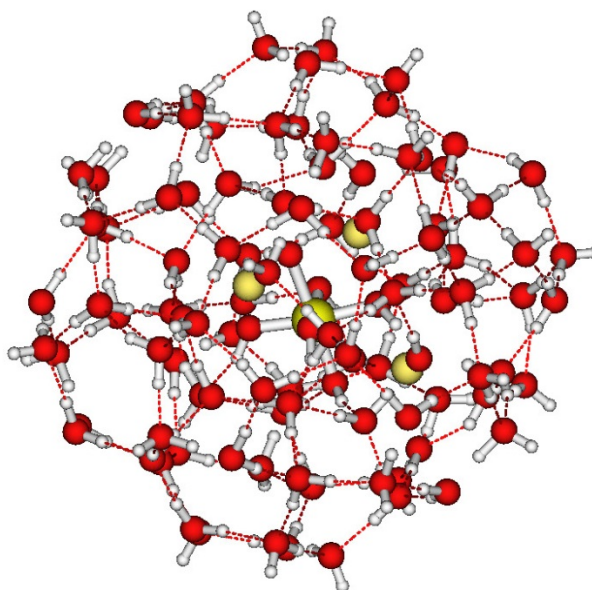
Fig. 3: $Ca_3[TcO(OH)_5]^{3+}$ species surrounded by 100 water molecules

[1] R. Guillaumont, T. Fanghänel, J. Fuger, I. Grenthe, V. Neck, D. Palmer, M. H. Rand, Update on the Chemical Thermodynamics of U, Np, Pu, Am and Tc. Vol.5 of Chemical Thermodynamics(2003), Amsterdam: Elsevier.
[2] E. Yalcintas, PhD thesis, Karlsruhe Institute of Technology (2015).
[3] A. Baumann, Diploma thesis, Karlsruhe Institute of Technology (2014).
[4] E. Yalcintas, A. Bauman, X. Gaona, M. Altmaier, H. Geckeis (2015), poster presentation Migration 2015.
[5] V. Neck, M. Altmaier, Th. Rabung, J. Lützenkirchen, Th. Fanghänel, Pure Appl. Chem. 81 (2009) 1555.
[6] M., Altmaier, V., Neck, T. Fanghänel, Radiochimica Acta, 96 (2008) 541
[7] D. Fellhauer, PhD thesis, Karlsruhe Institute of Technology (2013)
[8] S. R. Langhoff, C. W. Bauschlicher Jr., L. G.M. Pettersson, Chemical Physics 132 (1989) 49.
[9] E. Breynaert, C. E. A. Kirschhock, A. Maes, Dalton Trans. 43 (2009) 9398.

VIOLATION OF BADGER'S RULE FOR THE ANO$_2^{2+}$ IONES (AN=U, NP, PU): A QUANTUM CHEMICAL STUDY

R. Polly[(1)], B. Schimmelpfennig[(1)], P. Lindqvist-Reis[(1)]

[(1)] Institut für Nukleare Entsorgung, Karlsruher Institut für Technologie, Campus Nord, Postfach 3640, D-76021 Karlsruhe

The hexavalent state is the prevalent oxidation state for uranium in aqueous systems under oxic conditions, where it occurs as a linear, dioxo uranyl cation, $[O=U=O]^{2+}$. Under oxidizing conditions also neptunium and plutonium form linear neptunyl and plutonyl cations. Their linear geometry is a result of participation of the 5f orbitals in the actinyl multiple bonds. These bonds are strong and rather unreactive, making the oxo groups to weak Lewis bases. However, the reactivity and the Lewis basicity of the oxo groups depend strongly on the ligands in the equatorial plane and their binding to the metal. By effective σ-donation hydroxide and carbonate ligands are able to polarize the actinyl bond through cis-destabilization and thus increase the Lewis basicity of the oxo groups [1-3]. Such destabilization is reflected by an increase of the actinyl bond distance and a decrease of the symmetric actinyl stretch frequency [3]. If we instead consider a series of actinyl complexes from UO_2^{2+} to PuO_2^{2+}, for example their aqua ions $[AnO_2(H_2O)_5]^{2+}$, the observed changes are counterintuitive and in fact violate Badgers's rule [4]. In this case the rule predicts an increase of the actinyl stretch frequency and the bond force constant on going from uranium to plutonium as the interatomic An=O distance decreases; however, the opposite trend is observed, the stretch frequency and bond force constant decrease down the series [5]. Violation of Badgers's rule is also observed for the corresponding actinyl nitrate, carbonate, and chloride complexes [5-7]. Although it is quite obvious that the origin causing the effect must be of electronic nature, a satisfactory explanation has not yet been established in the literature, despite the effect has been observed and reported by several researchers over the years [6-7].
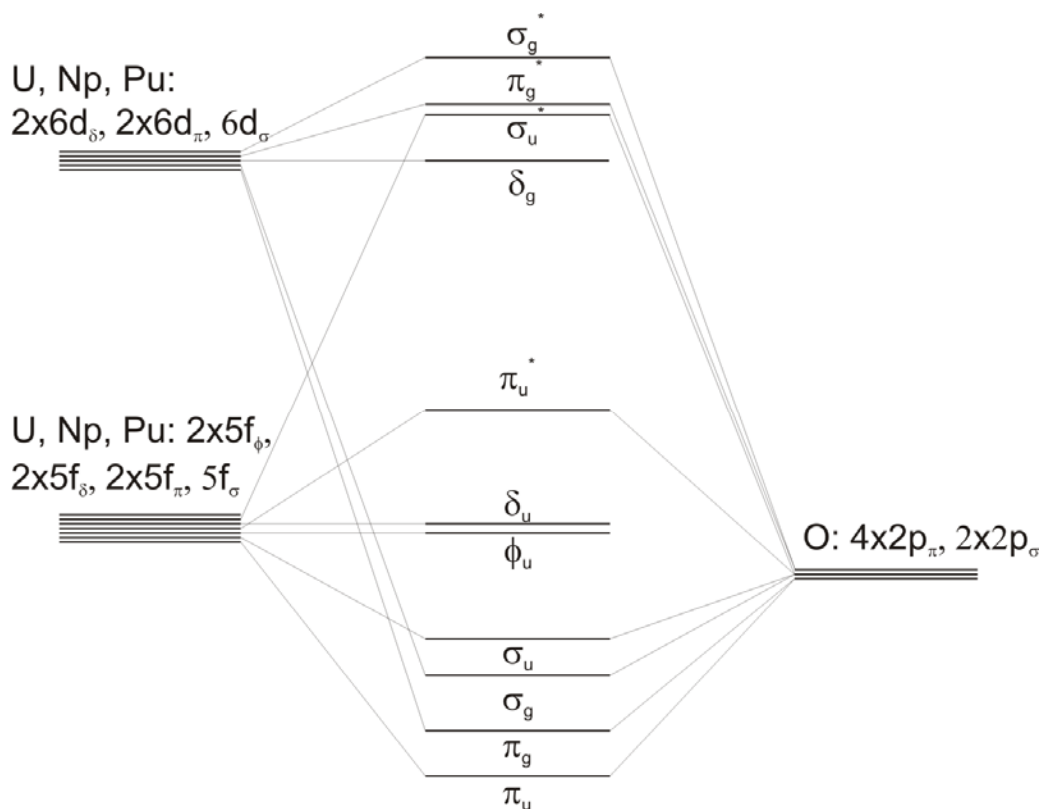
Fig. 1: Qualitative molecular orbital scheme for the AnO$_2^{2+}$ ions

In accord with these experimental findings this 'opposite trend' is also found by theory. Density functional calculations (DFT) of the vibrational

frequencies in $[AnO_2(NO_3)_2(H_2O)](H_2O)$ crystals clearly revealed that the bond lengths decrease from UO_2^{2+} to NpO_2^{2+} and PuO_2^{2+} but the corresponding symmetric vibrational frequencies show an peculiar decrease for the symmetric vibrational frequencies. Already DFT calculations in the gas phase on UO_2^{2+}, NpO_2^{2+} and PuO_2^{2+} revealed the same systematic for these frequencies. Since this effect is already observable in the gas phase we carried out a detailed study of the vibrational frequencies of these three species in the gas phase to understand this peculiar trend in detail.

A crucial role in this effect can be ascribed to the behavior of the 5f electrons of U^{6+}, Np^{6+} and Pu^{6+} which are $5f^0$, $5f^1$ and $5f^2$ systems. The 12 2p electrons of O^{2-} completely occupy the 4 electronic states (π_g, π_u, σ_g, σ_u) of the AnO_2^{2+} species (see Fig. 1) which are formed from the 2p orbitals of oxygen and the 5f and 6d orbitals of the An ions (see Fig. 1). For UO_2^{2+} the ϕ_u and δ_u orbitals remain unoccupied, but for NpO_2^{2+} the ϕ_u is occupied and for PuO_2^{2+} both are singly occupied. This near degeneracy of the ϕ_u and δ_u orbitals or PuO_2^{2+} leads to the strong multireference character of the PuO_2^{2+} ground state.

Accordingly we use multireference ab initio methods like Complete Active Space Self Consistent Field (CASSCF) and Multi Reference Configuration Interaction (MRCI) calculations to understand the violation of Badger's rule in UO_2^{2+}, NpO_2^{2+} and PuO_2^{2+}.

For the CASSCF calculations we set the 1s2s2p3s3p3d4s4p4d4f5s5p5d6s6p orbitals of the An^{6+} ions and the 1s2s orbitals of oxygen inactive and used an active space consisting of all the 5f and the $6d_\sigma$ and $6d_\pi$ orbitals of the An^{6+} ions and the 2p orbitals of oxygen. Hence we correlated 12, 13 or 14 electrons in a total of 16 active orbitals for all three species. As basis sets we empoyed the Atomic Natural Orbital (ANO) basis sets of Roos for the actinides. Due to the large negative charge of the oxygens we had to employ very diffuse basis functions and used Dunnungs doubly augmented d-aug-cc-pVTZ for oxygen.

Since the UO_2^{2+}, NpO_2^{2+} have ground states which can in a very good approximation be described by a single determinant, we also applied CCSD(T) for these species and determined the vibrational frequencies beyond the harmonic approximation to rule out whether anharmonic effects might play a role in the observed effect. This is not the case for PuO_2^{2+} which has a clear multireference ground state due to the near degeneracy of the ϕ_u and δ_u orbitals. Hence the application of DFT or CCSD(T) is not possible for PuO_2^{2+}.

Based on the CASSCF calculations we attribute the peculiar behavior of the symmetric vibrational frequencies to a change of the bonding character from UO_2^{2+}, NpO_2^{2+} to PuO_2^{2+}. Additional population analysis gives further insight into this peculiar behavior.

[1] Arnold, P. L.; Jones, G. M.; Odoh, S. O.; Schreckenbach, G.; Magnani, N.; Love, J. B. Nat. Chem., 2012, 4, 221-227.
[2] Lewis, A. J.; Yin, H.; Carroll P. J.; Schelter, E. J. Dalton Trans., 2014, 43, 10844-10851.
[3] Vallet, V.; Wahlgren, U.; Grenthe, I. J. Phys. Chem. A. 2012,116,12373-12380.
[4] Badger, R. M., J. Chem. Phys., 1934, 2, 128-131.
[5] Skripkin, M., *et al.*, unpublished results, European FP7 TALISMAN project (JRP TALI-C01-07).
[6] Clark, D. L., *et al.*, abstracts of papers of the Am. Chem. Soc., Volume 243, 60-NUCL.
[7] Schnaars, D. D., *et al.* Inorg. Chem., 2013, 52, 14138-14147.

SORPTION OF THORIUM ONTO GRANITE AND ITS CONSTITUENT MINERALS

Y. Iida, T. Yamaguchi, T. Tanaka, K. Hemmi

Nuclear Safety Research Center, Japan Atomic Energy Agency, Tokai, Ibaraki, 319-1195, Japan

Retardation of radionuclide migration by sorption onto a host rock is one of the main geologic factors that influence performance of a radioactive waste disposal system. Performance assessment calculations for hypothetical high-level radioactive waste repositories show that ^{229}Th which is a member of the neptunium series (4n+1) is one of the radionuclides dominating the long–term radiological hazard. Thorium exists only in the tetravalent oxidation state independent of the redox conditions of the groundwater. The dominant aqueous species of Th were estimated to be hydroxide–carbonate complexes in reference groundwaters for the performance assessment from thermodynamic calculations [1].

The sorption behavior of Th onto granite and its major constituent minerals, quartz, feldspar and mica, were investigated by batch sorption experiments. One gram of $Th(NO_3)_4$ nH_2O was dissolved in 10 cm^3 volume of 0.1 mol dm^{-3} HCl. Diluting 0.1 cm^3 volume of the solution to 10 cm^3 with 0.1 mol dm^{-3} HCl, Th stock solution was prepared. Experimental solutions were prepared by adding the Th stock solution into 0.01, 0.1 or 0.2 mol dm^{-3} $NaHCO_3$ solutions.The rock and mineral samples (0.1 g) were immersed in a 10 cm^3 volume of the experimental solutions in polypropylene test tubes.The pH of the sample suspension was adjusted to 6–12 with NaOH solution or HCl. The sample suspensions were agitated once a day. After two weeks, the suspensions were filtered through 10,000 NMWL ultrafilters. The concentrations of Th were determined by ICP–MS.

Distribution coefficients, K_d (m^3 kg^{-1}), for granite are shown in figure 1. The K_d value decreased with increased carbonate concentrations and showed the minimal value at pH 9–10. This sorption tendency was seen for all the rock and mineral samples, and it was likely due to forming the hydroxide–carbonate complexes of Th in the solutions. The order of sorbability for Th was mica > feldspar > quartz ≈ granite.

The sorption behaviors of Th were analyzed by the triple–layer surface complexation model with the Visual Minteq computer program. The inner–sphere surface complexation of Th was assumed [2,3]. Based on the Th aqueous species, the surface species were estimated as follows[4].

$$2\equiv SOH + Th^{4+} = (\equiv SO)_2Th^{2+} + 2H^+$$

$$\equiv SOH + ThOH^{3+} = \equiv SOTh^{3+} + H_2O$$

$$\equiv SOH + Th(OH)_2^{2+} = \equiv SOThOH^{2+} + H_2O$$

$$\equiv SOH + Th(OH)_4(aq) = \equiv SOTh(OH)_3^{0} + H_2O$$
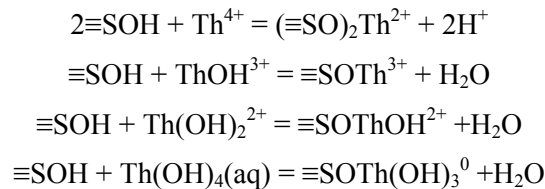
The caluclation results were able to explain the experimental results reasonably well (Fig. 1).
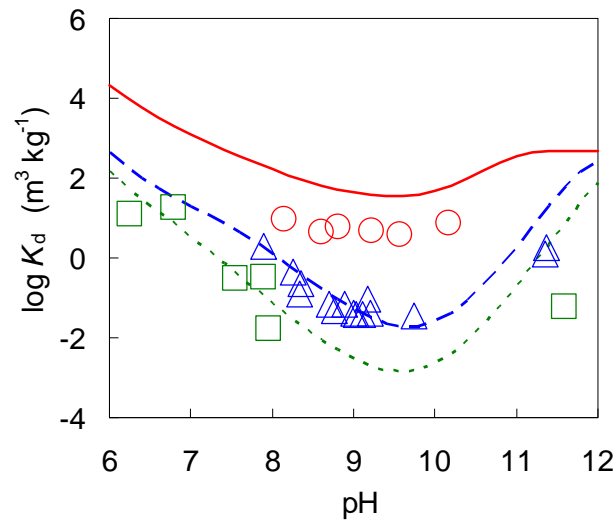
Figure1. The distribution coefficients (K_d) of Th onto granite. The circles, triangles and squares represent the data obtained at 0.01 mol dm^{-3}, 0.1 mol dm^{-3} and 0.2 mol dm^{-3} NaHCO$_3$ respectively. The curves represent the results of the triple layer model calculations.

[1] T. Yamaguchi et al., Radiochim. Acta, 102(11): 999–1008 (2014).
[2] P. Reiller et al., Radiochim. Acta, 91(9), 513–524 (2003).
[3] Z. Hongxia et al., Colloids Surf. A, 278, 46–52 (2006).
[4] M. H. Bradbury et al., Geochim. Cosmochim. Acta, 69, 875–892 (2005).

ROLE OF BENTONITE COLLOIDS AND DESORPTION KINETICS IN TRANSPORT OF CESIUM AND AMERICIUM IN A GROUNDWATER/FRACTURE FILL SYSTEM

T. Dittrich[1], H. Boukhalfa[1], P. Reimus[1]

[1]*Earth and Environmental Sciences Division, Los Alamos National Laboratory, P.O. Box 1663, Mail Stop J966, Los Alamos, NM 87545*

Americium and cesium are known to readily sorb to mineral surfaces found on mobile colloids and geologic media [1,2,3]. We investigated the role of mobile bentonite colloids and sorption kinetics to help quantify transport mechanisms important for upscaling in time and distance to help determine the long-term fate and transport of radionuclides to aid in risk assessment. We selected the fractured and geochemically altered granodiorite at the Grimsel Test Site (GTS) in Switzerland as a model crystalline rock repository system because the system has been thoroughly studied and field experiments involving radionuclides have already been conducted. This system provides a unique opportunity to compare lab experiments with field-scale observations.

Grimsel fracture fill material (FFM) and FEBEX bentonite were characterized (e.g., BET, SEM/EDS, QXRD), and batch and breakthrough column experiments were conducted. Synthetic groundwater that matched the natural water chemistry at the Grimsel site was prepared in the lab. FFM and bentonite samples were crushed, rinsed, sieved, and equilibrated with synthetic groundwater. Bentonite was sodium saturated and settled for 2 weeks to yield a stable suspension. 100 mg L^{-1} bentonite suspensions were equilibrated with Am or Cs and injected through Teflon® microcolumns with 1-5 g of FFM. After normalized effluent concentrations(C/C_0) reached 1, radionuclide-free solutions and/or bentonite suspensions were injected to observe the desorption and release behavior of the sorbed radionuclides.

Aliquots of effluent were measured for pH, colloid concentration, and total and dissolved radionuclides. Unanalyzed effluent from the first column was then injected through a second column of fresh material. For Am, the process was repeated for a third column. Breakthrough results were modeled with a multi-site/multi-rate FORTRAN or MATLAB code [2,3,4,5,6] to elucidate the sorption rate coefficients and binding site densities of the bentonite colloids and fracture fill material. For Am, nearly 50% of the sorbed Am was exchanged from the colloids to the fracture fill material in each of the three columns. Colloids were transported nearly conservatively with a filtration rate constant (k_f) of 0.01-0.02 h^{-1}. The Am desorption rate constants were 0.096, 0.098, and 0.091 h^{-1} for the first, second, and third columns, respectively [6]. Mean residence times were 6-7 h and Peclet numbers ranged from 5-10. When rate constants are normalized to either the FFM mass to solution volume ratio or the FFM surface area to solution volume ratio, the rate constants in these microcolumn experiments are in excellent agreement (~0.002 to 0.003 ml/g-hr) with batch experiments conducted by Huber et al. (2011) [8]. Cs results were similar to Am with repeat injections exhibiting the same desorption rate constants for the first and second columns with similar residence times and Peclet numbers as with Am. The first column breakthrough curves for Am and Cs are shown in Fig. 1.

[1] K. Iijima, T. Tomura, M. Tobita, Y. Suzuki (2010). Distribution of Cs and Am in the solution-bentonite colloids-granite ternary system: effect of addition order and sorption reversibility. *Radiochim. Acta* **98**, 729-736.

[2] Wang, Y., A. Miller, E. Matteo, P. Reimus, M. Ding, T. Dittrich, L. Zheng, J. Houseworth, P. Zhao, A. Kersting, Z. Dai, M. Zavarin (2013). *Experimental and Modeling Investigation of Radionuclide Interaction and Transport in Representative Geologic Media*. US DOE Used Fuel Disposition Report. FCRD-UFD-2013-000314. pp. 44-76.

[3] T.M. Dittrich (2012). *The Role of Desorption Kinetics and Physical Heterogeneity in the Colloid Facilitated Transport of Cesium and Strontium Through an Unsaturated Quartz Porous Medium*. PhD Dissertation. Department of Civil and Environmental Engineering. University of Colorado-Boulder, Boulder, CO.

[4] T.M. Dittrich, P.W. Reimus (2015). Uranium transport in a crushed granodiorite: Experiments and reactive transport modeling. *J. Contam. Hydrol.* **175/176,** 44-59. doi.org/10.1016/j.jconhyd.2015.02.004

[5] T.M. Dittrich, P.W. Reimus (2013) Experimental evaluation of actinide transport in a fractured granodiorite. *Proceedings of the 14th International High-Level Radioactive Waste Mangement Conference*. American Nuclear Society, LaGrange Park, IL, pp. 473-480.

[6] T.M. Dittrich, J.N. Ryan, J.E. Saiers (2011) Role of desorption kinetics on colloid-facilitated transport of cesium and strontium. *Abstr. Pap. Am. Chem. S.* **242,** 1155.

[7] T.M. Dittrich, C.W. Gable, S. Karra, N. Makedonska, S.L. Painter, and P. Reimus (2014). Laboratory investigation of colloid-facilitated transport of americium by bentonite colloids in a granodiorite system. *Crystalline and Crystalline International Disposal Activities.* US DOE Used Fuel Disposition Report. FCRD-UFD-2014-000495. pp. 69-89.

[8] F. Huber, P. Kunze, H. Geckeis, T. Schäfer (2011). Sorption reversibility kinetics in the ternary system radionuclide-bentonite colloids/nanoparticles-granite fracture filling material. *Appl. Geochem.* **26**, 2226-2237.
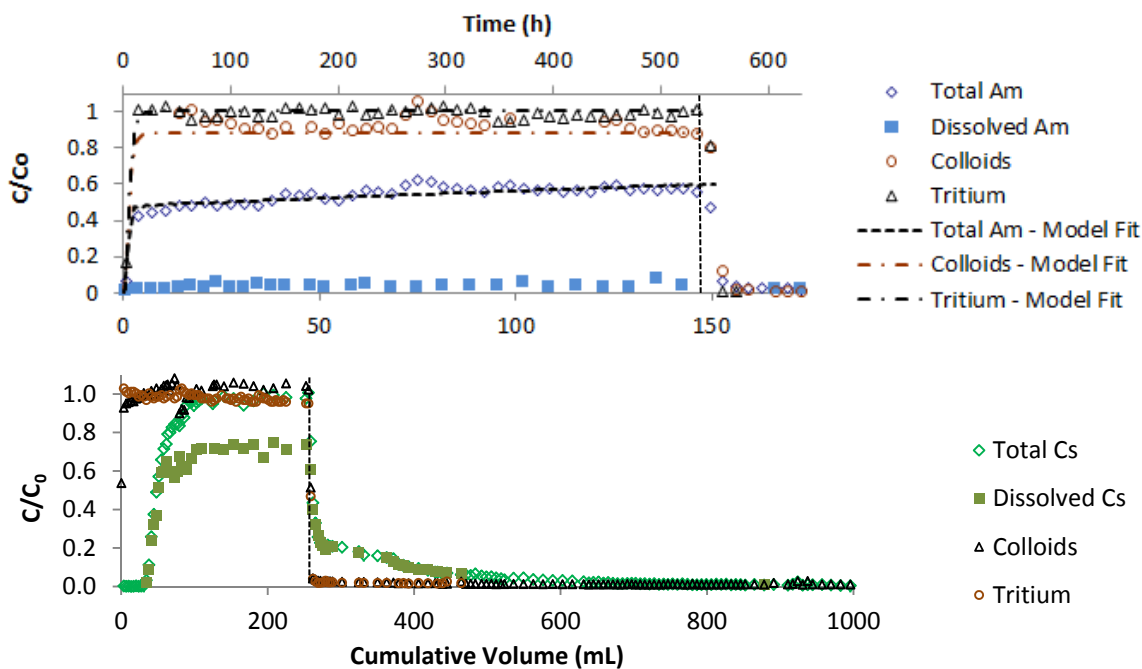
Figure 1. Americium (top) and cesium (bottom) colloid-facilitated transport showing normalized total and dissolved radionuclide concentrations, colloid concentrations, and tritium (conservative tracer). Vertical lines denote when colloid and radionuclide suspension was switched to colloid- and radionuclide-free background solution.

DESORPTION OF CESIUM FROM RIVER SEDIMENTS AND AGGREGATION OF SEDIMENT PARTICLES IN THE BRACKISH WATER REGION OF RIVER SYSTEMS

K. Fujiwara, K. Iijima, M. Terashima, Y. Tachi

Japan Atomic Energy Agency, Fukushima, Fukushima, Japan

Due to the accident of the Fukushima Dai-ichi Nuclear Power Plant, radioactive cesium (Cs) was released in a wide range of areas in and around the Fukushima prefecture, and the deposited Cs was migrated through mountainous forests, rivers, reservoirs to estuaries. Thus, the chemical condition and mechanism governing transport behavior of Cs should be investigated to predict the behavior of Cs in the natural system. It is considered that the most of the Cs was adsorbed to soil particles and migrated through the currents such as rivers. In the brackish water region near the river mouth where a cognate ion (Na, K) concentration increases due to the mixture of seawater, two dynamic evolutions influencing Cs behavior are expected. Firstly, the soil has an ion exchange sites, Cs adsorbed onto ion exchange sites of soil particles is likely to be desorbed. Secondly, decreasing of electrostatic repulsion among clay particles causes aggregation of particles leading to deposition with Cs. In this report, Cs desorption and aggregation of particles such as clays was examined using the seawater of the estuary in the coast and the sediments of the riverbed.

All the desorption and aggregation experiments were conducted under the aerobic atmosphere. The riverbed sediments and estuary seawater of Ukedo and Odaka River running through coastal area of Fukushima and to the Pacific Ocean were used. Sediments were sequentially fractionated by means of sieves of 2 mm and 63 μm, and the fraction under 2 μm was removed by gravity settling. The desorption experiments were carried out by the batch method at solution / solid ratio of 100 mL/g. After aging with periodical hand-shaking for the required contact time ranging from 1 d to 90 d, solid samples were collected by using 0.45 μm membrane filter and dried after washing by de-ionized water. The filtrate was collected in 50ml polypropylene container (8 cm x5 cm) and dried up. Cs concentration of each sample was measured with a Ge semiconductor detector. The aggregation experiments used the fraction under 2 μm. The samples were suspended in the de-ionized water and the time dependences of particle size distribution after spiking the seawater were observed by means of laser diffraction particle size analyser and digital microscope.

In the case of riverbed sediments of 2 mm – 63 μm and 63 μm – 2 μm, the desorption ratios of Cs in seawater were around 40% and 10-20%, respectively. In the case of under 2 μm, no significant desorption was observed. The desorption ratio reached at the steady state around one week. After over 1 month, each sample solutions were exchanged to the fresh seawater, however, further desorption was not observed in all samples. It is considered that the sediment particles have irreversible or kinetically controlled sorption sites even in the relatively large fractions.

Fig.1 shows the suspension sample under 2 μm about 0 and 10 minutes after spiking the seawater. It is considered that particles were quickly aggregated to up to around 20 μm within 10 minutes. On the other hand, a part of particles were still suspended without aggregation even after a few days. The XRD measurements suggested that these suspended particles were mainly composed of SiO_2, while aggregates contained some clay minerals. The samples of Odaka river showed similar behavior. It can be concluded that Cs transported by river systems with soil particles may be partly desorbed and deposit caused by the aggregation of particles near the river mouth.

Figure1. Time dependences of the suspension sample under 2 μm after spiking the seawater.

About 0 min   10 mins
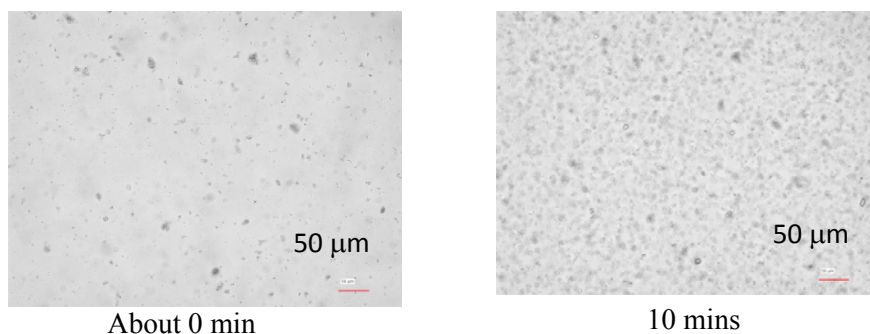
IMPLICATIONS OF DESORPTION EXPERIMENTS FOR COLLOID-FACILITATED PLUTONIUM TRANSPORT

J.D. Begg, M. Zavarin, A. B. Kersting

Glenn T. Seaborg Institute, Physical & Life Sciences, Lawrence Livermore National Laboratory, 7000 East Avenue, Livermore, CA 94550, USA

Plutonium (Pu) release to the environment through nuclear weapon development and the nuclear fuel cycle is an unfortunate legacy of the nuclear age. Accordingly, the behavior of Pu in both surface and sub-surface waters is a topic of continued interest. Recent work demonstrating the importance of colloid facilitated Pu transport has led to renewed study into the adsorption/desorption interactions of Pu with environmentally relevant minerals.

We examined the stability of Pu(IV) adsorbed on colloidal-sized particles of the clay mineral montmorillonite. Plutonium, at an initial concentration of 1×10^{-10} M, was adsorbed onto the clay at pH values 4, 6, and 8 under oxic conditions. Flow-cell desorption experiments were then performed with Pu-free solutions at the corresponding pH. The flow rates were varied in order to investigate the kinetics of desorption and gain a mechanistic understanding of the desorption process. The results indicate a pH dependence to Pu desorption; the extent of desorption was minimal at pH 4.

A simple model was developed to simulate the known Pu redox transformations occurring on the surface of minerals and quantify the various Pu adsorption, desorption, and redox rates. By populating the model parameters as much as possible with existing literature values and results from other experiments performed in our lab, we were able to generate good fits to the data.

The model values have allowed us to make predictions about the residence time of Pu associated with clay mineral colloids in subsurface environments. We generated half-lives for Pu adsorbed on montmorillonite on the order of years. These timescales are consistent with estimated 20-40 year transport times for colloid associated Pu at the Nevada National Security Site (NNSS; formerly the Nevada Test Site)[1] but do not necessarily support transport time on the order of 100s of years.

1. Kersting, A. B.; Efurd, D. W.; Finnegan, D. L.; Rokop, D. J.; Smith, D. K.; Thompson, J. L., Migration of plutonium in ground water at the Nevada Test Site. *Nature* **1999,** *397*, (6714), 56-59.

NEPTUNIUM(V) SORPTION ONTO MONTMORILLONITE AND BENTONITE COLLOIDS AND THE INFLUENCE OF COLLOIDS ON Np(V) TRANSPORT

O. Elo[1)*], P. Hölttä[1)], N. Huittinen[2)], J. Lehto[1)]

[1)] *University of Helsinki, Department of Chemistry, Laboratory of Radiochemistry,*
P. O. Box 55, 00014 University of Helsinki, Finland
[2)] *Helmholtz-Zentrum Dresden-Rossendorf, Institute of Resource Ecology,*
Bautzner Landstr. 400, 01328 Dresden, Germany

In Finland, the SNF repository is going to be at the depth of 450 m in the crystalline bedrock in Olkiluoto at Eurajoki the site proposed by Posiva Oy. The bentonite buffer in EBS consists mainly of montmorillonite which, like other aluminosilicates is known to retain radionuclides, thus, contributing to the retention or immobilization of them. Long-lived Np-237 (2.144×10^{-6} a) in the pentavalent oxidation state forms a neptunyl cation NpO_2^+, which is rather soluble, poorly sorbed and readily mobile making it highly relevant for research concerning SNF repository safety. The potential relevance of colloids for radionuclide transport is highly dependent on the formation of stable and mobile colloids in different environmental conditions and the interaction of radionuclides with the formed colloids. The aim of this work was to investigate the sorption of neptunium on montmorillonite and bentonite colloids and the influence of bentonite colloids on neptunium transport by means of batch sorption and column experiments.

The materials used in this work were Nanocor PNG Montmorillonite (98 %) and a colloid dispersion made from MX-80 bentonite powder. In the previous study, the interaction of neptunium with Na-montmorillonite purified from MX-80 bentonite and corundum (α-Al$_2$O$_3$) was investigated [1]. Corundum was used as a reference mineral in order to study the aluminol surface sites present on clay minerals, which are regarded as the main adsorption sites for radionuclide attachment [2]. We conducted batch sorption experiments as a function of pH (4 – 11) and neptunium concentration 1×10^{-9} to 5×10^{-6} M. The solid-liquid ratio was studied to obtain an optimum mineral concentration needed to conduct batch sorption experiments, in which the amount of montmorillonite is not the limiting factor for the neptunium sorption. Solid concentrations of 0.5 g/l and 5 g/l were used for montmorillonite and 3.3 – 4.0 g/l for bentonite colloids. All sorption experiments were performed under carbonate-free N$_2$-atmospere in 10 mM NaClO$_4$ or NaCl. The samples were made by adding a small aliquot of concentrate montmorillonite or colloid stock solution, Np-237 tracer and a background electrolyte to 20 ml polyethylene vials. The solution was buffered to the desired pH and after one week equilibration time the solid was separated from the liquid by centrifugation and 1 mL aliquots were taken immediately for liquid scintillation counting (Perkin Elmer Tri-Carb 3100 TR liquid scintillation counter).

The effect of bentonite colloids on neptunium transport in granite crushed rock and drill core columns [3] was studied without and with the presence of colloids. Water was pumped through the column at different flow rates using a peristaltic pump to control the water flow rate. A tracer pulse was injected into the water flowing system using an injection loop and the out flowing tracer was collected using a fraction collector. The hydraulic properties in the columns were determined using a conservative tracer without colloids. The column experiments were performed in 10 mM NaClO$_4$.

Np(V) sorption onto bentonite colloids, Na-montmorillonite (MX-80) and corundum in 10 mM NaClO$_4$ is shown as a function of pH in Figure 1. Sorption onto bentonite colloids was rather weak (20 %) at pH 8 and higher adsorption occurred only above pH 10. Sorption isotherms as a function of Np(V) concentration seen in Figure 2 indicates that corundum has sorption capacity for Np(V) higher than that of montmorillonite or bentonite colloids.
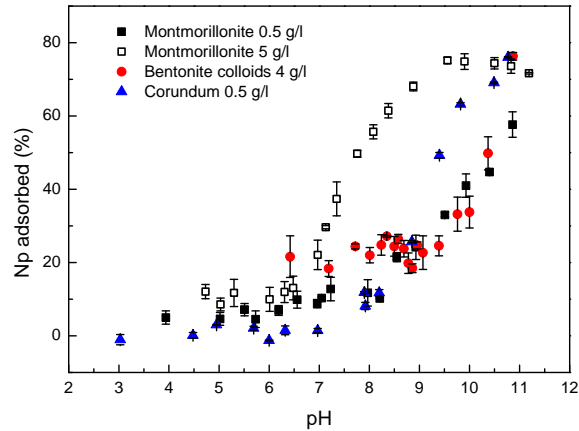
Figure 1. 10^{-6} M Np(V) adsorption onto bentonite colloids, Na-montmorillonite and corundum as a function of pH in 10 mM NaClO$_4$
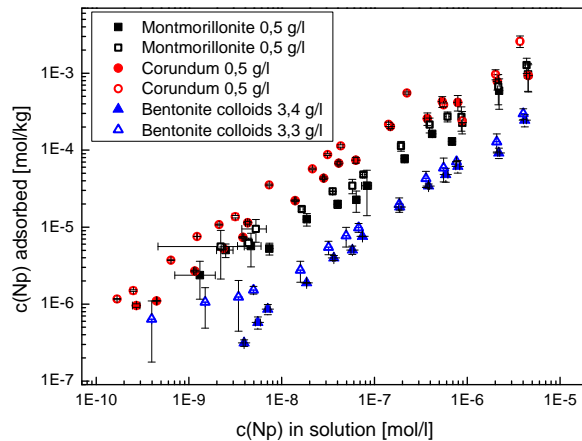
Figure 2. Np(V) adsorption onto corundum, montmorillonite and bentonite colloids as a function Np(V) concentration at pH 8 (solid symbols) and 9 (open symbols) in 10 mM NaClO$_4$ and Np(V) concentration of 10^{-9} to 5×10^{-6} M.

In environmentally relevant conditions for SNF repository, at pH 8, corundum, montmorillonite and bentonite colloids have low and almost similar adsorption capacities for neptunium. The pH and ionic strength can have a great influence on the speciation of actinides, thus batch sorption results are an important source of data for further studies using specific methods. The results from batch sorption and column experiments will be presented and the importance of bentonite colloids on the migration of neptunium will be discussed. This research has received funding from the European Atomic Energy community's Seventh Framework Programme (FP7/2007-2011) under grant agreement n° 295487.

[1] O. Elo, N. Huittinen, K. Müller, A. Ikeda-Ohno, F. Bok, A.C. Scheinost, P. Hölttä and J. Lehto. "Batch sorption and spectroscopic speciation studies of Np-237 on montmorillonite and corundum." Manuscript.

[2] D.R. Turner (1998). Clays Clay Miner. 46 (3): pp. 256-269.

[3] P. Hölttä, M. Siitari-Kauppi, A. Leskinen and A. Poteri (2008). Phys. Chem. Earth 33, 14–16: 83–990.

PU TRANSPORT AT THE NEVADA NATIONAL SECURITY SITE: FIELD EVIDENCE, EXPERIMENTAL DATA, AND CONCEPTUAL MODELS

M. Zavarin, C. Joseph, P. Zhao, J. Begg, M. Boggs, and A.B. Kersting

Glenn T. Seaborg Institute, Physical & Life Sciences Directorate, Lawrence Livermore National Laboratory, L-231, P.O. Box 808, Livermore, CA 94550, USA

The migration of plutonium in groundwater (e.g. Mayak, RU [1], Nevada National Security Site (NNSS, formerly Nevada Test Site), USA [2], and Hanford Site, USA [3]) and surface water (e.g. Rocky Flats, USA [4], Little Forest Burial Ground, AU [5]) has been documented at various locations in the world. In nearly all cases, colloid-facilitated Pu transport has been identified as the dominant mechanism leading to this migration. Importantly, Pu concentrations downgradient from contaminated sites have been consistently low. Both solubility constraints and colloid stability limits likely minimize the migration potential of Pu. Nevertheless, development of a credible conceptual model has been hampered by the lack of experimental data. The single most important process controlling Pu migration in groundwater is Pu stability and desorption from migrating colloids.

To elucidate the mechanisms controlling Pu transport, we have investigated Pu adsorption/desorption rates on montmorillonite and other mineral colloids under controlled laboratory conditions. Pu desorption rates are slow enough that colloid-facilitated transport of adsorbed Pu is possible at the field scale (km distances and decade timescales). Organic matter surface coatings on mineral surfaces could further decrease desorption rates and enhance colloid-facilitated transport [6,7]. However, these data also suggest that Pu concentrations and transport distances will be inherently limited and very sensitive to the desorption rates and flow velocities in the field.

One additional process that may be relevant at the NNSS and under hydrothermal repository conditions is Pu incorporation into secondary mineral colloids during rock alteration. This co-precipitation phenomenon could yield a truly irreversible association of Pu with colloids. This process has been investigated through long-term hydrothermal alteration experiments. Nuclear melt glass collected from underground nuclear tests from the NNSS was hydrothermally altered at 25, 80, 120, and 200°C for nearly three years to mimic processes occurring in the field. Gram quantities of Pu-containing glass were suspended in $NaHCO_3$/NaCl solutions and placed in large volume (600 mL) Ti Parr bomb vessels. The solution and solid phase was sampled at 1.3, 1.8, and 2.7 years.

The colloidal material produced from hydrothermal alteration of the original melt glass consists of secondary clays and zeolites (Figure 1). Although the concentration and composition of the colloids varied with temperature and time, the total Pu activities in solution remained low and were never more than 1 nCi/L (EPA maximum contaminant level for alpha-emitting radionuclides is 0.015 nCi/L). These results provide an upper limit for Pu concentrations at NNSS (Table 1).
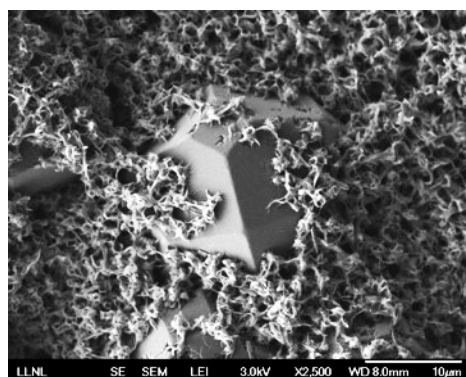
Figure 1. Glass equilibrated with pH 8 $NaHCO_3$/NaCl water at 200C for 3 yrs leads to nearly complete alteration to smectite and zeolite secondary phase colloids.

Follow-on Pu desorption experiments using EDTA extraction revealed that only 2 to 10% of the total Pu associated with the colloidal fraction can be easily desorbed within 3 days. This suggests that the majority of the Pu may be partitioned into alteration phases and inaccessible to desorption processes. Thus, colloid-facilitated

transport of Pu at NNSS may, in part, be controlled by physical filtration processes rather than adsorption/desorption kinetics. However, longterm desorption experiments are still needed to quantify desorption rates and the extent of irreversibility as these rates will determine the fundamental limit of colloid facilitated Pu transport at the NNSS.

Table 1. Summary of Pu concentrations and colloid loads in hydrothermal alteration experiments.

	colloid load			Pu concentration			% colloidal*		
	days			days			days		
	457	644	994	457	644	994	457	644	994
	g/L			pCi/L			percent		
25 ℃	0.000	0.002	0.000	0.7	1.6	0.4	79	88	71
80 ℃	0.011	0.013	0.003	44.2	54.4	58.2	94	94	21
140 ℃	0.239	0.259	0.073	342.5	373.2	304.8	79	90	70
200 ℃	0.070	0.150	0.062	313.7	800.1	125.2	90	68	45

* >20 nm particle size

[1] Novikov, A. P., S. N. Kalmykov, S. Utsunomiya, R. C. Ewing, F. Horreard, A. Merkulov, S. B. Clark, V. V. Tkachev, and B. F. Myasoedov (2006), Colloid transport of plutonium in the far-field of the Mayak Production Association, Russia, Science, 314(5799), 638-641.
[2] Kersting, A. B., D. W. Efurd, D. L. Finnegan, D. J. Rokop, D. K. Smith, and J. L. Thompson (1999), Migration of plutonium in ground water at the Nevada Test Site, Nature, 397(6714), 56-59.
[3] Buck, E. C., D. A. Moore, K. R. Czerwinski, S. D. Conradson, O. N. Batuk, and A. R. Felmy (2014), Nature of nano-sized plutonium particles in soils at the Hanford Site, Radiochimica Acta, 102(12), 1059-1068.
[4] Santschi, P. H., K. A. Roberts, and L. D. Guo (2002), Organic nature of colloidal actinides transported in surface water environments, Environmental Science & Technology, 36(17), 3711-3719.
[5] Payne, T. E., J. J. Harrison, C. E. Hughes, M. P. Johansen, S. Thiruvoth, K. L. Wilsher, D. I. Cendón, S. I. Hankin, B. Rowling, and A. Zawadzki (2013), Trench 'Bathtubbing' and Surface Plutonium Contamination at a Legacy Radioactive Waste Site, Environmental Science & Technology, 47(23), 13284-13293.
[6] Boggs, M. A., Z. Dai, A. B. Kersting, and M. Zavarin (2015), Plutonium(IV) sorption to montmorillonite in the presence of organic matter, Journal of Environmental Radioactivity, 141, 90-96.
[7] Tinnacher, R. M., J. D. Begg, H. Mason, J. Ranville, B. A. Powell, J. C. Wong, A. B. Kersting, and M. Zavarin (2015), Effect of Fulvic Acid Surface Coatings on Plutonium Sorption and Desorption Kinetics on Goethite, Environmental Science & Technology.

MIGRATION OF TRITIUM IN THE LOIRE RIVER ESTUARY: HIGHLIGHT ON ORGANICALLY BOUND TRITIUM IN THE ENVIRONEMENT

O. Péron[1*], C. Gégout[1], B. Reeves[1], L. Pastor[2], E. Fourré[3], F. Siclet[2], C. Landesman[1], G. Montavon[1]

[1]*SUBATECH, UMR 6457, EMN, 4 rue Alfred Kastler, 44307 Cedex 3 Nantes, France*
[2]*EDF, LNHE, 6 quai Watier, 78400 Chatou Cedex, France*
[3]*LSCE, Orme des Merisiers, CEN Saclay, 91191 Gif sur Yvette Cedex, France*

The radioactive isotope of hydrogen, *i.e.* tritium (^{3}H or T), is important to consider in radioecology. Tritium is a beta emitter with a radioactive half-life of 12.3 years. Tritium enters the water cycle in the environment (as HTO for tritiated water) and is tied to the photosynthesis and the metabolism of organic molecules (as OBT for Organically Bound Tritium). Then, it can be transferred to human body through food chain. The OBT is usually distinguished under two forms: tritium covalently bound to carbon atoms, which is supposed to be non-exchangeable (NE-OBT) and tritium bound to oxygen, sulphur or nitrogen, accessible to exchange (E-OBT). According to the ICRP (International Commission on Radiological Protection), NE-OBT presents a non-negligible remanence in the human body with a mean biological period of 40 days, depending on bio-molecular turnover. However this differentiation between NE-OBT and E-OBT is still a subject of discussion. Indeed, the IAEA (International Atomic Energy Agency) in his EMRAS [1] program suggests another definition where NE-OBT includes both covalently bound tritium and buried tritium. The latter is defined as tritium which occupies exchangeable positions in large bio-molecules but cannot be removed by rinsing with tritium-free water [2] for a question of accessibility. These considerations on the nature of the chemical bonds between the exchangeable hydrogen atoms and organic matter are very important. Indeed, tritium levels of the organic matter are most often compared to those of the water of the natural medium. Then, the understanding of the tritium speciation in the environment should enhance bioaccumulation interpretations. The "Livre blanc du tritium" [3] requested by the Nuclear Safety Authority (ASN, France) emphasizes the small impact that tritium releases have in France. However it also shows the need to carry out further study and research in order to supplement current data and knowledge on the behavior of tritium in the environment.

The two objectives of the project are (i) to propose a methodology for determining accurate exchange parameters (α) and (ii) to test it on field samples containing anthropogenic tritium.

In order to estimate the non-exchangeable OBT (NE-OBT) activity, the exchangeable pool of hydrogen within the matrix has to be known.

$$\left(\frac{T}{H}\right)_{total-OBT} = \alpha \times \left(\frac{T}{H}\right)_{E-OBT} + (1-\alpha) \times \left(\frac{T}{H}\right)_{NE-OBT}$$

The fraction of exchangeable hydrogen (α) is determined thanks a dedicated experimental set-up [4]. It consists in a temperature and humidity controlled glove box where the matrix of interest is exposed to a specific atmosphere with a fixed T/H pressure ratio. This approach prevents the dissolution of soluble components which occurs when the exchangeable parameter is measured in the presence of water. The approach was first validated with a model system (cellulose) spiked with deuterated and tritiated vapour. First results quantifying the NE-OBT of cellulose samples will be presented.

Concerning the field samples, mud, sediment core and water samples were recovered from upstream and downstream of several nuclear power plants on the Loire River to the estuary (France). The Loire estuary is the outlet of a watershed where several nuclear power plants are located. Mud and sediment core samples were subjected to freeze-drying and combustion as pre treatment in order to recover free HTO and total OBT respectively. Free HTO (lyophilization water) and total OBT (combustion water) activities from mud samples range from 3.9 ± 0.6 to 26.1 ± 3.2 Bq.L^{-1} and from 10.3 ± 2.8 to 22.9 ± 3.4 Bq.L^{-1}, respectively. ^{3}H activity concentrations of a sediment core were also analysed. Free HTO and total OBT activities from sediment core sections range from 2.6 ± 0.5 to 4.1 ± 0.7 Bq.L^{-1} and from 1.3 ± 1.4 to 13.0 ± 0.4 Bq.L^{-1}, respectively. The overall values can be compared with the EU tritium indicator which is established at 100 Bq.L^{-1}. The average of ^{3}H

volume activities in precipitation over the continental surface in the Northern hemisphere was estimated to be < 3 Bq.L^{-1} in 2012. Quantifying the NE-OBT of these field samples will be the next step.

[1] EMRAS (Environmental Modelling of Radiological Safety) Program, "Modelling the Environmental Transfer of Tritium and Carbon-14 to Biota and Man". Final Report, Tritium and Carbon-14 Working Group. IAEA, Vienna, Austria 2010.

[2] Kim S.B., Baglan N., Davis P.A., "Current understanding of organically bound tritium (OBT) in the Environment", Journal of Environmental Radioactivity 126, 83-91 (2013).

[3] ASN. Livre blanc du tritium. Paris, 2010

[4] Schimmelmann, A., "Determination of the concentration and stable isotopic composition of non-exchangeable hydrogen in organic matter", Analytical Chemistry 63, 2456-2459 (1991).

AN OVERVIEW OF IN-SITU RADIONUCLIDES THROUGH DIFFUSION EXPERIMENT AT ONKALO UNDERGROUND FACILITY

M. Siitari-Kauppi[1], M. Voutilainen[1], K. Helariutta[1], P. Kekäläinen[1], H. Aromaa[1], K. Nilsson[2], P. Andersson[2], J. Byegård[2], M. Skålberg[2], A. Poteri[3], J. Luukkonen[4], L. Koskinen[4]

[1]*Department of Chemistry, University of Helsinki, P.O.Box 55, 00014 University of Helsinki, Finland* [2] *VTT, P.O.B. 1000, 02044 VTT, Finland*
[3]*Geosigma AB, P.O.Box 894, 75108 Uppsala, Sweden*
[4]*Posiva Oy, Olkiluoto, 27160 Eurajoki, Finland*

The final disposal of high-level nuclear waste has been considered to take place in crystalline granitic rock in Finland and the transport of radionuclides in the rock matrix has been subject to extensive research in the safety assessment of the deep geological repositories [1]. A project "rock matrix REtention PROperties" (REPRO) at ONKALO, the underground rock characterization facility in Olkiluoto, consists of an extensive series of in-situ experiments that are supplemented by other experiments from laboratory and estimates of the rock matrix retention properties [2]. The main objective of the REPRO is to investigate rock matrix retention properties under repository conditions and to demonstrate that assumptions that are applied in the safety case are in line with the site evidence.

One of these experiments, in-situ Through Diffusion Experiment (TDE), is planned to be launched during spring 2015. In TDE concentrated mixture of selected radionuclides is circulated for several years in a meter long packed-off section of a drill hole at a distance of 11–12 m from the tunnel wall. Breakthrough of the radionuclides is followed in two observation drill holes about 10 cm away from the injection drill hole. These observation holes are placed so that possible influence of the rock foliation on the diffusion properties could be studied. Decrease of radionuclide concentration in the injection hole is also followed to have more information on retention properties. A large number of supporting experiments are being performed in the laboratory using rock samples from the TDE experimental drill holes. These experiments provide parameters to be used for predicting and analyzing the in-situ experiment and they also give valuable information for sorting out differences between in-situ and laboratory data.

In the current plan the tracer cocktail includes both non-sorbing and sorbing radionuclides: HTO, ^{22}Na, ^{36}Cl, ^{133}Ba, and ^{134}Cs. Non-sorbing nuclides, HTO and ^{36}Cl, can be measured using liquid scintillation technique. As for sorbing nuclides, ^{22}Na, ^{133}Ba, and ^{134}Cs, gamma spectroscopy will be used. From these sorbing nuclides ^{22}Na is only slightly sorbing (distribution coefficient, $K_d = 1\times10^{-6}$–1×10^{-4} m^3/kg) while ^{133}Ba and ^{134}Cs are known to be strongly sorbing ($K_d = 1\times10^{-1}$–1×10^{-3} m^3/kg). The sorbing radionuclides are not expected to diffuse through the rock matrix into the observation holes, except possibly ^{22}Na, and thus the only information is coming from the decrease of their activity in the injection hole. However, previous studies have shown that the decrease will be much more apparent than that of non-sorbing nuclides.

Predictive modeling of TDE was done by solving diffusion equations in cylindrical coordinates with the appropriate initial and boundary conditions. The modelling was based on a non-sorbing nuclide and approximation of the test section by an infinitely long drill hole. In order to estimate timescales of the experiment, we plot the breakthrough curve at distance of the observation hole (r_1) together with conservative estimates for detection limits (low and high) (see Figure 1). Based on these limits detectable amounts of radionuclides will appear in the observation hole when $tD_p/r_1^2 = 0.3 - 0.7$. Here D_p is pore diffusion coefficient and t time from the injection. Three different laboratory techniques were used to measure D_p: Traditional through diffusion measurement using HTO, gas phase measurement using helium, and electrical formation factor measurements. According to these D_p values and the above interval estimated breakthrough will occur after 0.08 to 4.5 years (see Table 1).

In the experimental setup the total volume of the experimental holes (including tubing) is about 250 ml and the total activity and detection limit of HTO are 200 MBq and 0.5 Bq/ml, respectively. These lead to an initial concentration of 0.8 MBq/ml and to the result that relative concentrations of 1×10^{-6} could be detected in the observation hole. Furthermore, if we assume that the result from the HTO through diffusion measurement is the most representative, the breakthrough of HTO is expected to be observed after 0.2 years from the injection. For

[36]Cl similar analysis (the total activity: 5 MBq and detection limit: 0.1 Bq/ml) leads to expected detection of breakthrough after 0.25 years from the injection.
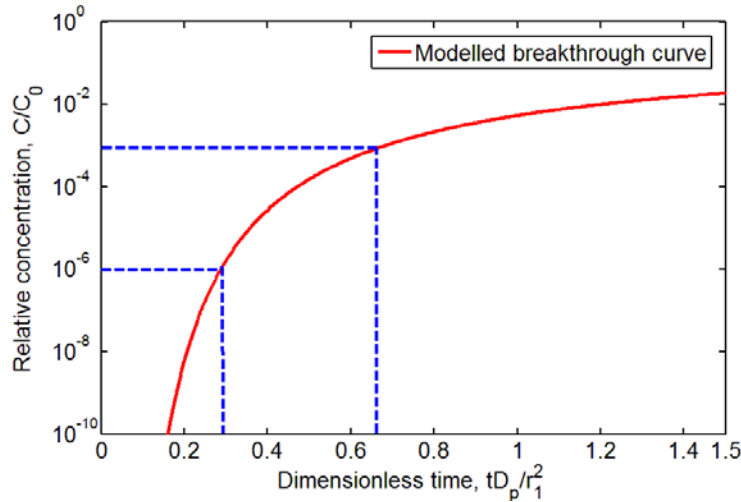
Figure 1. Predictive modeling of TDE shows that a detectable amount of tracer will appear in the observation hole when $tD_p/r_1^2 = 0.3 - 0.7$.

Table 1. Predicted breakthrough times determined for dimensionless times between 0.3 (t_{min}) and 0.7 (t_{max}) and different conservative estimates for D_p according laboratory studies [3].

	D_p [m^2/s]	t_{min} [y]	t_{max} [y]
Minimum	0.4×10^{-11}	1.9	4.5
He-gas average	1×10^{-11}	0.75	1.7
HTO average	4×10^{-11}	0.2	0.4
Formation factor average	6×10^{-11}	0.12	0.3
Maximum	10×10^{-11}	0.08	0.2

[1] Poteri, A., Nordman, H., and Pulkkanen, V.-M. (2014). "Radionuclide transport in the repository near-field and far-field." POSIVA 2014-02.
[2] Voutilainen, M., Poteri, A., Helariutta, K., Siitari-Kauppi, M., Nilsson, K., Andersson, P., Byegård, J., Skålberg, M., Kekäläinen, P., Timonen, J., Lindberg, A., Pitkänen, P., Kemppainen, K., Liimatainen, J., Hautojärvi, A. and Koskinen, L. (2014). "In-situ experiments for investigating the retention properties of rock matrix in ONKALO. Olkiluoto, Finland." Waste Management 2014 Conference Proceedings 40, 14258.
[3] Kuva, J., Voutilainen, M., Kekäläinen, P., Siitari-Kauppi, M., Timonen, J. and Koskinen, L. (2015). "Gas phase measurements of porosity, diffusion coefficient, and permeability in rock samples from Olkiluoto bedrock, Finland." Transp. Porous Med. 107(1): 187-204.

RadFLEx: RADIONUCLIDE FIELD LYSIMETER EXPERIMENT at the UNITED STATES DEPARTMENT OF ENERGY SAVANNAH RIVER SITE

Brian A. Powell[1], Daniel I. Kaplan[2], Laura Bagwell[2], Hilary P. Emerson[1], Fred Molz III[1], Kimberly Roberts[2], Michael Witmer[1]

[1]Department of Environmental Engineering and Earth Science, Clemson University, Anderson, SC 29625
[2]Environmental Science and Biotechnology Division, Savannah River National Laboratory, Aiken, SC 29808

A field scale radionuclide vadose zone transport experiment at the United States Department of Energy Savannah River Site is being operated by Savannah River National Labroatory and Clemson University scientists. In this experiment, radionuclides are buried in 61cm long x 10cm diameter lysimeters which are open to precipitation (Figure 1). Leachate is collected from these lysimeters approximately every three months to provide a measure of radionuclide transport. Most lysimeter sources are placed in triplicate to allow for descructive analysis of the source material and concentration profile within the soil after 2, 4, and 10 years. The radionuclide sources under investigation are (number in parentheses indicates number of active lysimeters):

1. Tc-99 contained within cement (2) and reducing grout (2)
2. Cs-137, Co-60, Ba-133, and Eu-152 in cement (3), reducing grout (3), and soil (3)
3. $Np^{IV}O_2(s)$ (2) and $Np^VO_2NO_3(s)$ (2)
- $Pu^VNH_4(CO_3)$ (6*)
- $Pu^{III}_2(C_2H_2)_3$ and $Pu^{IV}(C_2H_2)_2$ (9*)
- $Pu^{IVO2}(s)$ nanocolloids (4)

Consistent with data from previous field lysimeter experiments with Pu sources, there has been no Pu measured in the effluent from any lysimeter source (*1-3*). Lysimeters containing $Pu^VNH_4CO_3(s)$ with and without organic matter amendments to the soil have been destructively analyzed. The soil was extruded from the lysimeters in approximately 1.5 cm segments and analyzed for Pu. Preliminary data indicate that greater than 99% of the total Pu remained within the source. X-ray absorption spectroscopy indicates that after 2.5 years in the field, reduction of Pu(V) to Pu(IV) within the source occurred. Likely due to the relatively similar behavior of tetravalent actinides, there has been no breakthrough of neptunium in the effluent from the lysimeters containing $Np^{IV}O_2(s)$ sources. After approximately one year, neptunium was measured in the effluent of lysimeters containing $Np^VO_2NO_3(s)$ sources and the concentration of neptunium in the effluent has continued to increase in each quarterly sampling event.

Figure 1: Radionuclide Field Lysimeter Experiment (RadFLEx) at the USDOE Savannah River Site.

The most significant breakthrough occurred in the lysimeters containing Tc-99 with a total of 1 – 12 MBq (10-58% of the initial activity added) measured in the effluent of these lysimeters. After approximately one year of exposure to rainfall, the lysimeters were capped to await analysis of the Tc-99 distribution within the soil. Both upward and downward migration of Tc-99 was observed during destructive sampling. The upward migration was unexpected and is believed to be due to diffusion of Tc-99 in the unsaturated column during the approximately 9 months that passed between capping the Tc-99 lysimeters and performing the destructive analysis.

1. D. I. Kaplan *et al.*, *Environ. Sci. Technol.* **40**, 443 (Jan 15, 2006).
2. D. I. Kaplan *et al.*, *Environ. Sci. Technol.* **38**, 5053 (Oct 1, 2004).
3. D. I. Kaplan *et al.*, *Environ. Sci. Technol.* **41**, 7417 (Nov 1, 2007).

MULTISCALE CHEMISTRY OF U AND Pu AT CHERNOBYL, HANFORD, LOS ALAMOS, McGUIRE AFB, MAYAK AND ROCKY FLATS

Olga N. Batua[a], Steven D. Conradson[a,], Olga N. Aleksandrova[b], Hakim Boukhalfa[a], Boris E. Burakov[c], David L. Clark[a], Ken C. Czerwinski[d], Andrew R. Felmy[e], Juan S. Lezama-Pacheco[f], Stepan N. Kalmykov[g,h], Dean A. Moore[e], Boris F. Myasoedov[h], Donald T. Reed[a], Dallas D. Reilly[e], Robert C. Roback[a], Irina E. Vlasova[g], Samuel M. Webb[i], Marianne P. Wilkerson[a]*

[*]Synchrotron-SOLEIL, Saint-Aubin 91190, France
[a]Los Alamos National Laboratory, Los Alamos, NM 87545, USA
[b]Ural Federal University, Mira Street 19, Ekaterinburg, Russia
[c]V.G. Khlopin Radium Institute, 28, 2-nd Murinskiy Ave., St. Petersburg 194021, Russia
[d]University of Nevada, MSM 245 4505 S. Maryland Pkwy, Las Vegas, NV 89154, USA
[e]Pacific Northwest National Laboratory, PO Box 999 MSIN: K8-96 Richland, WA 99352, USA
[f]Environmental Earth System Sciences Department, 473 Via Ortega, Stanford University, Stanford CA, 94305-4216, USA
[g]Radiochemistry division, Chemistry department, Lomonosov Moscow State University, Leninskie Gory, Moscow 119991, Russia
[h]Frumkin Institute of Physical Chemistry and Electrochemistry of RAS, Leninsky av. 31, Moscow 119071, Russia
[i]SLAC National Accelerator Laboratory 2575 Sand Hill Road Menlo Park, California 94025, USA

The chemical speciation of hazardous elements is a crucial parameter in environmental risk assessment and remediation because it determines the transport and toxicological properties. This tenet applies to uranium and plutonium contamination that arguably constitute the most intractable environmental restoration problems at legacy sites from nuclear weapons production and testing as well as weapons and reactor accidents. Under oxic conditions the stable forms of Pu and U are PuO_{2+x} (actually $PuO_{2+x-y}(OH)_{2y} \cdot z(H_2O)$) and uranyl oxyhydroxides[1,2]. The assumption that U and Pu will form these compounds is, however, derived from laboratory studies of relatively simple systems, controverting indications of the much greater complexity expected in the environment[3,4].

A key assumption in predicting the migration of actinide contaminants is that once released to the environment the original materials will react quickly to form the thermodynamically stable species identified in laboratory experiments. To challenge this assumption, the Å and μm length scale chemical speciation of U and Pu in soil and concrete from Rocky Flats and in particles from soils from Chernobyl, Hanford, Los Alamos, Mayak, and McGuire Air Force Base were determined by a combination of X-ray Absorption Fine Structure (XAFS) spectroscopy and X-Ray Fluorescence (XRF) element maps. These experiments identify three correlations between the speciation and the source terms and histories of these samples: the $Pu(U)O_{2+x}$ from distinct Pu and U components that equilibrated with O_2 and H_2O under both ambient conditions and in fires or explosions; instances of U remaining as UO_{2+x} or U_3O_8 instead of oxidizing to U(VI); and mononuclear Pu-O species and novel PuO_{2+x}- or UO_{2+x}-type compounds incorporating additional elements most likely because the Pu/U were exposed to extreme chemical conditions such as acidic solutions released directly into soil or concrete that mobilized the exposed materials (see Figure 1).

The results identify both expected and novel aspects of the environmental chemistry of U and Pu. In some samples, particles that were in close proximity for decades exhibit different speciation with no indication of convergence to their presumed thermodynamic minima, implying that the observed species are the source terms that were inhibited from oxidation. In other samples they are present in unusual, non-PuO_{2+x} forms, or as the expected oxyhydroxides but with additional elements whose incorporation would have resulted from transitory local conditions and chemical activation resulting from the waste stream or perhaps in combination with chemistry enhanced by surface phenomena. Most importantly, they not only provide the molecular scale chemical speciation information that was incomplete in prior reports of complexity in their environmental chemistry but also suggest possible mechanisms for it that appear to recapitulate the source term and subsequent history after release. The absence of such information causes descriptions and predictions derived from laboratory experiments on pure actinide oxyhydroxide compounds to be incomplete. The accuracy of predictive models will therefore be

greatly enhanced by incorporating into both the codes and laboratory experiments from which they are developed the actual source term, disposal, and subsequent site chemistry that may produce unexpected species formed in these processes.
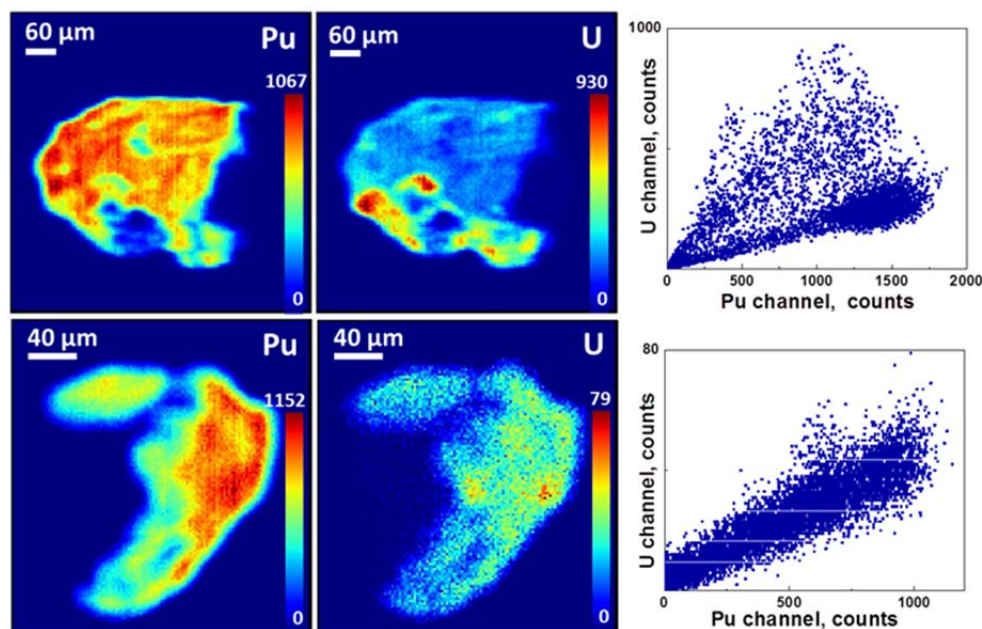
Fig. 1. **μ**-XRF maps of a Pu-U composite particles from McGuire and their Pu-U spatial correlations. One particle (top) is best described as a conglomerate of Pu-rich and U-rich particles that melded without significant mixing, whereas in a second particle (bottom) was presumably subjected to higher temperatures for a longer time the elements are intermingled to give a homogeneous mixture.

References

(1) Conradson, S. D.; Begg, B. D.; Clark, D. L.; den Auwer, C.; Ding, M.; Dorhout, P. K.; Espinosa-Faller, F. J.; Gordon, P. L.; Haire, R. G.; Hess, N. J.; Hess, R. F.; Keogh, D. W.; Morales, L. A.; Neu, M. P.; Paviet-Hartmann, P.; Runde, W.; Tait, C. D.; Veirs, D. K.; Villella, P. M., Local and nanoscale structure and speciation in the $PuO_{2+x-y}(OH)_{2y} \cdot zH_2O$ system. *Journal of the American Chemical Society* **2004,** *126*, (41), 13443-13458.
(2) Burns, P. C.; Finch, R., Uranium: Mineralogy, geochemistry and the environment. In *Reviews in Mineralogy & Geochemistry*, Mineralogical Society of America: Washington, DC, 1999; Vol. 38.
(3) Burns, P. C.; Ewing, R. C.; Navrotsky, A., Nuclear fuel in a reactor accident. *Science* **2012,** *335*, (6073), 1184-1188.
(4) Runde, W., The chemical interaction of actinides in the environment, *Los Alamos Science* **2000**, *26*, 392-411

DEVELOPING TECHNOLOGIES AT A SAVANNAH RIVER SITE TEST-BED TO FACILITATE USE OF ATTENUATION-BASED REMEDIES FOR CONTAMINATED GROUNDWATER

M.E. Denham[*], C.A. Eddy-Dilek, M.R. Millings, M.B. Amidon, and D.I. Kaplan

Savannah River National Laboratory, Aiken, South Carolina, USA

In 2007 a test-bed was established at the Savannah River Site (SRS) to develop and test technologies that facilitate implementation of attenuation-based remedies for contaminated groundwater. The test-bed, run by Savannah River National Laboratory (SRNL), was part of the Applied Field Research Initiatives funded by the DOE Office of Environmental Management's Technology Development Program. Attenuation-based remedies exploit natural attenuation mechanisms or engineered attenuation of contaminants to retard their migration and limit their risk to human health and the environment. For metals and long-lived radionuclides, this means leaving contaminants in the subsurface and requires a high burden of proof that the contaminants will remain in a state of low mobility for long periods of time. The SRS test-bed has focused on developing and testing characterization tools/approaches and long-term monitoring strategies, as well as remediation technologies to allow transition of contaminated sites from active remedies to more passive attenuation-based remedies that minimize costs but are also acceptable to regulators and stakeholders.

The test-bed at SRS is at a site formerly known as the F-Area Seepage Basins. These were three unlined basins into which approximately 7 billion liters of predominantly acidic low-level radioactive waste was disposed from 1955 to 1988. Mobile contaminants travelled through the unsaturated zone and reached the underlying aquifer, ultimately creating a plume with a footprint of 1 km^2 that resurfaces downstream in a near-by wetland and stream. The plume contaminants include tritium, ^{90}Sr, uranium isotopes, ^{129}I, ^{99}Tc, and nitrate. The migration of some of these contaminants is abetted by the acidic nature of the plume with pH values as low as 3.2. The plume is stratified, moving primarily in the bottom 3 meters of the water table aquifer with the migration path influenced by depressions in the top of the clay that separates the upper aquifer from a lower aquifer. The aquifer consists of fine to medium sands with minor kaolinite and goethite. The site is an excellent test-bed because of the well understood contamination history and the wealth of sediment characterization and groundwater monitoring data.

The model for developing new technologies to facilitate deployment of attenuation-based remedies is to integrate the more basic research of the DOE Office of Science (SC) and universities with the more applied research of industry and DOE Office of Environmental Management (EM). An example of this model is research to account for heterogeneity in aquifers, often an impediment to deployment of attenuation-based remedies. SRNL worked with Lawrence Berkeley National Laboratory (LBNL) and Oregon State University to develop the concept of reactive facies and their characterization using geophysics, push-pull tests, diffusion samplers, and acid-base titrations. Remediation technologies were also developed and tested is this way as illustrated by a field test by SRNL of a humate amendment for treatment of uranium in acidic plumes that was developed in the laboratory by LBNL. Collaboration between SC and EM is also being used to understand speciation of ^{129}I and potential remediation strategies at this test-bed. Bringing the expertise of basic and applied researchers together to work on the same site on specific problems associated with attenuation-based remedies has proven to be a successful and efficient way to bring ideas from concept to field testing.

IRON DIFFUSION IN A POROUS MEDIUM: REACTIVE TRANSPORT MODELING WITH DIFFERENT CODES

H. Seher, G. Bracke, H. Fischer, H. C. Moog

Gesellschaft für Anlagen- und Reaktorsicherheit (GRS) gGmbH, Schwertnergasse 1, 50667 Köln, Germany

Data from a laboratory experiment with diffusion of $FeCl_2$ and NaOH in an inert porous medium under anoxic conditions [1] is used to compare the capabilities of two different codes for reactive transport modeling: I) TOUGHREACT [2], and II) MARNIE coupled with ChemApp [3] or PHREEQC [4].

TOUGHREACT [2] developed by LBNL can model two phase flow processes for reactive transport calculations for a large variety of scenarios. The transport code MARNIE is developed by GRS to analyze the long term safety of repositories for high level nuclear waste in deep geological formations. MARNIE can be used for the modelling of the transport of contaminants within repositories in rock salt, which represent the currently favored host rock formation investigated in Germany [5]. The modeling can include a source term for the release of radionuclides from various waste forms e.g. spent fuel, vitrified waste, spent fuel from R&D reactors etc. and retardation of radionuclides e.g. in plugs and seals using the K_d-concept. In order to consider geochemical reactions of radionuclides during transport MARNIE has been coupled with the geochemical codes ChemApp [3] and PHREEQC [4].

For comparing the modeling capabilities of the codes a common thermodynamic database such as THEREDA [6] is needed. Since data from a diffusion experiment with iron is used, thermodynamic data for iron is a prerequisite. This data is currently added to THEREDA which will be released as an updated database in 2015.

The contribution will present and compare the current results of the study using the updated THEREDA database.

1. Seher, H.: Gegendiffusionsexperimente zur Bildung sekundärer Eisen(II)-Phasen aus wässrigen Lösungen in einer chemisch inerten porösen Polyethylenmatrix: Experimentelle Validierung geochemischer Modellrechnungen, Diplomarbeit, Lehrstuhl für Angewandte Geologie, Universität Karlsruhe, 2005.

2. Xu, T., Sonnenthal, E., Spycher, N., Pruess, K.: TOUGHREACT User's Guide, LBNL-55460, 2006.

3. Fischer, H., Martens, K.-H., Moog, H.C.: Kopplung des Transportprogrammes MARNIE mit der Programmierbibliothek ChemApp zur Durchführung thermodynamischer Gleichgewichtsrechnungen. GRS-A-3264, 2007.

4. Fischer, H., Seher, H., Bracke, G.: Untersuchungen zur Kopplung des Transportprogrammes MARNIE mit dem geochemischen Rechencode PHREEQC, GRS-334, ISBN:978-3-944161-14-3, 2014.

5. Larue, J., Baltes, B., Fischer, H., Frieling, G., Kock, I., Navarro, M., Seher, H.: Radiologische Konsequenzenanalyse, GRS-289, ISBN 978-3-939355-65-6, 2013.

6. Moog, H.C., Bok, F., Marquardt, C.M., Brendler, V.: Disposal of nuclear waste in host rock formations featuring high-saline solutions – Implementation of a thermodynamic reference database (THEREDA). Applied Geochemistry, DOI 10.1016/j.apgeochem.2014.12.016, 2015 (in Press).

REACTIVE TRANSPORT OF RADIONUCLIDES IN THE INTERFACE BETWEEN EBS AND THE HOST ROCK: MODEL DEVELOPMENT BY COUPLING LATTICE BOLTZMANN METHOD AND PHREEQC

Jung-Woo Kim[1], Je-Ho Min[2], Min-Hoon Baik[1]

[1] *Radioactive Waste Disposal Research Division, Korea Atomic Energy Research Institute, 989-111 Daedeokdaero, Yuseong-Gu, Daejeon 305-353, Rep. of Korea*
[2]*Korean Association for Radiation Application, 77 Seongsuil-ro, Seongdong-gu, Seoul 133-822, Rep. of Korea*

Geological disposal system of radioactive wastes generally includes engineered barrier system(EBS) and natural barrier system(NBS)[1]. From a safety standpoint, migration of radionuclides through the disposal system should be well understood. Bentonite, which has high swelling pressure and low permeability, is regarded as one of the most feasible buffer materials for the EBS, and a crystalline rock, which can have a fracture network, is frequently represented as an option for the host rock in many countries[2]. Owing to the two different materials, the hydrological and geochemical conditions are changed in the interface between EBS and the host rock. When the radionuclide migration is estimated in the interface, those transition conditions would be a challenging factor especially for the modeling purpose. In that context, a numerical model for the reactive transport of radionuclides in the interface between EBS and the host rock was developed by coupling lattice Boltzmann method(LBM) and PHREEQC in this study.

Firstly, the fluid flow and the solute transport were simulated by LBM and then the geochemical reactions at each lattice node were computed by PHREEQC at every time step. The overall procedure is depicted in Fig. 1. Key steps of LBM are streaming and collision of the particles. The BGK approximation for collision was used as the simplest approach using a single relaxation time. For the field-scale application, the gray-scale porous media was incorporated in LBM. That is, the lattice node properties reflected the local porosity or permeability, and a partial bounce back concept was applied[3]. In this context, the macroscopic variables, such as fluid density(ρ), fluid velocity($\mathbf{u}$), and solute concentration(C), should be modified as follows: $\rho = \sum f / V$, $\mathbf{u} = \sum \mathbf{e} f / \rho V$, and $C = \sum f_s / V$ where f and f_s is the particle distribution function of fluids and solutes, respectively, $\mathbf{e}$ is the discrete velocity vector, and V is the pore volume at each lattice node. PHREEQC module was coupled to LBM according to Charlton and Parkhurst's method[4] and the overall LBM-PHREQC model was coded using MATLAB.

For the verification of LBM-PHREEQC, a simple example of 1D reactive transport including the cation exchange was computed and the results were compared with the results from PHREEQC itself (Fig. 2). Both models could reveal that initially adsorbed Na$^+$ and K$^+$ were sequentially flowed out by cation exchange with Ca^{2+} which was injected, and then Ca^{2+} was flowed out just after the depletion of Na$^+$ and K$^+$. The difference between the results from PHREEQC and LBM-PHREEQC, especially for K$^+$ and Ca^{2+}, was presumably originated from the scale difference.

For more specific application of LBM-PHREEQC to the radioactive wastes, thermodynamic sorption of strontium on bentonite was investigated by considering ion exchange(IE) and surface complexation(SC) processes. From the results in Fig. 3, the sorption of Sr(II) on bentonite by ion exchange was dominant at low pH while surface complexation was dominant at high pH. This indicates that both sorption mechanisms should be considered at the same time in the interface between EBS and the host rock where the groundwater has nearly neutral pH.

Although the feasibility of LBM-PHREEQC was carefully confirmed in this study, it is still needed to study further about the upscaling.
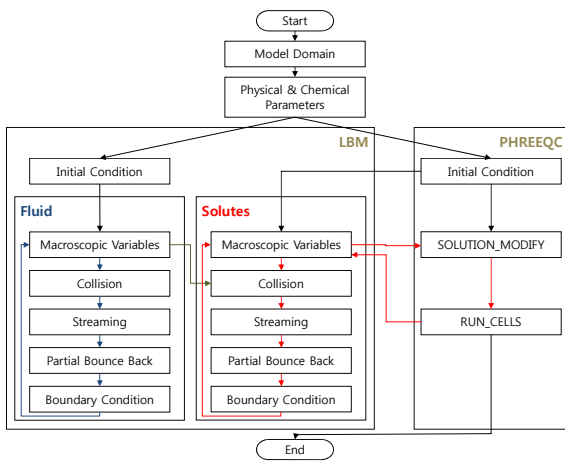
Figure 1. Overall procedure of LBM-PHREEQC.
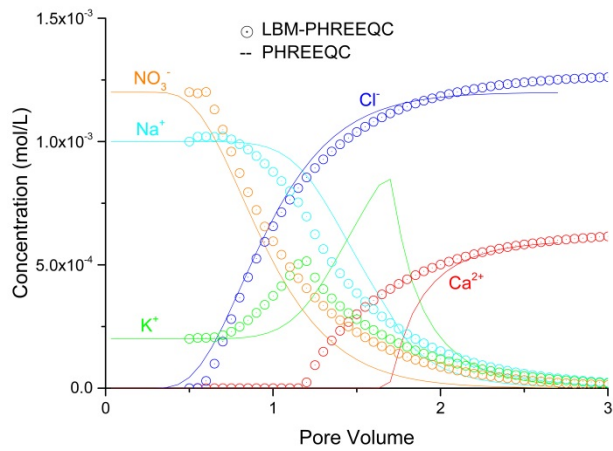
Figure 2. Examples of solute breakthrough in 1D reactive transport including the cation exchange: Comparison between results from PHREEQC only and LBM-PHREEQC.
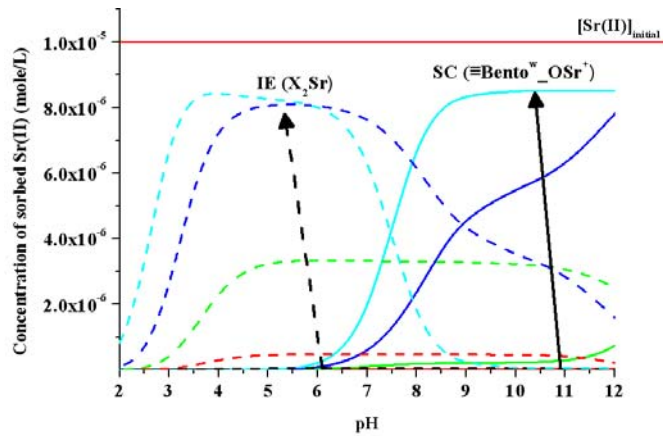
Figure 3. Concentration of Sr(II) sorbed on bentonite as a function of pH for each sorption mechanism, ion exchange(IE) and surface complexation(SC).

[1] KAERI, KAERI/TR-4525/2011 (2011).
[2] SKB, SKB/TR-11-01 (2011).
[3] S. Anwar, A. Cortis, M.C. Sukop, Progress in Computational Fluid Dynamics 8, 213 (2008)
[4] S.R. Charlton, D.L. Parkhurst, Computers & Geosciences 37, 1653 (2011).

DISSOLUTION RATES AND MECHANISMS OF URANYL OXYHYDROXIDE AND PHOSPHATE MINERALS IN FLOW-THROUGH COLUMN EXPERIMENTS

E. Reinoso-Maset[1,*], W. Um[2], J. Chorover[3], C. Steefel[4], P. A. O'Day[1]

[1]*Sierra Nevada Research Institute, University of California, Merced, CA, USA*
(*ereinoso-maset@ucmerced.edu)
[2]*Pacific Northwest National Laboratory, Richland, WA, USA*
[3]*University of Arizona, Tucson, AZ, USA*
[4]*Lawrence Berkeley National Laboratory, Berkeley, CA, USA*

Understanding dissolution, desorption and mineral transformation in simple systems at a molecular scale is crucial for improving predictions of uranium transport and fate in complex subsurface systems over time. In this work, the dissolution mechanisms and rates of two uranyl oxyhydroxide (compreignacite, $K_2(UO_2)_6O_4(OH)_6 \cdot 7H_2O$, and Na-compreignacite, $Na_2(UO_2)_6O_4(OH)_6 \cdot 7H_2O$) and two uranyl phosphate (meta-ankoleite, $KUO_2PO_4 \cdot 4H_2O$, and Na-autunite, $NaUO_2PO_4 \cdot 4H_2O$) minerals were investigated in flow-through column experiments using two different simulated groundwaters with low and high dissolved total carbonate (0.2 and 2.8 mM). Dissolution rates were measured for each mineral using 1 cm^3 columns filled with U-mineral:quartz mixture and leached upwards (0.037 mL min^{-1}) for up to 11 days, corresponding to 2000 pore volumes (PV). After the column reaction, solid samples were analyzed by EXAFS to identify changes in U speciation.

In the first 200 PV, high U release was correlated with K and Na release from the mineral structures, and congruent dissolution of P was also observed for the uranyl phosphate minerals. In the Na-compreignacite and low carbonate groundwater experiments, K from the input solution was strongly retained in the column. The EXAFS spectrum of reacted Na-compreignacite was best fit by linear combination of K-compreignacite and U(VI) sorbed on quartz reference spectra, suggesting the exchange or removal of Na from the mineral structure. In experiments with high dissolved carbonate, over 60% of total U was released from each mineral, whereas only 0.5% of total U was dissolved in low carbonate groundwater. In these latter systems, apparent steady state was reached at 800 PV for the uranyl oxyhydroxides, and pseudo-first order dissolution rates for K- and Na-compreignacite were $8.8 \cdot 10^{-13}$ and $2.5 \cdot 10^{-12}$ mol m^{-2} s^{-1} respectively. The U release from the uranyl phosphate minerals was one order of magnitude lower than the oxyhydroxides but showed a linear increase over time. The dissolution rate at 2000 PV was $7.1 \cdot 10^{-13}$ and $1.3 \cdot 10^{-12}$ mol m^{-2} s^{-1} for meta-ankoleite and Na-autunite respectively. Dissolution with high carbonate groundwater did not reach a distinct steady state after the length of the experiments.

Experimental and spectroscopic results suggest that in low carbonate systems the rate-determining step for K-compreignacite dissolution is desorption of uranyl from an altered surface layer. For Na-compreignacite, exchange of Na for K destabilized the mineral structure and enhanced dissolution rate. Higher dissolved carbonate significantly accelerated the dissolution of K- and Na-compreignacite, likely due to the formation of aqueous uranyl carbonate complexes, which equally controlled the dissolution mechanism for both minerals. Dissolution of meta-ankoleite and Na-autunite presented similar trend, but future spectroscopic analyses of the reacted columns will elucidate changes in the mineral phases and, consequently, potential differences in the dissolution mechanisms between uranyl phosphate end-members. Reactive transport modeling (Crunchflow) incorporating mineral dissolution, ion exchange, sorption and complexation reactions will also be reported.

DEVELOPMENT OF CHEMICAL SPECIATION MODELS INCORPORATING KINETICS AND TRANSPORT FOR THE INTERACTION OF RADIONUCLIDES AND DISSOLVED ORGANIC MATTER

L. Abrahamsen, N. Bryan, K. Smith

National Nuclear Laboratory, Chadwick House, Birchwood Park, Warrington WA3 6AE, UK

Chemically heterogeneous and polydisperse ligand mixtures such as humic acid (HA) and fulvic acid (FA) exhibit a range of metal ion binding sites and equilibrium constants. Generally, their incorporation into speciation and transport models is complex, because they have a distribution of metal ion affinity and protonation constants. The work described aims to couple an existing model of the interaction of metal ions with HA with the more versatile chemical speciation code PHREEQC, which includes a 1-D transport function. As well as transport, the model test case developed here also includes the effects of surface complexation, the kinetic properties of HA complexation, as well as the kinetic sorption and desorption of the complex.

An existing model for the interaction of metal ions with HA and FA is MODEL VII [1]. Combined with the speciation code WHAM (Windermere Humic Aqueous Model), it is referred to as WHAM-VII and can simulate these systems over a wide range of conditions. Although WHAM-VII can account for the interaction of radionuclides with humic substances whilst taking into account the effect of simple inorganic species formation, it cannot take into account many physico-chemical processes that are important, e.g. surface complexation, kinetics and transport. The chemical speciation code PHREEQC can simulate these effects, but it cannot take account of humic substance complexation directly.

HA molecules initially bind metal ions via an equilibrium process. This fraction is termed 'exchangeable' since the metal is still able to exchange with solution and can dissociate instantaneously. Over time, some metal transfers to a distinct, *non-exchangeable* fraction, and dissociation from this fraction is slow, regardless of the strength of the competing sink [2]. Depending on the rate of advection, these kinetic interactions could have an impact on migration rates. If the rate of flow is fast compared to the release of metal ions from the complex, then migration could be enhanced.

A PHREEQC model has been developed by incorporating a solution species that can mirror the predictions made by WHAM-VII, enabling complex speciation problems to be solved. This includes the equilibrium interaction between a metal ion and the humic species (derived from WHAM-VII), the kinetic processes controlling the speciation of the metal-HA complex (see below), the kinetic sorption of this complex onto a surface, the surface complexation of free metal onto the surface and the advection of the solution along a 1-D column. The processes are outlined in Figure 1.
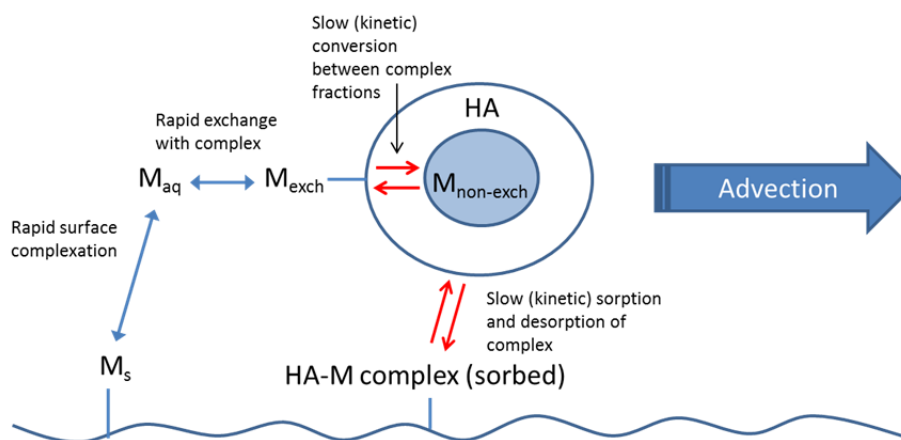
Figure 1 – Physico-chemical processes considered by the model

This novel modelling approach enables the assessment of the importance of dissolved organic complexants,

including natural organic matter in the form of HA, in controlling the solubility, sorption and migration of metallic pollutants in a range of effluent and environmental systems.

[1] Tipping, E; Lofts, S; Sonke, JE (2011). Environmental Chemistry, 8, 225-235.

[2] Bryan, ND; Abrahamsen, L; Evans, N; Warwick, P; Buckau, G; Weng, LP; Van Riemsdijk, WH (2012). App.Geochem. 27, 378-389.

RADIONUCLIDE MIGRATION IN LONG-TERM STORAGE CONCEPTS OF RADIOACTIVE WASTES ORIGINATED FROM AN URANIUM TREATMENT PROCESS

Marek Pękala, Salvador Jordana, Alba Valls and Lara Duro

Amphos 21, P. Garcia i Faria 49-51, 1-1, Barcelona E-08019 (Spain)

This work presents a reactive transport model developed to compare different concepts proposed for the long-term management options of the wastes currently existing in a natural uranium conversion site in the south of France. One of the concepts is surface storage, with a low permeability clayey capping, and the two others are sub-surface storages in geological host rocks from Oligocene.

Hydrogeological and geochemical conceptual models have been developed and numerically implemented in a coupled reactive transport code COMSOL-PhreeqC. Radioactive decay and ingrowth is also incorporated in the coupled model when relevant for the obtained conclusions. The model is focused on the calculation of the evolution of the system until 50,000 years after disposal closure and assesses the behaviour of Th, U, Pu, Tc, Ra, As, Cd, Mn, Mo, Ni, Pb and Se.

The geochemical model assumes equilibrium with calcite and gypsum and equilibrium with ferrihydrite and siderite to simulate the major composition of pore water. Redox is assumed to be controlled by the iron system, given the lack of agreement between the measured redox and the speciation of other redox pairs in the wastes and tailings, such as the nitrate/ammonia or the sulphate/sulphide systems (redox disequilibrium). This led towards the use of a thermodynamic database where the sulphate and the nitrate redox systems were de-coupled, meaning that sulphate was not allowed to be reduced to sulphide and nitrate was not allowed to be reduced to ammonia or other lower redox states. Given that microbial effects were not included, this is a sensible approach for this system.

An assessment of the chemistry of the different elements was conducted and a selection of the processes able to account for the retardation of the elements in the different domains of the system was made. Most of the trace components are present in too low concentrations as to form individual solid phases under the predominant chemical conditions, thus association with major components of the solid wastes is accounted for such as coprecipitation and sorption. This observation is consistent with experimental analyses of the waste materials.

The parameterisation of the geochemical processes was done on the basis of information available in the literature. Radioactive decay was implemented for 226Ra (ingrowth from 230Th and decay), after conducting an assessment of the relevance of decay and ingrowth processes over the 50,000 years of the simulation under the expected conditions of the systems.

The evolution of the concentration of the different elements at various monitoring points away from the disposal has been calculated. A sensitivity analyses on the different properties of the engineering barriers and the stability of the wastes has been also conducted by means of advanced 3D flow and transport simulations. Four general factors control the environmental impact reduction of the waste: 1) initial form in which the contamination is present (source term), 2) regional groundwater flow field, 3) retardation properties of the host rock, and 4) the presence of engineered barriers (which affect both local groundwater flow near the waste and retardation during transport).

REACTIVE TRANSPORT MODEL ACCOUNTING FOR (GEO-)CHEMICAL AND PHYSICAL PROCESSES TAKING PLACE IN THE NEAR-FIELD OF A GENERIC SPENT NUCLEAR FUEL REPOSITORY IN A DEEP CLAY ROCK FORMATION.

Sanjay Dubey[1, 2], Vanessa Montoya [1], Florian Huber[1], Volker Metz[1], Bernhard Kienzler [1]

[1] *Karlsruhe Institute of Technology, Institute for Nuclear Waste Disposal (KIT-INE), Karlsruhe, Germany*
[2] *Ecole des Mines de Nantes (EMN), Nantes, France*

Quantitative calculations of radionuclide release and migration are necessary to evaluate the safety of the different engineered barriers and geometry included in a geological disposal concept. The objective of this work is to develop a reactive transport model accounting for (geo-) chemical and physical processes taking place in the near-field of a generic spent nuclear fuel (SNF) repository in a deep clay rock formation. The modelling approach considers coupled processes which potentially occur during a period of thousands of years. The system studied is implemented in the iCP interface [1], which couples two different codes: the Finite Element code COMSOL Multiphysics V.5 [2] and the geochemical simulator PHREEQC v.3.1.7. [3].

Geometrical and physic-chemical properties (i.e. diffusion) in 2D have been implemented in COMSOL Multiphysics (see Fig 1). The (geo-) chemical conceptual model calculations has been setup in the geochemical modelling module PHREEQC v.3.1.7. Chemical reactions (precipitation/dissolution) of major components and radionuclides at equilibrium have been simulated using parameters and data from the thermodynamic database ThermoChimie v.9. [4]. Porosity changes due to mineral precipitation/dissolution and feedback on transport is taken into account. Steel corrosion is considered to be kinetically controlled and progressing with a constant rate and generation of magnetite and hydrogen is included in the model. Sorption mechanism (cation exchange and surface complexation) and competition effects with the major background dissolved elements (e.g. Ca, Mg, Fe, K and Sr) are also considered.
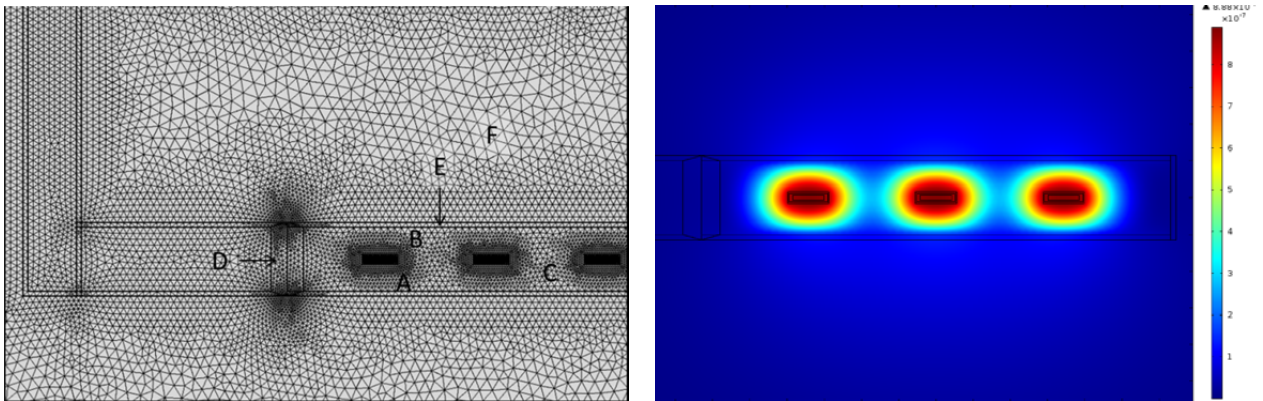
Figure1. (left) 2D -Geometry and computational mesh of the studied system, representing A) the SNF, B) the steel container, C) bentonite, D) cement plug, E) cement liner, F) Surrounding clay rock. (right) migration of $^{129}I^-$ after 100 years

Simulation calculations with respect to reactive transport processes in a fully saturated isothermal system of a mobile anion (e.g. $^{129}I^-$), a relatively mobile cation (e.g. $^{137}Cs^+$) and a less mobile safety relevant radionuclide (e.g. Am^{3+}) have been carried out. The studied multi-barrier system barrier is composed of the waste form (spent fuel), the steel canister, the bentonite buffer, the cement liner and cement sealing as well as the clay host rock in the vicinity of the repository. A mechanistic specific migration model is defined separately for each radioactive element in each barrier. As example, an initial concentration of $\sim 10^{-5}$ M for I and Cs^+ in the waste is assumed. $^{129}I^-$ presents the higher mobility, diffusing from the waste to the bentonite barrier resulting in concentration up to 3

x10^{-7} M in 100 years (see Figure 1). Cs$^+$ can diffuse and sorb in the different barriers. In contrast to these fast release elements iodine and caesium, the release of Am^{3+} from the waste is modelled by solubility of hydroxo-carbonate phases. Sorption and precipitation in the different barriers is taken into account. The computed results show that diffusion of Am^{3+} is significantly retarded in comparison to I$^-$ and Cs$^+$. Am is sorbed in a small region of the bentonite barrier. Calculations over thousands of years will be presented.

[1] Nardi A., Idiart, A., Trinchero, P., de Vries L. M., Molinero, J. (2014) Interface COMSOL -PHREEQC (iCP), an efficient numerical framework for the solution of coupled multiphysics and geochemistry, Computers & Geosciences 69, 10-21.

[2] COMSOL (2014) COMSOL-Multiphysics. Version 5.0, www.comsol.com

[3] Parkhurst and Appelo (2013) Description of input and examples for PHREEQC version 3—A computer program for speciation, batch-reaction, one-dimensional transport, and inverse geochemical calculations, U.S. Geological Survey

[4] Giffaut, E., Grivé, M., Blanc, P., Vieillard, P., Colàs, E., Gailhanou, H., Gaboreau, S., Marty, N., Madé, B., Duro, L. (2014). Andra thermodynamic database for performance assessment: ThermoChimie. Applied Geochemistry, 49, 225-236.

OVERVIEW OF THE BELGIAN RESEARCH PROGRAM ON RADIONUCLIDES MIGRATION FOR GEOLOGICAL DISPOSAL OF HLW-LL AND PRIORITIZATION OF REMAINING RESEARCH EFFORTS

S. Brassinnes[1)]

[1)]*ONDRAF/NIRAS, Belgian Agency for Radioactive Waste and Enriched Fissile Materials,*
B-1210 Brussels, Belgium

Deep geological disposal in plastic and poorly indurated clay formations is recommended by ONDRAF/NIRAS as a safe and feasible solution for the long-term management of HLW-LL (ONDRAF/NIRAS, 2011) but no political decision has been taken so far. In this context, the first Belgian Safety and Feasibility Case (SFC-1) is currently planned for 2019. In absence of a Belgian policy, this SFC will be generic and methodological but its timing and content may change in case of a policy decision.

The two presently considered potential host rocks, namely Boom Clay and the Ypresian clays, are marine clayey sediments consisting of detrital minerals with subsidiary authigenic minerals (e.g., glauconite, carbonates, …). Boom Clay is richer in pyrite and organic matter in comparison with the Ypresian clays whereas the Ypresian clays display a much higher smectite content (maybe partly authigenic) [2].

Considering the long-term evolution of the disposal system and of its environment, radionuclides will inevitably be released from the repository and will spread in the clayey geological barrier. Therefore, in order to build a sound and defensible safety case, it is necessary to understand the mechanisms and the processes that will govern the transport of these potentially hazardous substances, taken into account the peculiarities of each individual potential host rock (e.g., mineralogy, pore water chemistry…).

In the field, these clay layers look heterogeneous at various scales and hence, need to be adequately characterized for the purpose of geological disposal. Then, this detailed phenomenological characterization has to be properly abstracted taking into account up-scaling in space and time for the purpose of safety analysis allowing a treacable performance assessment abstraction process.

This contribution will give a broad overview of the current Belgian research program on radionuclides migration. This will include a description of the current knowledge on the various radionuclides transport in these two clay layers. Besides, the author will put an emphasis on the remaining open issues and possible knowledge gaps and their possible consequences on the safety case. Considering the limited resources, research efforts have to be pragmatically prioritized in the perspective of the stepwise approach aiming at building a safe and publicly acceptable repository.

[1] ONDRAF/NIRAS, NIROND-TR 2011-02FR, 263pp (2011).

[2] ONDRAF/NIRAS, NIROND-TR NIROND-TR 2013-12E, 411pp (2013).

ADDRESSING TECHNICAL AND POLICY CHALLENGES FOR REMEDIATION OF METALS AND RADIONUCLIDES WITHIN COMPLEX VADOSE ZONE ENVIRONMENTS

D. Wellman[1], M.H. Lee[1], M.J. Truex[1], M. Freshley[1]

(1)*Pacific Northwest National Laboratory, Richland. Washington, USA*

Deep vadose zone contamination is a significant issue in many regions of the world. While direct contact with the contamination does not threaten human health or the environment due to its depth in the vadose zone, movement of contamination from the deep vadose zone to the groundwater creates the potential for exposure and risk to receptors. Therefore, while the deep vadose zone does not necessarily require restoration, limiting flux from contaminated vadose zone is key to protecting groundwater resources and downgradient receptors.

Although remediation of deep vadose zone contamination is important, technical issues complicate the decision process for remedial actions. For example, remediation of metal and radionuclide contamination is complicated by heterogeneous contaminant distribution and the preferential saturation-dependent flow in heterogeneous sediments. These complications have generally rendered attempts to remove the contamination unsuccessful; and as a result, the magnitude of contaminant discharge (mass per time) from the vadose zone to the groundwater must be kept low enough by natural attenuation (e.g., adsorption processes or radioactive decay) or through remedial actions (e.g., contaminant mass or mobility reduction) to meet the groundwater concentration goals.

Regulations are another important consideration. Remediation of deep vadose zone contamination typically is linked to regulatory cleanup goals for groundwater, and as such, remediation technologies need to be considered within the regulatory context. A key concept here is that contaminant transport mechanisms through the vadose zone can attenuate the overall contaminant flux to the groundwater, and vadose zone contamination may not necessarily require remediation if the natural flux results in sufficiently low contaminant concentrations in the groundwater. In other cases, however, remediation to control transport, enhance attenuation mechanisms, or remove contaminants may be needed to limit flux so groundwater or surface water protection standards are maintained.

The inherent complications of deep vadose zone environments also provide opportunities for remediation:
- Incremental enhancements may meet remediation goals, given typically slow unsaturated flow conditions.
- Long times enhance opportunities for interactions with sediments and remediation amendments because of slow transport rates.
- Capillary forces resist movement in some cases and hold contaminants in fine-grained units
- The driving force for water flow, recharge from surface infiltration, can be controlled and reduced by surface structures (e.g., infiltration barriers).
- Gas-phase advection for distribution of remediation amendments can potentially be effective over large zones of influence.
- Water added in relatively small quantities, although increasing the downward driving force, will only minimally impact the overall rate of movement.

The challenge of deep vadose zone remediation is to reach an acceptable rate of contaminant transport while dealing with considerable uncertainties associated with estimating and measuring contaminant transport at the field scale. However, this also provides an opportunity to target remediation strategies for the vadose zone to mitigate the source of contamination and reduce transport to receptors, rather than meeting a specific concentration measured at some location within the vadose zone. This approach, however, requires technology development, methods, and protocols to demonstrate that groundwater will remain uncontaminated or that contamination will remain below levels of concern in the future, and achieve in situ remedial performance that is sufficient to support a remedy decision.

This presentation (1) reviews major processes for viable remediation of deep vadose zone metal and radionuclides that form the practical constraints on remedial actions and (2) provides an overview of how these principles are being practiced to address technetium and iodine contamination at the Hanford Site.

REASSESSMENT OF THE IMPACT OF MICROBIAL ACTIVITY ON THE PERFORMANCE OF THE WASTE ISOLATION PILOT PLANT

J. Swanson[*], J.-F. Lucchini, M. Richmann, D. Reed

Actinide Chemistry & Repository Science Program, Repository Science & Operations, Los Alamos National Laboratory,1400 University Drive, Carlsbad, NM USA

The projected impact of microbial activity on the performance of the Waste Isolation Pilot Plant has changed little from the initial certification period to the most recent recertification application submitted in 2014 [1-3]. The areas of greatest concern were, and still are: 1) carbon dioxide generation from the consumption of organic waste; 2) bioreduction of actinides; and 3) biocolloid migration potential. Over time, the reasoning behind certain model assumptions has changed somewhat (e.g., methanogenesis initially accounted for >90% of all carbon dioxide generated; currently, it is not included in the model), but the overall conservativism remains unchanged. Reviews of microbial survival and activity in high ionic strength matrices and recent work on WIPP-indigenous microorganisms suggest that the gas generation model is more conservative than originally thought. This overview is intended to support this claim by presenting data on the microbial ecology at the WIPP site and by summarizing current work into how both emplaced and indigenous microorganisms may affect actinide fate under WIPP-relevant conditions.

The indigenous WIPP microbial community can be divided into near- and far-field compartments, with the chief determinant of community structure being sodium chloride concentration. Halophilic archaea of the order *Halobacteriales* dominate near-field (halite) and high-salt conditions (Figure 1); while, bacteria dominate the far-field (overlying aquifer) and low-salt conditions [4]. Only aerobic incubations of WIPP halite have yielded growth; although DNA sequence analysis shows the genes encoding denitrification are present in one WIPP haloarchaeal isolate.
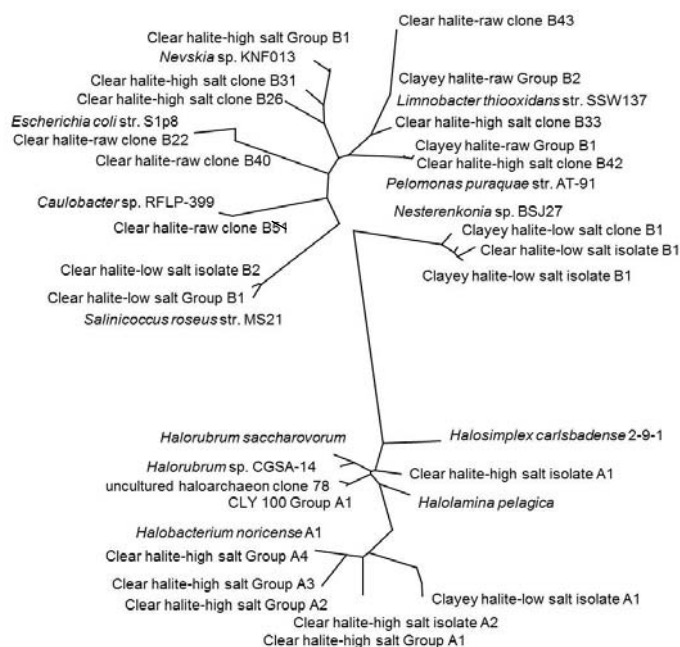
Figure 1. Phylogenetic tree of bacterial (top) and archaeal (bottom) DNA sequences from halite isolates and clone libraries. Sequences were retrieved from clear and clayey halites incubated in low and high-salt media, as well as from raw halite samples.

Organisms in the far-field may have a greater impact on actinide migration, should the repository horizon be breached. Cultures of far-field samples were positive under aerobic, nitrate-reducing, iron-reducing, and sulfate-

reducing conditions, suggesting that waste transformation with concomitant carbon dioxide generation, actinide reduction, and biocolloid formation in this compartment are possible [4]. Still, since bacterial structural diversity decreases as ionic strength increases, it is uncertain what the effect of moving from high to low ionic strength will be on biocolloid transport, especially for haloarchaea which may lyse at lower salt concentrations. For bacterially induced actinide reduction, our studies show that indirect reduction, via fermentation, dominates at higher ionic strength, due to the microbial ecology of that space.

Access to waste destined for the WIPP has yielded a third relevant community comprising microorganisms introduced with the emplaced waste (Figure 2). Because of close proximity with the waste, these organisms are likely to be radioresistant and may already be associated with actinides. Additionally, they may play a role in waste transformation prior to repository inundation. Further research on these organisms is underway.
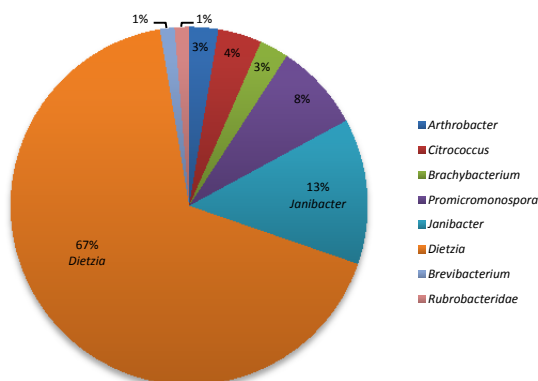
Figure 2. Phylogenetic distribution of organisms detected in WIPP-destined low-level radioactive waste.

Given a low-diversity community with limited metabolic capabilities, the projected rates of carbon dioxide production under near-field repository conditions can be deemed optimistic. If actinides migrate into the far-field, they may be reduced directly or indirectly by indigenous organisms there. Biocolloid enhancement of migration by indigenous organisms is likely to be less than projected by PA, but uncertainty exists as to the role of the emplaced organisms.

[1] U.S. Department of Energy. 2004. Title 40 CFR Part 191 Compliance Recertification Application for the Waste Isolation Pilot Plant. DOE/WIPP 2004-3231. Carlsbad, NM: Carlsbad Field Office.

[2] U.S. Department of Energy. 2009. Title 40 CFR Part 191 Subparts B and C Compliance Recertification Application 2009, Appendix PA, Attachment SOTERM. DOE Carlsbad Field Office. Carlsbad, NM.

[3] U.S. Department of Energy. 2014. Title 40 CFR Part 191 Subparts B and C Compliance Recertification Application 2014, Appendix SOTERM-2014. DOE Carlsbad Field Office. Carlsbad, NM.

[4] Swanson JS, Simmons KA, Norden D, Reed DT. 2013. Microbial Characterization of Halite and Groundwater Samples from the WIPP. Report LA-UR-13-26280. Los Alamos National Laboratory; Carlsbad, NM.

CHARACTERIZATION OF TRU WASTE DRUMS TO ASSESS MECHANISMS OF METHANE GENERATION

[1]D. T. Reed, [1]J.S Swanson, [1]M.K. Richmann, [2]T.H. Johnsen, [2]L.R. Frost and [2]T.L. Clements

1. *Los Alamos National Laboratory, 1400 University Drive, Carlsbad NM, 88220, USA.*
2. Transuranic Waste Projects, CH2M-WG Idaho, LLC, Idaho Falls, Idaho, USA.

A detailed microbial and qualitative radiolytic assessment was performed on Idaho National Laboratory (INL) transuranic (TRU) samples from drums ARP-60106 (drum 6) and ARP-60109 (drum 9) to establish the cause of methane gas production observed in these two WIPP-bound TRU waste drums. They had been in the underground for over 50 years prior to excavation and re-packaging for shipment. These two drums exhibited high methane gas generation rates that prevented their shipment to the WIPP site. Since other such drums may be found, it was important to evaluate the mechanism of gas generation with the idea of developing a treatment strategy to mitigate or eliminate methane production. This mechanistic study has broader implications to the WIPP waste emplacement [1] and permanent disposal in that microbial effects impact current WIPP PA implementation and the production of methane in the WIPP underground is an operational consideration for mine safety.

In all, six ~ 10 g samples were taken from each of the two drums. These were taken with relatively few precautions to minimize microbial contamination and had been splayed in air twice to inhibit what was thought to be anaerobic microbial gas generation prior to the sampling that was done. The samples obtained were shipped to the Los Alamos labs located in Carlsbad NM. It was verified, prior to the subsequent analyses performed, that significant methane generation continued to occur under both oxic and anoxic conditions and the presence of oxygen was not a significant factor in the rates of gas generation observed (see Figure 1).

Figure 1 Methane and CO_2 gas production for the anoxic sample #6 from both drums ARP 60106 and ARP 60109 as a function of time.

The first mechanism evaluated was the possibility that the gas generation being observed was microbial in origin. Methanogens are known producers of methane and are ubiquitous in subsurface environs where anaerobic conditions and the right mix of organic nutrients exist. Although very small levels of DNA were found in the samples (See Figure 2), it was concluded that microbial processes could not account for the immediate gas production being observed. This conclusion is based on the very low microbial populations observed overall, and the absence of DNA signatures for the microorganisms that directly account for methane gas generation (i.e. methanogens). These results do not discount that the origin of the methane could be biogenic in nature (either within the drums or present in the subsurface). But this source of gas production is currently not present in the TRU waste and does not account for what is seen in the headspace analysis and in our laboratory studies. The DNA found was amplified to establish the nature of the microorganisms present and some isolates have been identified (see Figure 3) although these studies are ongoing.

The second mechanism qualitatively evaluated was the possibility that the source of methane production was the radiolytic decomposition of the organic content in the waste drums. This had been initially discounted base on back-of-the-hand calculations but there was not good quantitative data on the moles of methane production as a function of the mass of waste. The actinide content of the TRU waste was measured by dissolving known quantities of the waste and analyzing for Am and Pu using ICP-MS. Experiments were performed to evaluate the mole to mass ratio and steps were taken to sterilize the samples to isolate chemical/radiolytic sources from microbial ones. These radiolytic pathways are also discounted as the immediate source of high methane in the two TRU waste samples. The methane "production" observed does not correlate with measured alpha activity (high activity samples have the lower methane production). The G values calculated, if one assumes a radiolytic
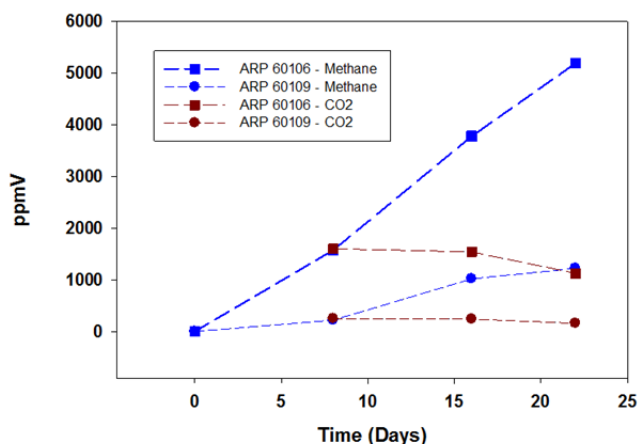
pathway, are unreasonably high and also support the assertion that radiolysis is not the immediate/current source of methane although over time in the subsurface this could be a source that was somehow trapped in the TRU waste.
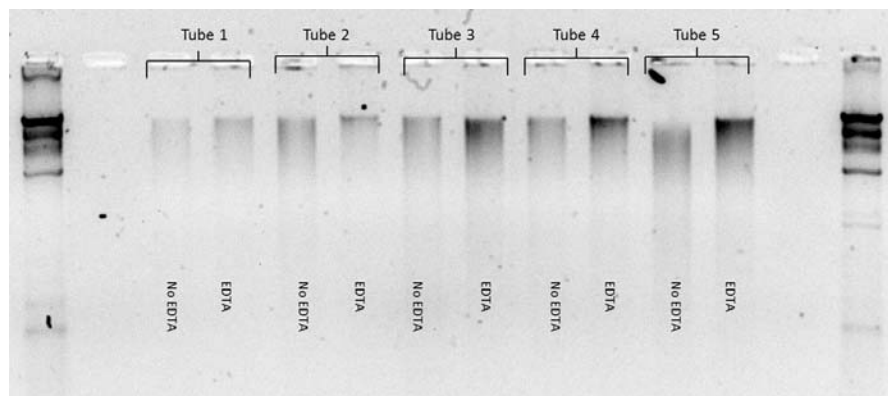
Figure 2. Genomic DNA extracted from tubes 1-5 of Drum 6. Outer lanes, λHindIII DNA digest (size marker).
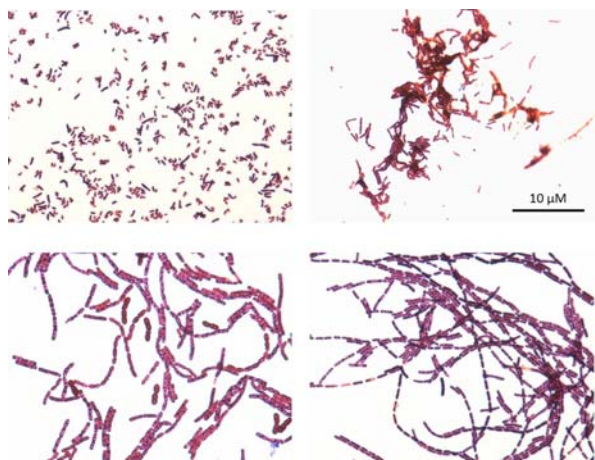
Figure 3. Gram-stained images of four bacterial isolates from Drum 6 under aerobic conditions.

The overall conclusion is that microbial and radiolytic pathways cannot account for the methane levels/production that were observed in samples ARP 60106 and ARP 60109. The best, but somewhat speculative, interpretation of the immediate source of methane is that there is a slow outgassing step that is occurring (so regardless of how the methane got there, it is now trapped in the waste and is released when new surfaces are exposed). This interpretation, although it explains much of our data, is supported by longer-term gas generation data that show a steady and rapid decrease in the amount of methane observed.

A side benefit of this overall study is that it confirmed the validity of the waste source data used to estimate waste contents as well as provided insights to the impact of the "stress" of TRU waste on the indigenous microbial community as well as the microbial "inoculum" that is being introduced to the WIPP site when the TRU drums are emplaced.

References

[1] J.S. Swanson, K. Simmons, D. Norden and D.T. Reed. "Microbial Characterization of Halite and Groundwater Samples from the WIPP." Los Alamos Report LA-UR-13-26280. Los Alamos National Laboratory, Los Alamos NM, USA (2013).

USING WATER TO DECONTAMINATE ROCK SALT AT THE WASTE ISOLATION PILOT PLANT, NEW MEXICO, USA

R. Demmer[1], S. Reese[1], R. Nelson[2] and A. Van Luik[2]

[1]*Battelle Energy Alliance, Idaho National Laboratory, Idaho Falls, Idaho 83415, USA*
[2]*US Department of Energy, Carlsbad Field Office, Carlsbad, New Mexico 88220, USA*

The Waste Isolation Pilot Plant (WIPP) is a U.S. Department of Energy transuranic (TRU) waste deep geologic repository. The repository permanently isolates defense related TRU waste from the biosphere by placing it in a bedded salt formation, the Salado, at about 655 m below the Chihuahuan desert of southeastern New Mexico, near the city of Carlsbad. WIPP has disposed of more than 86,000 m^3 of TRU waste in more than 165,000 containers.

After nearly 15 years of operations, on February 14, 2014, a waste drum breached, likely due to a runaway chemical reaction between the nitrate salt waste form and organic materials used to condition the waste at the site of generation, before being shipped to WIPP for disposal. This reaction produced heat and gas and expelled combustion products into the underground air, contaminating portions of the underground facility mostly with [241]Am and lesser levels of plutonium. Figure 1 shows the extent and degree of contamination based on radiological surveys through December 2014.
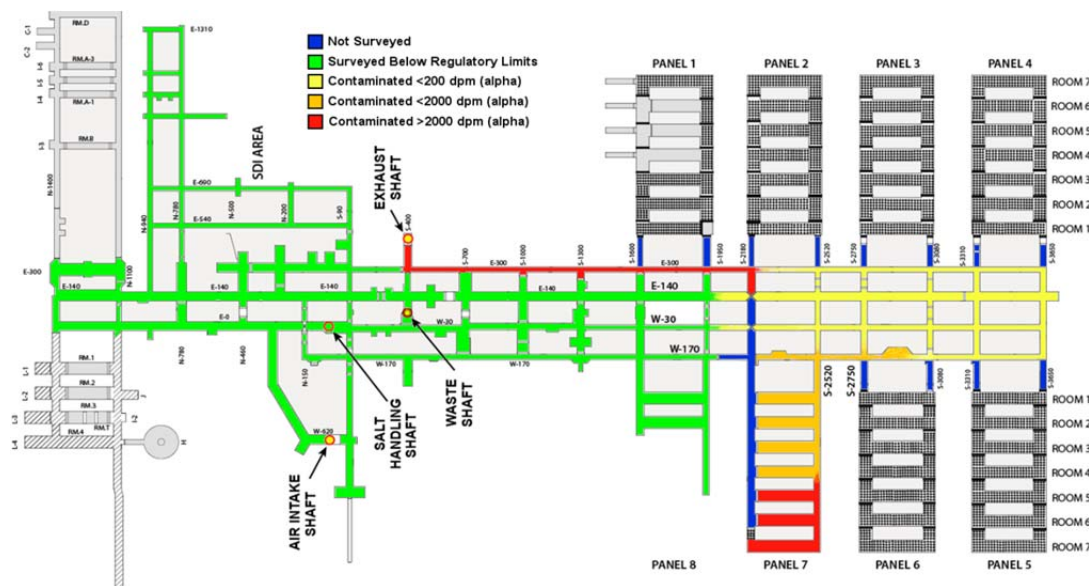
Figure 1: Schematic of Waste Isolation Pilot Plant underground, showing measured levels of contamination (regulatory limits refers to DOE Order 458.1-Radiation Protection of the Public and the Environment-limits of 20 dpm/100cm^2 removable alpha and 100 dpm/100cm^2 total alpha)

Several methods were evaluated for removing fine waste particles from the salt surfaces it contacted as the particulate laden air stream exited the underground (Reese et al., 2015). The method that stood out in terms of ease, rapidity and decontamination efficiency was the use of a water spray.

The test using water spray was performed using a surrogate fine insoluble powder as well as [241]Am in aqueous solution applied to the salt surfaces in droplets. The fractured, porous salt imbibed some of the liquid and thus attenuated the measurable alpha radiation to about 13% of the alpha radioactivity added to the surface. A steel plate was used in the same manner, with no porosity, to allow the attenuation by the salt to be estimated. Water spray washing reduced that detectable count fraction further, to 0.7% or less (removing ≥ 95% of the measurable alpha radiation). The finely powdered surrogate material was removed from the salt surface at about 98% efficiency. Whether the actinide waste form was a dry powder or an aqueous suspension in a droplet, water-washing was a very efficient decontamination method for a salt surface.

Figure 2. Salt test coupon and water washing technique used in the laboratory

Based on experience with fine surrogate contaminant particulates applied to the salt coupons, it is expected that in a real repository decontamination application, the contaminant on the rock walls will became entrained in and removed with about <1 millimeter of salt surface dissolved by the water spray. By adjusting the aerial application rate of water used, the runoff from the walls can be controlled to assure it carries the contaminants to several millimeters below the porous (broken) salt floor. This is followed with placement of a strong fabric and fresh layer of salt over the floor to assure no resuspension. This approach decontaminates without creating secondary waste streams.

Given the observation that a dilute suspension of americium was transported into the interior of the salt coupons, additional work that may be useful is to study the interaction between rough rock salt walls and particulates containing americium under different humidity conditions. The interaction of high relative humidity and the salt coupon surfaces rendered them "sticky" in the laboratory. In a ventilated, working repository, the hygroscopic salt results in a thin brine surface layer, when relative humidity is high (greater than ~75%). Since the repository walls are fractured and porous, this moisture also penetrates into the salt, thereby enhancing pathways for very small particles on the rock surface to penetrate more deeply. When the air becomes very dry again, what has moved into the interior of the salt will remain there. Also, the recrystallized salt on the surface can trap micron-scale particulate as it dries. With a mean path length of about 20 microns for the 5MeV alpha decay of Am-241, the direct frisk measured levels are attenuated by the recrystallized salt coating the remaining surface-bound contaminants. Repository wall contamination would likely be largely removed from the surface over time even without water washing, decreasing the measurable alpha radiation levels at a rate far exceeding that due to radioactive decay alone.

This release incident at WIPP was an operational one. Its occurrence has no negative implications for the use of salt as a repository host rock or for the use of deep geologic repositories to permanently remove risk from the biosphere. In fact this release incident and its decontamination process illustrate yet another positive aspect of using rock-salt as a repository host rock: it is relatively easy to decontaminate.

Reese, S., R. Demmer, M. Ancho, 2015, "Decontamination Methods Testing for the Waste Isolation Pilot Plant," Paper 15691, Waste Management Symposium 2015, March 15-19, 2015, Phoenix, Arizona, USA

PERMANENT GEOLOGIC ISOLATION OF ACTINIDES IN A SALT REPOSITORY: UPDATE OF THE WIPP SAFETY CASE

D. T. Reed, M.K. Richmann, J.S. Swanson, T. Dittrich, and J.F. Lucchini

Actinide Chemistry and Repository Science Program, Repository Science and Operations, Los Alamos National Laboratory, 1400 University Drive, Carlsbad NM, 88220, USA.

The Waste Isolation Pilot Plant (WIPP) transuranic repository remains a cornerstone of the U.S. Department of Energy's (DOE) nuclear waste management effort. Although the project is currently dealing with operational issues that led to a shutdown of operations, the long-term safety case for the permanent disposal of transuranic (TRU) waste remains intact and was largely unaffected. The WIPP is now pursuing its third recertification (submitted in March 2014) and there remain ongoing discussions about possible expanded missions and additional nuclear repository concepts in a Salt geology within the United States. Research to strengthen the scientific basis of the safety case for actinide containment in high ionic-strength brine systems continues and is ongoing.

An understanding of the actinide and brine chemistry in the WIPP is needed to address the low-probability scenario that brine inundation and release could occur due to human intrusions and is driven by regulatory requirements for the repository license case. The overall ranking of actinides, from the perspective of potential contribution to release from the WIPP, is: Pu ~ Am > U >> Th and Np and remains unchallenged from past recertification. An updated inventory of the predicted TRU content and key waste constituents is given in the Table below. The oxidation state distribution of key multivalent actinides, which is based on expert opinion and the predicted redox environment, also remains unchanged: U – 50% U(IV) and 50% U(VI); Pu – 50% Pu(III) and 50% Pu(IV); with Am/Cm as the III oxidation state and thorium as the IV oxidation state. These actinide/analog oxidation states are the focus of the site-specific redox and solubility studies being performed.

Table 1. Projected Actinide Inventory and Key Waste Constituents in the WIPP [1]

Actinide	Activity in Ci	Mass in Kg
Th	7.04	1.35×10^4
U	528	2.26×10^5
Np	23.2	32.5
Pu	2.02×10^6	1.20×10^4
Am	7.05×10^5	203
Cm	9.97×10^3	0.122
Waste Material		**Total Mass (Kg)**
Iron-Based metals/alloys		4.91×10^7
CPR (Cellulosic/Plastic/Rubber)		1.54×10^7
MgO (Engineered Barrier)		5.14×10^7
Organic Ligands (Citrate)		7.78×10^3
Organic Ligands (EDTA)		3.76×10^2

In this recertification cycle, thorium solubility studies in brine were completed; substantial progress was made on the characterization of indigenous microorganisms and the investigation of key actinide-microbial interactions; and the performance assessment (PA) approach to define the contribution of colloidal species to the actinide source term was re-examined and updated. These data [2-6] continue to extend our understanding of high ionic-strength actinide chemistry and strengthen and improve the scientific basis for the safety case for a nuclear repository in salt.

Colloidal Contributions and Effects of Organic Chelating Agents on the Solubility of thorium in WIPP brine

Further studies have been completed to establish the effects of organics and understand the colloidal nature of the thorium species observed in site-specific simulated brine systems. We have previously reported [5] that long times (greater than two years) are needed for thorium concentrations to approach model-predicted equilibration values and these data qualitatively agree with results reported elsewhere [7]. The underlying reason for this long-term equilibration in WIPP brine is not yet fully understood. Further studies explore the relationships between ionic strength and the lesser brine constituents on the colloids formed. In addition, the effects of organic chelating agents on this process as well as the overall solubility of thorium were investigated. The organic complexants do not, in the end, lead to a significant increase in the thorium solubility although metastable complexes can be formed and persist.

Microbial Characterization and Interactions with Actinides

Significant progress has already been reported in the microbial characterization of WIPP-indigenous (salt and nearby brines) microorganisms [2, 3]. This will be summarized and updated. Current work extends this to sequence the genomic and metagenomic DNA of select isolates and samples to determine the presence of genes that encode the enzymes necessary for specific metabolic pathways. Growth and stress responses of microorganisms to specific actinide species are being explored to establish and further understand the mechanisms that lead to actinide toxicity. Additionally, the biosorption of specific isolates towards Np(V), Th(IV) and Nd/Am(III) were extended to a broader pH range and work is ongoing to look at structure-specific features of this sorptive process [4,6].

Colloidal fraction of the actinides in the WIPP

The mineral, intrinsic and microbial contributions to the WIPP mobile colloidal actinide source term model [6] continue to be re-examined under conditions specific to the WIPP safety case. Colloidal species can potentially contribute to the WIPP actinide source term and are currently accounted for in WIPP PA. Data for all key actinides as well as further and more detailed interpretation of the biocolloidal contribution will be updated.

In all, there is continued progress towards establishing more realism in the WIPP PA models and these strengthen the safety case for nuclear waste disposal in a salt repository.

References

[1] Van Soest, G. *Performance Assessment Inventory Report – 2012* (PAIR 2012). INV-PA-08, LANL-CO\Inventory Report, Los Alamos, NM: Los Alamos National Laboratory (2012).
[2] Swanson et. al., *Geomicrobiology Journal*, vol. 30:3, 189-198 (2013).
[3] Swanson et al.,   Los Alamos National Laboratory report LA-UR-13-26280. Los Alamos National Laboratory, Los Alamos NM, USA (2013).
[4] Ams et al. *Geochimica et Comoschimica Acta*, vol. 110: 45-57 (2013).
[5] Borkowski et al., Los Alamos National Laboratory report LA-UR 12-24417, Los Alamos National Laboratory, Los Alamos NM, USA (2012).
[6] Reed et al., Los Alamos National Laboratory report LA-UR 13-20858, Los Alamos National Laboratory, Los Alamos NM, USA (2013).
[7] Altmaier et al., *Radiochimica Acta*, vol. 92: 537–43 (2004).

FAST RADIONUCLIDE RELEASE FROM THE WASTE FORM "USED NUCLEAR FUEL"

Bernhard Kienzler

Institut für Nukleare Entsorgung (INE), Karlsruhe Institute of Technology (KIT), Germany

In many countries, used nuclear fuel is considered as a waste form to be disposed in the deep underground. The radionuclide source term from used nuclear fuel was under investigation since decades. However, as a result of cost optimization, the fuel burn-up has increased to a range above 50 GWd/t_{HM}, in the last years. These burn-ups require higher initial enrichments in ^{235}U and consequently, the used fuels have different compositions. The 7th FP Collaborative Project FIRST-Nuclides tackled the challenge of realistically describing the release of the first batch of radionuclides from disposed spent nuclear fuel upon canister failure (fast/instant release fraction). This first release consists of radionuclides which are (1) segregated from the fuel matrix such as iodine and cesium and (2) are usually highly soluble and mobile in the groundwater. The degree of segregation and the accessibility of the phases within the fuel rods depend on operational parameters of the nuclear power plants (NPP). As repositories need to take the fuel from different types of NPPs using fuels of different initial enrichments, burn-ups, power ratings, heat ramps, poisoning, etc. a comprehensive study of the fast releases of radionuclides from 12 different types of high burn-up LWR fuel have been elaborated.

The presentation summarizes the outcome of the FIRST-Nuclides project with respect to the characterization and properties of the fuel samples, the fission gas releases and the radionuclide releases in contact with groundwater for different sample preparations and sample sizes, such as clad fuel pellets, unclad fragments and powders. Experiments cover the time dependent leaching of fission products under different redox conditions up to one year duration. The obtained release data are related to operational parameters of the NPP in order to allow estimation of the source term for a complete repository.

The experimental results obtained in the project FIRST-Nuclides are discussed with respect to previous findings and approaches. Correlations of the release data with burn-up, fission g gas release and with time are discussed for pressurized (PWR) and boiling water reactors (BWR). Conclusions are drawn on the dependency of the fast release on the power plant operational parameters, on the leaching conditions, on the transition between the fast release and the significantly slower UO_2 matrix corrosion as well as on modelling the mobilization of radionuclides along the grain boundaries after penetration of water into the fuel sample and the subsequent migration along the wetted fractures and grain boundaries.

Acknowledgement

LEACHING TEST OF ACTINIDE ELEMENTS FROM SIMULATED FUEL DEBRIS TO SEAWATER

A. Kirishima[1], M. Hirano [1], T. Sasaki [2], D. Akiyama[1], N. Sato[1]

[1] *Institute of Multidisciplinary Research for Advanced Materials (IMRAM), Tohoku University, 1-1 Katahira, 2-chome, Aoba-ku, Sendai 980-8577, Japan*
[2] *Department of Nuclear Engineering, Kyoto University, Kyoto daigaku-Katsura, Nishikyo-ku, Kyoto 615-8540, Japan*

On March 11, 2011, a mega earthquake followed by a tsunami resulted in a loss of coolant accident at Fukushima Daiichi nuclear power station (NPS) operated by Tokyo Electric Power Company (TEPCO). After the NPS black out, over 4000 tons of seawater were injected into the high temperature reactor cores for the emergency cooling. However, this post-accident effort to remove heat was insufficient, resulting in the melting of the nuclear fuel and its subsequent reaction with zirconium alloy cladding. The main component of melted nuclear fuel debris is expected to be a solid solution of uranium and zirconium oxide ($=Zr_yU_{1-y}O_2$) containing a variety of fission products (FPs) and minor actinides (MAs). Water-soluble FPs in the damaged fuel or fuel debris such as $^{137/134}$Cs and ^{90}Sr were released into the cooling water from the damaged reactor cores. In addition, actinide isotopes such as ^{238}Pu, ^{239}Pu, ^{240}Pu, ^{241}Am and ^{244}Cm were detected in the treated water of Simplified Active Water Retrieve and Recovery System (SARRY) in concentrations of 2.1 x 10^{-3} Bq/ml (^{238}Pu), 8.3 x 10^{-4} Bq/ml (^{239}Pu + ^{240}Pu), 5.6 x 10^{-4} Bq/ml (^{241}Am), 6.3 x 10^{-4} Bq/ml (^{244}Cm) respectively. From the isotopic composition, it was confirmed that the detected Pu was released from the reactors in Fukushima Daiichi NPS [1]. Although the concentrations of these actinide nuclides are currently very low, the existence of actinide elements in the contaminated water have serious impact for the management of radioactive waste released from the de-commissioning process of Fukushima Daiichi NPS, since actinide elements have high radiotoxicity and very long lifetime. The source of the actinides in the contaminated water is suspected to be fuel debris existing in the unit 1, 2 and 3.

For understanding of leaching behavior and chemical speciation of these major FP elements from the NPS fuel debris, we conducted an experimental study using natural Fukushima seawater and a neutron-irradiated solid solution of UO_2 and ZrO_2 [2, 3]. The chemical and physical properties of the fuel debris originated in the Fukushima NPS is expected to be different from those of normal light water reactor spent fuel (LWR-SF), so that the leaching behavior of actinide elements in the debris to water should differ from that in normal LWR-SF. Additionally, at the initial stage of the accident, huge amount of seawater was directly injected into the reactor cores for the emergency cooling, which made the actinide leaching more complicated due to the variety of seawater components.

Therefore, in this study, a simulated fuel debris consisting of UO_2-ZrO_2 (U:Zr = 1:1 in atomic ratio) [2, 3] solid solution doped with ^{137}Cs, ^{237}Np, ^{236}Pu and ^{241}Am tracers was synthesized, and agitated leaching tests were conducted. The synthesized simulated fuel debris was immersed and shaken in natural seawater collected at a coast 11 km away from Fukushima Daiichi NPS. For comparison, the same leaching test was conducted for pure water. The brief leaching test conditions were T = 25 °C, solid-liquid ratio = 4 g/l and test duration was up to 60 days. The ratio of tracers leached into seawater from the simulated fuel debris by the agitated leaching test for 4 days was evaluated to be 0.09% for U, 0.01% for Np, 0.01% for Pu, 0.01% for Am and 35.39 % for Cs as determined by alpha or gamma spectroscopy of the soluble fraction. Figure 1 shows a comparison of the leaching ratios between from the simple mixture of UO_2 and ZrO_2 and from the simulated fuel debris (solid solution). The result of the leaching tests indicated that the leaching ratio from the simulated fuel debris can be simply written as (large) Cs >> U > Np ≈ Am ≈ Pu (small), and the leaching of Cs and the actinides are clearly supressed by the formation of a solid solution between UO_2 and ZrO_2 as shown in Figure 1. The latter result implies that the leaching of actinides from the real fuel debris in the reactor unit 1-3 in Fukushima Daiichi NPS is expected to be suppressed in comparison with the leaching from normal LWR-SF. Additionally, the leaching ratio of U into seawater tended to be higher than those into pure water, which seems to reflect the difference of carbonate ion concentrations in seawater and in pure water.
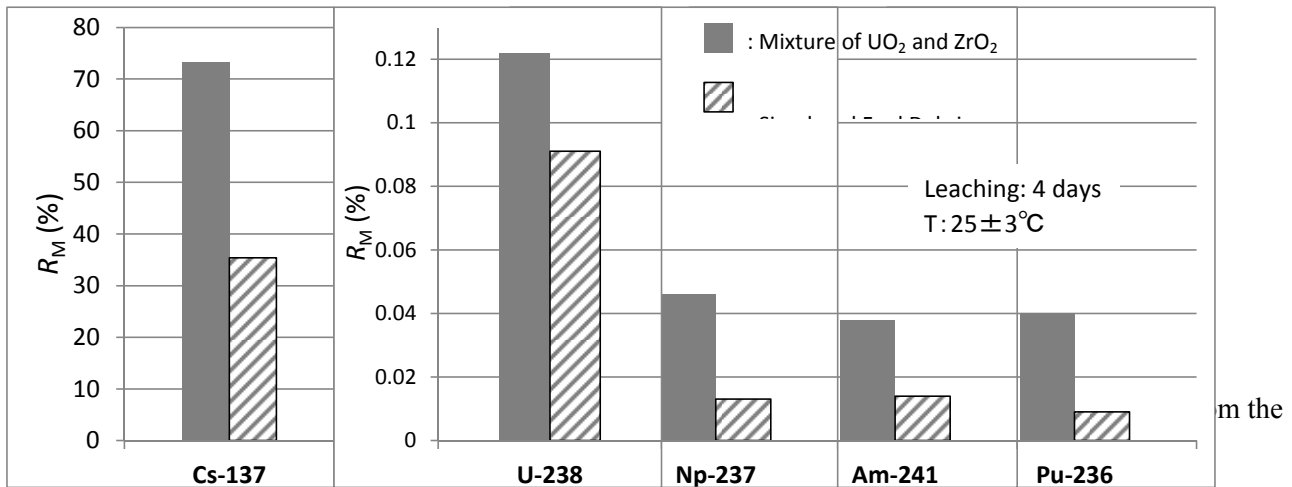
Figure 1 Comparison of the leaching ratios between from the simple mixture of UO_2 and ZrO_2 and from the simulated fuel debris (solid solution). This figure will be published in [4].

[1] Secretariat of the Council for the Decommissioning of TEPCO's Fukushima Daiichi Nuclear Power Station, Progress Status and Future Challenges of Mid-and-Long-Term Roadmap toward the Decommissioning of TEPCO's Fukushima Daiichi Nuclear Power Station Units 1 – 4. Tokyo: Japanese Ministry of Economy, Trade and Industry (METI); November 28, 2013. (in Japanese) .

http://www.meti.go.jp/earthquake/nuclear/pdf/131128/131128_01ss.pdf

[2] A. Kirishima, T. Sasaki, N. Sato. "Solution chemistry study of radioactive Sr on Fukushima Daiichi NPS site." J. Nucl. Sci. Technol. 52: 151-160 (2015).

[3] T. Sasaki, Y. Takeno, A. Kirishima, N. Sato . "Leaching test of gamma-emitting Cs, Ru, Zr, and U from neutron-irradiated UO_2/ZrO_2 solid solutions in non-filtered surface seawater" J. Nucl. Sci. Technol. 52: 146-150 (2015).

[4] A. Kirishima, M. Hirano, T. Sasaki, N. Sato. "Leaching of Actinide Elements from Simulated Fuel Debris to Seawater" J. Nucl. Sci. Technol. –in press- DOI:10.1080/00223131.2015.1017545.

THE EFFECT OF RADIATION DAMAGE ON THE STRUCTURE, CHEMISTRY AND SOLUBILTY OF SIMULATED UK AGR SPENT NUCLEAR FUELS

A. Popel [1], M. E. Bowden [2], A. S. Lea[2],T. M. Wiestra[2], E. S. Ilton[2], D. J. Edwards[2], Z. Heisl[3] , W.E. Lee[3], I. Farnan[1],

[1]*Department of Earth Sciences, University of Cambridge, Downing Street, Cambridge, CB2 3EQ, UK*
[2] *Environmental and Molecular Sciences Laboratory, Pacific Northwest National Laboratory, Richland, WA 99352*
[3] *Department of Materials Science, Imperial College, London SW7 2AZ*

The impending closure of nuclear fuel re-processing facilities in the United Kingdom has meant that spent nuclear fuel arising from the UK's Advanced Gas Cooled Reactors (AGRs) will need to be disposed of in a geological repository. A large body of research exists on the long-term durability of spent nuclear fuel arising from light water reactors (LWR), which predominate in the global generation of nuclear energy. However, there are potential chemical and structural differences in the spent fuel arising from operational differences such as graphite moderation and CO_2 coolant, elevated temperature, as well as physical differences such as cladding and pellet shape that may cause deviations from LWR behaviour. To investigate these effects AGR fuel with burn-ups of 25 GWd/THM and 43 GWd/THM has been simulated with depleted uranium and fission products representing the fuel at a time 100 years after being removed from the reactor. To simulate the effect of radiation damage, a portion of each sample was irradiated to a fluence of 4.8×10^{15} ions/cm^2 with 92 MeV Xe.

This study concentrates on the effect of radiation damage on the micro-structure and chemistry of UO_2 and UO_2 simfuels and the subsequent effect this has on their aqueous durability. To our knowledge, the only previous explicit study of the effect of radiation damage on UO_2 dissolution was carried out by Matzke [1]. In this previous study, UO_2 disks were irradiated with 40 keV Kr and an order of magnitude increase in the solubility of the UO_2 compared with an unirradiated reference sample was observed. Here, irradiated and unirradiated disks of plain UO_2 and UO_2 simfuel pellets have been characterised by X-ray photoelectron spectroscopy (XPS), transmission electron microscopy (TEM) and atomic force microscopy (AFM) before anoxic dissolution tests. The irradiations in this study simulate the effect of fission fragments (92 MeV Xe). The irradiations were carried out without anoxic controls and the XPS reveals a large contribution of U^{5+} due to surface oxidation of the samples. Irradiation did not alter the degree of hyperstoichiometry imposed by atmospheric oxidation in the UO_2 or the simfuel samples to the depth probed by XPS. X-ray diffraction, with a greater penetration depth, was able to characterise a reduction in crystallite size following irradiation from ~ 80 -100 nm to ~ 30 -40 nm with ~ 0.25% increase in lattice parameter for the irradiated material. The unirradiated, doped simfuels showed a reduction in lattice parameter compared with plain UO_2. TEM examination of focused ion beam sections profiling the peak damage area of the irradiated UO_2 and UO_2 simfuels showed a lower dislocation density for the simfuel compared with the plain UO_2. All samples were characterised for their surface area using AFM and subjected to a single pass flow through (SPFT) tests under strictly anoxic conditions to discriminate between the dissolution of the atmospherically oxidised layer and the subsequent anoxic dissolution of the radiation damaged layer (7 μm depth) for irradiated and unirradiated UO_2 and UO_2 simfuels.

[1] Matzke, H. (1992). "Radiation damage-enhanced dissolution of UO_2 in water." J. Nucl. Mat. 190:101-106

MOX SPENT NUCLEAR FUEL CORROSION PROCESSES UNDER WASTE DISPOSAL CONDITIONS

C. Jégou[1], M. Odorowski[1,2], L. De Windt[2], V. Broudic[1], M. Magnin[1],
M. Tribet[1], S. Peuget[1], C. Martin[3]

[1] *Commissariat à l'Energie Atomique et aux Energies Alternatives, Centre de Marcoule,
DEN/MAR/DTCD/SECM/LMPA, 30207 Bagnols-sur-Cèze Cedex*
[2] *MINES ParisTech, Centre de Géosciences, Equipe Hydrodynamique et Réactions,
35 rue St Honoré, 77305 Fontainebleau*
[3] *Agence Nationale pour la gestion des Déchets Radioactifs, 1/7 rue Jean Monnet,
92298 Chatenay-Malabry Cedex*

Many studies have been conducted in recent decades on the alteration of UOX spent fuel under long term interim storage and direct geological disposal conditions. For UOX spent fuel the processes of corrosion and alteration under irradiation and various environmental conditions are quite well known and are the subject of a broad international consensus [1,2,3]. However the available data on MOX (Mixed-OXide) spent fuel are more limited particularly with respect to the heterogeneous Mimas® MOX fuel. The microstructure observed on this type of MOX fuel revealed the presence of three zones with different plutonium contents and microstructures arising from the fabrication process (dilution of a UO_2 and PuO_2 oxide blend in UO_2 powder) and from the origin of the UO_2 powder. Although the mechanisms are likely to be close to those of the UOX fuel it is still necessary to study the specificity of MOX fuels [4].

To clarify these mechanisms, leaching experiments were performed on MOX fuels (unirradiated MOX fuel with an initial Pu/[Ox] enrichment of 6.6 wt% and MOX spent nuclear fuel with a burn-up of 47 Gwd/t_{HM}) under various irradiation conditions (mainly alpha for the unirradiated fuel and under an   mixed irradiation field for the MOX47 fuel), in waters of different chemical compositions (deionized and carbonated waters, synthetic clayey water) and in the presence or not of environmental materials (iron foil simulating the metal canister and its corrosion products). For each experiment, solution samples were taken over time and Eh and pH were monitored. The uranium in solution was assayed using a kinetic phosphorescence analyzer (KPA), plutonium and fission products were analyzed by radiochemical route. Major cations were analyzed by ICP-AES and anions by ionic chromatography. At the end of the experiment, the un-irradiated pellets, the spent fuel fragments and the iron foils were characterized by SEM, EDX, EPMA and Raman spectroscopy in order to identify secondary phase precipitations.

About the experimental results, under alpha irradiation the uranium concentrations in the bulk solution show a great similarity of behaviour for simple UO_2 and heterogeneous MOX fuels regardless of the chemical composition of the water. The different surface characterizations show that the surrounding UO_2 matrix was much more sensitive to dissolution than the Pu aggregates, which appear to be more stable over time; this does not argue in favor of a significant contribution from the aggregates to the releases in solution. Moreover the uranium concentrations decrease by several orders of magnitude between a carbonated water and a synthetic clayey water containing iron. The influence of iron depends on the redox gradients between the fuel surface and the surrounding environment. On this point the nature of the irradiation field is an important parameter. For the MOX spent fuel the oxidative dissolution is not inhibited in the presence of iron, this is not the case under a predominant alpha irradiation field located at the fuel surface.

All these data allows to propose a schematic representation of the heterogeneous MOX spent fuel alteration mechanisms including heterogeneity, irradiation fields, groundwater, corroded waste package… Future steps will aim to integrate the environment materials such as argillite of the french geological repository site.

[1] Shoesmith, D. W. J. Nucl. Mater. **282**, 1–31 (2000).
[2] Poinssot, C. et al. *Synthesis on the Spent Fuel Long Term Evolution CEA Report CEA-R-6084* Vols I and II (2001).
[3] Grambow, B et al. MICADO (Model Uncertainty for the Mechanism of Dissolution of Spent Fuel in Nuclear Waste Repository) european project report. From EUR 24597 report (1-56) (2010).
[4] Ewing, R.C. Nature Materials. **14**, 252-257 (2015).

A NEW VIEW ON THE U(VI) DIFFUSION THROUGH COMPACTED BENTONITE:
REVELATIONS FROM A 6-YEAR STUDY

C. Joseph[1)*], J. Mibus[2)‡], P. Trepte[2)§], C. Müller[2)], V. Brendler[2)], A.B. Kersting[1)], M. Zavarin[1)]

[1)]*Glenn T. Seaborg Institute, Physical & Life Sciences Directorate, Lawrence Livermore National Laboratory, L-231, P.O. Box 808, Livermore, CA 94550, USA*

[2)]*Helmholtz-Zentrum Dresden-Rossendorf e.V., Institute of Resource Ecology, P.O. Box 510119, 01314 Dresden, Germany*

[‡] *present address: Nagra, Hardstrasse 73, CH-5430 Wettingen, Switzerland*

[§] *present address: LSI Sachsen GmbH & Co. KG, BioInnovationsZentrum Dresden, Tatzberg 47, 01307 Dresden, Germany*

With regard to the safe long-term storage of high-level nuclear waste in repositories in deep geological formations, safety assessment studies are essential to investigate the migration behavior of actinides, such as uranium, released from the waste into the surrounding geo- and biosphere. Bentonite is discussed as potential backfill material, which properties (e.g., swelling pressure, density, porosity) can have a significant effect on the diffusive transport of species within a repository.

For a time period of six years the U(VI) diffusion through compacted MX-80 bentonite was investigated as a function of clay dry bulk density (ρ =1.3, 1.6, 1.9 g/cm^3). The clay rock contained natural uranium with a fraction of (13 ± 0.1) ppm. The experiments were conducted under aerobic conditions at room temperature. The clay was compacted in stainless steel diffusion cells [1]. These were connected to a source reservoir, containing the tracer ^{238}U(VI) ($c_0 = 1 \times 10^{-6}$ M), and a tracer-free receiving reservoir, respectively. As background electrolyte complex model pore water [2] was used whose composition differed slightly depending on the clay density (pH 8, $I =$ 0.3 M). After 2457 days the diffusion experiment was stopped and the uranium clay depth profiles were determined by abrasive peeling [3]. Diffusion parameters were determined by modeling [4, 5].

Speciation calculations [6] revealed that independent of pore water type and water sampling time always the $Ca_2UO_2(CO_3)_3$(aq) complex [7] was the dominant U(VI) species in solution (83-90%). This neutral complex was assumed to be the main diffusing U(VI) species in the system. As effective transport porosity, ε_{eff}, the value for HTO was assumed in the U(VI) diffusion model, although one can expect that ε_{eff}(U(VI)) is smaller than ε_{eff}(HTO) regarding to the size of the molecules and their respective access to the clay interlayers. However, the used value of ε_{eff} has no significant impact on the modeled U(VI) diffusion parameters, since the U(VI) sorption onto the clay is dominating [8].
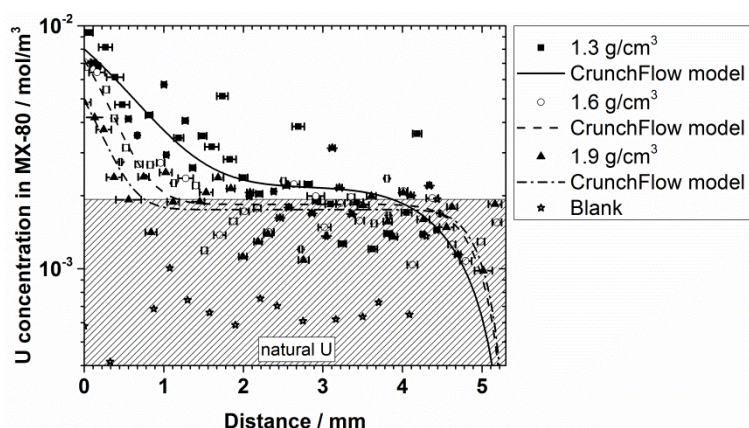
Figure 1. Concentration depth profile of uranium in MX-80 as a function of clay dry density [9].

Under consideration of the natural uranium background in MX-80 it was estimated that U(VI) diffused about 2 mm, 1 mm, and 0.7 mm deep in the clay at $\rho =$ 1.3, 1.6, and 1.9 g/cm^3, respectively (cf. Figure 1). The distribution coefficients modeled are very low (K_d = 5.8-2.6×10^{-3} m^3/kg). This can be attributed to

Ca$_2$UO$_2$(CO$_3$)$_3$(aq) which is known to sorb only weakly onto clay [10]. For the same system batch sorption experiments were performed using a solid-to-liquid ratio (S/L) of 2.5 g/L [11]. The K_d values obtained were about one order of magnitude higher than the K_d values of the present study. Probably, the S/L ratio was too small. Such a dependence of K_d on the S/L ratio was previously described for the U(VI) sorption onto clay [10]. However, the K_d values of the present study differ only by a factor of three from the K_d values published by Glaus and Van Loon [12] for the U(VI) diffusion through compacted montmorillonite in calcareous NaClO$_4$ solutions for I = 0.1 M, 0.5 M, which can be regarded as in very good agreement.

For determination of the apparent U(VI) diffusion coefficient, D_a, two fitting approaches were applied. 1) Fitting of the uranium depth profiles: About two orders of magnitude lower D_a values were obtained than any published D_a value so far, in particular, for "short-term" diffusion studies conducted for less than one year. 2) Fitting of the out-diffusion of natural uranium into the receiving reservoir solution: D_a values are in very good agreement with literature data [12, 13]. This discrepancy shows that the in- and out-diffusion of U(VI) in MX-80 has to be regarded independently in this study.

The reason for these substantial different results could be a reduction of clay porosity far below the percolation threshold by formation of a clay-gel in the pores after longer time scales as just recently reported for MX-80 [14], which leads to a decrease in pore connectivity and would hinder or even stop the through-diffusion of U(VI). However, the out-diffusion or leaching of U(VI) from the clay would still be possible. The experiments show the value of long-term diffusion experiments, since migration determining processes may occur or be visible only at longer time frames. In addition, it shows the excellent retention capacity of bentonite for weakly sorbing U(VI) species.

[1] L. R. Van Loon, et al., Appl. Geochem. 18, 1653 (2003).
[2] L. R. Van Loon, et al., Deliverable (D-N°: 2.5.20), Reporting period: 01/01/04 - 31/12/07, European Commission - Community Research (2007).
[3] L. R. Van Loon, J. Eikenberg, Appl. Radiat. Isot. 63, 11 (2005).
[4] C. Steefel, CrunchFlow, Lawrence Berkeley National Laboratory (2011).
[5] J. Doherty, PEST, Watermark Numerical Computing (2003).
[6] C. M. Bethke, S. Yeakel, The Geochemist's Workbench®, Hydrogeology Program, University of Illinois (2010).
[7] G. Bernhard, et al., Radiochim. Acta 89, 511 (2001).
[8] C. Joseph, et al., Geochim. Cosmochim. Acta 109, 74 (2013).
[9] C. Joseph, et al., Geochim. Cosmochim. Acta in preparation (2015).
[10] C. Joseph, et al., Chem. Geol. 284, 240 (2011).
[11] C. Nebelung, V. Brendler, Annual Report 2008, FZD-511, Forschungszentrum Dresden-Rossendorf, Institut für Radiochemie, Dresden (2009).
[12] M. A. Glaus, L. R. Van Loon, Clays in Natural & Engineered Barriers for Radioactive Waste Confinement - 5th International Meeting, Andra, Montpellier, 885 (2012).
[13] K. Idemitsu, et al., Mater. Res. Soc. Symp. Proc. 412, 683 (1996).
[14] L. M. Keller, et al., Appl. Clay Sci. 104, 150 (2015).

THE IMPORTANCE OF CATION EXCHANGE SPECIES FOR THE DIFFUSIVE BEHAVIOUR OF MODERATELY AND STRONGLY SORBING RADIOELEMENTS IN COMPACTED ILLITE

M.A. Glaus, B. Baeyens, M. Marques Fernandes, L.R. Van Loon

Laboratory for Waste Management, Paul Scherrer Institut, CH-5232 Villigen PSI, Switzerland

The assessment of the diffusive behaviour of moderately and strongly sorbing radioelements in compacted argillaceous media is difficult because almost no data for effective diffusion coefficients (D_e [m^2 s^{-1}]) are available from the open literature and because surface diffusion may also be effective for such species. The extent of surface diffusion effects depends on a variety of basic system properties, such as the type of clay, its bulk dry density and the chemical composition of the equilibrium solution. It was hypothesised that surface diffusion is restricted to smectite clay minerals at rather high bulk dry densities [1]. However we recently showed that these effects are also important for compacted illite in which the interlayer space is collapsed by intercalation of dehydrated potassium ions [2].

The present work is focused on variations of the fractional occupancies of the different cation sorption sites in illite. According to current sorption models the uptake of cationic species on the surfaces of negatively charged clay minerals is effectuated by cation exchange and surface complexation reactions [3], the dominance of which is mainly governed by pH, ionic strength and metal loading. We present the results of diffusion experiments with Zn(II) and Eu(III), in which the background concentration of the stable element was varied resulting in different degrees of saturation of the different sorption sites. For this purpose defined amounts of stable isotopes of the test metal cations were added to the clay mineral before preparation of the compacted test specimens. These "stable isotope conditions" are compared to experiments in which no stable isotopes were added. Measureable backgrounds of stable isotopes were also present in the latter experiments owing to impurities originating from accessory minerals in illite and/or from the tracer stock solutions. For simplicity these are denoted to as "trace conditions" in the following.

Fig. 1A shows the diffusion results obtained for Zn^{2+} in illite compacted to bulk-dry densities of ~1700 kg m^{-3}. The experiments were carried out at pH 5 and at various levels of background concentrations of the stable Zn isotope and NaClO$_4$. At "stable isotope conditions" D_e values were linearly correlated with the respective solid-liquid distribution ratios (R_d [L kg^{-1}]), which were also evaluated from the diffusion experiments. Previously published results [2] obtained at "trace conditions" of $^{65}Zn^{2+}$ are also shown in Fig. 1A. The correlation between D_e and R_d values was almost completely absent in this latter group of data.

We hypothesised previously that the species bound to the cation exchange sites are mobile, while those in the surface complexation sites are immobile [2]. Changing the ratio of mobile surface species to aqueous phase species has thus a direct influence on D_e, while changing the ratio of immobile species to aqueous phase species has no influence on D_e. The observed correlation of D_e and R_d values in the new data at "stable isotope conditions" suggests therefore that the majority of surface species are mobile. Sorption modelling (Fig. 1B) shows the areas of predominance of these surface species. The model parameters used in Fig. 1B were obtained from sorption experiments using disperse illite suspensions [4]. In agreement with the position of the R_d values relative to the modelled sorption isotherms for the surface complex species we conclude that the surface mobility has to be attributed predominantly to Zn species on the cation exchange sites. At "trace conditions" the changes in D_e upon a given variation of the NaClO$_4$ concentration is similar to that observed at "stable isotope conditions". Also the absolute values of D_e are rather comparable. Under such conditions the ratio of cation exchange species to aqueous phase species is thus similar to the respective ratio at "stable isotope conditions". However R_d values are rather insensitive to changes in NaClO$_4$ concentrations because they are largely dominated by species on the surface complexation sites. If these species were mobile, the expected D_e values would be larger by orders of magnitude than those observed at "stable isotope conditions". The data measured at "stable isotope conditions" complementhus our data measured at "trace conditions" and hence fully support the general concept of potentially different surface mobilities for different surface species.

The confirmation of this concept has strong implications for the prediction of the mobility in the geosphere of moderately and strongly sorbing radioelements under realistic repository conditions. Diffusion dominated transport is described by Fick's second law which relates the time and space derivatives of species concentration

(c [mol m^{-3}]) via the apparent diffusion coefficient (D_a [m^2 s^{-1}]) as a proportionality factor (ε being the total clay porosity [m^3 m^{-3}] and ρ_{bd} its bulk dry density [kg m^{-3}])

$$\frac{\partial c}{\partial t} = D_a \frac{\partial^2 c}{\partial x^2} = \frac{D_e}{\varepsilon + \rho_{bd} R_d} \frac{\partial^2 c}{\partial x^2} \tag{1}$$

For an appropriate assessment of the D_a values, knowledge on strong and weak interactions between the radionuclide and the clay surface is needed. While the specific surface complexation species mainly govern the total amount of the surface inventory and thus R_d values, D_e values are largely influenced by the extent of the formation of cation exchange species. An adequate knowledge of both the selectivity coefficients for cation exchange and the respective equilibrium constants for the formation of surface complexes is thus required for a reliable prediction of the migration behaviour of moderately and strongly sorbing radionuclides.

Figure 1. Plot A shows the relationship between D_e and R_d values measured in diffusion experiments with ^{65}Zn^{2+}
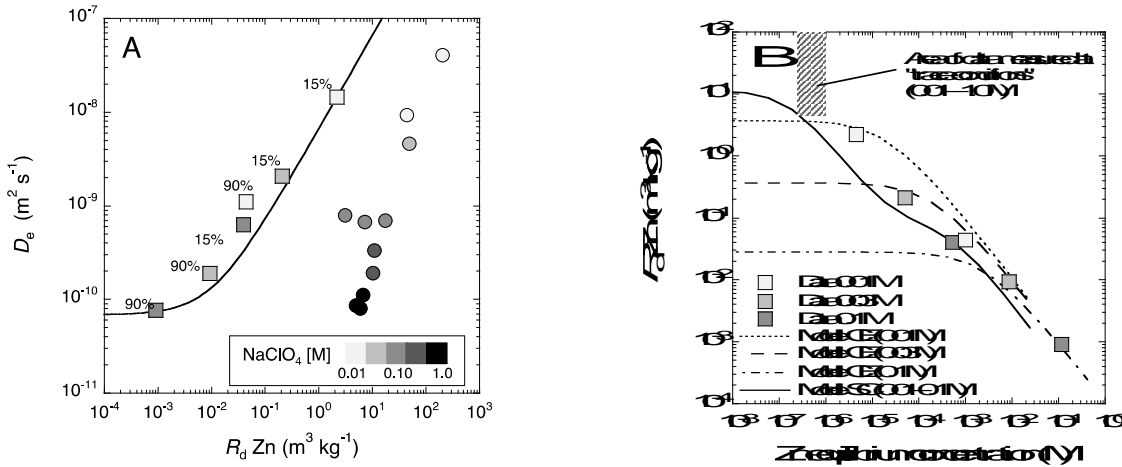
in compacted illite at pH 5 and various concentrations of NaClO$_4$ at "stable isotope conditions" (squares) and at "trace conditions" (circles, data from [2]). The data labels give the relative degree of saturation of the cation exchange sites with Zn. The model curve represents the linear correlation between D_e and R_d values for a parallel flux model of a surface and an aqueous phase species according to [5]. Plot B shows the position of these data on the sorption isotherms for cation exchange (CE) and surface complexation species (SC) for the various concentrations of NaClO$_4$ specified in the legends.

References:

1. Shackelford, C.D., *The ISSMGE Kerry Rowe Lecture: The role of diffusion in environmental geotechnics.* Canadian Geotechnical Journal, 2014. **51**(11): p. 1219-1242.

2. Glaus, M.A., et al., *Enhanced mass transfer rates for Sr^{2+}, Co^{2+} and Zn^{2+} in compacted illite caused by cation diffusion in the electrical double layer.* Submitted to Geochimica et Cosmochimica Acta, 2015.

3. Bradbury, M.H. and B. Baeyens, *A mechanistic description of Ni and Zn sorption on Na-montmorillonite .2. Modelling.* Journal of Contaminant Hydrology, 1997. **27**(3-4): p. 223-248.

4. Kupcik, T., et al., *Sr(II), Co(II) and Zn(II) sorption onto Na-illite: batch sorption studies and modelling.* in preparation, 2015.

5. Gimmi, T. and G. Kosakowski, *How mobile are sorbed cations in clays and clay rocks?* Environ. Sci. Technol., 2011. **45**(4): p. 1443–1449.

THE INFLUENCE OF PH ON DIFFUSION OF $^{99}\text{TcO}_4^-$ AND $^{75}\text{SeO}_3^{2-}$ IN BEISHAN GRANITE, CHINA

C.L. Wang[(1)], C. Li[(1,2)], C.L. Liu[(1)*]

1.Beijing National Laboratory for Molecular Science, Radiochemistry & Radiation Chemistry Key Laboratory for Fundamental Science, College of Chemistry and Molecular Engineering, Peking University, Beijing 100871, P.R. China

2. State Nuclear Security Technology Center, Beijing 100037, P.R. China

Deep geological disposal based on the 'multi-barrier system' is internationally accepted to be the most effective way in isolating the high-level radioactive wastes (HLW) from biosphere for a long period [1]. To make sure the wastes can be isolated in a long time scale, it is necessary to carry out the pre-safety assessment of the repository [2], and the migration and transportation behaviors of key radionuclides in geological barriers are an important part that should be investigated in the pre-safety assessment. In China, Beishan area (Gansu province) has been pre-selected as an important research site for the potential HLW repository, and Beishan granite is a vital pre-selected host rock [3].

When radionuclides release from a repository, it might pass through the near field, the far field and finally enter the biosphere and contribute to the total radiation dose of the population close the potential repository. Along the path way, different regions may present different hydro-geochemical conditions, which might affect the properties of geological barriers, and when radionuclides interact with granite surfaces, their diffusion or migration would be influenced by the surface properties of granite. As is well-known, the surface of minerals would be positively or negatively charged due to different pH values, and density of the charges is also significantly controlled by pH. Moreover, the species distribution of radionuclides is strongly depend on the pH and Eh values of the system, which will further affect the solubility and migration behaviors of radionuclides in the geological disposal repository.

^{99}Tc and ^{79}Se are key fission products present in HLW which have a high probability to release off from the repository. $^{99}\text{TcO}_4^-$ which has high mobility in geological environments is the predominant species under non-reducing condition, whereas ^{79}Se is a redox-sensitive element which can exist in five oxidation states (0, −1, −2, +4 and +6) and its solubility and mobility in the environment are largely depend on the oxidation state and chemical form which is controlled by the surrounding Eh-pH conditions [4].

In order to gain a better understanding of the diffusion and migration mechanisms of key radionuclides ^{99}Tc and ^{79}Se in the granitic rocks, and provide data to the performance assessment for the potential geological repository for HLW in China, the influence of the Beishan granite/groundwater system pH on diffusion of $^{99}\text{TcO}_4^-$ and $^{75}\text{SeO}_3^{2-}$ was investigated by through-diffusion technique. $NaClO_4$ solution was used as background solution and to control the ionic strength. The surface charge of Beishan granite in various pH was investigated by potentiometric titration experiment. The experimental data were fitted with a finite difference scheme procedure DKFIT, which was based on the Fick first law, to get the effective diffusion coefficient De of $^{99}\text{TcO}_4^-$ and $^{75}\text{SeO}_3^{2-}$ in Beishan granite.

The results of De values at different pH for $^{99}\text{TcO}_4^-$ and $^{75}\text{SeO}_3^{2-}$ in Beishan granite were shown in Figure 1. It can be seen that the effective diffusion coefficient D_e of $^{99}\text{TcO}_4^-$ in Beishan granite hardly changed with pH in atmosphere condition at room temperature, and the values were 9.7×10^{-13} m^2/s $\sim 1.3 \times 10^{-12}$ m^2/s when the pH ranged from 3 to 10. Moreover, the distribution coefficient K_d of $^{99}\text{TcO}_4^-$ in Beishan granite decreased while the pH increased.

On the other hand, the De values of $^{75}\text{SeO}_3^{2-}$ in Beishan granite varied from 8.5×10^{-14} m^2/s to 4.8×10^{-13} m^2/s when the pH ranged from 2 to 8.5, and the results indicated that the values of De decreased with pH increasing when the pH is lower than 6, whereas, when the pH is higher than 6, the De values increased with increased pH. These results may be explained by the species distribution of ^{99}Tc and ^{79}Se, as well as surface properties especially the surface charge of Beishan granite at different pH values.
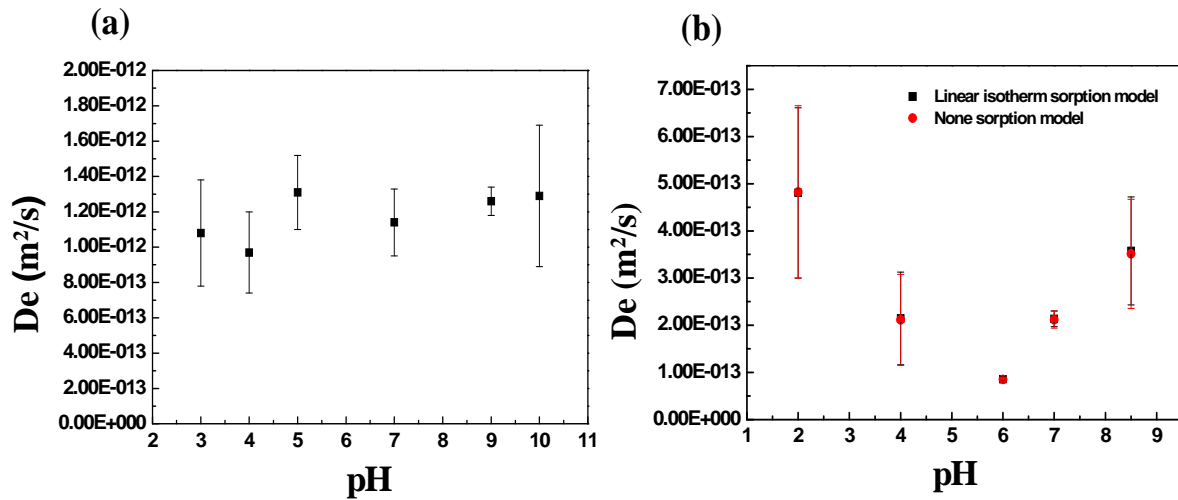
Figure1. De values of $^{99}TcO_4^-$ (a) and $^{75}SeO_3^{2-}$ (b) in Beishan granite as a function of pH

[1]   Ewing, R. C., RADIOACTIVE WASTE:Less Geology in the Geological Disposal of Nuclear Waste. *Science* **1999,** *286*, (5439), 415-417.

[2]   Chapman, N.; Hooper, A., The disposal of radioactive wastes underground. *Proceedings of the Geologists' Association* **2012,** *123*, (1), 46-63.

[3]   Yuemiao, W. J. S. R. C. W. G. Y. J. Y. W. Z. L., Deep geological disposal of high-level radioactive wastes in China. *Chinese Journal of Rock Mechanics and Engineering* **2006,** *25*, (4), 649-659.

[4]   Charlet, L.; Kang, M.; Bardelli, F.; Kirsch, R.; Géhin, A.; Grenèche, J.-M.; Chen, F., Nanocomposite pyrite–greigite reactivity toward Se (IV)/Se (VI). *Environmental Science & Technology* **2012,** *46*, (9), 4869-4876.

BEHAVIOR OF ^{36}Cl IN IRRADIATED NUCLEAR GRAPHITE WASTE: CONSEQUENCES FOR INVENTORIES AND TREATMENT IN VIEW OF DISPOSAL

N. Toulhoat[1,2], N. Moncoffre[1], N. Bérerd[1,3], Y. Pipon[1,3], A. Blondel[1,*], N. Galy[1], P. Sainsot[4], J.N. Rouzaud[5], D. Deldicque[5], M.R. Ammar [6]

[1] Université de Lyon, Université Lyon 1, CNRS/IN2P3, UMR5822, (IPNL), France
[2] CEA/DEN, Centre de Saclay, France
[3] Université de Lyon, UCBL IUT A, département chimie, France
[4] Université de Lyon, Université Lyon 1, LaMCoS, INSA Lyon, CNRS UMR5259, France
[5] Laboratoire de Géologie de l'Ecole Normale Supérieure, Paris, UMR CNRS ENS 8538, France
[6] CNRS, UPR 3079 CEMHTI, 45071 Orléans Cedex 2, France, France
* now at Agence nationale pour la gestion des déchets radioactifs, Châtenay-Malabry, France

Nuclear graphite has found widespread use in many areas of nuclear technology based on its excellent moderator and reflector qualities. Thus, since the sixties, several first generation commercial nuclear reactors (UNGG, MAGNOX, AGR) using natural uranium fuel, CO_2 cooled and graphite moderated were built. Many of these reactors are now being decommissioned and over 23000 tons of irradiated graphite waste is waiting for management all over the world. Neutron irradiation of graphite results in the production of radionuclides such as ^{14}C and ^{36}Cl, these radionuclides being a key issue regarding the management of the irradiated graphite waste because they might be dose determining at the outlet. Whatever the management option (purification, storage or disposal), a previous assessment of the radioactive inventory has to be made.

This study is devoted to ^{36}Cl. Chlorine is present as an impurity and is not uniformly distributed in the nuclear graphite matrix. It tends also to be more enriched close to open pores especially when the maintenance stages of the nuclear reactors are performed under air. ^{36}Cl activity is low but, due to the high mobility of chlorine in the disposal clay, it could result in a dose peak at the outlet. Thus, in order to be able to control and to limit a potential dissemination of chlorine during dismantling and in the repository, it is necessary to collect information about ^{36}Cl location and speciation in graphite, after reactor closure. This information is also necessary for the further disposal dimensioning.

Our work is the fruit of a cooperation performed within the European Carbowaste project of the Euratom 7th framework program. Based on our work, this presentation proposes a state of the art on the knowledge related to the behavior of ^{36}Cl from reactor operation to repository conditions.

According to the results of Poncet & Petit [1] using identification calculation–measurement process, significant amounts of ^{36}Cl have been released during reactor operation. Thus, the goal of this work is to elucidate the mechanisms responsible for its release in reactor and consequently to understand the behavior of ^{36}Cl during reactor operation. As the detection limits of usual spectroscopic methods are generally not adequate to detect the low concentration levels (< 1 ppm) of the radionuclides, we used an indirect approach based on the implantation of ^{37}Cl, to simulate the presence of ^{36}Cl. Virgin nuclear graphite samples from the SLA2 UNGG reactor was implanted with ^{37}Cl at a concentration of some at.ppm used to simulate ^{36}Cl displaced from its original structural site through recoil. Experiments were carried out to simulate and to elucidate the respective and synergistic effects of temperature, radiolytic corrosion and irradiation on chlorine depletion during reactor operation.

Using many complementary techniques for treatment (temperature annealing, irradiation) or analysis of the samples, (gas chromatography, SIMS, RBS, Raman microspectrometry, XPS, SEM), following main results have been obtained:

The effects of temperature solely induce a release of ^{37}Cl of around 25% of the initial implanted quantity within a few hours at maximum reactor temperatures of 500°C implying that temperature is responsible for a part but not all the depletion of the ^{36}Cl inventory occurring during reactor operation. Temperatures as high as 1400°C are necessary to totally remove ^{37}Cl.

Thus, the impact of irradiation and its synergistic effects with temperature on chlorine release were also investigated. Both ion irradiation and gamma photon irradiation were explored.

-       The collisions of the impinging neutrons with the graphite matrix carbon atoms induce mainly ballistic damage. However, a small part of the recoil carbon atom energy is also transferred to the graphite lattice through electronic excitation. Thus, using ion irradiation performed at different facilities with dedicated irradiation cells, we have been able to simulate the effects of these different irradiation regimes in synergy with temperature. The results show that "moderate" electronic excitations and ionizations, i.e. for electronic stopping powers ranging up to 700keV/µm which corresponds to the usual range in UNGG reactors, do not promote ^{37}Cl release. On the contrary, ballistic damage highly promotes ^{37}Cl release at temperatures lower than 400°C due to the mobility of interstitials. The release reaches 30% from 200°C. It slows down above 400°C due to the recombination of interstitials and vacancies but remains higher than the release solely induced by temperature. The role played by the concomitant graphite reordering induced by temperature on chlorine release during irradiation has been clearly evidenced by Raman microspectrometry studies.

-       The impact of gas radiolysis has also been investigated using gamma photons (at room temperature) or ions (at 500°C). Graphite samples put in contact with a gas representative of the UNGG gas thus were irradiated with gamma photons on one hand and with $^{4}He^{++}$ ions on the other hand. The comparison of the results show that, in absence of methane, when the free radicals formed through gas radiolysis are produced at the gas/heated graphite interface, the radiolytic corrosion of the graphite surface proceeds. This should therefore be another important factor responsible for ^{36}Cl release in graphite moderated CO_2 cooled reactors [2].

Finally, our experiments allow getting more insight about the ^{36}Cl inventory that has to be considered for further disposal. They put in evidence the respective or synergistic roles of temperature and irradiation inducing a zoning of ^{36}Cl depletion in the moderator. Thus, ^{36}Cl should be more depleted in region of high neutron flux and high temperature and less depleted in less irradiated and colder parts of the irradiated graphite.

Moreover, our studies allowed us to infer that chlorine is mainly bound to carbon in nuclear graphite. Two main trapping sites of chlorine have been identified: a low energy one located at the crystallite and grain edges (close to the open pores) from which chlorine is easily de-trapped and released through the micro and macroporosities (the open porosity is around 25%); a high energy site located inside the crystallites for which more energy and therefore a temperature higher than 1100°C is required to allow chlorine de-trapping and diffusion.

A consequence is that, in view of irradiated graphite waste purification of ^{36}Cl, an annealing process at temperatures higher than 1300°C in non-oxidizing atmosphere could be beneficial.

Finally, our findings are in excellent agreement with the results of C. Pichon et al. [3] on the behavior of ^{36}Cl during irradiated graphite leaching experiments suggesting the presence of two kinds of chlorine: a labile fraction present in the macroporosity on one hand and a fraction located in the microporosity or closed porosity on the other hand.

[1] B. Poncet & L. Petit, J. Radioanal. Nucl. Chem (2013) 298:941-953 Method to assess the radionuclide inventory of irradiated graphite waste from gas cooled reactors
[2] A. Blondel, PhD thesis, Effets de la température et de l'irradiation sur le comportement du chlore 37 dans le graphite nucléaire : Conséquences sur la mobilité du chlore 36 dans les graphites irradiés, University Claude Bernard Lyon-I, December 19, 2013, LYCEN – T2013-15, N° d'ordre 323-2013
[3] C. Pichon, C. Guy, J. Comte, ATALANTE 2008 Montpellier (France) May 19-22, 2008, ^{36}Cl and ^{14}C behaviour in UNGG graphite during leaching experiments

SYNTHESIS AND DETERMINATION OF THE THERMODYNAMIC
PROPERTIES OF COFFINITE

<u>N. Dacheux</u> [(1)], S. Szenknect [(1)], A. Mesbah [(1)], T. Cordara [(1)], N. Clavier [(1)], C. Poinssot [(2)], X. Guo [(3)], S.V. Ushakov [(3)], S. Labs [(4)], H. Curtius [(4)], C. Den Auwer [(5)], J. Lozano-Rodriguez [(6)], D. Bosbach [(4)], P.C. Burns [(7)], A. Navrotsky [(3)], R.C. Ewing [(8)]

[(1)] *Institut de Chimie Séparative de Marcoule, ICSM - UMR 5257 CEA / CNRS / UM / ENSCM, Site de Marcoule – Bât. 426, BP 17171, 30207 Bagnols-sur-Cèze cedex, France*

[(2)] *CEA, Nuclear Energy Division, DRCP/DIR, CEA Marcoule, Bât. 400, BP 17171, 30207 Bagnols-sur-Cèze cedex, France*

[(3)] *Peter A. Rock Thermochemistry Laboratory and Nanomaterials in the Environment, Agriculture, and Technology Organized Research Unit, University of California, Davis, CA 95616, USA*

[(4)] *Institute of Energy and Climate Research (IEK-6), Nuclear Waste Management, Forschungszentrum Jülich GmbH, 52425 Jülich, Germany*

[(5)] *Institut de Chimie de Nice, UMR 7272, Nice Sophia-Antipolis University, 28 av.de Valrose, 06108 Nice cedex 2, France*

[(6)] *HZDR, Institute of Resource Ecology, the Rossendorf Beamline at ESRF, P.O. Box 220, 38043 Grenoble, France*

[(7)] *Department of Civil and Environmental Engineering and Earth Sciences, University of Notre Dame, Notre Dame, IN 46556, USA*

[(8)] *Geological Sciences and Center for International Security & Cooperation, Stanford University, Stanford, CA 94305-2115, USA*

Coffinite, $USiO_4$, and associated solid-solutions are expected to play an important role in the direct disposal of spent nuclear fuel in an underground repository. Indeed, coffinite is the second most abundant U^{4+} mineral on Earth, and its formation by the alteration of the UO_2 may control the release of radionuclides from nuclear fuels to the environment. However, the thermodynamic properties associated with coffinite, especially the solubility constant, have remained poorly defined. Indeed, the few available thermodynamic data related to the coffinite formation or solubility are hardly reliable since none were determined experimentally by direct solubility measurements [1-4].

One of the reasons is that most of the natural samples of coffinite are very fine-grained ($\approx$ 5 μm) [5] and in intimate intergrowths with other U-minerals, while solubility studies require pure single-phase $USiO_4$. Despite its abundance in nature, the synthesis and characterization of pure single-phase coffinite has eluded researchers for decades. In order to circumvent this problem, an indirect method based on solubility measurements of $Th_{1-x}U_xSiO_4$ samples was first envisaged. The preparation of $Th_{1-x}U_xSiO_4$ uranothorite solid solutions under hydrothermal conditions was successfully undertaken [6,7]. The analysis systematically demonstrated the formation of pure $Th_{1-x}U_xSiO_4$ solid-solutions for $0 \leq x \leq 0.4$, although multiple phases formed at higher uranium incorporation concentrations.

Based on the first results obtained for the uranothorite solid-solution and in order to understand why coffinite is abundant in nature and so difficult to synthesize, we examined the experimental conditions under which coffinite can be reproducibly synthesized and efficiently formed in mixtures of $USiO_4$ / UO_2 / SiO_2. In fact, the formation of coffinite results from the complex interplay between pH, T, Si:U ratio and heating time. The pH is definitively the dominant parameter in the stabilization of coffinite, In fact, the pH must be adjusted to a range between 10 and 12.5 in order to stabilize an appropriate uranium silicate complex $U(OH)_3(H_3SiO_4)_3^{2-}$ in solution, that is a precursor of uranium silicate colloids and then finally of coffinite. Moreover, in this pH range, the largest yield of coffinite (as compared with the two competing by-product phases: nanometer-scale UO_2 and amorphous SiO_2) was obtained for T = 250°C, t = 7 days, and 100 % of excess silica. However, this synthesis always led to an equilibrium between $USiO_4$, UO_2 and SiO_2 (as observed in natural samples) [8].

Because the samples of $Th_{1-x}U_xSiO_4$ (with x > 0.4) were always found to be polyphase, a purification procedure based on three successive cycles, including dissolution steps in acidic (0.01M HNO_3) then in a basic media

(0.01M KOH), was successfully developed in order to prepare purified uranothorite and coffinite samples over the entire compositional range [9].

The second step of the study was dedicated to the acquisition of thermodynamic data for coffinite. Its solubility constant was first determined by extrapolation from the solubility of several purified $Th_{1-x}U_xSiO_4$ solid-solutions. Considering the solubility constant of thorite ($\log*K_S^o(ThSiO_4, cr) = -5.62 \pm 0.08$), on the one hand, and that of various $Th_{1-x}U_xSiO_4$ solid solutions (with x < 0.5), on the other hand, a first estimate led to $\log*K_S^o(USiO_4, cr) = -6.1 \pm 0.2$ [10]. Solubility experiments were thus completed on purified coffinite then on several phases assemblages containing coffinite ($USiO_4 + UO_2$, $USiO_4 + SiO_2$, $USiO_4 + UO_2 + SiO_2$) in under saturated experiments (0.1M HCl, Ar-atmosphere or air). The previously determined solubility constant was confirmed to be $\log*K_S^o(USiO_4, cr) = -6.13 \pm 0.37$, in good agreement with the results from the extrapolation of data on the solid-solution series. Thermodynamically, coffinitization of UO_2 occurs at 298K, under reducing conditions, at near-neutral pH, for an H_4SiO_4 activity above 10^{-2}. Under these conditions, coffinite must precipitate and controls the concentration of tetravalent uranium in solution. The value of $_{r,ox}G°(298K)$ obtained (15.6 ± 3.4 kJ.mol^{-1}) indicates unambiguously that coffinite is less stable than a quartz-uraninite mixture at 298K, but also that the equilibrium may be easily reversed at slightly higher temperatures [11].

Finally, thermodynamics of formation of coffinite were examined. The enthalpy of formation was obtained by high temperature oxide melt solution calorimetry in two different solvents: $3 Na_2O - 4 MoO_3$ and $2 PbO - B_2O_3$. The calorimetric data confirmed the thermodynamic metastability of coffinite with respect to a mixture containing UO_2 (uraninite) and SiO_2 (quartz) ($H_{f,ox} = 25.6 \pm 3.9$ kJ.mol^{-1}). The associated standard enthalpy of formation from the elements was evaluated to be: -1970.0 ± 4.2 kJ.mol^{-1} at 298K. When heated, coffinite slowly decomposes to U_3O_8 and SiO_2 starting around 450 °C in air and thus exhibits poor thermal stability. This energetic metastability explains why coffinite cannot be synthesized directly from uraninite and quartz by heating, but can be made by low temperature precipitation in aqueous and hydrothermal environments [12].

[1] Grenthe, I.; Fuger, J.; Konings, R. J. M.; Lemire, R. J.; Muller, A. B.; Nguyen-Trung, C. and Wanner, H., «Chemical Thermodynamics of Uranium». North Holland Elsevier Science Publishers B.V.: Amsterdam, The Netherlands, 1992; Vol. 1, p 715

[2] Guillaumont, R.; Fanghänel, T.; Fuger, J.; Grenthe, I.; Neck, V.; Palmer, D. A. and Rand, M. H., «Update on the chemical thermodynamics of uranium, Neptunium, Plutonium, Americium and Technetium». North Holland Elsevier Science Publishers B.V.: Amsterdam, The Netherlands, 2003; Vol. 5, p 919.

[3] Langmuir, D., Geochimica et Cosmochimica Acta 1978, 42, 547-569.

[4] Hemingway, B. S., «Thermodynamic properties of selected uranium compounds and aqueous species at 298.15K and 1 bar and at higher temperatures. Preliminary models for the origin of coffinite deposits.» ; US Geological Survey: 1982; p 89.

[5] Deditius, A. P.; Utsunomiya, S.; Ewing, R. C., Chemical Geology 2008, 251, 33-49.

[6] Costin, D. T.; Mesbah, A.; Clavier, N.; Szenknect, S.; Dacheux, N.; Poinssot, C.; Ravaux, J.; Brau, H. P., Progress in Nuclear Energy 2012, 57, 155-160

[7] Costin, D. T.; Mesbah, A.; Clavier, N.; Dacheux, N.; Poinssot, C.; Szenknect, S.; Ravaux, J., Inorganic Chemistry 2011, 50, 11117-11126

[8] Mesbah, A.; Szenknect, S.; Clavier, N.; Lozano-Rodriguez, J.; Poinssot, C.; Den Auwer, C.; Ewing, R.C.; Dacheux, N., Inorganic Chemistry, submitted.

[9] Clavier, N.; Szenknect, S.; Costin, D. T.; Mesbah, A.; Ravaux, J.; Poinssot, C.; Dacheux, N., Journal of Nuclear Materials, 2013, 441, 73-83.

[10] Szenknect, S.; Costin, D. T.; Clavier, N.; Mesbah, A.; Poinssot, C.; Vitorge, P.; Dacheux, N., Inorganic Chemistry 2013, 52, 6957-6968.

[11] Szenknect, S.; Mesbah, A.; Cordara, T.; Clavier, N.; Brau, H.P.; Le Goff, X.; Poinssot, C.; Ewing, R.C.; Dacheux, N., Geochimica et Cosmochimica Acta, submitted.

[12] Guo, X.; Szenknect, S.; Mesbah, A.; Labs, S.; Clavier, N.; Poinssot, C.; Ushakov, S.V.; Curtius, H.; Bosbach, D.; Ewing, R.C.; Burns, P.C.; Dacheux, N.; Navrotsky, A., Proceedings of the National Academy of Sciences, 2015, 112, 6551-6555.

CURIUM(III) AND EUROPIUM(III) INCORPORATION IN LANTHANIDE PHOSPHATE CERAMICS FOR CONDITIONING OF RADIOACTIVE WASTES

N. Huittinen[1], Y. Arinicheva[2], J. Holthausen[2], M. Schmidt[1], S. Neumeier[2], T. Stumpf[1]

[1]*Helmholtz-Zentrum Dresden-Rossendorf, Institute of Resource Ecology, Bautzner Landstraße 400, 01328 Dresden, Germany*
[2]*Forschungszentrum Jülich GmbH, Institute of Energy and Climate Research, Nuclear Waste Management and Reactor Safety (IEK-6), 52425 Jülich, Germany.*

The high-level radioactive waste (HLW) from spent nuclear fuel reprocessing facilities is currently immobilized in borosilicate glass. The vitrification process is well established and the flexible glass matrix is able to incorporate a very large range of elements present in the waste solution [1]. With the development of partitioning strategies, enabling the extraction of long-lived fission products and minor actinides (MA) from the PUREX raffinate, specific waste streams will be created that may require durable host matrices for their safe disposal. Especially for MA immobilization, some ceramic materials have been envisioned as host materials due to their thermal stability, high radiation tolerance, and chemical durability [2].

Lanthanide phosphate ceramics ($LnPO_4$) are able to incorporate radionuclides in well-defined atomic positions within the crystal lattice [3] up to high (27 %) loadings [2]. The existence of very old natural analogues containing high concentrations of uranium and thorium shows that the crystalline phosphate structure is very tolerant towards self-irradiation damages as well as chemical weathering [4]. The dehydrated, high-temperature $LnPO_4$ phases are known to crystallize in two distinct structures, depending on the ionic radius of the lanthanide cation: the larger lanthanides from La^{3+} to Gd^{3+} crystallize in the nine-fold coordinated monazite structure with a low symmetry, while the smaller lanthanides Tb^{3+} to Lu^{3+} form tetragonal, eight-fold coordinated xenotime structures.

In the present study we have used site-selective time-resolved laser fluorescence spectroscopy (TRLFS) to investigate the influence of the host cation radius as well as the crystal structure of the ceramic (monazite vs. xenotime) on the incorporation of the trivalent metal ions Eu^{3+} and Cm^{3+}. We have synthesized pure monazites and xenotimes doped with 500 ppm Eu^{3+} or 50 ppm Cm^{3+} by precipitation of $LnPO_4$ from a 0.3-0.5 M lanthanide nitrate solution with phosphoric acid followed by sintering of the precipitate at 1450°C to obtain the crystalline ceramic. The laser spectroscopy was performed either with a pulsed Nd:YAG-pumped tunable optical parametric oscillator or dye laser setup at cryogenic temperatures (~ 10 K). Excitation and emission spectra as well as luminescence lifetimes were collected for all measured samples.

Results on Eu^{3+}-doped monazites show very narrow excitation spectra (Figure 1, left) for all investigated phases ($LaPO_4$, $SmPO_4$, $GdPO_4$), indicating a complete incorporation of the dopant within the monazite crystal structure independent of the host cation radius. The emission spectra show a maximum splitting of the $^7F_1$ and $^7F_2$ bands (Figure 1, right), confirming the incorporation of Eu^{3+} on the low symmetry cation sites in the monazites.

The xenotime structure is not able to fully incorporate the europium ion within the crystal lattice. The excitation spectrum of Eu^{3+}-doped $LuPO_4$ in Figure 2 shows two regions of europium intensity that, upon excitation, decay with very different lifetimes. The broad signal in the wavelength region 575-580 nm corresponds to an ill-defined, partially hydrated europium species with a lifetime of approximately 580 μs (1.2 H_2O). The species at 583.00 nm has a lifetime of 2700 μs indicating a full loss of the europium hydration sphere upon incorporation. The emission spectrum at this excitation wavelength shows a 2 and 4-fold splitting of the $^7F_1$ and $^7F_2$ bands, respectively, which is expected for an ion within the tetragonal cation site in the xenotime structure.
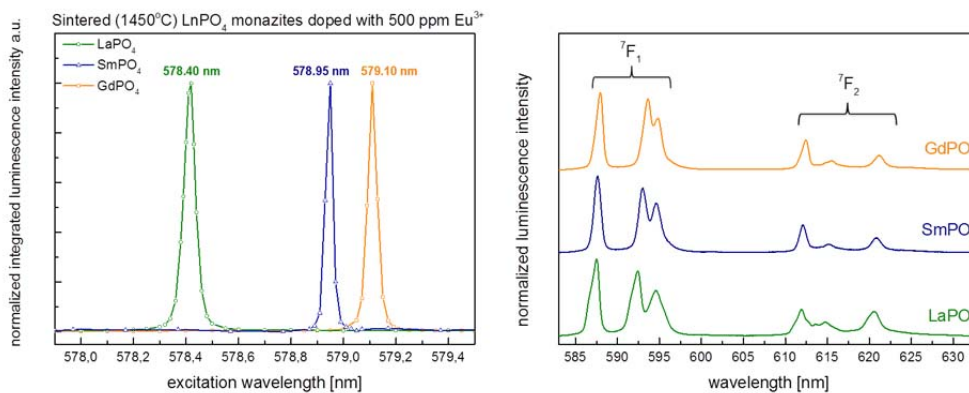
Figure 1. Excitation spectra (left) and emission spectra (right) of Eu^{3+} doped monazites.
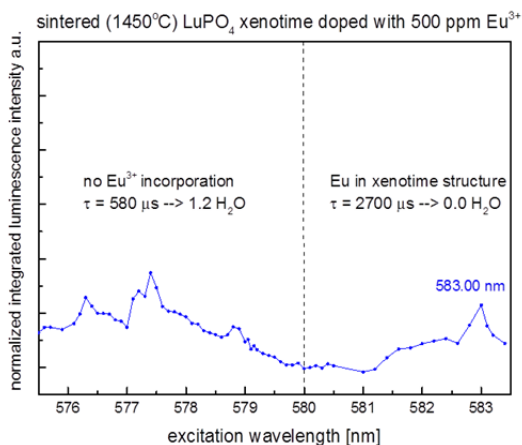
Figure 2. Excitation spectrum of Eu^{3+}-doped LuPO$_4$ xenotime.

Our results demonstrate the importance of spectroscopic methods to probe the local environment of a guest cation within a solid matrix. According to our results, monazites can be considered as suitable host matrices for the immobilization of trivalent actinides. The xenotime structure on the other hand is not an ideal host for the larger lanthanide or actinide dopants due to the structure mismatch that does not allow for a complete guest ion substitution within the ceramic structure.

[1] D. Caurant, P. Loiseau, O. Majérus, V. Aubin-Chevaldonnet, I. Bardez, A. Quintas (2009). "Glasses, glass-ceramics and ceramics for immobilization of highly radioactive nuclear wastes." In: Glasses, Glass-Ceramics and Ceramics, Nova Science Publishers, Inc.

[2] G. R. Lumpkin (2006). "Ceramic waste forms for actinides." Elements 2: 365-372

[3] K. S. Holliday, C. Babelot, C. Walther, S. Neumeier, D. Bosbach, Th. Stumpf (2012). "Site-selective time resolved laser fluorescence spectroscopy of Eu and Cm doped LaPO$_4$." Radiochim. Acta 100: 189-195

[4] A.-M. Seydoux-Guillaume, R. Wirth, A. Deutsch, U. Schärer (2004). "Microstructure of 24-1928 Ma concordant monazites; implications for geochronology and nuclear waste deposits." Geochim. Cosmochim. Acta 68: 2517–2527.

ADVANCED MICROANALYTICAL CHARACTERIZATION OF THE (BA,RA)SO$_4$ SOLID SOLUTION WITH APT AND TEM

J. Weber[1], F. Brandt[1], M. Klinkenberg[1], U. Breuer[2], A. Savenko [2], J. Barthel[3], D. Bosbach[2]

[1] *Institute of Energy and Climate Research, Nuclear Waste Management and Reactor Safety IEK-6, Forschungszentrum Jülich, 52425 Jülich, Germany.*
[2] *Central Institute for Engineering, Electronics and Analytics, ZEA-3, Forschungszentrum Jülich, 52425 Jülich, Germany.*
[3] *Central Facility for Electron Microscopy, RWTH Aachen University, 52074 Aachen / Ernst Ruska-Centre for Microscopy and Spectroscopy with Electrons (ER-C), Research Centre Jülich, 52425 Jülich, Germany.*

In some scenarios for the direct disposal of spent fuel Ra dominates the dose in the far future evolution of the repository (>100.000 years) [1]. It is well known that BaSO$_4$ and RaSO$_4$ form a solid solution. BaSO$_4$ is a possible secondary phase, which may precipitates due to the contact of Ba originating from Cs decay within the spent fuel with sulphate-containing water in the repository [1, 2]. As Ba accumulates at the grain boundaries of the spent fuel, it is more accessible than Ra. Therefore BaSO$_4$ may precipitate before Ra comes into contact with water [2]. Subsequently Ra may enter a system which is close to the thermodynamic equilibrium with BaSO$_4$ [1].

In order to investigate this system, barite recrystallization experiments in the presence of Ra were conducted under close-to-equilibrium conditions [4, 5, 6, 7]. For these experiments a high-purity barite synthesized by precipitation was used. A significant decrease of the Ra concentration was observed and a homogeneous uptake of Ra into the crystal volume was detected in agreement to thermodynamic predictions [5, 6, 7, 8].

So far, the spatial resolution of the microscopic analysis (Time-of-Flight Secondary Ion Mass Spectrometry and Scanning Electron Microscopy) applied was not sufficient to unravel the details of the Ra uptake [8]. Here, we present the method development for the detailed nanoanalytical characterization of solids from macroscopic Ra uptake experiments and parallel Ra-free reference experiments.

By the combination of the state-of-the-art techniques atom probe tomography (APT) and transmission electron microscopy (TEM) a deeper insight into the barite crystal properties could be achieved. The APT analyses were conducted with a LEAP 4000X HR. APT provides chemical information about the sample based on time-of-flight mass spectrometry with almost atomic resolution in 3D [9]. A voltage or laser pulse is applied to the needle-shaped sample (50 - 70 nm diameter) which were prepared by a focused ion beam technique (FIB). The TEM and scanning transmission electron microscopy (STEM) characterization was carried out on FIB-lamellae using an FEI Tecnai G^2 TEM for high resolution imaging of the sample structure. A spherical aberration corrected FEI Titan 80-300 TEM was used to obtain structural information with atomic resolution.

The FIB preparation for barite and (Ba,Ra)SO$_4$ solid solutions was established and improved on a reference sample from a Ra-free experiment, indicating a macroporosity and layered structures within the barite single crystals (Figure 1a). The layered structures are oriented parallel to defined crystallographic directions of barite and often parallel to the outside faces of the crystals. These structures were clearly visible by high-angle annular dark-field (HAADF) STEM imaging (Figure1 b). Additionally, by variation of the lamellae preparation for TEM between cross-section and plan-view it was possible to verify that this feature is three-dimensional.

Several possible reasons for the generation of such contrast features in HAADF-STEM were investigated systematically to identify the origin of the observed layers. Contrast changes can be caused by differences in crystal orientations or chemical composition, stacking faults as well as by regions of lower density or thickness of the TEM lamella. According to our TEM investigations regions of lower density with a round shape are the most likely explanation.

Chemical characterization of Ra-free reference samples with APT also showed layered structures which could be attributed to the detection of H$_2$O, H$_3$O, Na and Cl. Their concentrations are inversely correlated with the Ba concentration. Furthermore, Sr was detected in correlation with the Ba-concentration. By combination of the

results obtained by TEM and APT we conclude that the layered structures are fluid inclusions which are present in distinct layers.

No changes in the layered inclusions or the size and number of macropores were detected within the first 127 days of the Ra free reference experiment. In contrast, the parallel samples from Ra uptake experiments indicate a change in the average number, shape and size of the macropores with time. Besides, the layered inclusions are not present in distinct layers within the Ra containing sample after 127 days. Thicker and thinner regions containing fluid inclusions were observed instead. Therefore it can be assumed that the changes in the macroporosity as well as in the layered inclusions are related to the uptake of Ra. It needs to be proven if the layered inclusions perform as paths for the Ra uptake and therefore explain the kinetic of the uptake. The here presented approach is promising to solve this question.
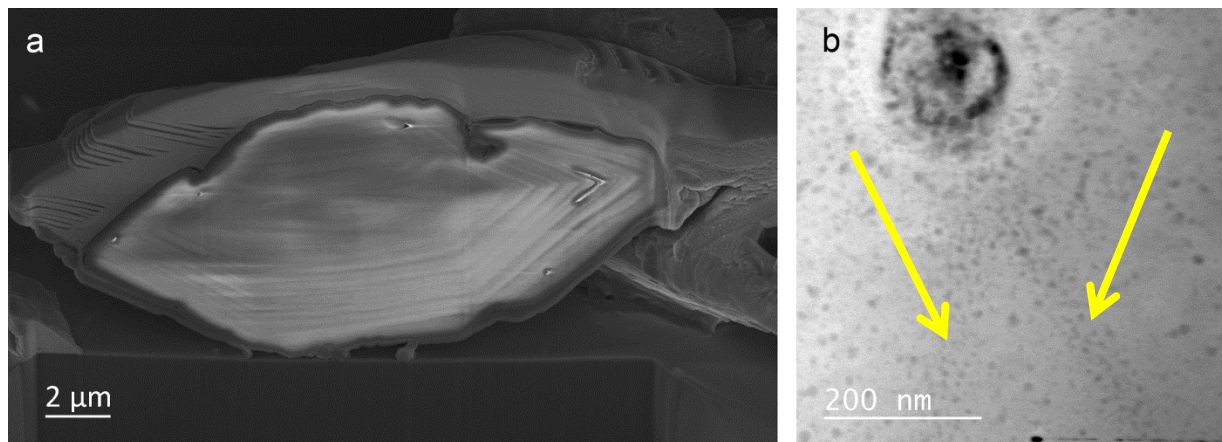
Figure1. a) SEM image of a cross-section of a barite particle after FIB showing the layered structure of a barite particle from a Ra-free reference experiment

b) HAADF STEM image of the layered structure in detail. Dark dots represent areas with lower density. The arrows indicate the layers of dark dots.

[1] S. Norrby, J. Andersson, B. Dverstorp, F. Kautsky, C. Lilja, R. Sjöblom, B. Sundström, Ö. Toverud, S. Wingefors. SKB report. ISSN 1104-1374 (1997).
[2] J. Bruno, R.C. Ewing, Elements, 2, 343-349 (2006).
[3] H.A. Doerner, W.M. Hoskins, J. Am. Chem. Soc., 47, 662-675 (1925).
[4] D. Bosbach, M. Böttle, V. Metz, SKB TR-10-43 (2010).
[5] E. Curti, K. Fuijiwara, K. Iijima, J. Tits, C. Cuesta, A. Kitamura, M.A. Glaus, W. Müller, Geochim. Cosmochim. Acta, 74, 3553-3570 (2010).
[6] V.L. Vinograd, F. Brandt, K. Rozov, M. Klinkenberg, K. Refson, B. Winkler, D. Bosbach, Geochim. Cosmochim. Acta, 122, 398-417 (2013).
[7] F. Brandt, E. Curti, M. Klinkenberg, K. Rozov, D. Bosbach, Geochim. Cosmochim. Acta, Accepted (2015).
[8] M. Klinkenberg, F. Brandt, U. Breuer, D. Bosbach, Environ. Sci. Technol., 48, 6620-6627 (2014).
[9] T.F. Kelly, D.J. Larson, Annu. Rev. Mater. Res., 42, 1-31 (2012).

SORPTION OF Eu(III)/Cm(III), Np(V) AND U(VI) ONTO CLAY MINERALS UNDER SALINE CONDITIONS. EXPERIMENT AND MODELING IN NaCl, CaCl$_2$ AND MgCl$_2$ MEDIA

A. Schnurr[1], R. Marsac[1], M. Marques[2], Th. Rabung[1], J. Lützenkirchen[1], X. Gaona[1], B. Baeyens[2], H. Geckeis[1]

[1]*Institute for Nuclear Waste Disposal (INE), Karlsruhe Institute of Technology (KIT), 76131 Karlsruhe, Germany*

[2]*Laboratory for Waste Management (LES), Paul Scherrer Institute (PSI), 5232 Villigen, Switzerland*

Actinide retention at clay mineral surfaces is a well established process, which has been intensely investigated in the context of nuclear waste disposal (e.g. [1], [2], [3]). Up to now, however, no mechanistic sorption model exists that reliably describes actinide uptake at elevated ionic strength (> 1 M). Such conditions are to be expected e.g. in the vicinity of a repository in rock salt formations, in the Jurassic and lower Cretaceous clay rock layers in Northern Germany [4] or in sedimentary rocks in Canada [5], all identified as potential host rocks for the disposal of high level nuclear waste.

Within the present study, the uptake of actinide/lanthanide (Eu(III) ([152]Eu quantification by γ-counting), Cm(III), Np(V) ([237]Np quantification by LSC and HR-ICP-MS) and U(VI) ([238]U quantification by ICP-MS) by illite (IdP), montmorillonite (SWy) and a synthetic iron free montmorillonite (IfM) was investigated in dilute to concentrated saline systems (0.1 – 4.0 M NaCl; 0.06 – 2.0 M MgCl$_2$ and CaCl$_2$) in the absence of carbonate (Ar glovebox). Eu(III), Np(V), U(VI) batch sorption and Cm(III) time-resolved laser fluorescence spectroscopy (TRLFS) experiments were carried out for 3 < pH$_c$ < 12 (for MgCl$_2$ solutions up to pH$_c$ = 9).

Ionic strength has a small impact on log K_D values in NaCl systems under near-neutral to hyperalkaline pH conditions (Fig. 1, (a)). Only under acidic pH conditions where cation exchange is the dominating binding mechanism a significant decrease of Eu(III) sorption is observed with increasing NaCl concentration. Unlike in the NaCl system, a significant decrease in the extent of uptake is observed in all solutions with elevated Mg/CaCl$_2$ concentrations ([Mg/CaCl$_2$]$_{max}$ = 2.0 M; Fig. 1, (b)). Nonetheless, log K_D (K_D in L·kg^{-1}) values remain high (log $K_D \geq 4.5$) for all systems in the pH$_c$ range 8 - 11. TRLFS studies do not indicate any significant change in the first coordination sphere of Cm(III) at a given pH$_c$ if ionic strength is increased. As a consequence, we do not expect any change in the surface speciation of Cm(III) at elevated ionic strength compared to a previous study at low background electrolyte concentration [6]. Identical surface species are assumed and Eu(III) uptake data are sufficiently well described using the 2SPNE SC/CE approach calibrated at lower ionic strength. The impact of elevated ionic strength on the activities of solutes and of water is taken into account by applying the Pitzer approach.

Sorption data for Np(V) and U(VI) is shown in figure 1 (c) and (d) respectively. The actinyl-cations exhibit no significant ionic strength dependency over the whole pH range. As expected Np(V) sorption is relatively low compared to the other systems starting at pH$_c$ ~ 8 (> 20%) and approaching quasi quantitative retention (> 95%) at pH$_c$ > 10. Nevertheless, the sorption data does not change between 0.1 and 4.0 M NaCl background electrolyte concentration and/or due to the variation of the metal concentration of about two orders of magnitude.

The shape of the sorption edge for U(VI) uptake is very similar to the one for Eu(III), but it is shifted towards more acidic conditions as a result of the stronger hydrolysis of U(VI). Notably, under the experimental conditions no significant outer-sphere complexation (ion-exchange) of U(VI) at low pH occurs. A pronounced uptake (>20%) can be observed at pH$_c$ > 4. The retention of U(VI) onto the clay minerals is quasi quantitative (> 99.5%) within the pH range (6 < pH$_c$ < 11), where the aqueous speciation of uranium is mostly dominated by UO$_2$(OH)$_3^-$. At pH$_c$ > 11, the sorption of U(VI) decreases steadily as a result of the increasing predominance of the species UO$_2$(OH)$_4^{2-}$. Calculations applying the 2SPNE SC/CE approach for U(VI) sorption are in accordance with experimental data upto pH$_c$ ~ 7. However, model results suggest decreasing U(VI) sorption at higher pH$_c$ and a pronounced ionic strength dependency, which is not compatible with the experimental results.

It can be concluded that even under high ionic strength conditions clay minerals exhibit a strong retardation for tri-, penta-, and hexavalent radionuclides in absence of carbonate. The predictive modeling generally is in good agreement with experimental findings. Additional work is on-going to address the disagreement between the experimental and model data observed under alkaline to hyperalkaline pH conditions.
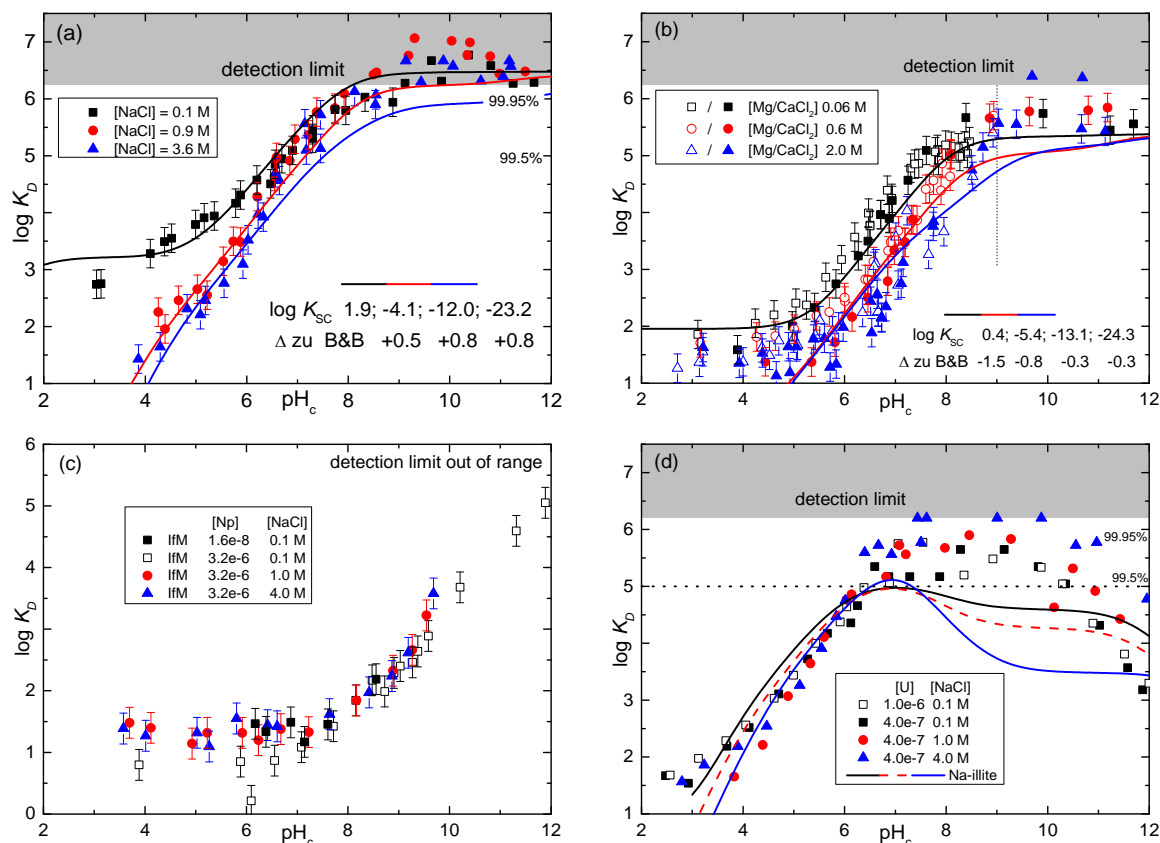
Figure 1: Sorption edges of Eu(III) ($[Eu]_{tot} = 2 \cdot 10^{-7}$ M; (a), (b)) onto IdP, Np(V) ($[Np]_{tot} = 1.6 \cdot 10^{-8}$, $3.2 \cdot 10^{-6}$ M; (c)) onto IfM and U(VI) ($[U]_{tot} = 4 \cdot 10^{-7}$ M, $1 \cdot 10^{-6}$ M; (d)) onto IdP in saline media. Solid lines corresponding to model calculations using 2 SPNE SC/CE with K_D values expressed in L·kg^{-1}.

References

[1] M. H. Bradbury, B. Baeyens, Geochim. Cosmochim. Acta 66, 2325 (2002).
[2] X. Tan, et al., Molecules 15, 8431 (2010).
[3] H. Geckeis, et al., Chem. Rev. 113, 1016 (2013).
[4] W. Brewitz, Zusammenfassender Zwischenbericht, GSF T 114 (1980).
[5] P. Fritz, S. K. Frape, Chem. Geol. 36, 179 (1982).
[6] Th. Rabung, et al., Geochim. Cosmochim. Acta 69, 5393 (2005).

Acknowledgement

IMPACT OF SLOW PROCESSES CLOSE TO EQUILIBRIUM ON RADIONUCIDE MIGRATION

B. Grambow[1]*, T. Suzuki[1], D. Bosbach[2], D.A. Kulik[3], K. Spahiu[4], L. Duro[5]

[1]*Subatech (Mines-Nantes, Université de Nantes, CNRS-IN2P3),4 rue Alfred Kastler, 44307 Nantes, France*
[2]* Institute of Energy and Climate Research (IEK-6) – Nuclear Waste Management and Reactor Safety, Research Centre Jülich GmbH, 52425 Jülich, Germany*
[3]* Paul Scherrer Institut, Laboratory for Waste Management, 5232 Villigen PSI, Switzerland*
4) Swedish Nuclear Fuel and Waste Management Co., 10124 Stockholm, Sweden
5) Amphos 21, Pg. Garcia i Fària, 49-51, 08019 Barcelona, Spain

This paper summarizes the key results of the recent European project SKIN. The objectives of the project were to study the slow processes influencing radionuclide mobility in close-to-equilibrium scenarios in a detailed and systematic manner in relation to surface properties, surface site detachment/attachment kinetics, irreversible sorption and surface incorporation, for cases relevant to the assessment of radionuclide mobility in nuclear waste repository sites.

Emphasis was on the temporal evolution of surface detachment and attachment rates on minerals and the coupling of surface equilibrium with slow bulk phase diffusion/ recrystallization processes of trace element partitioning (incorporation in mineral volume or release). This concerns kinetic studies, thermodynamic evaluations of solid solution/ aqueous solution equilibrium, trace- and major element relations, structural and morphological observations and modelling. Aged and non-aged solid/water systems studied both experimentally (isotopic exchange…) and by modelling include carbonates, silicates, oxides, sulphates and cement phases.

The term "equilibrium" does hardly ever apply to the overall system, but only to some sub-systems, hence, we speak of "local" or "partial" equilibrium under conditions of global disequilibrium. For example, even though minerals like calcite or barium sulphate are in solubility equilibrium with the aqueous solution, this is not necessarily true for minor/trace components of the system, such as radionuclides. The example of radium incorporation in barite has shown that the presence of trace elements like Ra in aqueous solution can lead to a complete recrystallization of the solid under apparent solubility equilibrium.

Crystallographic distinction between lattice-compatible and incompatible elements alone is not sufficient to assess the potential for radionuclide incorporation in a host mineral such as carbonate. The example of aqueous Se(IV)-calcite system shows that even for those structurally incompatible elements, a strong uptake can occur at the surface and in the sub-surface region, leading to enrichments million times higher than in the bulk mineral phase. Such entrapment phenomena are strongly dependent on the degree of supersaturation.

Radionuclides from nuclear waste behave in many aspects similar to the non-radioactive isotopes present in the natural environment or to homologue chemical elements. The natural isotopes are involved in the overall geochemical mass transfer processes between various solid and fluid phases. These processes are often ongoing for hundreds of millions of years. How long it will take to incorporate the radionuclides from the nuclear waste in the pre-existing geochemical cycle? The SKIN project has opened the door to study such very slow processes close to equilibrium, using the concept of sub-surface entrapment in mineral solid solutions. However, the link between growth of crystalline solid phases and their capacity for entrapment of trace elements needs to be more clearly established. We are still not capable to quantify the exchange pool of mineral volumes along the transport path and the degree of incorporation of radionuclides from waste in the global exchanges in the mineral-water system. Nevertheless, we know that the present sorption models, taking the surface as inert, largely underestimate the available exchange pool, and ignore the irreversible uptake. More quantitative approaches need to be developed to assess the magnitude of the safety margins. Finally, a large knowledge base for the significance of entrapment processes in trace element transport is hidden in natural and archaeological analogue systems. It should be possible to use the scientific tools generated in the SKIN project to analyse entrapment processes occurring in natural chemical gradients in a quantitative manner.

SORPTION OF TRIVALENT RARE EARTH ELEMENTS ON CALCITE

S. E. Peschel[1]*, M. Schmidt[1], S. Hofmann[2], J. E. Stubbs[3], P. J. Eng[3]

[1]*Helmholtz-Zentrum Dresden-Rossendorf, Institute of Resource Ecology, Dresden, Germany*
[2] *Karlsruhe Institute of Technology, Institute for Nuclear Waste Disposal, Karlsruhe, Germany*
[3] *Center for Advanced Radiation Sources, University of Chicago, Chicago, IL, USA*

Calcite plays a significant role in the safety assessment of nuclear waste disposal sites. It can be found at these sites in the near field as a secondary phase (e.g. by weathering of the geochemical barrier) and as a constituent mineral in the surrounding rocks. Geochemically, calcite has the potential to adsorb ions at its surface as well as substitute guest ions with an ionic radius similar to calcium, such as americium and curium, in its crystal lattice. The influence of different dissolved cations on the incorporation process was investigated by Schmidt et al. [1]. They showed with time-resolved laser fluorescence spectroscopy (TRLFS) and Eu(III)/Cm(III) that there exists a coupled substitution mechanism (one Eu(III)/Cm(III) and one Na(I) ion replace two Ca(II) ion). Recently, Hofmann et al. [2] showed that the sorption of trivalent lanthanides and actinides can be affected by anionic ligands like nitrate. Atomic force microscopy indicated that the presence of $NaNO_3$ forms a "gel-like layer" with lower crystallinity but unknown composition on the surface of calcite crystals. TRLFS with Eu(III) revealed the incorporation of the Eu(III) ions in this layer, instead of an incorporation directly into the calcite lattice.

The transuranic elements are subject of intensive research because of their importance in long term safety assessments of nuclear waste disposal. Their long half-lives and their high radiotoxicity make them particularly interesting. The rare earth element yttrium served as a nonradioactive homologue, as its ionic radius and chemical behavior are similar to americium and curium.

We used two surface specific high resolution X-ray reflectivity techniques, crystal truncation rod (CTR) measurements and resonant anomalous X-ray reflectivity (RAXR). The experiments were run *in situ*, with the mineral in contact with a thin solution layer on the crystal surface. CTR results in an overall electron density profile from both, the first layers of the crystal bulk and the adsorbed water layer (including sorbed species). RAXR yields the near surface distribution of a distinct element, in this case Y(III).

For our experiments we used freshly cleaved (along the (104) plane) calcite crystals, which were stored in calcite saturated solution (CSS). The sample is reacted with Y(III) over a course of ~ 170 hours and transferred to the diffractometer. We can detect low quantities [~ 0.05 Y/A_{UC} (A_{UC} = area of the calcite unit cell ~ 20.20 Å²)] of adsorbed Y on the calcite surface with more than one species with an average height of ~ 3 Å. In a second step the sample is then flushed with a CSS containing 10 mM $NaNO_3$. After a relatively short contact time with $NaNO_3$ (approx. 48 h) Y is no longer detectable, and consequently must have desorbed from the calcite surface entirely.

CTR experiments for longer contact times with $NaNO_3$ show that nitrate quickly affects the water sorption structure on calcite. The formation of the "gel-like layer" observed by Hofmann et al. [2] is slower, and its formation can be verified after 14 days of exposure to $NaNO_3$.

[1] M. Schmidt, T. Stumpf, M. Marques Fernandes, C. Walther, T. Fanghänel, Angew. Chem. Int. Ed. Engl. 47, 5846 (2008)

[2] S. Hofmann, K. Voïtchovsky, M. Schmidt, T. Stumpf, Geochim. Cosmochim. Acta 125, 528 (2014).

WATER MEDIATED DIFFERENTIAL BINDING OF STRONTIUM AND CESIUM CATIONS IN SOIL ORGANIC MATTER

Biswajit Sadhu,[(1)]Mahesh Sundararajan,[(2)] Tusar Bandyopadhyay[(2)] and K. S. Pradeepkumar[(1)]

[1]Radiation Safety Systems Division, Bhabha Atomic Research Centre, Mumbai – 400 085. India

[2]Theoretical Chemistry Section, Bhabha Atomic Research Centre, Mumbai – 400 085. India

Retention of radionuclides in soil largely depends on chemical and biological reactivity of soil components. Soil Organic matter (SOM) is one of its essential component which is known to alter the mobility of radionuclide cations like Cs^+ and Sr^{2+}in the post nuclear accidental scenario.[1] Radionuclide-SOM interaction also controls their availability into soil solution that modulates their soil to plant transfer factor.[2] Shedding light on the possible interaction mechanisms at the atomic level of these two ions with SOM is thus vital to explain their transport behavior via soil horizons and for the design of new ligands for efficient extraction of radionuclides.

In this study, we have performed state-of-the-art multi-scale modeling using metadynamics (MtD), molecular dynamics (MD) simulations and density functional theory (DFT) based calculations to understand the binding mechanism of strontium (Sr^{2+}) and cesium (Cs^+) radionuclide cations to fulvic acid (FA), a model for SOM (Figure 1).
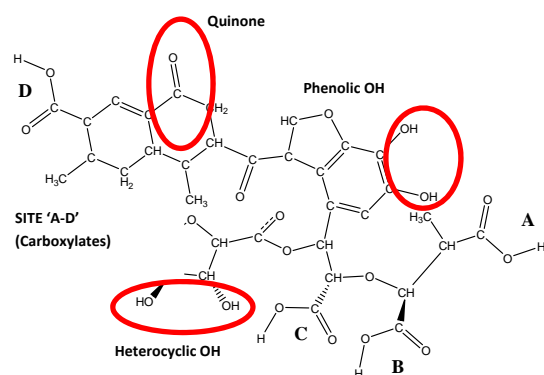
Figure 1. Model Structure of FA
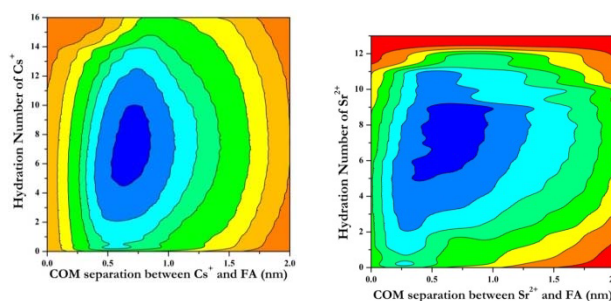
Figure 2. Free energy landscapes of (a) Cs-FA and (b) Sr-FA complexes from MtD simulations. Energy increases from blue to red in the free energy

At first, the most probable binding site of FA is initially evaluated based on the proton affinity and relative energetics study. Using 100 ns of metadynamics simulation, free energy landscapes (Figure 2) were generated for both the radionuclide cations to shed light on the probable binding mechanism (Figure 3). Our studies predict that interaction of Cs^+ to FA is very weak as compared to Sr^{2+}. The water-FA interaction is largely responsible for the weak binding of Cs^+ to FA, which leads to the outer sphere complexation of the ion with FA thus Cs^+ mainly remain diffused in the bulk (blue minima 6 Å away from FA, Figure 2). For Sr^{2+}, the interaction between Sr^{2+} and FA is stronger and thus can surpass the existing secondary non-bonding interaction between coordinated waters and FA leading to inner sphere complexation of the ion with FA (blue minima tilted towards FA), akin to the uranyl binding to FA.[3]

Finally, most frequently occurred conformations of cation bound FA structures are extracted from MtD generated trajectory to perform equilibrium MD simulation and DFT calculations. As an important conclusion, we find that entropy plays a dominant role for Cs^+ binding to FA, whereas Sr^{2+} binding is an enthalpy driven process (Table 1). The participation of functional groups other than carboxylate also plays a significant role to reduce the migration of both radionuclides. Due to this differing binding mechanism of the two radionuclide cations to FA, Cs^+ cation is predicted to be more mobile in the presence of SOM which can leach into the soil solution and eventually available for plant uptake, whereas Sr^{2+}mobility can be controlled by SOM. Our predicted results are found to be in excellent agreement with the available experimental data on complexation of Cs^+ and $Sr^{2+}$with SOM. [4-5]

Model	Ion	ΔH	$T\Delta S$	ΔG
FA (C)	Cs^+	-15.32	-19.20	+3.88
	Sr^{2+}	-15.50	-5.10	-10.40

Table 1. Thermodynamic quantities (kcal mol^{-1}) of optimized metal-FA complexes.
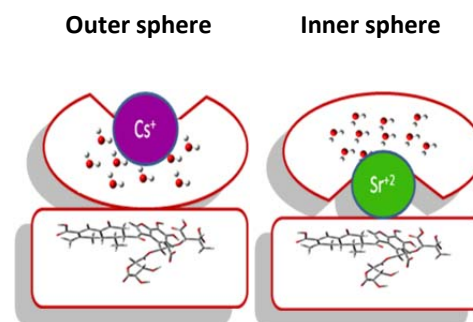
Figure 3. Differential binding mechanism

[1] Stohl, A. P. Seibert, G. Wotawa, D. Arnold, J. F. Burkhart, S. Eckhardt, C. Tapia, A. Vargas, and T. J. Yasunari (2011). "Xenon-133 and caesium-137 releases into the atmosphere from the Fukushima Dai-ichi nuclear power plant: determination of the source term, atmospheric dispersion, and deposition." Atmos. Chem. Phys. Discuss., 11: 28319-28394.

[2] Sanchez, A. L. S. N. Wright, E. Smolders, C. Naylor, P. A. Stevens, V. H. Kennedy, B. A. Dodd, D. L. Singleton, and C. L. Barnett (1999). "High plant uptake of radiocesium from organic soils due to Cs mobility and low soil K content" Environ. Sci. Technol, 33: 2752-2757.

[3] Sundararajan, M. G. Rajaraman, and S. K. Ghosh (2011). "Speciation of uranyl ions in fulvic acid and humic acid: a DFT exploration." Phys. Chem. Chem. Phys., 13: 18038-18046.

[4] Helal, A. A.; H. A. Arida, H. E. Rizk, and S. M. Khalifa (2007). "Interaction of cesium with humic materials: A comparative study of radioactivity and ISE measurements." Radiokhimiya, 49: 458-463.

[5] Xu, X. A. G. Kalinichev, and J. Kirkpatrick (2006) "^{133}Cs and ^{35}Cl NMR spectroscopy and molecular dynamics modeling of Cs^+ and Cl^-complexation with natural organic matter." Geochem. Cosmochim. Acta, 70: 4319-4331.

U₃O₈ AND AMORPHOUS UO₂(OH)₂ SOLUBILITY AT ELEVATED TEMPERATURE IN SODIUM CHLORIDE BRINE

M.K. Richmann, A. Hayes, T. Sontag, and D. T. Reed

Actinide Chemistry and Repository Science Program, Repository Science and Operations,
Los Alamos National Laboratory, 1400 University Drive, Carlsbad NM, 88220, USA.

The permanent disposal of defense high-level nuclear waste or spent fuel in a salt repository will lead to elevated temperatures. It is important, by analogy with the WIPP safety case, to know the concentration of mobile actinide species as a function of temperature to account for actinide release in the event of low-probability human intrusion scenarios. An understanding of uranium speciation and solubility, especially in the case of spent fuel, is a key to predicting wasteform behavior should brine inundation occur.

The predicted repository-scale increase in temperature is dependent on the final repository design and heat loading but is typically estimated to be ~ 40°C (to ~ 70°C) for defense high-level waste and as high as ~130°C (to ~ 160°C) for spent fuel [1]. These temperatures will impact water movement and availability within the host rock prior to inundation, but will also lead to a heating of the brine introduced into the repository that will interact with the waste at elevated temperature.

Herein we report the results of temperature-variable studies with two uranium phases: crystalline U₃O₈ and amorphous uranyl hydroxide. In WIPP-related studies at room temperature [2] the amorphous uranyl hydroxide phase was found to be the solubility-controlling phase. U₃O₈ is an identified early intermediate phase in the reactive dissolution of uranium dioxide (i.e., spent fuel). The overall research strategy was to use the phase transition of the crystalline uranium oxide phase to the amorphous phase as an indicator of rate of reaction as the temperature is varied and link this to the observed uranium speciation and solubility. Experimental results for 30 to 90°C in 5 M sodium chloride are reported but these are ongoing experiments and there are plans to extend this to higher temperatures to cover the full temperature range for the HLW/SF repository case.

U₃O₈ was prepared by direct calcination of UO₂(NO₃)₂*6H₂O. This was done by heating stepwise in a furnace to 750°C. This led to the formation of crystalline U₃O₈ (see Figure 1) that was confirmed by XRD (Bruker D8 Advance XRD with LynxEye detector). Uranium (VI) hydroxide was prepared by the precipitation of dissolved uranyl from 3 M NaCl brine solution at near-neutral pH using PIPES to buffer/control the pH. For the experiments performed, XRD analysis was used to track phase evolution; ICP-MS (Agilent 7500 ce ICP-MS) was used to analyze for uranium and verify brine composition; pH was measured using a Ross combination electrode and corrected for ionic strength [4] and dissolved carbonate concentration was determined by GC analysis (Bruker 430 GC configured with a CO₂-methane conversion reaction cell and FID detector) of the gas phase for carbon dioxide following acidification of the brine sample.
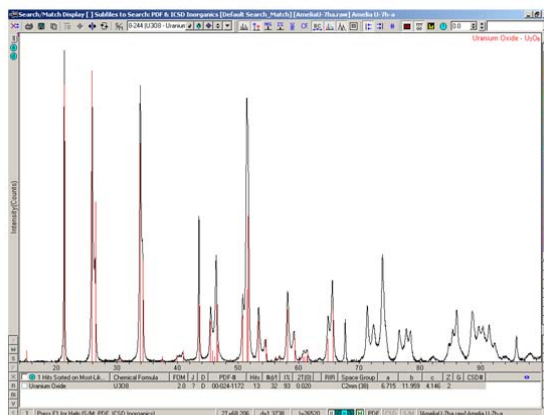
Figure 1. XRD analysis of synthesized U₃O₈

Experiments were performed in 5 M NaCl, which is a simplified brine [2], in the pH range of 4-12 and in the presence and absence of carbonate at 30, 60 and 90°C. Approximately 20 mM bicarbonate/carbonate was initially added and confirmed to be present at pH > 9. This was 6 mM at pH 6 and < 1 mM at pH = 4. The uranium concentration at 30°C is shown in Figure 2a. At this temperature, no significant solid phase transition from the oxide to the hydroxide was noted and the uranium concentration data showed significant hysteresis. The solubility of the uranium was consistently higher for the oxide phase by almost an order of magnitude. Speciation is dominated by carbonate complexation at the higher pH as expected.

At 60°C, although the hydroxide precipitate phase remained essentially unchanged, significant phase transformation was noted for the oxide. Uranium solution data are shown in Figure 2b and indicate that the measured solubility is converging with time although not yet completely at equilibrium after 20 days.

At 90°C, the phase transition is occurring more rapidly but increased hysteresis was noted rather than convergence in the solution data. These higher rate data are not understandable and the higher temperature data remains the focus on ongoing studies.
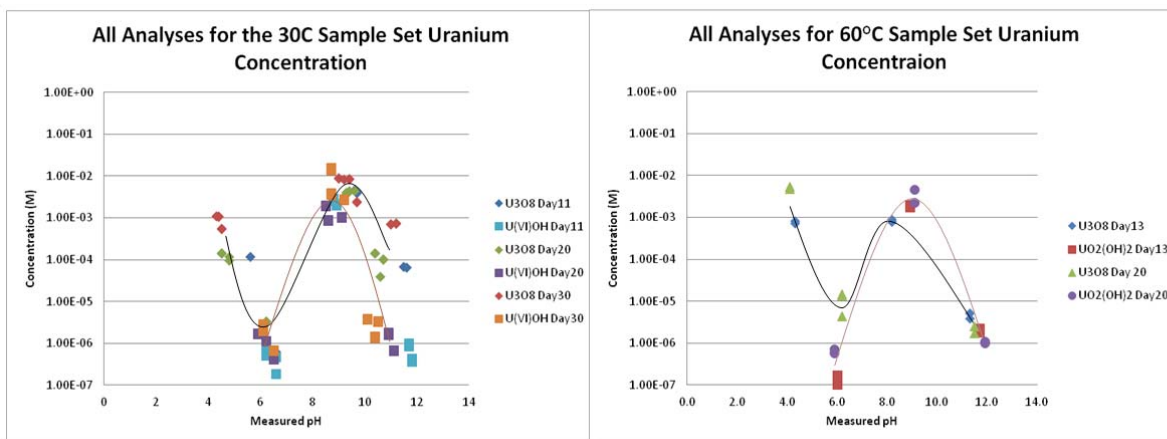
(a)   (b)

Figure 2.   Uranium concentration data (10 nm filtration and analysis by ICP-MS) are show for the 30 and 60°C experiments. Triplicate experiments were performed and averaged together.

The solution data shown are consistent with a carbonate dominated system that shows an increase in uranium concentration through pH 9 due to carbonate complexation with hydrolysis dominating at high pH. The measurable rate of phase conversion, observed visually and confirmed by XRD, is identified as a good indicator of the rate of reaction and time to equilibration. These data are in agreement with our prior long term solubility studies [3-4] that show ~ 30 day equilibration times for under and oversaturation approaches to solubility at room temperature and clearly link the solution chemistry changes to the phase and the corresponding solution data. Experiments to address ionic strength effects on the rate of phase transition and further establish the effects of higher temperature are in progress and will be summarized.

References

[1] Clayton and Gable, SAND report, Sandia National Laboratories (2009)

[2] Lucchini et al., "Uranium(VI) Solubility in WIPP Brine." LANL-CO report LA-UR 13-20786, Los Alamos National Laboratory, Los Alamos NM, USA (2013)

[3] Lucchini et al., *Radiochimica Acta* **101**, 391-398 (2013)

[4] Lucchini et. al., "WIPP Actinide-Relevant Brine Chemistry."   Los Alamos Report LA-UR-14-21612. Los Alamos National Laboratory, Los Alamos NM, USA (2012)

EFFECT OF SUPERPLASTICIZERS ON Ni BEHAVIOUR AT HYPERLAKALINE CONDITIONS

D. García[1,2], M. Grivé[1], L. Duro[1], S. Brassinnes[3], J. de Pablo[2]

[1]Amphos21, Passeig de Garcia i Fària 49-51, 08019, Barcelona, Spain
[2]Fundació CTM Centre Tecnològic, Environmental Technology Area, Plaça de la Ciència, 2,08243, Manresa, Spain
[3]Belgian Agency for Radioactive Waste and Enriched Fissile materials (ONDRAF/NIRAS), Belgium.

Hyperalkaline conditions developed in cementitious environments can cause chemical transformations of polymeric SuperPlasticizers (SPs) (degradation, aging, etc.) with the subsequent production of small organic compounds with new chemical properties [1]. A number of investigations indicate that radionuclides form stable complexes with some organic compounds [2, 3 and references there in]. It is thus expected that those small organics ligands (i.e. gluconate, isosaccharinate…) can play an important role in transporting radionuclides through the near and far field of a radioactive waste repository [4]. Therefore, the understanding on the nature and strength of the interactions between radionuclides and organic admixtures present in the concrete formulations (and their degradation products) deserves focused studies. It is in this field where this study is framed.

The effect of a polycarboxylic ether (PCE) based SP (i.e. glenium® 27) on the solubility of $Ni(OH)_2(s)$ was investigated. Three different media were considered: 1) concrete synthetic porewater (CSPW) without organic compounds, 2) leachates of concrete samples without SPs, and 3) leachates of concrete samples containing glenium® 27. CSPW was prepared according to [5], while concrete leachates were obtained after contacting crushed concrete (based on CEM I formulation) with MilliQ water for 30 days at a solid/liquid ratio of 10 g/L. Those waters were characterised in terms of pH (Crison 52-22 electrode), cations (ICP-OES Thermo Scientific, iCap 6000 series and ICP-MS Agilent Technologies, 7500 CX) and anions (IC, Dionex, model ICS 2000).

Solubility experiments were set up under both, under- and oversaturation conditions under $N_2(g)$ atmosphere (Jacomex, GP[Concept]-II-S). Commercial $Ni(OH)_2(s)$ (ACROS, analysis grade) was used in the under-saturation experiments. Those experiments were set up by contacting 2 g of commercial $Ni(OH)_2(s)$ with 50 mL of media (either CSPW or the leachates), S/L ratio of 40g/L. Solution pH was unaltered after the addition of the solid. The experiments were manually shaken daily over a period of several months. Oversaturation experiments consisted in mixing 4mL of a $Ni(OH)_2$ solution (0.1M HNO_3) with 40mL of media (CSPW or the leachates). After few seconds the formation of a characteristic green solid suspension was observed suggesting the formation of nickel hydroxide. The pH of the solution was kept nearly equal as the one of the initial media. At given time intervals, aliquots of the samples were collected and filtered through 0.45 and 0.22μm Nylon filters, acidified and analysed for Ni concentration by ICP-MS. Obtained results are shown in Figure 1and Figure 2.

In CSPW media, equilibrium was always reached before 80 days of contact time (Figure 1). In the case of the solubility experiments with the leachates, whose composition is somewhat complex than CSPW media, equilibria was not completely reached even after 120 days (Figure 2). In either case, obtained results are in fair agreement with previous published studies [6, 7].

After 120 days of contact time, no relevant differences between solubility measurements in leachates of concrete samples with or without SPs in their formulations were observed, in agreement with the very similar TOC levels measured in both cases. From this observation, it can be concluded that the release of small organic compounds from concrete, due to the SPs degradation or aging to the solution, is negligible after 120 days. Additional leaching experiments at longer times and solubility experiments with variable SPs spikes in aqueous solution are ongoing. Preliminary results (not shown) seem to indicate that the presence of SPs in the solution drastically increases the solubility of Ni.
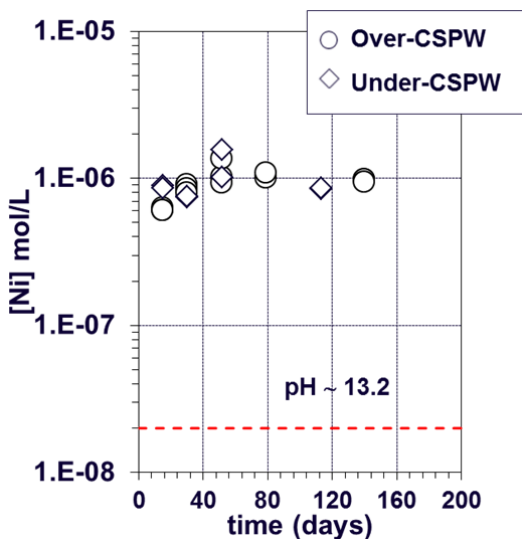
Figure 1. Ni (mol·l^{-1}) as a function of time (days) in over and under saturation experiments. Those results have been obtained in CSPW media, pH~13.2. Red dashed line stands for the equipment Limit Of the Quantification (LOQ).
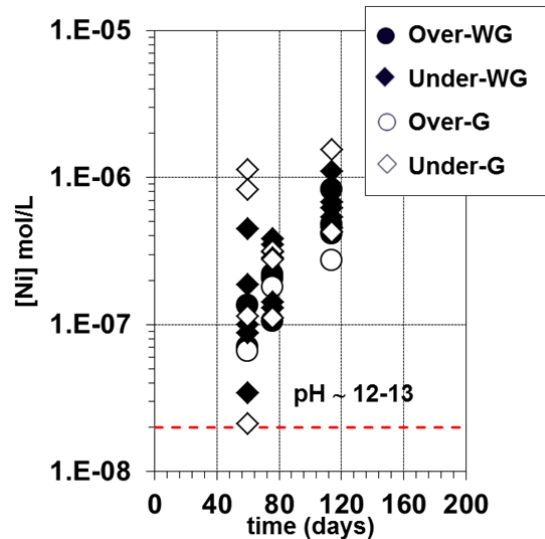
Figure 2. Ni (mol·l^{-1}) as a function of time (days) in over and under saturation experiments. Those results have been obtained in concrete leachates media, WG (samples non-containing SPs) G (samples containing SPs), pH~12-13. Red dashed line stands for the equipment Limit Of the Quantification (LOQ).

In summary, the results indicate that, once SPs is included in the concrete formulation, this polymeric material is stabilized (e.g. adsorbed into the cement phases) and negligible mobilization effects on the behaviour of a trace radionuclide like Ni could be observed. However, if SPs are released to the solution, they cause an important enhancement of the solubility of Ni at hyperalkaline conditions.

[1] M. A. Glaus, L.R. Van Loon, PSI Report 04-02 (2004).
[2] M. Andersson, et al., POSIVA Working Report 2008-29 (2008).
[3] X. Gaona, et al., J. Contam. Hydrol. 102, 217-227 (2008).
[4] L. Duro, et al., SKB R-12-15 (2012).
[5] T. Stumpf, et al., J. Colloid Interface Sci. 276(1), 118–124 (2004).
[6] K. Gayer, A. Garrett, J. Am. Chem. Soc. 71(9), 2973–2975 (1949).
[7] S. Mattigod et al., J. Solution Chem. 26(4), 391–403 (1997).

CORROSION TESTS OF COMMERCIAL UO$_2$ BWR SPENT NUCLEAR FUEL: MODELING OF THE INSTANT RELEASE FRACTION

Albert Martínez-Torrents[1], Rosa Sureda[1], Daniel Serrano-Purroy[2], Laura Aldave de las Heras[2], Alexandra Espriu[3], Ignasi Casas[3], Stefaan Van Winckel[2], Joan de Pablo[1,3]

[1]*Fundació CTM Centre Tecnològic, 08242 Manresa, Spain*
[2]*European Commission, Joint Research Centre, Institute for Transuranium Elements, 2340 D-76125 Karlsruhe, Germany*
[3]*Universitat Politècnica de Catalunya (UPC), 08034 Barcelona, Spain*

Irradiation of the nuclear fuel produces a segregation of determined fission products from the center to the exterior of the fuel. This segregation creates an accumulation of these radionuclides (RN) in the gap between the fuel and the cladding, in fractures, in bubbles and in the grain boundaries. A fraction of these elements segregated during the irradiation dissolve faster than the matrix, which is known as instant release fraction (IRF). The Perfomance Assessment (PA) of spent nuclear fuel (SNF) storage considers the IRF to be one of the main sources of radiological risk [1]. In the present study, corrosion tests were performed on two different UO$_2$ BWR SNF using cladded pieces and powdered fuel. The fuel powder from the center (CORE) and the periphery of the pellet (OUT) was separated in order to study the effect of the RN segregation and the high burn-up structure (HBS) [2,3].

The fuels used in the experiments had a burn-up (BU) of 42 and 54 GWd(tHM)$^{-1}$. The average linear power rate (W/cm) was 215 and 160 and the fission gas release (%) was 2.3 and 3.9, respectively. A fraction of particles with a diameter size of 40-100 μm was used. The leaching solution used was a carbonated solution (1mM NaHCO$_3$+19mM NaCl) with a pH of 8.4±0.1. The experiments were performed under oxidizing conditions at a temperature of 25±5°C. The solution was continuously stirred and it was renewed several times during the experiments. Samples were taken for different contact times.

The cumulative moles released in solution were calculated considering the total amount of an element *i* removed in each sampling. The cumulative Fraction of Inventory in Aqueous Phase (FIAP) was calculated taking into account the RN inventory determined experimentally for each cladded segment and the powder fractions.

The FIAP was normalized to the total surface area (FNS$_i$) and to the FIAP$_U$ of uranium (FNU$_i$) for each element *i*. The release of uranium was considered as the release of the matrix. The IRF was calculated subtracting the FIAP$_U$ of uranium from the FIAP$_i$ of an element *i*.

Cs, Rb and Sr showed faster dissolution than the matrix in the experiments and therefore were attributed to the IRF. In all the cases Cs presented the highest release. In the powder experiments Mo and Tc presented an IRF that lasted only some days and after that the release was attributed to the phase of Tc and Mo trapped in the matrix and the ε-particles [4].

During the first hours a high RN release was observed followed by a slower release during the rest of the days. The high release was attributed to the RN trapped in gap, cracks, and grain boundaries initially available to water corrosion. The second contribution was assumed to be due to the internal grain boundaries.

The IRF normalized to the surface area is shown in Table 1. Rb and Sr segregated fractions, are mainly accumulated in the grain boundaries [4,5], therefore the IRF normalized was similar for the cladded segments and the powder fractions. The accumulation of Cs in the gap and cracks is higher than for the other elements presented [4,5], so the IRF normalized should be higher for the cladded segment than for the powder fractions as it was observed for the 54BWR fuel. The 42BWR fuel had lower BU and FGR, hence our hypothesis is that the contribution of the gap and cracks was not enough to make a difference between the cladded segments and the powder fractions and the release of Cs of each 42BRW experiment was similar.

Table 1. IRF normalized to surface area after 200 days.

IRF norm. (%) m^{-2}	42BWR Segment	42BWR CORE	42BWR OUT	54BWR Segment	54BWR CORE	54BWR OUT
Rb	$(2.5\pm0.4)\times10^{-4}$	$(1.7\pm0.7)\times10^{-4}$	$(2.2\pm1.0)\times10^{-4}$	$(1.1\pm0.2)\times10^{-4}$	$(1.2\pm0.6)\times10^{-4}$	$(2.6\pm1.3)\times10^{-4}$
Sr	$(1.3\pm0.2)\times10^{-5}$	$(1.5\pm0.7)\times10^{-4}$	$(1.7\pm0.8)\times10^{-4}$	$(1.1\pm0.2)\times10^{-4}$	$(1.8\pm0.9)\times10^{-4}$	$(1.6\pm0.8)\times10^{-4}$
Cs	$(3.0\pm0.1)\times10^{-4}$	$(4.5\pm2.0)\times10^{-4}$	$(4.0\pm1.9)\times10^{-4}$	$(1.0\pm0.1)\times10^{-3}$	$(3.2\pm1.7)\times10^{-4}$	$(3.3\pm1.6)\times10^{-4}$

[1] D.Serrano-Purroy, F. Clarens, E. González-Robles, J.P. Glatz, D.H. Wegen, J. de Pablo, I. Casas, J. Giménez and A. Martínez-Esparza, J. Nucl. Mater. 427 249-258 (2012).

[2] J.P. Hiernaut, T. Wiss, J.Y. Colle, H. Thiele, C.T. Walker, W. Goll, R.J.M. Konings, J. Nucl. Mater. 377, 313-324 (2008).

[3] D. Serrano-Purroy, I. Casas, E. González-Robles, J.P. Glatz, D.H. Wegen, F. Clarens, J. Giménez, J. de Pablo, A. Martínez-Esparza, J. Nucl. Mater. 434 451-460 (2013).

[4] SKB, SKB Technical Report TR-99-07 (1999).

[5] L. Johnson, C. Poinssot, C. Ferry and P. Lovera, NAGRA Technical Report 04-08 (2004).

NP(V) SORPTION AND SOLUBILITY IN HIGH PH CALCITE CONTAINING SYSTEMS

K.F. Smith[(1),(2)], N.D. Bryan[(2)], G. Law[(3)], K. Morris[(1)]

(1)Research Centre for Radwaste Disposal and Williamson Research Centre, School of Earth, Atmospheric and Environmental Sciences, The University of Manchester, Oxford Road, Manchester, M13 9PL, United Kingdom.
(2)National Nuclear Laboratory, Chadwick House, Risley WA3 6AE, United Kingdom
(3)Centre for Radiochemistry Research, School of Chemistry, The University of Manchester, Oxford Road, Manchester, M13 9PL, United Kingdom

In the UK, it is likely that much of the intermediate level radioactive waste inventory will be encapsulated in grout. These wasteforms will then be emplaced in a Geological Disposal Facility backfilled with cementitious material, which may contain limestone [1]. Further, calcite is a relatively common mineral in the subsurface. Upon resaturation of the repository, the interaction of the cementitious materials with groundwater will create a region of high pH (> pH 10.5) [2]. Therefore, there is an interest in studying radionuclide interactions with calcite. Here, we have studied Np(V) interactions with calcite under conditions representative of an evolving cementitious repository.

The behaviour of Np(V) in hyperalkaline / calcite systems was studied over a range of concentrations (1.62 x 10^{-3} - 1.62 µM) and in two synthetic, high pH cement leachates. The cement leachates were selected to be representative of the chemical conditions expected in a young (pH 13.3, Na^+, K^+, Ca^{2+}; YCL) and old (pH 10.5, Ca^{2+}; OCL) cementitious geological disposal facility. These systems were studied using a combination of batch sorption and solubility experiments, X-ray absorption spectroscopy and modelling to describe their equilibrium, kinetic and speciation behaviour.

In calcite equilibrated old and young cement leachates, the solubilities were 9.68 and 0.084 µM Np(V), respectively. This was consistent with the formation of a $Np(V)O_2OH_{(am, fresh)}$ solid phase in the old leachate. However, the solubility in the YCL system could not be explained with respect to the known neptunium phases $NpO_2OH_{(am, fresh)}$ and $NpO_2OH_{(am, aged)}$ or Np_2O_5, which suggested that another phase was forming and controlling the solubility. In pH 13.3 NaOH solutions, Np(V) solubility decreased with increasing calcium concentration, indicating that calcium is involved in solubility control in the YCL system, at least on the timescale of a several months. Analysis of solubility data in conjunction with EXAFS analysis suggests that a Np containing becquerelite-like structure may be the solubility controlling phase in the YCL system.

The sorption of Np(V) to the calcite was observed across a range of Np concentrations and solid to solution ratios. Sorption isotherm data for both YCL and OCL systems at an apparent steady state are shown in Figure 1. Analysis of these data suggested that a combination of surface complexation and precipitation was probably responsible for the observed Np(V) removal in the YCL system. In the OCL system, sorption across a range of concentrations was dependent on solid to solution ratio and thus binding site density, and these data were successfully modelled using a surface complexation model based on the approach of van Cappellen et al [3], which assumed the formation of a monodentate Np(V)-calcite surface complex ($>CO_3NpO_2$) with a log K of 2.42 and a binding site concentration of 0.15 sites / nm^2.

The kinetics of Np(V) removal were also studied, with all systems showing slow sorption kinetics with reaction times of weeks to reach equilibrium. In the old cement leachate system, these kinetics were successfully modelled assuming a colloidal or unavailable form that was slow to dissolve. Such behaviour has been seen previously in U(VI) high pH calcite systems [4].
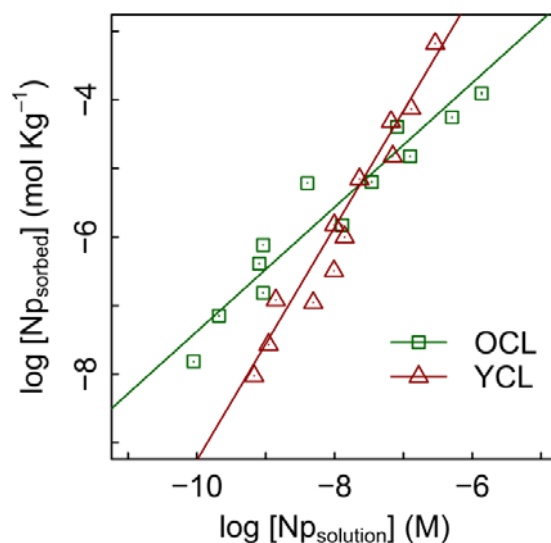
Figure1. Sorption isotherms from OCL and YCL batch sorption experiments. Lines represent linear fits to the data with gradients of 0.90 ± 0.12 and 1.69 ± 0.20 L Kg^{-1} for OCL and YCL systems, respectively.

[1] McCarter, W., Crossland, I., Chrisp, I., 2004. Hydration and drying of Nirex Reference Vault Backfill. Building and Environment, 39, 211_221.

[2] Braney, M.C., Haworth, A., Jefferies, N.L., Smith, A.C., 1993. A study of the effects of an alkaline plume from a cementitious repository on geological materials. *J. Contam. Hydrol.* 13, 379-402.

[3] van Cappellen, P., Charlet, L., Stumm, W., Wersin, P., 1993. A surface complexation model of the carbonate mineral-aqueous solution interface. *Geochim. Cosmochim. Acta*. 55, 3505-3518.

[4] Smith, K., Bryan, D., Swinburne, A., Pieter, B., Shaw, S., Natrajan, L., Mosselmans, F., Morris, K., 2015, U(VI) behaviour in hyperalkaline calcite systems. *Geochim. Cosmochim. Acta*. 148**,** 343-359.

THE SOLUBILITY OF RaSO$_4$ AND UPTAKE OF RADIUM BY BaSO$_4$ AT T = 25 - 90 °C

F. Brandt[1], K. Rozov[1], M. Klinkenberg[1], D. Bosbach[1]

[1] *Institute of Energy and Climate Research, IEK-6 Nuclear Waste Management, Forschungszentrum Jülich GmbH, 52425 Jülich, Germany*

Radium plays an important role for the radiological impact of a geological repository for spent nuclear fuel. In some scenarios for the direct disposal of spent nuclear fuel, ^{226}Ra dominates the dose after 100,000 years [1]. Radium has a high affinity to barite (BaSO$_4$) which is also likely to form as a result of the reaction between sulfate bearing ground waters and Ba present as a fission and decay product in spent fuel. Several recent studies have shown that (Ba,Ra)SO$_4$ solid solutions are forming under close-to-equilibrium conditions expected for this system in a nuclear waste repository [2,3,4]. The presence of these solid solutions can lower the radium solubility by several orders of magnitude, depending on the amount of BaSO$_4$ present in the system. Radium is also a naturally occurring radioactive material (NORM) of high environmental relevance. The decay of ^{226}Ra produces the radioactive noble gas radon which has a short half-life and is the largest contributor to an individual's background radiation dose [5]. In NORM, radium is a common impurity associated with barite which forms during geothermal energy production or in produced waters from gas and oil production.

A thermodynamic model which describes the behavior of the RaSO$_4$-BaSO$_4$-H$_2$O system at ambient conditions was derived based on atomistic simulations by Vinograd et al. [6]. The aim of the present study was to extend this (Ba,Ra)SO$_4$ solid solution - aqueous solution model to elevated temperatures. Particularly, the objective was to improve the knowledge about the solubility of the pure RaSO$_4$ end-member for the temperature range 25 - 90 °C. The existing data can only be applied to describe the solubility of RaSO$_4$ as linear function of temperature for T = 25 - 50 °C, assuming a simple van't Hoff approach. However, at T $\geq$ 50 °C, due to the analogy with BaSO$_4$ a non-linear solubility-temperature relationship with a maximum of the RaSO$_4$ solubility is expected [7]. This hypothesis still was not proved due to the absence of experimental data for the solubility of RaSO$_4$ above 70 °C.

Here we are presenting new results from recrystallization experiments with two different types of BaSO$_4$ (Sachtleben and Aldrich) in the presence of radium in aqueous solution performed at room temperature and elevated temperatures. For this purpose pure BaSO$_4$ was equilibrated at room temperature, 70 °C and at 90 °C with an aqueous solution containing 0.1 mol/L NaCl and 5 · 10^{-6} mol/L radium. Depending on the solid/liquid ratio and on the temperature a constant radium concentration in the aqueous phase was reached after a few hundred days and was attributed to equilibrium between solid and aqueous phase. A regular (Ba,Ra)SO$_4$ solid solution model as proposed by Vinograd et al. [6] was applied in order to calculate the activities of Ra^{2+} and SO$_4^{2-}$ at the given experimental conditions using the GEMS-PSI code package [8]. As a result, solubility constants of RaSO$_4$ at 70 and 90 °C were estimated. By combination with literature data [7] new values for S^o_f, H^o_f, C$_p^o$ for RaSO$_4$ were obtained. As a result, a reasonable model which reproduces the behavior of the Ba-Ra-SO$_4$-H$_2$O system in the range T = 25 - 90 °C can be applied in the safety assessment for the direct disposal of spent fuel elements.

[1] Norrby S. et al., 1997, SKI Statens Kaernkraftinspektion (Sweden).
[2] Curti E. et al., 2010. Geochim. Cosmochim. Acta 74, 3553-3570.
[3] Klinkenberg M. et al., 2014, Environ. Sci. Technol. 48, 6620-6627.
[4] Brandt F. et al. 2015, Geochim. Cosmochim. Acta, in press
[5] Keith S. et al., 2012, U.S. Dep. Heal. Hum. Serv.
[6] Vinograd V. L., et al., 2013, Geochim. Cosmochim. Acta 122, 398-417.
[7] Brown P. L et al., In: Uranium Past and Future Challenges. Springer International Publishing. pp. 553–564.
[8] Kulik D. A et al. , 2012, Comput. Geosci. 17, 1-24.

ESTIMATION AND THERMODYNAMIC ANALYSIS OF NATURAL THORIUM, URANIUM, AND REE CONCENTRATIONS IN GROUNDWATER AT HORONOBE URL

T. Sasaki[1], T. Koukami[1], H. Amamiya[2], H. Murakami[2], Y. Amano[2], T. Iwatsuki[3], T. Mizuno[2], T. Kobayashi[1], A. Kirishima[4]

[1] *Department of Nuclear Engineering, Kyoto University, Kyoto daigaku-Katsura, Nishikyo, Kyoto 615-8540, Japan*
[2] *Horonobe Underground Research Center/GIRDD, JAEA, Horonobe, Hokkaido 098-3224, Japan*
[3] *Tono Geoscience Center/GIRDD, JAEA, Akeyo-cho, Mizunami, Gifu 509-6132, Japan*
4) *IMRAM, Tohoku University, Katahira 2-1-1, Aoba, Sendai 980-8577, Japan*

For thermodynamic analysis of the trace amounts of actinides and lanthanides in groundwater, concentrations of Th, U, and rare earth elements (REEs) were investigated at Horonobe Underground Research Laboratory (URL), Hokkaido, Japan. Groundwater was sampled in anaerobic condition directly from a packed section in the boreholes drilled to 140 m and 250 m depth in drift. The colloidal distribution was checked by an on-site batch ultrafiltration unit using 0.2 m or 10 kDa membranes that maintain almost equal hydraulic pressure and temperature. Unfiltered groundwater was also collected for comparison.

One liter of the groundwater sample stocked in clean Teflon-coated bottle was acidified immediately with ultrapure nitric acid, and heated overnight at 80 °C. The metal concentrations were measured by inductively coupled plasma mass spectrometry (ICP-MS, PerkinElmer, ELAN DRCII). Since the concentrations of the elements in the groundwater samples are extremely low, they were pre-concentrated using a chelating resin disk (3M Empore Disk Cartridge). After conditioning, 1 L sample was injected onto the disk, and all the metal ions were recovered using 10 mL of 1.5 M HNO_3, where the recovery was 100±10 % in the preliminary analysis tests.

Figure 1 shows the Th concentrations of groundwater processed in Horonobe URL. The Th concentration decreased with decreasing pore size (unfiltered > 0.2 m > 10 kDa) because tetravalent Th with colloids and suspended particles in groundwater should have been removed by ultrafiltration. The concentration of "dissolved" Th^{4+} was similar to that of surface seawater. Meanwhile, U concentration in groundwater was much lower than that in seawater due to the lower E_h condition. Under the reported physicochemical conditions of various parameters (pH, Eh and concentration of inorganic components such as chloride, carbonate and phosphate [1]), both Th and U concentrations could be estimated by thermodynamic calculations [2], assuming that the soluble solid phases are restricted to $ThO_2(cr)$ and $UO_2(cr)$, respectively.

The concentrations of REEs in accordance with the Oddo-Harkins rule were also very low (Figure 2), and significant colloidal distribution for lighter REEs was observed. In the thermodynamic analysis, the lanthanide phosphate was assumed to be a solid phase. This tendency might be explained by the following equation for solid solution-aqueous solution equilibrium in phosphate co-precipitation of REE series in saline groundwater [3].

Figure 1. Th concentration measured at Horonobe URL and thermodynamic estimation of the species.

$$K_{sp}^0(LnPO_4) \propto \{K_{sp}^0(La)^{X_{La}} K_{sp}^0(Ce)^{X_{Ce}} \cdots K_{sp}^0(Lu)^{X_{Lu}}\} \times \{\alpha_{LaPO_4}^{X_{La}} \alpha_{CePO_4}^{X_{Ce}} \cdots \alpha_{LuPO_4}^{X_{Lu}}\}$$

where $K_{sp}(M)$ are the solubility products of pure REE phosphates, X_M indicates a solid mole fraction for REE on the co-precipitate surface, and is the solid phase activity.
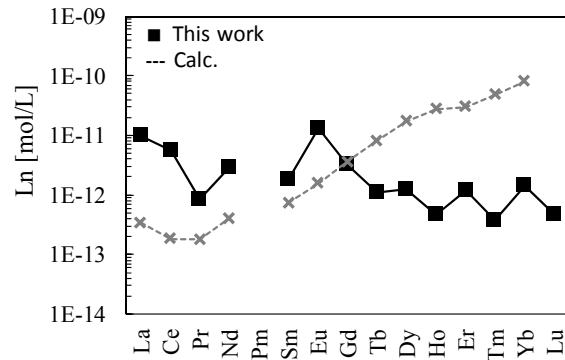
Figure 2. REE concentrations measured at Horonobe URL (140 m) and solubility estimation by assuming each K_{sp} of Ln(PO$_4$) to be a solid phase.

[1] Amano, Y., et al., "Data of groundwater from boreholes, river water and precipitation for the Horonobe Underground Research Laboratory Project; 2001-2010", JAEA-Data/Code 2011-023 (2011).

[2] a) M. Rand, et al., Chemical Thermodynamics of thorium, In: Chemical Thermodynamics Vol. 11, OECD Publications, Paris, France (2007), b) T. Fanghänel, et al., Update on the Chemical Thermodynamics of Uranium, Neptunium, Plutonium, Americium and Technetium, In: Chemical Thermodynamics Vol. 5, Elsevier, North Holland, Amsterdam (2003)

[3] Liu, X., et al., "Rare earth and yttrium phosphate solubilities in aqueous solution", Geochim. Cosmochim. Acta, 61 (1997) 1625-1633.

TEMPERATURE EFFECT ON THE SOLUBILITY
AND SOLUBILITY PRODUCT OF Th AND Zr HYDROXIDES

T. Kobayashi[1)], T. Sasaki[1)], H. Moriyama[2)]

[1)] *Department of Nuclear Engineering, Kyoto University,*
Kyoto daigaku-Katsura,Nishikyo, Kyoto 615-8540, Japan
[2)] *Research Reactor Institute, Kyoto University,*
Kumatori-cho, Sennan-gun 590-0494, Osaka, Japan

As a decay heat emission from the high level radioactive waste or spent nuclear fuel will be transferred to surrounding barrier systems of the disposal site, actinide elements leached from the waste form are exposed to elevated temperature condition in the early failure scenario. For the evaluation of potential temperature impact on the migration behaviour of actinides, it is necessary to establish a comprehensive thermodynamic model for the solubility of tetravalent actinides. The solubility of tetravalent actinides (An^{IV}) is often controlled by sparingly soluble amorphous hydroxide ($An^{IV}(OH)_4(am)$) at 25°C and described using relevant thermodynamic constants [1]. Under elevated temperature condition, $An^{IV}(OH)_4(am)$ are subject to dehydrate and crystallize to a solid phase with higher crystallinity [2]. Accordingly, for the thermodynamic description of the solubility of $An^{IV}(OH)_4(am)$ at elevated temperature, both temperature dependence of thermodynamic constant and possible solid phase transformation need to be taken into account. The present study focused on the solubility of $Zr(OH)_4(am)$ and $Th(OH)_4(am)$ in the temperature range from 5 to 60°C. Characterizing the solid phase after aging at different temperature, solubility product values were determined and their temperature dependence was discussed.

Stock solutions of Th and Zr perchlorate were prepared from $Th(NO_3)_4 \cdot 4H_2O$ and $ZrCl_4$ and diluted to the Th and Zr concentrations of 0.01 mol/dm^3 (M). Sample solutions at given hydrogen ion concentration (pH_c) were then prapared by oversaturation method [3,4]. The ionic strength (I) was fixed at $I = 0.5$ by adding appropriate amount of $NaClO_4$. The sample solutions were stored in temperature chambers controlled at 5, 40 and 60°C for given aging time. After the aging, the sample solutions were taken from the chambers and placed and kept in a thermostat contolled at a certain measurement temperature ranging from 5 to 60°C. The pH_c measurement and ultrafiltration (3k - 100k Da filter membrane) of the sample solutions were performed under controlled temperature. Th and Zr concentrations were then determined by ICP-MS with a detection limit of about 10^{-8} M for both elements. For solid phase analysis, X-ray diffraction (XRD) patterns and small-angle X-ray scattering (SAXS) spectra were collected after the separation of the solid phase.

Th solubility after aging at 60°C and measured at 25°C in the acidic pH range significantly decreased from those of $Th(OH)_4(am)$ kept at 25°C [4]. Similar to the Th solubility aged at 90°C [2], the crystallization of initial $Th(OH)_4(am)$ was thought to proceed to form a solid phase with higher crystallinity. On the other hand, Th solubility in the acidic to neutral pH_c and size distribution of colloidal species showed similar results between different measurement temperatures from 25 to 60°C. The solubility product (K_{sp}) for $Th(OH)_4(s)$ formed after aging at 60°C was determined at each measurement temperature using the literature data of hydrolysis constant ($\beta_{m,n}$) and ion product of water (K_w) [5,6]. The K_{sp} value for $Th(OH)_4(s)$ formed at 60°C was found to increase with temperature. By assuming the simple van't Hoff expression, the enthalpy of reaction ($\Delta_r H$) below was determined.

$$Th^{4+} + 4OH^- \Leftrightarrow Th(OH)_4(s,ag)$$
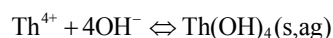
where, $Th(OH)_4(s,ag)$ denotes a solid phase formed at a certain aging temperature (ag = 60°C). Similar experiment was perfomed for Zr with different aging temperatures. The $\Delta_r H$ for Th and Zr solid phases formed at different temperature was discussed for the thermodynamic description of Th and Zr solubility under a given elevated temperature.

[1] R. Guillaumont, et al., *Update on the chemical thermodynamics of uranium, neptunium, plutonium, americium and technetium. Chemical Thermodynamics. Vol. 5,* Elsevier, Amsterdam (2003).
[2] D. Rai, D. A.,Moore, C. S.,Oakes, M., Yui, Radiochim. Acta 88, 297 (2000).
[3] T. Sasaki, T. Kobayashi, I. Takagi, H. Moriyama, Radiochim. Acta 94, 489 (2006).
[4] T. Kobayashi, T. Sasaki, I. Takagi, H. Moriyama, J. Nucl. Sci. Technol., 46, 1085 (2009).
[5] M. Rand, et al., *Chemical thermodynamics of thorium. Chemical Thermodynamics. Vol. 11*, Elsevier, Amsterdam (2009).
[6] W. Stumm and J. J. Morgan, *Aquatic chemistry: chemical equilibria and rates in natural waters*, A Wiley-Interscience publication (1996).

SOLUBILITY OF SELENIUM IN THE PRESENCE OF IRON
UNDER REDUCING CONDITIONS

R. Doi[1)], K. Uchikoshi[2)] and H. Beppu[2)]

[1)]*Japan Atomic Energy Agency(JAEA), 4-33, Muramatsu, Tokai, Ibaraki, 319-1194, Japan*
[2)]*Inspection Development Company Ltd., 3129-37, Hibara, Muramatsu, Tokai, Ibaraki, 319-1112, Japan*

Selenium (Se) is one of the key elements in the safety assessment of the geological disposal system because ^{79}Se is the long-lived fission product. Because of slow diffusional transport and nearly nonexistent sorption due to the anionic nature of Se species, it is expected that the solubility phenomenon will control Se concentrations in repository environments. Predictions based on the available thermodynamic data[1] suggest that under reducing repository environments $FeSe_2$(cr) is the expected solubility-controlling solid of Se. However, Iida et al.[2] reported that in the Se solubility experiments performed in the presence of Fe under reducing conditions where HSe^- was the predominant species, the Se concentration was controlled by amorphous or minor amount of crystalline Se although X-ray diffraction (XRD) analysis of the solid samples from the equilibrated suspensions showed the presence of $FeSe_2$(cr). This is contrary to the predictions based on the above mentioned thermodynamic data. Whether $FeSe_2$(cr) controls the Se concentration in the region where Se_4^{2-} is the predominant species is still questionable. Thermodynamic calculations of the Se solubility in simulated porewaters showed that estimated solubility of crystalline Se is around 3 orders of magnitude higher than that of $FeSe_2$(cr)[3], suggesting that determination of the solubility-controlling solid of Se significantly impacts on the Se solubility. Kitamura et al.[1] selected the equilibrium constant (K^0) for the dissolution reaction of $FeSe_2$(cr) as tentative value because of the uncertainty of the quality of the data. For these reasons, the primary objective of this study is to determine the solubility-controlling solid of Se under reducing conditions. In this study, solubility experiments of Se were performed from oversaturation direction in the presence of Fe under reducing conditions where $FeSe_2$(cr) and Se_4^{2-} are thermodynamically stable.

Three grams of metallic Se were washed in 0.01 mol/dm^3 NaOH to remove soluble impurities such as SeO_2. The washed metallic Se was dissolved in 14 mol/dm^3 NaOH at 353 K. This solution was filtered through 0.45 μm membrane filters to remove the solid material. Seven grams of metallic Fe were washed in 0.05 mol/dm^3 HCl to remove organic substances. The washed metallic Fe was dissolved in 2 mol/dm^3 HCl. This solution was filtered through 0.45 μm membrane filters to remove the unreacted metallic Fe. Samples for solubility experiments were prepared by adding aliquots of Se and Fe filtrates into deionized water. The initial concentrations of Se and Fe were 0.011 mol/dm^3 and 0.012 mol/dm^3, respectively. The pH of the samples was adjusted between 5 and 9 using 10.0 mol/dm^3 HCl. Reducing conditions were maintained using hydrazine monohydrate. Solubility experiments were performed in 50 cm^3 glass vials under nitrogen atmosphere in a controlled atmosphere glove box (O_2<1ppm). The glass vials were stored in a constant temperature oven. The temperature was maintained at 348 K inside the oven to promote the formation of $FeSe_2$(cr). After several different equilibration periods, ranging from 29 to 217 days, aliquots of the aqueous phase were withdrawn and filtered through ultrafilters with an effective 10,000 molecular-weight cutoff. Filtrates were acidified with HNO_3 and stored until they were analyzed for Se and Fe using ICP-MS. The precipitate was separated by a 0.45 μm membrane filter and dried at 348 K inside the oven until this was characterized by XRD analysis.

The Se concentration as a function of equilibration periods indicated that Se concentrations were similar at different equilibration periods. The steady-state concentrations and the fact that most solubility reactions show rapid precipitation/dissolution kinetics at elevated temperatures such as those used in this study, suggest the attainment of equilibrium in our system. The redox potential (Eh) and pH of the equilibrated suspensions ranged from -175.5 to -4.9 mV vs. SHE and 6.0 to 8.2, respectively. Based on the thermodynamic data[1], Se_4^{2-} and Fe^{2+} are thermodynamically stable in this region. The dissolution reaction of Fe_nSe with these species can be described as

$$4Fe_nSe(cr) \rightleftharpoons 4nFe^{2+} + Se_4^{2-} + (8n-2)e^- \ .$$
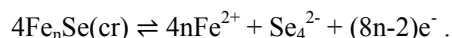
Interpretations using the specific ion interaction theory model showed that the relationship between Eh and the measured concentrations of Se and Fe could be interpreted well when in the above equation n = 0.50 ± 0.01 and $\log_{10}K^0$ = -17.28 ± 0.07. The $\log_{10}K^0$ value calculated from the available thermodynamic data[4][5][6] agrees with that determined here. Only $FeSe_2$(cr) was detected as the Se solid phase by XRD analysis of the

solid samples from the equilibrated suspensions. Therefore, we conclude that $FeSe_2(cr)$ is most likely the solubility-controlling solid of Se under these conditions.

[1] A. Kitamura et al., JAEA-Date/Code 2014-009 (2014).
[2] Y. Iida et al., article soumis à MOFAP La Baule (2007).
[3] A. Kitamura et al., proceedings of the 13th ICEM, ICEM(2010-40172), Tsukuba (2010).
[4] Å. Olin et al., North Holland Elsevier Science Publishers B. V. (2005).
[5] R. J. Lemire et al., OECD Publications (2013).
[6] Y. Iida et al., J. Nucl. Sci. Technol. 47, No. 5, 431 (2010).

DISSOLUTION OF CRYSTALLINE ThO$_2$ – STUDY OF DISSOLUTION PROCESS WITH INITIAL ^{229}Th SPIKE

E.Myllykylä [1)*], T.Lavonen[1)], K.Ollila [1)], L.Koivula[2)], D.Lumen [2)], J.Knuutinen [2)], M.Siitari-Kauppi[2)]

[1)]*VTT Technical Research Centre of Finland Ltd, P.O. Box 1000, FI-02044 VTT, Finland*
[2)]*Department of Chemistry, Laboratory of Radiochemistry, University of Helsinki, A.I.Virtasen aukio 1, 00014 Helsingin yliopisto, Finland*

The objective of this study was to investigate the solubility and initial dissolution rate of crystalline ThO$_2$. The research was mainly performed as a part of the EU project, REDUPP, and was later continued under national program. REDUPP aimed for better understanding of the dissolution processes of the oxides, ThO$_2$, CeO$_2$, and UO$_2$, which are isostructural with fluorite, the structure of UO$_2$ matrix of spent nuclear fuel.

In literature, the solubility values of ThO$_2$, as well as the hydrolysis constants of thorium show great discrepancies [1]. Thorium's tendency to undergo polynucleation and colloid formation, its strong absorption to surfaces, and the low solubility of both Th^{4+} hydroxide and hydrous oxide are the main reasons for the observed discrepancies. The solubility values have been observed to depend on the crystallinity of ThO$_2$, but the surface phenomena of the oxide may also play a role in the dissolution.

Prior to the experiments, the sintered ThO$_2$ pellets were made to meet an ideal composition and microstructure similar to the fluorite structure of UO$_2$ fuel. Making of the pellets is described in detail elsewhere [2]. The surface analyses, performed prior to the solubility experiments, showed a microstructure similar to UO$_2$ fuel pellets; randomly oriented crystals with grain size from 10 to 30 μm.

In this study the aim was to evaluate the dissolution of ^{232}Th from the solid phase and precipitation/sorption of the ^{229}Th tracer from the solution. The dissolution experiments were conducted with 2 to 4 mm particles or a single pellet (3.8 mm x 8.7 ø mm) in 0.01 M NaCl in an Ar glove-box. Parallel experimental series was conducted in the same solution using ^{229}Th spike (10^{-9} mol/L) at the beginning of the experiment to study the reversibility of surface reactions.

Table 1. Experimental matrix with 2 to 4 mm particles and solid pellets.

Experiment	Solid	m(^{232}ThO$_2$)	Solution	^{229}Th spike
A	pellet	2	0.01 M NaCl	1·10^{-9} M
B	pellet	2	0.01 M NaCl	1·10^{-9} M
C	pellet	2	0.01 M NaCl	-
D	pellet	2	0.01 M NaCl	-
E	crushed	0.5	0.01 M NaCl	1·10^{-9} M
F	crushed	0.5	0.01 M NaCl	1·10^{-9} M
G	crushed	0.5	0.01 M NaCl	-
H	crushed	0.5	0.01 M NaCl	-

The concentration of dissolved ^{232}Th and the isotopic ratio of ^{229}Th/^{232}Th in the nonfiltered samples were analysed with High Resolution (HR)-ICP-MS (Element 2 by ThermoScientific). The analyses were performed using standard solutions with known concentrations diluted from AccuTrace^{TM} Reference Standard SQS-01. A control sample for the analysis was prepared from standard CLMS-1 solution by SPEX. In addition, all the blank, standard and control samples contained a known amount of an internal standard, indium. Analyses of Th were performed by using low resolution (R≈ 300). The detection limit for thorium was between 1·10^{-12} mol/L and 4·10^{-12} mol/L depending on the solution matrix and daily efficiency of the instrument. For some selected liquid samples the isotopic ratio was also analysed with alpha spectrometric method. Thorium was coprecipitated from solution with CeF prior to alpha detection.

In the end of the experiments the solid pellets were also analysed by alpha detection. Most of the alpha particles are absorbed inside the pellets and therefore a well-defined simulation is crucial for correct activity measurement. Samples were studied with silicon semiconductor detectors in the vacuum chambers and the collected alpha spectra from Th isotopes were compared to the spectra obtained from simulations performed with AASI-program. Monte Carlo- based program AASI (Advanced Alpha-spectrometric Simulation) is designed by Radiation and nuclear safety authority of Finland. With these simulations we could determine the amount of decays in the pellets.
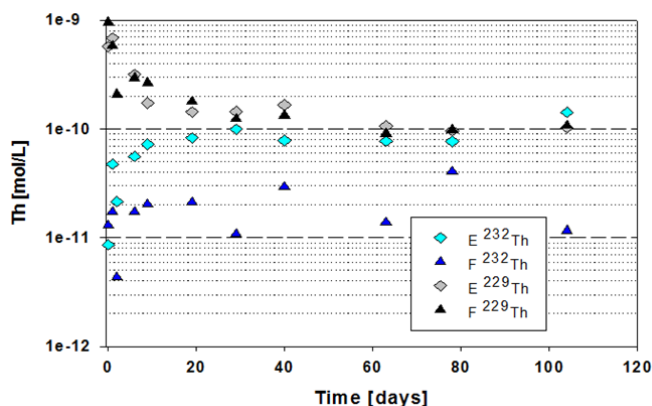
Figure1. The evolution of Th concentrations in the experimental series with crushed ThO_2 particles with ^{229}Th spike (E and F in Table1).

HR-ICP-MS enabled the detection of Th down to 10^{-12} mol/L. The results of these experiments show that for ThO_2 the process of dissolution/precipitation occurs simultaneously and demonstrates reversibility. In the end of the experiments the ^{229}Th/^{232}Th ratio in liquid phase approaches 1. It should be noticed that the dissolution/precipitation sparingly soluble oxides might continue even after the solubility limit of the oxide has been achieved. The continuation of dissolution despite the equilibrium is relevant when considering the disposal of spent nuclear fuel.

[1] J. Vandenborre, B. Grambow, A. Abdelouas, Inorg. Chem. 29, 8736-8748 (2010).
[2] E. Myllykylä et al., Radioch. Acta (submitted 2014, accepted 2015)

EXPERIMENTAL DETERMINATION OF SOLUBILITY OF NEODYMIUM HYDROXIDE IN HIGH IONIC STRENGTH SOLUTIONS AT 298.15 K UNDER WELL-CONSTRAINED CONDITIONS: COMPARISON WITH MODEL PREDICTIONS[A]

Yongliang Xiong[1], Leslie Kirkes[1], Cassie Marrs[1]

[1] *Sandia National Laboratories (SNL)[B], 4100 National Parks Highway, Carlsbad, NM 88220, U.S.A.*

$Nd(III)$ is a good non-radioactive analog for actinides in +III oxidation state $(An(III))$[1]. Therefore, $Nd(III)$ has been studied extensively for the investigation of the chemical behaviors of $An(III)$[1]. In the review performed by Baes and Mesmer [2], the authors reviewed solubility experiments on $Nd(OH)_3(s)$ prior to 1976. Since then, there have been several solubility experimental studies of $Nd(OH)_3(s)$ in literature [e.g., 3-7]. However, few solubility studies were conducted in high ionic strength solutions that are applicable to nuclear waste disposal in salt formation environments [5]. In this presentation, we report the experimental results from our long-term solubility studies on $Nd(OH)_3(s)$ under well constrained conditions in high ionic strength solutions relevant to salt formation environments.

Our long-term solubility experiments equilibrium was approached from undersaturation at 298.15 K, using high-purity crystalline $Nd(OH)_3(s)$ synthesized according to the procedure described by Wood et al. [6]. As detailed in Wood et al. [6], many other synthesis methods suffer from various shortcomings, which would result in difficulty/uncertainty interpreting solubility data. Therefore, starting with well-defined high-purity material is of fundamental importance to the success of solubility experiments. In synthesis of $Nd(OH)_3(s)$, high purity Nd_2O_3 was first loaded into Paar® reaction vessels with deaerated DI water, and then the reaction vessels were sealed in a glovebox under a positive pressure of an inert gas. The reaction vessels were then removed from the glovebox and placed into a muffle furnace. $Nd(OH)_3(s)$ was synthesized by reacting the high purity Nd_2O_3 with the deaerated DI water at 473.15 K in Paar® reaction vessels for a period of two weeks. Following the synthesis step, the reaction vessels were then transferred back into the glovebox, and were opened for drying in an atmosphere of inert gas. This synthesis method assures the complete conversion of Nd_2O_3 to $Nd(OH)_3(s)$, as demonstrated by XRD and SEM-EDS characterizations. Note, the deaerated DI water used in the synthesis was prepared by vigorously bubbling high purity Ar or N_2 gas through the DI water for a minimum of 30 minutes in the glovebox. This deaeration process was intended to remove any dissolved CO_2 and therefore ensure the synthesis process was not contaminated by carbonate.

In our solubility experiments, approximately 0.3 grams of $Nd(OH)_3(s)$ were placed into serum bottles and 100 mL of supporting solutions with the desired ionic strength, were added to the serum bottles in the glovebox, and the filled serum bottles were sealed with clip caps. The supporting solutions consisted of 4.4 and 5.0 mol•kg^{-1} NaCl solutions where mol•kg^{-1} refers to concentration on molal scale, i.e., moles per 1000 g of water. All supporting solutions were prepared from reagent grade chemicals from Fisher Scientific, or its associated vendors, and deaerated DI water. In our solubility experiments, hydrogen ion concentrations (i.e., pmH, hydrogen ion concentrations on molal scale) were not adjusted, rather the pmH was controlled by the dissolution of $Nd(OH)_3(s)$, as the pmH range, buffered by the dissolution of $Nd(OH)_3(s)$ in high ionic strength solutions, had not been determined in previous studies.

Solution samples were periodically withdrawn from the experiments to determine if the system had reached equilibrium. Before each sampling, pH readings were taken for each experiment. In each sampling, about 3 mL of solution samples were taken from each experiment, and the solution samples were filtered through a 0.2 m filter, and transferred into pre-weighed 10 mL Grade A volumetric flasks. After filtration, masses of each solution sample were determined with a balance precise to the fourth decimal place. Samples were then immediately acidified with 0.5 mL of the Optima® Grade HNO_3 from Fisher Scientific, and diluted to 10 mL with DI water. Prior to chemical analyses for Nd using the PerkinElmer NexION 300D ICP-MS, and for Na using the PerkinElmer Optima 3300 Dual View (DV) ICP-AES, aliquots from the afore-mentioned acidified samples were further diluted to an appropriate ionic strength.

The measured pH readings were converted to hydrogen ion concentrations on molar scale (i.e., pcH) based on the correction factors determined in reference [8], and pcH's were converted to pmH's according to the equations in reference [9]. The final measurements for this study included sodium, neodymium, chloride, and hydrogen ion molal concentration data.

The results from our long-term solubility experiments indicate that the pmH range (~9.6 — ~9.7) exhibited by the dissolution of $Nd(OH)_3(s)$ is similar to that controlled by the dissolution of brucite in high ionic strength solutions [10]. The measured solubility of $Nd(OH)_3(s)$ in 4.4 and 5.0 mol•kg^{-1} NaCl solutions, were compared with the model-predicted solubilities of $Am(OH)_3(s)$. In the model prediction, solubility values in

equilibrium with Am(OH)$_3$(s) in the above solutions are predicted by using the Waste Isolation Pilot Plant (WIPP) thermodynamic model [11-15]. The comparison demonstrated that the model-predicted values were in good agreement with the measured Nd(OH)$_3$(s) solubility data.

[1] G. R. Choppin, J. Radioanaly. Nucl. Chem. 273, 695 (2007).
[2] C. F. Baes Jr., R. E. Mesmer, The Hydrolysis of Cations, John Wiley, New York (1976).
[3] R. J. Silva. Report LBL-15055, Lawrence Berkeley Laboratory, Berkeley (1982).
[4] L. Rao, D. Rai, A. R. Felmy, Radiochim. Acta 72, 151 (1996).
[5] F.I. Khalili, V. Symeopoulos, J.-F. Chen, and G.R. Choppin, Radiochim. Acta 66/67, 51 (1994).
[6] S.A. Wood, D.A. Palmer, D.J. Wesolowski, and P. Bénézeth, The aqueous geochemistry of the rare earth elements and yttrium. Part XI. The solubility of Nd(OH)$_3$ and hydrolysis of Nd^{3+} from 30 to 290 ^{o}C at saturated water vapor pressure with in-situ pH$_m$ measurement. In Hellmann, R. and Wood, S.A., ed., Water-Rock Interactions, Ore Deposits, and Environmental Geochemistry: A Tribute to David Crerar, Special Publication 7, The Geochemical Society, pp. 229–256 (2002).
[7] V. Neck, M. Altmair, T. Rabeng, J. Lutzenkirchen, T. Fanghanel, Pure Appl. Chem. 81, 1555 (2009).
[8] D. Rai, A.R. Felmy, S.I. Juracich, L.F. Rao, Report SAND94-1949, Sandia National Laboratories, Albuquerque, New Mexico (1995).
[9] Y.-L. Xiong, H.-R. Deng, M.B. Nemer, S. Johnsen, Geochim. Cosmochim. Acta 74, 4605 (2010).
[10] Y.-L. Xiong, Aquatic Geochim. 14, 223 (2008).
[11] Babb, S.C., and Novak, C.F., "User's Manual for FMT Version 2.3: A Computer Code Employing the Pitzer Activity Coefficient Formalism for Calculating Thermodynamic Equilibrium in Geochemical Systems to High Electrolyte Concentrations." Albuquerque, NM: Sandia National Laboratories (1997).
[12] Y.-F. Wang, "WIPP PA Validation Document for FMT (Version 2.4), Document Version 2.4." Sandia National Laboratories, Carlsbad, New Mexico, USA (1998).
[13] E. Giambalvo, L.H. Brush, Y.-L. Xiong, "Role of actinide solubility in assessing performance of the Waste Isolation Pilot Plant" EOS, Trans. American Geophysical Union, 83(47), U11B-02 (2002).
[14] Y.-L. Xiong, E.J. Nowak, L.H. Brush, Geochim. Cosmochim. Acta 69, A417 (2005).
[15] Y.-L. Xiong, E.J. Nowak, L.H. Brush, A.E. Ismail, J.J. Long, "Establishment of uncertainty ranges and probability distributions of actinide solubilities for performance assessment in the Waste Isolation Pilot Plant." Materials Res. Soc. Symp. Proc. 1265, 15-20 (2010).

INTERACTION OF Np(V) WITH BORATE IN DILUTE TO CONCENTRATED ALKALINE NaCl AND MgCl₂ SOLUTIONS

K. Hinz, M. Altmaier, X. Gaona, D. Fellhauer, D. Schild, H. Geckeis

Karlsruhe Institute of Technology, Institute for Nuclear Waste Disposal, Germany

Neptunium-237 is a long-lived ($t_{1/2} = 2.14 \times 10^6$ years) redox-sensitive actinide relevant in the long-term safety assessment of nuclear waste repositories. Np(V) is expected to control the chemistry of Np in the early stage after repository closure whereas tetravalent Np(IV) is relevant under more reducing conditions. A thorough understanding of Np(V) aqueous chemistry is of special importance in the unlikely event of water intrusion in a repository. This understanding must be extended to concentrated salt brines when considering repositories in rock salt formations or certain sedimentary bedrocks with high salinity. Boron can be present in high concentrations in the intruding brines of salt-based repositories as well as a part of the emplaced waste. The interaction of Np(V) with borate is a relevant research topic in view of radionuclide retention processes and the possible impact of complexation/solubility phenomena on the mobilization of actinides into the biosphere.

The interaction of Np(V) with borate in chloride containing solutions was investigated by a combination of solubility measurements, UV–vis/NIR spectroscopy and solid phase characterization. All experiments were conducted under inert gas (Ar) atmosphere at $22 \pm 2°C$. Np(V) solubility was investigated in independent batch experiments from undersaturation conditions with ~ 8–14 mg of freshly precipitated $^{237}NpO_2OH(am)$ solid phase per sample. Samples were prepared in 0.1–5.0 M NaCl and 0.25–3.5 M MgCl₂ with $0.04\,M \leq [B]_{tot} \leq 0.16\,M$ and $8 \leq pH_m \leq 9$. All systems were equilibrated for up to 270 days; pH_m and m_{Np} (LSC) were monitored at regular time intervals. After attaining equilibrium conditions, selected solid phases were characterized by XRD, XPS and SEM–EDX. Additional UV–vis/NIR experiments with $\sim 1 \times 10^{-4}$ M $^{237}Np(V)$ per sample were performed in 0.25–3.5 M MgCl₂ solutions with $8 \leq pH_m \leq 9$.

A slight increase in Np(V) solubility is observed in NaCl solutions with $8 \leq pH_m \leq 9$ and $[B]_{tot} = 0.04$ M, indicating the possible formation of a Np(V)–borate complex in solution (Fig. 1). Complex formation is further confirmed by UV–vis/NIR, where a red shift and peak broadening is observed in MgCl₂ systems. Similar to previous observations made for Nd(III) under analogous experimental conditions [1], a distinct decrease in solubility occurs in dilute to concentrated NaCl solutions with higher boron concentration ($[B]_{tot} = 0.16$ M) and $pH_m \leq 9$ (Fig. 1). A similar decrease in Np(V) solubility occurs in dilute MgCl₂ systems, but not in concentrated MgCl₂ brines where a strong competition of Mg^{2+} for borate complexation is expected.
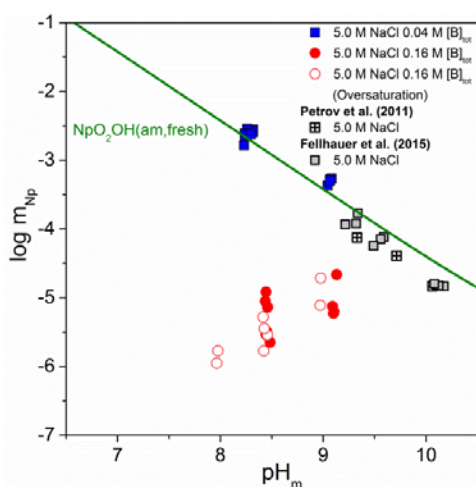
Fig. 1. Experimentally measured Np(V) solubility in 5.0 M NaCl in absence [2–3] and presence of borate ($[B]_{tot}$ = 0.04 and 0.16 M) [this work]. Solid line corresponding to the solubility of NpO₂OH(am,fresh) in 5.0 M NaCl calculated according with NEA–TDB selection [4].
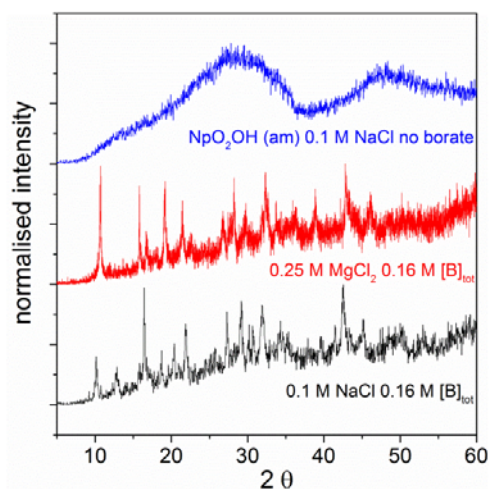
Fig. 2. Diffractograms of solubility-controlling Np(V) solid phases in the absence and presence of borate ($[B]_{tot}$ = 0.16 M).

The decrease in solubility observed in NaCl and MgCl₂ is accompanied by a clear change in the color of the solid phase (from greenish to white) and the slope of the solubility curve (log m_{Np} *vs.* pH_m). The newly formed

solid phase shows distinct XRD patterns (Fig. 2), confirming its crystalline character in contrast to the amorphous $NpO_2OH(am)$. XPS further indicates the stoichiometric participation of boron and Na^+/Mg^{2+} in the secondary phase formation. This solid phase transformation constitutes a previously unreported retention mechanism for the highly mobile Np(V).

[1] Hinz, K., Altmaier, M., Gaona, X., Rabung, T., Schild, D., Richmann, M. Reed, D. T., Alekseev, E. V., Geckeis, H., (2015), New Journal of Chemistry, 39, 849-859.

[2] Petrov, V.G., Gaona, X., Fellhauer, D., Dardenne, K.., Kalmykov, S.N., Altmaier, M., (2011) Migration Conference, Beijing China.

[3] Fellhauer, D. (2015), Personal communication.

[4] Guillaumont, F.J., Fanghänel, Th., Fuger, J., Grenthe, I., Neck, V., Palmer, D.A., Rand, M. A.,(2003) Elsevier, Amsterdam.

SOLUBILITY BEHAVIOR OF NpO_2(am,hyd) AND PuO_2(am,hyd) IN DILUTE TO CONCENTRATED NaCl SOLUTIONS

J. Schepperle, D. Fellhauer, X. Gaona, <u>M. Altmaier</u>, H. Geckeis

Karlsruhe Institute of Technology, Institute for Nuclear Waste Disposal, Germany

Reliable long term safety assessment of a repository for high level radioactive waste requires a precise analysis of possible future events, which might compromise the safety of a potential repository site. From this perspective the intrusion of aqueous solutions or groundwater into a repository is of major concern, as this may lead to the corrosion of the waste containers and the formation of aqueous, i.e. mobile, radionuclide species in the near field. In order to assess if the latter are transported to the far-field or the environment over the long term, a profound knowledge of the basic geochemical processes of radionuclides in aqueous solutions (e.g. solubility behavior, complexation, redox, sorption, colloid formation etc.) as well as the corresponding thermodynamic data are mandatory. Actinide elements, especially the long-lived alpha emitting isotopes of plutonium and neptunium, are relevant in this context. In the present work, the solubility and hydrolysis behavior of Np(IV) and Pu(IV) is experimentally investigated, which are the most stable oxidation states under the reducing conditions expected in a deep underground repository on the long term. Although several studies exist on this topic (see e.g. Neck et al. [1]), some aspects have not been solved and remain open for these systems: a) solubility data for NpO_2(am,hyd) and PuO_2(am,hyd) are missing for $3 < pH < 6$, thus hindering a comprehensive description of Np(IV) and Pu(IV) solubility behavior in this pH region; b) comprehensive solubility studies with NpO_2(am,hyd) and PuO_2(am,hyd) that cover a wide range of background electrolyte concentrations and pH values are so far not available; c) almost all available solubility data for NpO_2(am,hyd) and pH > 6 are reported with large uncertainty.

Batch solubility experiments with $^{237}NpO_2$(am,hyd) and $^{242}PuO_2$(am,hyd) were performed from undersaturation over a broad range of pH_m values ($-\log m_{H^+} = 2–13$) and ionic strengths ([NaCl] = 0.1 mol L^{-1}–5.0 mol L^{-1}) under well-defined redox conditions (addition of reducing chemicals). The corresponding AnO_2(am,hyd) solid phases were obtained by precipitation from an electrochemically prepared Np^{4+} stock solution with NaOH (Np), or by slow "reductive precipitation" of PuO_2^{2+} with hydroquinone (Pu), respectively. Phase separation was performed by ultrafiltration (10 kD, 2 nm), although in some samples an aliquot of the clear supernatant was also collected. Samples were analyzed for pH_m, redox potential (with pe = 16.9 E_H), and An concentration (liquid scintillation counting, LSC, or sector field inductively coupled plasma mass spectrometry, SF-ICPMS) over a period of 23 weeks. The results were compared to thermodynamic model calculations based on the database of the NEA-TDB [2].

The $pe+pH_m$ conditions determined in pH neutral and alkaline samples were in the thermodynamic stability field of An(IV). As expected, the solubility of NpO_2(am,hyd) and PuO_2(am,hyd) under these conditions were below the detection limit of LSC ($1\cdot10^{-8}$ mol L^{-1} for ^{237}Np, $1\cdot10^{-9}$ mol L^{-1} for ^{242}Pu). All samples are currently analyzed by the more sensitive SF-ICPMS (detection limit ca. $1\cdot10^{-12}$ M) to quantify the An(IV) concentration in this pH region, and evaluate the relevant equilibrium reaction AnO_2(am,hyd) + 2 $H_2O \rightleftharpoons$ $An(OH)_4$(aq). First results for Np in 0.1 mol L^{-1} NaCl reveal a pH independent Np(IV) concentration of log [Np(IV)] ≈ -9.8, which is in good agreement with the model calculations, see figure 1. In acidic solutions, the solubility of Np(IV) and Pu(IV) is systematically increasing with decreasing pH value. In the case of Np (measured redox conditions are in the stability field of Np(IV)), the slope of the experimental solubility curve is in fair agreement with the one calculated for NpO_2(am,hyd). The experimental Pu concentration in the acidic samples were, however, clearly above the calculated value for the equilibrium PuO_2(am,hyd) $\rightleftharpoons$ Pu(IV)(aq). Based on the results of a solvent-extraction analysis, the observed deviations are due to major contribution of trivalent Pu species in the aqueous phase which formed during the course of the experiment. The result is unexpected as no reducing chemical was added to the acidic Pu samples, and points to the need for further investigation. With respect to the intended thermodynamic evaluation of the data, a comprehensive determination of the Pu and Np oxidation state distribution in all acidic samples by capillary electrophoresis (CE) coupled to SF-ICPMS is currently ongoing. After completion of this work, the study will be extended to carbonate containing solutions using the same NpO_2(am,hyd) and PuO_2(am,hyd) solid phases to comprehensively investigate the Np(IV)-OH-CO_3 and Pu(IV)-OH-CO_3 systems. First results will be shown at the Migration conference.
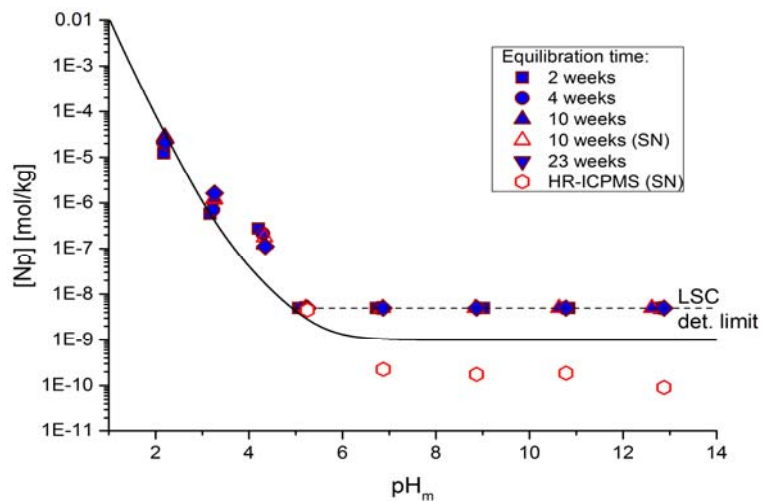
Figure 1. Experimental and calculated (solid line) solubility of NpO_2(am,hyd) in 0.1 mol L^{-1}. Closed symbols: after 10 kD (ca. 2 nm) ultrafiltration. Open symbols: untreated supernatant.

[1] V. Neck, J. I. Kim (2001), "Solubility and hydrolysis of tetravalent actinides", Radiochimica Acta 89: 1–16.

[2] R. Guillaumont, Th. Fanghänel, J. Fuger, I. Grenthe, V. Neck, D. Palmer "Update on the Chemical Thermodynamics of Neptunium and Plutonium", Elsevier, Amsterdam, 2003.

FORMATION, STABILITY AND SOLUBILITY OF MIXED Nd–OH–Cl(s) PHASES IN CONCENTRATED NaCl, MgCl₂ AND CaCl₂ SOLUTIONS

M. Herm, X. Gaona, D. Fellhauer, V. Metz, M. Altmaier, H. Geckeis

Karlsruhe Institute of Technology, Institute for Nuclear Waste Disposal, Germany

In safety analyses for deep geological nuclear waste repositories a reliable prediction of the chemical behavior of actinides in aqueous solutions is necessary. Although geological or geo-technical barrier systems may retard or prevent formation water from contacting the waste, intrusion of aqueous solutions into a repository has to be taken into account within the long-term evolution of these facilities. Porewater in certain sedimentary bedrocks as well as water potentially intruding salt rock repositories will be characterized by high ionic strength and high Na^+, Mg^{2+}, K^+ and Cl^- concentrations. In addition, the corrosion of cementitious waste forms in $MgCl_2$ dominated brines may lead to high $CaCl_2$ concentrations and highly alkaline pH conditions. Trivalent (An^{III}) and tetravalent (An^{IV}) actinides are assumed to prevail under the reducing conditions expected after the closure of a deep geological repository for nuclear waste.

An appropriate knowledge of the solubility controlling solid phases is mandatory in source term estimations and for accurate geochemical calculations. $An^{III}/Ln^{III}(OH)_3(s)$ phases are normally considered as solubility limiting solid phases of trivalent actinides/lanthanides in dilute to concentrated saline systems in the absence of complexing ligands. The successful synthesis of ternary $An^{III}/Ln^{III}–OH–Cl(s)$ phases has been reported in structural studies, but no thermodynamic data has been derived so far for these systems [1, 2]. The formation and stability of these solid phases can have relevant implications in the source term of repository concepts where high chloride concentrations are expected.

In a first part of this work, the transformation of $Nd(OH)_3(s)$ into a ternary Nd–OH–Cl solid phase was experimentally assessed in NaCl (5.61 m), $MgCl_2$ (0.25–5.15 m) and $CaCl_2$ (3.91 m) systems as a function of pH ($7.5 \leq pH_m \leq 9.6$) and temperature ($T = 22$ and 80°C). Experiments at $T = 22$°C were performed under argon atmosphere, whereas those at $T = 80$°C were conducted with autoclaves in presence of air. Note that in $MgCl_2$ solutions, the maximum pH_m ($pH_{max} \approx 9$) is limited by brucite or $Mg_2(OH)_3Cl \cdot 4H_2O(s)$ precipitation.

Solid phase characterization (XRD and SEM-EDS, see Figure 1) shows a clear transformation of the initial solid phase into $Nd(OH)_2Cl(s)$ in $MgCl_2$ systems at $T = 22$ and 80°C. The transformation is enhanced at high m_{Cl^-} and low pH_m (≈ 8), whereas it does not occur in 2.67 m $MgCl_2$ and pH_{max} (≈ 8.9). No solid phase transformation takes place either in 5.61 m NaCl ($pH_m = 9.3$) and 3.91 m $CaCl_2$ ($pH_m = 9.6$), indicating that these m_{Cl^-} and/or pH_m conditions are beyond the thermodynamic stability of $Nd(OH)_2Cl(s)$.

In a second part of the present study, the thermodynamic properties of $Nd(OH)_2Cl(s)$ were assessed. Therefore batch solubility experiments were performed under argon atmosphere at room temperature using the $Nd(OH)_2Cl(s)$ phase synthesized at $T = 22$°C. Experiments were performed from undersaturation in 5.61 m NaCl, 2.67 m, 3.87 m, 5.15 m $MgCl_2$, 3.91 m $CaCl_2$ and $7.5 \leq pH_m \leq 13$. In a second set of experiments, $Nd(OH)_3(s)$ and $Nd(OH)_2Cl(s)$ were mixed and equilibrated under pH-unbuffered conditions with analogous background electrolyte and salt concentrations.

The comparison of $Nd(OH)_2Cl(s)$ and $Nd(OH)_3(s)$ solubility under virtually the same conditions [this work, 3] shows significantly lower m_{Nd} (up to 1.5 log_{10}-units) in equilibrium with $Nd(OH)_2Cl(s)$ in 2.67–5.15 m $MgCl_2$ and 3.91 m $CaCl_2$ at $pH_m \leq 8.8$ (see exemplarily Figure 2). On the contrary, no differences in aqueous concentrations in experiments with $Nd(OH)_2Cl(s)$ and with $Nd(OH)_3(s)$ are observed in 5.61 m NaCl within $7.5 \leq pH_m \leq 13$. The combination of the experimental solubility data determined in this work in $MgCl_2$ and $CaCl_2$ solutions with the Pitzer activity model derived in [3] allows the quantification of $log_{10} {}^*K^\circ_{s,0}$ for $Nd(OH)_2Cl(s)$. pH measurements in the "mixing experiments" with both solid phases being present give direct insight of $log_{10} {}^*K^\circ_{s,0}$ based on the thermodynamic equilibrium $Nd(OH)_2Cl(s) + H_2O \Leftrightarrow Nd_{aq} \Leftrightarrow Nd(OH)_3(s) + Cl^- + H^+$ and corresponding equation $log_{10} {}^*K'_{s,0}(Nd(OH)_2Cl(s)) = log_{10} {}^*K'_{s,0}(Nd(OH)_3(s)) - pH_m + log_{10} m_{Cl^-}$, provided that $pH_m^{mix} \leq pH_{max}$ in $MgCl_2$ solutions. The combination of both datasets permits an accurate quantification of the solubility product of $Nd(OH)_2Cl(s)$:
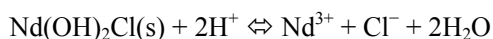
$$Nd(OH)_2Cl(s) + 2H^+ \Leftrightarrow Nd^{3+} + Cl^- + 2H_2O \qquad\qquad log_{10} {}^*K^\circ_{s,0} = 10.56 \pm 0.10$$

The newly characterized solid phase can play a relevant role in controlling the solubility of An^{III}/Ln^{III} under repository systems with high chloride concentrations. Although kinetically rather slow, the transformation $An^{III}/Ln^{III}(OH)_3(s) \rightarrow An^{III}/Ln^{III}(OH)_2Cl(s)$ is enhanced at $m_{Cl^-} \geq 5.34\,m$ and $pH_m \leq 8.8$.
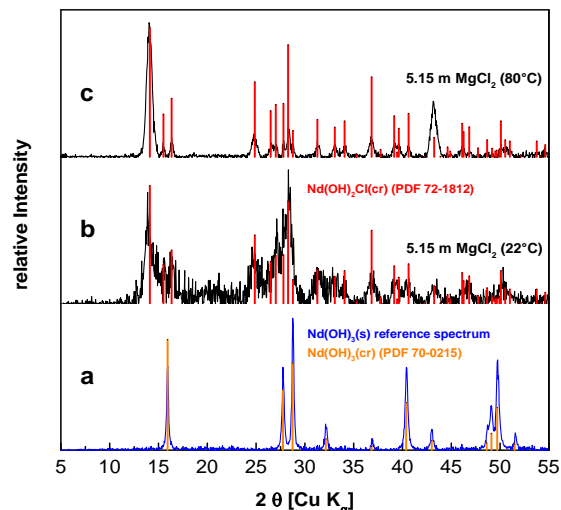
Figure 1: Exemplary XRD pattern of $Nd(OH)_3(s)$ starting material (a) and solid phases recovered from experiments in $5.15\,m$ $MgCl_2$ at 22°C (b) and 80°C (c) showing clearly the reflexes of $Nd(OH)_2Cl(s)$.
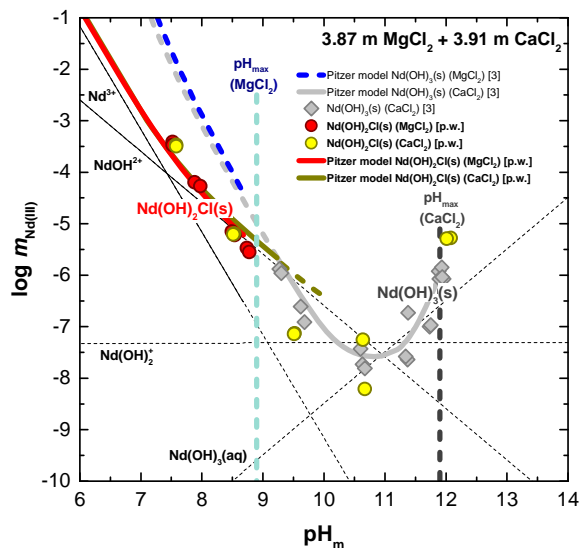
Figure 2: Experimentally measured solubility of Nd(III) in $3.87\,m$ $MgCl_2$ and $3.91\,m$ $CaCl_2$. Reference solubility data of $Nd(OH)_3(s)$ [3] is included for comparison. Thick solid lines corresponding to the solubility of $Nd(OH)_2Cl(s)$ ($pH_m \leq 9.2$) and $Nd(OH)_3(s)$ ($pH_m > 9.2$) calculated with the thermodynamic and (Pitzer) activity models reported in [3] and derived in this work. Thin lines show the aqueous speciation underlying $Nd(OH)_2Cl(s)$ solubility curve in the respective systems.

[1] R. A. Zehnder, D. L. Clark, B. L. Scott, R. J. Donohoe, P. D. Palmer, W. H. Runde, D. E. Hobart, Inorg. Chem. 49, 4781–4790 (2010).

[2] V. I. Bukin, Dokl. Akad. Nauk SSSR 207, 1332–1335 (1972).

[3] V. Neck, M. Altmaier, Th. Rabung, J. Lützenkirchen, Th. Fanghänel, Pure Appl. Chem. 81, 1555–1568 (2009).

THERMODYNAMIC DESCRIPTION OF Tc(IV) IN Tc^{4+}–Na^+–K^+–Mg^{2+}–Ca^{2+}–H^+–Cl^-–OH^-–H_2O SYSTEMS: APPLICATION TO REPOSITORY-RELEVANT CONDITIONS

E. Yalcintas, A. Baumann, X. Gaona, M. Altmaier, H. Geckeis

Karlsruhe Institute of Technology, Institute for Nuclear Waste Disposal, Germany

Technetium–99 is a β–emitting radionuclide produced in nuclear reactors by the fission of [235]U and [239]Pu. Due to its significant inventory in spent nuclear fuel, long half-life ($t_{1/2}$ ~211.000 a) and redox-sensitive character, ^{99}Tc is a very relevant radionuclide in Performance Assessment exercises of repositories for radioactive waste disposal. Under sub-oxic/oxidizing conditions, technetium exists as the highly soluble and mobile pertechnetate anion (TcO_4^-). In reducing environments, Tc(IV) prevails forming sparingly soluble hydrous oxides ($TcO_2 \cdot xH_2O(s)$). The later redox state is expected to dominate the aqueous chemistry of Tc in the reducing conditions predicted for deep geological repositories. In this framework, an appropriate understanding of the solubility and hydrolysis of Tc(IV) in dilute to concentrated saline systems is required for an accurate assessment of technetium source term in repositories for radioactive waste disposal.

The solubility of Tc(IV) was investigated from undersaturation conditions in 0.1–5.61 m NaCl, 0.1–4.58 m KCl, 0.25–5.15 m $MgCl_2$ and 0.25–5.25 m $CaCl_2$ solutions in the pH_m range 1.5–14.6. Experiments were performed at 22 ± 2°C in Ar gloveboxes with < 2 ppm O_2. Strongly reducing conditions (pH + pe < 4) were chemically set for each independent solubility sample with $Na_2S_2O_4$, $SnCl_2$ or Fe powder. All investigated systems were equilibrated for up to 600 days. Technetium concentration, pH_m and E_h values were monitored at regular time intervals. Thermodynamic equilibrium was assumed after repeated measurements with constant [Tc] and pH_m. After attaining equilibrium conditions, the redox speciation of technetium in the aqueous phase was quantified for selected samples using solvent extraction with TPPC and XANES analysis. Solid phases of selected batch experiments were also characterized by XRD, SEM–EDS and quantitative chemical analysis. Additional solubility experiments were conducted in "simulated systems", based on reported ground water and cementitious pore water compositions with complex mixtures of NaCl–KCl–$MgCl_2$–$CaCl_2$.

Solid phase characterisation and solubility data indicate that $TcO_2 \cdot 1.6H_2O(s)$ is the solid phase controlling the solubility of Tc(IV) in all the evaluated systems. The combination of solvent extraction and XANES analysis confirms the predominance of Tc(IV) in the aqueous phase, independently of the salt system and concentration. The solubility of $TcO_2 \cdot 1.6H_2O(s)$ decreases with a well-defined slope of –2 in acidic dilute systems. The same slope is retained in concentrated brines, although a very significant increase in the solubility (up to 4 orders of magnitude) is observed with increasing ionic strength. A newly derived chemical model based on these solubility data in combination with spectroscopic evidences reported in the literature [1], best explains this increase considering the formation of the previously unreported trimeric technetium species $Tc_3O_5^{2+}$. In the near-neutral pH region, the pH-independent behaviour of the solubility is consistent with the chemical reaction $TcO_2 \cdot 1.6H_2O(s)$ $TcO(OH)_2(aq) + 0.6\ H_2O$ with a $\log_{10} {}^*K^\circ_{s,TcO(OH)2}$ in good agreement with the current NEA–TDB data selection [2]. The amphoteric behaviour of Tc(IV) is confirmed by the formation of the species $TcO(OH)_3^-$ in dilute NaCl and KCl systems with $pH_m \geq 11$. The same speciation is retained in concentrated alkaline NaCl and KCl solutions, although a decrease in solubility compared to dilute systems takes place due to ion interaction processes. Changes in the aqueous speciation are observed in concentrated alkaline $MgCl_2$ and $CaCl_2$ brines, where the formation of $Mg_3[TcO(OH)_5]^{3+}$ and $Ca_3[TcO(OH)_5]^{3+}$ ternary species are proposed based on the slope analysis of the corresponding solubility curves and the comparison with previous observations available for An(IV) and Zr(IV) [3, 4] in concentrated $CaCl_2$ solutions. The formation of these species has been recently validated by quantum chemical calculations performed at KIT–INE [5].

Based on the newly generated experimental data, comprehensive chemical, thermodynamic and activity models using both SIT and Pitzer approaches are derived for the system Tc^{4+}–Na^+–K^+–Mg^{2+}–Ca^{2+}–H^+–Cl^-–OH^-–H_2O at 25°C. These data complement and significantly extend the current thermodynamic selection of the OECD Nuclear Energy Agency (NEA–TDB) [2]. Tc(IV) solubility investigated in "simulated systems" is in good agreement with qualitative predictions based on pure systems.

[1] Vichot, L., Fattahi, M., Musikas, C. and Grambow, B., Tc(IV) chemistry in mixed chloride/sulphate acidic media. Formation of polyoxopolymetallic species, Radiochimica Acta, 91, 263-271, (2003).

[2] Guillaumont, R., Fanghänel, T., Neck, V., Fuger, J., Palmer, D. A., Grenthe, I. and Rand, M. H., Update on the chemical thermodynamics of uranium, neptunium, plutonium, americium and technetium, ed. OECD Nuclear Energy Agency. Vol. 5. North-Holland, Amsterdam, Elsevier, (2003).

[3] Brendebach, B., Altmaier, M., Rothe, J., Neck, V. and Denecke, M. A., EXAFS study of aqueous Zr(IV) and Th(IV) complexes in alkaline $CaCl_2$ solutions: $Ca_3[Zr(OH)_6]^{4+}$ and $Ca_4[Th(OH)_8]^{4+}$, Inorganic Chemistry, 46, 6804-6810, (2007).

[4] Altmaier, M., Neck, V. and Fanghänel, T., Solubility of Zr(IV), Th(IV) and Pu(IV) hydrous oxides in $CaCl_2$ solutions and the formation of ternary Ca-M(IV)-OH complexes, Radiochimica Acta, 96, 541-550, (2008).

[5] Polly, R., Schimmelpfennig, B., Yalcintas, E., Gaona, X. and Altmaier, M., Hydrolysis of Tc(IV) and formation of ternary Na/Ca-Tc(IV)-OH species in $NaCl/CaCl_2$ systems: a quantum chemical study, in Migration Conference, Santa Fe, USA (2015).

EXPERIMENTALLY DETERMINED SOLUBILITY OF Nd(OH)$_3$ AT HIGH TEMPERATURE AND pH[A]

J. Icenhower, L. Kirkes, C. Marrs

Sandia National Laboratories (SNL), Carlsbad Programs Group, 4100 National Parks Highway, Carlsbad, NM 88220, USA[B]

Numerous studies have attempted to determine Nd(OH)$_3$ solubility [1-8], where Nd^{3+} is a non-radioactive proxy for Am^{3+} and Pu^{3+}. However, few investigations have been carried out to ascertain Nd(OH)$_3$ solubility in alkaline, high ionic strength solutions, and at temperatures above ambient. The investigation of Wood et al. [1] determined the temperature dependence of Nd(OH)$_3$ up to 290 °C, but they did not attempt to determine the pH and ionic strength dependence for conditions appropriate for the Waste Isolation Pilot Plant (WIPP). They found that the dominant Nd^{3+} specie at pH values greater than 8 and 30 °C is Nd(OH)$_3^0$. Because aqueous solutions in disposal vaults will interact with cement, the pH of the solution may rise to high values (>12). The specie Nd(OH)$_4^-$ is likely to exist at high pH, but has not yet been observed experimentally. Therefore, obtaining solubility data at high pH conditions is necessary to understand the potential mobility of actinides under some repository conditions.

Nd(OH)$_3$ crystals were synthesized in the laboratory using the methods outlined in Wood et al. [1]. Low temperature (≤90 °C) solubility experiments are being carried out in a low fO$_2$ and fCO$_2$ environment. The initial experiments are being carried out in 1 mM NaCl solutions in 100 mL polypropylene bottles. The Nd(OH)$_3$ crystals will dissolve for ~30 days at 30 °C and then the temperature will be raised to 90 °C. A small amount of dissolved Gd^{3+} (5-100 ppb) will be added as a tracer of the precipitation process. Because the solubility of Nd(OH)$_3$ is retrograde [1], as it is for other rare earth element hydroxides [9], increasing the temperature will cause precipitation of new material on the cores of the surviving crystals (homogeneous nucleation). The newly precipitated Nd(OH)$_3$ material will contain trace Gd^{3+} substituting for the Nd^{3+}. The presence of Gd^{3+} will be easily detected using SEM-EDS or electron microprobe with x-ray mapping capability, demonstrating growth from solution. Additional experiments will quantify the solubility of Nd(OH)$_3$ as a function of pH at fixed ionic strength, followed by determination of the ionic strength dependence.

High temperature (100 to 250 °C) experiments are being conducted in specially-designed "Hi-TAC" equipment. The 1-liter vessels are constructed of titanium and are designed to withdrawal aqueous samples at constant T and P. Assembly of the reactors containing deaerated solution and Nd(OH)$_3$ crystals take place in a glove box. Solubility of Nd(OH)$_3$ are being approached from both undersaturated and supersaturated conditions. Experiments over a pH- (8 − 12) and ionic strength (1 mM − 5 M) interval are planned. The data will be used to parameterize the equation relating solubility to temperature, pH and ionic strength for crystalline Nd(OH)$_3$. Preliminary results will be presented and discussed in the context of waste isolation in salt repositories.

[1] S. A. Wood et al., Water-Rock Interactions, Ore Deposits, and Environmental Chemistry (R. Hellman, S. A. Wood, eds.), The Geochem. Soc., Special Publ. no. 7, 229 (2002).
[2] J.-F. Lucchini et al., J. Alloys Comp. 444-445, 506 (2007).
[3] V. Neck, et al., Pure Appl. Chem. 81, 1555 (2009).
[4] L. Rao, D. Rai, A. R. Felmy, Radiochim. Acta 72, 151 (1996).
[5] R. S. Tobias, A. B. Garrett, J. Amer. Chem. Soc. 80, 3532 (1958).
[6] R. J. Silva, Lawrence Berkeley National Laboratory, LBL-15055 (1987).
[7] L. R. Morss, C. M. Haar, S. Mroczkowski, J. Chem. Thermo. 21, 1079 (1989).
[8] D. Rai, et al., Radiochim Acta 58/59, 9 (1992).
[9] S. Deberdt, et al., Chem. Geol. 151, 349 (1998).

REDOX CHEMISTRY AND SOLUBILITY OF PLUTONIUM UNDER HYPERALKALINE REDUCING CONDITIONS

A. Tasi[1], X. Gaona[1], M. Böttle[1], D. Fellhauer[1], K. Dardenne[1], M. Grivé[2], J. Bruno[2], K. Källström[3], M. Altmaier[1], H. Geckeis[1]

[1]Karlsruhe Institute of Technology, Institute for Nuclear Waste Disposal, Germany
[2]Amphos 21 Consulting S.L., Passeig Garcia i Fària, 49-51, 1-1, 08019 Barcelona, Spain
[3]Svensk Kärnbränslehantering AB, Avd. Låg-och medelaktivt avfall, Box 250, 101 24 Stockholm, Sweden

An accurate knowledge of the aquatic chemistry and thermodynamics of actinides is fundamental in the safety assessment of repositories for nuclear waste disposal. One of the internationally accepted options for the final disposal of nuclear waste involves the emplacement in deep geological formations where reducing conditions are expected to develop in the post-closure period mainly due to steel corrosion processes. In the case of low and intermediate level wastes (L/ILW), the preferred concept involves the use of cementitious materials for the stabilization of the waste and construction purposes. The interaction of these materials with groundwater buffers the pH in the alkaline to hyperalkaline range ($10 \leq$ pH ≤ 13.3) over a very long time-scale.

Due to its presence in both L/ILW and high level waste (HLW), long half-live ($t_{\frac{1}{2}}$ ^{239}Pu = $2.41 \cdot 10^4$ a) and redox-sensitivity, plutonium is an element of highest relevance in the context of nuclear waste disposal. The formation of Pu(III) and Pu(IV) is expected under the reducing conditions foreseen in a deep underground repository [1]. The sparse knowledge on the thermodynamic data limits the NEA–TDB thermodynamic selection increasing the uncertainties associated to Pu(III) and Pu(IV) aqueous species and solid compounds expected under alkaline pH conditions [2]. This leads to a rather ill-defined Pu(IV) / Pu(III) redox border, which could induce to an ill assessment of the chemical behaviour of Pu under these conditions. In this context, it is of great importance to carefully study the redox-behaviour of Pu under repository relevant conditions.

All experiments were conducted at $T = 22 \pm 2$ °C in Ar glove boxes with O_2 concentration below 2 ppm. The isotopic composition of Pu used in the experiments was 99.4 wt. % ^{242}Pu, 0.58 wt. % ^{239}Pu, 0.005 wt. % ^{238}Pu and 0.005 wt. % ^{241}Pu. We prepared solubility experiments in undersaturation conditions with 0.2 mg (per batch sample) of a well-characterized PuO_2(am,hyd) solid phase. Redox conditions were buffered with 2 mM hydroquinone (pe + pH$_m$ ~ 10) or $SnCl_2$ (pe + pH$_m$ ~ 2). The (pe + pH$_m$ ~ 10) redox conditions are considered as a "reference state" with predominance of Pu(IV) both in the aqueous and solid phases. The very reducing conditions set by $SnCl_2$ are representative of those expected in underground repositories where large amounts of steel are present. Ionic strength was maintained constant with 0.10 M NaCl–NaOH solutions and pH$_m$ was varied from 8 to 13. pH$_m$ and E_h were regularly monitored with a combination glass and a combined Pt and Ag/AgCl reference electrode, respectively. Plutonium concentrations in the aqueous phase were determined after 10 kD ultrafiltration by Liquid Scintillation Counting (LSC) using the signal of the low-energetic β-emitter ^{241}Pu. Plutonium concentrations in the clear supernatant were also measured without phase separation to determine the presence of Pu(IV) colloids. We carried out the solid phase characterization before and after the solubility experiments by using XRD, XPS, SEM–EDX and TEM. The redox state and the molecular environment of Pu in the solid phase were further evaluated by XANES/EXAFS following the Pu L$_{III}$ edge (18057.0 eV) recorded in X-ray fluorescence detection mode at the INE-Beamline for Actinide Research at the ANKA synchrotron light source, KIT Karlsruhe. The spectra were calibrated against the first inflection point in the XANES spectrum of a Zr metal foil (17998.0 eV).

The XRD and EXAFS measurements confirm the (micro-) crystalline character of the original Pu(IV) solid phase. Rietveld analysis of the XRD data indicates an average crystal (domain) size of 4 ± 1 nm. Preliminary EXAFS results suggest that the original solid phase remains unaltered in alkaline to hyperalkaline hydroquinone systems. The solubility of Pu (after 10 kD ultrafiltration) at $8 \leq$ pH$_m \leq 13$ in the presence of hydroquinone and $SnCl_2$ remains very close to or at the detection limit of LSC ($10^{-8.8}$ M) in all the samples. No clear hints of a reductive dissolution of PuO_2(am,hyd) in the presence of $SnCl_2$ can be observed with the available data, although the use of SF–ICP–MS coupled with an ultracentrifugation separation step is planned in order to improve the detection limit for Pu (to ~10^{-12} M). Plutonium concentrations (~10^{-8} M) clearly above the LSC detection limit are measured in the supernatant solutions without phase separation both in hydroquinone and $SnCl_2$ systems, and may indicate the presence of Pu(IV) colloids as described in the literature [1].

[1] Neck V., Altmaier M., Fanghänel Th., 2007. Solubility of plutonium hydroxides/hydrous oxides under reducing conditions and in the presence of oxygen. C. R. Chimie, 10, 959-977.

[2] Guillaumont R., Fanghänel T., Neck V., Fuger J., Palmer D.A., Grenthe I., Rand M.H., 2003. Chemical Thermodynamics Vol. 5. Update on the Chemical Thermodynamics of Uranium, Neptunium, Plutonium,Americium and Technetium. OECD, NEA-TDB, Elsevier, North Holland, Amsterdam.

SOLUBILITY OF URANYL MINERALS UNDER URANYL CLUSTER FORMING AQUEOUS CONDITIONS

Haylie Lobeck, Enrica Balboni, Peter C. Burns

Department of Civil and Environmental Engineering and Earth Science,
University of Notre Dame, 301 Stinson-Remick Hall, Notre Dame, IN 46556, USA

The solubility of actinide materials in aqueous solutions is important in industrial-scale processes of the nuclear fuel cycle, including in situ leaching of U ore, recovery of U from mined and crushed ore, purification of uranium prior to enrichment and fuel fabrication, and reprocessing of irradiated nuclear fuel. Solubility of irradiated fuel is also of paramount importance in a core-melt incident such as happened in three reactors at Fukushima, Japan, which were subsequently cooled with seawater. The solubility of uranium minerals is of fundamental importance in the genesis of complex uranium mineral assemblages in nature deposits, and in the transport of uranium contamination through the environment. Finally, dissolution of uranium-based used nuclear fuel into water in a geologic repository is a potential pathway for release of the inventory of radionuclide to the environment.

Uranyl minerals such as the phosphates autunite and torbernite, the silicates uranophane and boltwoodite, the oxyhydrates schoepite and becquerelite, and the vanadate carnotite, generally have low aqueous solubilities under a broad range of pH conditions. Water in contact with these minerals will typically contain less than 200 ppm U, and considerably less in the case of uranyl phosphates, vanadates, and peroxides. In general, the aqueous speciation of uranyl in such systems is rather pH dependent, and includes various uranyl carbonates and products of hydrolysis reactions.

Where counterions such as Na or K are combined with uranyl and peroxide, with the latter due to the radiolysis of water by natural or anthropogenic radiation, uranyl peroxide cage clusters can form and persist in aqueous solution. We have shown that these clusters can contain from 16 to 124 uranyl polyhedra, and have diameters in the range of 1.5 to 4.0 nm. They incorporate hydroxyl, phosphate, pyrophosphate, nitrate, oxalate, transition metal polyhedra, etc. in most cases, in addition to peroxide. Once formed, these clusters behave very differently in solution, as compared to small species. They are anionic and have associated counterions, and can result in uranium concentrations in solution that exceed 100,000 ppm under some conditions.

Uranyl mineral aqueous solubility data has been measured under conditions where simple uranyl aqueous species dominate speciation. We are interested in the dissolution behavior of such minerals under conditions that are conducive to formation of nanoscale cage clusters, and hypothesize that mineral dissolution may be greatly enhanced under such conditions. We are conducting solubility experiments for uraninite, schoepite, uranophane, and several uranyl phosphates. Each experiment is done in aqueous solution with several pH values, in the absence of peroxide, and then again at the same pH conditions in the presence of peroxide at several different concentrations. Clusters that form in solution are characterized by electrospray ionization mass spectrometry, and the concentration of uranium and other ions in solution is measured using inductively coupled plasma optical emission spectrometry. Results to date indicate formation of uranyl peroxide cage clusters in solution significantly enhances the dissolution of these uranyl minerals, with as much as two orders of magnitude more uranium found in solution under cluster-forming conditions, as directly compared to experiments lacking peroxide that are otherwise identical.

STRUCTURES OF NEPTUNIUM PEROXIDE CLUSTERS

Rachel Lopez and Peter C. Burns

Department of Civil and Environmental Engineering and Earth Sciences,
University of Notre Dame, 301 Stinson-Remick Hall, Notre Dame, IN 46556, USA

Neptunium-237 is of considerable importance for nuclear waste management because of its very long half-life (2.14 million years) and its relatively high aqueous solubility in its pentavalent and hexavalent oxidation states. Like U(VI), both Np(V) and Np(VI) form linear dioxo cations in water, but unlike U, the pentavalent oxidation state is the most stable for Np. Whereas one might reasonably imagine that the aqueous and solid state chemistry of Np(V) will be similar to U(VI), various recent studies have demonstrated significant departures in their properties. Most notable is the tendency for Np(V) to form cation-cation interactions, in which an O atom of a neptunyl ion coordinates another neptunyl ion at the equatorial position of a bipyramid.

Over the past decade an extensive family of uranyl peroxide nanoclusters has been developed by our group. More than 100 clusters have been isolated that contain as many as 124 uranyl polyhedra and have diameters in the 1.5 to 4.0 nm range. These clusters self-assemble in aqueous solution at room temperature, have high aqueous solubility, and can persist in solution for at least many months.

In 2005 we reported the formation and crystallization of a neptunyl peroxide cage cluster containing 24 neptunyl ions (Np24) that is analogous to U24. However, unlike for U24, it is possible that Np24 contains Np in two different oxidation states – pentavalent and hexavalent. In 2005 we crystallized Np24 in a tetragonal space group, such that there were only 3 symmetrically distinct Np cations in the cluster. Although the Np-O bond lengths suggested the possibility of mixed valence states, the symmetry averaging prevented definitive identification of Np(V) and Np(VI).

We have recently focused a renewed effort on the synthesis of neptunyl peroxide cage clusters, and have been able to crystallize Np24 in a monoclinic space group. In this structure, there are 12 symmetrically distinct neptunyl ions. Analysis of the corresponding Np-O bond lengths of the neptunyl ions has shown that several are about 1.73 Å, some are at about 1.84 Å, and others are at intermediate values. The short and long Np-O bond lengths are indicative of Np(VI) and Np(V), respectively, and the intermediate values suggest averages of these two oxidation states. The presence of two Np oxidation states in Np24 may have important implications for its stability and properties. For example, the crystals containing Np24 are very dark in color, which suggests electron delocalization.

We continue to expand our synthetic effort to produce additional neptunyl peroxide cage clusters. Current efforts are focused on plausible clusters that contain pyrophosphate and oxalate, as extensive uranyl cage clusters containing these ligands have been isolated. We are also interested in determining the extent to which Np(V) or Np(VI) can substitute for uranyl ions in uranyl peroxide cage clusters, as this may have significant implications for the mobility of Np in a nuclear waste repository or in a contaminated subsurface environment.

SOLUBILITY OF UN/UC UNDER AQUEOUS URANYL CLUSTER FORMING CONDITIONS

Sarah Hickam and Peter C. Burns

Department of Civil and Environmental Engineering and Earth Sciences,
University of Notre Dame, 301 Stinson-Remick Hall, Notre Dame, IN 46556, USA

Over the past decade we have developed a family of more than 100 nanoscale uranyl peroxide clusters that spontaneously self-assemble in aqueous solution. Most of these are cage clusters, with both the inner and outer surfaces defined by uranyl ions. These anionic clusters contain as many as 124 uranyl ions, and have diameters in the range of 1.5 to 4.0 nm. They persist in aqueous solution for months, and even remain stable under intense gamma irradiation.

The radiolysis of water by radiation, either natural or anthropogenic, readily causes formation of peroxide that can then combine with uranyl to form cage clusters. The uranyl peroxide minerals studtite and metastudtite clearly demonstrate that natural conditions can cause the formation of sufficient peroxide for precipitation of uranyl peroxide solids. Where water contacts irradiated nuclear fuel, such as following the core-melt accidents that occurred at Fukushima, Japan in 2011, much more peroxide can be expected because of the intense radiation fields. For example, uranyl peroxide minerals have been reported on Chernobyl "lava" that resulted from the 1986 accident in Ukraine.

A fascinating property of uranyl peroxide cage clusters is that they are highly soluble in aqueous solution, much more so than uranyl minerals in general. As such, they may be important in the transport of uranium subsequent to nuclear accidents, as well as in contaminated environments and a geological repository. We are currently interested in understanding the impact of uranyl peroxide clusters in aqueous solution on solid phase solubility. Specifically, we hypothesize that U-based solids may exhibit very high solubilities under conditions that permit the formation of uranyl peroxide cage clusters in contacting solution.

We are currently examining the solubility of UN, a possible nuclear fuel form for future-generation reactors, in aqueous solutions. It has previously been demonstrated that UN can be dissolved in concentrated nitric acid. We hypothesize that its dissolution will be significant in aqueous solution under mildly alkaline conditions in the presence of peroxide, which will facilitate formation of cage clusters.

We have obtained well-characterized UN from Los Alamos National Laboratory, and are commencing a series of studies of its aqueous solubility. Measurements will be conducted for several different solution pH values, both in the presence and absence of peroxide. Cage clusters that form in the aqueous solution will be characterized by electrospray ionization mass spectrometry, and inductively coupled mass spectrometry will be used to measure the concentration of U and other ions in solutions that contact the UN. Concentrations for aqueous solutions in contact with UN with and without peroxide will provide for a direct comparison of solubility under cluster-forming conditions and in the absence of clusters. Various quantities of peroxide will be used to determine conditions of maximum dissolution, as peroxide will serve both as an oxidant for uranium and a cluster-forming agent.

COMPLEXATION OF F-ELEMENTS WITH HUMIC CARRIERS –
HOW DYNAMIC IS THE EQUILIBRIUM ?

H. Lippold, J. Lippmann-Pipke

Helmholtz-Zentrum Dresden – Rossendorf, Institute of Resource Ecology, 04318 Leipzig, Germany

In the far-field of a repository, complexation with dissolved humic matter can be crucial in controlling the mobility of actinides in case of their release [1, 2]. For transport modeling, all interactions in the system metal / humic substance / solid surface are presumed to be dynamic equilibrium processes where association and dissociation run permanently. For metal-humic complexes, however, there are indications of a growing resistance to dissociation over time [3-7]. It is thus questionable whether full reversibility is actually given for this interaction. So far, the existence of a dynamic equilibrium has never been proven. In this study, the isotope exchange principle was employed to gain direct insight into the inner dynamics of the complexation equilibrium, including kinetic stabilization phenomena.

Purified humic acids were contacted with terbium(III) as an analogue of trivalent actinides. The systems contained the radioisotope ^{160}Tb at a very small amount, whereas concentrations of non-radioactive ^{159}Tb were varied at a high level, covering a binding isotherm up to the state of saturation. Owing to the high metal loads, flocculation of humic colloids generates a solid-liquid system where adsorbed amounts of ^{160}Tb can be determined by radiometric analysis of the supernatant. ^{159}Tb and ^{160}Tb were introduced simultaneously or consecutively (^{159}Tb followed by ^{160}Tb or vice versa). Contact times with both isotopes were varied within a range of 3 months.

In a first series of experiments, ^{160}Tb was contacted with humic acid that had been pre-equilibrated with ^{159}Tb at a range of concentrations. Adsorbed amounts of ^{160}Tb were found to be equal to those obtained if both isotopes were introduced at the same time, i.e., the radioisotope represented the solid-liquid distribution of total Tb throughout the binding isotherm, including the plateau region where all available binding sites are occupied. Obviously, there is a permanent exchange of free and humic-bound Tb – evidence of a dynamic equilibrium. The rate of exchange was very high, regardless of how long ^{159}Tb and humic acid had been in contact prior to the addition of ^{160}Tb. There were no indications of stabilization processes.

Completely different results were obtained if the small amount of ^{160}Tb (strictly, $[^{160}Tb]Tb$) was added first, followed by saturation with non-radioactive ^{159}Tb. For representing the solid-liquid distribution of total Tb in a dynamic equilibrium, the radioisotope was expected to be partly desorbed since the bound fraction of total Tb is lower in the plateau region of the binding isotherm. Desorption occurred in fact (Fig. 1a), but at much lower rates than those observed for the equilibration process in the reverse procedure. Moreover, the rates proved to be dependent on the time of pre-equilibration with ^{160}Tb (increasing hindrance of desorption, Fig. 1b). The existence of kinetic stabilization processes was thus substantiated. Evidently, they are confined to the most reactive sites, occupied by the radiolabeled fraction of Tb.

Fitting the time-dependent course of isotope exchange according to first-order kinetics was only successful if at least two components with different rate constants were assumed, suggesting that the very small fraction of sites occupied by $[^{160}Tb]Tb$ ($\sim 1/10^6$) is still only partly affected by the slow exchange kinetics ($\sim 1/3$ slow component). Nonetheless, this is of relevance since just such extremely low metal loads are to be considered. Extrapolating the fits indicates that it takes up to 2 years until equilibrium is attained. This is, however, a short period compared to the time scale to be covered in predictive transport models. Very low flow velocities must be taken into account. Therefore, metal exchange between humic carriers and mineral surfaces cannot be neglected, notwithstanding the observed stabilization process since complexation is not restricted in its reversibility.
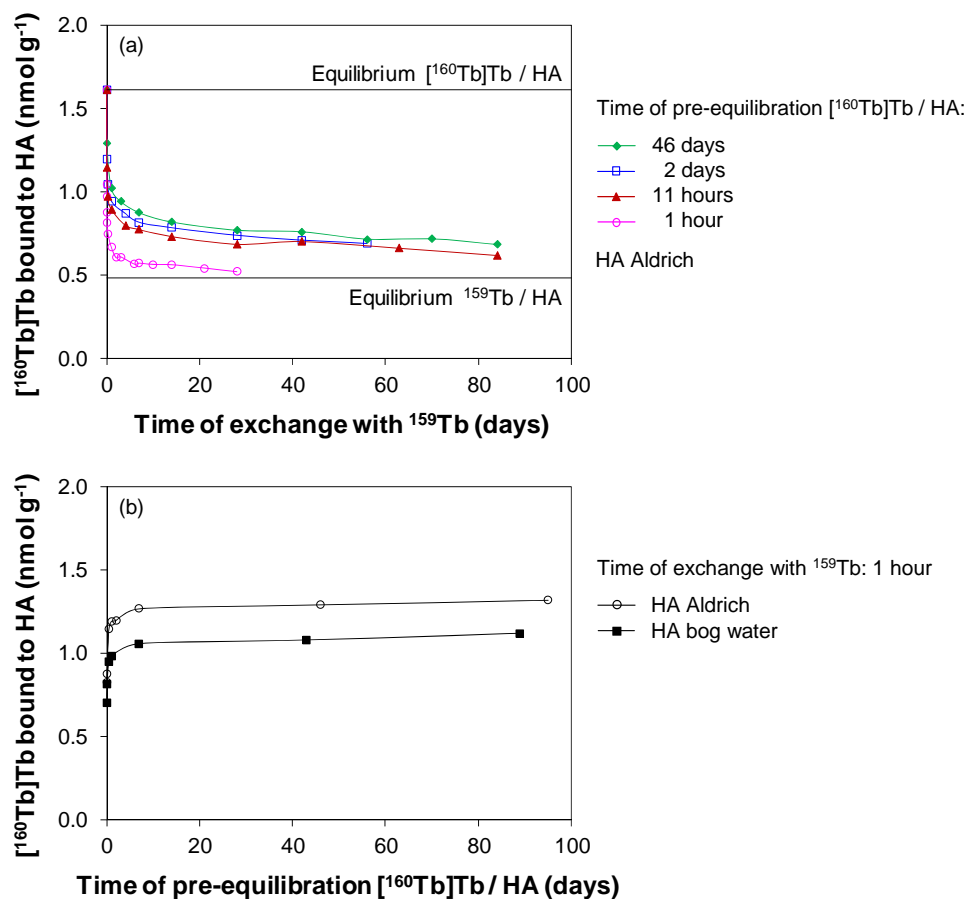
Figure 1. Amount of [160Tb]Tb bound to humic acids (HA) after saturating with non-radioactive 159Tb, shown as a function of exchange time for different pre-equilibration times (a) and as a function of pre-equilibration time for a fixed exchange time of 1 hour (b) (1 nM [160Tb]Tb, 2 mM 159Tb, 0.5 g L^{-1} HA, 0.1 M NaClO$_4$, pH 4.0).

[1] K. H. Lieser et al., Radiochim. Acta 49, 83 (1990).
[2] G. R. Choppin, Radiochim. Acta 58/59, 113 (1992).
[3] L. Rao et al., Radiochim. Acta 66/67, 141 (1994).
[4] R. Artinger et al., J. Contam. Hydrol. 35, 261 (1998).
[5] S. J. King et al., Phys. Chem. Chem. Phys. 3, 2080 (2001).
[6] H. Geckeis et al., Environ. Sci. Technol. 36, 2946 (2002).
[7] H. Lippold et al., Appl. Geochem. 27, 250 (2012).

A NOVEL COF MATERIAL CONTAINING C-C TRIPLE BONDS: SYNTHESIS AND APPLICATION AS A SELECTIVE SOLID-PHASE EXTRACTANT FOR SEPARATION OF URANIUM

Xiaoyu Yang[(1,2)], Chiyao Bai[(2)], Shoujian Li[(2)]*

[(1)] *Beijing National Laboratory for Molecular Science, Radiochemistry & Radiation Chemistry Key Laboratory for Fundamental Science, College of Chemistry and Molecular Engineering, Peking University, Beijing 100871, P.R. China*
[(2)]*Department of Chemistry, Sichuan University, Jiuyanqiao Wangjiang Road, Chengdu 610064, PR China*
Author for correspondence sjli000616@163.com

With the rapid development of nuclear energy, the reprocessing of spent nuclear fuel has become an important activity. Separation and recovery of uranium from various uranium-containing aqueous systems are of great scientific and practical significance, not only in reutilization of uranium resources and sustainable development of nuclear energy, but also for protection of both human health and ecological security. To extract uranium efficiently, high selectivity and large adsorption capacity are needed for the material and method. Compared with traditional method, solid-phase extraction (SPE) has its advantages including higher enrichment factors, low consumption of reagents (especially organic solvent), minimal secondary waste generation and so on [1]. A solid phase extractant usually consists two parts, the solid phase matrix and the functional component. Commonly used solid-phase matrices include Al_2O_3, SiO_2, polymer resin, or diatomaceous earth. Polymer resin and carbonaceous materials exhibit several shortcomings in practical application, such as low surface area, poor performance in high temperataure environments, and low stability in acidic environments or high radiation fields.

For these reasons, covalent organic frameworks (COFs) as a new type of solid-phase extractant matrix are being developed and applied to the separation and enrichment of uranium in simulated spent fuel solution. COFs are a type of porous organic materials which are composed by light elements such as C, H, O, N, or B via strong covalent bonds [2]. Such materials possess the advantages of low density, large surface area, tunable pore size and structure, and high thermal and chemical stability [3].

In this study, a novel COF-based material (COF-Y) containing large amounts of acetylene C-C triple bonds was prepared for the first time by using a simple and effective synthetic method, in which the cheap and commercially available raw materials, propargyl alcohol, and triethylamine. The three step preparation of the solid-phase extractant is illustrated in Scheme 1. In the first step, 2,4-hexadiyne-1,6-diol is synthesized from propargyl alcohol in air based on simple Glaser Coupling reaction with the alkali triethylamine, tetramethylethylenediamine (TMEDA), and a CuI catalyst. In the second step, 2, 4-hexadiyne-1,6 -diol and trimesoyl chloride undergo a condensation reaction with triethylamine (to capture acid) in an ice water bath to produce the COF-Y. In a final step, oxidizing agents including $KMnO_4$ and H_2O_2 were used to add additional oxygen atoms to COF-Y.
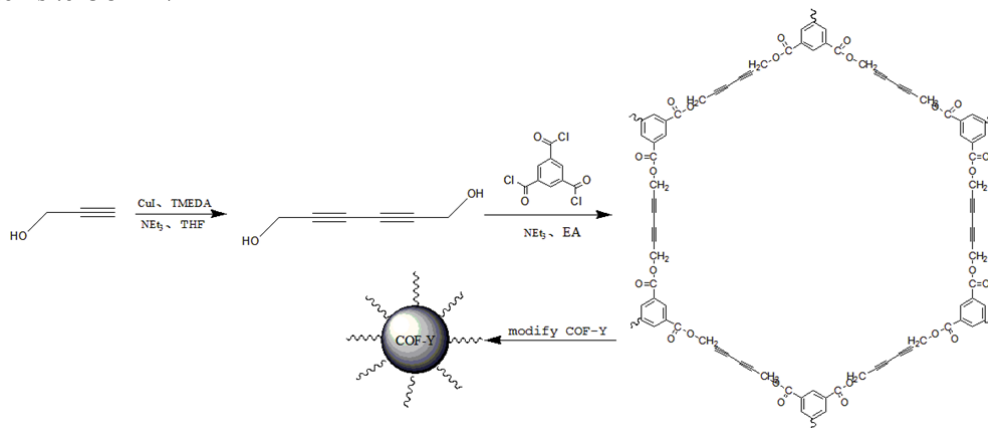
Scheme 1. Schematic illustration of the preparation of COF-Y

FT-IR spectroscopy shows characteristic bands at 1740 cm^{-1} attributed to an ester C=O bond, and 2150 cm^{-1} assigned to the C-C triple bond of the acetylene unit. SEM images of COF-Y clearly show a large number of spherical nanoparticles.

To evaluate the sorption selectivity of COF-Y for uranium, sorption experiments were performed in a simulated nuclear industrial effluent containing the uranyl ion and 11 additional undesired cations (Figure 1). In the presence of competing cations, the total sorption capacity of COF-Y is 0.91 mmol g^{-1} for all ions, the sorption capacity for UO_2^{2+} reaches 0.27 mmol g^{-1} and is 29.68% of the total sorption amount.
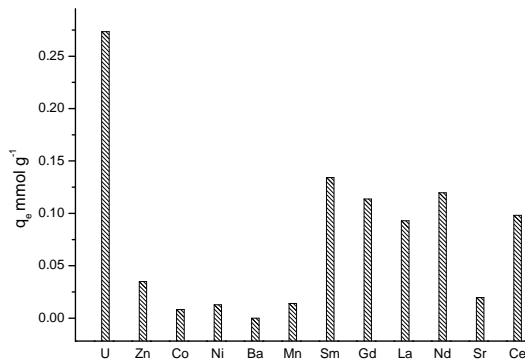
Figure 1. Competitive adsorption capacities of coexistent ions on COF-Y
($C_0 \approx 100$ mg L^{-1}, pH = 4.5, t = 120 min, V = 25 mL, T = 298.15 K, and w = 10 mg)

The batch sorption experiments demonstrate that the sorption of uranium by COF-Y is rapid and efficient. The method of synthesizing COF-Y material provides another choice for preparation of solid phase extractant that possesses the ability of selective sorption for uranium and other metal ions.

[1] Y.S. Zhao, C.X. Liu, M. Feng, et al. J. Hazard. Mater. 176 (2010) 119–124.
[2] A. Thomas, Angew. Chem. Int. Ed. 49 (2010) 8328–8344.
[3] A.P. Cote, A.I. Benin, N.W. Ockwig, O.M. Yaghi, et al. Science. 310 (2005) 1166–1170.

URANYL COMPOUNDS TEMPLATED BY PROTONATED AMINES: SYNTHESIS, STRUCTURES, AND PROPERTIES

X. L. Qiao, Q. Q. Zhu, L. H. Wang, C. L. Liu*

[1] *Beijing National Laboratory for Molecular Sciences, Radiochemistry & Radiation*
[2] *Chemistry Key Laboratory for Fundamental Science, College of Chemistry and Molecular Engineering, Peking University, Beijing 100871, China*

In the last two decades metal−organic frameworks (MOFs) have been extensively studied due to their very wide spectrum of properties, functionalities, and possible applications[1]. In uranyl bearing hybrid materials` research area, there is an emerging realization that MOFs can display diversity in their physical properties and critical phenomena or phase transitions, probably as rich as that in traditional materials. We noted that cations of alkaline and alkaline-earth metals and small protonated ammoniums have been investigated[2]. The introduction of protonated amines can fill the gaps, balance charges, and form a large hydrogen bonding network with the host molecules, thereby stabilizing the structure. Moreover, it may play a guiding role in the process of structure formation of the crystal. Protonated amines have rarely been explored in uranyl−oxalate/formate systems, though they have been used as templates in constructing uranyl phosphates[3] and some other uranium−organic frameworks recently[4]. Our group have devoted to the systematic study of uranyl compounds templated by protonated amines in the two areas, in order to explore their structures and properties, which could indicate their potential applications. We have performed the study on the systems of ammonium uranyl oxalates/formates. The combination of these building blocks, ammoniums, uranyl and oxalate/formate, yielded crystalline solids consisting of mono-/di- nuclear, chains, and sheets of uranyl oxalate/formate anions, templated by ammonium cations. The compounds displayed structural diversity, various packing patterns and a plenty of hydrogen bonding motifs involving cations, anions and lattice water.

Crystal-to-crystal transformations contain the structural alternations, which are of significant potential in applications in nuclear waste management[5], ion-exchange[6,3b], ionic conductivity[7], photochemistry[3], and so on. In our researches, the two systems of $[dabcoH_2]^{2+}/[pipH_2]^{2+}$−uranyl−oxalate, where $[dabcoH_2]^{2+}$ is the cation of doubly protonated 1,4-diazabicyclo-[2.2.2]-octane (dabco) and $[pipH_2]^{2+}$ the doubly protonated piperazine (pip), each having two crystalline products, showed similar and reversible crystal-to-crystal transformations between the two product crystals controlled by the ratio of reactants or building blocks in aqueous solutions(figure1,a) [8]. The four compounds in pairs are $[dabcoH_2][UO_2(C_2O_4)_2(H_2O)]\cdot2H_2O$ (dabco1) and $[dabcoH_2][(UO_2)_2(C_2O_4)_3(H_2O)_2]\cdot2H_2O$ (dabco2), and $[pipH_2][UO_2(C_2O_4)_2(H_2O)]\cdot4H_2O$ (pip1) and $[pipH_2][(UO_2)_2(C_2O_4)_3(H_2O)_2]\cdot2H_2O$ (pip2). Besides the cations and lattice water, dabco1 and pip1 contain mononuclear anions of $[UO_2(C_2O_4)_2(H_2O)]^{2-}$, whereas dabco2 and pip2 possess dinuclear anions of $[(UO_2)_2(C_2O_4)_3(H_2O)_2]^{2-}$, and in all structures, the uranium ion shows a pentagonal bipyramid environment made up of equatorial oxalate, water, and apical oxygen.

The ammonium metal formate frameworks (AMFFs), being a class of MOFs, exhibit unique dielectric and ferro-/antiferro-electricities (DE/FE/AFE) properties, which could coexist or combine with other properties such as magnetism[9]. We obtained an ammonium uranyl formate framework of formula $[(C_2H_5)_4N][U_2O_4(HCOO)_5]$, prepared by using components of tetraethylammonium, uranyl, and formate[10]. The compound possesses a layered structure of anionic uranyl−formate wavy sheets and intercalated $(C_2H_5)_4N^+$ cations. The sheet consists of pentagonal bipyramidal uranyl cations connected by equatorial anti−anti and anti−syn $HCOO^-$ bridges, and it has a topology of $3^3\cdot4^3\cdot5^4$ made of edge-sharing square and triangle grids. It underwent a para-electric (PE) to FE transition at ~200 K, with the lattice symmetry changed from high-temperature (HT) tetragonal P$\bar{4}$21m to low-temperature (LT) monoclinic P21, caused by the freezing of the flip motion of a disordered formate ligand and the related shift of the cation with respect to the anionic sheets(figure1,b). VT luminescent spectroscopy, differential scanning calorimetry (DSC), and dielectric studies characterized the phase transition, and the structure−property relationship was established.
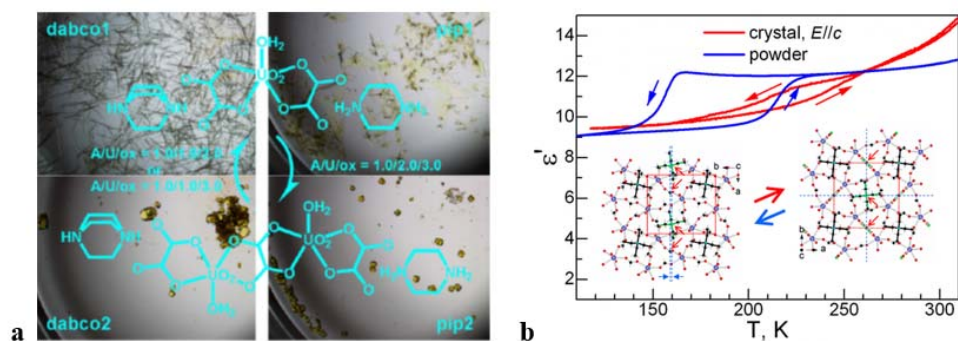
Figure1. a: Morphologies of crystals of the four compounds, dabco1, dabco2, pip1, and pip2, and the transformations controlled by the A/U/ox ratio; b: Temperature-dependent traces of the dielectric permittivities: crystal capacitor with the applied E∥c and powder capacitor.

[1] (a) H.C. Zhou, et al., Chem. Rev. 112, 673(2012); (b) A. B. Cairns, A. L. Goodwin, Chem. Soc. Rev. 42, 4881(2013).
[2] Cambridge Structural Database, Version 5.33; Cambridge Crystallographic Data Centre: Cambridge, U.K., 2012.
[3] (a) P. O. Adelani, et al., Cryst. Growth Des. 11, 3072(2011); (b) W. T. Yang, Inorg. Chem. 51, 11458(2012).
[4] M. B. Andews, C. L. Cahill, Chem. Rev. 113, 1121(2013).
[5] (a) P. C. Burns, et al., Science, 335,1184(2012); (b) C. R. Armstrong, et al., Proc. Natl. Acad. Sci. U.S.A. 109,1874(2012).
[6] (a) P. O. Adelani, T. E. Albrecht-Schmitt, Angew. Chem., Int. Ed. 49, 8909(2010); (b) P. O. Adelani, T. E. Albrecht-Schmitt, Inorg. Chem. 50, 12184(2011).
[7] D. Grohol, et al., Inorg. Chem. 35, 5264(1996).
[8] L. H. Wang, et al., Cryst. Growth Des. 13, 2597(2013).
[9] (a) S. Chen, et al., Inorg. Chem. Front. 1, 83(2014); (b) W. Li, et al., Chem. Soc. 134, 11940(2012).
[10] Q. Q. Zhu, et al., Inorg. Chem. 53, 8708(2014).

EFFECTS OF ORGANIC ADDITIVES ON THE SORPTION AND MOBILITY OF RADIONUCLIDES IN CEMENTITIOUS MATERIALS: EXPERIMENTAL DETERMINATION AND COMPUTATIONAL MOLECULAR MODELING

I. Androniuk[1)], C. Landesman[1)], A. G. Kalinichev[1)], P. Henocq[2)]

[1)]*Laboratoire Subatech (UMR 6457), Ecole des Mines de Nantes,*
4 rue Alfred Kastler, BP 20722, 44307 Nantes cedex 03, France.
[2)]*ANDRA – Agence nationale pour la gestion des déchets radioactifs,*
1-7, rue Jean-Monnet, 92298 Châtenay-Malabry cedex, France.

Cementitious materials are extensively used in the design and construction of radioactive waste repositories in the last decades due to their high barrier and immobilization properties. One of the ways to enhance the durability, porosity and workability of cement is to introduce various types of organic admixtures into the structure (0.1-2% wt). However, the presence of organic matter in the cement pore water can influence the radionuclide mobility: organic molecules can form water-soluble complexes and compete for sorption sites at the cement surface. Our study is designed to get detailed understanding of the mechanisms of such interaction on the molecular level.

The investigated model cement system has three components. First, synthetic pure C-S-H phases with different C/S ratios: 0.83; 1.0; 1.4 (models for cement degradation steps) were chosen as a representative material in this project. Secondly, gluconate is chosen as an organic additive model as a simple well-described molecule stable in highly alkaline solutions. The third component, U (VI), is a representative of the actinide series. Previous studies [e.g., 1-2] were focused mostly on the influence of admixtures on hydration processes, while much less efforts were made [e.g., 3-5] to understand and explain their postproduction effects for radioactive waste storage applications. The development of quantitative description of these effects on the molecular scale is the primary objective of the project.

Study on binary systems (C-S-H/gluconate, HCP/gluconate [4], C-S-H/U (VI) [6]) provides basic reference data for the investigation of more complex ternary system (C-S-H/gluconate/U (VI)). The interactions between model components are studied by means of different experimental techniques and computational molecular modeling approaches. The composition of the solid phase is determined through elemental analysis (ion chromatography, ICP-MS) and pH measurements of the equilibrated solution. The data on sorption and desorption kinetics and isotherms for gluconate and for U (VI) on C-S-H with different C/S ratios (0.83, 1.0, 1.4) are presented in this work. There is a noticeable influence of C/S on gluconate sorption: it sorbs better on C-S-H with higher C/S ratio. Gluconate labeled with ^{14}C was used to improve the sensitivity of analytical detection techniques (scintillation liquid counting) for low concentration range (10^{-8} mol/l – 10^{-5} mol/l). In parallel, atomistic models are developed for Ca^{2+}/gluconate and UO_2^{2+}/gluconate aqueous solutions, corresponding to different pH values (concentration of OH^-) in the bulk liquid phase and on the surface of several C-S-H phases. Structural, energetic, and dynamic aspects of the sorption processes on surface of cement are quantitatively modeled by molecular dynamics technique, following the previously developed approaches [7].

Gluconate molecule is a good starting model for investigation of interaction mechanisms on molecular scale. More complex system involving polycarboxylate superplasticizer (PCE) instead of gluconate will be studied as a next step. This comb-shaped polymer with adsorbing anionic backbone and nonadsorbing side chains is a representative of a typical industrial admixture. PCE labeled with ^{14}C will be used to study interactions at low concentrations.

[1] Lesage, K. et al. Adv. in Cem. Res. art.nr. DOI: 10.1680/adcr.13.00087 (2014).
[2] Zingg, A. et al. J. of Coll. and Int. Science 323, 301-312 (2008).
[3] Wieland, E. et al. App. Geochem. 19, 119-135 (2004).
[4] Glaus, M.A.; Van Loon, L.R. PSI Bericht Nr. 04-02 (2004).
[5] Ferrari, L. et al. J. of Coll. and Int. Science 347, 15-24 (2010).
[6] Tits, J. et al. Dalton Transact. 44, 966-976 (2015).
[7] Kalinichev, A.G. et al. Cem. and Conc. Res. 37, 337-347 (2007).

LOADING EFFECT ON Eu(III) BINDING TO GROUNDWATER HUMIC ACID: APPLICATION OF NICA-DONNAN MODEL

M. Terashima[1]*, T. Saito[2], T. Ishii[3], Y. Akagi[3], Y. Tachi[1]

[1]*Radioactive Waste Processing and Disposal Research Department, Japan Atomic Energy Agency (JAEA),4-33 Muramatsu, Tokai, Ibaraki, 319-1194, Japan*
[2] *Advanced Science Research Center, Japan Atomic Energy Agency (JAEA), 2-4 Shirakata Shirane, Tokai, Ibaraki, 319-1195, Japan*
[3]*Energy Project & Technology Center, Mitsubishi Materials Corporation, 1002-14 Mukohyama, Naka, Ibaraki, 311-0102, Japan*

To enhance credibility for the long-term performance of geological disposal system for high-level radioactive waste, uncertainty analyses for key uncertainties related to radionuclide migration in natural barrier and their application to in-situ condition are important issues. Because natural organic matter such as humic substances (HS) in groundwater is one of such uncertainties, its effect on the migration of radionuclides in natural barrier needs to be assessed quantitatively. Modeling of radionuclide bindings to HS in groundwater is essential for the assessment. The Non-Ideal Competitive Adsorption (NICA)-Donnan model of which generic parameters have been developed [1, 2] is one of the most useful models for modeling of metal-ion bindings by HS in a variety of solution conditions. However, it is not always true that such model can be useful for all HS, because most of generic parameters have been developed for HSs from soil and river, which have metal binding characteristics different from groundwater HS [3]. On the other hand, it is known that the binding affinity can enhance with reducing loading level (i.e., concentration ratio of metal ion and binding site of HS), due to heterogeneity of binding sites in HS [4]. This loading effect is important for modeling radionuclide bindings to HS in groundwater, in which concentration of radionuclides can be low due to their solubility limits. However, understanding of applicability of the NICA-Donnan model to modeling of radionuclide bindings by groundwater HS at low loading level is currently incomplete. In this study, the Eu^{3+} binding to humic acid (HA) isolated from deep groundwater (depth -250 m) in Horonobe URL site, Hokkaido, Japan, were evaluated at low loading level using the solvent extraction method [5,6], and were then compared with calculation values derived by the NICA-Donnan model with generic or specific binding parameters.

Apparent formation constant ( ), which were evaluated by the solvent extraction method, was converted into distribution coefficient, due to direct comparison between experiment and calculation. A logarithmic distribution coefficient of Eu^{3+} to the groundwater HA ($\log K_{HA\_Eu}$), which was obtained from the experiment, was linearly increased with reducing the loading level. Comparison of these experimental values with the calculation values derived by using the generic parameters showed that the calculation values were 3 to 4 times larger than the experimental values. However, the $\log K_{HA\_Eu}$ values calculated using the specific parameters in bindings of H^+ and Eu^{3+} well interpreted the experiments. These confirm that, for the groundwater HS, the specific parameters are necessary for the realistic modeling. On the other hand, the $\log K_{HA\_Eu}$ value at the lowest level (1.8×10^{-5}), which was calculated using the specific parameters, was one order of magnitude higher than the experimental value. As binding sites at each loading level were characterized by analysis using the NICA-Donnan model, 99.9% of Eu^{3+} was bound to hydroxyl type sites of HA whereas carboxyl groups of HS acted as a binding site in a dominant fashion at higher loading level. This indicates that the specific binding parameters for hydroxyl type sites could be overestimated. Thus, at low loading level, the NICA-Donnan model parameters might need to be improved for more realistic modeling of radionuclide binding by groundwater HS.

[1] C.J. Milne, et al., Environ. Sci. Technol. 35, 2049 (2001). [2] C.J. Milne, et al., Environ. Sci. Technol. 37, 958 (2002). [3] M. Terashima, et al., J. Nucl. Sci. Technol. 49, 804 (2012). [4] R. Marsac, et al., Geochim. Cosmochim. Acta 74, 1749 (2010). [5] T. Kubota, et al., Radiochim. Acta 90, 569 (2002). [6] T. Sasaki, et al., Am. J. Anal. Chem. 3, 462 (2012).

THE THERMODYNAMICS OF THE COMPLEXATION OF Cm(III) WITH CHLORIDE IN ALKALINE AND EARTH-ALKALINE SOLUTIONS AT ELEVATED TEMPERATURES

C. Koke[1),2)], A. Skerencak-Frech[1),2)], P.J. Panak[1),2)]

[1)] *Institut für Nukleare Entsorgung, Karlsruher Institut für Technologie, 76021 Karlsruhe, Germany*
[2)] *Physikalisch-Chemisches Institut, Universität Heidelberg, 69120 Heidelberg, Germany*

The long-term safety assessment of a nuclear waste repository in deep geological formations requires a well-founded thermodynamic description of the processes relevant for the migration and retention of the actinides. In the past, a broad variety of complexation reactions of actinides in their most important oxidation states were studied. The stability constants (log β^0_n) and the thermodynamic data ($\Delta_r H^0_m$, $\Delta_r S^0_m$) are listed in thermodynamic databases.[1] However, the majority of this data is valid only for 25°C. Due to the radioactive decay, temperatures above 25°C are expected in the near field of a repository for high level nuclear waste. These conditions will have a distinct impact on the geochemistry of the actinides. Thus, thermodynamic data for the actinides at T ≥ 25°C is of high importance for a comprehensive long-term safety assessment. Besides clay and granite, rock salt formations are considered as potential host rocks for a nuclear waste repository due to their high heat conductivity and gas retention. In the accident scenario of water intrusion into the repository, salt brines with high concentrations of chloride are expected. Only little information is available on the complexation of trivalent actinides with Cl⁻ at high salinity and increased temperature. Thus, in the present work the thermodynamics of Cm(III) chloride complexes are investigated by time resolved laser fluorescence spectroscopy in diluted to saturated solutions of LiCl, NaCl, CaCl₂ and MgCl₂ at T = 20 to 200 °C.

The molar fractions of the various Cm(III) chloride complexes are determined as a function of T and Cl⁻ by peak deconvolution of the emission spectra. As an example, the speciation of Cm(III) in LiCl solution is displayed in figure 1 as a function of [Cl⁻]$_{total}$ at T = 20 and 100 °C.
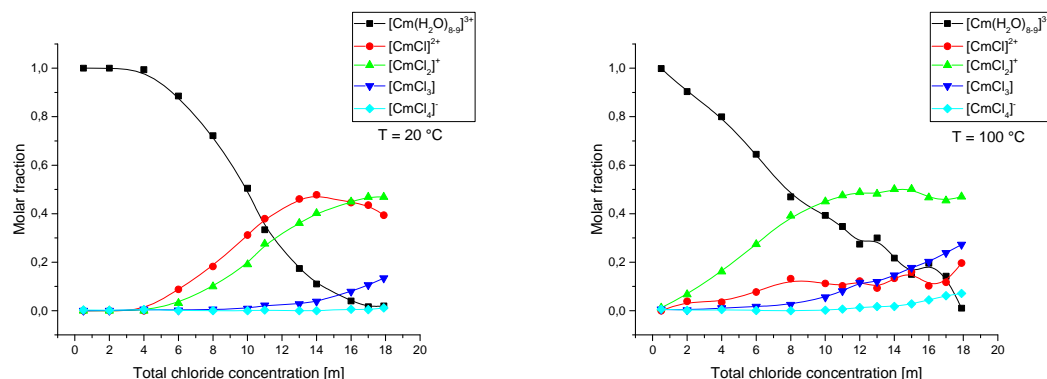
Fig. 1: Molar fractions of [CmCl$_n$]$^{3-n}$ in aqueous LiCl solution (c_m(LiCl) = 0.5 to 17.9 m) at 20 and 100 °C.

At 25°C, no Cm(III) chloride complexes are present at [Cl⁻] < 4.0. At higher chloride concentration the [Cm(Cl)]$^{2+}$ and [Cm(Cl)₂]$^+$ complexes are formed, being the dominate species at [Cl⁻] > 11 m. Additionally, a small fraction of the [Cm(Cl)₃] is present at very high [Cl⁻]. At increased temperatures the Cm(III) chloride complexes start to form at distinctively lower Cl⁻ concentrations. In particular, the formation of the [Cm(Cl)₂]$^+$ complex is fostered at higher temperatures, while the [Cm(Cl)]$^{2+}$ and [Cm(Cl)₃] complexes are only minor species. Additionally, a [Cm(Cl)₄]⁻ complex, which is not observed at ambient temperatures, forms at very high [Cl-] and T. Using the specific ion-interaction theory (SIT) the conditional log $\beta'_2(T)$ are fitted in the range of I_m < 6.0 m, yielding log $\beta^0_2(T)$ and $\Delta\varepsilon_{02}$. To fit the data over the entire studied ionic strength range, the Pitzer model is applied to determine the thermodynamic stability constants of all Cm(III) chloride complexes as well as the cationic and neutral interaction parameters for Cm^{III}/M (M = Li, Mg, Ca) in the respective alkaline and earth-alkaline media. The temperature-dependency of the log $\beta^0_n(T)$ is fitted by Van't-Hoff-based regression and the thermodynamic functions ($\Delta_r H^0_m$, $\Delta_r S^0_m$, $\Delta_r C^0_{p,m}$) are determined. The results show positive values for the standard reaction enthalpies and entropies of the different [CmCl$_n$]$^{3-n}$ complexes, indicating entropy driven complex formation. The herein determined log $\beta^0_n(T)$, and $\Delta_r H^0_m$, $\Delta_r S^0_m$, $\Delta_r C^0_{p,m}$ are in good agreement with previously published data.[2,3] Also, the log $\beta_n(T)$ correspond values of various Ln(III) chloride complexes.[4,5]

This paper provides a detailed spectroscopic and thermodynamic study on the formation of Cm(III) chloride complexes in various saturated saline media over a very large temperature range. The present work elaborates

on previous basic studies and shows that increased temperature will have a distinct impact on the geochemical behaviour of trivalent actinides. Ligands which form only weak complexes at ambient temperatures may increase strongly in their complexation strength at higher temperatures. The present results contribute to a better understanding of the geochemistry of trivalent actinides in saline brines and allow for a better estimation of their behaviour in naturally occurring (e.g. NaCl) and geotechnical employed (brucite/$MgCl_2$) highly concentrated chloride brines at high temperatures. Thus, the herein determined thermodynamic data is an integral part for a comprehensive long-term safety assessment of a salt rock based nuclear waste repository for heat-producing waste.

[1] R. Guillaumont, T. Fanghänel, J. Fuger, I. Grenthe, V. Neck, D. A. Palmer, M. H. Rand, *Update on the Chemical Thermodynamics of Uranium, Neptunium, Plutonium, Americium and Technetium*, Nuclear Energy Agency, North Holland Elsevier Science Publishers B.V., Amsterdam, The Netherlands, **2003**.

[2] M. Arisaka, T. Kimura, R. Nagaishi, Z. Yoshida, *Journal of Alloys and Compounds* **2006**, *408-412*, 1307.

[3] A. Skerencak-Frech, D. R. Fröhlich, J. Rothe, K. Dardenne, P. J. Panak, *Inorganic chemistry* **2014**, *53*, 1062.

[4] C.H. Gammons, S.A. Wood, A.E. Williams-Jones, *Geochimica Acta* **1996**, *23*, 4615.

[5] S.A. Stepanchikova, G.R. Kolonin, Russian *Journal of Coordination Chemistry* **2005**, *31*, 207.

EXAFS STUDY OF $K_4Th(C_2O_4)_4$ AND $Th(C_2O_4)_2$

Ashwani Kumar[1], A.K.Yadav[2], D.Bhattacharya[2], S.N.Jha[2] and B.S.Tomar[1]

[1]*Radioanalytical Chemistry Division,* [2]*Atomic and Molecular Physics Division,*
Bhabha Atomic Research Centre, Mumbai 400085

Complexation of actinides by anions present in ground water is one of the pathways for their migration. Thorium can be used as an analogue for tetravalent actinides, such as Pu(IV), while oxalic acid is one of the common anions present in ground water. In the present work Extended X-ray Absorption Fine Structure (EXAFS) has been used to study thy molecular structure of solid compounds formed between Th(IV) and oxalate. Depending upon the experimental conditions, Th(IV) can be precipitated as thorium oxalate ($Th(C_2O_4)_2$) or potassium thorium oxalate ($K_4Th(C_2O_4)_4$). Polycrystalline compounds were prepared following the procedures given in the literature [1]. EXAFS measurements were carried out at the Energy-Scanning EXAFS beamline (BL-9) in transmission mode at the INDUS-2 Synchrotron Source (2.5 GeV, 100 mA) at RRCAT, Indore, India [2]. Samples of appropriate weight, estimated to obtain a reasonable edge jump were taken in powder form and mixed thoroughly with cellulose powder to prepare homogenous pellets of 15 mm diameter.

Figure1 shows the normalised EXAFS spectra of $K_4Th(C_2O_4)_4$ and $Th(C_2O_4)_2$ at the Th L3-edge. L_3 edges are assigned to the $2p_{3/2}$ to 6d electric dipolar transition with a strong white line peak due to empty 6d states. The enlarged portion of white line is shown in inset of the figure 1. The peak intensity of white line is higher in $K_4Th(C_2O_4)_4$ than $Th(C_2O_4)_2$. The $\chi(R)$ versus R spectra, generated (Fourier transform range k=3.0-10.0 $Å^{-1}$) from the $\mu(E)$ versus E spectra are shown in figure 2. The first peak in the $\chi(R)$ versus R spectrum of $Th(C_2O_4)_2$ at Th L_3-edge is due to ~10 oxygen atoms (at 2.43 Å) surrounding the Th atom and the small peak after the first main peak is due to 8 carbon atoms at 3.18 Å. However in case of $K_4Th(C_2O_4)_4$, the first peak has contribution of 2 oxygen shells with ~8 oxygen atoms at 2.42 Å and ~2 oxygen atoms at 2.53 Å. It can be seen that the intensity of the second peak is higher in case of $K_4Th(C_2O_4)_4$ than that for $Th(C_2O_4)_2$, which is also reflected in the fitting results that show more carbon atoms in case of the former compound.
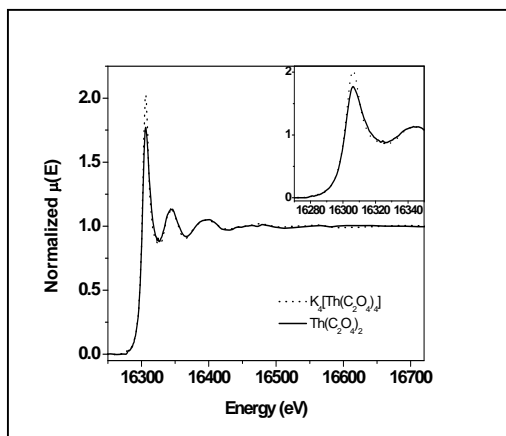
Figure 1. Normalized EXAFS spectra of $Th(C_2O_4)_2$ and $K_4Th(C_2O_4)_4$, at Th L_3

Figure 2. $\chi(R)$ vs R
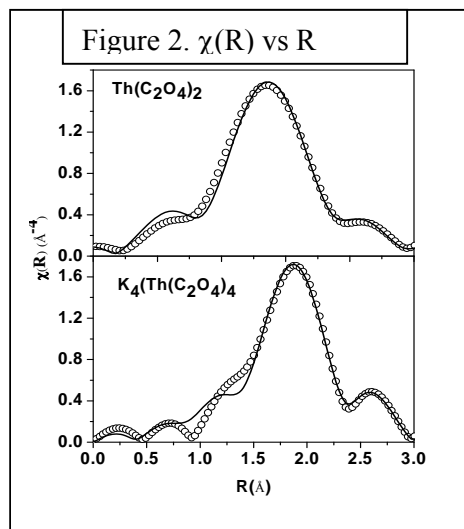
[1] A. Frederic et al., *Inorganic Synthesis*, Vol. 8, Ed. Henry F. Holtzlaw, McGraw Hill Inc., (2007).
[2] S. Basu et al. *J. Phys.: Conf. Ser.,* 493 (2014), 012032.

COMPLEXATION OF NEPTUNYL (NpO_2^+) ION WITH HYDROXAMIC ACIDS IN 0.1 M NaClO₄ MEDIUM

D. Rama Mohana Rao, Neetika Rawat, B. S. Tomar

Radioanalytical Chemistry Division, Bhabha Atomic Research Center, Mumbai – 400085, India

[237]Np is one of the important minor actinides present in high level waste (HLW) generated during the reprocessing of spent nuclear fuel owing to its long half-life ($t_{1/2} = 2.14 \times 10^6$ y) and alpha emitting property. The existence of [237]Np as NpO_2^+, in its most stable (V) oxidation state, reduces its interaction with various geological components thereby increasing its mobility in environment. Migration of Np in environment depends on its interaction with the various natural organic and inorganic ligands. Pyoverdins are a special group of bio-ligands having high affinity for actinides mainly due to the presence of hydroxamate and catechol functional groups in their binding site. In order to understand the interaction of NpO_2^+ with pyoverdines it is necessary to investigate its complexation with selected ligands with relevant functionality, viz., hydroxamic acids of varying structures, as model compounds.

In the present work, the complexation of Np(V) by different hydroxamic acids (HA) namely acetohydroxamic acid (AHA) and Salicylhydroxamic acid (SHA), has been studied specrophotometrically. The f-f transition of NpO_2^+ (982 nm) was monitored to determine the stability constants of its complexes with HAs. In both the cases, the intensity of absorption peak decreases with ligand concentration whereas no shift in λ_{max} was observed (fig 1). As f-f transitions are symmetry forbidden, the decrease in intensity can be related to the increase in symmetry around the Np centre upon complexation whereas constancy of λ_{max} can be attributed to the absence of direct participation of 'N' in metal ion bonding. The analysis of spectrophotometric data reveals the formation of 1:1 and 1:2 complexes in both the cases, while no protonated complex was observed indicating the deprotonation of hydroxyl group during binding with NpO_2^+. The large variation in stability constant of NpO_2^+- AHA and NpO_2^+- SHA (Table 1) cannot be explained on the basis of their basicity (pK_a) thereby suggesting different mode of binding in the two complexes. Owing to the presence of hydroxyl group at ortho position in SHA, NpO_2^+ can possibly interact with hydroxyl group to form seven membered ring. In order to understand the exact structure of these complexes, computational studies on NpO_2^+-HA complexes are in progress.

Table 1. Stability constants (log (β) of Np(V) with hydroxamic acids

Complex	NpO_2^+- AHA (pKa= 8.70)	NpO_2^+- SHA (pKa=9.08)
ML	2.65 ± 0.10	6.48 ± 0.05
ML$_2$	4.70 ± 0.11	9.48 ± 0.12
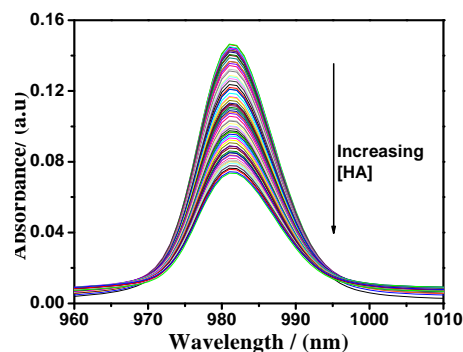
Fig 1. Spectrophotometric titration of NpO_2^+ (3.96×10^{-4} M) with SHA (0.05 M) at pH 4 in 0.1 M NaClO₄)

DETERMINATION OF THE COMPLEXATION ENTHALPY OF HUMIC ACID BY CALORIMETRIC TITRATION

S. Kimuro[(1)], A. Kirishima[(1)], D. Akiyama[(1)], N. Sato[(1)]

[(1)] *Institute of Multidisciplinary Research for Advanced Materials, Tohoku University, 1-1 Katahira, 2-Chome, Sendai 980-8577, Japan*

Humic substances (HS) are heterogeneous mixture of high-molecular-weight organic materials formed by humification of animals, plants and microbes. HS are believed to play an important role in the transportation of cations in environment, and are confirmed to be present even in the deep underground where radioactive wastes are planned to be disposed. While HS have many functional groups in the molecular, carboxyl and phenolic hydroxyl groups interact strongly with variety of metal cations by forming complexes, with heavy metal and actinide ions. Stable HS complexes are formed, which may change the geochemical properties of these ions including mobility, solubility and oxidation states. Therefore HS are expected to affect the migration of radionuclides released from the disposed radioactive waste. Thus, numerous attempts have been carried out to model and describe the interaction of HS with metal cations.

The reaction enthalpy (ΔH) and entropy (ΔS) are fundamental thermodynamic quantities for a discussion of reaction mechanism. However, in terms of interaction of humic acid with cation, only few studies reported these quantities. Most of previous studies reported only equilibrium constants corresponding with Gibbs free energy (ΔG). Besides, the calorimetric titration is a promising technique for the determination of the reaction enthalpy by direct measurement in the solution system. In our previous study, potentiometric titration and calorimetric titration were applied to the reactions of dicarboxylic acids with Uranium (VI) and Europium (III) [1, 2]. Thus, the better understanding of reaction mechanism was achieved by accurate determination of ΔG, ΔH, and ΔS by calorimetric titration technique. For this reason, we applied calorimetric titration technique to the interaction of humic acid with Copper (II) ion. It is commonly recognized that copper exists in deep groundwater. Thus, the binding of copper ion to HS become the competitive reaction between the binding actinide ions to HS. In addition, copper ion concentration in the solution system can be precisely measured by potentiometric titration using a copper ion selective electrode. Hence, many researchers have investigated the availability of complexation model to the interaction of HS with copper. However, there is no study which determined ΔH and ΔS in various pH and the ionic strength by direct method using calorimetric titration technique. Therefore, the purpose of this study is to achieve the accurate determination of ΔG, ΔH and ΔS in the protonation and the complexation of humic acid by combination of the equilibrium model, potentiometric titration and calorimetric titration. Furthermore, the reaction mechanism is discussed from the consideration of obtained thermodynamic quantities.

Two kinds of humic acids were investigated in this study, they are, Elliot Soil and Waskish Peat purchased from IHSS (International Humic Substances Society). Additionally, polyacrylic acid (PAA) was chosen as chemical analog of polyelectrolyte. The apparent protonation constant and the apparent complexation constant were determined by potentiometry. Our previous study reported that the logarithm of the apparent protonation constant and complexation constant are described by the following equations [3].

$$\log K_{i,app}^{p} = \log K_{pi} + m_{pi}pcH - b_{p}\log[Na^{+}] \quad (1)$$

$$\log K_{app}^{c} = \log K_{c} + a_{c}\log\alpha - b_{c}\log[Na^{+}] - m_{c}\log[M] \quad (2)$$

Where pcH is the negative logarithm of the absolute hydrogen ion concentration, $[Na^{+}]$ is the bulk sodium ion concentration in the background electrolyte solution, which is equal to the ionic strength of the back ground solution, [ML] and [M] are the concentrations of bound and free metal ions, and α is the degree of dissociation of the functional groups in HS. The two groups of apparent protonation constants, $K_{1,app}^{p}$ and $K_{2,app}^{p}$, were employed for the protonation of carboxyl and phenolic hydroxyl groups, respectively. The $\log K_{pi}$, m_{pi}, b_{p}, $\log K_{c}$, a_{c}, b_{c}, and m_{c} are characteristic constant parameters of the cation and HS.

Then, the reaction heat of de-protonation and complexation were measured by iso-thermal titration calorimeter (TAM-III) to determine the protonation enthalpy and the complexation enthalpy. The protonation enthalpy was calculated by fitting the following equation (3), and the complexation enthalpy was calculated by fitting the equation (4).

$$dQ_i = \Delta H_p\left(\nu_i^{HR} - \nu_{i-1}^{HR}\right) + \Delta H_{OH^-}\left(\nu_i^{OH^-} - \nu_{i-1}^{OH^-}\right) \quad (3)$$

$$dQ_i = \Delta H_c\left(\nu_i^{CuL} - \nu_{i-1}^{CuL}\right) + \Delta H_p\left(\nu_i^{HR} - \nu_{i-1}^{HR}\right) + \Delta H_{OH^-}\left(\nu_i^{OH^-} - \nu_{i-1}^{OH^-}\right) \quad (4)$$

In these equations, dQ_i denotes the reaction heat at i-th titration step, and ν_i^X is the mole amount of species 'X' existing in the reaction vessel after i-th titration step. ν_i^X was calculated using solution volume and the stability constants determined by the potentiometric titration. The dissociation enthalpy of H_2O (ΔH_{OH^-}) was adopted the reported value in NIST database [4]. Thermodynamic quantities of complexation of Elliot Soil at pCu =4.5 is shown in Figure 1.

From the obtained thermodynamic values, it is revealed that the protonation and the complexation reaction of humic acid was characterized by the polyelectrolyte effect and the heterogeneity. The protonation mechanism of humic acid was discussed in our previous study [5]. Moreover, the reaction enthalpies of humic acid were changed by pH and the ionic strength of bulk solution, while many study reported that the complexation enthalpy, which estimated by equilibrium constant, does not depend on pH of bulk solution.
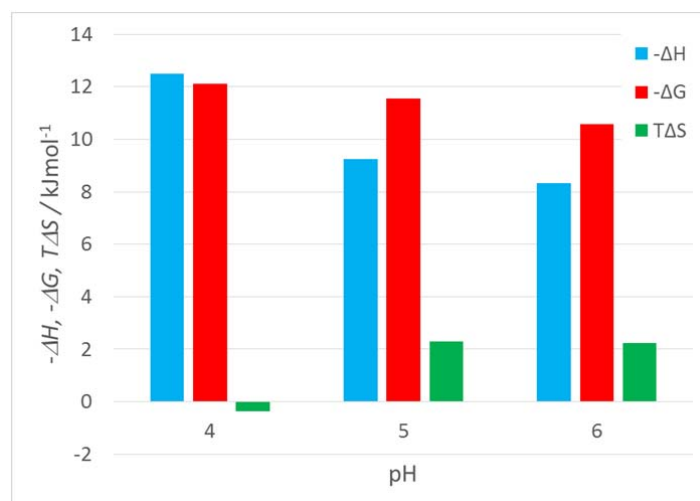
Figure 1. Thermodynamic quantities of complexation of Elliot Soil at pCu =4.5

[1] A. Kirishima, Y. Onishi, N. Sato and O. Tochiyama, "Determination of the thermodynamic quantities of uranium (VI)-carboxylate complexes by microcalorimetry", J. Chem. Thermodyn. 39 (2007) 1432-1438.
[2] H. Kitano, Y. Onishi, A. Kirishima, N. Sato and O. Tochiyama, "Determination of the thermodynamic quantities of complexation between Eu (III) and carboxylic acids by microcalorimetry", Radiochim. Acta 94 (2006) 541-547.
[3] A. Kirishima, T. Onishi, N. Sato and O. Tochiyama, "Simplified modelling of the complexation of humic substance for equilibrium calculations", J. Nucl. Sci. Technol., Vol. 47, No. 11, (2010) 1044-1054.
[4] NIST Standard Reference Database 46 Version 8.0 (2004).
[5] S. Kimuro, A. Kirishima, N. Sato, "Determination of the protonation enthalpy of humic acid by calorimetric titration technique", J. Chem. Thermodyn. 82 (2015) 1-8.

ACID-BASE CHEMISTRY OF HUMIC SUBSTANCES AT DIFFERENT TEMPERATURES

Q. Jin, Z. Guo*, G. Wang, W. Wu

School of Nuclear Science and Technology, Lanzhou University, Lanzhou, 730000, China.

Humic substances (HSs) have important influences on processes in the environment, such as pH buffing, metal binding and transport, and nutrient control [1-5]. Acid-base chemistry of HSs at elevated temperatures may be necessary to better understand the migration of radionuclides in the near-field of deep geological repository of high level radioactive waste.

In the present study, both proton binding equilibrium and kinetics of humic acid (HA) and fulvic acid (FA) from different sources were investigated at 273, 293 and 313 K, respectively. Acid-base titrations were performed at ionic strengths of 0.01-0.4 mol/L, and the equilibrium data were fitted by NICA-Donnan model [1]. The standard enthalpy changes were estimated from fitting parameters of NICA-Donnan model via the van't Hoff equation, which may enable the acid-base chemistry at other temperatures to be predicted. The proton dissociation kinetics of HA and FA were strongly pH-dependent and the dissociation rates were increased with increasing temperature, which was in agreement with forward- and back-titration hysteresis.
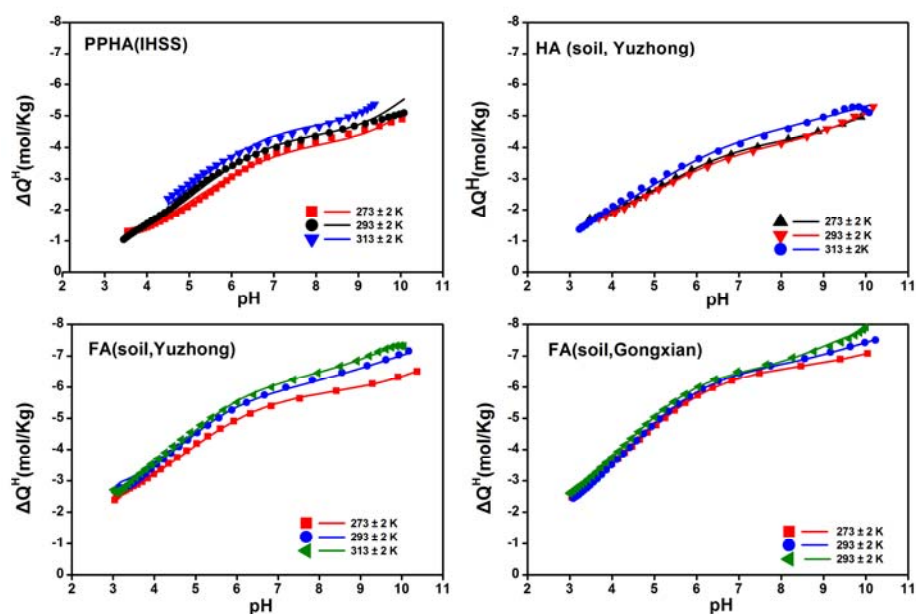
Fig.1 Acid-base titration data of HA and FA at different temperatures, $I = 0.05$ mol/L.

[1] D.G. Kinniburgh, W.H. van Riemsdijk, L.K. Koopal, M. Borkovec, M.F. Benedetti, M.J. Avena, Colloid Surf. A 151, 147(1999).
[2] E. Tipping, Cation Binding by Humic Substances. Cambridge University Press, 2002.
[3] M.A. Schlautman, J.J. Morgan, Geochim. Cosmochim. Acta 58, 4293(1994).
[4] C.J. Milne, D.G. Kinniburgh, E.Tipping, Environ. Sci. Technol. 35, 2049(2001).
[5] N.D. Bryan, L. Abrahamsen, N. Evans, P. Warwick, G. Buckau, L. Weng, W.H.Van Riemsdijk, Appl. Geochem. 27, 378(2012).

THE IMPACT OF AQUEOUS PHASE DEGRADATION PRODUCTS FROM POLYVINYL CHLORIDE ON DEEP GEOLOGICAL DISPOSAL OF INTERMEDIATE LEVEL WASTE

P. A. Davies [1], M. Cowper [3], N. D. M. Evans [1], J. Hinchliff [1], D. Read [1], N. L. Thomas [2]

[1] *Department of Chemistry, Loughborough University, Loughborough, Leicestershire, LE11 3TU*
[2] *Department of Materials, Loughborough University, Loughborough, Leicestershire, LE11 3TU*
[3] *Nuclear Services, AMEC Foster Wheeler, Building 150, Harwell, Oxford, OX11 0QB*

Polyvinyl chloride (PVC) is a common plastic that has been used historically in the nuclear industry in varying roles, including as protective clothing, tenting material and glove-box posting bags. This has resulted in an abundance of PVC materials in UK intermediate level waste (ILW) streams. Plutonium Contaminated Material (PCM) at Sellafield Ltd contains 2,800 t representing 81% of all PVC in the UK nuclear waste inventory. According to the present concept for the disposal of ILW in the UK, this waste will be disposed of in a cementitious geological disposal facility (GDF) and, owing to the chemical conditions and temperatures expected, together with ionising radiation the PVC will degrade over time to form low density non-aqueous phase liquids (LNAPLs) [1]. These LNAPLs could be released from the waste containers and, being of low density, are likely to migrate through groundwater towards the surface, via porosity and fractures. It has been hypothesised that the migration of these radionuclides from the near field may be affected by adsorption or by solubility enhancements brought about by partitioning into the buoyant NAPL phase [2]. Previous work has shown that PVC degradation products result in solubility enhancements of radionuclides such as Am(III) and Pu(IV) of between 2 and 3 orders of magnitude [3].

The aim of this project is to improve confidence in the understanding of the potential formation of organic complexants from PVC additives present in ILW, under conditions relevant to the near field of a GDF. The study focusses on the degradation of three phthalic acid ester (PAE) plasticisers, commonly used in PVC formulation (di-ethylhexyl phthalate (DEHP), di-isodecyl phthalate (DIDP) and di-isonyl phthalate (DINP)) in CEM1 Portland cement and Nirex Reference Vault Backfill (NRVB) solutions. The study includes an experiment involving gamma irradiation (dose to 1 MGy) of these phthalates and a Weston Vinyls formulated PVC at temperatures up to 80 °C (GDF relevant conditions). Analysis of the degradation products formed is presented as well as a characterisation of the original non-degraded Weston Vinyls PVC formulation. A variety of techniques including gas chromatography mass spectrometry (GC-MS), scanning electron microscopy (SEM)/ energy-dispersive X-ray analysis (EDXA), nuclear magnetic resonance spectroscopy (NMR) and Fourier-transform infrared spectroscopy (FT-IR) have been used for characterisation. The results presented here focus on the effect of the organic degradation products on the solubility and sorption characteristics of key safety-related radioisotopes of Ni, U and Pu with these components.

Initial results from the irradiation experiment show that significant degradation occurs, which increases with elevated temperature. From non-purgeable organic carbon (NPOC) analysis of the aqueous phase of the irradiated PVC and plasticiser samples, the NPOC concentration increases to a maximum at doses between 500 – 750 kGy (~4700 mg/dm^3 in PVC and ~650 – 800 mg/dm^3 in the plasticisers samples) and then decreased as absorbed dose increased further to 1000 kGy (Figure 1). The decrease in NPOC observed at higher doses is attributed to the formation of low molecular mass products, which tend to be gaseous and evaporate during the degradation process.
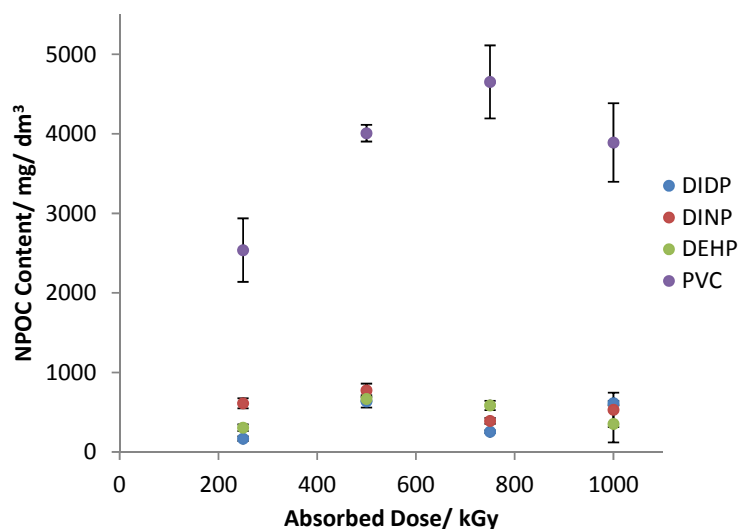
Figure 1. NPOC data of irradiated samples

Gas chromatography mass spectrometry (GC-MS) analysis of the irradiated samples has been conducted to identify degradation products in both the PVC and PAE plasticiser samples. The main products found are shown in Table 1 (N.B. components identified in the Phthalic Acid Ester Plasticiser samples were also identified in the PVC). An alcohol (ethyl hexanol) and the carboxylic acid variant that have been identified in the DEHP samples are a result of the hydrolysis of the ester group in the plasticisers. The PVC samples show production of a large quantity of phenol, benzoic acid and other phenol derivatives, as do the ester plasticisers. The elevated temperature samples (50 °C) show similar degradation products but at higher concentrations.

Sample type	Key Peak Retention Times/ min[-1]	Component(s) Identified
Phthalic Acid Ester Plasticiser	7.11	Ethyl hexanol + other isomers
	7.62	2-ethyl hexanoic acid/ 2-ethyl hexanoic acid anhydride
	8.47	Isophthalaldehyde
	9.07	Phthalamic acid, phthalic acid, phthalic anhydride, monoethyl ester phthalic acid
PVC	6.75	Phenol + other derivatives
	7.98	Benzoic acid
	9.56	2,4-bis(1-methylethyl)- phenol
	10.42	Azelaic acid
	11.63	[1,1'-biphenyl]-2,5-diol

Table 1. Degradation components identified in the GC-MS analysis of irradiated samples

[1] I. Mersiowsky, M. Weller and J. Ejlertsson, *Fate of Plasticised PVC Products under Landfill Conditions: a Laboratory-Scale Landfill Simulation Reactor Study*, Water Research, **35**(13), p 3063-3070, 2001.
[2] V. Smith, S. Magalhaes and S. Schneider, *The Role of PVC Additives in the Potential Formation of NAPLs,* AMEC Report AMEC/PPE/2834/001, 2012
[3] M. Cowper, *The Impacts of Aqueous Phase Degradation Products from PVC Additives*, AMEC Report SF6604 Issue 02 2013

THE SUITABILITY OF POLYCARBOXYLATE SUPERPLASTICISERS IN CEMENTITIOUS GROUT ENCAPSULATION OF NUCLEAR WASTE

M. Isaacs[1], J. Hinchliff[1],, S. D. Christie[1], J. D. Holt[1], S. E. Taylor[1], S.Edmondson[2], M. Siitari-Kauppi[3], D. E. MacPhee[4,], D. Read[1]

[1] *Department of Chemistry, Loughborough University, Loughborough, LE11 3TU, UK*
[2] *School of Materials, University of Manchester, Oxford Road, Manchester, M13 9PL, UK*
[3] *Laboratory of Radiochemistry, University of Helsinki, Helsinki, FI-00014, Finland*
[4] *Department of Chemistry, University of Aberdeen, Meston Building, King's College, Aberdeen AB24 3UE, UK*

The UK uses cement grout encapsulation for the long term storage of low and intermediate-level nuclear waste. Cementitious backfill is also envisaged as part of a multi-barrier system for a future geological disposal facility. The use of superplasticisers in both applications is desirable owing to their ability to increase the workability of a cement paste, as well as allowing a reduction in the amount of water required in the mix. Interest in the current generation of superplasticisers, polycarboxylate 'comb' polymers, in waste-form production has required confirmatory studies on their possible effects on radionuclide behaviour. It has been shown previously that the presence of superplasticisers in high pH systems can increase the solubility of U(VI), Pu(IV)[1,] Ni(II), Am(III), Th(IV) and Np(V)[2] by as much as four orders of magnitude; these are minimum values since, in some experiments, the radionuclide concentrations were inventory limited. There is also evidence that superplasticisers can cause rejection of radionuclides from a cement during the curing process leading to significant radionuclide concentrations in bleed water and failure to bind the radionuclide homogeneously throughout a sample [3].

This work examines the impact of superplasticisers and other common additives found in superplasticiser blends (biocides, viscosity modifying agents and de-foaming agents) on the solubility, mobility and leaching properties of nickel, uranium, plutonium and americium. Four commercial superplasticisers were tested in this work in addition to two new materials synthesised specifically for the project. The synthesised materials were produced using a free radical aqueous polymerisation [4,5] and purified via dialysis so that only the high molecular weight polymers are present in the experiments. Two cements blends were used in this work: 9:1 GGBS:OPC and 3:1 PFA:OPC.

A series of solubility tests in cement-equilibrated water were performed in order to determine the effect of each superplasticiser on the solubility of the above radionuclides. When superplasticiser was added, solubility increased by as much as four orders of magnitude in concordance with previous work.

Leaching tests include experiments on intact monoliths, disaggregated material and samples subject to prior gamma irradiation, in which the blocks were exposed to 1MGy of radiation over a period of   . Radionuclide concentrations have been measured in the bleed water from small scale cement blocks doped with U(VI), Pu(IV), Ni(II) and Am(III). In slag cement samples made with the commercial superplasticisers up to 10% of the total radionuclide inventory added to the blocks was present in the bleed water. No detectable radionuclides were found in samples made with the synthesised superplasticisers, those with additives or in fly ash cement samples. Notwithstanding the effect on solubility in free solution and with the exception of bleed, no radionuclide leaching was observed from any of the blocks.

Radial through-diffusion tests were performed in which a spike of each respective radionuclide was placed in a central well drilled in a cement monolith and the block placed in cement-equilibrated water[6]. No breakthrough was found over a six month period; the absence of radionuclide migration has been confirmed by digital autoradiography.

A number of supplementary experiments have been carried out to further understand the effect of superplasticiser composition on the microstructure of cured cement. Porosity has been measured by both argon pycnometry to obtain gas ('total porosity') and by injection of ^{14}C-labelled methyl methacrylate followed by polymerisation to measure the accessible porosity. Pore water squeezing has also been carried out at pressure up to 4,000psi in order to determine the concentration of organics in the pore water.

[1] Effect of ADVA Cast 551 on the Solubility of Plutonium (IV) and Uranium (VI). A.P. Clacher and M.M. Cowper, Serco/TAS/003145/001 Issue 2, 2011
[2] Solubility Studies: Effect of Adva Cast 551 in Low Concentration, A.P. Clacher, T. Marshall and S.W. Swanton, Serco, NPO004236, December 2010

[3] A, J. Young, A. E. Milodowski, P. Warwick, D. Read. Behaviour of radionuclides in the presence of superplasticiser. Advances in Cement Research, 2013, 25(1)

[4] J. Plank, K. Pöllman, N. Zouaoui, P.R. Andres, C. Schaefer. Synthesis and performance of methacrylic ester based polycarboxylate superplasticizers possessing hydroxy terminated poly(ethylene glycol) side chains. Cement and Concrete Research, 2008, 38

[5] W. Fan, F. Stoffelbach, J. Reiger, L. Regnaud, A.Vichot, B. Bresson, N. Lequeux. A new class of organosilane-modified polycarboxylate superplasticizers with low sulfate sensitivity. Cement and Concrete Research, 2012, 42

[6] M. Felipe-Soltelo, J. Hinchliff, N.Evans, P.Warwick, D.Read. Sorption of radionuclides to a cementitious backfill material under near-field conditions. Mineralogical Magazine, 2012, 76(8)

RADIATION EFFECT OF IONIC LIQUIDS AND RELATED EXTRACTION SYSTEM

Yinyong Ao, Jing Peng, Jiuqiang Li, Maolin Zhai

Radiochemistry and Radiation Chemistry Key Laboratory of Fundamental Science, College of Chemistry and Molecular Engineering, Peking University, Beijing 100871, P. R. China

The room-temperature ionic liquids (RTILs) with negligible vapour pressure, excellent thermal and chemical stability have been considered as novel "green" solvents in the reprocessing of spent nuclear fuel. Studies on the radiation effect and recycling of RTILs are of great importance before their practical application.[1-3] In this work, we investigate systematically the radiation effect of two widely used hydrophobic RTILs [C_4mim]X and [C_4mim]X-based extraction systems, where [C_4mim]$^+$ is 1-butyl-3-methylimidazolium and X is hexafluorophosphate (PF_6^-) and bis(trifluoromethylsulfonyl)imide ([NTf_2]$^-$), respectively. The trace acidic radiolytic products of [C_4mim]X were found and identified by analyzing D_2O-washed samples of γ-ray irradiated ionic liquids for the first time. The results of EXAFS indicated that the Sr coordination environment in Sr-crown ether complexes did not change when the extraction was carried out using irradiated [C_4mim][NTf_2] as solvent, and acidic radiolytic products were responsible for the decrease of Sr^{2+} partitioning in irradiated [C_4mim][NTf_2]. The Sr^{2+} partitioning could be simply recovered by washing irradiated [C_4mim][NTf_2] with water. The radiolysis of crown ether/[C_4mim]X and N-heteropolycyclic ligands/[C_4mim]X systems were studied by UPLC/Q-TOF-MS and high-resolution ESI-MS. The main radiolytic products of extactants were identified, and their radiolysis mechanisms were proposed. Compared with traditional extraction system, these extraction systems based on RTILs show higher radiation stability. Moreover, special irradiation equipment was designed and used to investigate the α-radiation effect of [C_4mim]X with He$^+$ beams. The water-soluble radiolytic products of [C_4mim][NTf_2] under He$^+$ beam irradiation were analyzed, and found that they were similar to those by γ-rays irradiation, but their yield was much less than that by γ-rays irradiation, which was attributed to the recombination of [C_4mim][NTf_2] radical cations in track by high linear energy transfer radiations of He$^+$ beam. These results indicate that [C_4mim]X and their extraction system have high radiation stability, suggesting their potential application in spent nuclear fuel reprocessing.

Reference

1. D. Allen, G. Baston, A. E. Bradley, T. Gorman, A. Haile, I. Hamblett, J. E. Hatter, M. J. F. Healey, B. Hodgson, R. Lewin, K. V. Lovell, B. Newton, W. R. Pitner, D. W. Rooney, D. Sanders, K. R. Seddon, H. E. Sims and R. C. Thied, *Green Chem.*, 2002, **4**, 152-158.

2. L. Berthon, S. I. Nikitenko, I. Bisel, C. Berthon, M. Faucon, B. Saucerotte, N. Zorz and P. Moisy, *Dalton Trans.*, 2006, 2526-2534.

3. G. Le Rouzo, C. Lamouroux, V. Dauvois, A. Dannoux, S. Legand, D. Durand, P. Moisy and G. Moutiers, *Dalton Trans.*, 2009, 6175-6184.

INTERACTION OF GLUCONATE WITH An(III)/Ln(III) IN DILUTED TO CONCENTRATED MgCl$_2$ SOLUTIONS

A. Tasi[1], X. Gaona[1], Th. Rabung[1], B. Kutus[2], I. Palinko[2], P. Sipos[2], M. Altmaier[1], H. Geckeis[1]

[1]*Karlsruhe Institute of Technology, Institute for Nuclear Waste Disposal, Germany*
[2]*University of Szeged, Faculty of Science and Informatics, Materials and Solution Structure Research Group, Hungary*

In the long term safety assessment of repositories for radioactive waste disposal, the event of water intrusion and consequent formation of aqueous systems needs to be evaluated. In the case of repositories in rock salt formations, aqueous solutions (brines) are dominated by NaCl and MgCl$_2$. The use of brucite-based backfill material in such repository concepts is responsible for the buffering of pH$_m$ to ~9. Gluconic acid (C$_6$H$_{12}$O$_7$, HGH$_5$) is a poly–hydroxocarboxylic acid expected in repositories for low and intermediate–level radioactive waste as a component in the formulation of cement and cementitious materials. Gluconic acid is also considered as close analogue of iso-saccharinic acid (ISA), the main product of cellulose degradation under hyperalkaline conditions. Radionuclide solubility and sorption in cementitious and saline systems can be affected by the presence of these ligands. Formation of stable An(III)/Ln(III)–gluconate binary complexes has been reported in the literature [1]. The presence of Ca(II) enhances complex stability through formation of ternary species with An(III)/Ln(III) in the hyperalkaline pH range [2]. Despite the relevance of Mg(II) in several repository concepts for radioactive waste disposal, no studies assessing the role of Mg(II) in An(III)/Ln(III)–gluconate complexation have been conducted so far.

All samples were prepared and stored at 22 ± 2 °C in Ar glove boxes (O$_2$ content < 2 ppm). Undersaturation solubility experiments with Nd(OH)$_3$(am) were conducted in independent batch samples with 0.25 M, 1.00 M, 2.50 M, 3.50 and 4.50 M MgCl$_2$ as background electrolyte. The pH$_m$ (–log m$_{H^+}$) of the solutions was buffered to 8 and ~9 (pH$_{max}$) with 20 mM TRIS and Mg(OH)$_2$(s) (converting to Mg$_2$(OH)$_3$Cl·4H$_2$O(cr) above 2 M MgCl$_2$), respectively. The total concentration of gluconate in each of the series was varied according with 10^{-4} M $\leq$ [GH$_5^-$]$_{tot}$ $\leq$ 0.1 M. The total concentration of Nd(III) in the aqueous solution was quantified by ICP–MS after 10 kD ultrafiltration, whereas [GH$_5^-$]$_{tot}$ in solution was measured as total organic carbon (TOC). Solid phases before and after solubility experiments were characterized by XRD. TRLFS measurements were performed with $1 \cdot 10^{-7}$ M of Cm(III) per sample in MgCl$_2$ (0.25 M and 4.50 M) solutions. The concentration of gluconate in all samples was increased to 0.10 M by step–wise additions of concentrated NaGH$_5$ stock solutions.

The solubility of Nd(OH)$_3$(am) in MgCl$_2$ solutions is clearly affected by gluconate in weakly alkaline conditions. A strong increase in Nd(III) solubility (more than 2 log$_{10}$-units) is observed in 0.25 M MgCl$_2$ solutions with pH$_m$ = 9 and increasing gluconate concentration. The effect of gluconate on Nd(III) solubility is weaker in 1.0 M and 2.5 M MgCl$_2$, and becomes negligible at higher MgCl$_2$ concentration due to the competition between Mg(II) and Nd(III) for gluconate. TRLFS data show distinct Cm(III) spectra in the absence and presence of gluconate, clearly hinting towards the formation of Cm(III)–gluconate complexes. A single isosbestic point is observed in the spectra collected in 0.25 M MgCl$_2$ at pH$_m$ = 8, indicating the formation of a single Cm(III)–gluconate species. Furthermore, the formation of a 1:2 complex can be suggested from the magnitude of wavelength-shift observed in the presence of gluconate (~9 nm in 0.25 M MgCl$_2$ and pH$_m$ = 8). Note that the participation of two gluconate ligands in the complex formation with Cm(III) has been reported in a recent study in hyperalkaline CaCl$_2$ solutions (pH$_m$ = 12), where the formation of ternary Ca–Cm(III)–gluconate species was confirmed in combination with solubility data [2]. Ternary Mg–Cm(III)–gluconate species can possibly play a role in the less alkaline MgCl$_2$ systems, although further experimental efforts are needed to confirm this hypothesis. Note that the interaction of gluconate with Mg(II) in binary systems was found to be weaker than that in the analogous Ca(II) systems. In spite of the strong affinity of gluconate towards hard cations such as actinides, this study confirms the minor impact of this ligand on the solubility of An(III) in concentrated MgCl$_2$ brines relevant for disposal concepts in rock salt formations.

[1] Tits, J., Wieland, E., Bradbury, M. H., Applied Geochemistry, 20, 2082-2096 (2005).
[2] Gaona, X., Rojo, H., Rabung, T., García-Gutiérrez, M., Missana, T., Altmaier, M. (2015). This conference.

STRUCTURAL TRENDS AND PROPERTY CORRELATION IN LANTHANIDE AND ACTINIDE CHROMATES

Alexandra A. Arico

Florida State University, Department of Chemistry, 95 Chieftan Way, Tallahassee, Fl. 32304

A series of trivalent lanthanide chromates that illustrate structure-type as a function of ionic radius have been prepared under hydrothermal conditions. An excess of lanthanide starting material in a concentration of 0.2mmol is added to 0.075mmol each of Cs_2CrO_4 and $Cs_2Cr_2O_7$. These are loaded into 23mL Parr autoclaves with 2mL of deionized water and heated at a temperature of 200 degrees Celsius for 48 hours, with a cooling period following thereafter of 48 hours. The crystals that form are washed with deionized water, isolated, washed with ethanol, and dried in air. Single crystals are structurally characterized using a Bruker APEX II Quest X-Ray Diffractometer for unit cell determination and for full collections of diffraction data. Final structures are determined using SHELX XP and XPREP software. Three different space groups in the monoclinic crystal system and one space group in the triclinic crystal system emerge as a consequence of the contraction of the ionic radii in the $4f$ elements. The early lanthanides crystallize in the centrosymmetric space group $P2_1/c$ with formulae $CsLn(CrO_4)_2$ (Ln = La, Pr). Both lanthanide centers have 9-coordinate geometry. The next two lanthanides crystallize in the non-centrosymmetric space group Pc with the formulae $CsLn(CrO_4)_2$ (Ln = Nd, Sm). Both lanthanide centers adopt distorted 8-coordinate geometry. The late lanthanides crystallize in the centrosymmetric space group $P2_1/n$ with formulae $Ln_2(CrO_4)_2(OH)_2$ (Ln = Eu, Gd, Ho, Dy, Er, Tm, Yb). These lanthanide centers have distorted 8-coordinate geometry with two different sites for each lanthanide center. Every structure present in this series edge- and corner- shares with chromate tetrahedra to form sheets in a 3D network. Cesium cations charge balance in the interlayer channels that form. Terbium deviates from the structure type seen in the later lanthanides and crystallizes in the triclinic space group P-1 with formula $Tb_2(CrO_4H_2)(OH)_4$. Two Tb sites are present, one with 8-coordinate geometry and one with 9-coordinate geometry, wherein the 2 types of polyhedral both edge- and face- share asymmetrically. All of the compounds in this series are either orange or red-orange, with the exceptions being $CsNd(CrO_4)_2$, which is green, and $Tb_2(CrO_4H_2)(OH)_4$, which is yellow. Solid-state UV-Vis-Near-IR absorbance data show broad, very intense charge transfer bands in both compounds, wherein each coincide with the appropriate wavelengths in the visible region. These structural trends and absorbance anomalies show interesting behavior when f-elements are complexed with d^0 transition metal oxides.

ESTIMATION OF COMPLEXATION CONSTANTS BETWEEN ACTINIDES AND SIMPLE CARBOXYLIC ACIDS IN SOLVENT MEDIA COMPOSED OF WATER AND METHANOL

K. Bennett[(1)], C-H. Graser[(2)], C. M. Marquardt[(2)], S. B. Clark[(1)]

[(1)]*Department of Chemistry, Washington State University, Pullman, Washington 99164, United States*
[(2)]*Institute of Nuclear Waste Disposal, Karlsruhe Institute of Technology, Karlsruhe 76021, Germany*

The determination of complexation constants is traditionally accomplished by use of established techniques such as solvent extraction, potentiometry, spectrophotometry, and calorimetry. The use of these techniques result accurate determinations of complexation constants, but can be time consuming, labor intensive, and higher concentrations of samples are needed. Capillary electrophoresis inductively coupled plasma mass spectrometry (CE-ICP-MS) has recently been established as an additional method to find complexation constants [1-3]. This method is uniquely suited for use with radioactive materials, as it involves very small quantities of materials, resulting in increased safety when compared to traditional approaches.

Little data exists to describe the complexation of f-elements in mixed solvent media such as water:methanol. CE-ICP-MS is a method uniquely suited to finding this information for radioactive samples. In this work, this method has been used to estimate complexation constants between actinides of various oxidation states and simple carboxylic acids in solvent media water and methanol. The actinides that were used were Cm(III), Np(V), and U(VI), while the carboxylic acids used were acetic acid, α-hydroxyisobutyric acid (HIBA), and 2-hydroxy-2-methylbutyric acid. The goal of these studies are to find initial complexation constants between the actinides and carboxylic acids in a range of methanol concentrations. This basic data will elucidate the impact of solvent composition on complexation.

In an electric field, the mobility of charged species is affected by many parameters, including charge and size of the individual species. Consequently, complexes of the actinides in different oxidation states can be separated because their migration times in the capillary are different. As the ratio of ligand to cation changes, the degree of complexation also changes, which affects the overall size of the species. This trend enables a correlation between species mobility or migration rate with ligand concentration, and hence degree of complexation. In our study, the carboxylate ligands form relatively labile complexes with the f-elements, and the individual complexes with a given cation are not separated from each other. Instead, cations of different charges are separated from one another, but all the species associated with a given cation travel together in a single band. Thus, for our work, an average mobility for all of the species formed between a given ligand and metal cation is observed by capillary electrophoresis and the elements are detected by the ICP-MS [4]. The following equation is used to estimate the mobility of each species as well as the complexation constants for a system containing a trivalent metal and forming three metal-ligand species [1]:

$$\mu_{ave} = \frac{\mu_{M^{3+}} + \mu_{ML^{2+}}\text{ß}_{101}[L] + \mu_{ML_2^+}\text{ß}_{102}[L]^2 + \mu_{ML_3}\text{ß}_{103}[L]^3}{1 + \text{ß}_{101}[L] + \text{ß}_{102}[L]^2 + \text{ß}_{103}[L]^3}$$

In a solvent composed of 10% (v/v) methanol, the mobility of the observed species decreased as a result of an increasing HIBA concentration. As the ligand concentration increases, a proportional increase in higher order complexes is expected, leading to a decrease in charge of the species and an increase in species size. Potentiometric titrations were also conducted to determine the pKa of each ligand in different solvent compositions of methanol and water, which enabled calculation of the deprotonated ligand concentration from the total ligand concentration used for each solvent composition. Complexation constants were estimated for the actinide-HIBA system in 10% (v/v) methanol and are shown in Table 1.

Table 1. Estimation of complexation constants between actinides and α-hydroxyisobutyric acid[a]

	log ß$_{101}$	*log* ß$_{102}$	*log* ß$_{103}$
Cm^{3+}	3.1 ± 0.2	5.0 ± 0.1	5.7 ± 0.3
NpO_2^+	3.1 ± 0.4	4.9 ± 0.4	6.5 ± 0.4
UO_2^{2+}	3.3 ± 0.3	5.1 ± 0.3	6.7 ± 0.3

[a]Reported error is 3σ. T = 25 ± 1 °C. Ionic strength is 0.1 M.

[1] J. Petit, et al., Electrophoresis, 31, 355 (2010).
[2] S. Topin, J. Aupiais, P. Moisy, Electrophoresis, 30, 1747 (2009).
[3] S. Topin, et al., Anal. Chem., 81, 5354 (2009).
[4] J. E. Sonke, V. J. M. Salters, J. Chrom. A, 1159, 63 (2007).

FUNCTIONALIZED MAGNETIC MESOPOROUS SILICA NANOPARTICLES (MMSNs) FOR BINDING URANIUM AND TECHNETIUM FROM AQUEOUS MEDIA

Dien Li[1)], Daniel I. Kaplan[1)], Steve M. Serkiz[1)], Sarah C. Larsen[2)], Shani Egodawatte[2)]

[1)] *Savannah River National Laboratory, Aiken, SC 29808, United States*

[2)] *University of Iowa, Iowa City, IA 52242, United States*

Uranium is the most common radioactive contaminant in the DOE complex, and at U mine / processing sites. There are two common oxidation states of U in natural environments and waste streams, U(IV) and U(VI). U(VI) is normally more mobile, bioavailable, and toxic than U(IV). The aqueous U(VI) species exhibits little or no adsorption to sediments under pH < 4 or pH > 8 aqueous conditions commonly found in the environment (*e.g.*, Savannah River Site (SRS) and the Hanford Site), which leads to yet-unresolved problems for remediation of U. In addition, technetium-bearing nuclear wastes continue to increase rapidly, and Tc may inadvertently be introduced into the environment during nuclear power production and from leaks at waste storage facilities. For example, Tc is a key risk driver in SRS and other DOE waste management sites (*e.g.*, the Hanford Site and ORNL). Technetium is present as an anionic TcO_4^- species under most of these environmental conditions, and the TcO_4^- anion has essentially near-zero adsorption to common mineral sorbents, is mobile and difficult to be immobilized.

In this study, MMSNs were synthesized using a surfactant-template method in the presence of magnetite nanoparticles. The surfaces of the MMSNs were then functionalized using selected functional molecules that can more effectively bind and immobilize U or Tc under environmental conditions at which sediments or other sorbents are usually not effective. The functionalized MMSNs were evaluated for U removal from pH 3.0 and pH 9.6 artificial groundwater under ambient conditions using batch experiments. The adsorption coefficient, K_d (mL/g), was calculated using this formula:

$$K_d = \frac{C_0 - C}{C} \times \frac{V}{M}$$

where C_0 and C are the initial and final U concentrations in the solution, respectively, V is the volume of groundwater (mL) and M is the mass of MMSNs (g).

Figure 1. K_d values of the functionalized MMSNs for U removal from pH = 3 (A) and pH = 9.6 (B) artificial groundwater
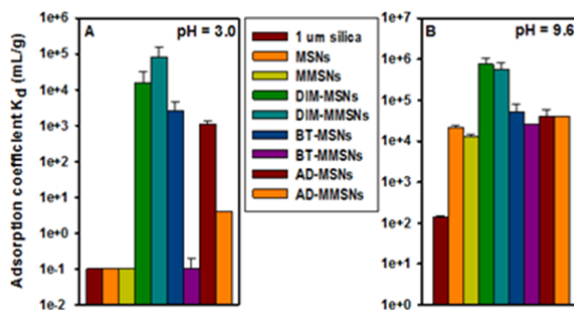
The functionalized MMSNs are very effective for U removal from pH = 3 or pH = 9.6 groundwater under atmospheric $P_{CO2} = 10^{-3.5}$ atm. At pH = 3, U removal was as much as 99%, K_d values increased by 4 to 6 orders of magnitude compared to most of common minerals and non-grafted MMSNs, U concentrations decreased to ~100 µg/L. At pH = 9.6, U removal was nearly 100%, K_d values increased by 2 to 4 orders of magnitude compared to most of common minerals. They removed U from pH = 9.6 groundwater to as low as <0.7 µg/L, which is much lower than the U Maximum Contaminant Level of 30 µg/L regulated by EPA. Synchrotron XAS analyses indicated that the MMSNs-bound U existed primarily as U(VI), indicating that these may be highly effective sorbents, even under oxidizing conditions. In addition, these functionalized MMSNs had moderate K_d values (~300 mL/g) for Tc removal from pH = 3.0 groundwater.

CHARACTERIZATION OF NATURAL ORGANIC MATTER (NOM) DERIVED FROM DIFFERENT LAYERS WITHIN THE BOOM CLAY FORMATION AND THEIR RADIONUCLIDE INTERACTION

U. Kaplan[1], M. Bouby[1], Th. Rabung[1], T. Kupcik[1], D. Schild[1], P. Kaden[1], C. Bruggeman[2], D. Durce[2], N. Maes[2], S. Brassinnes[3], T. Schäfer[1]

(1) Institute for Nuclear Waste Disposal (INE), Karlsruhe Institute of Technology, D-76021 Karlsruhe, Germany
(2) Belgian Nuclear Research Centre SCK·CEN, Boeretang 200, 2400 Mol, Belgium
(3) ONDRAF/NIRAS, Belgian Agency for Radioactive Waste and Enriched Fissile materials, Geological Disposal, R&D, Avenue des Arts, 14, 1210 Bruxelles, Belgium

In Belgium, deep geological disposal of nuclear waste is envisaged by ONDRAF/NIRAS, the Belgian Agency for Radioactive Waste and enriched Fissile Material, in poorly indurated clay formations like the Boom Clay (BC) or Ypresian clays (http://www.ondraf-plandechets.be). These host rocks have favourable intrinsic properties promoting the retention of radionuclides (low hydraulic conductivity, reducing redox capacity, slightly alkaline character, high specific surface area, cationic exchange capacity and plasticity). Organic material (OM) is present in 1 to 5% wt in BC [1]. Knowing the possible interactions with radionuclides (RNs), this organic material has to be properly characterized. Accordingly, to complement the Belgian research program conducted so far, this research focuses on a better determination and characterization of the mobile size fraction of dissolved organic matter (DOM) currently present and to be expected within the lifespan of the repository (i.e., taking into account the possible geochemical evolution).

Practically, this work concentrates on the size distribution and natural metal association determination of 1) current pore water DOM and 2) DOM released from solid clay samples (data not presented here). The pore waters and solid clay samples are representative of different horizons of the Boom Clay formation in Mol under present-day conditions (i.e., 15 mM $NaHCO_3$).

Boom Clay pore waters are sampled from three piezometers: Spring (1 sample), Morpheus (4 samples), EG/BS (1 sample) located in the HADES underground research laboratory at Mol. Spring is representative of a given layer (horizontal drilling). EG/BS represents several layers as a bulk (vertical drilling over ~15m). The Morpheus piezometer samples pore water from different horizons representing different naturally occurring variations within Boom Clay; F4: bulk clay with low DOC, F8: bulk double-band silt, F12: bulk silt, F20: bulk clay with high DOC. The pore waters are directly sampled in Swagelok containers under anoxic conditions and kept closed until sample measurements.

Detailed investigations were carried out by DOC analysis and Asymmetrical Flow Field-Flow Fractionation coupled to a UV-Visible spectrophotometer and an ICP-MS detector (AsFlFFF/UV-Vis/ICP-MS; for details see e.g. [2]) before or after (sequential) ultra-filtration (UF). Complementary analyses were done by High Pressure Size Exclusion Chromatography coupled to a UV-Visible spectrophoto-meter (HPSEC/UV-Vis). Sequential UF consists of using UF cartridges rinsed before use with ultra-pure water 3 times at 3,500 rpm during 35 min. The cut-offs used are 100 kDa, 30 kDa, 10 kDa and 1 kDa. All the BC pore waters and the leachate suspensions from the solid clay disc samples are sequentially ultra-filtrated as indicated. The different filtrates are placed in glass vials and stored at 4°C in a fridge.

Boom Clay pore water. DOM size distributions obtained by UF, AsFlFFF/UV-Vis/ICP-MS and HPSEC/UV-Vis are consistent with each other. Results agree with DOC analysis on the different isolated fractions. The analyses show that the OM present in all the BC pore waters analyzed is smaller than 70 kDa or ~ 11 nm.. The inorganic element analysis reveals the OM-association of several elements like Mg, Mn, Sr and traces of lanthanides (Lns) and actinides (e.g. U, Th). Fe was only detected in EG/BS pore water.

Time Resolved Laser Fluorescence Spectroscopy (TRLFS). For investigating the binding properties of DOM towards trivalent actinides TRLFS experiments were performed by adding Cm(III) as a fluorescence probe. The influence of carbonate as a strong competing ligand was further studied. First experiments were done by using EG/BS pore water. All investigated samples (Cm(III) + carbonate, Cm(III) + DOM, and Cm(III) + DOM + carbonate) of the EG/BS pore water show a similar fluorescence fingerprint, with Cm(III) emission spectra significantly different compared to the aquo ion. The redshift of the emission peak maximum from 593.8 nm (Cm(III) aquo ion) to ~603 nm indicates a strong metal ion complexation by groundwater DOM or carbonate ligands. Based on the peak maximum a clear differentiation between Cm(III)-DOM and Cm(III) carbonato complexes is not possible, as both ligands as well as their mixtures show quite comparable fluorescence spectra under EG/BS groundwater conditions. However, complexation of Cm(III) by DOM and

excitation at 355 nm results in a pronounced energy transfer from the organic molecule to the metal ion that is very helpful for elucidating the Cm(III) speciation. Based on the high fluorescence intensities at this excitation wavelength in presence of DOM, it can be concluded that Cm(III)-DOM complexes are the dominant species even if carbonate is simultaneously present. Further on, mixed Cm(III)-carbonato-DOM complexes are absent based on our laser spectroscopy results. In addition, we tested the DOM size effect on Cm(III) fluorescence spectra. Two sets of experiments were performed, one by adding Cm(III) to different size fractions of DOM, the other by sequential filtration of DOM when Cm(III) was added in advance. Both experiments provided identical TRLFS results. Thus, the binding properties of the different size fractions of EG/BS DOM are identical or at least very similar.

Acknowledgement

References

[1] C. Bruggeman, M de Craen, "Boom Clay natural organic matter", Status report 2011, SCK.CEN-ER.206, External Report, June 2012.

[2] Bouby, M.; Geckeis, H.; Lützenkirchen, J.; Mihai, S.; Schäfer, T., Interaction of bentonite colloids with Cs, Eu, Th and U in presence of humic acid: A flow field-flow fractionation study. Geochim. Cosmochim. Acta 2011, 75, (13), 3866-3880.

SELENIUM UPTAKE BY CEMENTITIOUS MATERIALS: EFFECT OF THE REDOX STATE

J. Tits[1], H. Rojo[1,2], A. C. Scheinost[3], B. Lothenbach[4], E. Wieland[1]

[1]*Laboratory for Waste Management, Paul Scherrer Institute, Villigen-PSI, Switzerland*
[2]*Institute for Nuclear Waste Disposal, Karlsruhe Institute of Technology, Karlsruhe, Germany*
[3] *Institute of Resource Ecology, Helmholtz-Zentrum Dresden-Rossendorf, Dresden, Germany*
[4] *Laboratory for Concrete and Construction Chemistry, Empa, Dübendorf, Switzerland*

Safety assessment studies for low- and intermediate level nuclear waste (L/ILW) repositories predict selenium-75 to be an important dose-determining radionuclide due to its long half-live and its presence in the anionic form resulting in weak retention by many common near- and far field minerals [1]. However, such predictions ignore the potential uptake by positively charged anion exchangers present in the cementitious near-field of a L/ILW repository, such as ettringite and AFm phases (hydrocalumite), a group of Ca, Al–layered double hydroxides.

The objective of this work is to investigate the immobilisation of Se under the alkaline and reducing conditions existing in a cement-based repository (-230mV < E_h < -750 mV, 10.0 < pH < 13.5). Under these conditions, Se(IV) and Se(-II) are the dominating redox states and the aqueous Se speciation is dominated by anionic species SeO_3^{2-}, HSe^- and a series of polyselenides, mainly Se_2^{2-}, Se_3^{2-} and Se_4^{2-} [2].

Sorption and co-precipitation experiments were carried out under alkaline conditions ($10 \leq pH \leq 12.5$) with the most common cement phases such as calcium silicate hydrates (C–S–H phases) and AFm phases ($[Ca_2Al(OH)_6][X^{n-}]_{1/n}\cdot(H_2O)_m$), X being CO_3^{2-}, SO_4^{2-}, OH^-, Cl^-). C–S–H phases were synthesized by co-precipitating CaO and SiO_2 at varying ratios (C:S ratios). Pure AFm phases containing different types of anions were synthesized by co-precipitating tricalcium aluminate (C_3A) with different Ca salts of the form $CaX_{2/n}$. Sorption experiments were performed by mixing aliquots of ^{75}Se-labelled Se(IV) or Se(-II) solutions with suspensions of C-S-H and AFm phases and allowing them to equilibrate for periods between 1 day and 2 months. Se(IV) incorporation in AFm interlayers was studied by co-precipitating C_3A with $CaSeO_3$ or CaSe and $CaX_{2/n}$ at various ratios. Se(-II) was obtained by electrochemical reduction of Na_2SeO_3 in 1 M NaOH at a redox potential of -1.2 V (SHE). Sorption and co-precipitation experiments with Se(-II) were performed in inert atmosphere glove boxes (O_2 partial pressure < 1.0 ppm) and in the presence of 0.01 M hydrazine to avoid re-oxidation of Se(-II) by traces of O_2 present in the experimental systems. The redox state of selenium in solution was determined with UV-Vis spectrometry. To assess the redox state of the sorbed Se, Se K-edge XANES and EXAFS spectra were collected at the ROBL beamline at ESRF, France. XRD examinations were carried out using Co–Kα radiation; the angular scan was varied between 5–90° 2θ with a step size of 0.017° and a count time of 65 s per step.

Kinetics studies showed that the processes controlling the sorption of both Se(IV) and Se(-II) with all cement phases are attaining a steady state within one day suggesting that fast ion-exchange or surface complexation mechanisms are involved in the Se uptake.

Se(IV) and Se(-II) sorption onto C–S–H phases was found to be weak, demonstrated by solid/liquid distribution ratios (R_d values) ranging between $5 - 50$ L kg^{-1} for both oxidation states. This weak sorption behaviour is attributed to the presence of mainly negatively charged sorption sites on the surfaces of the C-S-H particles in the pH region under investigation, resulting in an electrostatic repulsion between the anions and the mineral surfaces. Se(IV) sorption isotherms on C–S–H phases were linear over a loading range between $\sim 10^{-6}$ mol kg^{-1} and $\sim 10^{-2}$ mol kg^{-1} indicating that one single type of sorption sites is responsible for the uptake (Figure 1a). The non-linear sorption behaviour of Se(-II) on C-S-H phases suggests the presence of several sorption mechanisms, which are not yet understood (Figure 1b).

AFm phases were found to be much more effective in removing Se(IV) and Se(-II) from solution than C–S–H phases. At trace loadings, R_d values ranged between 500 L kg^{-1} and $2 \cdot 10^4$ L kg^{-1} for both redox states. These higher R_d values suggest that sorption onto AFm phases is not controlled by a simple surface complexation mechanism as in the case of C–S–H phases. Furthermore, Se(IV) and Se(-II) uptake by AFm phases was found to depend strongly on the type of interlayer anions and thus on the interlayer distance: the highest R_d values were measured for Se(IV) and Se(-II) sorption onto AFm-OH-CO_3 and AFm-SO_4 having basal spacings of 8.20Å and 8.93Å, respectively. Much lower R_d values were determined in the case of AFm-CO_3 and AFm-Cl_2 with smaller basal spacings of 7.58Å and 7.88Å, respectively. These observations together with the high R_d values are clear evidence for anion-exchange as the dominating sorption process for Se(IV) and Se(-II) onto AFm phases. The non-linear shape of the Se(IV) sorption isotherms measured on AFm phases (Figures 1a and 1b) further suggests the presence of at least two different types of sorption sites. Finally, X-ray

diffraction studies of AFm samples obtained from co-precipitation experiments with increasing Se(IV) : $X_{2/n}$ ratios (X = CO_3^{2-} or X=$(OH-CO_3)^{2-}$) indicated that the Se(IV) immobilisation at high loadings is taking place through dissolution of the original AFm phase and precipitation of a new, separate AFm-SeO_3 phase. It is concluded that, at low loadings, Se(IV) and Se(-II) sorption onto AFm phases might take place through anion exchange in the AFm interlayers, whereas at high loadings, in the case of Se(IV), a new AFm-SeO_3 phase is formed.

The present results highlight the ability of the AFm phases present in cementitious materials to remove Se(IV) and Se(-II) from solution and thus to reduce the mobility of selenium under the reducing conditions prevailing in a L/ILW repository.
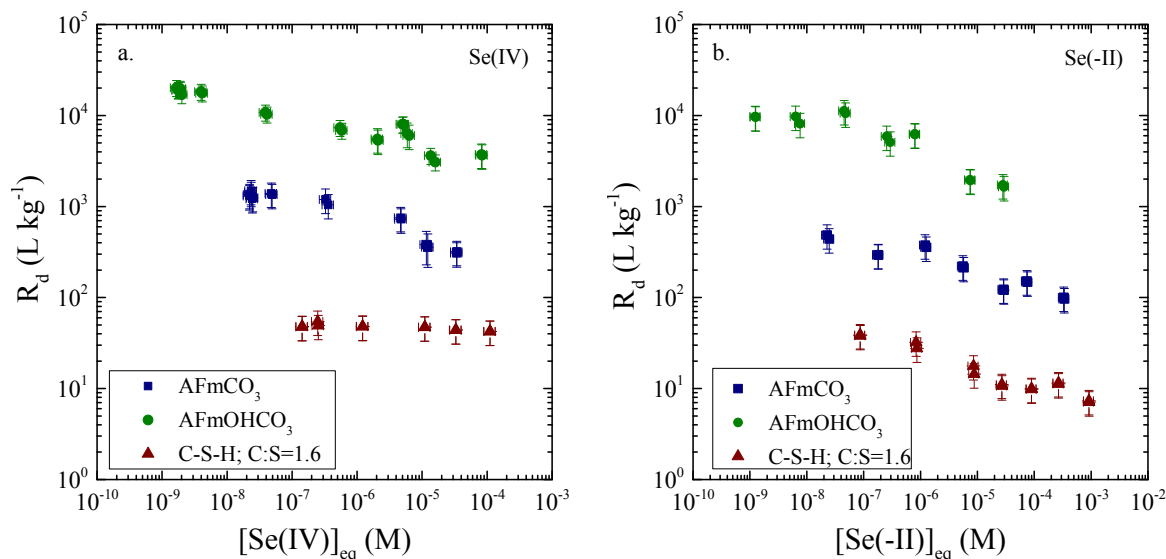
Figure 1. Se(IV) (a) and Se(-II) (b) sorption isotherms for a C-S-H phase with a C:S ratio of 1.6 (pH = 12.5), for AFm-CO_3 (pH = 11.6), and for AFm-OH-CO_3 (pH = 12.2).

[1] Nagra (2002). Project Opalinus Clay. Safety report. Demonstration of disposal feasibility for spent fuel vitrified high-level waste and long-lived intermediate level waste (Entsorgungsnachweis). Nagra Technical Report, NTB 02-05, Nagra, Wettingen, Switzerland.

[2] Olin, Å., Noläng, B., Osadchii, E. G., Öhman, L.-O., and Rosén, E. (2005). Chemical thermodynamics of selenium. NEA, Issy-Les Moulineaux, France.

INFLUENCE OF TITANIUM SUBSTITUTION AND IRON REDOX CHEMISTRY ON THE SORPTION OF ACTINDES BY TITANIUM-DOPED IRON OXIDE (Fe$_{3-x}$Ti$_x$O$_4$) NANOPARTICLES

E. Wylie[1], B. Powell[1]

[1] *Department of Environmental Engineering and Earth Sciences, Clemson University, 342 Computer Court, Anderson, SC 29625*

Titanoferrous magnetites form naturally by Ti(IV) replacement in magnetite (Fe$_3$O$_4$), particularly in sediments derived from igneous rocks such as basalt [1]. A series is produced by replacement of Fe(III) by Ti(IV) in the unit cell yielding a complete solid solution of Fe$_{3-x}$Ti$_x$O$_4$ from magnetite (x = 0) to ulvospinel (x = 1) [1]. As Fe(III) is replaced by Ti(IV), a reduction of the unit cell Fe(III) to Fe(II) occurs for charge balance. This results in a proportional increase in the Fe(II)/Fe(III) ratio to values greater than that of stoichiometric magnetite (0.5). The distribution of Fe(II) and Fe(III) between the A and B sites depends on x and results in a range of magnetic, electronic, and structural properties. Previously, a series of titanomagnetite nanoparticle suspensions have been produced at room temperature under anoxic conditions with x values ranging from 0.00 to 0.40 according to [1]

$$(1+x)Fe^{2+} + (2-2x)Fe^{3+} + xTi^{4+} + 8OH^- \Leftrightarrow Fe_{3-x}Ti_xO_4 + 4H_2O$$
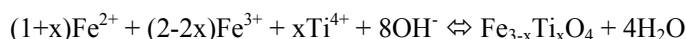
In those studies, titanomagnetites were implicated as a phase controlling radionuclide mobility in the Hanford subsurface and exhibited a high reductive capacity for both Tc(VII) and U(VI) under anoxic conditions [2, 3].

In the present study, we are examining the sorption properties and reductive capacity of these particles with respect to the light actinides (Th(IV), U(VI), Np(V)) and Eu(III). In addition to their adsorption/reduction properties under anoxic conditions, we are interested in desorption/oxidation when the particles are subjected to oxidizing conditions. Batch sorption data suggests that at pH 3, U and Np sorption increases with increasing titanium content (higher Fe(II)/Fe(III) ratio) (Figure 1). Acid extraction followed by LaF$_3$ coprecipitation indicated that, under anaerobic conditions, U and Np were sorbed as tetravalent species on the titanomagnetite surface. TEM and XAS experiments are underway to determine the Np coordination environment and examine the potential for NpO$_2$ surface precipitates. These data will compliment previously published uranium-titanomagnetite XANES/XAFS data [3]. Additionally, a rapid release of radionuclides from the nanoparticles was observed when the suspensions were subjected to an oxidizing environment. A systematic study will be presented that examines this re-oxidation step and the effects of 'aging' on the process.
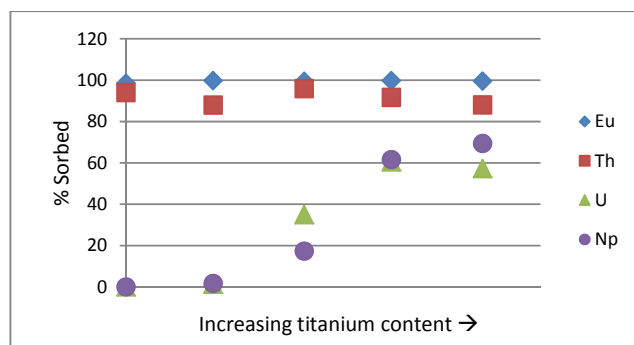
Figure1. Titanomagnetite sorption of actinides and Eu at pH 3

[1] Pearce, C.I., et al., Journal of Colloid and Interface Science. 387, 24 (2012).

[2] Liu, J., et al., Geochimica Et Cosmochimica Acta. 92, 67 (2012).

[3] Latta, D.E., et al., Environmental Science & Technology. 47, 4121 (2013).

REDOX CHEMISTRY AND SOLUBILITY OF Fe IN REDUCING ALKALINE TO HYPERALKALINE CONDITIONS: Fe(0)–Fe$_3$O$_4$–Fe(II)$_{aq}$ SYSTEM

M. R. González-Siso[1], X. Gaona[2], L. Duro[1], D. Schild[2], M. Lagos[2], G. Darbha[2], N. Finck[2], M. Altmaier[2], J. Bruno[1]

[1]*Amphos 21 Consulting S.L., Passeig Garcia i Faria, 49-51, 1-1a, 08019 Barcelona, Spain*
[2]*Karlsruhe Institute of Technology, Institute for Nuclear Waste Disposal, Germany*

The Swedish Final Repository (SFR) is used for the final disposal of low- and intermediate-level radioactive-waste. The quantitative assessment of the chemical evolution of the SFR repository is essential to establish reliable performance assessment models. According to recent modelling work [1], the ingress of groundwater in SFR repository will impose highly alkaline and strongly reducing conditions. These are mainly the consequence of the dissolution and subsequent alteration of cement combined with the initial aerobic corrosion of the iron content of the repository and its anoxic corrosion once oxidants have been depleted. Magnetite (Fe$_3$O$_4$) has been identified as one of the main products resulting from the anoxic corrosion of metallic iron and steel. Thermodynamic data selected in the NEA–TDB database for this solid phase are based on calorimetric studies [2]. Kinetics have been reported to hinder the solubility equilibrium of magnetite at room temperature under acidic to near-neutral pH-conditions, due to the reversible transformation equilibrium between -Fe$_3$O$_4$(cr) and -Fe$_2$O$_3$(cr). Furthermore, the NEA–TDB database does not select any neutral or anionic hydrolysis species of Fe(II) and Fe(III), which are expected to dominate the aqueous chemistry of Fe under hyperalkaline conditions.

In the present study, the solubility of magnetite was investigated at 22 ± 2 °C under inert gas (Ar) atmosphere (O$_2$ < 2 ppm). Batch solubility experiments were performed from undersaturated conditions with hydrothermally prepared -Fe$_3$O$_4$(cr) [3]. Independent samples were prepared within $8 \leq pH_c \leq 13$ ($pH_c = -\log [H^+]$) in 0.1 M NaCl–NaOH solutions. Three different redox systems were defined: S1. -Fe$_3$O$_4$(cr); S2. -Fe$_3$O$_4$(cr) + Fe(cr) and S3. -Fe$_3$O$_4$(cr) + 0.01 M SnCl$_2$. pH, pe (as pe = 16.9·E_h) and [Fe]$_{tot}$ were monitored at regular time intervals. Dissolved [Fe]$_{tot}$ was measured after 10 kD ultrafiltration by Sector Field ICP–MS at medium and high resolution mode. Solid phases of selected solubility samples (pH$_c$ = 9, 12.5) were characterized by XPS, XRD, SEM–EDS and AFM.

Very low and reproducible E_h values ($0 \leq (pe+pH) \leq +2$) are measured for the magnetite systems in the presence of SnCl$_2$. The redox conditions in the system Fe(cr)– -Fe$_3$O$_4$(cr) evolve from (pe+pH$_c$) ~ −1 (at $8 \leq pH_c \leq 9$) to (pe+pH$_c$) ~ +3 (at $12 \leq pH_c \leq 13$). Together with SEM–EDS observations, these results imply the possible passivation of the Fe(cr) surface under hyperalkaline pH conditions. Pure magnetite systems retain higher E_h values throughout the complete pH-range evaluated, (pe+pH$_c$) ~ +4. XRD confirms the presence of magnetite in all samples. XPS measurements indicate that both the starting material and most of the samples after initiated the solubility experiment have a content of 28 ± 3 % Fe(II) in relation to Fe$_{tot}$ on the solid surface, thus approaching the value ideally expected for pure magnetite (33.3 %). The Fe(II) content increases to 34 ± 3 % in the more reducing samples (presence of SnCl$_2$), where traces of Fe(0) are also observed. A particle size of 60–120 nm is quantified by SEM–EDS, AFM and XRD, without significant changes appearing with respect to the initial material. A very significant decrease in the solubility with a log [Fe]$_{aq}$ *vs.* pH$_c$ slope of −2 / −3 takes place within $8 \leq pH_c \leq 9.5$. For the same pH-region, the solubility significantly increases with decreasing E_h, according with the sequence S2 > S3 >> S1. A solubility control exerted by the reaction -Fe$_3$O$_4$(cr) + 8H$^+$ + 2e$^-$ $\Leftrightarrow$ 3Fe^{2+} + 4H$_2$O is proposed for this pH region. Aqueous iron concentration above pH$_c$ ~10 remains below 10^{-7} M and shows relatively large dispersion, but qualitatively confirms the formation of negatively-charged Fe(II) hydrolysis species above pH$_c$ ~11.5.

[1] Duro, L., Domènech, C., Grivé, M., Roman-Ross, G. Bruno, J and Kallström, K. (2014). Appl. Geochem. Vol. 49, pp. 192-205.

[2] Lemire, R., Berner, U., Musikas, C., Palmer,D., Taylor, P., Tochiyama, O. (2013) Chemical Thermodinamics 13a. Chemical Thermodynamics of Iron. NEA OECD

[3] Schwertmann, U., Cornell, R.M. (2000). Weinheim; New York: Wiley-VCH.

INFLUENCE OF RADIATION DAMAGE ON SORPTION CAPACITY AND REDOX REACTIVITY OF SHEET SILICATES IN A GDF ENVIRONMENT

C.I. Pearce[1]*, W.R. Bower[2], J.F.W. Mosselmans[3], A.D. Smith[4], S.M. Pimblott[4], A.P. Sims[1], A. Yorkshire[1], R.A.D. Pattrick[2]

[1]Dalton Nuclear Institute & School of Chemistry, The University of Manchester, UK
[2]Research Centre for Radwaste Disposal & Williamson Research Centre, School of Earth, Atmospheric and Environmental Sciences, The University of Manchester, UK
[3]Diamond Light Source, Harwell, UK
[4]Dalton Cumbrian Facility, Dalton Nuclear Institute, Westlakes Science Park, UK

Phyllosilicates will be at the frontline of the battle to safely contain radioactive wastes in a geological disposal facility (GDF) for hundreds of thousands of years. It is essential that we understand how clays and micas behave in a GDF where, apart from physicochemical conditions, they will be subjected to radiation damage over long timescales. Radiation damage will affect the physical integrity of these materials, and therefore their interaction with escaped radionuclides. Phyllosilicates will play a major role in containment in two critical areas of a GDF: (i) as the principal component of the engineered back-fill material surrounding steel/copper canisters containing the highest level radioactive wastes; and (ii) in the far-field where clays and micas will be the most reactive constituents of the host lithology. Understanding radiation damage effects across the components of both engineered and natural 'barriers' is highlighted as a major requirement for the UK's GDF safety assessment [1].

We have used controlled α-particle irradiation with the 5MV tandem ion accelerator at the Dalton Cumbrian Facility (NDA/University of Manchester), coupled with microfocus XAS/XRD (I18, Diamond Light Source) to obtain insights into radiation damage effects in model phyllosilicates [2]. Analysis of biotite mica after receiving a cumulative dose of $\sim 10^{16}$ He^{2+} ions over an area of $\sim 1.4 cm^2$ reveals the development of new domains of damaged biotite structure with evidence of high densities displaced atoms due to nuclear collisions. The structural integrity of clay minerals and micas, in particular the interlayer spacing, is highly susceptible to α-particle radiation damage; XRD studies demonstrate the vulnerability of interlayers to collapse even at relatively low doses. Fe K-edge XANES spectra show clear changes in short range order with a shift in the white line to lower energies, indicating a lowering of the average binding energy and therefore an increase in the electron density of the Fe component in the phyllosilicate structure as a result of α-particle bombardment. Adsorbed redox-active species have the potential to react with this structural Fe and reductive precipitation is likely to have a significant influence on the migration behaviour of redox-active radionuclides in the GDF.

Due to their characteristic swelling properties, which results in high sorption capacity for radionuclides, phyllosilicates are expected to play a key role in retaining risk-driving elements within the GDF. In the present study, our aim is to examine the effect of α-particle damage in biotite, chlorite and natural dioctahedral smectites - montmorillonite, beidellite and nontronite – on sorption capacity and redox reactivity with respect to Tc(VII) (as the TcO_4^- pertechnetate anion), U(VI) (as the UO_2^{2+} uranyl cation) and Se(IV) (as the SeO_3^{2-} selenate anion). We will build on an understanding of the effect of α-radiation damage on the physical integrity and oxidation state of model phyllosilicates, extending into radiation-induced effects on sorption capacity and redox reactivity; this will be required to predict the long-term ability of phyllosilicates to perform their safety function of retaining radionuclides in the GDF near and far field.

[1] NDA/RWMD/009NDA Radioactive Waste Management Directorate Proposed Research and Development Strategy (2008)

[2] R.A.D. Pattrick et al. Mineralogical Magazine, 77, 2867–2882 (2013).

REDUCTION OF SE(IV) AND U(VI) BY IRON SULPHIDES: CONTROLLING FACTORS ON THE FINAL PRODUCTS

M. L Kang [(1)], B. Ma [(2)], F. Bardelli [(2)], F. R Chen [(3)], L. Charlet [(2)], C. L Liu [(4)]

[(1)] *Sino-French Institute of Nuclear Engineering and Technology, Sun Yat-sen University, Zhuhai 519082, China*
[(2)] *Environmental Geochemistry Group, ISTerre, University of Grenoble I, 38041 Grenoble, France*
[(3)] *Key Laboratory of mineralogy and Metallogeny, Guangzhou Institute of Geochemistry, Chinese Academy of Sciences, Guangzhou, 510640, China*
[(4)] *Radiochemistry and Radiation Chemistry Key Laboratory for Fundamental Science, College of Chemistry and Molecular Engineering, Peking University, Beijing, 100871, China*

Selenium (^{79}Se, $T_{1/2} = 3.77 \times 10^5$a) and uranium concerned in geological disposal of high-level radioactive waste (HLRW) are redox sensitive that can occur in several oxidation states. In reducing environments, their mobility in the geosphere is greatly attenuated [1, 2]. Therefore, redox reactions are important for assessing the risks of a nuclear waste repository, remediating a contamination site, forming Se/U ore deposits, and global U/Se cycling.

Pyrite (FeS_2) is the Earth's most widespread and abundant sulphide mineral and occurs in a range of geological environments, such as hydrothermal, sedimentary, and igneous settings [3]. In addition, pyrite occurs in granite and claystone, which are widely considered as host rocks for potential nuclear waste repositories [4, 5]. Pyrrhotite ($Fe_{1-x}S$, $0<x<0.125$), a major species among iron sulphides, is often accompanied by pyrite, marcasite, and magnetite [6]. From a thermodynamic point of view, both pyrite and pyrrhotite can reduce Se(IV) and U(VI) to $FeSe_2$ and UO_2, respectively (Figure 1).
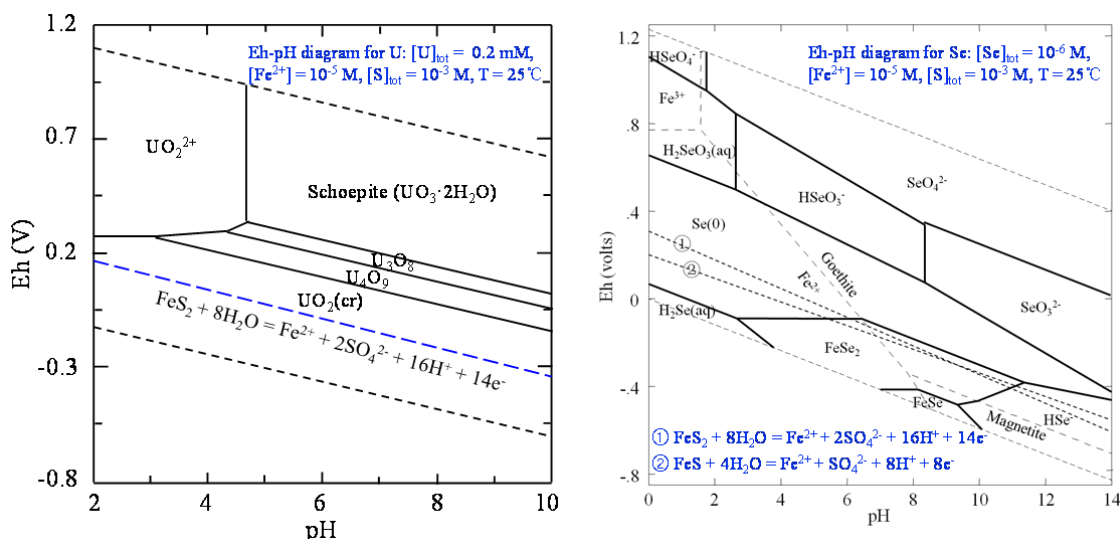
Figure1. Eh vs pH predominance diagrams for U (left panel) and Se (right panel).

In contrast to the thermodynamic calculations, as well as the prevalence of iron selenide phases observed in soil, sediments, and ore deposits, laboratory experiments performed on Se(IV) reduction by natural pyrite and pyrrhotite have found that Se(0) was the reaction product [7-9]. Formation of $FeSe_2$ was only observed on nanocomposite pyrite-greigite [10] and selenide-doted pyrite [11]. Our recent studies indicated that $FeSe/FeSe_2$ can be oxidized to Se(0) by Se(IV) with fast kinetics [12], and the reactivity of $FeSe_2$ is stronger than that of pyrite [13]. These observations indicate that reaction kinetics plays a significant role on the formation of $FeSe_2$ for Se(IV) reduction by iron sulphides. A more recent study further indicated that pH and reaction time also influence the final products (paper in preparing).

Theoretically, pyrite can reduce U(VI) to UO_2 in a wide pH range, however, a mixed U(IV) and U(VI) product (e.g., $U_3O_8/U_4O_9/U_3O_7$) was only observed at pH 6.21-8.63 and 4.52-4.83 for synthetic and natural pyrite, respectively [14]. The inhibition mechanism for U(VI) reduction by pyrite was analysed.

In summary, these studies give insight into the possible controls on the redox process of Se(IV) and U(VI) in the geosphere where iron sulphides present.

[1] Chen, F. R.; Burns, P. C.; Ewing, R. C. (1999). "^{79}Se: geochemical and crystallo-chemical retardation mechanisms." Journal of Nuclear Materials 275(1): 81-94

[2] Ragnarsdottir, K. V and Charlet, L. Uranium behaviour in natural environments. In Environmental Mineralogy: Microbial Interactions, Anthropogenic Influences, Contaminated Land and Waste Management; Cotter-Howells, J. D., Campbell, L. S., Valsami-Jones, E., Batchelder, M., Eds.; Mineralogical Society of Great Britain and Ireland: Middlesex 2000; pp 245-289

[3] Vaughan, D. J and Lennie, A. R (1991). "The iron sulfide minerals - their chemistry and role in nature". Science Progress 75 (298): 371-388

[4] Baeyens, B.; et al. In situ physico-chemical characterisation of Boom clay. In Radioactive Waste Management and the Nuclear Fuel Cycle; Harwood Academic Publishers: New York 1985; Vol. 6, pp 391−408.

[5] Gaucher, E.; Robelin, C.; Matray, J. M.; Negral, G.; Gros, Y.; Heitz, J. F.; Vinsot, A.; Rebours, H.; Cassagnabere, A.; Bouchet, A. (2004). ANDRA underground research laboratory: interpretation of the mineralogical and geochemical data acquired in the Callovian-Oxfordian formation by investigative drilling. Physics and Chemistry of the Earth 29 (1), 55-77

[6] Janzen, M. P.; Nicholson, R. V.; Scharer, J. M. (2000). "Pyrrhotite reaction kinetics: Reaction rates for oxidation by oxygen, ferric iron, and for nonoxidative dissolution." Geochimica et Cosmochimica Acta 64(9): 1511-1522

[7] Kang, M. L.; Chen, F. R.; Wu, S. J.; Yang, Y. Q.; Bruggeman, C.; Charlet, L. (2011). Effect of pH on Aqueous Se(IV) Reduction by Pyrite. Environmental Science & Technology 45 (7): 2704-2710

[8] Kang, M. L.; Bardelli, F.; Charlet, L.; Géhin, A.; Shchukarev, A.; Chen, F. R.; Morel, Marie-Christine.; Ma, B.; Liu, C. L. (2014). Redox reaction of aqueous selenite with As-rich pyrite from Jiguanshan ore mine (China): reaction products and pathway. Applied Geochemistry 47: 130-140

[9] Ma, B.; Kang, M. L.; Zheng, Z.; Chen, F. R.; Xie, J. L.; Charlet, L.; Liu, C. L. (2014). The reductive immobilization of aqueous Se(IV) by natural pyrrhotite. Journal of Hazardous Materials 276: 422-432

[10] Charlet, L.; Kang, M. L.; Bardelli, F.; Kirsch, R.; Géhin, A.; Grenèche, Jean-Marc.; Chen, F. R. (2012). Nanocomposite pyrite−greigite reactivity toward Se(IV)/Se(VI). Environmental Science & Technology 46: 4869-4876

[11] Diener, A.; Neumann, T.; Kramar, U.; Schild, D. (2012). Structure of selenium incorporated in pyrite and mackinawite as determined by XAFS analyses. Journal of Contaminant Hydrology 133: 30-39

[12] Kang, M. L.; Ma, B.; Bardelli, F.; Chen, F.; Liu, C. L.; Zheng, Z.; Wu, S. J.; Charlet, L. (2013). Interaction of aqueous Se(IV)/Se(VI) with FeSe/FeSe$_2$: Implication to Se redox process. Journal of Hazardous Materials 248-249: 20-28

[13] Ma, B.; Nie, Z.; Liu, C. L.; Kang, M. L.; Bardelli, F.; Chen, F. R.; Charlet, L. (2014). Kinetics of FeSe$_2$ oxidation by ferric iron and its reactivity compared with FeS$_2$. Science China-Chemistry 57 (9): 1300-1309

[14] Yang, Z. W.; Kang, M. L.; Ma, B.; Xie, J.; Chen, F. R.; Charlet, L.; Liu, C. L. (2014). Inhibition of U(VI) Reduction by Synthetic and Natural Pyrite. Environmental Science Technology 48 (18): 10716-10724

CHANGES TO URANIUM REDOX PROCESSES DUE TO SORPTION ONTO OR INCORPORATION INTO FE-BEARING MINERALS

Y. Wen[1], D. Hood[1], D. Renock[2], L. Shuller-Nickles[1]

[1]*Environmental Engineering and Earth Science, Clemson University, 342 Computer Court, Anderson, SC 29625, USA*
[2]*Department of Earth Sciences, Dartmouth College, 6105 Fairchild Hall, Hanover, NH 03755, USA*

Aqueous speciation of actinides, particularly oxidation state, controls mobility in aqueous systems. The mobility of aqueous actinyl species may be limited via incorporation into the bulk mineral or sorption onto mineral surfaces. In either case, the interaction between the actinyl and the mineral will alter the redox potential of the actinide species. Reduction to the tetravalent form on the mineral surface, in turn, reduces the mobility of the species. Of particular interest is the role of Fe-bearing minerals on the redox behavior of uranyl in aqueous systems. Fe-bearing minerals, such as hematite, have been shown to irreversible sorb aqueous uranyl, which can ultimately reduce to tetravalent U [1]. In addition, uranyl incorporated into hematite can be stabilized as U(V) longer than uranyl sorbed onto hematite [2]. In both cases, the Fe-bearing mineral hematite facilitates the stabilization of the uranium speciation, ultimately limiting mobility of the radionuclide.

In this work, we present an investigation of the effect of incorporation into hematite on the redox potential of uranyl, as well as the role of Fe-bearing minerals and aqueous Fe(II) concentration on the redox potential of aqueous uranyl species. The redox behavior of incorporated and sorbed uranium is investigated by coupling quantum-mechanical calculations with cyclic voltammetry (CV) measurements. Uranium-doped hematite powder was synthesized according to Duff et al. and Ilton et al. [2,3]. The resulting powder was rinsed several times using a carbonate wash followed deionized water to remove sorbed uranyl. The wash solutions were analyzed using ICP-MS for U and Fe content. The synthesized powders were analyzed using X-ray Diffraction and electron microscopy techniques. XRD results show shifts in the peak positions indicating changes to the unit cell parameters, likely caused by incorporation of U into the bulk structure. Additional peaks were present, indicating the possible presence of clarkeite, $(Na)(UO_2)O(OH)\cdot H_2O$; however, no evidence of this phase was observed from the microscopy. The symmetry of clarkeite (*R-3m*) and hematite (*R-3c*) are related in the ordering along the c-axis observed in the hematite structure. Thus, the presence of peaks associated with clarkeite in the XRD spectrum is indicative of the mechanism of U incorporation into hematite, which is supported from quantum-mechanical calculations.

The CV experiments are conducted using a standard three-electrode configuration, where the working electrode is a mineral powder microelectrode (PME). Compared with traditional mineral electrodes (either bulk or powder), the PME is easy to prepare, free of adhesive, and can efficiently limit mass transfer effects [4]. In addition, the PME enables for a wider scan range and higher scan rates, allowing for the investigation of a wider range of redox processes [5]. For both the sorbed and incorporated CV experiments, the system is preconditioned for 30 minutes at -0.25 V and scanned between ± 0.7 V with a scan rate of 50 mV/s. Under these conditions, initial reduction of U(VI) to U(IV) is observed based on the presence of the oxidation peak upon a positive voltage sweep. Subsequent scans shows the cycling between the U(VI)/U(V) redox couple. The anodic peak areas (1.12 E-08 J/s for incorporated uranium *versus* 1.35 E-08 J/s for sorbed uranium) indicate that comparable amounts of U(IV) are oxidized in both systems. However, the U(IV)/(VI) anodic peak potential is shifted from ~0.25 V for sorbed U to ~0.15 V for incorporated U. This shift indicates the favorability of U(IV) on the hematite surface *versus* incorporated into the hematite phase. The role of Fe(II) on the U redox potential was further evaluated via studies of aqueous uranyl on hematite, magnetite, and pyrite PMEs with changing Fe(II) concentration. Figure 1 shows the change in the U(IV)/U(VI) anodic peak on a magnetite PME with changing Fe(II) concentration, which indicates that the Fe(II) spiked into the solution facilitated U(VI) reduction during preconditioning.
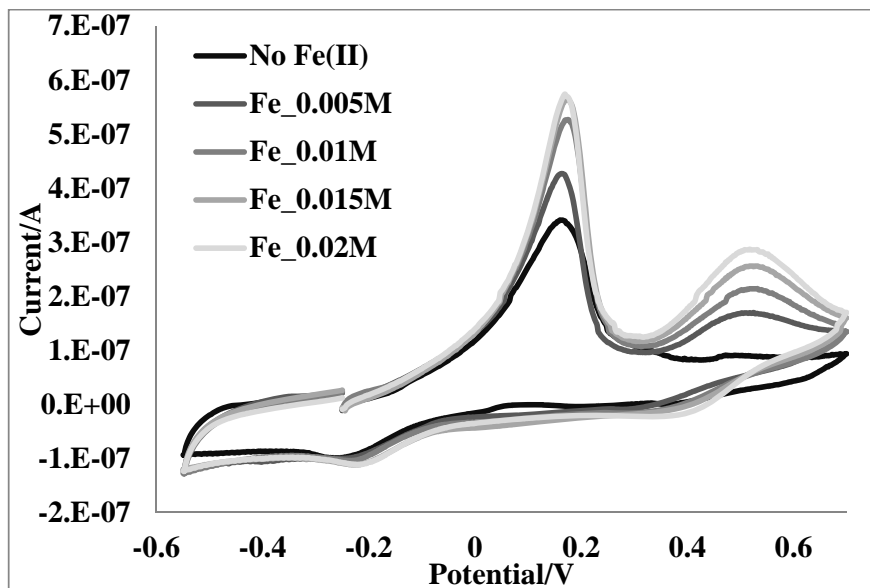
Figure 1. CV highlighting the U(IV)-U(VI) and Fe(II)-Fe(III) anodic peaks formed during initial cycle after spiking (and equilibrating) the analyte with increasing amounts of Fe(II).

References:

[1] Jeon, B.H.; Dempsey, B.A.; Burgos, W.D.; Barnett, W.O.; Roden, E.E. *Environmental Science and Technology* **2005**, *39*, 5642-5649.
[2] Ilton, E.S.; Pacheco, J.; Bargar, J.; Shi, Z.; Liu, J.; Kovarik, L.; Engelhard, M.; Felmy, A. *Environmental Science and Technology* **2012,** *46,* 2498-2436.
[3] Duff, M.; Coughlin, J.; Hunter, B. *Geochimica et. Cosomochimica Acta* **2002,** *66,* 3533-3547.
[4] Cachet-Viver, C; Vivier V.; Cha, C.; Nedelic, N.; Yu, L. *Electrochimica Acta.* **2001,** *47,* 181-189.
[5] Renock, D.; Mueller, M.; Yuan, K.; Ewing, R.; Becker, U. *Geochimica et. Cosmochimica Acta* **2013,** *118,* 56-71.

GENERATION AND STABILITY OF BENTONITE COLLOIDS

V. Suorsa[1], P. Hölttä[1], O. Elo[1], J. Lehto[1]

[1]University of Helsinki, Department of Chemistry, Laboratory of Radiochemistry, P. O. Box 55, FI-00014 University of Helsinki, Finland.

In Finland, the repository for spent nuclear fuel (SNF) will be excavated at a depth of about 500 meters in the fractured crystalline bedrock in Olkiluoto at Eurajoki, the site proposed by Posiva Oy. The spent uranium fuel placed in the final disposal tunnels in copper iron canisters will be surrounded with bentonite clay, which is assumed to be a potential source of colloids due to bentonite erosion. Colloids may effect on the migration of radionuclides and colloid-facilitated transport may be significant to the long-term performance of a spent nuclear fuel repository. The potential relevance of colloids for radionuclide transport is highly dependent on the release and stability of colloids in different chemical environments and their interaction with radionuclides. The objective of this work was to determine the bentonite erosion and stability of colloids generated from bentonite clay, which mainly consists of montmorillonite.

The bentonite materials investigated in the experiments were MX-80 Volclay powdered bentonite (76 % montmorillonite) or bentonite pellets and Nanocor PGN Montmorillonite (98 %). In batch type experiments, 1 g of bentonite powder or two pellets were placed in a sample tube where 50 mL of solution was added. The reference groundwater used was low salinity granitic Allard (I = 4.2 mM) and OLSO (I = 0.517 M), which simulates the current saline groundwater in Olkiluoto in oxic conditions. Diluted OLSO, NaCl and $CaCl_2$ electrolyte solutions (I = 1 mM – 0.1 M) were used to determine the stability of colloids as a function of ionic strength. The samples were stored for the sampling with and without agitation and the colloidal particle fraction was separated by centrifugation. The colloid generation and stability were followed as a function of time by analysing pH, particle size distribution applying the photon correlation spectroscopy (PCS) method and Zeta potential applying the dynamic electrophoretic mobility (Malvern Zetasizer Nano ZS). Colloid concentration was estimated using a standard series made from bentonite colloids and a count rate obtained PCS measurements or by analyzing the aluminum content of montmorillonite using ICP-MS.

Mean Zeta potential of colloids generated from bentonite powder in diluted OLSO reference groundwater is presented as a function of time in Figure 1 and the cumulative particle concentration in Figure 2. The cumulative particle concentration of colloids generated from bentonite pellets in 4.2 mM Allard and 1 mM OLSO, NaCl and $CaCl_2$ solutions without agitation are presented in Figure 3 and with gentle agitation in Figure 4. The colloidal dispersion has remained stable in low salinity solutions so far for almost four years and noticeable colloid generation occurred only in the most diluted (1 and 5 mM) solutions. The bentonite generation was significantly increased with the slow agitation. A thin layer between bentonite suspension and colloidal fraction was formed as a result of bentonite erosion via gel phase. The stability of bentonite colloids depended strongly on the ionic strength of the medium and the valence of the cation. Colloids were smaller and more stable in monovalent (Na^+) than in divalent (Ca^{2+}) dominated solutions. In low salinity solutions, high negative Zeta potential values, lower than -20 mV, indicated the existence of stable colloid dispersion. In more saline solutions, Zeta potential values were near zero indicating particle aggregation and instable colloids.

The results from bentonite colloid stability experiments are given and the importance of bentonite colloids to the migration of radionuclides in environmentally relevant conditions for SNF repository is discussed.
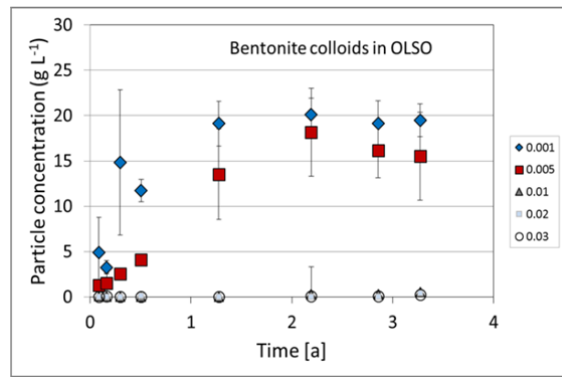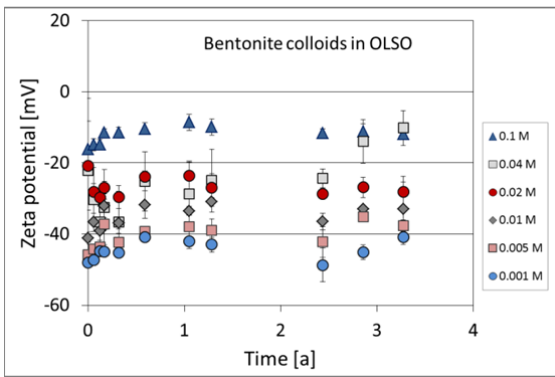
Figure 1 (left). Mean zeta potential of colloids generated from bentonite powder in diluted OLSO reference groundwater.

Figure 2 (right). Cumulative particle concentration of colloids generated from bentonite powder in diluted OLSO reference groundwater.

Figure 3 (left). Cumulative particle concentration of colloids generated from bentonite pellets in 4.2 mM Allard and 1 mM OLSO, NaCl and CaCl$_2$ solutions without agitation.

Figure 4 (right). Cumulative particle concentration of colloids generated from bentonite pellets in 4.2 mM Allard and 1 mM OLSO, NaCl and CaCl$_2$ solutions with gentle agitation.

SPECTROSCOPIC STUDIES ON U(IV) NANOPARTICLE FORMATION

UNDER MILD ACIDIC CONDITIONS

W. Cha[*], H.-R. Cho, E. C. Jung

Nuclear Chemistry Research Division, Korea Atomic Energy Research Institute,
989-111 Daedeok-daero, Yuseong-gu, Daejeon 305-353, Republic of Korea

Tetravalent uranium (U(IV)) is generally considered to form much less mobile phases than those of U(VI) owing to the low solubility of U(IV) solids. Recently, biotic or abiotic U(VI) reduction processes have been reported to result in the production of U(IV) nanoparticles (NPs) [1, 2], which may play an important role in uranium migration in an anaerobic groundwater environment. The concentration of dissolved U(IV) species including colloidal NPs or organic ligand complexes can be significant, as demonstrated in our previous studies on the microbe-mediated transformation of uranium [3, 4]. However, information regarding the role of dissolved U(IV) species (e.g., U^{4+} and $U(OH)^{3+}$) during their conversion process to U(IV) NPs is still limited. In this study, our aim is to investigate the kinetics of U(IV) NP formation from dissolved U(IV) species under mild acidic conditions ($\geq$ pH 2) and monitor the physico-chemical properties of the produced NPs, such as particle size, crystallinity, and redox states.

The kinetics of U(IV) hydrolysis reactions leading to the NP formation was monitored in situ using temperature-controlled cell blocks installed in a UV-Vis spectrophotometer. The U(IV) stock solution prepared by the electrochemical reduction of U(VI) in $HClO_4$ was diluted in an aqueous $NaClO_4$ medium to obtain various mild acidic samples ($\geq$ pH 2) and to initiate U(IV) hydrolysis and NP formation under argon atmosphere. The absorbance of the characteristic absorption bands of U^{4+} and $U(OH)^{3+}$ was measured over time and quantitatively analyzed. A monotonic increase of the background absorption was also examined as an indication of U(IV) NP(am) formation.

$$U^{4+} \rightarrow UOH^{3+} \rightarrow U(OH)_n^{4-n\,(n\geq2)} \rightarrow UO_2 \cdot xH_2O(am) \rightarrow UO_2(cr)$$
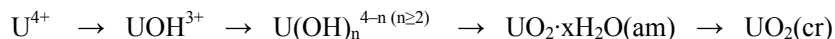
At an early stage the formation of intermediate U(IV) hydrolysis products, i.e., $U(OH)_n^{4-n\,(n\geq2)}$ is evident based on the growth of new absorption bands (λ_{max}, 260 nm and 669 nm) identified in this study. Although the corresponding hydrolysis product is not assigned yet, it is likely that its steady-state concentration is a key determinant of the NP formation rate, i.e., $d[UO_2 \cdot xH_2O(am)]/dt$. The dependency of the reaction rates on pH and temperature, and the candidate species responsible for the new absorption bands will be discussed in detail in this presentation. A TEM analysis of the collected NPs at different growth stages clearly demonstrates the production of the crystalline U(IV) NPs and the increase in the primary particle size (approximately 2 - 10 nm) over time. Additionally, the laser-induced breakdown detection (LIBD) technique is used to monitor the overall sizes of the primary particle aggregates (e.g., 80 - 500 nm).

The redox state of the produced NPs was also examined using time-resolved laser-induced fluorescence spectroscopy (TRLFS). Without the addition of reducing agents, the oxidation of U(IV) NPs was observed for NP samples aged up to several months in argon atmosphere. At pH 3.0 ± 0.1 the luminescece spectra resulting from the produced U(VI) species exhibit major spectral maxima at 493.0, 515.6 and 539.0 nm (λ_{ex} = 355 nm, $[U]_{total}$ = 1.1 x 10^{-4} M) with a lifetime of ~39 μs, which are distinct from those of UO_2^{2+} and U(VI) hydrolysis species [5, 6]. To discuss the speciation of U(VI) during this oxidation process we will determine the concentration of U(IV) and U(VI) using the previously developed method [4] and further analyze U(VI) luminescence spectra at various solution pHs.

[1] Y. Suzuki, S. D. Kelly, K. M. Kemner, J. F. Banfield, Nature 419, 134 (2002).
[2] D. R. Lovely, E. J. P. Phillips, Y. A. Gorby, E. R. Landa, Nature 350, 413 (1991).
[3] S. Y. Lee, W. Cha, J.-G. Kim, M. H. Baik, E. C. Jung, J. T. Jeong, K. Kim, S. Y. Chung, Y. J. Lee, Chem. Geol. 370, 40 (2014).
[4] W. Cha, S. Y. Lee, E. C. Jung, H.-R. Cho, M. H. Baik, J. Radioanal. Nucl. Chem. 302, 1127 (2014).
[5] V. Eliet, G. Bidoglio, N. Omenetto, L. Parma, I. Grenthe, J. Chem. Soc. Faraday Trans. 91, 2275 (1995).
[6] G. Bernhard, G. Geipel, V. Brendler, H. Nitsche, J. Alloy. Compd. 271-273, 201 (1998).

EVIDENCE FOR ORIENTATED ATTACHMENT GROWTH PROCESSES IN
THE HANFORD TANK SLUDGE

E. C. Buck,[*] R. S. Wittman, C. Z. Soderquist, B. K. McNamara

*Radiochemical Processing Laboratory, Pacific Northwest National Laboratory, 902 Battelle Blvd.,
Richland, WA, 99353, USA*

Approximately 190 million curies of radioactive material is currently stored at the Hanford Site in underground storage tanks. Most of the waste in these tanks is expected to be retrieved, treated onsite, and properly disposed of in proposed high-level and low-level repositories. The sludge waste in the tanks is highly heterogeneous. X-ray diffraction analysis of the sludge indicates that a sizeable fraction of the waste consists of very small amorphous and/or semi-crystalline particles. These particles have been examined by various micro-analytical methods, including electron microscopy, and their small size and variable composition has been confirmed [1-4].

The orientated attachment (OA) of colloids and nano-particles is now recognized as an important mechanism of crystal growth in many systems [5]. However, the mechanism of attachment and alignment processes remain poorly understood. We examined the nature of nano-particles from Hanford sludge, looking for potential evidence of OA processes. Surprisingly, we find little evidence of particle growth in these systems in spite of the lengthy time that these colloidal suspensions have existed.
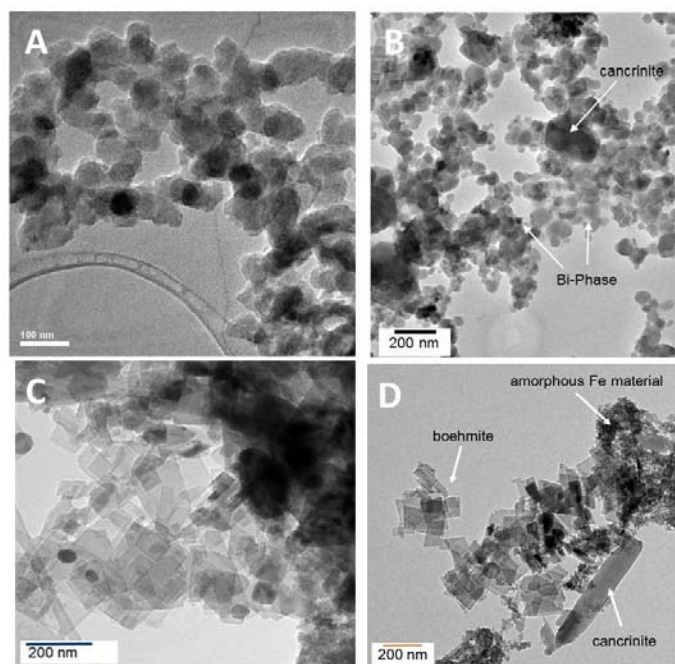
Figure 1. (A and B) Bismuth phosphate derived wastes showing particle agglomeration, (C and D) REDOX cladding waste sludge showing the nature of boehmite particles in the sludge.

Wastes from the bismuth phosphate separation processes have been found to contain an iron bismuth phase, possibly related to bismuthoferrite $[BiFe^{3+}_2(SiO_4)_2(OH)]$. This phase is present as agglomerates ranging up in size from a few nanometers (see Figure 1A and 1B). Cancrinite was identified with EDS and electron diffraction as large euhedral particles in many wastes. The lack of any ripening of these phases is extraordinary given the conditions of formation and duration in the Tanks.

Aluminum was added to the steel storage tanks, in part, to control corrosion by buffering the pH through dissolution/precipitation reactions involving minerals such as gibbsite $[Al(OH)_3]$ and boehmite (AlOOH), which are known to be the most prevalent aluminum-bearing minerals in Hanford high-level nuclear waste sludge (see Figure 1C and 1D). Reynolds and co-workers have also demonstrated that dawsonite $[NaAl(OH)_2CO_3]$ is another common Al-bearing phase in the Hanford tank sludge [4]. High concentrations of Al will be a problem for the planned internment of the high-level nuclear waste sludge in glass: although

aluminum is an essential component for a durable glass, excess aluminum is detrimental. Most aluminum phases will be dissolved and removed through caustic leaching; however, the boehmite nanoparticles in the sludge have been found to be extremely resistant to caustic leaching in spite of their small size.

TEM examination of these systems has failed to identify evidence of OA processes. It is possible that the lack of crystal growth may be due to the role of radiolysis in this environment. In this paper, we will present evidence of OA growth processes in the sludge wastes and describe the possible role of radiolysis on this system.

[1] Rapko B. M., Lumetta, G. J., Deschane, J. R., Peterson, R. A., Process Development for Permanganate Addition During Oxidative Leaching of Hanford Tank Sludge Simulants. *Separation Science and Technology* **43**(2008) 2840-2858.

[2] Lumetta, G. J., Rapko, R. M., Removal of Chromium from Hanford Tank Sludges. *Separation Science and Technology* **34**(1999)1495-1506.

[3] Cantrell, K. J., Um, W., Williams, B. D., Bowden, M. E., Gartman, B. N. Lukens, W. W., Buck, E. C., Mausolf, E. J., Chemical Stabilization of Hanford Tank Residual Waste. *Journal of Nuclear Materials* **446** (2014) 246-256

[4] Reynolds, J. G., Cooke, G. A., Herting, D. L., Warrant, R. W., Evidence for dawsonite in Hanford high-level nuclear waste tanks, *J. Hazard. Mater.* **209-210** (2012) 186-192.

[5] Li, D., Nielson, M. H., Lee, J. R. I., Frandsen, C., Banfield, J. F., De Yoreo, J. J., Direction-specific interactions control crystal growth by oriented attachment, *Science*, **336** (2012) 1014-1018.

THE INFLUENCE OF pH ON DIFFUSION OF ^{129}I AND ^{79}Se IN BEISHAN GRANITE UNDER AEROBIC AND ANAEROBIC CONDITION

USING THE "CAPILLARY METHOD"

J.G. He[1], B. M[1], W.Y. Tian[1], L.Y. Qi[1], Liu[1,*]

1.Beijing National Laboratory for Molecular Science, Radiochemistry & Radiation Chemistry Key Laboratory for Fundamental Science, College of Chemistry and Molecular Engineering, Peking University, Beijing 100871, P.R. China

The deep geological disposal is the best way to deal with high level radioactive waste (HLW) in the world and the multi-barrier concept was adapted to overcome the disposal difficulties of HLW into geological formations. It is imperative to investigate the diffusion and the migration of radionuclides in the clays or host rocks for assessing the long-term performance of radioactive waste repositories [1]. In China, Gansu Beishan has been pre-selected as the site for the potential HLW repository and Beishan granite is the most important host rock.

The 'in-diffusion' method is a vital way to study the diffusion behavior of radionuclides. The results from the capillary method show that it is a fast and easy method to study the diffusion and the migration of radionuclides in the clays or host rocks [2]. The method allows us to study the influence of pH、temperature、Ionic strength、isotopic carrier、anaerobic condition and irradiation simultaneously. Fission product ^{129}I and ^{79}Se have very long half-life and mostly exists as anions under environmental conditions of geological repository. Iodine presents as iodide in the whole pH spectrum in aqueous solution under 298 K when the Eh is between +0.2 and -0.2 V [3]. Chemical forms of Se in natural waters are governed by various physicochemical factors including oxidation–reduction status、pH and adsorption behavior. Oxidation of the less soluble forms of Se such as selenides and elemental Se^0 leads to the more soluble anions. This study was focused on the selenite anion (SeO_3^{2-}), since it is expected to be very mobile in rocks found around the underground depositories (clays or granite) whose major components present a very low affinity toward anions [4].

In the past work, the influence of pH、temperature、Ionic strength、isotopic carrier and Iodine ion concentration on the diffusion of ^{129}I in compacted bentonite have been studied using capillary method systematically and this study mainly focuses on the diffusion of ^{129}I and ^{79}Se in Beishan granite.

One of the first objectives was to investigate the pH influence during the diffusion of ^{129}I and ^{79}SeO_3^{2-}$. By fitting the experimental data using a procedure provided by Xiangyun Wang, we can obtain the apparent diffusion coefficient Da and distribution coefficient K_d of ^{129}I and ^{79}SeO_3^{2-}$ in Beishan granite. On the other hand, so for, there are few researchers to study the diffusion of key nuclides under anaerobic condition. Therefore, some work about the diffusion of ^{129}I and ^{79}SeO_3^{2-}$ under anaerobic condition to investigate the influence of oxygen during the diffusion have been done.

The final results indicate that pH doesn't affect the diffusion of ^{129}I, and the apparent diffusion coefficient Da of ^{129}I is about to 10^{-9} m²/s under aerobic or anaerobic condition. Nevertheless, pH and oxygen have a great impact on the diffusion of ^{79}SeO_3^{2-}$. The Da values at different pH for ^{75}SeO_3^{2-}$ in Beishan granite was shown in Figure 1. On one hand, we can see that the apparent diffusion coefficient Da presented a decreasing tendency firstly, then increased to a platform and the apparent diffusion coefficient Da have a maximum value when the pH is about 5 with the pH increasing either aerobic or anaerobic condition. On the other hand, it can be seen that the apparent diffusion coefficient $D_a (10^{-11} m^2/s)$ of ^{75}SeO_3^{2-}$ under anaerobic condition is larger than the apparent diffusion coefficient $D_a (10^{-12} m^2/s)$ of ^{75}SeO_3^{2-}$ under aerobic condition one order of magnitude in Beishan granite. Moreover, the distribution coefficient K_d of ^{75}SeO_3^{2-}$ on Beishan granite show the opposite tendency while the pH increased. These results can be explained by the adsorption behavior and redox. We know that the content and the form of some reducing ion such as Fe^{2+} will be different under anaerobic and aerobic conditions with different pH so that the adsorption behavior and the redox will affect the diffusion.
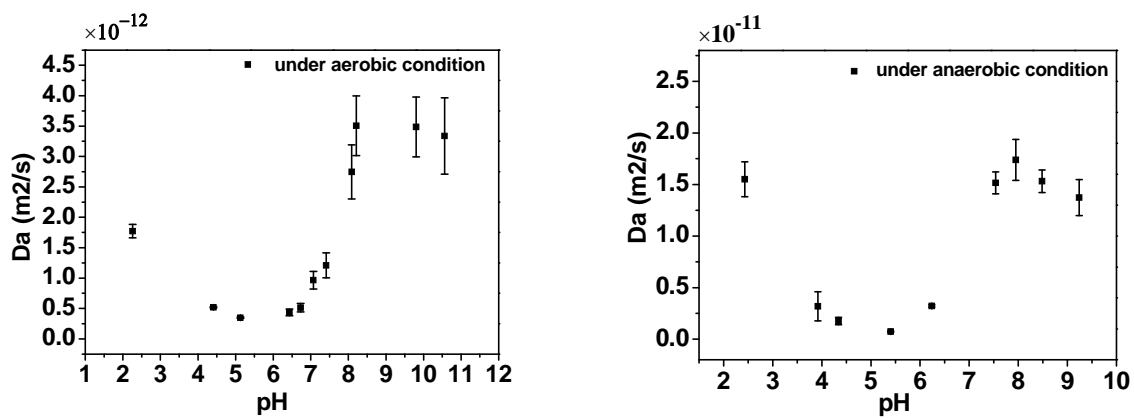
Figure1. Da value of $^{75}SeO_3^{2-}$ in Beishan granite as a function of pH under aerobic and anaerobic condition

[1] Lee, C.-P., et al., *Diffusion of cesium and selenium in crushed mudrock.* Journal of Radioanalytical and Nuclear Chemistry, 2009. **279**(3): p. 761-768.

[2] Wang, X.K., et al., *The concentration and pH dependent diffusion Of Cs-137 in compacted bentonite by using capillary method.* Journal of Nuclear Materials, 2005. **345**(2-3): p. 184–191.

[3] Wenyu Tian, et al., *The effect of ionic strength on the diffusion of 125I in Gaomiaozi bentonite.* Journal of Radioanalytical and Nuclear Chemistry, 2012.

[4] Duc, M., G. Lefèvre, and M. Fédoroff, *Sorption of selenite ions on hematite.* Journal of Colloid and Interface Science, 2006. **298**(2): p. 556-563.

ANISOTROPY OF DIFFUSION THROUGH BOOM CLAY

<u>Y. Akagi</u>[1], N.Watanabe[2], T. Kozaki[2], S. Ueta[1],
H. Kato[1], S. Shimoda[1], M. Ochs[3], S. Brassinnes[4]

[1]*Mitsubishi Materials Corporation, Naka Energy Research Center,*
1002-14 Mukohyama, Naka-shi, Ibaraki-ken, 311-0102 Japan,
[2] *Hokkaido University Faculty of Engineering, Laboratory of Nuclear and Environment Materials,*
Kita 13, Nishi 8, Kita-ku, Sapporo, Hokkaido, 060-8628 Japan,
[3]*BMG Engineering Ltd/Arcadis, Ifangstrasse 11, CH-8952 Schlieren, Zürich, Switzerland,*
[4]*ONDRAF/NIRAS, Geological Disposal, R&D,*
Avenue des Arts 14, 1210 Saint-Josse-ten-Noode, Belgium

The Boom Clay formation is one of the potential host rocks for the geological disposal of radioactive waste in Belgium. It has a remarkable bedding structure and the sediment strata are sub-horizontal in the region of interest. For the performance assessment of potential disposal systems, it is very important to acquire the data for water movement and nuclide migration. Among these data, hydraulic conductivity, diffusion coefficients of non-sorbing elements and anisotropy of permeability and diffusion are the most fundamental parameters. The hydraulic conductivities of various Boom Clay layers have been measured for many years. In case of less sandy material such as the Putte and Terhagen members in the Boom Clay, the average hydraulic conductivity parallel to the Boom Clay strata is approximately two times larger than the average hydraulic conductivity vertical to the strata [1]. Diffusion coefficients for an inert tracer were measured in high pressure-percolation experiments using tritiated water. The pore diffusion coefficients were calculated from the dispersion coefficients by a linear function formula [2]. The calculated diffusion coefficient parallel to horizontally oriented strata, D_h, were found to be two to three times larger than the diffusion coefficient vertical to the strata, D_v [3]. However, the direct measurement of the diffusion coefficient in experiments using passive diffusion has not yet been conducted. At the same time, only few Boom Clay samples have been analysed to date, and further data are needed to allow an evaluation of the variability of diffusion properties within the Boom Clay formation.

We conducted different diffusion experiments in the laboratory to measure D_h and D_v of several Boom Clay samples. The specimens for the experiments were prepared from different Boom Clay cores drilled from the Belgian underground research laboratory, HADES, located in Mol. The diffusion experiments were carried out using two different types of experimental set-ups. In-diffusion experiments were used to measure the apparent diffusion coefficient, Da [4]. Through-diffusion experiments were used to measure the effective diffusion coefficient, De [5]. In both diffusion experiments, both horizontally and vertically oriented specimens were examined. Synthetic Boom Clay water [6] was used in all experiments.

Figure 1 shows a typical experimental set-up of an in-diffusion experiment. A trace amount of tritiated water was placed in the center of the specimen to allow the diffusion of tritiated water toward both ends of the specimen. After an appropriate length of time had elapsed, the concentration profile in the specimen was analysed and the apparent diffusion coefficients were calculated from the profile. Figure 2 shows the apparent diffusion coefficients measured in in-diffusion experiments. The values of Da_h are approximately three times larger than those of Da_v, showing clearly anisotropy of diffusion.

In the present contribution, effective diffusion coefficients measured in through-diffusion experiments are reported and compared to apparent diffusion coefficients. The effect of geometric structure of clay layer and other findings are further discussed with respect to heterogeneity/homogeneity of the Boom Clay.

Boom Clay
(imaging horizontal sample)

Tracer (HTO)
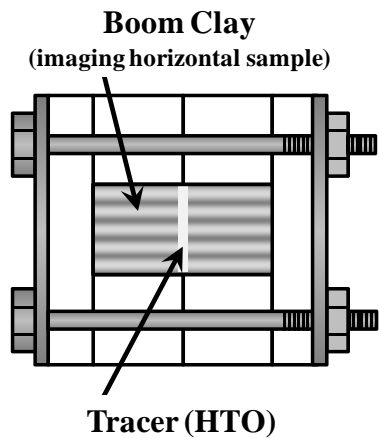
Figure 1. Typical experimental setting of
an in-diffusion experiment.
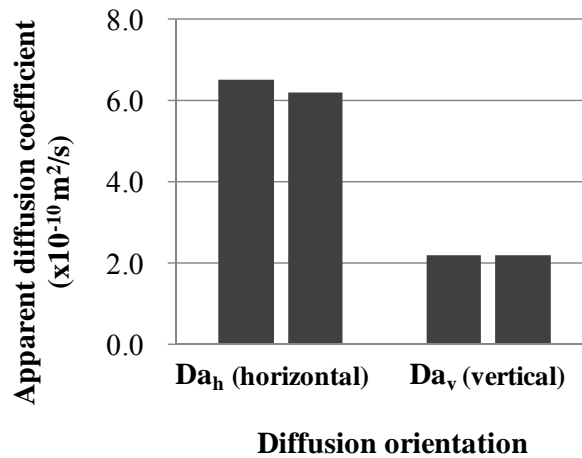
Figure 2. Apparent diffusion coefficient of
Boom Clay.

[1] Yu L., Gedeon M., Wemaere I., Marivoet J., De Craen M. (2011). "Boom Clay Hydraulic Conductivity – a synthesis of 30 years of research." External Report of Belgian Nuclear Research Centre, SCK•CEN-ER-122.

[2] Put M. J., Monsecour M. (1991). "Estimation of the migration parameters for the Boom clay formation by percolation experiments on undisturbed clay cores." Material Research Society Symposium proceedings 212: 823-829.

[3] Bruggeman C., Maes N., Aersten M., De Canniére P. (2009). "Tritiated water retention and migration behaviour in Boom Clay." ONDRAF/NIRAS report, NIROND-TR 2009-16E.

[4] Kozaki T., Sato Y., Nakajima M., Kato H., Sato S., Ohashi H. (1999). "Effect of particle size on the diffusion behavior of some radionuclides in compacted bentonite." J. Nucl. Mater. 270: 265-272.

[5] Kato H., Muroi M., Yamada N., Ishida H., Sato H. (1995). "Estimation of effective diffusivity in compacted bentonite." Material Research Society Symposium proceedings 353: 277-284.

[6] De Craen M., Wang L., Van Geet M., Moors H. (2004). "Geochemistry of Boom Clay pore water at the Mol site." Scientific Report of Belgian Nuclear Research Centre, SCK•CEN-BLG-900.

DO DIFFERENT TYPES OF DIFFUSION EXPERIMENTS IN CLAY LEAD TO CONSISTENT RESULTS?

M. Aertsens, L. Van Laer, N. Maes

Institute for Environment, Health and Safety, Belgian Nuclear Research Centre, SCK•CEN, Boeretang 200, B-2400 Mol, Belgium

Clay layers are studied in many countries as possible host formations for the final disposal of nuclear waste. Transport of radionuclides in clays is dominated by diffusion. Therefore, it is essential to know the values of the parameters determining diffusive transport: (1) the apparent diffusion coefficient D_{app}, and (2) the capacity factor ηR, being the product of the diffusion accessible porosity η and the retardation factor R.

These transport parameters can be determined in lab experiments as well as in in-situ experiments. Classical lab experiments consist of (1) pure diffusion experiments, with a concentration gradient only, and (2) tests with an additional pressure gradient [1]. Through-diffusion and 'back to back diffusion' (where initially all tracer is in a thin slice between two clay cores) are examples of pure diffusion experiments. Back to back diffusion experiments with an additional pressure gradient are called 'percolation experiments'. In pulse migration experiments, a pulse of radionuclide tracer is injected at one side of a clay core. The tracer amount that elutes at the other side of the clay core by diffusion and advection is monitored as a function of time (breakthrough curve).

Consistency requires that each type of experiment leads to the same transport parameter values. Another necessity is that the same set of transport parameters predicts well all evolutions in the same experiment, e.g. in a through diffusion experiment: the evolution of the inlet concentration, the evolution of the outlet concentration and the tracer concentration in the clay at the end of an experiment. A factor complicating a consistency check of the type of experiment is the heterogeneity of natural clays. To avoid this problem, different types of experiments can be performed on the same core.

For Boom Clay a whole series of different types of experiments were conducted with HTO. Based on a series of thirty eight pulse injection experiments on Boom Clay cores sampled over the entire thickness of Boom Clay at Mol (Mol-1 coring) average values of $\eta R = 0.37$ and $D_{app} = 2.4 \ 10^{-10} \ m^2/s$ [2] were obtained. These values predict well the concentrations in two large-scale in-situ experiments [3, 4]. From these in situ experiments, D_{app} values were fitted in the range $D_{app} = 2.0 – 2.8 \ 10^{-10} \ m^2/s$ (fixed $\eta R = 0.37$) [3, 4]. Two back to back diffusion experiments lead to $D_{app} = 2.3 \ 10^{-10} \ m^2/s$ and $D_{app} = 3.6 \ 10^{-10} \ m^2/s$ respectively. Seven through diffusion experiments, where both the inlet and the outlet evolution are fitted simultaneously, lead to an average $D_{app} = 3.8 \ 10^{-10} \ m^2/s$ (about 50 % higher than the average from the pulse injection experiments) and $\eta R = 0.38$. Because this concerns an average of seven experiments, the higher D_{app} value cannot be attributed to heterogeneity alone. The model used for fitting the pulse injection experiments [5] underestimates the D_{app} value, because it considers the filters confining the clay cores as mixing volumes, while more recent experiments [6] show that diffusion through the filters must be taken into account. Therefore, the pulse injection experiments need to be reevaluated with an adapted model.

Also for Sr-85, different types of diffusion experiments on Boom Clay samples were done: a percolation experiment, an in situ experiment, three through diffusion experiments of the VC-CC type [7] and a diffusion experiment of the VC-VC type [7]. The experiments lead to a quite narrow range for D_{app} values: 6-11 10^{-12} m^2/s. However, the values for the capacity factor differ. The error on the capacity factors derived from the percolation and the in situ experiment is too large to consider these values reliable. In the through diffusion experiments, the evolution of the inlet concentration and of the outlet concentration as well as the tracer profile in the clay at the end of the experiments are all fitted simultaneously but this still leads to values for the capacity factors in the range 1000-8000.

In order to rule out the effect of heterogeneity, inherently present when using natural clay samples, studies are done on homogenized illite. Nine through diffusion experiments with strontium in illite lead to a higher apparent diffusion coefficient ($D_{app} \approx 0.9$-1.4 $10^{-11} \ m^2/s$) than a back to back experiment ($D_{app} = 1.8 \ 10^{-11}$ m^2/s). In a last step to check consistency between through diffusion and pulse injection tests, both techniques are performed on the same clay cores (samples from Ypresian clays (Kallo-1 drilling) with HTO and iodide (through diffusion tests on-going).

Summarizing, for the presently available results, the different (types of) diffusion experiments generally lead to the similar values for the apparent diffusion coefficient within a range of roughly 50 %.

ACKNOWLEDGEMENT

[1] M. Aertsens, P. De Cannière, K. Lemmens, N. Maes, H. Moors, Phys. Chem. of the Earth, 33, 1019 (2008).
[2] M. Aertsens, M. Put, A. Dierckx, in *Modelling of transport process in soils at various scales in time and space*, ed. J. Feyen, K.Wiyo, (Leuven, Belgium, 24-26 November 1999), 67.
[3] M. Aertsens, N. Maes, L. Van Ravestyn, S. Brassinnes,,Clay Minerals, 48-2, 153 (2013).
[4] E. Weetjens, N. Maes, L. Van Ravestyn, Geol. Soc. Special Publication , 400, 616 (2014).
[5] M. Aertsens, M. Put and A. Dierckx, J. Cont. Hydrology 61, 423 (2003).
[6] M. Aertsens, J. Govaerts, N. Maes, L. Van Laer, Mat. Res. Soc. Symp. Proc., 1475, 583 (2011).
[7] Takeda M., Nakajima H., Zhang M., Hiratshuka T., J. Cont. Hydrology, 97, 117 (2008).

FORMATION FACTOR AND PORE STRUCTURE OF CRYSTALLINE ROCK FROM OLKILUOTO OBTAINED BY ELECTRICAL METHODS AND C-14-PMMA AUTORADIOGRAPHY

J. Ikonen[(1)], J. Sammaljärvi[(1)], M. Voutilainen[(1)], M. Siitari-Kauppi[(1)] M. Löfgren[(2)] L. Koskinen [(3)]

[(1)] *Department of Chemistry, University of Helsinki, P.O. Box 55, 00014 University of Helsinki, Finland*
[(2)]*Niressa AB, P.O. Box 3081, 14503 Norsborg, Sweden*
[(3)]*Posiva Oy, Olkiluoto, 27160 Eurajoki, Finland*

Solute exchange between flowing groundwater and the pore water of the rock matrix is of importance for many types of contaminant transport problems, as well as for the characterisation of nuclear waste depositories. In sparsely fractured crystalline rock, such as gneiss and granite, the flowing groundwater is constrained to fractures that are surrounded by low-porous rock where the pore water is effectively stagnant. Radionuclides usually migrate in such rock at much lower speed than the velocity of the flowing water due to retention caused by matrix diffusion and sorption. A project "rock matrix REtention PROperties" (REPRO) at ONKALO, the underground rock characterization facility in Olkiluoto, consists of an extensive series of in-situ measurements that are supplemented by laboratory measurements and estimates of the rock matrix retention properties. Laboratory experiments for studying the formation factor, pore structure and the iodine diffusion were performed by electrical methods, C-14-PMMA autoradiography and electron microscopy. The aim was to connect the structure properties of the rock to formation factors from electrical methods.

Firstly, in the electrical formation factor (F_f) measurement, the porous system of the rock sample is saturated by electrolyte solution with known conductivity. By measuring the conductivity over the rock sample and by taking the ratio of the rock and electrolyte conductivity, the apparent formation factor is obtained from which the effective diffusion coefficient (D_e) can be derived [1]. Secondly, the iodine diffusivity (I D_e) was measured by through electromigration (TEM) technique. In both experiments the rock sample is placed between two compartments, and the electrical potential gradient over the sample is achieved by placing an electrode in each electrolyte and connecting the electrodes to a direct current power supply. In iodine TEM measurement one compartment contains electrolyte solution with high iodine concentration and the other contains electrolyte solution initially free of iodine. During the experiment, the iodine will migrate into the porous system of the rock with the electrical potential gradient as the main driving force. This way migration of iodine can be enhanced by a factor of 1000 compared to conventional through-diffusion methods in water phase.

The pore structure characterisation methods used here are C-14-PMMA autoradiography and electron microscopy. C-14-PMMA autoradiography method is based on impregnating C-14-labelled organic molecule into the rock and fixing it in place using polymerisation reaction. After the polymerisation, cross-section of the sample can be placed on autoradiographic film for imaging. The beta radiation from the labelled compound causes the film to darken in locations where it is present, and the intensity of this process is relative to the amount of C-14-MMA in that location. Therefore, optical densitometry and a set of C-14-PMMA activity standards can be used to establish the relationship between the gray scale values of the image and the spatial activity distribution in the sample. When the density of the sample material is known, the gray values of the image can be used to visualise the pore network and calculate porosity distribution of the sample on centimeter scale. The autoradiographed rock surfaces are analysed by electron microscopy to study the pore apertures and mineral specific porosities in more detail.

Two drill cores were studied, ONK-PP318, which is pegmatitic granite and ONK-PP323, which is veined gneiss. Porosity, formation factor, effective diffusion coefficient derived from formation factor and effective diffusion coefficients of iodine obtained using TEM method (I D_e) for these rocks are presented in table 1. Even though the porosity is low (~1 %) for both samples, the formation factors and effective diffusion coefficients are notably different. This can be explained by the different pore networks of the samples. ONK-PP318 has coarse grains with little intragranular porosity and there are large connected pores throughout the sample. This translates into more conductivity for water. There are also only a few mineral grains of high intragranular porosity. ONK-PP323 on the other hand has many medium sized grains with narrow cracks between them, and abundance of highly porous minerals. Medium sized grains and narrow pores mean that the path is constricted and tortuous. Both constrictivity and tortuosity are contained in the formation factor and the autoradiography highlights what the difference in formation factor values truly means.

Table 1. Porosity [2], formation factor (F_f), effective diffusion coefficient derived from formation factor (D_e) and effective diffusion coefficients of iodine obtained using TEM method (I D_e)

	Porosity / %	F_f	D_e / m²/s	I D_e / m²/s
ONK-PP318	0.50 mean with range of 0.30-0.75	$6.5\pm1.2\times10^{-4}$	$1.1\pm0.2\times10^{-12}$	$1.9\pm0.7\times10^{-12}$
ONK-PP323	0.73 mean with range of 0.30-1.30	$2.6\pm1.5\times10^{-4}$	$4.4\pm2.6\times10^{-13}$	$4.9\pm3.8\times10^{-13}$

[1] Löfgren, M, Neretnieks, I, 2006**.** Through-electromigration: A new method of investigating pore connectivity and obtaining formation factors. J. Contam. Hydrol, Vol. 87(3–4), pp. 237–252.

[2] Sammaljärvi, J., Ikonen, J., Voutilainen, M., Kuva, J., Lindberg, A., Siitari-Kauppi, M., Timonen, J., (2014). "Investigation of rock matrix retention properties. Supporting laboratory studies I: Mineralogy, porosity and pore structure." Posiva working report 2014-68.

TOMOGRAPHIC INVESTIGATION OF CAESIUM MIGRATION IN OLKILUOTO VEINED GNEISS AND GRIMSEL GRANODIORITE

J. Kuva[1], M. Voutilainen [2], J. Parkkonen [1], T. Turpeinen [1], M. Siitari-Kauppi [2], J. Timonen [1]

[1]University of Jyvaskyla, Department of Physics, P.O. Box 35, 40014 University of Jyvaskyla, Finland
[2] University of Helsinki, Department of Chemistry, P.O. Box 55, 00014 University of Helsinki, Finland

The Finnish plan for the final disposal of nuclear waste is an underground repository in crystalline bedrock in Olkiluoto. In the safety analysis of the repository, capacity of the bedrock to retard radionuclides if they leak into the groundwater is an important factor. There are still many uncertainties concerning e.g. groundwater transport routes and bedrock porosity, which have caused the present safety analyses to consciously underestimate the retarding capacity of the bedrock. To gain more information on how the heterogeneous microscopic structure affects retardation, we set out to study element intrusion into rock samples with X-Ray microtomography (XμCT).

For the tracer we wanted to choose an element that is relevant to the safety case, and has a high enough atomic number and density compared to the most common elements in rock minerals to be distinguishable from XCT images. In the safety assessment of the spent nuclear fuel on a long-term basis ^{135}Cs is classified as a second (high) priority radionuclide. After the closure of the repository anionic highly mobile elements are expected to be a major dose source for humans. However the importance of ^{135}Cs arises from its high content in the spent nuclear fuel and a long physical half-life of 2.3×10^6 years, even though it is considered relatively immobile. Furthermore, caesium has a highly mineral-dependent sorption coefficient, which makes the rock matrix heterogeneous with respect to caesium retardation. The high aqueous solubility of caesium as CsCl also allowed for a high enough concentration for the experiment. There are two on-going in-situ transport experiments (Olkiluoto, Finland and Grimsel, Switzerland) using caesium as one of the tracers. The main rock types selected for these studies are the same as in the in-situ experiments: veined gneiss from Olkiluoto and granodiorite from Grimsel. This way this study also serves as a supporting experiment for the in-situ experiments.

Three cubic samples, about $1\times1\times1$ cm^3 in size, of both rock types, were manufactured and imaged with a SkyScan 1172 XCT scanner with a pixel size of 6.1 μm at the University of Jyväskylä. Five of the six faces of the samples were sealed with epoxy resin, thus caesium would only diffuse from one face of the samples into the rock matrix. First scanning was done before immersion of the samples, then the samples were immersed into supersaturated aqueous CsCl solution. Second scanning was done after 141 days for first samples and after 249 days for second samples. The third samples will be in CsCl for one year. Migration velocity of caesium was thus followed by rescanning the samples after different amounts of contact time.

The post-immersion XCT images showed intrusion of caesium in the samples. By finding three corresponding points from the two scans of the same sample, and calculating a translation vector, images could be aligned since the scannings were done using the same exact parameters. Difference of the aligned images then showed exactly where caesium had migrated. It had migrated to the open pore space within highly porous mineral clusters and to biotite veins. In the Olkiluoto sample, caesium was migrated through the whole sample, also filling a microfracture in the sample, and there were areas of high caesium concentration corresponding to areas of high local porosity (see Figure 1). In the Grimsel sample caesium had migrated only a few mm into the sample. A few openings within biotite grains surrounding feldspars and quartz were filled with CsCl. There were no areas of high caesium concentration, as there are no high porosity areas in Grimsel granodiorite (see Figure 2). The results indicate that there is a highly connected pore network in the Olkiluoto sample forming fast migration paths for the diffusion of nuclides. In Grimsel sample the connectivity of the migration paths was less pronounced and highly porous patches behaving as sinks along transport pathway of elements did not appear.
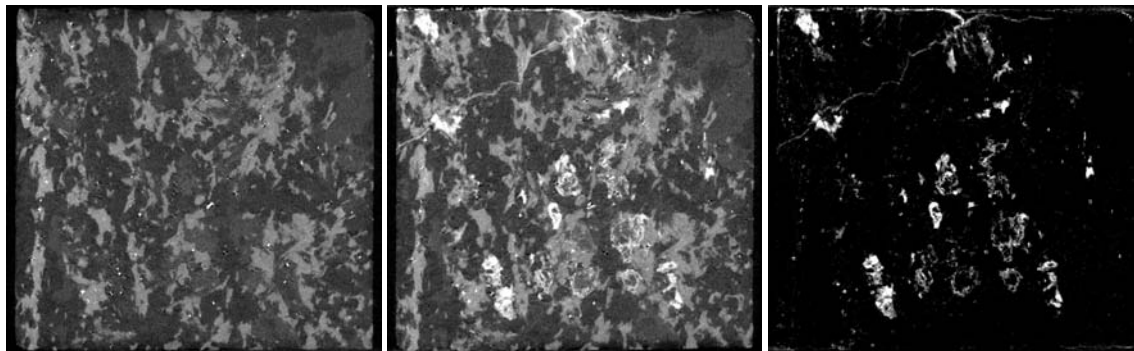
Figure1. Olkiluoto sample before CsCl immersion (left panel) and after 249 days contact time (middle panel). The difference of the two images (right panel) shows caesium intrusion throughout the sample. Caesium has infiltrated the sample from above. Sample size is $1 \times 1 \times 1$ cm^3.
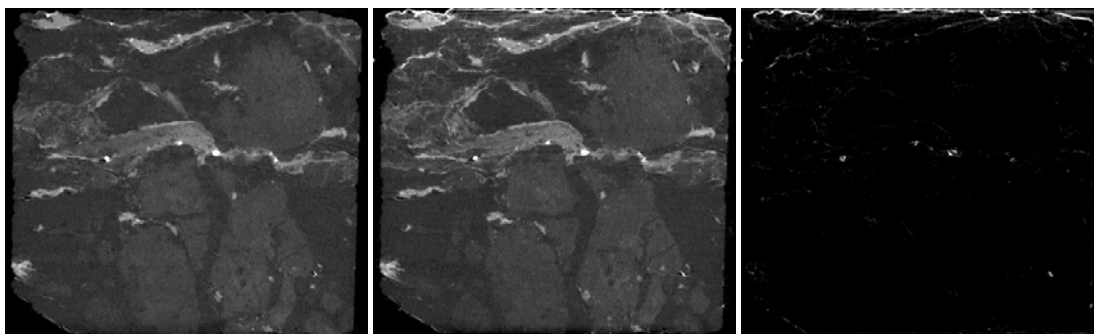
Figure 2. Grimsel sample before CsCl immersion (left panel) and after 249 days contact time (middle panel). The difference of the two images (right panel) shows caesium intrusion only a few mm deep into the sample. Caesium has infiltrated the sample from above. Sample size is $1 \times 1 \times 1$ cm^3.

EFFECT OF IONIC STRENGTH ON DIFFUSION BEHAVIOUR OF Sr^{2+} IN BELGIAN CLAY FORMATIONS

L. van Laer, C. Bruggeman, M. Aertsens, N. Maes

Belgian Nuclear Research Centre (SCK•CEN), Expert Group Waste & Disposal, Boeretang 200, Mol, Belgium

For the geological disposal program in Belgium, different clay formations (Boom Clay, Ypresian clays) and locations are still under consideration. Most studies were performed on Boom Clay at the Mol site. The pore waters of the Boom Clay located more to the west and the Ypresian clays are characterized by a higher ionic strength (IS) than the Boom Clay pore water at the Mol site [1-3]. Moreover, a significant seawater level rise due to, e.g. climate change, is a possible scenario in the future. This rise will likely imply also a replacement of the low IS water with seawater-type pore water (higher salinity and different composition).

Recently it was shown that the diffusion of Sr^{2+} and other sorbing cations (Zn^{2+} & Co^{2+}) is enhanced in purified Na-illite [4] due to the so-called 'surface diffusion' phenomenon. The enhanced diffusion can be attributed to the diffusion of the cations in the electrical double layer (EDL). This implies that cations which bind mainly via cation exchange (like Sr^{2+}), will experience a higher enhanced diffusion effect than cations which have surface complexation as dominant sorption mechanism (like Zn^{2+} and Co^{2+}). As the amount of 'mobile' cations in the electrical double layer depends on the ionic strength, this enhanced diffusion will decreace with an increasing ionic strength (decreasing EDL). In illite, a ten-fold increase in IS resulted in a decrease in the effective diffusion coefficient by one order of magnitude. From this point of view, it is necessary to compare the diffusion behaviour of the sorbing radionuclide Sr^{2+} in the two Belgian clay formations which differ in ionic strength (IS) ($IS_{Ypresican\ Clay} \approx 0.14$ M compared to $IS_{Boom\ Clay} \approx 0.015$ M for cores used in this study) but also in smectite content (with possibly authigenic smectite in the case of the Ypresian clays).

For the diffusion experiments with the Boom Clay, through-diffusion experiments were performed with clay cores of ± 30 mm, in contact with real pore water extracted from the Boom Clay (~ 0.015 M $NaHCO_3$) and spiked with ^{85}Sr in the source solution. The diffusion experiments with Ypresian clays are performed with synthetic pore water (0.12 M NaCl - 0.006 M Na_2SO_4) (experiments ongoing). The solution of the target reservoir is replaced frequently. At the end, the clay is sliced (per 200 μm) and analyzed on activity. Both, solutions and clay samples, are measured by gamma counting (Canberra Packard Cobra). The concentration changes in the source and target solution and the trace profile in the clay are fitted with COMSOL Multiphysics in order to determine the apparent diffusion coefficient (D_{app}) and the capacity factor α. The product of both parameters gives finally the effective diffusion coefficient (D_{eff}).

In order to evaluate enhanced double layer diffusion for both clays the ratio of D_{eff} (Sr) to D_{eff} (HTO) is used. For Boom Clay, there is clearly enhanced diffusion observed for Sr^{2+} with D_{eff} (Sr)/D_{eff}(HTO) = 84. In the Ypresian Clay where the ionic strength is 10 times higher, we expect that this ratio will be lower according to the observations for Na-illite. However, also the difference in mineralogy (clay content) and pore structure may have an impact on the diffusive behaviour.

ACKNOWLEDGEMENT

REFERENCES

[1] De Craen M., Wang L., Van Geet M., Moors H. (2004) Geochemistry of Boom Clay pore water at the Mol site, SCK•CEN-BLG990, SCK•CEN, Mol, Belgium.
[2] De Craen M., Wemaere I., Labat S., Van Geet M. (2006) Geochemical analysis of Boom Clay pore water and underlying aquivers in the Essen-1 borehole. SCK•CEN-ER-19, SCK•CEN, Mol, Belgium.
[3] Van Marcke P., Laenen B. (2005) The Ypresian clays as possible host rock for radioactive waste disposal: an evaluation, NIROND TR-2005-01, ONDRAF/NIRAS, Brussels, Belgium.
[4] Glaus M.A., Aertsens M., Appelo C.A.J., Kupcik T., Maes N., Van Laer L., Van Loon L.R. (submitted). Cation diffusion in the electrical double layer enhances the mass transfer rates for Sr^{2+}, Co^{2+} and Zn^{2+}. Submitted in Geochimica et Cosmochimica Acta.

SORPTION-DIFFUSION OF TRIVALENT LANTHANIDES/ACTINIDES IN SMECTITE RICH NATURAL CLAY

Sharayu Kasar[1], Sumit Kumar[1], R. K. Bajpai[2], B. S. Tomar[1]

[1]Radioanalytical Chemistry Division, [2] Technology Development Division
Bhabha Atomic Research Centre, Mumbai, India.
E-mail :bstomar@barc.gov.in

Smectite rich natural clay is considered as a potential buffer/backfill material in the deep geological repository. Low water permeability and high sorption characteristics of clay minerals have been the basis of this near unanimous choice. As the disposal arrangement is expected to retard the migration of radionuclides to the far-field areas over a long time period, for the safety analysis of a radioactive waste disposal site it is necessary to generate quantitative data on migration of radionuclides through the clay barrier. Smectite rich natural clay has been sourced from western part of India and based on its thermal, mechanical, and sorption characteristics, has been found a potential candidate for its usage in Indian proposed deep geological repository of nuclear high level waste [1-3].

In the present work, an in-diffusion study has been carried out for trivalent lanthanides/actinides using ^{152}Eu as a radiotracer. Diffusion experimental details are schematically shown in figure 1 below. Briefly, natural clay was washed and dried at the site and brought to the laboratory. Herein the clay lumps were crushed and sieved to < 90 μm size particles. Clay particles were contacted with 1 M NaCl overnight to form Na-clay and subsequently the clay particles were washed with Millipore water and dried to free flowing particles. Details of Clay characterization are given elsewhere [3]. The clay fraction was found to consist of mainly Smectite (95%). Clay was packed in the diffusion cells at a density of 1.6 g/cc and equilibrated with water. After a period of 1 month, a thin layer of radiotracer was applied between the two clay columns and allowed to again equilibrate for another 72 days. At the end of the tracer diffusion experiment, the clay column was sliced at nearly 0.5 mm thin slices and activity of ^{152}Eu present in each clay slice was measured using High purity Germanium detector based gamma spectrometry system.
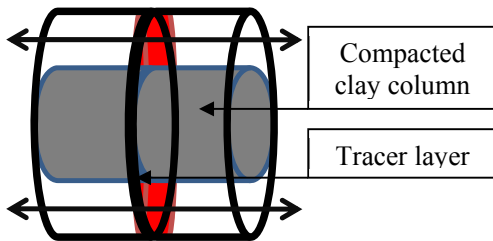
Figure 1. Schematic of diffusion cell

The depth profile of Eu in the clay column from initial tracer position was fitted into the thin film solution (eq. 1) of the Fick's second law of diffusion to get the apparent diffusion coefficient (D_a).

$$C(x,t) = \frac{C_0}{2\sqrt{\pi D_a t}} \exp\left(-\frac{x^2}{4 D_a t}\right)$$

(1)

Diffusion profile obtained in the present experiment is shown in figure 2. The log D_a calculated from the slope of the data is 1.3 ($\pm$0.1) $\times$ 10^{-13} cm^{2}s^{-1}.

Sorptive or retention capacity of the clay is an important factor in modifying the diffusive transport of the radionuclides in the bentonite clay. In the present experimental set-up, both the processes are coupled together and the net effect on radionuclide migration is reflected by the apparent diffusion coefficient (D_a).
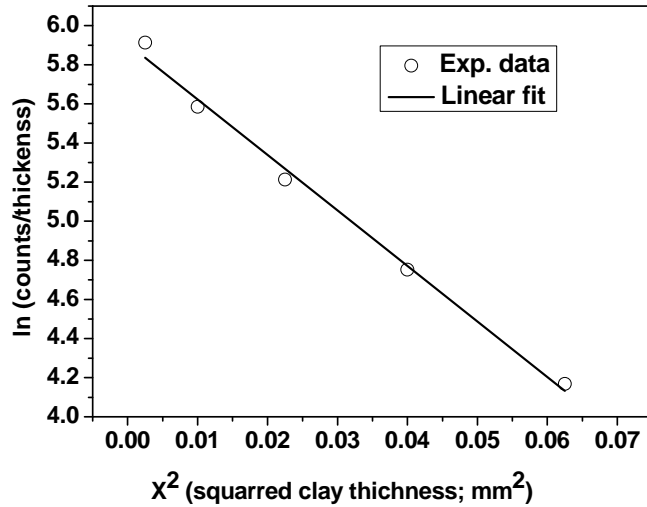
Figure 2. Depth profile of [152]Eu activity for the determination of apparent diffusion coefficient.

[1]Pente, A. S. (2010) Ph.D. thesis, Mumbai University.

[2] Kasar, S., Kumar, S. Kar, A. S., Bajpai, R. K., Kaushik, C. P., Tomar, B. S. (2014) Retention behaviour of Cs(I), Sr(II), Tc(VII) and Np(V) on smectite-rich clay, J. Radioanaly. Nucl. Chem. *DOI 10.1007/s10967-014-2943-2.*

[3] Kumar, S. Bajpai, R. K., Kaushik, C. P., Tomar, B. S. (2013) Americium sorption on smectite-rich natural clay from granitic ground water, Appl. Geochem. 35, 28-34.

UNDERSTANDING DIFFUSIVE TRANSPORT OF RADIOCAESIUM WITH DEPTH IN SOIL CONTAMINATED BY THE FUKUSHIMA NPP ACCIDENT

H. Sato [(1)], T. Niizato [(2)], S. Tanaka [(3)], H. Abe [(2)], and K. Aoki [(4)]

[(1)]Graduate School of Natural Science and Technol., Okayama Univ., Tsushima-naka 3-1-1, Kita-ku, Okayama-shi, Okayama 700-8530, Japan
[(2)]Sector of Fukushima Research and Develop., Japan Atomic Energy Agency, Okitama-cho 1-29, Fukushima-shi, Fukushima 960-8034, Japan
[(3)]Graduate School of Eng., Hokkaido Univ., Kita 13 Nishi 8, Sapporo, Hokkaido 060-8628, Japan
[(4)]Department of Construction, Japan Atomic Energy Agency, Ohaza Shirakata 2-4, Tokai-mura, Naka-gun, Ibaraki 319-1195, Japan

The accident at the Tokyo Electric Power Company (TEPCO) Fukushima Dai-ichi Nuclear Power Plant (1F-NPP) occurred following the Great East Japan Earthquake on March 11, 2011, and led to the release of volatile radionuclides (RNs), which were deposited on the surrounding environment (soils, forests, residential land, etc.) in the Fukushima pref. The inventory of RNs discharged by May 2011 is estimated to be approximately 900 PBq with this value converted to radioiodine (I-131) (500 PBq for I-131 and 10 PBq for Cs-137) [1]. This amount is equivalent to approximately 1/6th of the 5,200 PBq discharged by the Chernobyl Nuclear Power Plant accident which occurred in Apr. 1986 [2]. After the decay of short-lived I-131 (half-life $T_{1/2}$=8.021d), radiocaesium (Cs-134 ($T_{1/2}$=2.065y) and Cs-137 ($T_{1/2}$=30.07y)) [3] are now the main contributors to radiological dose rate.

This work was a research project related to distribution maps of radiation dose rate, which the Ministry of Education, Culture, Sports, Science and Technology (MEXT) has promoted as one countermeasure to the 1F-NPP accident, since Mar. 2011. Two investigations on the depth distribution of RNs in soil were conducted, in Jun. 2011 after about 3 months (1st investigation) [4] and during Feb. and Mar. 2012 after about 1 year (2nd investigation) following the 1F-NPP accident. In both investigations, the authors collected samples at 11 locations in the city of Nihonmatsu and the towns of Kawamata and Namie, which are located between 20 km and 60 km north-west from 1F-NPP. The apparent diffusion coefficients (D_a) of RNs were calculated from depth distributions near the surface layer of soil, and the distribution coefficients (K_D) of Cs-137 and I-131 on soil were obtained by a batch method in both investigations. The desorption experiments for both RNs at the end of sorption experiments were also conducted for 3 typical soils (sandy soil, clayey soil, organic soil) and those 3 kinds of elutriated components (clay, silt, sand and gravels) in the 2nd investigation. In addition, cation and anion exchange capacity measurements, mineral composition analysis by X-ray diffraction, etc. were also conducted in the 2nd investigation.

In both investigations, radiocaesium (Cs-134, Cs-137) were detected at all locations, and in the 1st investigation, Te-129m and Ag-110m were detected only at locations where radiation dose rates were high [4]. At many locations during the 1st investigation, more than 95% and 99% of the radiocaesium inventory distributed within 5 and 10cm deep in mainly sandy soil, respectively, and no evolution with depth was found between both investigations. On organic soil and soil of former farmland, more than 99% of the radiocaesium inventory distributed within 14cm deep in the 1st investigation [4], but in the 2nd investigation, more than 95% and 99% of the inventory distributed within 16cm and 20cm deep, respectively, and those distributions showed a tendency to gradually extend. Almost all D_a-values of radiocaesium derived from the 1st investigation were of the order 10^{-10} m^2/s, and tended to be higher in soil of former farmland and organic soil than in mainly sandy soil. However, all D_a-values derived from the 2nd investigation were, lower approximately of order 10^{-11} m^2/s. The K_D-values of Cs-137 on soil in the 1st investigation were in the range 2,080-61,000 ml/g, and a similar range of the K_D-values were obtained in the 2nd investigation. However, K_D-values on organic soil components were approximately one order of magnitude lower than those on other soils. These trends are qualitatively consistent with trend of changes in the depth distribution of radiocaesium, but are quantitatively inconsistent with the K_D-values. For example, considering the high K_D-values, the D_a-values should be 2 or 3 orders of magnitude lower than those obtained in both investigations, and large discrepancies are found between the K_D-values and the D_a-values. The cause for the high D_a-values is thought to be that the distributions include the effect of dispersion or permeation by advection following the deposition of RNs near the surface layer of soil. This high calculated D_a-values assumed that depth distributions following the initial deposition were formed mainly by a diffusion process.

Therefore, a theory to exclude the influence of early-time of dispersion or permeation by advection and derive D_a for only the diffusion process was considered based on the evolution of the depth distributions from the 1st to the 2nd investigation. Furthermore, K_D was calculated from the D_a and compared to the measured data. Finally, both parameters were calculated from the following relations.

$$D_a = -\frac{\tan\left\{\arctan\left(\frac{1}{b}\right) - \arctan\left(\frac{1}{a}\right)\right\}}{4(t_2 - t_1)} = -\frac{\tan\{\arctan(-4D_{a2}t_2) - \arctan(-4D_{a1}t_1)\}}{4(t_2 - t_1)} \qquad (1)$$

$$K_D = \frac{n_p(D^o - 3D_a)}{3\rho_d D_a} = \frac{n_p(D^o - 3D_a)}{3\rho_{th}(1 - n_p)D_a} \qquad (2)$$

Where, a and b are the slopes given by a plot of LnC (vertical axis) versus x^2 (horizontal axis) for elapsed time (t_1 and t_2), respectively, t_1 and t_2 the times elapsed after initial deposition of radiocaesium, respectively, D_{a1} and D_{a2} the apparent diffusion coefficients for elapsed times t_1 and t_2, respectively, n_p the porosity, $_d$ the dry density, $_{th}$ the solid density (solid particle density), and D^o the diffusion coefficient in free water.

In the analysis, physical parameters such as dry density and solid particle density were based on measured results, and the D^o for Cs^+ ions used 2.1×10^{-9} m^2/s (25°C). Figure 1 shows the calculated results of the D_a for Cs^+ ions versus soil type. The calculated results of D_a were of order 10^{-14} m^2/s, and the K_D-values calculated from the D_a-values were in the range of $K_D=10^4$-10^5 ml/g, which are consistent with the K_D-values measured by the batch method.
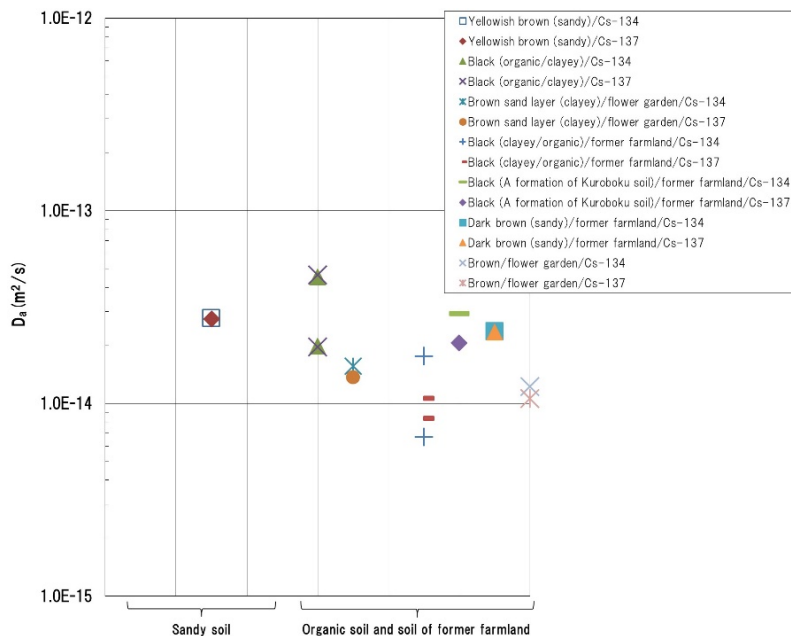
Figure 1. The calculated results of the D_a for Cs^+ ions versus the type of soil

[1] The National Diet of Japan Fukushima Nuclear Accident Independent Investigation Commission (NAIIC) Reports (July 5, 2012). "http://warp.da.ndl.go.jp/info: ndljp/pid/3856371/naiic.go.jp/en/ report/" July 21, 2014.
[2] Kato, H., Onda, Y. and Teramage, M. (in press). "Depth distribution of ^{137}Cs, ^{134}Cs, and ^{131}I in soil profile after Fukushima Daiichi Nuclear Power Plant Accident." J. Environmental Radioactivity.
[3] Japan Radioisotope Association. (2000). "Radioisotope Pocket Data Book, 9th Edition." Maruzen, Tokyo.
[4] Sato, H., Niizato, T., Amano K., Tanaka, S. and Aoki, K. (2013). "Investigation and research on depth distribution in soil of radionuclides released by the TEPCO Fukushima Dai-ichi Nuclear Power Plant Accident." Mater. Res. Soc. Symp. Proc. Vol.1518: 277-282.

ANALYSIS OF CESIUM DIFFUSION THROUGH MORTARS FROM DIFFERENT CEMENTS

M. García-Gutiérrez, T. Missana, M. Mingarro, U. Alonso

CIEMAT, Dpt. of Environment, Av. Complutense 40, 28040 Madrid (SPAIN)

Cement materials are widely used for stabilizing and conditioning of radioactive waste in low- and intermediate-level repositories. Cement determines the chemical and physical properties of the repository near-field for a long period of time, and provides alkaline conditions, which favour radionuclide immobilization by sorption and low solubility. Under these conditions, radionuclide transport takes place mainly by diffusion.

In this study, the adequacy of different types of cements to act as barrier to ^{137}Cs migration has been analysed. ^{137}Cs is a very important fission product in low and medium radioactive waste repository.

Four commercial cements (CEM I, II and IV (A and B) sulphate resistant) were used to obtain mortars with a cement:sand:water relation of 1:1.75:0.45. Synthetic pore water was prepared boiling Milli-Q water to minimize CO_2 content, contacting it with crushed and sieved mortar, and stirring until constant pH and conductivity are reached.

Diffusion experiments were performed using the in-diffusion (ID) method with constant tracer concentration in the reservoir, obtained spiking small quantity of tracer periodically. With this experimental configuration an analytical solution provided by Crank (1975) could be used to simulate the ^{137}Cs concentration profile within the sample. ^{137}Cs activity was measured through the gamma emission of the ^{137m}Ba in equilibrium with ^{137}Cs, using a Cobra-II auto-gamma Packard counter (NaI detector).

A first set of diffusion experiment lasted approximately 150 days but a short concentration profile, about 2-3 mm, was obtained. A second set of experiment lasted between 300 and 380 days and concentration profiles larger than 5 mm were obtained. In all the cases, the diffusion profiles were not well fitted by the simple analytical solution, but it could be interpreted as the superposition of two different profiles corresponding to Cs diffusion in different paths each with an apparent diffusion coefficient, D_a.

The higher D_a, leading to a larger penetration of Cs in the sample, corresponds to the transport through the connected larger pores of approximately 25% of Cs. The lower D_a, implies a shorter penetration of Cs through the cement matrix, but involves 75% of Cs. With this approach all the experimental results could be satisfactorily fit.

The D_a values range between $3 \cdot 10^{-15}$ m^2/s and $1 \cdot 10^{-13}$ m^2/s, being the difference between "high" and "low" D_a, in the same sample, up to one order of magnitude.

CEM IV A and B resulted as the most effective barrier to Cs migration

References

Crank J. (1975), The Mathematics of Diffusion, 2nd edition, Clarendon Press.

EFFECTS OF IRRADIATION ON THE BEHAVIOR OF ^{14}C IN NUCLEAR AND MODEL GRAPHITE: CONSEQUENCES FOR INVENTORY, DECONTAMINATION AND DISPOSAL

N. Galy[(1,2)], N. Toulhoat[(1,3)], N. Moncoffre [(1)], N. Bérerd[(1,4)], Y. Pipon[(1,4)], G. Silbermann[(1,2)], M.R. Ammar [(5)], P. Simon[(5)], J.N. Rouzaud[(6)], D. Deldicque[(6)], P. Sainsot[(7)],

[(1)] *Université de Lyon, Université Lyon 1, CNRS/IN2P3, UMR5822, (IPNL), France*
[(2)] *EDF/CIDEN, Lyon, France*
[(3)] *CEA/DEN, Centre de Saclay, France*
[(4)] *Université de Lyon, UCBL IUT A, département chimie, France*
[(5)] *CNRS, UPR 3079 CEMHTI, 45071 Orléans Cedex 2, France, France*
[(6)] *Laboratoire de Géologie de l'Ecole Normale Supérieure, Paris, UMR CNRS ENS 8538, France*
[(7)] *Université de Lyon, Université Lyon 1, LaMCoS, INSA Lyon, CNRS UMR5259, France*

Graphite is used in many types of nuclear reactors due to its ability to slow down fast neutrons without capturing them. Whatever the reactor design, the irradiated graphite waste management has to be faced sooner or later regarding the production of long lived radioactive species or radionuclides such as ^{14}C or ^{36}Cl that might be dose determining at the outlet after disposal. Thus, the first carbon dioxide cooled, graphite moderated nuclear reactors resulted in a huge quantity of irradiated graphite waste all over the world. Many of these reactors are now being decommissioned. In case of disposal, a particular attention is paid to ^{14}C due to its long half-life (T~5730 years) and as it is a major contributor to the radioactive dose. In addition, leaching experiments carried out on irradiated graphite issued from SLA2 UNGG French reactor have shown that, even if the quantity of ^{14}C released in the solution is low (less than 1% of the initial inventory), around 30% is in the organic form that would be mobile in repository conditions [1,2]. Thus, management solutions as graphite waste sorting or decontamination in order to reduce the initial radioactivity are also considered. In order to be able to choose the best management option, it is necessary to assess the radioactive inventory and gain information on ^{14}C location and speciation in the irradiated graphite. ^{14}C has two main production routes: i) transmutation of nitrogen (^{14}N(n,p)^{14}C) where nitrogen is mainly adsorbed at the surfaces of the irradiated graphite; ii) activation of carbon from the matrix (^{13}C(n,)^{14}C). The predominance of one reaction versus the other depends on the nitrogen content in the graphite. Significant quantities of ^{14}C and ^{14}N have been depleted during reactor operation mainly through radiolytic corrosion [3,4]. Thus, the remaining ^{14}C results mainly from ^{13}C of the carbon matrix. The separate and coupled effects of temperature and radiolytic corrosion on ^{14}C behavior in nuclear graphite during reactor operation have already been thoroughly investigated by [5] using ^{13}C implantation into virgin nuclear graphite issued from SLA2 reactor (to simulate ^{14}C displaced from its original structural site in the graphite matrix through recoil) in particular with a dedicated irradiation cell where a graphite sample was put in contact with a gas simulating the UNGG gas. We have thus shown that thermal annealing does not induce any migration of ^{13}C up to 1600°C (in inert atmosphere), even if the structure of the graphite is initially strongly disordered (around 6 dpa). A slight diffusion occurs from 1600°C. This diffusion might be linked to the reordering of the graphite structure and the "reorganization" of the implanted ^{13}C into carbon clusters for instance and argues in favor stabilization of ^{14}C in the graphite matrix through temperature. On the contrary, both temperature and irradiation effects tend to induce nitrogen migration towards the graphite "surfaces" (as pores for instance) where it is partially released or tends to form carbonitride complexes and several compounds such as C-N, C=N or C≡N. The migration and subsequent release occur all the more as the graphite structure is disordered (i.e. in the zones where the neutron flux is maximum) and the loss of ^{14}N may reach 65% of the initial amount.

Moreover, we have also confirmed that ^{13}C or ^{14}N located close to open pores could be easily removed through radiolytic corrosion at the gas/graphite interface. These results corroborate that ^{14}C mainly issued from ^{14}N and located close to free surfaces could have been released during reactor operation, mainly through radiolytic corrosion, thereby explaining the decrease of at least part of its inventory.

However, the consequences of neutron irradiation on the eventual release or stabilization of ^{14}C in the graphite matrix are not fully understood yet. Therefore, in order to elucidate the impact of neutron irradiation on ^{14}C behavior, we decided to carry out a systematic investigation of irradiation and its synergistic effects with temperature on nuclear graphite samples and model samples such as HOPG.

The collision of the impinging neutrons with the graphite matrix carbon atoms induces mainly ballistic damage. However, a small part of the recoil carbon atom energy is also transferred to the graphite lattice through electronic excitation. Thus, we simulated the effects of the different irradiation regimes in synergy with temperature by irradiating ^{13}C implanted graphite samples with different ions of different energies using

different facilities and dedicated irradiation cells. Moreover, as ^{13}C behavior might be strongly related to the modification of the graphite matrix structure, the structure modifications were also followed by Raman microspectrometry, when possible in *operando*, during irradiation. In all cases, the evolution of the implanted ^{13}C profiles has been followed by SIMS.

Following main information could already be gained: Irradiation carried out with He^{2+}, S^{9+} or I^{13+} ions, with energies ranging from a few MeV to 200 MeV, by increasing the electronic stopping power S_e, show that this regime disorders the graphite structure, all the more as S_e is high. At "moderate" electronic excitations and ionizations, i.e. for S_e ranging up to 700keV/μm which corresponds to the usual range in UNGG reactors, irradiation induces a disorder of the graphite structure that is compensated by the annealing effect of temperature. However, this regime does not promote ^{13}C release, neither in nuclear graphite nor in HOPG, as shown by the SIMS results. Even at higher S_e around 3700 keV/μm, the implanted ^{13}C does not migrate at a temperature as high as 1000°C. The reordering of the structure is evidenced by Raman microspectrometry analysis and might suggest that ^{13}C rearranges into new carbon structures. We also simulated the effects of ballistic damage by irradiating graphite samples with C^+ ions of 400keV and 600keV or Ar^+ ions of 800 keV producing atomic displacements ranging respectively from 0.5 to 4 dpa. The samples were heated at temperatures ranging from 200°C to 1000°C. The results show that whatever the initial structure disorder, the ballistic damage induces a high disorder of the structure which is strongly compensated by the annealing effects of temperature. SIMS data show that ^{13}C is not released. Thus, the whole set of results allow inferring that ^{13}C does not seem to be released whatever the irradiation regime even at high temperature.

Finally, extrapolating our results to the behavior of ^{14}C during reactor operation, we may conclude that graphite irradiation did not promote its release, contrary to what was observed for ^{36}Cl, for which ballistic damage promoted the loss [6]. Ballistic irradiation leads to bond breakage and fragmentation of the coke grains as well as the increasing disorientation of the crystallites in the grains that become smaller and smaller. But the typical UNGG temperatures (200°-500°C) reorder the graphite structure during irradiation, thereby probably stabilizing the ^{14}C into new carbon structures. Considering ^{14}C purification prior to disposal, annealing in inert gas would not lead to ^{14}C release, contrary to oxidizing conditions. However, the stabilization of ^{14}C into new carbon structures could be beneficial for disposal.

[1] L.Vendé PhD Thesis Ecole des Mines de Nantes, 2012, French. NNT 2012 EMNA0018 tel-00770671
[2] ANDRA (2012). Technical Report, Andra, FRPADPG.12.0020/A.
[3] B. Poncet and L. Petit, J. Radioanal. Nucl. Chem (2013) 298:941-953
[4] N. Moncoffre, N. Toulhoat, N. Bérerd, Y. Pipon, G. Silbermann, A. Blondel, N. Galy, P. Sainsot, J-N. Rouzaud, D. Deldicque, V. Dauvois, presented at the NuMat conference, October 27-30 2014, Clearwater,USA, submitted to J Nucl Mat special issue
[5] G. Silbermann PhD thesis, Université Claude Bernard Lyon I, 2013. French. tel-00954466
[6] N. Toulhoat, N. Moncoffre, N. Bérerd, Y. Pipon, A. Blondel, N. Galy, P. Sainsot, J.N. Rouzaud, D. Deldicque, J Nucl Mater 2015 doi:10.1016/j.jnucmat.2015.04.010

ANTHROPOGENIC PLUTONIUM-244 IN THE ENVIRONMENT: INSIGHTS INTO PLUTONIUM'S LONGEST-LIVED ISOTOPE

C. R. Armstrong and J.R. Cadieux

Nonproliferation Technology Section, Savannah River National Laboratory, Aiken, SC, USA, 29808

Owing to the rich history of heavy element production in the unique high flux reactors that operated at the Savannah River Site, USA (SRS) decades ago, trace quantities of plutonium with highly unique isotopic characteristics still persist today in the SRS terrestrial environment. Development of an effective sampling, processing, and analysis strategy enables detailed monitoring of the SRS environment, revealing plutonium isotopic compositions, e.g., ^{244}Pu (half-life: 81 million years), that reflect the unique legacy of plutonium production at SRS. This work describes the first long-term investigation of anthropogenic ^{244}Pu occurrence in the environment. Environmental samples consisting of a mixture of predominantly soils, mineral fragments, and organic debris, were taken in bulk at SRS over an eleven year period, from 2003 to 2014. Separation and purification of trace plutonium was carried out followed by three stage thermal ionization mass spectrometry (3STIMS) measurements for plutonium isotopic content and isotopic ratios. Significant ^{244}Pu was measured in all of the years sampled with the highest amount observed in 2003. The ^{244}Pu content (in 100 g samples) ranged from 31 femtograms (fg = 10^{-15} g) to over 4 picograms (pg = 10^{-12} g) in years 2006 and 2003 respectively. In all years, the ^{244}Pu/^{239}Pu atom ratios were significantly higher than global fallout, ranging from 0.004 to 0.698 in years 2009 and 2003 respectively.

BIOACCUMULATION AND SPECIATION OF EUROPIUM IN SPONGE *A. cavernicola*

M. Maloubier[1)*], H. Michel[1)], C. Moulin[2)], M. Monfort[2)], D. Shuh[3)], S.G. Minasian[3)], M-A. Tribalat[1)], O.P. Thomas[1)], M.Y. Bottein Dechraoui[4)], C. Den Auwer[1)]

[1)] *ICN, Institut de Chimie de Nice – UMR 7272, Parc Valrose, F06108 Nice cedex 2, France*
[2)] *CEA, DAM, DIF, F-91297 Arpajon, France*
[3)] *Lawrence Berkeley National Laboratory, Berkeley, California 94720*
[4)] *IAEA, Environment Laboratorie, 4 Quai Antoine Ier, MC-98000, Monaco*

Among the environmental compartments, the hydrosphere is ubiquitous and can transport compounds or elements over long distances. The fate of radionuclides in the marine environment remains a major concern in our modern societies [1], as exemplified by the recent event of Fukushima in 2011. Among the radionuclides of concern, actinides are the heaviest elements involved in nuclear activities. Some studies have already shown that actinides present in seawater can be strongly accumulated by some marine organisms without knowing their speciation [2-4]. They can be accumulated by phytoplankton, for example, and then transmitted up the food chain, to the fish until humans. Improving knowledge on the interaction between actinides and marine compartment is therefore essential to better understand the transfer mechanisms from the hydrosphere to the biosphere and to evaluate their global impact on humans. Among the organisms known to store heavy metals, marine sponges have already been identified as hyper-accumulators of several trace elements and are proposed in the case of this study as model biomonitor organisms.

We have focused on americium (III) as a representative of the heavier actinides about which very few data is available. It is also an element with a relatively simple RedOx chemistry compared to the earlier actinides like uranium, neptunium and plutonium. Yet because of the relatively high specific radioactivity of available 241- and 243-Am, europium (a stable lanthanide with chemical properties very close to that of americium) was also used as a chemical surrogate.

In a first step, the accumulation of trace and ultratrace amount of europium (III) and americium (III) respectively were investigated in the Mediterranean sponge *A. cavernicola*. This sponge is commonly found in the caves off the coasts of the Northwestern Mediterranean and previous studies have shown that it has a substantial capacity for metal accumulation [3]. The uptake curve of *A. cavernicola* exposed to a mix of stable and radiotracer ^{152}Eu on the one hand and radiotracer ^{241}Am on the other hand were estimated using a high-purity Ge gamma spectrometer. For europium, loads of 250 to 300 ppm in dry matter have been obtained. However the trend is linear and this suggests that sponges could accumulate more. In a second step, X-ray Absorption Spectroscopy (XAS) spectra at the europium L_{II}, L_{III} and K edges as well as Time-Resolved Laser-Induced Fluorescence (TRLIF) have been performed and speciation of accumulated europium has been assessed. A carbonate complex has been postulated. Furthermore, STXM (Scanning Transmission X-ray Microscopy) evidenced that europium precipitates are located everywhere in the sponge but with higher

concentration on its external surface. Those particles are close to 200 nm diameter. Moreover, TEM and fractional separation of sponge cells suggested that europium is located in the sponge tissue which is a spongine skeleton. This information could permit to understand the transfer mechanisms and to evaluate the impact on humans (toxicity) what is unknown at the moment.
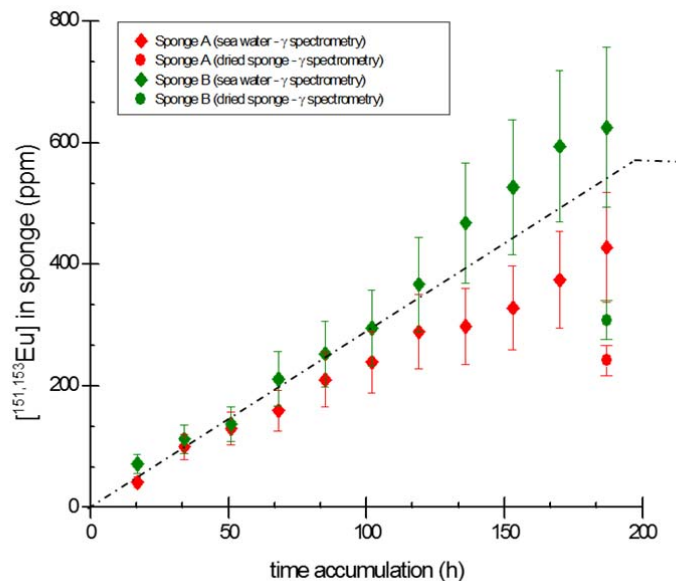
Figure 1: Europium uptake curve of two *A. cavernicola* exposed to [152]Eu and [151,153]Eu dissolved in seawater.

[1] Maher, K. et al., G., et al., "Environmental Speciation of Actinides", Inorg. Chem. 52, 3510 (2013).

[2] Johansen, M.P., et al., " Radiological dose rates to marine fish from the Fukushima Daiichi Accident : The first three years across the North Pacific", Environ. Sci. Technol., doi : 10.1021/es505064d.

[3] Genta-Jouve, G., et al., "Comparative bioaccumulation kinetics of trace elements in Mediterranean marine sponges", Chemosphere 89, 340 (2012).

[4] Stewart, G.M., et al., "The bioaccumulation of U-Th series radionuclides in marine organisms", U-Th series nuclides in aquatic systems 13, 269 (2008).

INTERACTION OF ANAEROBIC MONT TERRI OPALINUS CLAY BACTERIA WITH PLUTONIUM(VI)

H. Moll, A. Cherkouk, G. Bernhard

Institute of Resource Ecology, Helmholtz-Zentrum Dresden-Rossendorf e.V., P.O. Box 510119, 01314 Dresden, Germany

The Opalinus clay layer of the Mont Terri Underground Rock Laboratory (Switzerland) is one potential host rock tested for nuclear waste disposal [1]. Bacteria indigenous to such subterranean environments can affect the speciation and hence the mobility of actinides [2]. Thus various investigations [3-7] documented the manifold impact of bacteria on the speciation of plutonium. Plutonium can coexist in different oxidation states under environmental conditions which makes interaction studies in biological systems challenging.

Recently, we studied the interaction between Pu and *Sporomusa* sp. MT-2.99 cells at pH 6.1 with and without adding an electron donor (10 mM Na-pyruvate). This bacterium was isolated from Mont Terri Opalinus clay core samples. At pH 6.1, a moderate to strong impact of *Sporomusa* sp. cells on the Pu speciation was observed. In contrast to the electron donor free experiments, a clear enrichment of Pu(III) in the biomass (bioreduction) was observed in the presence of 10 mM Na-pyruvate. However, more information is necessary to understand the Pu interaction mechanism in the electron donor free experiments, i.e. the influence of biomass on the reduction of Pu(VI) in the biomass suspensions. In the present study, our focus lies on an improved understanding of the pH-dependent Pu redox chemistry in 0.1 M $NaClO_4$ with and without *Sporomusa* sp. MT-2.99 cells. The pH range was extended to 3, 4, and 7.

The experiments were performed anaerobically at *Sporomusa* sp. MT-2.99 dry biomass concentration of 0.33 $g_{dry\ weight}$/L and pH 3, 4 and 7 at 25 °C in 0.1 M $NaClO_4$. $[^{242}Pu]_{initial}$ was varied between 0.2 and 110 mg/L. The ^{242}Pu present in a) blank (no cells added), b) supernatant, and c) washed biomass re-suspended in 1 M $HClO_4$ were analyzed using UV-vis-NIR spectroscopy, solvent extraction, and liquid scintillation counting (LSC).

The time-dependent Pu concentrations measured in the supernatants were successfully fitted with bi-exponential decay functions and the time-dependent Pu oxidation state distributions by using mono-exponential decay or growth functions. Redox potential measurements indicated that the cells generated reducing conditions. This ability is pH-dependent (pH 3: 800 mV; pH 7: 535 mV). In the beginning, the biomass interacted with a Pu solution containing mainly Pu(VI) (60 %), Pu(IV)-polymers (19 %), and Pu(V) (12 %). In the blank samples at pH 4 the abiotical reduction of Pu(VI) is clearly by a factor of three lower than at pH 6.1. Hence the steady state concentration of Pu(VI) was with 30 % higher than at pH 6 (< 4 %). At pH 4 in the supernatants lower Pu(V) amounts (60 %) were measured than at pH 6 (88 %). Still 18 % of Pu(VI) remains in the supernatants indicating a lower capacity of the biomass to form Pu(V) compared to pH 6. Independently of pH an enrichment of tetravalent Pu (Pu(IV)-polymers and Pu(IV)) dominates the Pu oxidation state distribution in the biomass. However, a clear pH influence on both the amount of accumulated Pu and on the interaction process with the biomass could be proven.

[1] M. Thury, P. Bossart, Eng. Geol. 52,347-359 (1999).
[2] J.R. Lloyd, G.M. Gadd, Geomicrobiol. J. 28, 383-386 (2011).
[3] P. Panak, H. Nitsche, Radiochim. Acta 89, 499-504 (2001).
[4] M.P. Neu, et al., Radiochim. Acta 93, 705-714 (2005).
[5] H. Moll, et al., Radiochim. Acta 94, 815-824 (2006).
[6] J.C. Renshaw, et al., Biogeochemisty 94, 191-196 (2009).
[7] T. Ohnuki, et al., J. Nucl. Sci. Technol. 46, 55-59 (2009).

MICROBIAL REDUCTION OF URANIUM(VI) BY BACILLUS SP. DWC-2: MACROSCOPIC AND SPECTROSCOPIC STUDY

Xiaolong Li[1], Congcong Ding[1,2], Jiali Liao[1],Tu Lan[1], Feize Li[1], Liang Du[3], Jijun Yang[1], Yuanyou Yang[1], Dong Zhang[1], Jun Tang[1] and Ning Liu[1]

[1]*Key Laboratory of Radiation Physics and Technology, Ministry of Education; Institute of Nuclear Science and Technology, Sichuan University, Chengdu 610064, P. R. China;*
[2]*Key Laboratory of Biological Resource and Ecological Environment of the Ministry of Education, College of Life Sciences, Sichuan University, Chengdu 610064, P.R. China*
[3] *Institute of Nuclear Physics and Chemistry, CAEP, Mianyang 621900, P. R. China*

Over the last two decades, bioreduction has been considered as an environmentally friendly and greener alternative methods for uranium bioremediation since Lovley and co-workers reported that microbes can conserve energy for anaerobic growth via the reduction of U(VI) [1]. Microbial reduction of U(VI) to sparingly soluble U(IV) species under reducing conditions (e.g. subsurface) is an important mechanism for the uranium immobilization and for the formation of some uranium ores, and results in the significant decrease of its mobility and bioavailability [2]. Meanwhile, humic substances (or natural organic matter) are also known to be redox reactive and therefore can reduce redox-sensitive metals [3]. So, it is of particular interest that the possibility for humic substance or natural organic matter to mediate microbial reduction of metals and thus resulting in more rapid immobilization of these metals in soil and finally remediation of polluted site.

In the present work*, the bioreduction characteristics of U(VI) by *Bacillus* sp. dwc-2, one of the dominant bacterial species isolated from a potential disposal site of (ultra-) low uraniferous radioactive waste in Southwest China, in the presence or absence of electron donors under anaerobic conditions were investigated using transmission electron microscopy (TEM), energy dispersive X-ray (EDX) analysis, X-ray photoelectron spectroscopy (XPS) and X-ray absorption spectroscopy (XAS). Studies indicated that, at pH 8.2, about 16.0% of U(VI) at an initial concentration of 100mg/L uranium nitrate solution could be reduced by *Bacillus* sp. dwc-2 under anaerobic conditions, at room temperature. XPS results demonstrated that the uranium was present mixed valence states (U(VI) and U(IV)) after uranium bioreduction. Furthermore, the TEM and HRTEM analysis suggested that the reduced uranium was bioaccumulation as crystalline structure on cell wall and mainly within the cell. Besides, Uranium L_{III} edge XANES spectra obtained after U (VI) bioreduction by *Bacillus* sp. dwc-2 further demonstrated the presence of tetravalent uranium.

Acknowledgements

[1] D. R. Lovley, E. J. P. Phillips, Y. A. Gorby, E. R. Landa (1991). "Microbial reduction of uranium." Nature. 350: 413-416.
[2] Y. Suzuki, S. D. Kelly, K. M. Kemner, J. F. Banfield (2002). "Radionuclide contamination: Nanometre-size products of uranium bioreduction." Nature. 419: 134-134.
[3] B. H. Gu, J. Chen (2003). "Enhanced microbial reduction of Cr(VI) and U(VI) by different natural organic matter fractions." Geochim. Cosmochim. Acta. 67: 3575-3582.
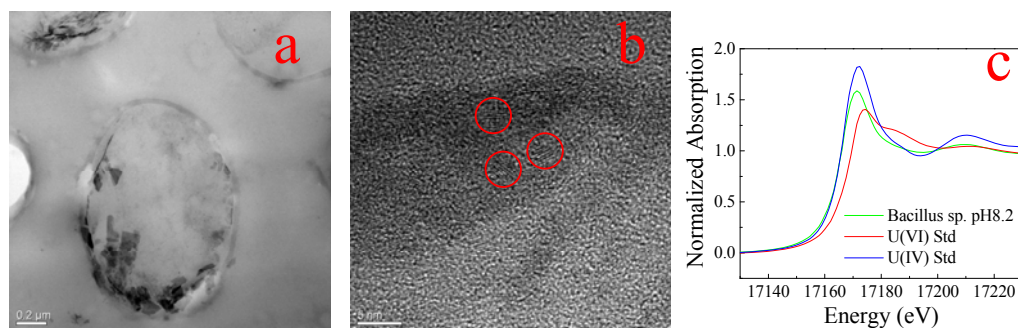
Figure 1. TEM (a) and HR-TEM(b) micrograph of *Bacillus* sp. dwc-2 cell after U(VI) bioreduction, Uranium L_{III} edge XANES spectra after U(VI) bioreduction by *Bacillus* sp. dwc-2 (c).

THE MICROBIAL IMPACT ON THE SORPTION BEHAVIOUR OF SELENITE IN AN ACIDIC NUTRIENT-POOR BOREAL BOG

M. Lusa[(1)], M. Bomberg[(2)], H. Aromaa[(1)], J. Knuutinen[(1)], J. Lehto[(1)]

[(1)] *Laboratory of Radiochemistry, Department of Chemistry, P.O. Box 55, 00014 University of Helsinki, Finland*

[(2)] *VTT Technical Research Centre of Finland, P.O. Box 1000, 02044 VTT, Finland*

In Finland, spent nuclear fuel will be disposed of in a deep bedrock repository situated on Olkiluoto Island. The long term safety of the nuclear fuel repository is based on several barriers, such as the copper sheeted waste canister, the bentonite clay protecting the canister and the bedrock of the repository. However, the radionuclides could escape from the repository, if the waste canisters were to lose their integrity and eventually migrate into the surface biosphere. In the repository area the post-glacial land uplift continues and as a result Olkiluoto Island will develop into an inland site after the next 6000 years [1][2]. According to the biosphere safety assessment, new bogs will form on the area at the same time period as the first potential radionuclide emissions from the repository to the surface ecosystem are possible, if the canisters would leak [2]. Lastensuo bog, situated 30 km inland from Olkiluoto, is considered to represent the mire type found in the Olkiluoto area in the future, and has therefore been chosen as an analogue biotope in biosphere safety assessment [3]. In the long-term safety assessment, [79]Se is classified as a high priority radionuclide when the possible radiation dose for humans in the future is considered [4].

The factors affecting the sorption behaviour of selenite SeO_3^{2-}, the probable form of selenium in these conditions, in the depth profile of Lastensuo nutrient-poor bog as well as the uptake of selenite by bacteria isolated from the bog was examined using batch experiments. The batch distribution coefficient (K_d) values of selenite decreased as a function of sampling depth of the bog profile and highest K_d values, on average 6700 L/kg dry weight (DW), were observed in the fresh surface moss and the lowest in the bottom clay (on average 1900 L/kg DW) (Fig. 1A). The highest sorption was observed at pH between 3 – 4 in all studied bog layers (Fig. 1B) and the K_d values were significantly higher in unsterilized samples than in sterilized samples, but anoxic conditions had only a minor effect on the K_d values (Fig 2A-B). *Pseudomonas* sp., *Burkholderia* sp., *Rhodococcus* sp. and *Paenibacillus* sp. strains isolated from the bog were able to remove selenite from the nutrient broth solution (1% Tryptone) (Fig. 3A). In addition, the incubation of sterilized surface moss, subsurface peat and gyttja samples with isolated bacteria increased the removal of selenite from the solution (Fig. 3B). Removal was most effective when *Pseudomonas* sp. or *Burkholderia* sp. strains were used. These results demonstrate the importance of bacteria for the removal of selenite from the solution phase in the bog environment, having a high organic matter content and a low pH.

A

B
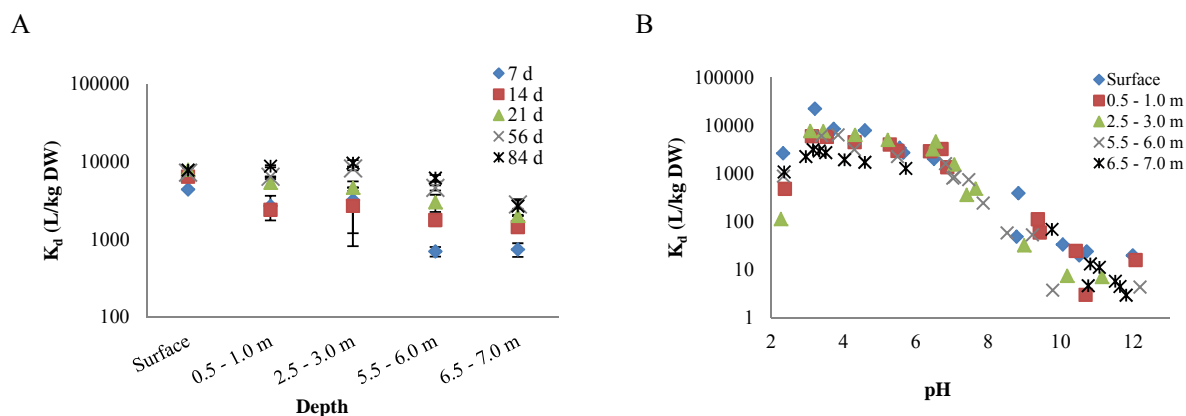
Figure1. A) The distribution coefficients (K_d) of selenite as function of bog depth. Incubation time 7 - 84 days. B) The K_d values of selenite as a function of pH in different bog layers.
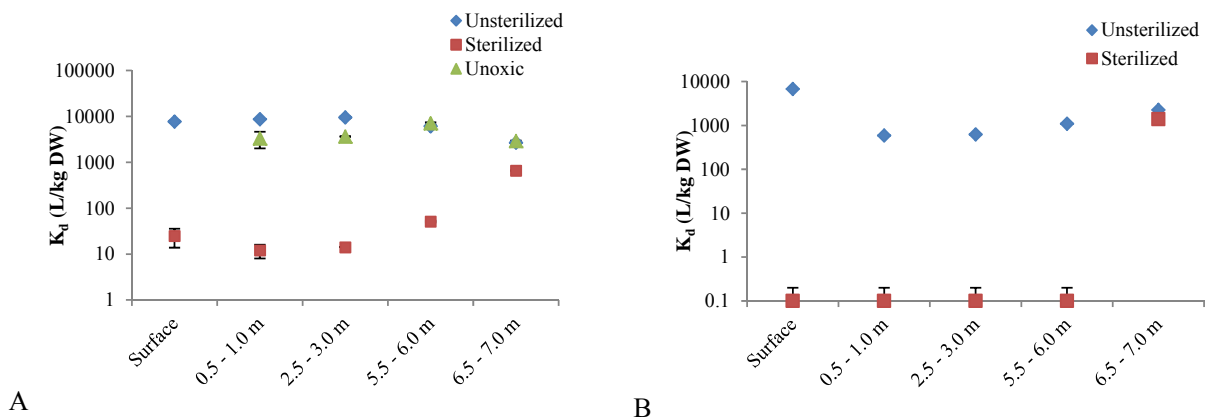
Figure 2. A) The K_d values of selenite in unsterilized and sterilized samples and under anoxic conditions at 20°C. B) The K_d values of selenite in unsterilized and sterilized samples at 4 °C.
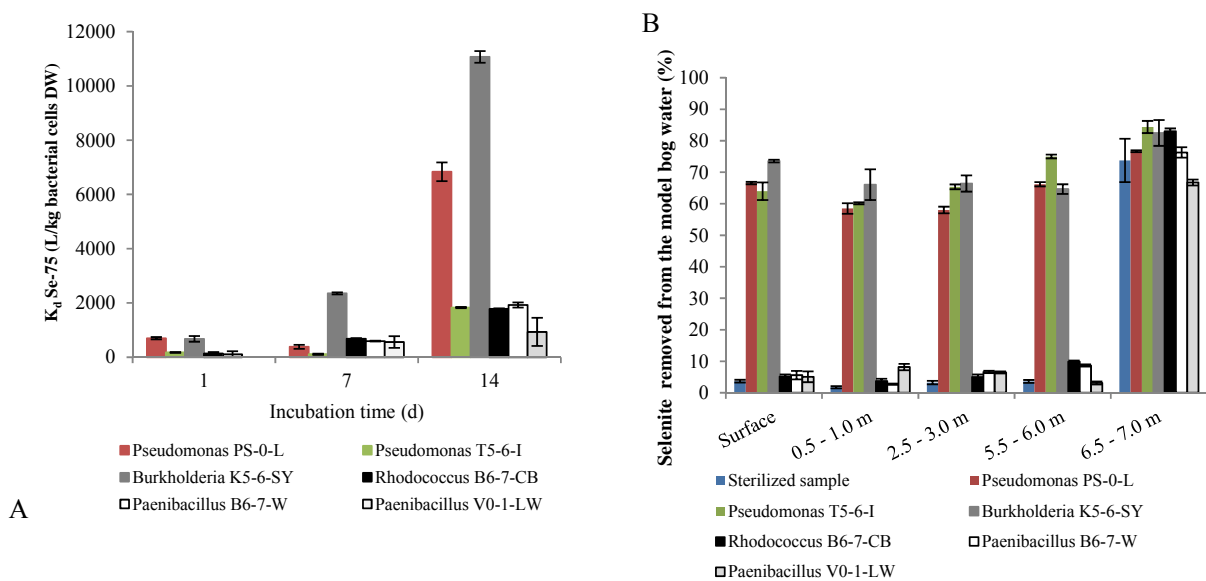
Figure 3. A) The uptake (L/kg DW) of selenite by bacteria isolated from the bog. B) Selenite removal (%) from the bog water model solution when 2 % sterilized surface moss, peat, gyttja or clay and different bacterial strains were added to the solution. T = + 20 °C, incubation time seven days.

[1] Haapanen, R., Aro, L., Helin, J., Ikonen, A.T.K., Lahdenperä, A-M. (2013). "Studies on Reference Mires: 1. Lastensuo and Pesänsuo in 2010-2011". Working Report 2012-102, Posiva Oy, Eurajoki, Finland.

[2] Posiva (2012). "Safety Case for the Disposal of Spent Nuclear Fuel at Olkiluoto—Description of the Disposal System 2012". Report POSIVA 2012–05, Posiva Oy, Eurajoki, 166 p. http://www.posiva.fi/

[3] Haapanen, R., Aro, L., Koivunen, S., Lahdenperä, AM., Kirkkala, T., Hakala, A., Helin, J., Ikonen, ATK. (2011). "Selection of Real-Life Analogues for Future Lakes and Mires at a Repository Site". Radioprotection, 46: 647-651.

[4] Helin, J., Hjerpe, T., Ikonen, A.T.K., (2010). "Review of Element Specific Data for Biosphere Assessment BSA – 2009". Working Report 2010-37, Posiva Oy, Eurajoki, Finland.

AN ANALOGUE STUDY FOR HEAVY METAL SORPTION ONTO BIOFILM IN THE DEEP SUBSURFACE ENVIRONMENT OF THE HORONOBE AREA, HOKKAIDO, JAPAN

Y. Amano[1]*, K. Ise[1], T. Ito[1], K. Nemoto[1], Y. Tachi[1]

[1]*Sector of decommissioning and Radioactive Wastes Management, Japan Atomic Energy Agency, 4-33 Muramatsu Tokai-Mura, Ibaraki, 319-1194 Japan*

Biofilms are ubiquitous in aquatic environments, and more than 99% of all microorganisms on Earth are living as biofilms. Solid-liquid interfaces are very important boundary in biofilm formation as they provide water for microorganism to form biofilm. In biofilm environments, heavy metals and radionuclide pollutants are removed by a variety of mechanisms, including biosorption, precipitation, mineralization, transformation, etc. Therefore, it is crucial to investigate natural biofilms to evaluate the mobilization of heavy metals including radionuclides in natural systems. High-level radioactive waste (HLW) and spent nuclear fuel (SF) from nuclear power generation must be disposed in a safe manner for at least 100,000 years until the radiation dose is reduced to the levels of natural radiation dose in subsurface environments. Microorganisms have been found ubiquitously in most subsurface environments, and biofilms can be expected to cover fracture surfaces in the subsurface environments and might have some influence on radionuclide transport, such as diffusion and sorption properties in host rocks. Therefore, it is necessary to evaluate and include microbial effects in performance assessments of geological disposal. Japan Atomic Energy Agency (JAEA) advances to establish general techniques for quantitative evaluation of microbial effects on radionuclide migration, which is one of the uncertain factors on long-term safety of the geological disposal. In this study, we characterized the geochemical and microbial properties of biofilm samples formed with groundwater from boreholes in the subsurface environment at Horonobe area, Japan. The biofilm samples were grown naturally into the sampling tubes made by nylon under in-situ geochemical conditions. The heavy metal sorption capacities of these biofilms were also determined to evaluate the effects of microorganisms on radionuclides transport in HLW systems.

Biofilm samples were collected from sampling tubes of two boreholes and naturally occurring on the gallary wall of the Horonobe Underground Research Laboratory at Horonobe area, Japan. The chemical composition of groundwater and biofilm samples were analyzed by absorption spectrophotometry and ICP-MS. The concentration of heavy metals, such as Co, Se, Cs, Ce, Nd, Eu, Gd, Th, U, etc., were analyzed by ICP-MS. The 16S rDNA of bacteria and archaea were analyzed to understand microbial community structure in the samples.

From the results of the heavy metal analyses, it is revealed that high content of heavy metals was accumulated in the biofilms, and each elements was not accumulated in quantity in the same proportion and had different sorption properties. The concentration of Ce, Nd, Eu, Gd in the biofilms were relatively high compared to the other elements, although the concentration in groundwater samples were extremely low. On the other hands, Se and Cs accumulated in the biofilms were detected relatively low concentration in spite of relatively high concentration in the groundwaters compared to the lantanoid elements. In addition, it is showed that sorption properties were different between each biofilm samples although the trend of heavy metal concentration were similar in each groundwater samples. We could find no discernible correlation between those elements accumulated in the biofilms and the composition of groundwaters. It is assumed that these differences depend on the microbial community structure that composed of biofilms. It is possible that the biofilms selectively accumulate heavy metals according to their metabolic activity. Analyses of 16S rDNA utilizing next generation sequencing indicates that the biofilms were dominated by the phylum Nitrospirae, Proteobacteria, JS1 as candidate division, and SM1 Euryarchaeon. Over 40% of the detected sequences belong to groups of uncultured microorganisms. These results possibly show the similar characteristics with natural biofilms formed on fracture-surfaces in the subsurface environments. Hence, it is necessary to evaluate mechanisms of interaction between heavy metals, microbial community structure and metabolic activities of biofilms.

INFLUENCE OF A HALOPHILIC ARCHAEUM TO URANIUM MIGRATION UNDER HIGHLY SALINE CONDITIONS

M. Bader, B. Drobot, K. Müller, T. Stumpf, A. Cherkouk

Helmholtz-Zentrum Dresden – Rossendorf, Institut of Resource Ecology, Bautzner Landstraße 400, 01328 Dresden, Germany

In Germany salt rock and clay are considered as potential host rock for the final repository of radioactive waste in deep geological formations. Both possibilities have in common that high saline conditions can occur. In clay deposits of Northern Germany pore water salt concentrations of 4.3 M were measured [1] and in salt rock the salt concentration is up to saturation. Despite these extreme environments some microbes are able to survive. To date little is known about the interactions of halophilic microorganisms with actinides and hence to the migration behavior. But for the safety assessment of the final repository it is important to know the impact of indigenous microorganisms. Microbes can interact with actinides in different ways [2]. Within this study, the sorption of uranium on the cell surface (so called biosorption) of *Halobacterium noricense* DSM 15987 cells was studied. This halophilic archaeum was chosen due to its worldwide occurrence in salt rock [3]. The reference strain was isolated in an Austrian salt mine [4] and similar species occurred also in the Waste Isolation Pilot Plant (WIPP, Carlsbad, New Mexico, USA) [3].

Biosorption studies were undertaken at pH 6.0 and a NaCl concentration of 3.0 M in dependence of uranium concentration, time and temperature. The uranium content in the supernatant after sorption was measured with ICP-MS (Inductively Coupled Plasma Mass Spectrometry). Both, supernatant and cell pellet, were analyzed with TRLFS (Time-resolved Laser-induced Fluorescence Spectroscopy) to get information about the formed complexes. Furthermore the cells were analyzed with Infrared Spectroscopy.

The results demonstrated that independent of the uranium concentration (10 – 120 μM) around 90 % of the added uranium was sorbed by the cells at room temperature. A time-dependent sorption study showed that this maximal sorption was reached after an incubation time of 42 h. A slightly faster sorption of added uranium could be seen at higher temperatures. Particularly at 50 °C, the maximal sorption was already reached after 24 h. In general, the obtained sorption curve indicated a two-step binding process of added uranium with a fast step within the first hours and a second slower one. For a uranium concentration of 100 μM the metal sorption rate of 37.5 ± 0.7 mg U(VI) per 1 g dry biomass of *Halobacterium noricense* DSM 15987 was determined .

Interestingly, with increasing time, uranium concentration and temperature the cells began to form agglomerates. Live/Dead staining (LIVE/DEAD® Bac Light™ Bacterial Viability Kit L7012, Molecular Probes) of cells after the biosorption with uranium showed that nearly all single cells were dead whereas agglomerated cells were alive. One conclusion is that this process is a kind of stress response to protect the cells themselves from environmental challenges.

The characterization of the formed cell-uranium-complexes with TRLFS indicated that uranium was bound to cellular carboxylic groups. This can be seen by comparing with literature spectra [5]. The obtained lifetimes of the uranyl complexes differed from those due to the quenching effect of the high chloride concentration to uranium luminescence. The binding of uranium to the carboxylic groups of the cell could be also verified with Infrared Spectroscopy.

[1] J. Larue, VerSi Endlagerung im Tonstein, Abschlussbericht 3607R02538 (2010).

[2] K. Morris, et al., Interactions of microorganisms with radionuclides 2, 101 (2002).

[3] J. S. Swanson, et al., Status report Los Alamos National Laboratory (2012).

[4] C. Gruber, et al., Extremophiles 8, 431 (2004).

[5] M. Vogel, et al., Sci. Total Environ. 409, 384 (2010).

MICROBIAL INDUCED CARBONATE PRECIPITATION FOR THE CAPTURE AND REMEDIATION OF TRIVALENT ACTINIDES AND LANTHANIDES

E. Johnstone, A. Cherkouk, M. Schmidt

Institute for Resource Ecology, Helmholtz-Zentrum Dresden-Rossendorf, 01328 Dresden, Germany

Biomineralization is the process by which minerals are produced by organisms. Microbial induced carbonate precipitation (MICP) is a fundamental example of biologically induced mineralization [1]. This occurs when the metabolic activities of bacteria chemically alter the surrounding environment facilitating the precipitation of carbonate minerals. Bacterial ureolysis is the most well-studied and basic pathway leading to MICP where urea is metabolized or degraded by urease enzyme containing bacteria, ultimately yielding ammonium and carbonate ions correlated with a rise in pH [2]. MICP has gained particular interest in applications for soil stabilization and subsurface barriers, limestone remediation, carbon dioxide sequestration, and groundwater remediation of heavy metals and radionuclides [3].

Near and far field studies of geological nuclear repositories are important for the better understanding of how radionuclides chemically behave under repository conditions and their potential interactions with the geo- and biosphere. Because of their long half-lives and high radiotoxicity, americium and curium are two problematic transuranic actinides (An) in spent nuclear fuel that pose a serious threat if released into the environment. Previous studies using Time-Resolved Laser Fluorescence Spectroscopy (TRLFS) have shown that Ca^{2+}-containing mineral phases, e.g., $CaCO_3$, are ideal for incorporation of trivalent Am/Cm and homologous trivalent lanthanides (Ln), i.e. europium, into the host material, thus retarding their environmental mobility [4]. Further investigations have also demonstrated that physicochemical differences between inorganic versus biogenically derived minerals may yield different interactions with these elements, which has important implications concerning their disposal and behavior in the biosphere [5].

In this work, the archetypal ureolyzing bacteria *Sporosarcina pasteurii* was used for the microbial induced precipitation of $CaCO_3$ in the presence of trivalent actinides and lanthanides under varying conditions. The reactions were monitored over time and the solution chemistry and resulting mineral were characterized by a variety of physicochemical techniques. In addition, batch as well as transport studies were performed to determine the static and dynamic interactions and kinetics of previously formed biominerals and trivalent An/Ln at the water-surface interface. Furthermore, TRLFS was used to determine the chemical environment and structural localization of the An/Ln(III) with the biominerals and compared to results from previous studies on pure inorganic $CaCO_3$ systems. Ultimately, this allows for the better understanding on how these elements interact with $CaCO_3$ originating from biomineralization and their fate within the biosphere.

[1] Y. Fujita, et. al., Geomicrobiol. J. 17, 305 (2000).
[2] N. K. Dhami, et al., Front. In Microbio. 4, 1 (2013).
[3] L. A. Warren, et. al., Geomicrobiol. J. 23, 213 (2001).
[4] M. Schmidt, et al., Angew. Chem. Int. Ed. 47, 5846 (2008).
[5] K. Holliday, et. al., Radiochim. Acta. 101, 267 (2013).

COPRECIPITATION OF RADIACTIVE STRONTIUM IN SEA WATER DURING FORMATION OF BIOGENIC CALCITE

T. Ohnuki[1]*, N. Kozai[1], F. Sakamoto[1], T. Saito[1], Q. Yu[1], M. Yamashita[2],
T. Horiike[2], S. Utsunomiya[3]

[1] *Advanced Science Research Center, Japan Atomic Energy Agency, 2-4,
Muramatsu, Tokai, Ibaraki 319-1195, Japan*
[2] *Rare Metal Bioresearch Center, Research Organization for Advanced Engineering Shibaura Institute of
Technology, 307 Fukusaku, Minuma-Ku, Saitama-shi Saitama 337-8570, Japan*
[3] *Department of Chemistry, Kyushu University, 6-10-1, Hakozaki, Fukuoka-shi, Fukuoka 812-8581,
Japan*

Many kinds of radionuclides were released by the Fukushima Daiichi Nuclear Power Plant (FDNPP) accident to environments[1]. Tremendous technological effort to deal with the effects of the FDNPP accident have been performed. Cesium-134 and ^{137}Cs were initially main radionuclides of concern for elimination from the contaminated ground and sea water in the area of FDNPP. More emphasis is now required on elimination of ^{90}Sr. Since sea water's salinity is high and contains high concentration of Ca and Mg, adsorption performance of Sr by sorbents including smectite decreases, compared to that in groundwater[2]. One of the possible method to eliminate ^{90}Sr is coprecipitation of Sr with carbonates minerals. Bacteria ureolysis is known to be able to in-situ eliminate Sr from groundwater by plroducing carbonates.[3,4]. We have studied the elimination of ^{90}Sr from sea water into biogenic calcite.

Biogenic calcite were produced at 30 °C by a maline microbe of TK2d. The liquid medium contained (per L) 3.74 g Maline broth, 20 g urea, 30 g NaCl. The medium was inoculated with the maline bacterium of TK2d with 5.0, 1.0. 0.1, and 0.02 mM $SrCl_2$ in erlenmeyer flask at 120 rpm. The initial pH value was adjusted to 7.6 ± 0.1 with 1 M NaOH or 1M HCl solution. Sr^{2+} concentrations were monitored by ICP-OES (ICP-OES; 720 Agilent Technologies, Inc., USA) during cultivation. After ten days incubation, most of Ca^{2+} in solution was removed. Biogenic precipitates were collected by filtration, repeatedly washed by distilled water. The precipitates and $SrCO_3$, coprecipitates of Ca-Sr carbonates, formed abiotically were observed by SEM and TEM. The coordination environment of Sr in the precipitates were analyzed by XAS.

When 1.0 mM Sr was dissolved in the solution, the time course of concentrations of Sr and Ca in the solution showed that the concentration of Ca gradually decreased to 0.8 mM with increasing time up to 6 days, followed by abrupt decrease of Ca up to 0.4 mM at the day 6, then decreased gradually to 0.1 mM. The concentration profile of Sr showed nearly the same time course as that of Ca. The concentration of Sr after 10 days was approximately 0.02 mM, indicating that most of Sr in the solution was eliminated within 10 days.

SEM and TEM analyses showed that needle shaped precipitates containing Ca and Sr was formed (Fig. 1) when 1.0 mM Sr was added in the solution with TK2d strain. The elemental mapping showed that Sr was present at the same position of Ca, indicating that Sr was coprecipitated with Ca. Precise analysis of the precipitates by TEM showed that the Ca and Sr bearing needle shaped precipitates of 2-3 m in size were polycrystalline aggregates of tens nm.

The XANES analysis of Sr in the precipitates showed that the XANES spectrum resembled with that of Sr coprecipitated with an abiotic Ca carbonates and differed from that in $SrCl_2$ and $SrCO_3$, indicating that Sr was neither adsorbed on the Ca carbonates, nor precipitated independently as $SrCO_3$, but was coprecipitated with $CaCO_3$. The FT of EXAFS spectrum showed that peaks of C and Sr were present in the FT and coordination number and distance from Sr were different from those in the FT of Sr in the abiotic coprecipitates of Sr-Ca carbonates. These results indicate that coordination environment of Sr in the biotic coprecipitates differs from that in the abiotic one.

Thus, biological coprecipitation of Sr with Ca carbonates is effective method for the elimination of radioactive Sr from saline solution.
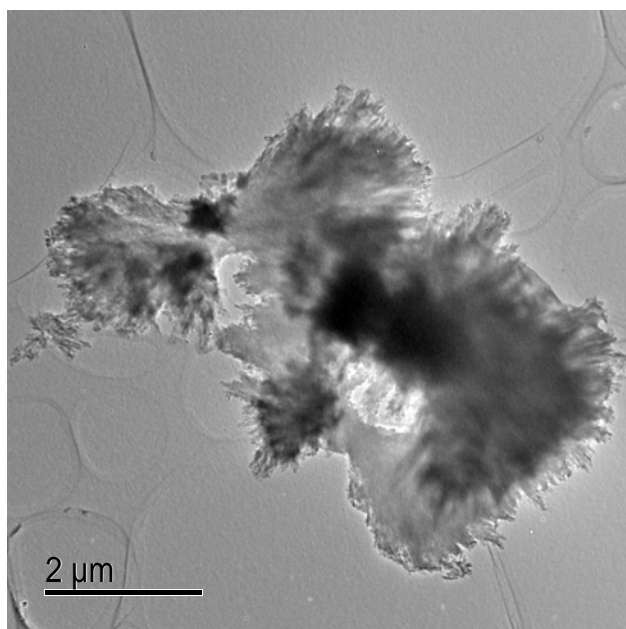
Fig. 1 TEM image of the biological precipitates containing Ca and Sr.

[1] K. Nishihara, et al., J. Nucl. Sci. Tecnol., 52, 301 (2015).
[2] T. Ohnuki, N. Kozai, Radiochim. Acta, 66/67, 327 (1994).
[3] Y. Fujita, et al., Geochim. Cosmochim. Acta 68, 3261(200).
[4] Y. Fujita, et al., Environ. Sci. Technol., 42, 3025(2008)

SORPTION AND REDUCTION OF PLUTONIUM BY SURFACE BOUND EXTRACELLULAR POLYMERIC SUBSTANCES

M. Boggs, Y. Jiao, Z. Dai, A. Kersting, M. Zavarin

Glenn T. Seaborg Institute, Lawrence Livermore National Laboratory, Livermore California

The present study examines sorption of Pu(V) and Pu(IV) to the surface of *Pseudomonas sp* cells isolated from the Nevada Nuclear Security Site, Nevada USA. The complexation and reduction of Pu was investigated in the presence and absence of cell-bound EPS. Surface-bound Pu species were characterized by transmission electron microscopy (TEM), and aqueous Pu-EPS complexes were examined by nuclear magnetic resonance spectroscopy (NMR).

Sorption of 10^{-10} M Pu(IV)/(V) to *Pseudomonus sp*. is shown in **Figure 1**. Sorption of Pu(IV) increased with cell density and was maximized at cell densities greater than 0.12 g_{cell}/L. The Pu(IV) sorption was independent of EPS presence - no effect on Pu(IV) sorption was observed between cells with EPS intact and those with EPS removed. Sorption of Pu(V) to cells with their EPS intact followed a similar trend to that of Pu(IV), increasing with cell density to a maximum at 0.1 g_{cell}/L. Pu(V) sorption significantly differed from that of Pu(IV) in that EPS affected cell sorption. Pu(V) sorption was limited to 20% when the cell bound EPS was removed, even at the highest cell densities studied.

Aqueous oxidation state analysis reveals that soluble Pu(V) was reduced within 48 hours in the presence of cells with EPS. No reduction occurred in Pu(V) sorption experiments where the EPS had been removed. The amount of Pu initially present as a reduced species coincides with the amount sorbed onto the cell and indicates a high affinity for reduced Pu species. From these studies it is apparent that EPS is a critical component to Pu-cell interaction.

To further investigate its influence on Pu complexation and reduction, EPS from *Pseudomonus sp* was harvested and purified. The near complete reduction of 4×10^{-9} M Pu(V) was observed at EPS concentration as low as 1 ppm. No reduction was observed in the absence of EPS, indicating that the EPS is the driving force behind Pu reduction. Complete reduction of 8×10^{-4} M Pu(V) was observed within 48 hours at EPS concentrations of 10 and 25 ppm. Despite the predicted solubility limit of Pu(IV) being far lower than the Pu concentrations used in these studies[1], the reduced Pu species remained soluble. The increased solubility may be attributed to the formation of soluble organic complexes upon reduction.

In order to determine if the surface sorbed Pu species is dependent on the initial oxidation state of Pu we examined the morphology and structure of Pu minerals formed on the cell surface using TEM. Surface bound Pu particles of less than 1 nm were observed on cells equilibrated with 1×10^{-5} M Pu(IV), independent of EPS. Conversely, no Pu mineralization was observed with up to 1×10^{-4} Pu(V). While there are clear morphological differences between the surface sorbed species we are not able to identify the surface species with TEM alone.

The complex composition of EPS makes the identification of specific binding and redox active sites difficult. By utilizing solution state NMR techniques we may gain greater insight into Pu complexation by EPS. Through the analysis of Pu equilibrated with EPS we are able to identify specific moieties involved in complexation. The formation and characterization of Pu EPS complexes will be discussed. Understanding these complexes is important as the chemical form of Pu will inevitably dictate its desorption rate from the cell surface as well as its environmental mobility.

Figure 1. Sorption of 1×10^{-10} M **A)** Pu(IV) and **B)** Pu(V) to whole cells of *Pseudomonas sp.* with (solid) and without EPS (hollow) at pH 6.5 in 0.01 M $NaClO_4$ after 48 hours. Error bars represent 2σ error calculated from triplicate samples.
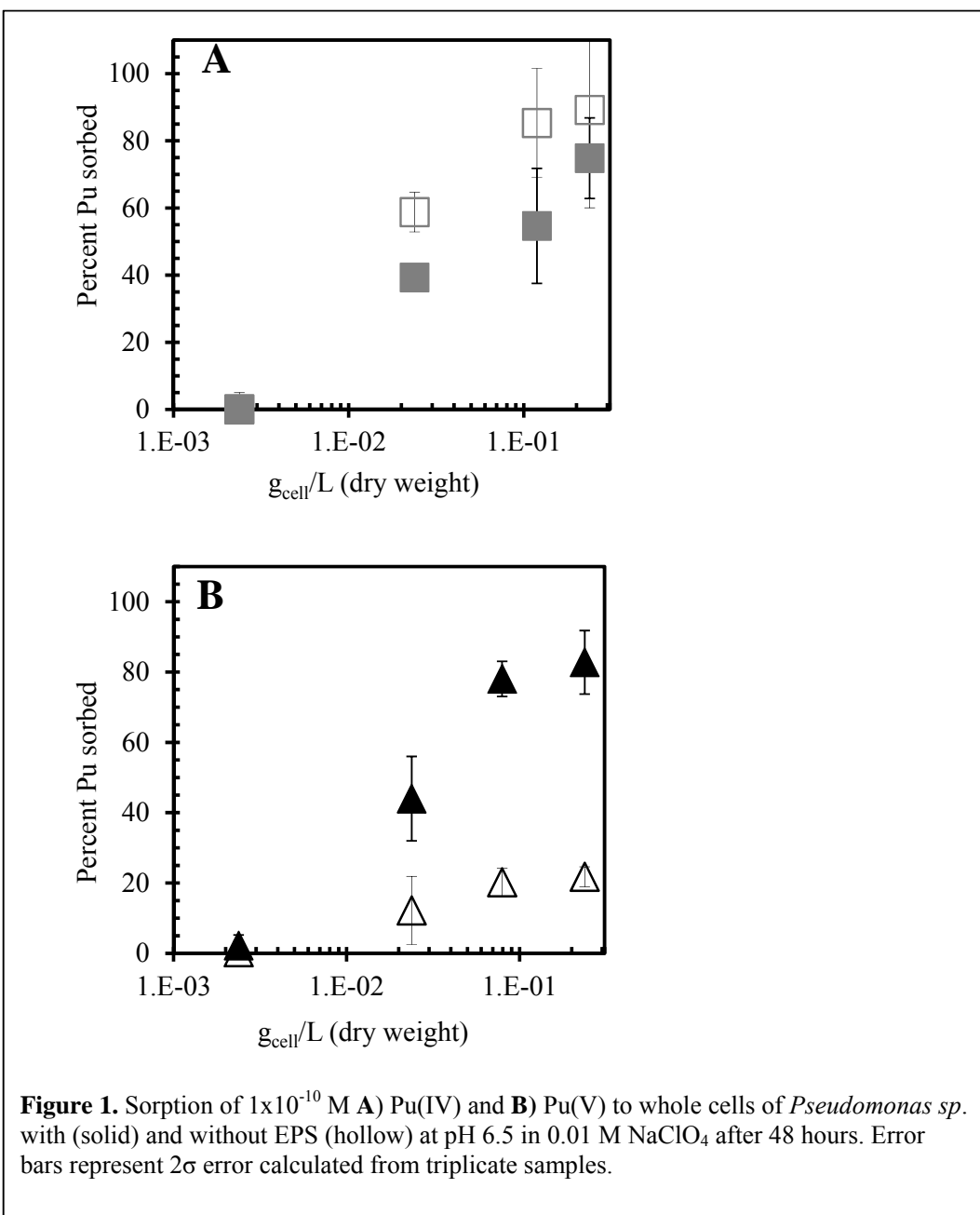
1. Neck, V.; Altmaier, M.; Fanghanel, T., Solubility of plutonium hydroxides/hydrous oxides under reducing conditions and in the presence of oxygen. *Comptes Rendus Chimie* **2007,** *10*, (10-11), 959-977.

BIOASSOCIATION OF ACTINIDES WITH MICROORGANISMS
IN HIGH IONIC STRENGTH BRINE SYSTEMS

J. F. Lucchini, D. T. Reed, M. K. Richmann, and J. S. Swanson

Repository Science & Operations Program,
Los Alamos National Laboratory, Carlsbad NM, 88220, USA

Bioassociation of actinides and redox-invariant analogs with microorganisms has been an increasing area of investigation in the Los Alamos National Laboratory (LANL) Repository Science & Operations (RSO) program in support of the Waste Isolation Pilot Plant (WIPP) recertification effort [1]. Because biocolloidal species are considered as a source term of the potential migration of actinides in the WIPP performance assessment [2], a better understanding of the interaction between actinides and microorganisms indigenous to high ionic strength systems is needed.

Halobacterium noricense, a halophilic archaeon, and *Chromohalobacter* sp. bacteria have been isolated from WIPP halite and brine [3]. The bioassociation of neodymium (Figure 1) and thorium, which are used as redox-invariant analogs for the +III and +IV actinide species respectively, with these two microorganisms were extensively studied in WIPP brine, over a broad range of pC_{H+}.
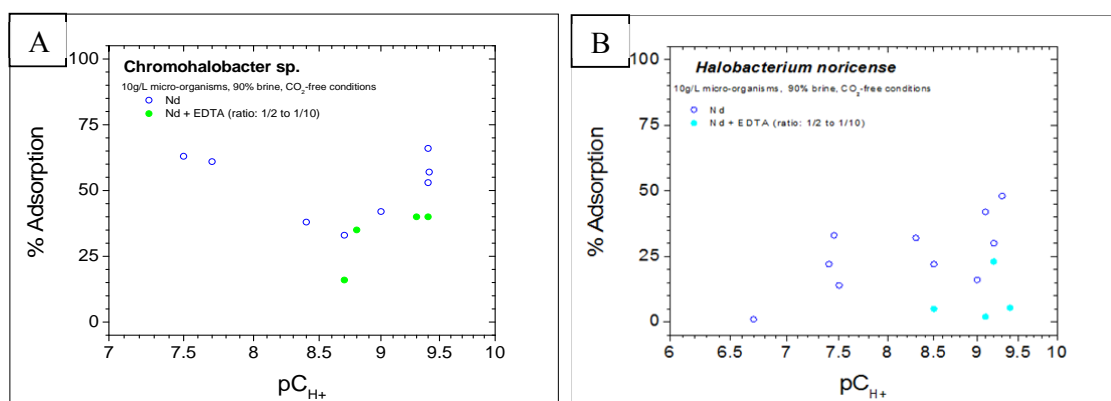
Figure 1. Adsorption of neodymium, an redox-invariant analog for the +III oxidation state of the actinides, to *Chromohalobater* sp. (A) and *Halobacterium noricense* (B) as a function of pC_{H+}, in carbonate-free brines and in the presence or the absence of EDTA.

Because of the presence of colloidal and hydrolysed species of neodymium (Nd) and thorium (Th) in high ionic strength systems at high pC_{H+} [4], only upper estimates of bioassociation with the two microorganisms were obtained. Relatively high and irreversible bioassociation with the bacteria was observed at high pC_{H+} (~80% for Th, ~60% for Nd). Bioassociation with the archaea was lower (~15% for Th, ~25% for Nd), with a different pattern across the investigated range of pC_{H+} (see Figure 1 for the Nd system). This result possibly indicates a difference in the nature of the bioassociation (extracellular, intracellular, different ligand at the cell surface) with the two microorganisms.

A similar conclusion was made from experiments on the interaction of neptunium (+V) with the two microorganisms in simplified brine (4 mol.L^{-1} sodium chloride). Bioassociation of neptunium with the archaea was relatively stable across the investigated range of pC_{H+} (Figure 2), and much lower (~10%) than the bioassociation with the bacteria (between 50% to 80% over the same range of pC_{H+}).

Future work is focused on the properties of the cell walls of the two organisms. A method previously developed for purifying cell envelopes from various isolates is being optimized for halophilic cultures [5]. The goal is to distinguish which type of uptake, intracellular (internal uptake) or extracellular (cell surface adsorption), is the predominant sorption process for each microorganism. Also, new bioassociation experiments using simplified systems (simplified brines, neptunium +IV, americium +III) are planned to determine the possible mechanisms involved in these interactions.
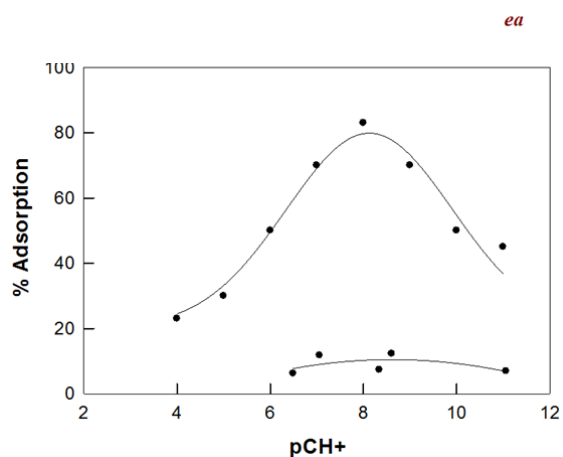
Figure 2. Adsorption of neptunium (+V) to *Chromohalobater* sp. (top curve) and *Halobacterium noricense* (bottom curve) as a function of pC_{H+} in carbonate-free brines.

[1] Ams, D. A., J. S. Swanson, J.E.S. Szymanowski, J.B. Fein, M. Richmann, D.T. Reed (2013). "The Effect of High Ionic Strength on Neptunium (V) Adsorption to a Halophilic Bacterium." Geochimica et Comoschimica Acta. 110: 45-57

[2] U.S. DOE, CRA-2014, Appendix PA, Attachment SOTERM, DOE/WIPP-14-3503, Carlsbad, NM. 2014

[3] Swanson, J.S., D.T. Reed, D.A. Ams, D. Norden, K.A. Simmons (2012). "Status Report on the Microbial Characterization of Halite and Groundwater Samples from the WIPP." Los Alamos National Laboratory Report, LA-UR-12-22824

[4] Reed, D. T., J. S. Swanson, J.F. Lucchini, M.K. Richmann (2013). "Intrinsic, Mineral and Microbial Colloid Enhancement Parameters for the WIPP Actinide Source Term." Los Alamos National Laboratory Report, LA-UR-13-20858

[5] Reitz, T., M.L. Merroun, A. Rossberg, R. Steudner, S. Selenska-Pobell (2011). "Bioaccumulation of U(VI) by *Sulfolobus acidocaldarius* under moderate acidic conditions." Radiochimica Acta. 99:543-553

LOW BACKGROUND RADIATION EXPERIMENTS (LBRE) ON BIOLOGICAL CELLS AT THE U.S. WASTE ISOLATON PILOT PLANT (WIPP) AND THE ITALIAN *Laboratori Nazionali di Gran Sasso*

G.B. Smith[1], H. Castillo[1] and A. Tabocchini[2]

[1]New Mexico State University-Department of Biology, Las Cruces, NM 88003.
[2]Istituto Superiore di Sanita, Roma, Italy.

An international collaboration has been initiated in order to investigate the biological effects of environmentally relevant levels of radiation on the growth, gene expression and enzymatic activity of cells ranging in complexity from bacteria (*Deinococcus radiodurans/Shewanella oneidensis*) to tissue cultures (*Cricetulus griseus* V-79 cells) to multicellular organisms (the nematode *Caenorhabditis elegans*). We are especially interested in addressing radiation effects "*from the other side of background*," that is by growing cells in the naturally-shielded and unique facilities in the underground laboratories at WIPP and Gran Sasso. The Gran Sasso group have pioneered work in radiation biology and health physics in documenting the mal-adaptive effects of depriving biological cells of normal levels of radiation in hamster and human cells (Satta et al. 2002; Carbone et al. 2009, Fratini et al. 2015). Similarly, the New Mexico State University group have documented deleterious effects of shielding cells from background radiation when bacteria were grown underground at WIPP (Smith et al. 2011, Castillo et al. 2015).

At WIPP, we incubate cells in a pre-World War II steel vault that lowers background radiation by about a factor of 400, to levels modeled by Monte Carlo N-Particle (MCNP) at ~0.2 nGy/hr. We have employed two types of controls in which cells are exposed to normal, background levels of radiation: they are grown aboveground (Smith et al. 2011) or they are grown underground with a natural source (KCl) of radiation added back to approximate background levels (Figure 1). When deprived of natural levels of radiation, the radiation sensitive bacterium, *Shewanella oneidensis*, upregulates expression of genes belonging to three different families of stress response genes for DNA repair, reactive oxygen species (ROS) scavenging and metal efflux pumps. After documenting the stress response, when we return the cells to radiation-sufficient conditions, the stress is allayed and the cells return to normal, control levels of gene expression and growth (Castillo et al. 2015).

We have initiated transcriptome analysis (RNA Seq) to document across the genome how many genes are responsive to the withdrawal of normal levels of radiation. Preliminary data shows the differential regulation of 272 and 172 known-function genes in both *S. oneidensis* and *D. radiodurans,* respectively*,* in response to below background radiation. As an example, *S. oneidensis* patterns of gene expression suggest, in general, that radiation-deprivation at WIPP increases the transcription of genes related to protein synthesis, signal transduction and transport processes while decreasing the transcription of genes involved in protein assembly (Figure 2). Since, according to the Linear No-Threshold (LNT) model, all levels of radiation are potentially harmful, it would be predicted that cells shielded from natural radiation levels would grow better and be less stressed. Results obtained at both the WIPP and Gran Sasso labs consistently reject this LNT-based hypothesis.

1. Carbone et al. 2009. The cosmic silence experiment: the putative adaptive role of environmental radiation. Rad. Environ. Biophys. 48:189-196.
2. Castillo et al. 2015. Stress induction in the bacteria *Shewanella oneidensis* and *Deinococcus radiodurans* in response to below-background ionizing radiation. Int. J. Rad. Biol. IN PRESS
3. Fratini et al. 2015. Low-radiation affects development of protection mechanisms in V79 cells. Radiat. Environ. Biophys. 54:183-194.
4. Satta et al. 2002. Influence of low background radiation on biochemical, biological responses in V79 cells. Rad. Environ. Biophys. 41:217-224.
5. Smith et al. 2011. Exploring biological effects of low level radiation from the other side of background. Health Phys. 100:263-265.
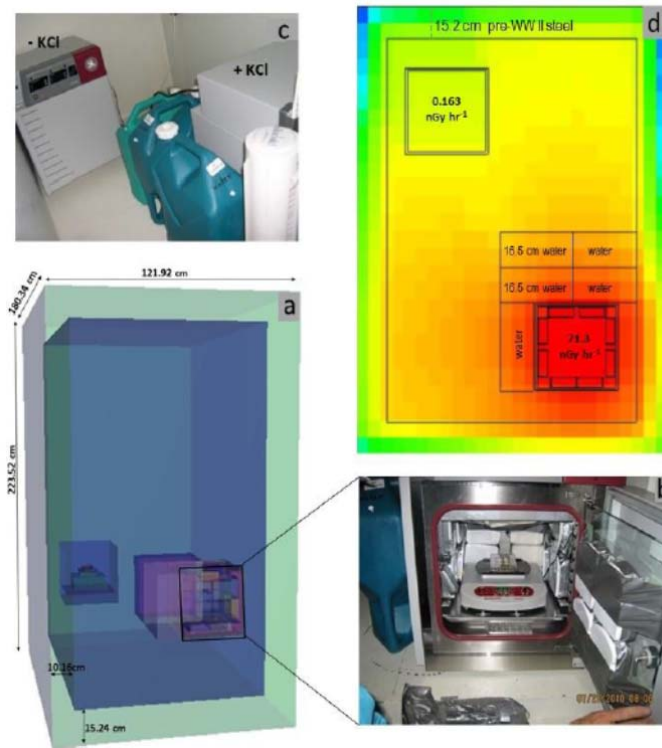
Figure 1. Pre-World War II vault (a) housing two incubators with and without a source of radiation (b,c) and a MCNP radiation heat map modeling the 400-fold difference between the two incubators.
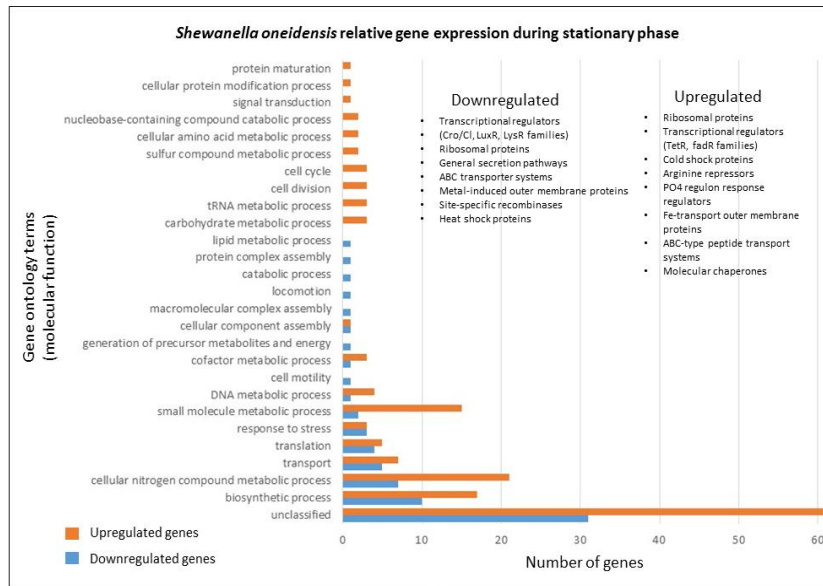
Gene enrichment analysis showing the functional classification (GO terms) of the differentially expressed genes in *S. oneidensis* grown at below-background radiation conditions.

Figure 2. Recent results of RNA-seq analysis of the entire genome that is transcribed, or expressed (ie. the "transcriptome") in *S. oneidensis* when grown at WIPP under radiation-deprived conditions.

References.

A RECORD OF URANIUM-SERIES TRANSPORT IN FRACTURED, UNSATURATED TUFF AT NOPAL I, SIERRA PEÑA BLANCA, MEXICO

J.S. Denton[(1†)], S.J. Goldstein [(1)], P. Paviet [(2)], A.J. Nunn [(1)], R.S. Amato [(1)], K.A. Hinrichs [(1)]

[(1)]Nuclear and Radiochemistry (C-NR), Los Alamos National Laboratory, MS J514, PO Box 1663, Los Alamos, New Mexico 87545
[(2)] Department of Energy, Office of Nuclear Energy, 19901 Germantown Road, Germantown, MD 20874
[†]Present address : Sellafield Ltd, Seascale, Cumbria, CA20 1PG, United Kingdom

Studies of U-series disequilibria within and around uranium deposits can provide valuable information on the extent and timing of actinide mobility via mineral-fluid interaction over a range of spatial and temporal scales. This can be useful in studies of analogues for high level nuclear waste repositories. In this study we characterize the geochemical evolution of one such analogue, the Nopal I uranium ore deposit (Peña Blanca, Chihuahua, Mexico), in terms of mineral fluid interactions as well as the role fractures play in U transport and retention. Samples of fracture-fill materials have been collected from a vertical drill core and surface fractures. High uranium concentrations in the fracture fill materials (12-7700 ppm) indicate U mobility and transport from the deposit in the past. U concentrations generally decrease with horizontal distance away from the ore deposit but show no trend with depth.

Isotopic activity ratios indicate a complicated geochemical evolution in terms of the timing and extent of actinide mobility. Uranium shows both open and closed system behavior, depending on both sample and time-scale. $^{234}U/^{238}U$ activity ratios are generally distinct from secular equilibrium and indicate some degree of open system U behavior during the past 1.2 Ma. However, calculated closed system ^{238}U-^{234}U-^{230}Th model ages are generally >313 ka for the surface fractures and >183 ka for the drill core samples, suggesting closed system behavior for U and Th over this most recent time period. Whole rock isochrons drawn for the drill core samples (Figure 1) show that at two of the three depths the fractures have remained closed with respect to U and Th mobility for >200 ka. However, open system behavior for U in the last 350 ka is suggested by the samples from 67 m depth. $^{231}Pa/^{235}U$ activity ratios within error of unity (Figure 2) suggest closed system behavior for U and Pa for at least the past 185 ka. $^{226}Ra/^{230}Th$ activity ratios range from 0.7 to 1.2 but are typically <1 (Figure 3), suggesting recent (<8 ka) radium loss and mobility due to ongoing fluid flow in the fractures. Overall, the mainly closed system behavior of U-Th-Pa over the past ~200 ka provides one indicator of the geochemical immobility of these actinides over long time-scales for potential nuclear waste repositories situated in fractured, unsaturated tuff.
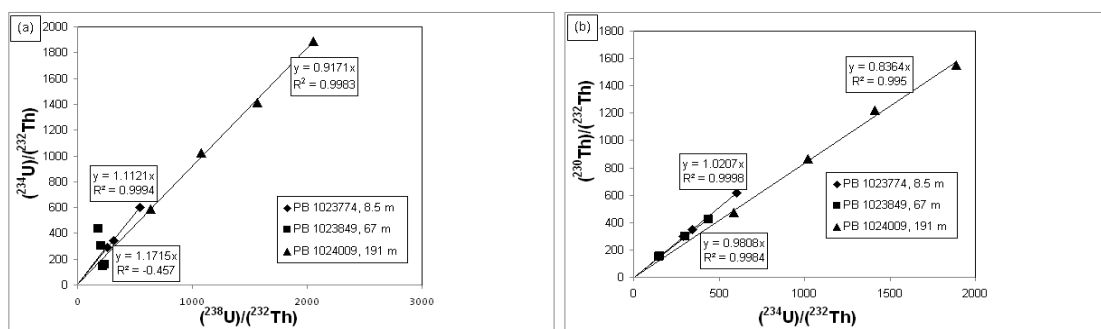
Figure1. Whole rock isochrons plotting (a) $^{234}U/^{232}Th$ activity ratio vs. $^{238}U/^{232}Th$ activity ratio and (b) $^{230}Th/^{232}Th$ activity ratio vs. $^{234}U/^{232}Th$ activity ratio. The isochron ages are 440 ± 30 ka for the near surface sample PB1023774 and 210 ± 20 ka for the deepest sample PB1024009. Sample PB1023849 at 67 m does not plot on the $^{234}U/^{232}Th$ vs. $^{238}U/^{232}Th$ isochron indicating open system behavior for U.
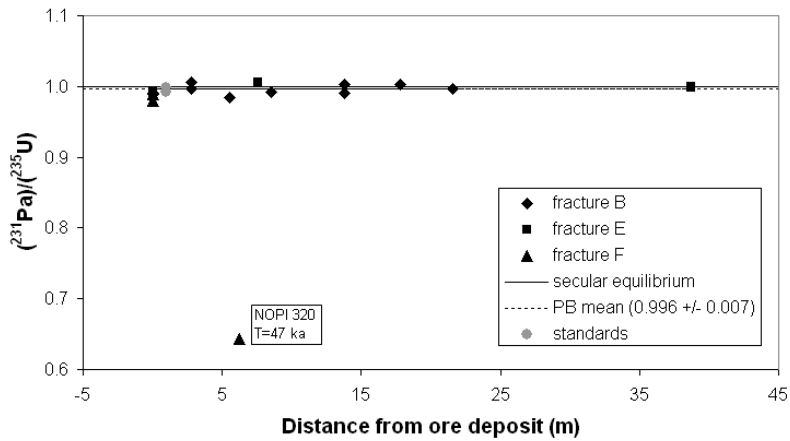
Figure2. Graph showing $^{231}Pa/^{235}U$ activity ratio as a function of distance from the ore deposit. The large majority of samples are within analytical uncertainty of secular equilibrium indicating closed system ^{235}U-^{231}Pa behavior and yield ^{231}Pa-^{235}U model ages >185 ka.
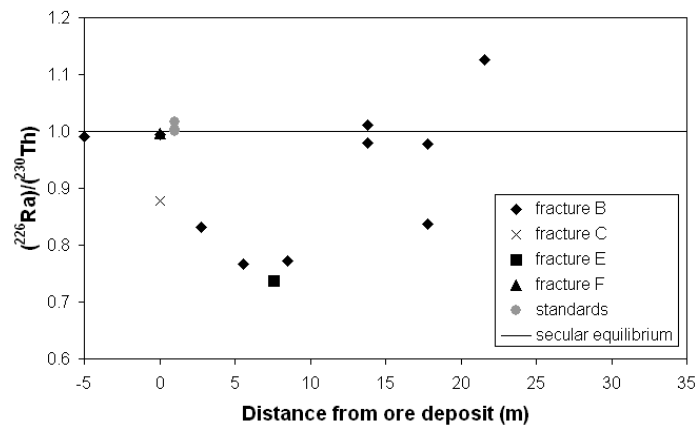
Figure3. Graph showing $^{226}Ra/^{230}Th$ activity ratio as a function of distance from the ore deposit. Deviations from secular equilibrium indicate some open system behavior for Ra, namely recent (<8 ka) ^{226}Ra loss relative to ^{230}Th. This evidence for Ra mobility agrees with prior vegetation [1] and UZ (unsaturated zone) groundwater studies [2] indicating high Ra mobility in the UZ near the deposit.

[1] Leslie, B.W., D.A. Pickett and E. Pearcy (1999). "Vegetation-derived insights on the mobilization and potential transport of radionuclides from the NOPAL I natural analog site, Mexico." Mat. Res. Soc. Symp. Proc. 555: 832-842.
[2] Goldstein, S.J., A.I., Abdel-Fattah, M.T. Murrell, P.F. Dobson, D.E., Norman, R.S. Amato and A.J. Nunn (2010). "Uranium-Series Constraints on Radionuclide Transport and Groundwater Flow at the Nopal I Uranium Deposit, Sierra Peña Blanca, Mexico." Environ. Sci. Tech. 44: 1579-1586.

THE NEA THERMOCHEMICAL DATABASE PROJECT: 30 YEARS OF ACCOMPLISHMENTS

M.-E. Ragoussi[(1)] and D. Costa[(1)]

[(1)]*Nuclear Energy Agency (NEA), Organisation for Economic Co-operation and Development (OECD)*
12, boulevard des Îles, 92130 Issy-les-Moulineaux, France
maria-eleni.ragoussi@oecd.org

The OECD NEA Thermochemical Database Project (TDB) was initiated in 1984 with the aim of creating a database of chemical thermodynamic values that would fill significant gaps in radionuclide chemistry and support the modelling requirements for performance assessments of radioactive waste disposal systems. The preparation of this database follows strict guidelines[i] to assure the high quality, consistency, reliability and CODATA-compatibility of the data provided. The projects, undertaken by TDB in five Phases, have continuously been supported by the participating organizations (mostly national nuclear waste authorities and institutions) through a well-structured organization. The fifth phase of TDB (Phase 5) was initiated in April 2014 and has duration of 4 years. The current membership is composed of fifteen organisations from twelve countries, which assign funds and in-kind resources.

This talk will describe the bases, scientific principles and organization of the TDB project, together with its evolution from its inception to the present organization as a semi-autonomous project under the aegis of the OECD NEA. Thirteen volumes of the *Chemical Thermodynamics Series* have so far been published and a great number of selected values have populated the electronic database, treating the most significant elements related to nuclear waste management and becoming an international reference in the field. The work carried out has resulted in the publication of major reviews on the chemical thermodynamics of inorganic species and compounds of U, Np, Pu, Am, Tc, Ni, Se, Zr, Th, Sn and Fe and on simple organic complexes of U, Np, Pu, Am, Tc, Ni, Se, and Zr with citrate, oxalate, EDTA and iso-saccharinic acid, as well as the publication of a state-of-the-art report on solid solutions of interest in nuclear waste management (Figure 1).[ii] The thermodynamic values that are selected for each treated element in all TDB review books become available on the Project's electronic database. Originating from the critical evaluation of chemical thermodynamics related to each element, the major reviews all go through a peer-review process by qualified experts before publication in order to ensure an independent view of the assessments made by the primary reviewers.

(i)

Year	
1985	A. B. Muller's NEA NWM-5 Report on "NEA Compilation of Chemical Thermodynamic Data for Minerals Associated with Granite"
1992	Uranium Review
1995	Americium Review
1998	Phase II Agreement
1999	Technetium Review
2001	Neptunium and Plutonium Review / TDB Workshop "Thermodynamic Data Bases in Performance Assessment"
2003	Update Review / TDB III Agreement
2004	Reprints of the Uranium and Americium Reviews
2005	Nickel, Selenium, Zirconium and Organic Ligands Reviews
2007	Solid solutions state-of-the-art report
2008	TDB IV Agreement
2009	Thorium Review
2010	Joint TDB-Sorption Symposium "From Thermodynamics to the Safety Case"
2013	Tin and Iron reviews / TDB-5 Agreement

(ii)

Figure 1. (i) Achievements of the TDB Project from 1985 to 2013; (ii) Cover of the latest publication of the Chemical Thermodynamics Series.

The current activities of the project are:

- *Chemical Thermodynamics of Iron (part II)*
- *Chemical Thermodynamics of Selected Ancillary Compounds*

- *Chemical Thermodynamics of Molybdenum*
- *State-of-the-Art report on the Thermodynamic Considerations for Cement Minerals*
- *2nd Update on the Chemical Thermodynamics of Uranium, Neptunium, Plutonium, Americium and Technetium*
- *High Ionic-Strength Solutions: State of the Art Report to Assess Modeling and Experimental Approaches*

The programme of work for Phase 5, approved by Project's Management Board (representatives of the 15 participating organizations), also contemplates the initiation of a state-of-the-art report on the thermochemical extrapolation of data to non-standard state temperatures.

THE OECD/NEA TDB ASSESSMENT OF THERMODYNAMIC DATA FOR ANCILLARY COMPOUNDS

M. H. Rand[1], J. Fuger[2], T. Gajda[3], D. A. Palmer[4], M.-E. Ragoussi[5]

[1]Winters Hill Consultancy, Dry Sandford, Abingdon, Oxon OX13 6JP, England
[2]University of Liège, B-4000, Liège, Belgium
[3]Department of Inorganic and Analytical Chemistry, University of Szeged, Hungary
[4]P.O. Box 390, Oliver Springs, Tennessee, TN 37840, USA
[5]OECD Nuclear Energy Agency (NEA), 12 Boulevard des Îles, 92130 Issy-les-Moulineaux, France

Within the scope of the OECD Nuclear Energy Agency (NEA) Thermochemical Database (TDB) Project, comprehensive assessments have been made of the thermodynamic data on many inorganic auxiliary species and common minerals [1].

The Review presents consistent data, at mainly ambient conditions, on the most important species in the following systems:

Aqueous   Aqueous solutions of P_2O_5, CO_2, SiO_2, B_2O_3, Al_2O_3, MgO, CaO,
        $MgSO_4$, $CaSO_4$, $MgCO_3$, $CaCO_3$, Na_2CO_3, K_2CO_3

Solids: SiO_2(four polymorphs), Al_2O_3, $Al(OH)_3$,
        (MO, $M(OH)_2$, MCl_2, MSO_4, MCO_3 for M = Mg and Ca), $Ca_3(PO_4)_2$,
        (M_2CO_3, $MHCO_3$, for M = Na and K)

Minerals: Two apatites, borax and two calcium borate hydrates, dolomite. For most of these,
        there are difficulties in giving any precise values, owing to the frequent use of
        appreciably non-stoichiometric samples and for borax, there seem to be no
        experimental data on the heat capacity.

In all cases, agreement for the values of standard enthalpies of formation and entropies of the solids([e.g. $Al(OH)_3$(gibbsite) and $MgCO_3$(magnesite)) has been achieved between the calorimetric and solubility data, albeit with one or two small changes in currently accepted basic data.

Other changes of note from currently accepted values are:

Revision of the data for (H_3PO_4(aq))

Revised data for all the aqueous silicate species, resulting from the adoption of a higher   solubility of quartz at 298.15 K (($1.81 \pm 0.10) \times 10^{-4}$ mol·kg^{-1}) rather than 1.0×10^{-4} mol·kg^{-1} used in earlier TDB reviews.

Adoption of higher values of C_p(CaO, cr) at high-temperatures, based on recent   studies.

[1] M. H. Rand, J. Fuger, T. Gajda, D. A. Palmer, Chemical Thermodynamics of Selected Ancillary Compounds, OECD Publishing, (to be published in 2016).

THE OECD/NEA TDB REVIEW ON MOLYBDENUM

H. Gamsjäger[1], M. Morishita[2], C. Musikas[3], N. Simon[4], M.-E. Ragoussi[5]

[1]Montanuniversität, Lehrstuhl für Physikalische Chemie, 8700 Leoben, Austria
[2]University of Hyogo, Department of Materials Science and Chemistry, Hyogo 671-2280, Japan
[3]Reviewer of the OECD/NEA TDB Review "Chemical Thermodynamics of Molybdenum"
[4]CEA/DTN/DTPA/LPC Cadarache, 13108 Saint-Paul-lez-Durance Cedex, France
[5] OECD Nuclear Energy Agency (NEA), 12 Boulevard des Îles, 92130 Issy-les-Moulineaux, France

Within the scope of the OECD Nuclear Energy Agency (NEA) Thermochemical Database (TDB) Project, a comprehensive review on the inorganic compounds and aqueous complexes of molybdenum (Mo) is being carried out.

THERMODYNAMIC PROPERTIES OF MOLYBDATE ION

Part of this work has concentrated on the thermodynamic properties of MoO_4^{2-}.

MoO_4^{2-}: Standard molar quantities of molybdate ion entropy, S_m^o, enthalpy of formation, $\Delta_f H_m^o$, and Gibbs energy of formation, $\Delta_f G_m^o$, are key data for the OECD/NEA TDB review on Mo [1].

$\Delta_f H_m^o(MoO_4^{2-})$ can be determined by measuring calorimetrically the enthalpy of dissolution of MoO_3(cr) in dilute aqueous MaOH solutions. For Ma = Li, Na, Rb, Cs, consistent values have been obtained and the weighted mean has been selected [2].

$$\Delta_f G^o(MoO_4^{2-}) = -RT_{ref} \ln K_{s,0}^o - n\Delta_f G^o(M^{2+/n}) + \Delta_f G^o(M_n MoO_4, \, cr) \qquad (1)$$

$K_{s,0}^o$ [3] and $\Delta_f G^o(M^{2+/n})$ [4] of M = Ca, Sr, Ba, Ag are well known and

$$\Delta_f G^o(M_n MoO_4, \, cr) = \Delta_f H^o(M_n MoO_4, \, cr) - T_{ref} \cdot \Delta_f S^o(M_n MoO_4, \, cr) \qquad (2)$$

Prerequisites for employing eq. (2) are accurate values for entropies of $M_n MoO_4$(cr) which have been determined recently [5]. For M = Ca, Sr, Ba, Ag, consistent values for $\Delta_f G^o(MoO_4^{2-})$ have been obtained and the weighted mean has been selected [2]. Now the standard entropy of formation follows from eq. (3).

$$\Delta_f S_m^o(MoO_4^{2-}) = [\Delta_f H_m^o(MoO_4^{2-}) - \Delta_f G_m^o(MoO_4^{2-})] / T_{ref} \qquad (3)$$

Finally the partial molar entropy of molybdate ion is given by eq. (4).

$$S_m^o(MoO_4^{2-}) = \Delta_f S_m^o(MoO_4^{2-}) + S_m^o(Mo, \, cr) + 2S_m^o(O_2, \, g) + S_m^o(H_2, \, g) \qquad (4)$$

AQUEOUS CHEMISTRY

- *Simple aqueous ions and redox potentials:* Mo(VI) is the main oxidation state in aqueous solutions. In acidic solutions it exists as species of the MoO_2^{2+} *cis*-dioxo cation and as MoO_4^{2-} tetrahedral anion at pH >7. An up-to-date Latimer diagram is proposed by us. Also, it has been observed that a kinetic barrier impedes many redox reactions in which a change of Mo polymerization degree occurs.

- *Hydrolysis of Mo(VI):* For $c_{Mo(VI)} < 10^{-4}$ mol·dm^{-3} the following simple path of MoO_4^{2-} protonation is accepted:

$$MoO_4^{2-} + H^+ \Rightarrow MoO_4H + H^+ \Rightarrow MoO_4H_{2(Td)} \Rightarrow MoO_2 \cdot (OH)_{2(Oh)} + H^+ + 2H_2O$$

$$\Rightarrow MoO_2(OH)^+ \cdot 3H_2O + H^+ \Rightarrow MoO_2^{2+} \cdot 4H_2O$$
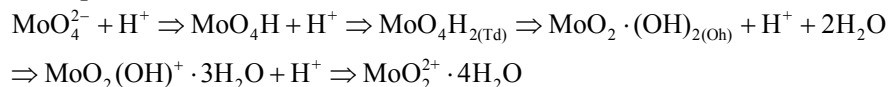
For $c_{Mo(VI)} > 10^{-4}$ mol·dm^{-3} polymerization of the octahedral Mo(VI) takes place with the addition of the first protons and the following is observed: $7 MoO_4^{2-} + 8 H^+ => Mo_7O_{24}^{6-} + 4 H_2O$.

The structure of $(NH_4)_6Mo_7O_{24}$ shows that $Mo_7O_{24}^{6-}$ anions form from octahedral Mo_6 moieties containing *cis*-MoO_2 species in which two O are situated at shorter distances than the remaining ones. The addition of more than 1.14 protons per Mo(VI) leads to more polymerized and less charged species, whose identification is still being studied. The reduction of these polymers leads to mixed-valence Mo(VI)-Mo(V) species.

- *Formation of heteropolyanions and complex formation with the actinides:* The Mo(VI) isopolyanions have high affinity for common ligands found in natural environments, such as silicates and phosphates. They form saturated heteropolyanions such as $PMo_{12}O_{40}^{3-}$, $SiMo_{12}O_{40}^{4-}$ (Keggin anions) or $P_2Mo_{18}O_{62}^{6-}$ (Dawson anion), whose unsaturated forms $PMo_{11}O_{39}^{7-}$, $SiMo_{11}O_{39}^{8-}$, $P_2Mo_{17}O_{61}^{10-}$ are strong ligands for the actinide ions. Thorough investigations have been carried out with the unsaturated hetero polytungstates, and in view of the common properties for Mo(VI) and W(VI) this topic seems important for actinide behavior in the presence of Mo(VI).

[1] H. Gamsjäger, C. Musikas, M. Morishita, W. Fürst, E. Königsberger, L.-C. Königsberger, N. Simon, L. Morss, Chemical Thermodynamics of Molybdenum, OECD Publishing, (to be published in 2016).

[2] H. Gamsjäger, M. Morishita, Pure Appl. Chem. (2015), in press.

[3] H. Gamsjäger, Pure Appl. Chem. 85, 2059 (2013).

[4] R. J. Lemire, U. Berner, C. Musikas, D. A. Palmer, P. Taylor, O. Tochiyama, Chemical Thermodynamics of Iron Part 1, Chemical Thermodynamics Series Vol. 13, OECD Publishing (2013), pp. 1082, Table IV-1.

[5] M. Morishita and H. Houshiyama, Mater. Trans. 56, (2015), in press.

CALCULATIONS OF NUCLIDES' SPECIES DISTRIBUTION BY CHEMSPEC IN GROUNDWATER OF HIGH LEVEL WASTE RADIOACTIVE DISPOSAL SITES

JingCheng Jiang, Meiling Jiang, Xiangyun Wang, Chunli Liu[*]

Beijing National Laboratory for Molecular Sciences, Radiochemistry & Radiation Chemistry Key Laboratory for Fundamental Science, College of Chemistry and Molecular Engineering, Peking University, Beijing 100871,China
Author for correspondence liucl@pku.edu.cn

With the development of nuclear energy, more and more high level radioactive waste (HLW) will be produced. HLW contains a lot of radionuclides, some of which are very poisonous, have long half-life and can give out large amounts of heat. Deep geological disposal is widely accepted to deal with HLW. HLW after vitrification will be put into the packaging container and then buried in repository about 500-1000m deep underground. This method is based on multiple-barrier model including solidification form, the canister, engineering barriers, and natural barriers. In this way, we hope totally seperate the radionuclides from the environment and protect the ecosystem. While the lfietime of repository is limited, the repository may be damaged by weathering, corrosion, degradation, and natural disasters year by year and then gives out harmful nuclides. As adsorption and migration behavior of a radionuclide is closely connected with its chemical forms in a given chemical environment, it is very essential to obtain its species distribution to study the adsorption and migration behavior.

For that reason, our research group independently wrote a species analysis software chemspec with fortran language. Seeing that Beishan area and Yamansu and Tianhu area are two of the most important preselected HLW disposal sites, species distribution of key radionuclides such as Uranium, Neptunium, Americium and so on has been calculated. A brief introduction to principles, structure and strategy of chemspec and part of calculation results are as follows.

Generally speaking, chemspec divides chemical materials in an aquatic system into two kinds, components and species. According to input files, chemspec searches all the possible species and output results after reaching convergence. In this progress, database, reaction model, calculation method and ionic strength coefficient are the most important parts. Chemspec adopts authoritative database taken from PSI, which includes 66 components and 448 species. This database covers thermodynamic data for Th, U, Np, Pu, Am, and many other high yield and long-lived fission product elements that are extremely important for HLW disposal [1]. In order to get good results, database is supposed to be preciese, comprehensive and updated in time. Usually datebase come from experiment data or empirical constants. Chemspec can deal with single or complex systems involving acid-base reaction, precipitation, redox reactions and complexation. Considering calculation method, mass balance equation is the core and more than four algorithms are used to solve the equation. Compared with other species analysis software like phreeqc, chemspec is more likely to reach convergence by automaticlly switching algorithm. Among different ion strength formula, chemspec can choose the best one when concentrations change.

The calculated results indicate that americium exists as trivalent Am(III) in Beishan groundwater and the species significantly change with pH values. Under acidic conditions, americium mainly exists as $AmSO_4^+$, $Am(SO_4)_2^-$ and Am^{3+}. While in neutral or weak alkaline condition, the main species is $AmCO_3^-$. When the solution is in strong alkaline condition, most of americium exists as Am(III). The concentration of different ions also have an influence on the speciation distribution of americium, and in the order of $HCO_3^- > F^- > SO_4^{2-} > Cl^-$. The solubility of americium is greatly affected by pH and HCO_3^- concentration. When pH value increases, the solubility of americium decreases. The solubility of americium in Beishan groundwater (pH = 7.56、Eh = 0 mV) is 2.01×10^{-7} mol/L.

The valence of plutonium in Beishan groundwater significantly change with pH and Eh, it can exist in four valence: Pu(III), Pu(IV), Pu(V), Pu(VI). With the pH and Eh value increases, the plutonium changes from low valence to high valence. Under acidic conditions, plutonium mainly exists as $PuSO_4^+$、$Pu(SO_4)_2^-$、Pu^{3+}、$PuCl^{2+}$ and $PuOH^{2+}$, while in alkaline conditions, the main species is $Pu(OH)_4$. The concentration of different ions also have an influence on the speciation distribution of Plutonium, and in the order of $HCO_3^- > F^- > SO_4^{2-}$ Cl^-. The solubility of Pu in Beishan groundwater is 3.88×10^{-11} mol/L and controlled by Pu(IV).

figure 1. species distribution of Am with pH   figure 2. species distribution of Pu with pH

[1] Wang Xiangyun (2009). "Chemical speciation code CHEMSPEC and its applications." Sci China Ser B-Chem. vol. 52 no. 11 2020-2032
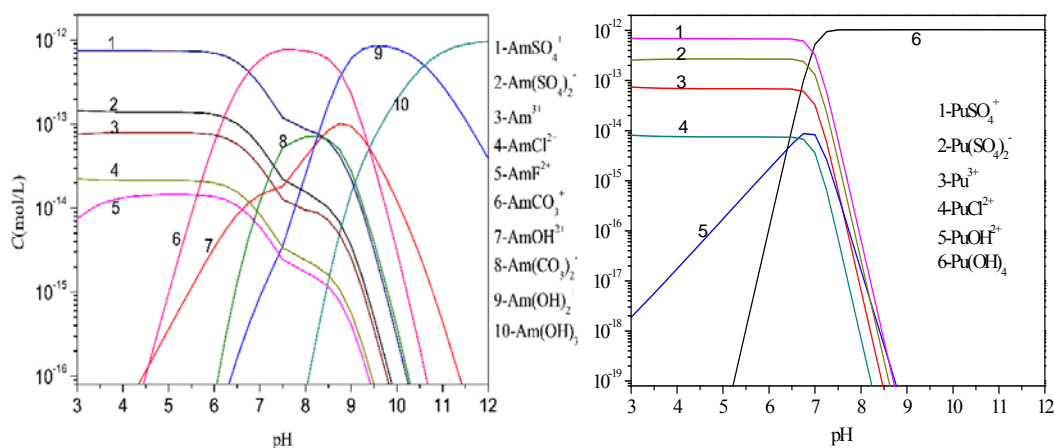
SORPTION PROPERTIES OF SEDIMENTARY ROCKS IN HIGHLY SALINE SOLUTIONS

T. Yang[(1)], P. Vilks[(2)], M. Hobbs[(1)]

[(1)]*Nuclear Waste Management Organization, 22 St. Clair Avenue East, Sixth Floor, Toronto, Ontario M4T 2S3, Canada*
[(2)]*Canadian Nuclear Laboratories, Whiteshell Laboratories, Pinawa, Manitoba, Canada, R0E 1L0*

The Nuclear Waste Management Organization's (NWMO) Adaptive Phased Management (APM) Technical Program is intent on advancing the understanding of solute migration in deep seated sedimentary and crystalline groundwater systems. In these systems, groundwaters may contain brines with total dissolved solid (TDS) concentrations up to 200-400 g/L (e.g., groundwaters in Southern Ontario [1]). As part of NWMO's Technical Program, a database of sorption coefficients (K_d) for Canadian sedimentary rocks (shale, limestone) and bentonite in saline solutions is being developed for the elements of interest for safety assessment, including C, Ni, Cu, As, Se, Zr, Nb, Mo, Tc, Pd, Sn, Cs, Eu, Pb, Bi, Ra, Th, Pa, U, Np, Pu, and Am [2, 3].

The approach for the development of the NWMO sorption database includes: (1) compilation of available sorption data from the open literature and international sorption databases that are relevant to Canadian sedimentary rocks and bentonite, in a setting that would include very saline Na-Ca-Cl solutions at near neutral pH; (2) experimental measurements of sorption coefficients for elements of interest onto Canadian sedimentary rocks (shale, limestone) and bentonite in a highly saline Na-Ca-Cl reference solution with TDS of 275 g/L by batch sorption tests and long-term diffusion sorption tests; and/or (3) surface complexation sorption modelling.

The K_d values for elements Li(I), Ni(II), Cu(II), Sr(II), Pb(II), Zr(IV), Eu(III) and U(VI) on Canadian sedimentary rocks (shale, limestone) and bentonite in highly saline reference brine solutions were determined by batch sorption tests using both single and multiple elements [4, 5]. The effects of salinity and pH on the sorption of these elements were investigated. The experimental measurements illustrated that the sorption K_d values of divalent elements Ni(II), Cu(II), and Pb(II) were 1 to 3 orders of magnitude lower in the brine reference solution (TDS=275 g/L) than in the dilute reference solution (TDS=0.49 g/L) due to the mass action effects, and the sorption K_d values of element U(VI) were a factor of 1.5-8 lower in the brine reference solution than in the dilute reference solution [5]. Short term (1 hour) sorption tests showed that the sorption of U(VI), Cu(II), and Zr(IV) increased with pH in the range of 5-8 [5]. Long-term diffusion tests were performed to study the sorption and migration properties of elements Li(I), Ni(II), Cu(II), Pb(II), and U(VI) in shale. The K_d values derived from the batch tests were consistent with K_d values estimated from the diffusive mass transport experiments in shale, providing confidence that the sorption K_d values obtained from the batch sorption tests can be applied to account for sorption in mass transport within shale [5].

Experimental measurements of sorption properties for elements Sn(IV), Zr(IV), Cs(I), Th(IV), and Pd(II) on Canadian sedimentary rocks (shale, limestone) and bentonite in the highly saline Na-Ca-Cl reference solution (with TDS of 275 g/L) under low O_2 conditions by both batch sorption tests and long-term diffusion sorption tests are underway. NWMO's sorption research program also includes the determination of sorption properties of Np(V) and Np(IV) onto bentonite, shale and illite, which is the main mineral in shale that sorbs radionuclides in shale from highly saline solutions. In addition, experimental measurements of the sorption of six key redox-sensitive elements Se(-II), As(III), Pu(III), U(IV), Tc(IV), and Np(IV) onto Canadian sedimentary rocks (shale, limestone) and bentonite in the highly saline Na-Ca-Cl solution (with TDS of 275 g/L) under reducing conditions are underway. NWMO's sorption database for these key elements will be updated with the experimental determined sorption coefficient values.

[1] Hobbs, M.Y., S.K. Frape, O. Shouakar-Stash and L.R. Kennell (2011). "Regional Hydrogeochemistry – Southern Ontario", Nuclear Waste Management Organization report NWMO DGR-TR-2011-12, Toronto, Canada.

[2] Vilks, P. (2011) "Sorption of Selected Radionuclides on Sedimentary Rocks in Saline Conditions – Literature Review". Nuclear Waste Management Organization report *NWMO* TR-*2011*-12, Toronto, Canada.

*[3] Vilks, P. (2015) "*Sorption of Selected Radionuclides on Sedimentary Rocks in Saline Conditions – Updated Sorption Values", *Nuclear Waste Management Organization report NWMO TR-2015-xx. Toronto, Canada (in preparation)*

[4] Vilks, P. N.H. Miller and K. Felushko (2011). "Sorption Experiments in Brine Solutions with Sedimentary Rock and Bentonite", Nuclear Waste Management Organization report *NWMO* TR-*2011*-11, Toronto, Canada.

[5] Vilks P. and N.H. Miller (2014). "Sorption Studies with Sedimentary Rock under Saline Conditions", Nuclear Waste Management Organization report NWMO TR-2013-22, Toronto, Canada.

HIGH IONIC-STRENGTH SOLUTIONS: STATE OF THE ART REPORT TO ASSESS MODELING AND EXPERIMENTAL APPROACHES

[1]D. T. Reed and [2]M. Altmaier

1. *Los Alamos National Laboratory, 1400 University Drive, Carlsbad NM, 88220, USA.*
2. *Karlsruhe Institute of Technology, Institute for Nuclear Waste Management, Karlsruhe, Germany.*

Within the scope of the OECD Nuclear Energy Agency (NEA) Thermochemical Database (TDB) Project, the preparation of a State of the Art Report (SOAR) to assess the modeling and experimental approaches used to describe high ionic-strength solutions has been envisaged, and development is herein reported. This state of the art report builds on past NEA-TDB documents [1] and will focus on ionic strengths $I \geq 3$ M where the Pitzer formulation [2,3], rather that the SIT approach, is recommended and usually applied. The focus of this SOAR update is on the nuclear waste disposal aspects that apply to repository concepts in bedded and domed salt Formations, although there is also relevance to other geologic disposal concepts where transient high ionic-strength aqueous conditions can exist. A comprehensive high quality and self-consistent Pitzer data set that can describe the aqueous actinide and brine chemistry for all predicted repository conditions is needed to address low-probability brine-inundation scenarios to support the safety case for a nuclear repository in salt [4].

A survey of the literature on the experimental parameter determination and modeling of high ionic-strength solutions showed that there are approaching 2000 publication on these topics (see Figure 1). More importantly many of these are relatively recent (since the year 2000) and are not comprehensively integrated into current data sets.
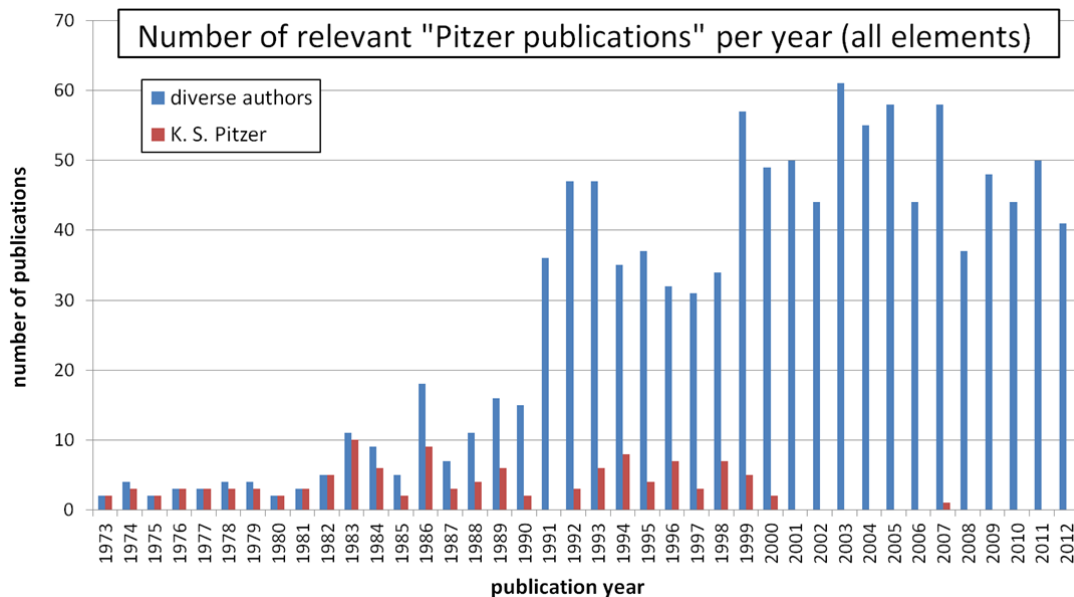
Figure 1:   Publications that center on the experimental measurement or modeling of Pitzer data since the development of the Pitzer approach in 1973.

The Pitzer literature that pertains to a nuclear repository in salt was divided into two categories: "Oceanic" for the main components of high ionic-strength brine and "Radionuclide/actinide" for the key radionuclides (and their analogs) that need to be addressed to support the safety case. The vast majority of the available literature deals with the brine chemistry associated with "oceanic" systems (~1000 species-specific) and this remains a very active area of research for a number of reasons outside of the nuclear repository application. The distribution of recent publication in this category is given in Figure 2 and show that there are new activity data being measured as well as new temperature-variable data being reported. All of these data were assessed

in the context of current database applications that are largely based on the Harvie-Møller-Weare data base [5].

Figure 2: Distribution of Pitzer articles in the general category of oceanic studies. Most new activity coefficient data measurements included temperature-variable studies. The vast majority of the papers was the application of the HMW Pitzer model, or optimized versions of this model, to site/system-specific high ionic-strength brines ("Model" designation above).
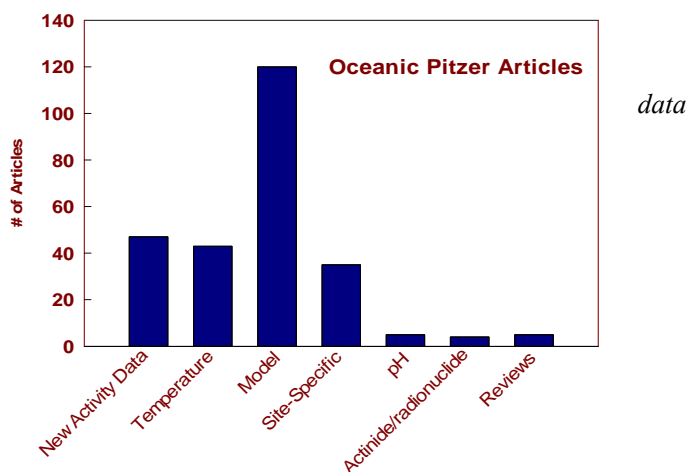
For the radionuclide/actinide data set, there are new data reported for all the key oxidation states of the actinides but there are significantly less literature publications (~65) on this key topic (see Figure 3).   There is especially a significant lack of temperature-variable data for the radionuclide/actinide data set as well as ternary species and a number of gaps exist in current database applications.   A critical assessment of these key data gaps will be provided.
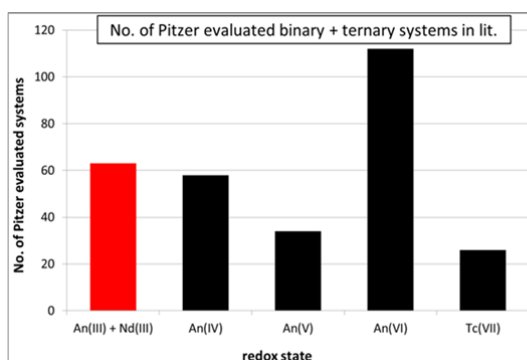
Figure 3.   Number of Pitzer-evaluated binary and ternary system references sorted by oxidation state.

References

[1] Allard et al. 1997. "Modelling in Aquatic Chemistry." OECD Publications, 724 pp., ISBN 92-64-15569-4.

[2] Pitzer, K.S. 1973. "Thermodynamics of Electrolytes. I. Theoretical Basis and General Equations." *Journal of Physical Chemistry, 77*, (2), 268–277. Washington, D.C.: American Chemical Society. TIC: 239503.

[3] Pitzer, K.S. 1991. "Ion Interaction Approach: Theory and Data Correlation." Chapter 3 of *Activity Coefficients in Electrolyte Solutions*. 2nd Edition. Pitzer, 152709 K.S., ed. Boca Raton, Florida: CRC Press. TIC: 251799.

[4] Reed, D.T. and M. Altmaier (eds.), "Proceedings of the Third International Workshop on Actinide and Brine Chemistry in a Salt-Based Repository (ABC-Salt III)," Los Alamos National Laboratory Report LA-UR-15-21114, Los Alamos, NM, USA (2015).

[5] Harvie, C.E.; Møller, N.; and Weare, J.H. 1984. "The Prediction of Mineral Solubilities in Natural Waters: The Na-K-Mg-Ca-H-Cl-SO4-OH-HCO3-CO3-CO2-H2O System to High Ionic Strengths at 25°C." *Geochimica et Cosmochimica Acta,48,* (4), 723-751. New York, New York: Pergamon Press. TIC: 239849.

HIGH PERFORMANCE REACTIVE TRANSPORT MODELING FOR UNDERSTANDING RADIONUCLIDE BEHAVIOUR IN FRACTURED CRYSTALLINE ROCKS AT SUB-MILLIMETER SCALE.

J. Molinero[1], G. Deissmann[2], P. Trinchero[1], H. Ebrahimi[1], D. Bosbach[2], B. Gylling[3], U. Svensson[4]

[1]AMPHOS 21 Consulting, Passeig de Garcia i Faria, 49-51, Barcelona, Spain
[2] Institute for Energy and Climate Research: Nuclear Waste Management and Reactor Safety (IEK-6) and JARA-HPC, Forschungszentrum Jülich GmbH, 52425 Jülich, Germany
[3]SKB Svensk Kärnbränslehantering AB, Besöksadress Blekholmstorget 30, Stockholm, Sweden
[4]CFE Computer-aided Fluid Engineering AB, Frankes väg 3, S-371 65, Lyckeby, Sweden.

The evolution of redox conditions in sparsely fractured crystalline rocks is an important and largely unresolved issue with respect to the assessment of the long-term geochemical conditions in deep geological repositories for nuclear wastes (e.g. [1-4]). The ingress of oxygen (i.e. oxygen-rich waters), especially in disruptive scenarios (e.g. due to faulting or earthquakes) or due to intrusion of glacial meltwaters (during/after glaciation events), into the repository may result in redox zonation and may create oxidizing conditions in the vicinity of the emplaced wastes. The penetration of oxygen can in consequence adversely affect the long-term repository performance due to (i) enhanced corrosion of metallic waste containers, (ii) increased matrix corrosion of and radionuclide release from the disposed spent fuel, which is a very stable waste form under the prevailing strongly reducing conditions, and (iii) an increase in the mobility of certain radionuclides (e.g. uranium, plutonium, technetium) that would be retained in the repository near-field under reducing conditions. However, the presence of (Fe^{II}-bearing) reduced minerals (such as pyrite, chlorite, and biotite) in the rock matrix or in fracture fillings may lead to oxygen consumption along the flow path and provide sufficient redox buffering to sustain strongly reducing conditions in the repository environment.

The (coupled) reactive transport simulation of redox transients and radionuclide behaviour into fractured rocks is computationally demanding and usually requires significant simplifications, since these simulations usually suffer stiffness and require a high spatially discretization as well as small time steps, for example due to (i) fast reaction kinetics, (ii) significantly different timescales of various hydrogeological and hydrogeochemical processes, (iii) the heterogeneous flow field and the heterogeneous distribution of minerals in fractures and the rock matrix, and (iv) the development of reaction fronts and high concentration gradients.

In this work, the reactive behaviour of oxygen in crystalline rocks and its consequences for radionuclide migration is investigated by means of High Performance Reactive Transport Modelling (HP-RTM) at sub-millimetre scale (mineral scale). The models use discrete fracture networks representing the micro-porosity of the rock, and a discrete representation of minerals thus avoiding an averaged equivalent porous media approach. A key scientific interest of these simulations is the evaluation of the validity of the macroscropic (continuum) approach, accepted and normally used to simulate this problem, by comparing with the computed results obtained in the sub-millimetre scale simulations with a realistic representation of the micro-fractures (discrete description) in the rock matrix.

The numerical tool used for the HP-RTM is named iDP (**i**nterface **D**arcyTools-**P**FLOTRAN). PFLOTRAN [5] is a next-generation, open source, reactive flow and transport simulator for modelling subsurface processes that has been developed by a consortium of National Research Laboratories of the Department of Energy of USA. PFLOTRAN has been built on top of well-known frameworks like MPI, PETSc and HDF. It has demonstrated peta-scale performance in simulations of uranium migration in the superfund Hanford 300 Area as part of the SciDAC-2 programme [6, 7]. On the other hand, DarcyTools [8] is one of the best codes available to simulate groundwater flow in crystalline, fractured rocks. DarcyTools has been developed by SKB, the Swedish Agency for nuclear waste management. Just like PFLOTRAN, DarcyTools is based on the finite volume method and uses MPI for its parallelization. These two simulation tools are combined by iDP, providing a common framework for coupling groundwater flow and geochemical processes in crystalline, fractured rocks. iDP is written in a modular, cross-platform and extensible way using Fortran and Python.

This work illustrates the use of iDP for improving the fundamental understanding of key processes for radionuclide transport in the geosphere. The simulations have been performed at the Jülich Supercomputing Centre, using JUQUEEN, one of the biggest supercomputers in the world. Numerical experiments demonstrate that reactive transport simulations scale properly up to thousands of computational cores, pointing out that HP-RTM is a very powerful methodological tool for future performance assessment exercises for deep geological repositories.

[1] Guimerà, J., Duro, L., Jordana, S., Bruno, J. (1999). Effects of ice melting and redox front migration in fractures rocks of low permeability. SKB Technical Report TR-99-19, Svensk Kärnbränslehantering AB.

[2] Guimerà, J., Duro, L., Delos, A. (2006). Changes in groundwater composition as a consequence of deglaciation. Implications for performance assessment. SKB Report R-06-105, Svensk Kärnbränslehantering AB.

[3] Sidborn, M., Sandström, B., Tullborg, E.L., Salas, J., Maia, F., Delos, A., Molinero, J., Hallbeck, L., Pedersen, K. (2010). SR-Site: Oxygen ingress in the rock at Forsmark during a glacial cycle. SKB Technical Report TR-10-57, Svensk Kärnbränslehantering AB.

[4] MacQuarrie, K., Mayer, K., Jin, B., Spiessl, S. (2010). Journal of Contaminant Hydrology, 112, 64-76.

[5] Lichtner, P.C., Hammond, G.E., Lu, C., Karra, S., Bisht, G., Andre, B., Mills, R., Kumar, J. (2014). PFLOTRAN User's Manual: A massively parallel reactive flow and transport model for describing surface and subsurface processes. 184 pp.

[6] Hammond, G.E., Lichtner, P.C. (2010). Water Resources Research, 46, W09527, 1-31.

[7] Hammond, G.E., Lichtner, P.C., Mills, R.T. (2014). Water Resources Research, 50, 208-228.

[8] Svensson, U., Ferry, M. (2014). DarcyTools: A Computer Code for Hydrogeological Analysis of Nuclear Waste Repositories in Fractured Rock. Journal of Applied Mathematics and Physics, 2014, 2, 365-383.

THE INFLUENCE OF STAGNANT WATER ZONE ON NUCLIDE TRANSPORT IN FRACTURED MEDIA

P.Shahkarami, L. Liu, L. Moreno, I. Neretnieks

Department of Chemical Engineering and Technology, KTH Royal Institute of Technology,
S-100 44 Stockholm, Sweden

This study presents the simulation results of the radionuclides release from a defective canister located in the near field of a hypothetical repository site, using NEAR3D [1]. The effect of stagnant water zones on the transport of radionuclides through the far field are then explored in detail by using the a 3D Channel Network Model (CHAN3D) [2] to generate the far field realisation as well as to determine the water travel times and the F-ratios for individual channels. These data are the essential underlying data needed for radionuclide transport calculations.

CHAN3D considers the major mechanisms that govern the nuclides transport, including advection and hydrodynamic dispersion along the fracture, sorption, diffusion into the rock matrix adjacent to the flowing channel, and radioactive chain decay. To account for the effects of stagnant water zone, the model developed by Shahkarami et al., 2015 [3] is incorporated into the CHAN3D to describe radionuclide transport through a heterogeneous fractured media consisting of an arbitrary number of channels with piecewise stochastic properties. The focus of the present study is on the far field release and the effect of stagnant water zone.

Figure 1 shows the release from the near filed. The releases from the far field are shown in figure 2 for two Cases (a) stagnant water zone is **not** considered and (b) stagnant water zone is considered.
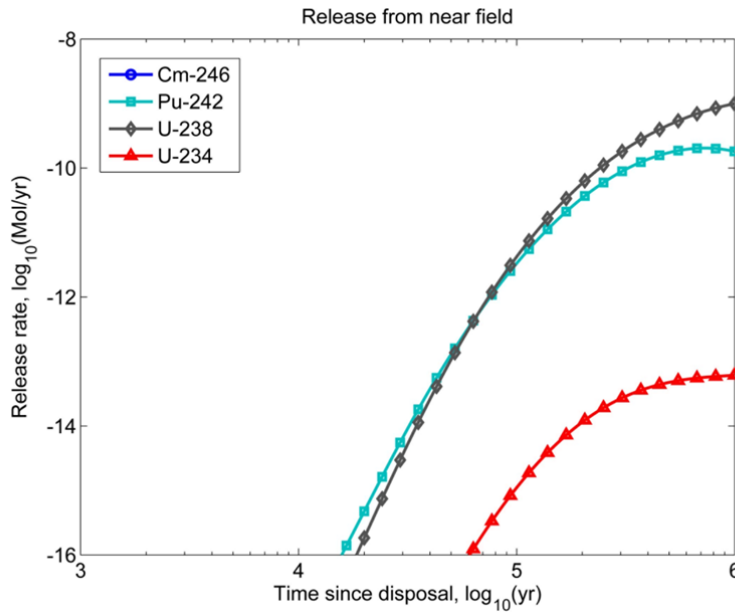
Figure1. Release from the near field
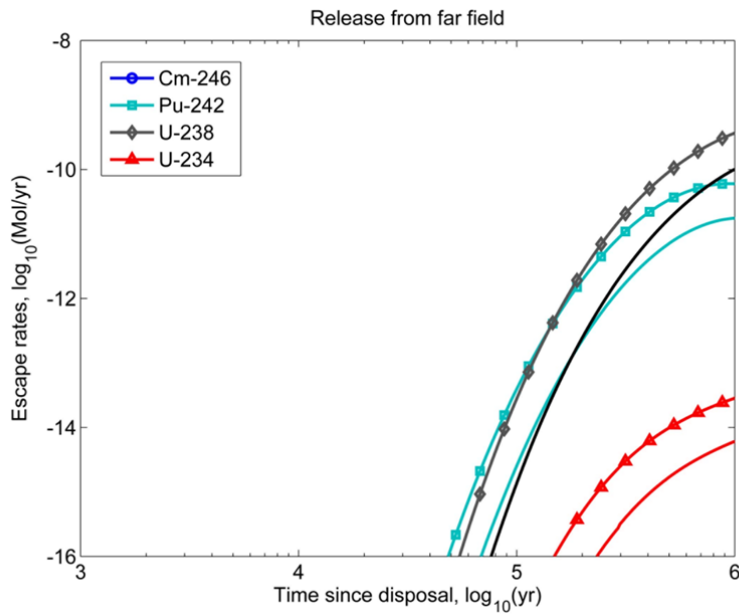
Figure2. Release from the far field, Case (a), line with markers, Case (b), solid lines

Compared to Case (a), Case (b) yields a decrease in the maximum concentration, C_{max}, and a significant increase in the arrival time, $t_{,arrival}$ (the first time that the nuclide is detected at the outlet. This comparison clearly shows the significant effect of the stagnant water zone on nuclide retardation for a stochastic case. It is, therefore, recommended to take this effect into account in understanding the results of field tracer experiments, and also in the performance assessment of repositories for spent nuclear fuel.

[1] L. Liu, L. Moreno, I. Neretnieks, B. Gylling, 2010. "A safety assessment approach using coupled NEAR3D and CHAN3D – Laxemar." SKB R-10-75, Svensk Kärnbränslehantering AB.

[2] L. Liu, L. Moreno, I. Neretnieks, B. Gylling, 2010. "A safety assessment approach using coupled NEAR3D and CHAN3D – Laxemar." SKB R-10-69, Svensk Kärnbränslehantering AB.

[3] P. Shahkarami, L. Liu, L. Moreno, I. Neretnieks, 2015. "Radionuclide migration through fractured rock for arbitrary-length decay chain: Analytical solution and global sensitivity analysis" Journal of Hydrology, 520: 448-460

DEMONSTRATING THE USE OF ASCEM TOOLS FOR COMPLEX GROUNDWATER TRANSPORT SIMULATIONS OF THE UNDERGROUND TEST AREA AT THE NEVADA NUCLEAR SECURITY SITE

E. Kwicklis, Z. Lu,T. Miller, D. Harp, K. Birdsell, P. Dixon, and A. Wolfsberg
Earth and Environmental Sciences Division, P.O. Box 1663, Mail Stop T003,
Los Alamos National Laboratory, Los Alamos, NM 87545

The Underground Test Area (UGTA) Activity is applying the Advanced Simulation Capability for Environmental Management (ASCEM) groundwater flow and transport code, Amanzi, to groundwater contamination problems at the Nevada National Security Site (NNSS), formerly the Nevada Test Site, where 828 underground nuclear tests were conducted between 1957 and 1992. The NNSS is characterized by complex geology involving fractured and faulted volcanic and carbonate aquifers, deep water tables, and numerous contaminant sources. Groundwater flow and transport models have been and will continue to be used to help locate monitoring wells and inform regulatory decisions to minimize risks to the public. The Amanzi code and related software for model calibration and uncertainty analyses developed by the Department of Energy's Environmental Management (DOE-EM) Program have been adapted for future application at the NNSS through a joint partnership where NNSS site experts and EM software developers have collaborated to bring new capabilities to the ASCEM software to address NNSS-specific issues and processes. The collaboration has enabled UGTA to benefit from a national state-of-the-art, high-performance computing initiative and has benefited ASCEM by furnishing a test bed that has helped inform code developers of additional code requirements that only actual field applications can provide.

A test-bed model for a 20-km by 35-km area of Pahute Mesa at the NNSS is currently being used for conceptual model development, and for calibration of site-specific hydrologic and radionuclide transport parameters. Figure 1 shows the hydrologic framework model below the water table within the test-bed model domain. The numerical mesh used to represent the domain includes 7.04 million nodes, 95 hydrostratigrahic units, and 44 faults. Figure 2 shows the network of faults included within the mesh. The talk will describe flow calibration and parameter estimation for the model using steady-state heads and pump test data from a dozen wells. Particle tracking simulations of radionuclide migration from 49 nuclear detonations will also be presented.
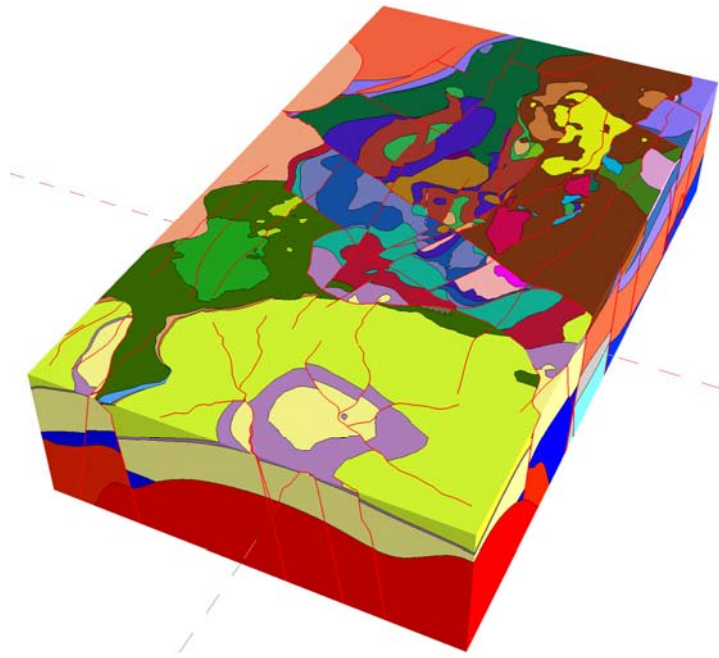
Figure 1. Hydrologic framework model in the Pahute Mesa test-bed model domain

Figure 2. Faults represented within the test-bed model domain

RADIONUCLIDE RELEASE FROM TANK WASTE RESIDUAL SOLIDS

D. H. Miller[1], K. A. Roberts[1], K. M. L. Taylor-Pashow[1], W. D. King[1], M. E. Denham[1], M. H. Layton[2], D. I. Kaplan[1] and D. T. Hobbs[1]

[1]Savannah River National Laboratory, Aiken, SC, USA
[2]Savannah River Remediation, Aiken SC USA

Current practice for closing high-level waste (HLW) tanks at the Savannah River Site (SRS) involves removing as much of the HLW as possible, disconnecting all transfer lines and penetrations into the tanks, and filling the internal volume of the tanks with grout. Performance assessment (PA) modeling of the time dependent release of radionuclides from closed HLW tanks uses a conceptual model in which pore water from the aging grout contacts the residual waste layer in the tank and dissolves radionuclides and other components of the waste solids. The model assumes that the pore fluid composition controls the solubility and waste release concentration of a particular radionuclide.

Simulation of grout aging identified three stages in which the pore waters have different pH values and redox potentials (E_h).[1] The earliest stage after breach of the steel tank liner features a reducing E_h and high pH condition referred to as reducing region II. The next stage features an oxidizing E_h and high pH condition referred to as oxidizing region II. The final stage features an oxidizing E_h and low pH condition referred to as oxidizing region III.

Waste release testing was identified as needed to provide additional information regarding the solubility assumptions used in the conceptual waste release model. The proposed testing was described generally in the SRS Liquid Waste Facilities Performance Assessment Maintenance Program FY2014 Implementation Plan.[2] This plan proposed that waste release experiments be performed with actual tank waste residuals after method development using surrogate materials. Based on this plan SRNL initiated testing to measure the release of key radionuclides from tank waste solids. Key findings from the testing completed to date with surrogates include the following.

- E_h potentials of simulated pore waters produced in these studies upon contact of synthetic infiltration water with surrogate tank closure solids are lower than those used in PA modeling.
- Addition of oxidizing reagents to pore water provides only transitory changes in E_h potentials and pH values.
- Under moderate reducing conditions, the quantity of Pu and U dissolved from the surrogate Tank 18 solids increased in pore water solutions that feature less reducing E_h and lower pH values.
- The presence of grout solids in the leaching tests generally reduced the dissolution of Pu and U from the surrogate Tank 18 solids.

[1] M. E. Denham and M. R. Millings, "Evolution of Chemical Conditions and Estimated Solubility Controls on Radionuclides in the Residual Waste Layer During Post-Closure Aging of High-Level Waste Tanks", Technical Report SRNL-STI-2012-00404, Aiken, SC, August 2012.

[2] K. H. Rosenberger, "Savannah River Site Liquid Waste Facilities Performance Assessment Maintenance Program FY2014 Implementation Plan", SRR Report SRR-CWDA-2013-00133, Aiken, SC, January 2014.

EXPERIMENTS AND THERMODYNAMIC MODELING IN THE Na^+-Cl^--Fe^{2+}-SO_4^{2-} SYSTEM TO HIGH IONIC STRENGTHS

Sungtae Kim[1], Martin B. Nemer [2], Taya Olivas [1], Je-Hun Jang [1]

[1]*Sandia National Laboratories, Defense Waste Management Programs, Carlsbad, NM 88220, USA*
[2]*Sandia National Laboratories, Albuquerque, NM 87123, USA*

The Waste Isolation Pilot Plant (WIPP) repository uses iron-based waste containers, in which lead (Pb) is sometimes present. These metals are expected to compete with actinide components for complexation of organic ligands such as citrate, ethylenediaminetetraacetate (EDTA) and oxalate in the repository. To estimate potential radionuclide release from the repository to the environment after closure, it is essential to determine the solubility of the radionuclides in the brine, which is affected by the ligands listed above. The solution chemistry for brines relevant to the WIPP repository is determined by using the Pitzer model [1,2] to evaluate activity coefficients. To date, the WIPP thermodynamic database does not incorporate iron nor lead species. As part of updating the thermodynamic database, the Pitzer interaction parameters iron and lead aqueous species are being determined. As a result, we present here the experimental data and theoretical derivation of the Pitzer interaction parameters that are relevant to the interaction of sulfate (SO_4^{2-}) with iron (II) species (Fe^{2+} and $FeOH^+$). The $Fe(OH)_3^-$/SO_4^{2-} iron species pair was excluded because negligible amounts of $Fe(OH)_3^-$ ions persist in pH ranges of 7.1-8.9. To mimic an environment consistent with the expected anoxic WIPP conditions, experiments have been performed inside a glovebox, where oxygen (O_2) concentrations were maintained below 3 ppm. Under anoxic condition, $Fe_2(OH)_3Cl(s)$ and $Fe(OH)_2(s)$ solids were synthesized by reacting $FeCl_2 \cdot 4H_2O$ with KOH and NaOH, respectively [3]. Products were confirmed using an x-ray diffractometer (XRD). About 0.7 gram of $Fe_2(OH)_3Cl(s)$ was added into X molal Na_2SO_4 brine solutions (X = 0.05, 0.38, 0.76, 1.14, 1.52, and 1.9), and these samples were labelled as Xm SO4-Fe(OH)2-1 and Xm SO4-Fe(OH)2-2 (1 and 2 represent replicates). About 2.0 grams of $Fe(OH)_2(s)$ were added into Y molal Na_2SO_4 + 0.15 molal NaCl brine solutions (Y = 0.01, 0.1, 0.5, 1, 1.5, and 1.8), and these samples were labelled as "YmNa2SO4+0.15NaCl-GR-Kinetics". These Xm SO4-Fe(OH)2-(1-2) and YmNa2SO4+0.15NaCl-GR-Kinetics sample reactors were aged over 3 years under anoxic conditions. Total iron (Fe(II)) concentrations were determined using an inductively coupled plasma atomic mission spectroscopy. The data was used to derive Pitzer interaction parameters of Fe^{2+}/SO_4^{2-} and $FeOH^+$/SO_4^{2-} binary ion pairs. EQ3NR version of EQ3/6 v.8.0a [4] and Python programming language, *EQ3CodeModule.py* [5], were used to calculate the aqueous speciation and saturation indices for given EQ3NR input files (*.3i files) by referencing known values of logK and Pitzer parameters. The optimized Pitzer interaction parameters of Fe^{2+}/SO_4^{2-} and $FeOH^+$/SO_4^{2-} binary ion pairs are implemented to assess the solubility of $Fe_2(OH)_3Cl$ and $Fe(OH)_2$ in Na^+-Cl^--Fe^{2+}-SO_4^{2-} system. Their adjusted solubilities are compared with experimentally analyzed total Fe(II) concentrations.

[1] PITZER, KS (1973). "Thermodynamics of Electrolytes. I. Theoretical Basis and General Equations." J. Phy. Chem. **77:** 268-277.

[2] PITZER, KS (1975). "Thermodynamcis of Electrolytes. V. Effects of Higher-Order Electrostatic Terms." J. Solution Chem. **4[3]:** 249-265.

[3] Nemer, MB et al. (2011). "Solubility of Fe2(OH)3Cl (pure-iron end-member of hibbingite) in NaCl and Na2SO4 brines." Chem. Geo. 280: 26-32.

[4] Xiong, Y-L, "WIPP Verification and Validation Plan/Validation Document for EQ3/6 Ver. 8.0a for Actinide Chemistry, Rev. 1" Carlsbad, NM: Sandia National Laboratories, ERMS 555358 (2011)

[5] KIRCHNER, TB (2012). "User's manual for the EQ3CodeModule", Carlsbad, NM: Sandia National Laboratories, ERMS 557360 (2012).

CEBAMA – A COLLABORATIVE PROJECT ON CEMENT-BASED MATERIALS, PROPERTIES, EVOLUTION, BARRIER FUNCTIONS, WITHIN THE EUROPEAN COMMISSION / HORIZION2020 FRAME

<u>M. Altmaier</u>[1], L. Duro[2], V. Montoya[1], B. Kienzler[1], J. Perrone[3], E. Holt[4], F. Claret[5], U. Mäder[6], B. Grambow[7], A. Idiart[2]

[1] *Karlsruhe Institute of Technology, Institute for Nuclear Waste Disposal, (KIT-INE), Germany*
[2] *Amphos21 Consulting SL, Barcelona, Spain,*
[3] *Amphos21 Consulting France, Paris, France*
[4] *Teknologian tutkimuskeskus VTT Oy, Espoo, Finland*
[5] *Bureau de recherches geologiques et minieres (BRGM), Paris, France*
[6] *Universität Bern, Bern, Switzerland*
[7] *Association pour la recherche et le developpement des methods et processus industriels (ARMINES), Paris, France*

Cebama is a research and innovation action granted by the European Atomic Energy Community in support of the implementation of the first-of-the-kind geological repositories. The 4-year project, started 1st of June 2015, is carried out by a consortium of 27 partners consisting of large Research Institutions, Universities, one TSO (Technical and Scientific Support Organizations), and one SME (small medium enterprise) from 9 EURATOM Signatory States, Switzerland and Japan. National Waste Management Organizations support Cebama by co-developing the work plan, participating in the End-User Group, granting co-funding to some beneficiaries, and providing for knowledge and information transfer.

Cebama addresses key issues of relevance for long-term safety and key scientific questions related to the use of cement-based materials in nuclear waste disposal applications. The scientific quality and impact of the project builds on joining the best expertise available to tackle these problems and emphasizing how the knowledge can be applied in the Safety Analysis and Safety Case. Cebama will extend the state-of-the-art with respect to integration of key scientific and long-term safety issues. Progress beyond the state-of-the-art is achieved by providing basic and trustworthy knowledge, modeling tools and arguments for the Safety Case.

Information about Cebama, such as key project events, main scientific results, open PhD positions and research highlights are available on the project website (www.cebama.eu).

The overall strategic objective of Cebama is to support the implementation of geological disposal by significantly improving the knowledge base for the Safety Case for European repository concepts. The scientific/technical research of Cebama is largely independent of specific disposal concepts and addresses different types of host rocks, as well as bentonite. Cebama is not focusing on one specific cementitious material, but aims at studying a variety of important cement-based materials in order to provide insight on general processes and phenomena which can then be easily transferred to different applications and projects. Specific objectives of Cebama are summarized as follows:

- **Perform experimental studies to understand the interface processes between cement-based materials and the host rocks (crystalline rock, Boom Clay, Opalinus Clay (OPA), Callovo-Oxfordian (COX)) or bentonite backfill and assess the impact on physical (transport) properties.**
  - Understand how chemical reactions affect porosity, and water and gas transport properties at the interface for the following systems.

- o Low pH cementitious component - crystalline rock
- o Low pH cementitious component - bentonite
- o Low pH cementitious component - OPA, COX
- o High pH cementitious component - crystalline rock
- o High pH cementitious component - bentonite
- o High pH cementitious component - OPA, COX, Boom Clay.

- These aspects are investigated by laboratory tests and up-scaling by utilization of in-situ tests (both ongoing and new tests).

- **Study radionuclide retention processes in high pH concrete environments. Radionuclides which have high priority from the scientific and applied perspective are selected.**
  - Analyze the retention of some specific radionuclides in high pH concrete environment, especially: Be, C, Cl, Ca, Se, Mo, I, Ra.
  - Assess the impact of chemical alterations (e.g., high pH concrete ageing, carbonation, transition from oxidizing to reducing conditions) on radionuclide retention.

- **Improve validity of numerical models to predict changes in transport processes as a result of chemical degradation. Support advanced data interpretation and process modelling, covering mainly issues responsible for the changes in transport properties.**
  - Allow improved interpretation of experiments on chemical interactions affecting porosity, and water and gas transport properties at both the bulk cementitious material and its interface with different host rocks by process level and mechanistic modelling.
  - Extrapolate modelling to system-level to modelling for Safety Case application.

Further objectives cover dissemination of key results to scientific and non-scientific oriented stakeholders as well as training and education of young professionals for carrying over the expertise into future implementation programmes.

Work in Cebama is organized in 3 scientific/technical work packages (WP): WP1 – *Experiments on interface processes and the impact on physical properties* (leader: E. Holt, F. Claret, U. Mäder; WP2 – *Radionuclide retention* (B. Grambow); WP3 – *Interpretation & Modelling* (A. Idiart). In addition, WP4 is on *Documentation, Knowledge Management, Dissemination and Training* (J. Perrone) and WP5 on *Management* (M. Altmaier, V. Montoya).

Cebama is offering the opportunity of external groups to join the project within the status of Associated Groups (AG). AGs will participate in Cebama at their own costs with specific scientific/technical contributions or particular information exchange functions. The AGs will be invited to the Annual Project Workshops and receive access to the public deliverables and scientific technical information obtained in the project (contact: marcus.altmaier@kit.edu).

A key activity of Cebama, open to all interested to participate, are the Annual Project Workshops which serve as an important forum for dissemination of the research performed within the project. The next Annual workshop will be organized by Amphos21, over at least 2 days in the week from May 8th 2016, in Barcelona, Spain. Exact dates and registration will be available in 2016 at Cebama website.

THERMAC – A JOINT PROJECT ON AQUATIC ACTINIDE CHEMISTRY AND THERMODYNAMICS AT ELEVATED TEMPERATURE CONDITIONS

M. Altmaier[1], X. Gaona[1], F. Endrizzi[1], V. Brendler[2], R. Steudtner[2], C. Franzen[2], S. Tsushima[2], P.J. Panak[3], A. Skerencak-Frech[3], S. Hagemann[4], F. Brandt[5], S. Krüger[6], E. Colàs[7], M. Grivé[7], T. Thoenen[8], D.A. Kulik[8]

[1] *Karlsruhe Institute of Technology, Institute for Nuclear Waste Disposal, (KIT-INE), Germany*
[2] *Helmholtz Zenter Dresden Rossendorf, Institute of Resource Ecology (HZDR-IRE), Dresden-Rossendorf, Gemany*
[3] *University of Heidelberg, Institute for Physical Chemistry, Heidelberg, Germany*
[4] *Gesellschaft für Reaktor und Anlagensicherheit (GRS), Braunschweig, Germany*
[5] *Jülich Research Center, Institute of Energy and Climate Research (IEK-6), Jülich, Germany*
[6] *Technische Universität München, Munich, Germany*
[7] *Amphos21 Consulting, Barcelona, Spain*
[8] *Paul Scherrer Institut, Laboratory for Waste Management (PSI-LES), Villigen, Switzerland*

The ThermAc project aims at extending the chemical understanding and available thermodynamic database for actinides, long-lived fission products and relevant matrix elements in aquatic systems at elevated temperatures. To this end, a systematic use of estimation methods, new experimental investigations and quantum-chemistry based information is intended. ThermAc has started in March 2015 and is projected for three years, running until 28.02.2018. The project is funded by the German Federal Ministry for Education and Research (BMBF) and is coordinated by KIT-INE. Within the collaborative project, the following German and international partners and researchers are involved:

- Karlsruhe Institute of Technology (KIT-INE, Germany)
- Helmholtz Zenter Dresden Rossendorf (HZDR-IRE, Germany)
- University of Heidelberg (Germany)
- Gesellschaft für Anlagen- und Reaktorsicherheit (GRS)
- Jülich Research Center (FZJ-IEK-6, Germany)
- Technische Universität München (Germany)
- Amphos21 Consulting (Spain)
- Paul Scherrer Institut (PSI-LES, Switzerland)

The ThermAc project is developed with the aim of improving the scientific basis for assessing nuclear waste disposal scenarios at elevated temperature conditions. In the case of disposal of highly active heat producing waste, the repository system is expected to feature elevated temperature conditions over a significant period of time, due to the high decay heat of the waste at an early stage of repository operation. If early canister failure occurs, radionuclides therefore may contact aquatic systems at higher temperature conditions. Adequate scientific tools must be available to assess the related chemical effects and their impact upon safety. A clear focus of ThermAc is on long-lived actinides in oxidation states III, V and VI, with selected fission products and important redox controlling matrix elements like Fe also receiving attention. Tetravalent actinides and detailed investigations of redox processes are excluded from the current ThermAc work programme. ThermAc addresses the temperature range from ~5°C up to ~90°C, focusing on systems at low or intermediate ionic strength. Only for selected cases with specific relevance or scientific interest, higher temperatures up to 200°C or highly concentrated salt brine solutions will be investigated. Chemical analogs for the actinide elements will be used, especially in order to gain information on solid phase transformation processes. Ion-interaction processes are treated with the Specific Ion Interaction theory (SIT), in agreement with the approach favored by the NEA-TDB project. Quantum chemical calculations are used to support the interpretation of experimental findings, and establish a fundamental understanding of chemical effects on a molecular level.

Within the scope of ThermAc, a significant impact can be realized within a strong collaborative and integrated concept with the following strategic components:

(1) Systematic use of estimation methods for thermodynamic data and model parameters
Using several different estimation methods both for aqueous species and solid phases, a "working database" will be set up for modeling selected reference systems at elevated temperatures. Focus is on simplified

systems at low or intermediate ionic strength. Based upon this newly derived thermodynamic basis, geochemical model calculations are performed and predictions on solubility and speciation made for selected reference systems at elevated temperature.

(2) Comprehensive experimental validation of the estimations
The estimations made in (1) are validated by new experimental studies using a set of complementary experimental approaches and analytical tools, including quantum chemistry. The ThermAc consortium features partners with a broad set of competences and available experimental techniques. The experimental studies established to validate the estimations focus on both aqueous and solid phases under strong variation of background electrolyte media, pH conditions, and temperature, allowing for a comprehensive picture of radionuclide solubility and speciation.

(3) Fundamental studies for improved process understanding of actinide chemistry at elevated T
Key processes which are likely to influence aquatic chemistry at elevated temperature conditions are investigated, like solid phase characteristics (e.g. changes in particle size), secondary phase formation processes, the relevance of intrinsic colloids, or ion-interaction processes. Following this approach, a qualitative, (semi)-quantitative assessment of relevant processes that are at present exceedingly difficult to be addressed within the explicit chemical/thermodynamic concepts and models used in (1) and (2) is possible, also serving as an anchoring point for the use of estimation methods.

(4) Comprehensive critical evaluation of the work performed within (1-3)
A key result from the comparison of predictions based upon estimation methods with new experimental data derived within ThermAc will be the assessment of the use of estimations methods to set up a workable thermodynamic database for elevated temperatures with high applicability to nuclear waste disposal issues. In this context it will be clarified, to which extent systems will remain critical with regard to available thermodynamic data, and which relevant processes at elevated temperatures are still not sufficiently understood.

ThermAc has a strong commitment to disseminate the outcome of the project to the international research community and interlink with similar R&D efforts and applied programs performed elsewhere. Given the scope and very large intrinsic complexity of investigating systems at elevated temperatures, establishing synergies and exchange with groups having complementary interests and competences at an international level seems mandatory. To this end, ThermAc offers the opportunity of external partners joining the consortium as Associated Groups. Associated Groups will join the ThermAc project at their own costs, receiving no financial support via the ThermAc project. Associated groups will have access to the results generated within ThermAc, are invited to the ThermAc project meetings which serve as main forum to present and discuss new results, have the opportunity to communicate their own expertise and research to the consortium and may join in bi- or multilateral cooperation with ThermAc partner institutions. For further information on Associated Groups to ThermAc, please contact the project coordinator at marcus.altmaier@kit.edu.

THE IMPACT OF RADIONUCLIDE EXPOSURE ON MICROBIAL COMMUNITIES AND SUBSEQUENT RADIONUCLIDE MIGRATION FROM A WASTE REPOSITORY: CASE STUDY OF THE WASTE ISOLATION PILOT PLANT

J. Swanson

Actinide Chemistry & Repository Science Program, Repository Science & Operations,
Los Alamos National Laboratory
1400 University Drive, Carlsbad, NM USA

The ability of microorganisms to affect radionuclide migration has long been recognized by those in the mining industry and the fields of waste management and environmental remediation. Microbial activity can result in the mobilization or immobilization of radionuclides by affecting their solubility and speciation.

Most radionuclides are not naturally occurring elements and have no known biological function. As a result, a microorganism's first exposure to a radionuclide may be due to an environmental insult. Although uranium occurs naturally, few phyla contain organisms that can respire on it, and data are lacking on respiration via transuranics. Still, it is clear that radionuclide reduction, mineralization and precipitation, and uptake occur, suggesting that radionuclide "sequestration" may be a microbe's main agenda.

Radioactive contamination may significantly alter the indigenous microbial community at an affected site because of many different stressors (e.g., pH extremes, radionuclides, co-contaminants), making it difficult to tell which stressor exhibited the greatest effect on community structure. Many have found *Actinobacteria* and *Firmicutes* to be dominant at radionuclide-contaminated sites, suggesting that these organisms are either tolerant or resistant [1-2]. Still others have noted Proteobacterial opportunists and recovery of diversity over time [3], and many seek to enrich specific members of this phylum for their remediation potential.

Because of significantly different site types (e.g., soil, groundwater, sediment, granite, clay, salt), a "one size fits all" assumption for radionuclide migration potential may not be valid. This is especially true for salt-based nuclear waste repositories, such as the Waste Isolation Pilot Plant (WIPP), where unique microbial ecology and repository conditions present a different perspective for microbially-induced radionuclide migration. In this setting, there are significant differences between microbial structural diversity spanning the two prokaryotic domains (*Archaea* and *Bacteria*) and even greater differences in functional diversity, both of which reflect their strategies for survival at high ionic strength. For example, incubations of WIPP groundwaters under iron-reducing conditions yielded less diverse communities as ionic strength increased and suggested different modes of metal reduction. Incubations of near-field (high ionic strength) halite samples under similar conditions yielded no growth.

As a consequence of ionic strength influence, redox reactions and transformations of radionuclides may be less important than for organisms in low ionic strength repository environments; while, biologically-induced precipitation and other effects on solubility may be more important. Biocolloid transport remains an uncertainty, although it may have an impact on the actinide source term in intrusion release scenarios.

This talk will provide a brief review of what is known about the microbial communities exposed to radionuclides in waste or at contaminated sites and how these organisms affect radionuclide migration. It will focus on the potential effects that microorganisms may have on salt-based nuclear waste repository performance using the WIPP near and far-field environments as examples of study. It will also address the potential roles of non-halophilic, waste-associated organisms on repository performance in a high-salt environment.
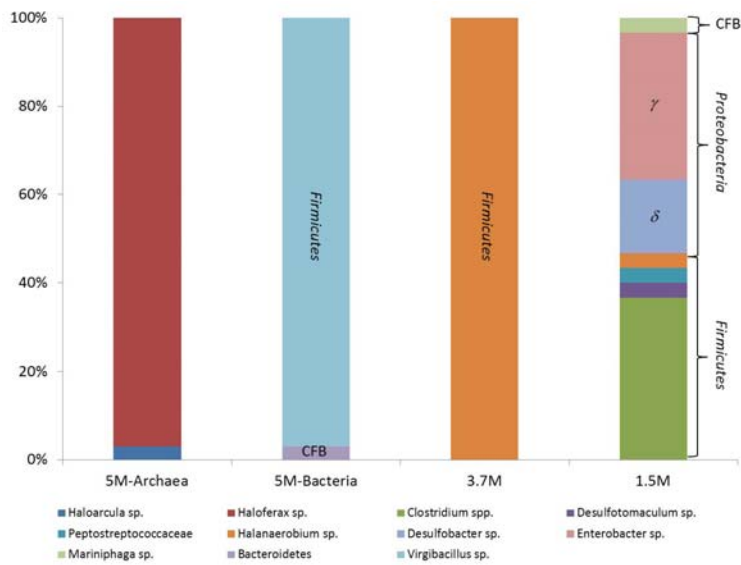
Figure 1. Resulting communities in iron-reducing enrichments of WIPP groundwaters.

1. Zavilgesky GB, Abilev SK, Sukhodolets VV, Ahmad SI. 1998. Isolation and Analysis of UV and Radio-Resistant Bacteria from Chernobyl. Journal of Photobiology B: Biology 43: 152-157.

2. Fredrickson JK, Zachara JM, Balkwill DL, Kennedy D, Li S-M W, Kostandarithes HM, Daly MJ, Romine MF, Brockman FJ. 2004. Geomicrobiology of High-Level Nuclear Waste-Contaminated Vadose Sediments at the Hanford Site, Washington State. Applied and Environmental Microbiology 70: 4230-4241.

3. Chapon V, Piette L, Vesvres M-H, Coppin F, Le Marrec C, Christen R, Theodorakopoulos N, Fevrier L, Levchuk S, Martin-Garin A, Berthomieu C, Sergeant C. 2012. Microbial Diversity in Contaminated Soils Along the T22 Trench of the Chernobyl Experimental Platform. Applied Geochemistry 27: 1375-1383.

THE BIO-REDUCTION OF URANIUM FOLLOWED BY ONE AND TWO PHOTON OPTICAL CONFOCAL MICROSCOPY

D. Jones[1], A.N. Swinburne[1], S. Botchway[2], A. Ward[2], J.R. Lloyd[3], L.S. Natrajan[1]

[1] *School of Chemistry, The University of Manchester, Oxford Road, M13 9PL, UK*
[2] *Central Laser Facility, Rutherford Appleton Laboratory, Harwell, OX11, 0QX*
[3] *School of Earth, Atmospheric and Environmental Sciences, The University of Manchester Oxford Road, M13 9PL*

The contamination of land with radionuclides is an ongoing problem for the nuclear industry impacting on many sites due to accidental spillage or nuclear weapons testing in addition to pollution due to mining and other activities.[1] Of the contaminants, uranium dominates the radionuclide inventory causing concern due to its long half-life, chemical and environmental toxicity.[2] Under oxic conditions, uranium is most commonly found in the +VI oxidation state as the mobile uranyl cation $[UO_2]^{2+}$.[2] Alternatively the +IV oxidation state dominates in anoxic environments, forming, for example, an insoluble crystalline uraninite species.[3]

Certain bacteria have been known to respire under anaerobic conditions, by coupling the reduction of U(VI) to U(IV) to the oxidation of organic matter. Luminescence spectroscopy can be used to distinguish between the oxidation states of uranium, since both the spectral fingerprint/features and luminescence lifetime are readily distinguished in solution.[4,5] We have been developing the use of luminescence spectroscopy to study redox reactions and environmental fate of uranium in model conditions, and here demonstrate the first example of two photon absorption and emission studies of simple uranyl(VI) salts to image biosorption of uranyl onto bacteria. Further insight into the mechanisms of biosorption coupled with microbially-catalysed redox reactions can be gained through the use of confocal microscopy techniques, such as one and two photon FLIM (fluorescence lifetime image mapping) and PLIM (phosphorescence lifetime image mapping). These powerful techniques offer the potential to image redox reactions occurring *in situ*, proving an excellent and sensitive probe to assess the coordination environment of uranium during the bioreduction process.[6]

Geobacter sulfurreducens and *Shewanella oneidensis* are the focus of this study; both are anaerobic, Gram-negative bacteria known for their metal reduction capabilities. For the first time, one and two photon luminescence spectroscopy has been used to study the uranium reduction *in situ,* following the fate of uranyl(VI) during the bioreduction process. Furthermore, we have shown that luminescence microscopy can be used to study the mechanism of electron flow in these systems, when combined with mutants lacking key electron transport proteins. 3D confocal microscopy data will be presented alongside data from other complementary techniques, helping us interpret the bioreduction mechanisms in the two contrasting model metal-reducing bacteria.
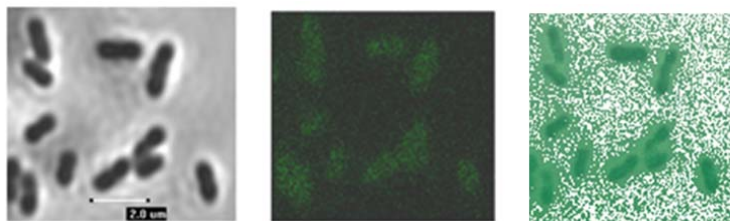
Figure 1: Left to right: brightfield image, fluorescence image and overlaid brightfield and fluorescence image of *Geobacter sulfurreducens* containing uranyl acetate at time =0 following one photon excitation at 405 nm.

1 S. Chakraborty, F. Favre, D. Banerjee, A. C. Scheinost, M. Mullet, J. J. Ehrhardt, J. Brendle, L. Vidal and L. Charlet, *Environmental Science & Technology*, 2010, **44**, 3779.
2 S. A. George, A. M. Whittaker and D. M. Stearns, *Chem. Res. Toxicol.*, 2011, **24**, 1830.
3 D. R. Lovley, *Annu. Rev. Microbiol.*, 1993, **47**, 263.
4 E. Hashem, A. N. Swinburne, C. Schulzke, R. C. Evans, J. A. Platts, A. Kerridge, L. S. Natrajan and R. J. Baker, *RSC Adv.*, 2013, **3**, 4350.
5 M. P. Redmond, S. M. Cornet, S. D. Woodall, D. Whittaker, D. Collison, M. Helliwell and L. S. Natrajan, *Dalton Trans.*, 2011, **40**, 3914.
6 E. Baggaley, S. W. Botchway, J. W. Haycock, H. Morris, I. V. Sazanovich, J. A. G. Williams and J. A. Weinstein, *Chem. Sci.*, 2014, **5**, 879.

DEMONSTRATING THE POTENTIAL FOR MICROBIAL TRANSFORMATION OF IODINE IN HANFORD GROUNDWATER

B. Lee[1], J. Ellis [1], E. Eisenhauer [1], S. Saurey [1], D. Saunders [1], M. H. Lee [1]

(1)Pacific Northwest National Laboratory, Energy and Environment Directorate, Richland, WA, USA

The Hanford Site in Washington is the most contaminated nuclear site in the United States. Radioactive iodine (^{129}I), a fission product generated during plutonium production, has been discharged from disposal cribs, trenches and pits in the 200 West area of the Hanford Site. This discharge is responsible for the majority of ^{129}I contamination found in the groundwater [1]. Radioactive iodine (^{129}I) is of environmental concern due to its long half-life (1.6×10^7 years), toxicity, and mobility in the environment [2]. The 200 West Area contains two separate plumes (200-ZP-1 and 200-UP-1 Operable Units) covering 1,500 acres where ^{129}I concentrations average 3.5 pCi/L. Speciation analysis shows that iodate (IO_3^-) comprises 70.6% of the iodine present, and organo-iodide and iodide (I^-) comprise 25.8% and 3.6% respectively. Based on thermodynamic considerations, iodide would be expected to be the dominant species in Hanford groundwater [3]. Understanding microbial impacts on iodine speciation in Hanford groundwater is important because species will affect interaction with sediments in the subsurface and ultimately transport.

Understanding microbial effects on iodine in the Hanford subsurface is important for two primary reasons: 1) microbes may have oxidized iodide thought to be in waste disposed to current species profile; and 2) microbial transformation of iodine will affect the fate and transport of species currently found in groundwater. To determine the potential for microbial transformation of iodine, PVC traps containing Ringold sediments were incubated in the groundwater at high, low (distal portions of plume) and background (outside the plume) for approximately 50 and 150 days. Once the traps were retrieved enrichment for iodine transforming microbial communities, and molecular analyses were performed to determine diversity within the plume and the potential for iodine biotransformation through the identification of microbial species previously shown to transform iodine.

Microbial diversity within the Hanford groundwater was determined from sediment traps that were incubated in Hanford groundwater containing, high, low or no iodine. Clone libraries showed that regardless of location in the plume and the time of incubation, the plume communities were dominated by *Alpha-, Beta-,* and *Gamma-proteobacteria* (Fig. 1). Organisms such as *Rhizobiales* (*Alphaproteobacteria*) were identified and have been previously described for their ability to reduce iodate. Bacterial diversity was greatest in wells from the high iodine portions of the plume.

A number of bacteria have been isolated from the plumes that are able to transform iodine, either through reduction of iodate or oxidation of iodide. An iodate reducing organism, designated as *Agrobacterium tumefaciens* strain AD35, was isolated from bio-trap material incubated for 50 days in a high ^{129}I concentration plume. Iodate (200 µM) was reduced by 36.3% in micro-aerobic cultures and 47.8% in anaerobic cultures in the presence of 10mM nitrate, which was reduced 81.4% and 80.9% respectively. Iodate was also shown to be reduced by 84.0% and 69.2% in microaerobic and anaerobic growth conditions respectively with nitrate spiking into the growth media. No iodate reduction was demonstrated without nitrate present. These data indicate there is a coupled reduction of nitrate and iodate by strain AD35. Results presented allow us to develop an understanding of iodine speciation throughout the Hanford Site, along with providing novel microbial systems for the bioremediation of iodine and also nitrate, which is not well understood to date.

A number of bacterial isolates from the sediment traps have also been shown to have the ability to oxidize iodide to molecular iodine (I_2). Isolates classified as *Pseudomonas*, *Agrobacterium*, *Arthrobacter*, *Shinella*, *Bacillus*, *Enterobacter* and *Microbacterium* by 16S rRNA were shown to oxidize iodide at different efficiencies. While only a small amount of the total iodide was oxidized to molecular iodine, levels of oxidation were comparable to the µM quantities found in the Hanford groundwater. Since organo-iodine is often created during oxidation of iodide, organic iodine analyses are currently being performed. These results indicate that microbes may be involved in oxidation of iodide found in waste disposed of at the Hanford site to the species distribution currently found in the Hanford groundwater.

These results indicate that microbes are present in the Hanford subsurface that can affect the speciation of iodine, through reductive or oxidative processes. These results are important because different iodine species react differently with sediments which will in turn affect migration in the aquifer.
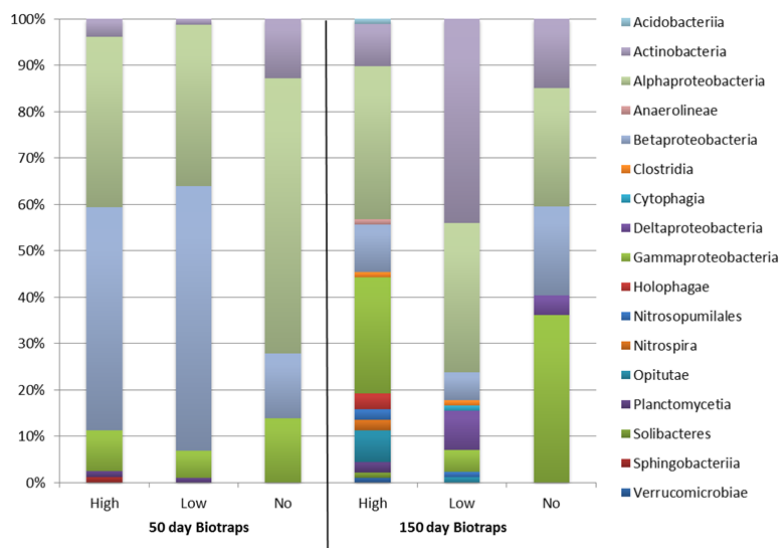
Fig. 1. Percent abundance of bacterial families identified in clone libraries that were developed from sediments that were incubated in iodine contaminated groundwater.

[1]   Zhang, S., et al. (2013). "Iodine-129 and Iodine-127 Speciation in Groundwater at the Hanford Site, U.S.: Iodate Incorporation into Calcite." Environmental Science & Technology 47(17): 9635-9642.

[2]   Councell, T. B., et al. (1997). "Microbial reduction of iodate." Water, Air, and Soil Pollution 100(1-2): 99-106.

[3]   Kaplan, D. I., et al. (2013). "Radioiodine Biogeochemistry and Prevalence in Groundwater." Critical Reviews in Environmental Science and Technology 44(20): 2287-2335.

THE EFFECTS OF ANTHROPOGENIC ORGANIC SUBSTANCES ON THE MIGRATION OF RADIONUCLIDES THROUGH CEMENTITIOUS MEDIA RELEVANT TO GEOLOGICAL WASTE DISPOSAL

J. Hinchliff, M. Felipe-Sotelo, M. Isaacs, P. Davies, N.D.M. Evans, D. Read

Chemistry Department, Loughborough University, LE1 3TU, United Kingdom

The presentation is an overview of several years of research undertaken at Loughborough University into the behaviour of cements intended as grout and backfill within a deep geological disposal facility (GDF). Focus is placed on a range of anthropogenic organic materials, previously known or potentially likely to have an effect on radionuclide retardation.

The present concept for the disposal of intermediate and some low level radioactive waste (ILW and LLW respectively) in the UK is based on a multi-barrier GDF concept. Most ILW will be conditioned by encapsulation in a cementitious grout containing pulverised fuel ash (PFA) and/or ground granulated blast furnace slag (GGBS) and packaged in stainless steel containers prior to deep disposal. The vaults will be backfilled with a cementitious admixture; the NRVB (Nirex Reference Vault Backfill [1]) is one possible material. Cementitious grouts and backfill play an important role within the multi-barrier concept; a key safety function is their contribution to chemical containment by maintaining an alkaline pH and providing surfaces for the adsorption of radionuclides. This local environment is expected to limit aqueous concentrations and inhibit the release of the actinides and other relevant ions from the engineered barrier system into the host rock [2, 3]. However, it is also known that the presence of certain types of organic material, either in the barrier system or the waste itself, could enhance solubility [4]. These organic materials may be present as cellulose degradation products (CDP) or plasticisers (from PVC and other polymers) in the waste, they may arise from decontamination operations at nuclear facilities, e.g. EDTA or citrate, and they are also used in construction materials, for example in the form of superplasticisers in concrete structures [5].

Consequently, it is important to understand how the cementitious media will interact with a range of organic substances and radionuclides to build confidence in predictions of the behaviour over the very long timescales necessarily considered in GDF post-closure safety assessments. The research includes a series of long duration diffusion experiments, which are being carried out to assess the migration of relevant radioisotope cations and anions in various oxidation states (SeO_3^{-2}, I^-, Cl^-, Cs^+, Ni^{2+}, Ca^{2+}, Sr^{2+}, Am^{3+}, Eu^{3+}, Th^{4+}, Pu^{4+} and UO_2^{2+}), in addition to advection, leaching, solubility and degradation studies.

A radial diffusion method, which involves submerging small cylinders of the cementitious admixtures in equilibrated water, has been developed as part of the research. A similar radial advection technique has been used in parallel to simulate the re-saturation phase following repository closure and to supplement the slower diffusion experiments. The cylinders can be manufactured easily, to a variety of relevant specifications and can be doped, via a central well, with a slurry or solution of the materials of interest. The experiments, which provide reproducible results, have been undertaken using CDP, plasticisers and superplasticisers, present in either the cement media or the surrounding solutions. Where diffusion is rapid, the fate of the migrating ions is determined by measuring the concentration increase in the surrounding water. Back-fitting the concentration profile found in solution allows diffusion coefficients to be calculated for monolithic samples. Significant differences have been found between the partition coefficients (R_d) determined with this methodology and literature values obtained on pulverised materials. Where migration is slow, digital autoradiography on axially cut sections of the cylinders is used to determine the migration profile of the radionuclides within the cement. In experiments where no migration has occurred, the solids from the central well are recovered and any alteration of mineral phases and physical changes to the cementitious media are identified using scanning electron microscopy (SEM), X-ray tomography, powder X-ray diffraction (XRD), Raman spectroscopy, nuclear magnetic resonance (NMR), XANES and EXAFS.

As anticipated, with such a large number of radionuclides, oxidation states and organic materials in combination the results show pronounced differences in migration behaviour. Monovalent radioisotopes, both cations and anions, were found to migrate rapidly through the cement [6]. Divalent nickel was immobile in the absence of CDP but mobilised where these were present. Uranium, americium and europium did not migrate under any of the experimental conditions applied and, in the case of uranium at least, the secondary phases responsible could be identified. Although little attention has been paid in the past to the effect of organic ligands on anionic radionuclides, these studies show that CDP can have a deleterious effect on the retardation of iodide [6] and chloride [7], neither of which behave as conservative tracers in purely inorganic systems.

CDP are shown to produce substantial enhancement of Ni, Th, Se(IV), Eu and U(VI) solubility, between 1 and 3 orders of magnitude, over and above that expected from consideration of constituent compounds (e.g. isosaccharinic acid). Studies carried out in the presence of strong ligands such as EDTA and citrate show a marked increase in the solubility of Ni, Th and U(IV/VI) under cementitious conditions, 2 to 4 orders of magnitude higher than calculated using published stability constants [8]. The latter are almost invariably obtained under acidic or near neutral conditions. These studies reveal that new constants need to be defined for the ligands under hyperalkaline conditions in order to avoid significant underestimation of metal solubility.

The presence of superplasticisers in the cement admixtures caused increase bleeding of pore water during the curing process. Both types of commercial superplaticisers tested here (polycarboxylate 'comb' polymers and sulfonated melamine formaldehyde superplasticisers) caused leaching of up to 10% of the loaded amount of radionuclides, namely Ni(II), U(VI), Pu(IV) and Am(III) in the bleed water. However, after the curing process neither further leaching, nor breakthrough of any of the radionuclides in through-diffusion experiments was observed. The synthesis of tailor-made superplasticiser using radical aqueous polymerisation proved successful in reducing radionuclide mobilisation due to bleed. Finally, radiolytic and thermal degradation products of plastic polymers (PVC and PAE) under alkaline conditions include a wide range of compounds including phthalic type species phthalamic acid, phthalic acid, phthalic anhydride, monoethyl ester phthalic acid and isophthalaldehyde. Some of these compounds have been shown to increase solubility of radionuclides, including Pu(IV), Am(III), Th(IV), U(IV/VI) and Ni(II) [9].

The findings presented here constitute a substantial body of solubility, sorption and degradation data that will contribute significantly to the assumptions and calculations made when undertaking post closure safety assessments.

[1] United Kingdom Nirex Limited (1997). "Development of the Nirex Reference Vault Backfill." Report on current status in 1994, Nirex Science report S/97/014

[2] Nuclear Decommissioning Authority (2010). "Geological disposal: Near-field evolution status report". NDA Report NDA/RWMD/033

[3] Nuclear Decommissioning Authority (2010). "Geological disposal: Radionuclides behaviour status report." NDA Report NDA/RWMD/034

[4] N.D.M. Evans, T.G. Heath (2004). "The development of a strategy for the investigation of detriments to radionuclide sorption in the geosphere." Serco Assurance Report SA/ENV-0611

[5] DECC (Department of Enery & Climate Change) and NDA (Nuclear Decommissioning Authority) (2011). "The 2010 UK radioactive waste inventory: Main report." Report by Pöyry Energy Limited for DECC (RRN 10D/985) and NDA (NDA/ST/STY(11)0004)

[6] Felipe-Sotelo, M. Hinchliff, J. Drury, D. Evans, N. Williams, S. and Read, D. (2014). "Radial diffusion of radiocaesium and radioiodide through cementitious backfill." Phys. Chem. Earth. 70-71: 60-70

[7] E. van Es, J. Hinchliff, A. E. Milodowski, L. Field, M. Felipe-Sotelo, N. Evans, D. Read. "Retention of chlorine-36 by a cementitious backfill" submitted to Mineralogical Magazine 2015

[8] M. Felipe-Sotelo, C. Jacklin, M. Edgar, T. Beattie, P. Warwick, N.D.M. Evans, D. Read. "Effect of anthropogenic organic complexants on the solubility of Ni, Th, U(IV) and U(VI)" submitted to Journal of Hazardous Materials 2015

[9] M. Cowper. (2013) "The Impacts of Aqueous Phase Degradation Products from PVC Additives." AMEC Report SF6604 Issue 02

THE ROLE OF DISSOLVED ORGANIC MATTER IN BOOM CLAY PORE WATER COMPOSITION

D. Durce, C. Bruggeman, N. Maes, L.Van Ravestyn

Belgian Nuclear Research Centre (SCK•CEN), Expert Group Waste&Disposal,
Boeretang 200, B-2400 Mol, Belgium

Organic matter is an important component of soil and sediments and its distribution over the solid and the solution is known to control the fate of trace metals and contaminants in the environment. Solid or particulate organic matter immobilize the contaminants acting as a sorption phase while dissolved organic matter (DOM), mobile, was notably shown to transport metals [1, 2] and radionuclides [3-5]. Boom Clay (BC), a potential host rock for deep geological nuclear waste disposal in Belgium, contains 1 to 5 wt% of OM of which ~10 % was observed to be soluble in BC pore water. The association of DOM with major and trace elements is believed to, at least partly, control their concentration in pore water. However, in low-porous media, such as BC, DOM is not entirely mobile and is partitioned between a mobile fraction, that in BC corresponds to molecular weight (MW) < 20 kDa and an immobile fraction (MW > 20 kDa) which is trapped in the pores of the rock. The role played by DOM on the pore water composition depends therefore on: 1/ the concentration of DOM, 2/ the ability of the elements to associate with DOM and 3/ the mobility of this association.

These three points were investigated by a set of batch leaching experiments performed in ultrapure water, in a synthetic pore water to mimic *in situ* conditions and in higher saline conditions to study perturbed conditions. The release of DOM and of major and trace cations in solution were followed as a function of the electrolyte composition. The association DOM-cations was evaluated with the aid of ultracentrifugation. As shown in Figure 1 (right), the release of DOM depends on the electrolyte composition, the increase of salinity decreasing the concentration of DOM. Figure 1 (left and right) also reveals that the concentration of major cations (Na, K, Ca, Mg, Li) were independent of DOM content and mainly controlled by solubility and ion exchange equilibrium. On the other hand, transition metal concentrations in the solution, such as Ni and Cu, were clearly correlated with DOM content and were removed by ultracentrifugation. Aluminium, phosphor and iron were also present in colloidal form and probably associated with DOM.

The determination of the size of DOM species to which the cations preferentially associate is currently investigated by means of ultracentrifugation which will allow determining the mobility of the DOM-cation association.
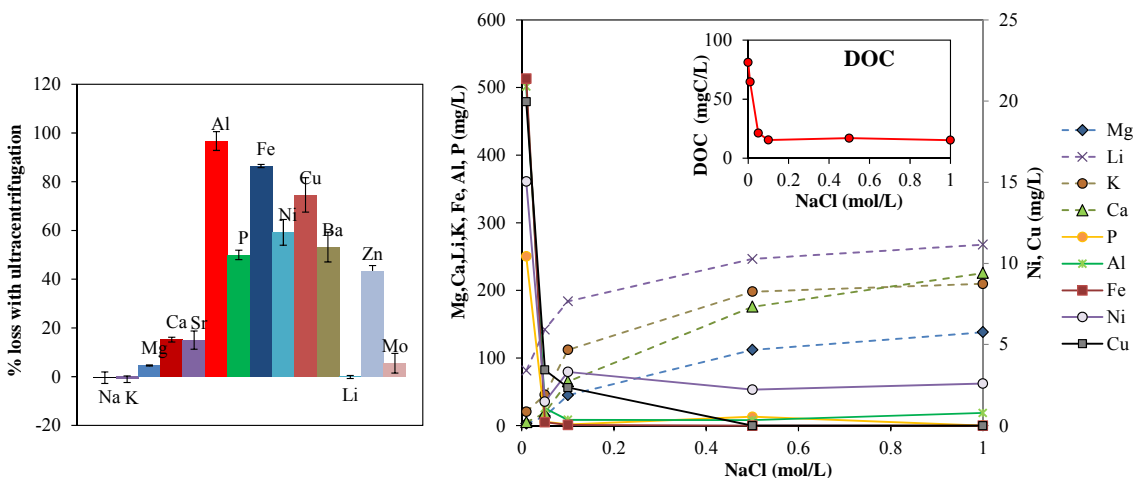
Figure 1. On the left: percentage of element released from BC in synthetic pore water that sedimented after ultracentrifugation at 35000 × g for 1h. On the right: concentration of element and DOC released from BC in contact with various NaCl solutions.

ACKNOWLEDGEMENT

[1] Kalmykova, Y., S. Rauch, A.-M. Stromvall, G. Morrison, B. Stolpe, and M. Hassellov, *Colloid-Facilitated Metal Transport in Peat Filters.* Water Environment Research, 2010. **82**(6): p. 506-511.

[2] Paradelo, M., P. Perez-Rodriguez, D. Fernandez-Calvino, M. Arias-Estevez, and J.E. Lopez-Periago, *Coupled transport of humic acids and copper through saturated porous media.* European Journal of Soil Science, 2012. **63**(5): p. 708-716.

[3] Warwick, P.W., A. Hall, V. Pashley, N.D. Bryan, and D. Griffin, *Modelling the effect of humic substances on the transport of europium through porous media: a comparison of equilibrium and equilibrium/kinetic models.* Journal of Contaminant Hydrology, 2000. **42**(1): p. 19-34.

[4] Maes, N., C. Bruggeman, J. Govaerts, E. Martens, S. Salah, and M. Van Gompel, *A consistent phenomenological model for natural organic matter linked migration of Tc(IV), Cm(III), Np(IV), Pu(III/IV) and Pa(V) in the Boom Clay.* Physics and Chemistry of the Earth, Parts A/B/C, 2011. **36**(17–18): p. 1590-1599.

[5] Mibus, J., S. Sachs, W. Pfingsten, C. Nebelung, and G. Bernhard, *Migration of uranium(IV)/(VI) in the presence of humic acids in quartz sand: A laboratory column study.* Journal of Contaminant Hydrology, 2007. **89**(3–4): p. 199-217.

COMPLEXATION OF TRIVALENT ACTINIDES AND LANTHANIDES WITH CLAY-ORGANIC LIGANDS AT T = 20 – 90°C

A. Skerencak-Frech[(1)], D. Froehlich[(2)], M. Maiwald[(2)], M. Trumm[(1)]. J. Rothe[(1)], K. Dardenne[(1)], P. J. Panak[(2)]

[(1)]*Institut für Nukleare Entsorgung (KIT-INE), Postfach 3640, D-76021 Karlsruhe*
[(2)] *Universität Heidelberg, Im Neuenheimer Feld 253, D-69120 Heidelberg*

Clay formations are considered as host rocks for a nuclear waste repository in deep geological formations. Studies on the composition of the pore waters of different clay rocks (e.g. Callovo-Oxfordian (COX), Opalinus Clay (OPA)) show that low molecular weight organic compounds (LMWOC) like acetate, propionate and lactate constitute a large fraction of the total dissolved organic matter (DOM; χ_{LMWOC}(COX) = 0.88, χ_{LMWOC}(OPA) = 0.36).[1,2] These compounds are potential ligands for trivalent actinides and may influence their migration behaviour. Although the complexation of An(III) with different LMWOC has been studied in the past, the majority of these studies is limited to ambient temperatures.[3] Due to the radioactive decay, temperatures well above 25°C will be present in the near-field of a repository for high-level nuclear waste for a considerable time span. Detailed thermodynamic data for An(III)-LMWOC complexes at 25°C and at increased temperatures contribute to the long-term safety assessment of certain nuclear waste repository scenarios under discussion.

In the present work the thermodynamics and structure of complexes of Cm(III) and Am(III) with different small clay-organic ligands (formate, acetate, propionate, lactate, oxalate) are studied at T = 20 – 90°C by time resolved laser fluorescence spectroscopy (TRLFS), extended x-ray absorption fine structure spectroscopy (EXAFS) and quantum-chemical calculations. The conditional stability constants (log K'_n(T)) of the different Cm(III) ligand complexes are determined as a function of the ligand concentration and the ionic strength (I_m). Thereby, the ionic strength is varied in the range of I_m = 0.5 – 4.0 with NaClO$_4$, NaCl and CaCl$_2$. The log K'_n(T) values are extrapolated to the reference state (I_m = 0.0) with the Specific Ion Interaction Theory (SIT) approach, yielding the respective thermodynamic constants (log K^0_n(T)). Also, the binary ion-ion-interaction parameters (ε_T(i,k)) of the different Cm(III) ligand complexes with the ions of the background electrolytes are determined. The temperature dependency of the log K^0_n(T) values is fitted with the integrated Van't Hoff equation and the respective thermodynamic functions ($\Delta_r H^0_m$, $\Delta_r S^0_m$) are calculated. The Am(III) acetate and lactate complexes are studied by EXAFS spectroscopy at different pH (1 – 6) and at T = 25°C and 90°C. The molecular structure (coordination number and mode, O and C distances) of the different complexes are determined by iterative transformation factor analysis. The results are in excellent agreement with the TRLFS data and provide additional information on the complexation mechanism. The structure of the Cm(III) oxalate complexes is studied by ab initio calculations in the gas phase and molecular dynamic simulations in a box containing 1000 H$_2$O molecules. The results provide detailed insights into the coordination mode and bond angles of the different [Cm(Ox)$_n$]$^{3-2n}$ (n = 1,2,3,4) species and provide an explanation for observed trends in the thermodynamic functions of the complexes.

The results show that all simple carboxylic ligands, which lack a functional group in α-position (formate, acetate, propionate), coordinate in a bidentate mode via the two oxygen atoms to the metal ion ("end-on"). The log K^0_n(T) of the complexes of Cm(III) with acetate and propionate are comparable. The values for formate are slightly lower by ~1.0. Furthermore, the log K^0_n(T) values of these complexes show similar temperature dependencies. Contrary to this, lactate and oxalate, with its additional α-functional groups, bind in a side-on coordination mode to An(III) and form a five-membered chelate ring. This results in distinctively stronger complexes and higher stability constants. Thereby, the stability constants for the oxalate are by over 2 orders of magnitude higher than the lactate complexes. Also, the temperature dependency of log K^0_n(T) for the chelating ligands differs from the simple carboxylic ligands, showing a decrease with increasing T. As an example, the log K^0_1(T) values for the different Cm(III) complexes determined in this work are compared in figure 1.

The different binding modes of the ligands are also reflected in the thermodynamic functions of the different Cm(III) complexes. The $\Delta_r H^0_m$ for the simple carboxylic ligands are all positive, with values ranging from 5 to 40 kJ/mol. Contrary, the ligands with a α-functional group show in general exothermic standard reaction enthalpies. The reason for this is the stronger complex formation and an accompanying release of more binding energy. The formation of the [Cm(Ox)$_n$]$^{3-2n}$ (n > 1) species is endothermic. This is attributed to the change of the sign of the charge of the complex and stronger electrostatic repulsion. For all Cm(III) complexes which are studied in the present work positive values for $\Delta_r S^0_m$ (~ 50 – 150 J/molK) are determined. The changes in $\Delta_r S^0_m$ for different Cm(III) oxalate species observed in this work are explained by

molecular dynamic simulations, showing the change of the degrees of freedom of the complexes as successive ligands are added to the first coordination sphere.
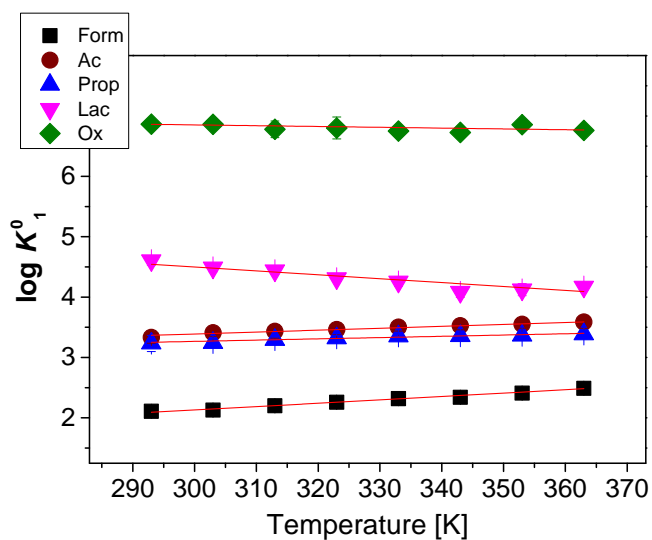
Figure 1. log $K^0_1(T)$ values for the complexes $[Cm(Form)]^{2+}$, $[Cm(Ac)]^{2+}$, $[Cm(Prop)]^{2+}$, $[Cm(Lac)]^{2+}$ and $[Cm(Ox)]^+$ as function of the temperature

This work presents a detailed multi-method study of the complexation of trivalent actinides with clay-organic ligands at increased temperatures (20 – 90°C) and in different ionic media ($NaClO_4$, $NaCl$, $CaCl_2$). Correlations of the presence of different functional groups of a ligand with the structure and the thermodynamic properties of the resulting An(III) complexes are derived. Thus, the results provide detailed insights into the complexations mechanisms and are important for a process understanding of these reactions on the molecular scale. The thermodynamic data and binary ion-interaction parameters derived in this work contribute to a comprehensive description and modelling of the migration of trivalent actinides from a potential nuclear waste repository.

[1] Courdouan, et al, *Appl. Geochem.*, **22**, 1537-1548, (2007)

[2] Courdouan, et al, *Appl. Geochem.*, **22**, 2926-2939, (2007)

[3] Hummel, et al, *NEA-TDB: Chemical Thermodynamics of Compounds and Complexes of U, Np, Pu, Am, Tc, Se, Ni and Zr with Selected Organic Ligands, OECD NEA-TDB, Vol. 9*, (2005)

FORMATION AND STRUCTURAL ANALYSIS OF TERNARY Mg-UO$_2$-CO$_3$ COMPLEXES USING TRLFS AND EXAFS

J.-Y. Lee[1], X. Gaona[2], M. Vespa[2], K. Dardenne[2], J. Rothe[2], T. Rabung[2], M. Altmaier[2], J.-I. Yun[1]

[1] Department of Nuclear and Quantum Engineering, KAIST
219 Daehak-ro, Yuseong-gu, Daejeon 305-701, Republic of Korea
[2] Institute for Nuclear Waste Disposal (INE), Karlsruhe Institute of Technology (KIT),
Karlsruhe, P.O. Box 3640, D-76021 Karlsruhe, Germany

The predominant presence of ternary uranium(VI) carbonate complexes in natural groundwater systems has been intensively discussed owing to the considerable amount of earth-alkaline metal ions and carbonate ions omnipresent in natural groundwater and the exceptionally high formation constants of several Me-UO$_2$-CO$_3$ species (Me = Ca, Mg, Ba, Sr). Recently, the formation of Mg-UO$_2$-CO$_3$ species was reported with respect to spectroscopic properties [1] and chemical thermodynamic data [1-3]. However, the presence of the second Mg(II)-bound uranium(VI) complex is still uncertain even though the existence of the complex Mg$_2$UO$_2$(CO$_3$)$_3$(aq) is highly expected in analogy to the reported presence of other Me$_2$UO$_2$(CO$_3$)$_3$(aq) (Me = Ca, Ba, Sr) complexes [1,2]. The objective of the present work is to investigate the formation behavior and spectroscopic properties as well as the molecular structure of ternary Mg-UO$_2$-CO$_3$ complexes by means of time-resolved laser fluorescence spectroscopy (TRLFS) and extended X-ray absorption fine structure (EXAFS).

Aqueous samples were prepared under aerobic condition using chemicals with analytical grade purity. The concentration of uranium(VI) was maintained at 10^{-3} M. Aqueous carbonate concentration was initially set to 5×10^{-2} M with Na$_2$CO$_3$ and the samples further equilibrated with ambient air. The acidity was controlled at pH = 8.2 using TRIS and HCl. The magnesium ion concentrations in aqueous solutions were controlled in the 8×10^{-4} M to 0.1 M range with MgCl$_2$·6H$_2$O. Ionic strength was maintained at 0.1 mol/L by adding Na/HCl except for the samples with high magnesium ion concentration. For the excitation of Mg-UO$_2$-CO$_3$ samples, a fourth harmonic (266 nm) of Nd:YAG laser was utilized. The fluorescence signal was measured by ICCD camera coupled with Czerny-Turner type spectrometer. U-L$_{III}$ EXAFS spectra were recorded in X-ray fluorescence detection mode at the INE-Beamline for actinide science, ANKA synchrotron radiation source, KIT Karlsruhe.

As illustrated in Fig. 1(a), the fluorescence intensity of formed uranium(VI) complexes formed at pH 8.2 showed an increasing tendency with raising the magnesium ion concentration, clearly representing the chemical reaction between Mg^{2+} ions and uranium(VI) species. Fig. 1(b) shows the fluorescence peak wavelengths of uranium(VI) species located at 467, 485, 506, 528, and 551 nm. The uranium(VI) complexes observed in the present work were assigned to be ternary Mg-UO$_2$-CO$_3$ complexes according to determined fluorescence peak wavelengths, which are in good agreement with data [1] reported by Geipel et al. Moreover, two different fluorescence lifetimes of 19 ± 2 ns and 52 ± 4 ns were found, based on fits of the bi-/tri-exponential fluorescence decay curve. The uranium(VI) complex having relatively short fluorescence lifetime was identified to be MgUO$_2$(CO$_3$)$_3$$^{2-}$, regarding the reported fluorescence lifetime (18.2 ± 2.7 ns [1]) of that species. However, the second uranium(VI) complex with longer fluorescence lifetime could not be directly attributed to the Mg$_2$UO$_2$(CO$_3$)$_3$(aq) species due to the lack of available spectroscopic data. The slope analysis coupled with iterative methods was employed to determine the coordination number of magnesium metal ions bound to Mg-UO$_2$-CO$_3$ complexes. The slope analysis for Mg-UO$_2$-CO$_3$ samples in terms of fluorescence intensity at relatively low magnesium concentration was conducted, and the coordination number of magnesium ions found to be 1.07 ± 0.08, indicating the presence of one magnesium ion as in MgUO$_2$(CO$_3$)$_3$$^{2-}$. The slope at relatively high magnesium ion concentration was evaluated to be 1.96 ± 0.13, representing that two magnesium ions were bound to the second Mg-UO$_2$-CO$_3$ complex, which could be assigned as Mg$_2$UO$_2$(CO$_3$)$_3$(aq). The formation constants of those uranium(VI) species were determined to be log β^0_{113} = 26.0 ± 0.1 and log β^0_{213} = 28.8 ± 0.3 using the specific ion interaction theory (SIT) for the MgUO$_2$(CO$_3$)$_3$$^{2-}$ and the Mg$_2$UO$_2$(CO$_3$)$_3$(aq) complexes, respectively.

Extended x-ray absorption fine structure (EXAFS) analysis performed at the INE Beamline for Actinide Research at ANKA was complementarily utilized to investigate the molecular structure of Mg-UO$_2$-CO$_3$ complexes, as represented in Fig. 1(c). The U-L$_{III}$ EXAFS data revealed almost identical molecular structures between Ca-UO$_2$-CO$_3$ and Mg-UO$_2$-CO$_3$ species except for the shorter atomic distance of U-Mg (ca. 3.82 Å) compared with that of U-Ca (ca. 4.15 Å) owing to the smaller effective ionic radius of magnesium ion compared with calcium ion.
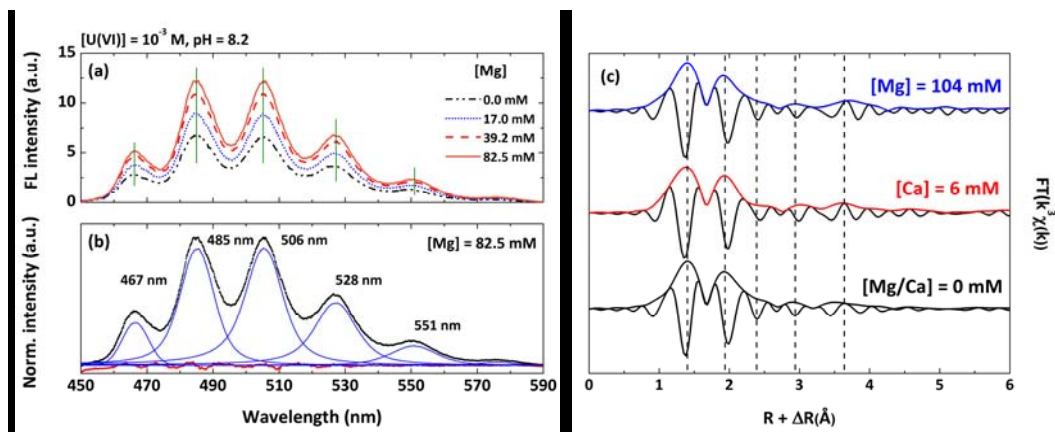
Fig. 1: (a) Fluorescence spectra and (b) fluorescence peak wavelengths of ternary Mg-UO$_2$-CO$_3$ species at various magnesium metal ion concentrations and (c) fourier transform of uranium L$_{III}$-edge k^3-weighted EXAFS spectra for Me-UO$_2$-CO$_3$ complexes (Me = Mg/Ca)

[1] G. Geipel, S. Amayri, and G. Bernhard, Spectrochim. Acta, Part A 71(1), 53 (2008)

[2] W. Dong and S. C. Brooks, Environ. Sci. Technol. 40(15), 4689 (2006)

[3] F. Endrizzi and L. Rao, Chem.-Eur. J. 20(44), 14499 (2014)

RECENT RAMAN SCATTERING STUDIES OF RADIOLYTIC ALTERATION ON SOLID/FLUID INTERFACES: IN SITU MEASUREMENTS UNDER ION BEAM IRRADIATION ON UO₂ AND NUCLEAR GRAPHITES

P. Simon[(1)], A. Canizarès[(1)], G. Guimbretière[(1)], M.R. Ammar[(1)], N. Raimboux[(1)], M.F. Barthe[(1)], F. Duval[(1)], R. Omnée[(1)], C. Corbel[(2)], B. Muzeau[(2)], E. Mendes[(2)], R. Mohun[(3)], L. Desgranges[(3)], M. Magnin[(4)], C. Jégou[(4)], N. Galy[(5)], N. Toulhoat[(5)], N. Moncoffre[(5)]

[(1)]*CNRS, CEMHTI UPR3079, Univ. Orléans, F-45071 Orléans, France*
[(2)] *Laboratoire des Solides Irradiés, CNRS-CEA-Ecole Polytechnique, ,F-91128 Palaiseau, France*
[(3)] *CEA/DEN/DEC, Cadarache Research Center, 13108 Saint-Paul-lez-Durance Cedex, France*
[(4)] *CEA/DEN/DTCD, Marcoule Research Center, 30207 Bagnols-sur-Cèze Cedex, France*
[(5)] *IPNL, CNRS/IN2P3, UMR 5822, Université de Lyon, F-69622 Villeurbanne cedex, France*

A better knowledge of the mechanisms of alteration of solids under radiolytic conditions is a key point for the long term storage of spent fuels and other materials of nuclear plants. Many experimental and numerical approaches have already been developed in this goal, giving noticeable information for these topics. The radiolysis conditions can be performed by radioactive species or by ion beam techniques. The former way is closer to the conditions of the problematics of long term storage, the latter one is easier for experimental conditions and safety rules, and allows to simulate in shorter times the conditions of high fluences, too long at the lab scale, provided the extrapolation of this change of time scale be reasonable. Nevertheless these experiments with ion beams can be used as model conditions for the study of some specific mechanisms. Moreover they are more and more instrumented with *in situ* measurement, giving access to the kinetics of mechanisms and to possible embedded schemes of alteration, with intermediate species. We present here a review of recent *in situ* Raman scattering characterizations of alteration of materials in radiolytic conditions, performed with He^{2+} beams at CEMHTI cyclotron (Orleans, France)[1].

Firstly we will detail a device developed for the study of UO_2/H_2O interfaces. The framework of this study is the behavior of nuclear spent fuel in long term underground storage. The He^{2+} beam is sent onto a depleted UO_2 ceramic disk. The output side is a water slab closed by a silica window. He^{2+} ions are stopped very close to the UO_2 surface, where water is radiolyzed. On the other side of the silica window a Raman probehead is positioned. The typical behavior of Raman records on the interface is as follows: after some tens of minutes of irradiation, new lines appear, due to U(VI) compounds studtite $UO_2O_2.4H_2O$ and schoepite $UO_3.2H_2O$, on the interface. The growth of these lines is rather regular, even after stopping the irradiation. Besides, a detailed analysis with Principal Component Analysis has evidenced spectral features which increase during irradiation, and decrease after stopping it: mainly H_2O_2 but also uranyl complexes.

More recently, a second experimental device was developed, aiming to characterize nuclear graphites used as moderator in the French UNGG reactors. The behavior and the mobility of long period radioactive species such as [36]Cl need a better understanding for solutions of long-term storage. This is studied through the study of model graphites implanted with [37]Cl (simulating [36]Cl) [5] and exposed to simultaneous conditions of temperature, gas pressure and irradiation corresponding to the working conditions of CO_2 gas-cooled UNGG reactors. The sample environment is a cell combining such conditions, in order to monitor by *in situ* Raman scattering the radiolysis-assisted degradation mechanisms of graphite, which govern the chlorine mobility. First results of this new system will be reported at the conference.

These two examples of *in situ* Raman scattering in radiolysis conditions aim to illustrate to efficiency of the method, which can be applied to many other materials and/or irradiation conditions. Even if such methods with ion beams must be considered carefully when extrapolating their conditions of high flux and short times to problematics of long-time storage or 'real' nuclear materials, they can nevertheless shed new light on alteration mechanisms. Moreover, these studies of model materials can be used as elementary bricks to understand the very complex Raman spectra of industrial materials such as MOX spent fuels [6].

[1] A. Canizarès, et al., (2012). J. Raman Spectr. 43: 1492-1497.
[2] G. Guimbretière, et al., (2012). Applied Physics Letters 100: 251914.
[3] L. Desgranges, G. Baldinozzi, P. Simon, G. Guimbretiere, A. Canizares, (2012). J. Raman Spectr. 43: 455-458.
[4] L. Desgranges, G. Guimbretière, P. Simon, C. Jegou, R. Caraballo, (2013). NIMB 315: 169-172.
[5] A. Blondel, et al., (2014). Carbon 73: 413-420.
[6] C. Jegou, et al., (2015). J. Nucl. Mater. 458: 343-349.

INTERACTION OF FERROUS IRON WITH IRON RICH CLAY MINERALS WITH IMPLICATIONS FOR REDOX-REACTIONS WITH POLYVALENT RADIONUCLIDES

K.M. Rosso[1], V. Alexandrov[1], A. Neumann[2], C.I. Pearce[3], O. Qafoku[1], R.N. Collins[4], M. M. Scherer[5]

[1]Pacific Northwest National Laboratory, Richland, WA 99352; [2]Newcastle University, Newcastle upon Tyne, NE1 7RU, UK; [3]University of Manchester, Manchester M13 9PL, UK; [4]UNSW Water Research Centre, University of New South Wales, Sydney, NSW 2052, Australia; [5] University of Iowa, Iowa City, IA 52242

Due to its uniquely poised redox chemistry and natural abundance, iron is arguably the most important transition metal in the Earth's crust. It occurs as discrete accessory minerals, nanoparticles, and aquatic ions, as well as being widely dispersed in diverse silicate mineral structures. With respect to subsurface fate and transport of redox-active radionuclide contaminants such as U(VI) and Tc(VII), an important form of iron is that residing in iron-rich clay minerals such as ferruginous smectite. This form is unique because it can act as a source of, or sink for, electron equivalents while remaining resistant to phase change due to topotactic charge compensation,[1] thus behaving as a recyclable catalytic substrate for heterogeneous redox transformation of radionuclides. Developing a detailed understanding of the mechanisms and thermodynamics of Fe(II/III) redox cycling of iron in clay minerals is an important goal.

Redox equilibration between aqueous Fe(II) and clay structural iron under reducing conditions is a fundamental aspect of the system because of their expected geochemical coincidence and because previous work has established that redox cycling releases some of the structural iron through mild dissolution.[2] Strong and weak Fe(II) binding sites on ferruginous smectite such as nontronite have also been established, depending on pH,[2] and this sorbed Fe(II) is capable of reducing Fe(III) in the octahedral sheet (OS).[3-5] Subsequent electron transfer (ET) processes can result in the precipitation of Fe(III)-oxyhydroxides,[3] whose nucleation and growth pathway with respect to the clay structure remains unknown. Key knowledge gaps include: (i) the molecular identity of strong and weak sorbed Fe(II): (ii) the energetics and kinetics of electron exchange with structural Fe(III); (iii) the mechanism of charge compensation as the clay is reduced; and (iv) the reactivity of the mixed phase products towards radionuclide electron acceptors.

Exposure of ferruginous smectites containing Fe isotopes at natural abundance to 57Fe(II) solution showed a fast initial uptake of 57Fe with simultaneous release of 56Fe that slowed after 3 days and stabilized after about 50 days, indicating that Fe atom exchange had occurred. We calculated that 5−20% of structural Fe in the nontronites NAu−1 and NAu−2, and the smectite SWa−1 exchanged with aqueous Fe(II), which significantly exceeds the Fe atom layer exposed directly to solution. Fe $L_{2,3}$-edge x-ray absorption and magnetic circular dichroism spectroscopies reveal a mixture of ferrous and ferric iron that is magnetically ordered and octahedrally coordinated, consistent with iron comprising the OS of the clay.

Density functional theory (DFT) calculations were performed to gain molecular level insights into the heterogeneous reaction between aqueous Fe(II) and nontronite (010) and (110) edge and (001) basal surfaces.[6] Edge-bound Fe(II) adsorption complexes at different surface sites (ferrinol, silanol, and mixed) may coexist on both (010) and (110) edge facets, with complexes at ferrinol FeO(H) sites being the most energetically favorable and likely corresponding to the strong adsorption site previously observed. Calculation of the ET activation energy suggests that interfacial ET into dioctahedral Fe(III) sheets is at the clay edges and occurs predominantly, but not exclusively, through a proton-coupled ET process at ferrinol sites. No evidence for ET through the basal surface is found. The modeling indicates that Fe(II) adsorption and ET to FE in the OS should occur, consistent with the experimental observations, primarily at nontronite edges, as a pH-dependent process influenced by the protonation state of bridging ligands and the ability of the surface complex site to couple proton transfer to ET.[6]

Our finding of 5−20% Fe atom exchange suggests that exchange may be facilitated by migration of injected electrons through the OS to Fe sites predisposed to reductive release from edges. DFT calculations using a small polaron hopping model[7] show that, while rates of electron hopping are much slower than in iron oxides, they agree very well with values deduced from variable-temperature Mossbauer data[5] and indicate mobilities high enough at room temperature to explain the atom exchange observations. Comparison of the ET rates for Fe in the tetrahedral versus octahedral sheets, as well as between these sheets, shows that the dominant migration pathway is indeed within the OS. Protonation of structural OH groups mediating ET between the Fe ions, as one possible mechanism of charge neutralizing the reduced clay, is predicted to slow electron migration through the OS, and presumably therefore atom exchange, by increasing the reorganization energy and decreasing the electronic coupling that facilitates electron hopping.

When added to previous knowledge our combined experiments and computations suggest that aqueous Fe(II) and ferruginous smectites combine to form a reactive electron source for reduction of redox-active radionuclides under conditions that favor strong interaction of Fe(II) and radionuclides at particle edges. Mixed-valent structural iron is a dynamic constituent, and after redox reaction the precipitation of lower solubility iron or iron-radionuclide metal oxyhydroxide products at particle edges appears likely. Batch reactivity experiments of Tc(VII) and, for comparison, Cr(VI) oxyanions with a natural Fe-rich smectite at native groundwater pH (approximately 8) from a reducing zone in the Ringold Formation at the Hanford Site, U.S.A., shows that under these conditions the structural Fe(II) is not reactive with Tc(VII) but is reactive over days of contact with more oxidizing Cr(VI). Added Fe(II) is rapidly sorbed to the clay and while no reactivity enhancement is observed towards Tc(VII), the rate of Cr(VI) reduction becomes significantly faster. Thus in addition to the redox potential gradient for reaction, our research on model systems indicates that major factors affecting ET rates and possibly product phases that form will also include: (i) pH, through its effect on speciation, redox potential gradient, and charge densities at clay edges; (ii) the nature and structure of the local environment at particle edges; and (iii) the degree of covalency of the bonds between Fe and ligands mediating ET processes. The research on model and natural Fe-rich clay systems is ongoing, and will assess the role and reactivity of excess Fe(II), which after edge site saturation presumably comprises the weaker bound more reversibly exchangeable species relative to more strongly interacting edge bound Fe(II).

[1] Manceau, A.; Lanson, B.; Drits, V. A.; Chateigner, D.; Gates, W. P.; Wu, J.; Huo, D.; Stucki, J. W., Oxidation-reduction mechanism of iron in dioctahedral smectites: I. Crystal chemistry of oxidized reference nontronites. *American Mineralogist* **2000,** *85* (1), 133-152.

[2] Jaisi, D. P.; Liu, C. X.; Dong, H. L.; Blake, R. E.; Fein, J. B., Fe^{2+} sorption onto nontronite (NAu-2). *Geochimica et Cosmochimica Acta* **2008,** *72* (22), 5361-5371. DOI: 10.1016/j.gca.2008.08.022.

[3] Neumann, A.; Olson, T. L.; Scherer, M. M., Spectroscopic evidence for Fe(II)-Fe(III) electron transfer at clay mineral edge and basal sites. *Environmental Science & Technology* **2013,** *47* (13), 6969-6977. DOI: 10.1021/Es304744v.

[4] Neumann, A.; Wu, L.; Li, W.; Beard, B. L.; Johnson, C. M.; Rosso, K. M.; Frierdich, A. J.; Scherer, M. M., Atom exchange between aqueous Fe(II) and structural Fe in clay minerals. *Environmental Science & Technology* **2015**. DOI: 10.1021/es504984q.

[5] Schaefer, M. V.; Gorski, C. A.; Scherer, M. M., Spectroscopic evidence for interfacial Fe(II)-Fe(III) electron transfer in a clay mineral. *Environmental Science & Technology* **2011,** *45* (2), 540-545. DOI: 10.1021/Es102560m.

[6] Alexandrov, V.; Rosso, K. M., Insights into the mechanism of fe(II) adsorption and oxidation at Fe-clay mineral surfaces from first-principles calculations. *Journal of Physical Chemistry C* **2013,** *117* (44), 22880-22886. DOI: 10.1021/Jp4073125.

[7] Alexandrov, V.; Neumann, A.; Scherer, M. M.; Rosso, K. M., Electron exchange and conduction in nontronite from first-principles. *Journal of Physical Chemistry C* **2013,** *117* (5), 2032-2040. DOI: 10.1021/Jp3110776.

U REDOX STATE AND SPECIATION OF U COPRECIPITATED WITH MAGNETITE NANOPARTICLES: HIGH RESOLUTION XANES, EXAFS, XPS AND TEM STUDY

I. Pidchenko[1], D. Schild [1], T. Yokosawa [1], K. Kvashnina [2], N. Finck [1], T. Schäfer [1],
J. Rothe [1], H. Geckeis [1] and T. Vitova [1]

[1]*Institute for Nuclear Waste Disposal (INE), Karlsruhe Institute of Technology, PO 3640, 76021 Karlsruhe - Germany*
[2] *European Synchrotron Radiation Facility (ESRF), 6 Rue Jules Horowitz, BP 220, 38043 Grenoble Cedex - France*

Long-term storage of high-level radioactive waste is associated with potential radioecological hazards. One chemical element of high interest is uranium (U), which can mainly exists as a mobile U(VI) (oxidizing conditions) and sparingly soluble U(IV) (reducing conditions) species. It is expected that the main inorganic reducing agent for U(VI) in the environment are ferrous species in magnetite, formed on the steel canisters surface as an intermediate iron (Fe) corrosion product [1]. Results obtained from laboratory experiments for the interaction of U(VI) with magnetite nanoparticles point to partial reduction of U(VI) [2] or the formation of ~3 nm uranium dioxide (UO_2) particles on the surface layer [3]. The evidence for U(VI) reduction to intermediate U(V) state was found with no direct evidence of U(IV), which is in contradiction with thermodynamic calculations [4]. Continuous interaction and related phase dissolution/recrystallization processes can also lead to U redox changes and structural U incorporation into Fe oxides, resulting in U immobilization [5]. U redox state and speciation analyses are still very challenging due to simultaneous formation of several different species in such mineral systems. New advanced spectroscopic methods for characterization of such systems will provide more precise results from speciation studies. The main goal of our investigation is to assess the U M_4 edge high energy resolution X-ray absorption near edge structure (HR-XANES) spectroscopy technique for detection of U(V) possibly co-existing with U(IV) and U(VI) under reducing conditions on/in Fe containing minerals. The U M_4 edge HR-XANES has an advantage compared to the conventional U L_3 edge XANES, as the measured spectra are less dominated by core-hole lifetime broadening effects and therefore have narrower spectral features [6-8]. This technique facilitates the detection of minor contribution of one oxidation state in mixtures.

We have investigated the U redox states and speciation in a set of samples where U coprecipitated with magnetite nanoparticles (~ 20 nm) with U concentrations varying in the 1000-10000 ppm range (1000, 3000, 6000 and 10000 ppm). In addition to U M_4 edge HR-XANES, U L_3 edge extended X-ray absorption fine structure (EXAFS), X-ray photoelectron spectroscopy (XPS) and transmission electron microscopy (TEM) techniques have been applied. The studied system models the interaction of U(VI) with magnetite in aqueous solution, important for the understanding of the retarding effect of Fe corrosion products on U in the context of deep geological spent nuclear fuel disposal. These spectroscopic results can be compared with thermodynamic calculations and geochemical models describing this interaction.

After 10 days U interaction with magnetite U M_4 edge HR-XANES results indicate the formation of U(IV), U(V) and U(VI) mixtures in varying ratios, depending on the initial U loading. Going from 10000 to 3000 ppm, the U(VI) content decreases continuously and is no longer found in the 1000 ppm sample. At the same time the U(IV) and U(V) fractions increase. U(V) is stabilized as the main U redox state in the 1000 ppm sample along with a smaller U(IV) contribution. After 20 days of contact time XPS data show the predominance of U(IV) and U(V) species in the 6000 ppm sample. However, mostly U(V) and some U(IV) is found for the 1000 ppm sample. For all samples aged for 240 days U L_3 XANES and EXAFS strongly suggest the formation of a UO_2 phase, UO_2 is the dominating species in the 10000 ppm sample with U-O bond distance 2.33 Å as determined by EXAFS. UO_2 crystalline clusters with about 5 nm size formed on the surface of the magnetite nanoparticles are also found by TEM in the 10000 and 3000 ppm samples. The major and minor contributions of U(V) and U(IV), respectively, for the 1000 ppm sample after 240 days confirm the assumption that the U redox kinetics has completed within less than 10 days at this U concentration. EXAFS analyses reveal U(V)-Fe interaction in the second U coordination sphere, which substantially increases from the 10000 to 1000 ppm sample and is the dominating species in the 1000 ppm sample.

Our results confirm that U(V) can be long-term stabilized for (at least 240 days) adsorbed on or incorporated in magnetite nanoparticles. We propose a phase transformation mechanism coupled to short and long-term U redox kinetics during interaction of the U with magnetite nanoparticles [9].

[1] Jeon, B.H., Dempsey, B.A., Burgos, W.D., Barnett, M.O., Roden, E.E. (2005). "Chemical reduction of U(VI) by Fe(II) at the solid-water interface using natural and synthetic Fe(III) oxides." Environmental Science & Technology, 39(15): 5642-5649

[2] Missana, T., Garcia-Gutierrez, M., Fernndez, V. (2003). "Uranium(VI) sorption on colloidal magnetite under anoxic environment: Experimental study and surface complexation modelling." Geochimica et Cosmochimica Acta, 67(14): 2543-2550

[3] Scott, T.B., Allen, G.C., Heard, P.J., Randell, M.G. (2005). "Reduction of U(VI) to U(IV) on the surface of magnetite." Geochimica et Cosmochimica Acta, 69(24): 5639-5646

[4] Ilton, E.S. Boily, J.F., Buck, E.C., Skomurski, F.N., Rosso, K.M., Cahill, C.L., Bargar, J.R., Felmy, A.R. (2010). "Influence of Dynamical Conditions on the Reduction of U-VI at the Magnetite-Solution Interface." Environmental Science & Technology, 44(1): 170-176

[5] Huber, F. Schild, D., Vitova, T., Rothe, J., Kirsch, R. and Schäfer, T. (2012). "U(VI) removal kinetics in presence of synthetic magnetite nanoparticles." Geochimica et Cosmochimica Acta, 96: 154-173

[6] Vitova, T., Denecke, M.A., Göttlicher, J., Jorissen, K., Kas, J.J., Kvashnina, K., Prüßmann, T., Rehr, J.J., Rothe, J. (2013). "Actinide and lanthanide speciation with high-energy resolution X-ray techniques." Journal of Physics: Conference Series, 430 (1), art. no. 012117

[7] Kvashnina, K.O., Butorin, S.M., Martin, P., Glatzel, P. (2013). "Chemical State of Complex Uranium Oxides." Physical Review Letters, 111(25)

[8] Vitova, T. Green, J.C., Denning, R.G., Löble, M., Kvashnina, K., Kas J.J., Jorissen, K., Rehr, J.J., Malcherek, T., Denecke, M.A. (2015). "Polarization Dependent High Energy Resolution X-ray Absorption Study of Dicesium Uranyl Tetrachloride." Inorganic Chemistry, 54(1): 174-182

[9] Pidchenko, I., Schild, D., Yokosawa, T., Kvashnina, K., Finck, N., Schäfer, T., Rothe, J., Geckeis, H. and Vitova, T. (2015). In preparation.

RADIOLYTIC LEACHING OF PU-DOPED UO$_2$ PELLETS IN THE ENVIRONMENTS OF CLAYEY GROUNDWATER AND IRON CANISTER

M. Odorowski[1,2], C. Jégou[1], L. De Windt[2], V. Broudic[1], C. Martin[3]

[1]*CEA/DEN/DTCD/SECM/LMPA, 30207 Bagnols-sur-Cèze Cedex, France*
[2]*MINES ParisTech, Centre de Géosciences, Equipe Hydrodynamique et Réactions,*
35 rue St Honoré, 77305 Fontainebleau, France
[3]*Agence Nationale pour la gestion des Déchets Radioactifs, 1/7 rue Jean Monnet,*
92298 Chatenay-Malabry Cedex, France

The safety assessment of direct disposal of spent fuel in a nuclear waste repository requires understanding the chemical interactions between the fuel and its environment. In particular, the chemical reactions between the fuel and the pore water from the host rock, possibly intruding after the breakdown of the steel canister, have to be understood and the resulting radionuclide release has to be quantified. The French National Radioactive Waste Management Agency (Andra) has selected a Callovian-Oxfordian (COx) clay formation for repository. This reducing environment is interesting due to the low solubility of uranium and plutonium under such conditions. However, the alpha activity of spent fuel may locally disrupt the reducing conditions by inducing alpha radiolysis of the surrounding water, and thus producing oxidizing species like H_2O_2. These species may cause the oxidizing dissolution of the fuel matrix and the subsequent release of radionuclides in the environment.

Several leaching experiments of UO$_2$ pellets doped with alpha-emitters ($^{238/239}$Pu) were carried out in order to quantify the effect of environmental parameters (pore water chemistry, redox properties of the environment, presence of iron). These leaching experiments were realized with different kind of UO$_2$ pellets to reproduce the evolution of the alpha activity in a spent fuel sample (with a burnup of 47 GWd/T$_{iHM}$) from 50 to 10 000 years. The studied system was gradually made more complex. The first experiments were conducted in carbonated water [1]. Synthetic COx water representative of the repository pore water composition was then used. Finally, a coupon (foil) of metallic iron was introduced in the system to simulate steel canister corrosion. For each experiment, solution samples were taken over time and Eh and pH were monitored. The uranium in solution was assayed using a kinetic phosphorescence analyzer (KPA). Major cations were analyzed by ICP-AES and anions by ionic chromatography. At the end of the experiment, the pellets and the iron foils were characterized by SEM, EDX, and Raman spectroscopy in order to identify secondary phase precipitations.

The experimental results were compared to those obtained using the reactive transport model developed with the HYTEC code. The model takes into account the H_2O_2 production rate at the surface of the pellet, the UO$_2$ matrix dissolution rate as a function of the oxidizing species (H_2O_2 and O_2) concentrations, the generalized corrosion of a metallic iron foil (with H_2 generation), the complexation and redox aqueous reactions, the precipitation of secondary phases (carbonates, hydroxides and silicates) and species diffusion. The thermodynamic constants were selected from the ThermoChimie database [2] and kinetic constraints were added from the literature on the oxidative and anoxic dissolution of Fe(0) and UO$_2$. The H_2O_2 production kinetic constant versus α-activity was preliminarily estimated by ChemSimul calculations, considering the H_2O_2 alpha primary yield in pure water.

Experimental results showed a significant influence of the presence of iron on uranium concentration in the leaching solution, which was very low compared to simpler systems and close to UO$_2$ solubility limit. Surfaces analyses revealed the precipitation of calcium carbonates (aragonite, calcite, chukanovite) on the iron foil, as well as iron hydroxide (akaganeite) and silicates on the UO$_2$ pellets. These results are discussed and a dissolution mechanism of Pu-doped UO$_2$ pellets in clayey groundwater in the presence of metallic iron is proposed: the presence of iron inhibits the oxidizing dissolution by consuming H_2O_2 and precipitating Fe(III)-hydroxide at the extreme surface of UO$_2$. To assess the relevance of the proposed mechanism, reactive-transport simulations were performed using the HYTEC model developed. The calculated concentration of uranium was close to the UO$_2$ solubility limit and the model also correctly led to the precipitation of carbonates onto the iron coupon as well as of Fe(III)-hydroxides onto the UO$_2$ surface detected by the SEM. Modeling demonstrated that the coupling or competition between the rate of radiolytic H_2O_2 production at the pellet surface and the rate of Fe(II) diffusion towards the pellet, induced by iron corrosion, was a key factor controlling plutonium and uranium releases in the system.

[1] Muzeau, B. (2007). Mécanismes d'altération sous eau du combustible irradié de type UOX. PhD thesis, University of Paris XI, Orsay (France).

[2] Giffaut, E., Grive, M., Blanc, P., Vieillard, P., Colas, E., Gailhanou, H., Gaboreau, S., Marty, N., Made, B., Duro, L. (2014). "Andra thermodynamic database for performance assessment: ThermoChimie." Applied Geochemistry 49, 225-236.

GROUNDWATER FLOW AND TRANSPORT MODEL FOR THE PERFORMANCE ASSESSMENT OF THE AREA G LOW-LEVEL RADIOACTIVE WASTE DISPOSAL SITE AT LOS ALAMOS NATIONAL LABORATORY

P. Stauffer[1], R. Shuman[2], Z. Lu[1], T. Miller[1], D. Levitt[3], K. Birdsell[1], S. Chu[1], Z. Dai[1], B. Robinson[1], H. Viswanathan[1], and S. French[1]

[1]Los Alamos National Laboratory, P.O. Box 1663, Mail Stop T003,Los Alamos, NM 87545
[2]Avon, ME 04966[3]Neptune and Company, Inc., 1505 15th St. Los Alamos NM 87544

Los Alamos National Laboratory (LANL) generates radioactive waste as a result of various programmatic and research activities. Most is low-level radioactive waste that is disposed of at Technical Area 54, Area G. Waste disposal operations began at Area G in 1957 and have continued to the present. The majority of the waste is disposed of in large rectangular pits; disposal shafts are used for selected waste streams. In all, there are 35 disposal pits and 294 shafts at the 63-acre site. The U.S. Department of Energy Order (DOE) 435.1 requires that DOE field sites prepare and maintain site-specific radiological performance assessments and composite analyses (PA/CA) for low-level radioactive waste disposal facilities. This presentation describes modeling that supports the analysis of the groundwater pathway from the near-surface pits and shafts at Area G, through the unsaturated zone, into the regional aquifer beneath the site, and to potential downstream receptors.

Three-dimensional (3-D) groundwater flow and transport modeling is used to simulate the movement of radionuclides leached from the disposal units to exposure locations downgradient of Area G. Modeling is conducted using the process-level, multidimensional, finite-element porous flow and transport computer code FEHM. The 3-D site-scale model is used to trace the travel times of particles released from Area G and to generate conservative breakthrough curves. These breakthrough curves vary based on the source locations, the thicknesses of the geologic units present in the unsaturated zone, and the assumed infiltration rates through the disposal units. For the simulations, the disposal facility is divided into eight waste disposal regions to capture these spatial dependencies; each region represents an area where flow and contaminant transport behavior is different. Figure 1 shows the numerical grid at the surface along with the disposal pits and the eight waste disposal regions. In addition, 10 infiltration rates were considered for each of the 8 disposal regions. Infiltration rates are bounded through site data and Hydrus modeling. Figure 2 shows typical breakthrough curves for the site. The results of the 3-D simulations are further abstracted into probabilistic model runs with GoldSim, which calculates the potential doses associated with the full set of exposure pathways. This talk will describe 3-D flow and transport modeling, infiltration modeling, model abstraction, and ongoing uncertainty analyses including the effects of transient flow.
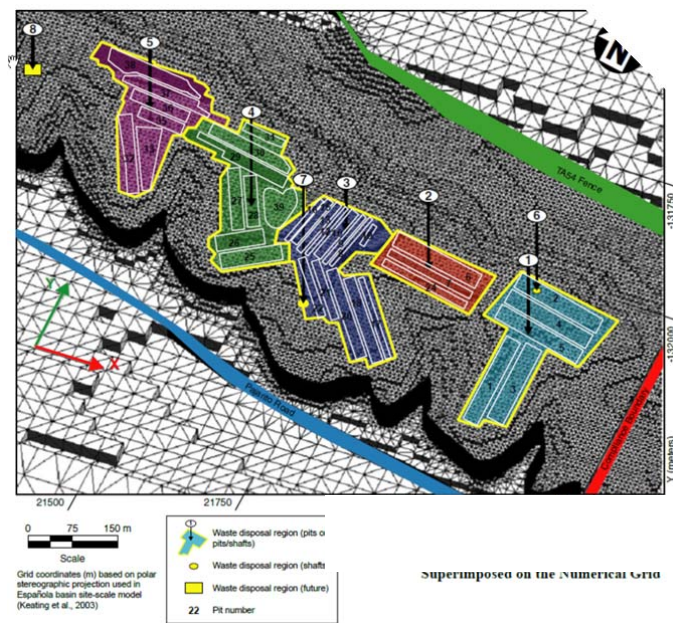

Figure 1. Waste Disposal Pits and Waste Disposal Regions Superimposed on the Numerical Grid
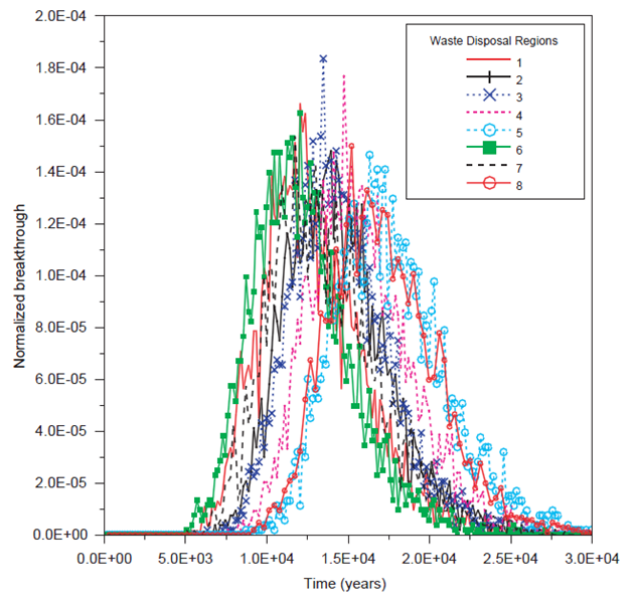
Figure 2. Example breakthrough Curves for Particles Released from All Waste Disposal Regions   (steady background infiltration rate of 0.5 mm/yr)

FEHM SIMULATIONS OF NON-STEADY FLOW AND TRANSPORT IN THE VADOSE ZONE OF THE SALIGNY SITE (ROMANIA)

Daniela Diaconu[(1)], Kay Birdsell[(2)], Crina Bucur[(1)], Alina Constantin[(1)], Cristina Dobrinoiu[(3)]

(1) Institute for Nuclear Research, Campului 1, Mioveni, 115400 - Romania,
(2) Los Alamos National Laboratory – USA
(3) University from Pitesti, Targului 1, Pitesti - Romania

Radioactive waste disposal, either near the surface or deep in a geological formation, is subject to public acceptability. Demonstration of site performance in ensuring long-term safety is a key element in getting public acceptance. Since modeling and numerical simulation are the tools available to predict long-term site performance, substantial effort has been dedicated to developing reliable computation models of water flow and radionuclide transport from the host site.

In the case of the Romanian site (Saligny site) selected for the proposed near surface disposal of operational LIL-SL and part of LL waste, particular attention was granted to the vadose zone, as the most important component of the multi-barrier system for limiting radionuclide release to the biosphere [1].

Water flow and contaminant transport modeling was performed using FEHM, HYDRUS 2D, ALLIANCE Platform, as part of collaborative projects with LANL-USA, SCK.CEN - Belgium, or CEA – France. Early on, the models built simulated steady-state flow and transport, and steady-state lateral flow. More recently non-steady flow using a time-variant flux derived from precipitation and evapotranspiration rates measured at the site has been modelled.

The simulation of non-steady flow and transport was run with FEHM_V2_20 [2] transferred to ICN under the Agreement on the Information Exchange and Collaboration for the Peaceful Use of Atomic Energy, signed with the U.S. Department of Energy in 1999, using site data validated on steady-state conditions.

The upper loess layer of the Saligny site is subject to large variations in moisture content [3]. The region has low precipitation and high evapotranspiration rates. During prolonged dry periods, which may last for 2 - 3 years, the near-surface, vadose-zone flux has an upward component. The model is intended to evaluate the possibility that H-3 and other radionuclides released from the repository could reach the surface and to define the conditions that would allow this process.

The non-steady model was also intended to validate the mass transport in the vadose zone of the Saligny site based on a tracer test launched at 0.5 m below the surface, in the upper loess layer. The tracer followed iodine migration, one of the important contributors to the annual individual dose.

FEHM predictions of transient flow were compared to the moisture content variations at three different depths near the surface (0.5 m, 1 m, 2 m and 3 m below the surface) and showed a very good ability of the code to properly solve not only the steady-state flow but also the non-steady flow for a large range of moisture contents (Figure 1) and especially at very low water flux values.

Time variation of the moisture content was measured by a special monitoring network designed and implemented in 2009 as part of the pre-operational monitoring program to record the hydrogeological characteristics as in-depth moisture content and matric potential variation in correlation with the meteorological parameters (precipitation rate, temperature, wind, humidity, etc). It consists in 5 pairs of sensors for water content and matric potential placed at 0.5m, 1 m, 2m and 3 m from the surface. Moisture measured by Time Domain Reflectrometry (TDR), matric potential measured by heat dissipation, together with meteo-station values for rain, wind, humidity, temperatures are hourly transmited by radio to the data acquisition module from the Meteorological Station in Bucharest.

Mass transport predictions were compared to iodine concentration profiles leading to calibration of dispersivity coefficients based on site-specific measurements.
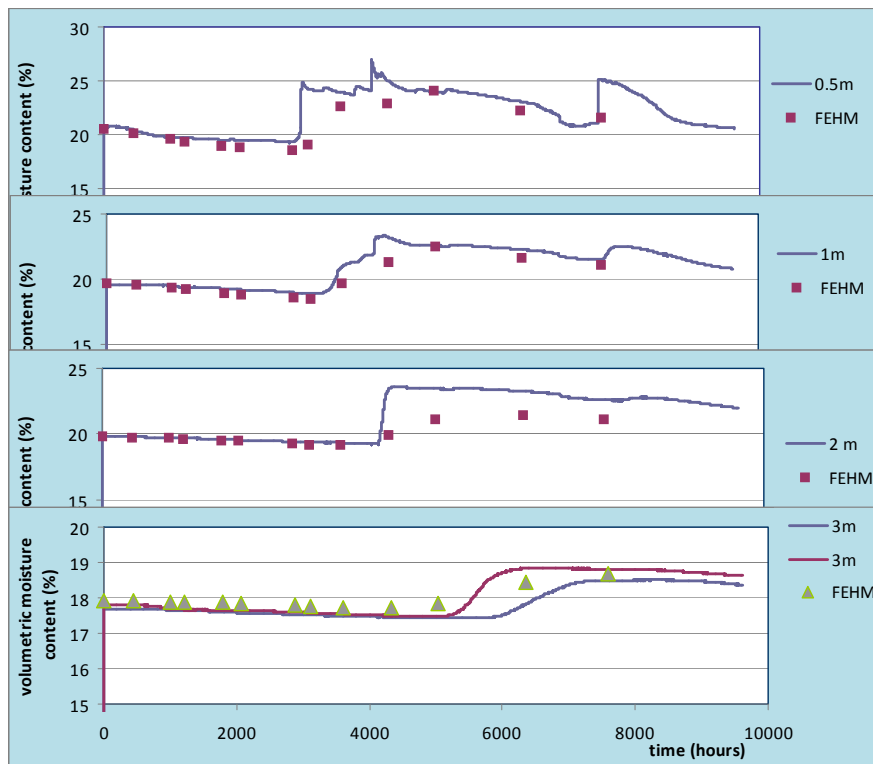
Figure 1. FEHM predictions of moisture content variations at four depths below the surface for non-steady flow

[1] D.Diaconu, K.H.Birdsell and G. Zyvoloski - Natural and Engineered Barriers in a Romanian Disposal Site for Low and Intermediate Level Waste", 9th ASME International Conference on Radioactive Waste Management and Environmental Remediation: Volumes 1, 2, and 3, Oxford, England, September 21–25, 2003, pp. 423-430

[2] Zyvoloski, G.A., Robinson B.A., Dash Z.V., and Trease - Methods for the FEHMN Application – A Finite-Element Heat- and Mass-Transfer Code", Los Alamos National Laboratory manuscript LA-13307_MS, 1997

[3] D.Diaconu, et al - Monitoring the Hydrogeological Characteristics of the Vadose Zone in the Saligny Site - Conference in Cryogenics and Isotopes Separations, Calimanesti–Caciulata, October 28-30, 2009

A NEW METHODOLOGY FOR UTILIZING MULTIDIMENSIONAL SMART K_d-MATRICES IN TRANSPORT PROGRAMS FOR LONG-TERM SAFETY ASSESSMENT

M. Stockmann[1)*], V. Brendler[1)], J. Schikora[1)], J. Flügge[2)], U. Noseck[2)]

[1)] *Helmholtz-Zentrum Dresden - Rossendorf, Institute of Resource Ecology, Dresden, Germany.*
[2)] *Gesellschaft für Anlagen- und Reaktorsicherheit (GRS) gGmbH, Braunschweig, Germany.*

Sorption on mineral surfaces is one important retardation process to be considered in long-term safety assessments for radioactive waste repositories. So far a conservative concept with temporally and spatially constant distribution coefficients (K_d-values) for each model unit is applied in the respective transport simulations.

In this work we describe a new methodology for integrating temporally and spatially variable distribution coefficients, so-called smart K_d-values, into the transport code r³t [1]. These smart K_d-values are pre-calculated with a bottom-up approach from mechanistic sorption models (namely surface complexation and ion exchange) and stored in a multidimensional matrix by coupling of three computer codes: PHREEQC [2], UCODE [3] and SimLab [4]. This strategy has numerous advantages over reactive transport codes: (1) One can calculate smart K_d-values for a reasonable number of environmental parameter combinations; (2) It is possible to perform uncertainty analysis based on such smart K_d-matrices; (3) In contrast to UCODE, SimLab also provides methods for global sensitivity analysis; (4) The overall methodology is much more efficient in computing time than a direct coupling of the geochemical speciation code with the transport code r^3t.

The capability of this new methodology is demonstrated for the sorption of repository-relevant radionuclides on a natural sandy aquifer [5] and is able to describe the sorption behavior in dependence of changing geochemical conditions quite well. Complex proof-of-concept scenarios were simulated for the sedimentary overburden of the Gorleben salt formation. Here, results for the upper aquifer are presented and discussed. As a prerequisite, the data processing of the field data [6, 7] is explained, including approximate correlations of environmental input parameters. Eventually, five environmental factors span the multidimensional parameter space for the K_d-matrices.

Smart K_d-distributions based on Latin-Hypercube samplings are given for different radionuclides covering the elements Am, Cs, Ni, Np[V], Ra, Se[VI], Th and U[VI]; with Am and Th also used as chemical analogues for Cm and Pu, respectively. They are then compared to constant values, determined in laboratory experiments [8], which have been used so far in transport calculations for long-term safety assessment. In a last step, ranked sensitivity indices are provided for all the investigated radionuclides to identify the most relevant environmental factors, which should be investigated in more detail in the future to improve both the data base and process understanding.

[1] E. Fein, GRS-Report 192, FKZ BMWi 02E9148/2 (2004).

[2] D.L. Parkhurst, C.A.J. Appelo, USGS Techniques and Methods, 6-A43 (2013).

[3] E.P. Poeter, et al., USGS Techniques and Methods 6-A11 (2005).

[4] A. Saltelli, et al., John Wiley and Sons, Chichester (2000).

[5] T. Brasser, et al., GRS-Report 248, BMBF-02C1144/54/64/74 (2008).

[6] H. Klinge, et al., Geol. Jb. C 71 (2007).

[7] W.-D. Grimm, BfS-Reports (1982-1994).

[8] D. Suter, et al., Proceedings DisTec 98, 581-584 (1998).

MODELING RADIONUCLIDE GAS TRANSPORT THROUGH EXPLOSION-GENERATED FRACTURE NETWORKS

A. Jordan[1], P. Stauffer[1], E. Rougier[2], E. Knight[2], D. Anderson[2]

[1] Computational Earth Sciences Group, Los Alamos National Laboratory, Los Alamos, NM 87545
[2] Solid Earth Geophysics Group, Los Alamos National Laboratory, Los Alamos, NM 87545

Underground nuclear explosions (UNEs) produce radionuclide gases which may be potentially detectable at the surface or in the atmosphere. A well-contained UNE does not immediately vent at the surface, but may produce late-time seepage on timescales of weeks to months of gases (such as Xe-133) that migrate under the influence of barometric pumping through explosion-enhanced fracture networks, while undergoing radioactive decay. Predicting the subsurface travel time, the (limited) window of opportunity for detection, and likely signal strength of signature radionuclide gases from UNEs is of considerable importance to monitoring for compliance with the Comprehensive Nuclear Test-Ban Treaty (CTBT), which provides stipulations for deploying equipment and personnel to help verify whether suspected UNEs by signatory countries are nuclear in nature.

Barometric pumping through explosion-fractured rock is investigated using a new sequentially-coupled hydrodynamic rock damage and gas flow and transport model (Figure 1). Fracture networks are produced for two different rock types (granite and saturated tuff) and three depths of burial (125, 250, and 390 m below ground surface) using a 2D radially symmetric hydrodynamic rock damage model. The fracture networks are integrated into a gas flow and transport numerical model and driven by several surface pressure signals of differing amplitude and seasonal variability. The complex effects of the subsurface fracturing regime on barometric pumping and gas transport are explored, including an explanation of the counter-intuitive result that some shallower explosions take longer and are less likely to seep than comparable deeper explosions.
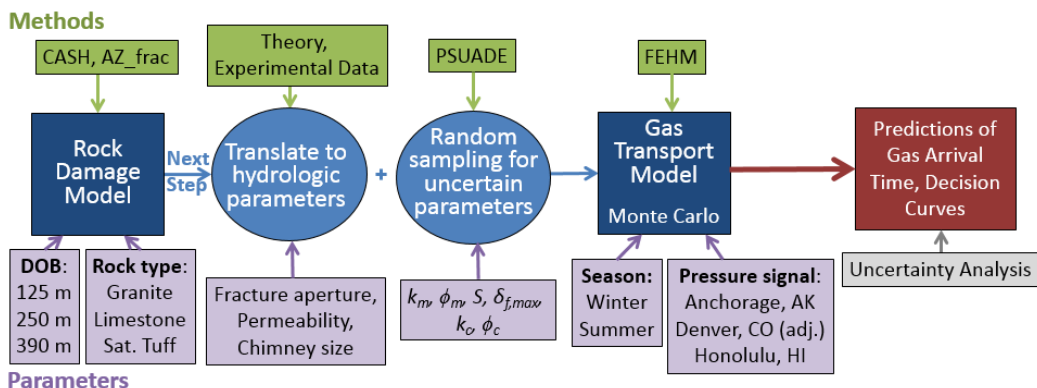
Figure 1. Overview of the integrated rock damage/gas transport model for predicting radionuclide gas seepage from underground nuclear explosions.

The mapping from rock damage to hydrologic parameters such as fracture and matrix permeability and porosity contains many uncertainties, especially in the case of an explosion at a site that is not geologically well-characterized. For this reason, we perform Monte Carlo simulations to explore the coupled effect of uncertainties on gas migration predictions of the following parameters: maximum fracture aperture, matrix permeability and porosity, saturation, and chimney porosity and permeability. Figure 2 shows Xe-133 concentration after 50 days of barometric pumping for one realization in the case of an UNE at 250 m depth of burial.
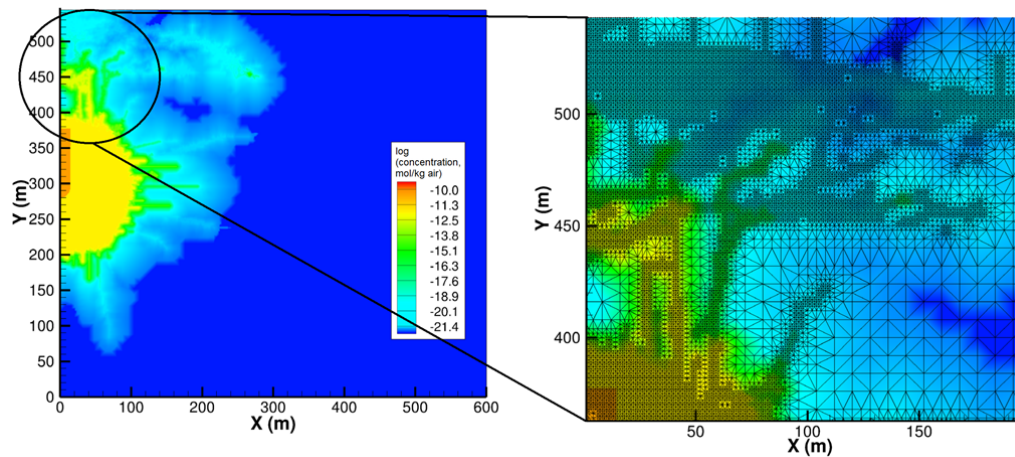
Figure 2. Xe-133 concentration 50 days after a 1 kt UNE in granite, for one realization.

The integrated fracture network approach provides a significant improvement in our capability of modeling gas seepage over simpler fracture models that have been used in the past ([1], [2], [3]). For gas seepage through rock damage produced by simulation of a 1 kt UNE in granite and saturated tuff, results of sensitivity analyses and Monte Carlo simulation across hydrogeologic parameter space show great differences as a result of the complex fracture network. Initial results suggest that modeling the fracture network accurately will be key to understanding the filtering of radionuclide gases through the subsurface to predict the delay in gas arrival at the surface, the window of opportunity for detection, and the distribution of gases spatially around the explosion cavity.

[1] Jordan, A. B., P. H. Stauffer, G. A. Zyvoloski, M. A. Person, J. K. MacCarthy, and D. N. Anderson (2014). "Uncertainty in Prediction of Radionuclide Gas Migration from Underground Nuclear Explosions." *Vadose Zone Journal*, *13*(10).

[2] Sun, Y., and C. R. Carrigan (2014). Modeling noble gas transport and detection for the Comprehensive Nuclear-Test-Ban Treaty. *Pure Appl. Geophys,* 171(3-5):735–750.

[3] Lowrey, J. D., S. R. Biegalski, A. G. Osborne, and M. R. Deinert (2013). Subsurface mass transport affects the radioxenon signatures that are used to identify clandestine nuclear tests. *Geophys. Res. Lett.* 40(1): 111-115.

OPTICAL IMAGING OF URANIUM SPECIES IN THE ENVIRONMENT; FROM FIRST PRINCIPLES TO APPLICATIONS

L.S. Natrajan[1)*], M.B. Andrews[1)], D.L. Jones[1)], M.A. Williams[1)], A.N. Swinburne[1)] J.R. Lloyd[2)], S. Shaw[2)], S.W. Botchway[3)], A.D. Ward[3)]

[1)]*Centre for Radiochemistry Research, School of Chemistry, The University of Manchester, Oxford Road, Manchester, M13 9PL, UK*
[2)]*School of Earth, Atmospheric and Environmental Sciences, The University of Manchester, Oxford Road, Manchester, M13 9PL, UK*
[3)]*The Science and Technology Facilities Council, Rutherford Appleton Laboratory, Harwell Oxford, Didcot, Oxfordshire, OX11 OQX, UK*

The world currently holds a substantial nuclear legacy arising from fission activities, with a large proportion of high activity wastes that pose a radiological threat to natural and engineered environments. The decision to dispose of these high level wastes (following separation) in a suitable geological disposal facility (GDF) has provided some of the most demanding technical, and environmental challenges facing the world in the coming century. In order to address these issues, we have begun a programme of work to establish a comprehensive understanding of the electronic properties and physical and chemical properties of the radioactive actinide metals using state of the art emission spectroscopic techniques[1,2] in order to probe actinide speciation at sub micron resolution over a given time period.

We will discuss the potential to use the inherent fluorescent properties of the uranyl cation to study redox speciation in uranium-containing environmental samples by one and two-photon confocal fluorescence and phosphorescence microscopy and lifetime image mapping. Previous studies carried out on crystalline samples have shown that uranyl species are capable of experiencing two-photon excitation. Here we study uranyl species in solution at room temperature and report fundamental properties such as quantum yield, two-photon excitation and emission spectra and two-photon cross sections. These capabilities are then applied to confocal fluorescence microscopy of uranyl in a range of bacterial and mineral samples, to study and map potentially useful process in (bio)remediation strategies including incorporation,[3] biosorption and the *in situ* enzymatic reduction of uranyl.[4]

[1] L.S. Natrajan, *Coord. Chem. Rev.*, 2012, **256**, 1583.

[2] L.S Natrajan, A.N Swinburne, M.B Andrews, S. Randall, S.L Heath, *Coord. Chem. Rev.*, 2014, **266–267**, 171.

[3] K.F. Smith, N.D. Bryan, A.N. Swinburne, P. Bots, S. Shaw, L.S. Natrajan, J.F.W. Mosselmans, F.R. Livens, K. Morris, *Geochimica et Cosmochimica Acta*, 2015, **148**, 343.

[4] D.L. Jones, M.B. Andrews, A.N. Swinburne, S.W. Botchway, A.D. Ward, J.R. Lloyd, L.S. Natrajan, *Chem. Sci.*, 2015, Advance Article, **DOI:** 10.1039/C5SC00661A.

SENSITIVE REDOX SPECIATION OF ELEMENTS RELEVANT TO NUCLEAR WASTE DISPOSAL BY CAPILLARY ELECTROPHORESIS HYPHENATED TO INDUCTIVELY COUPLED PLASMA SECTOR FIELD MASS SPECTROMETRY

C.-H. Graser [(1)], N. L. Banik [(1)], M. Lagos [(1)], C. M. Marquardt [(1)], R. Marsac [(1)], H. Geckeis [(1)]

[(1)] Institute for Nuclear Waste Disposal, Karlsruhe Institute of Technology, P.O. Box 3640,

76021 Karlsruhe, Germany

 The long-term safety assessment for nuclear waste repositories demands a detailed understanding of actinide (geo)chemistry. Advanced analytical tools are required to obtain experimental data as a basis for reliable chemical and thermodynamic models. The geochemical conditions especially the redox conditions in the vicinity of a nuclear repository control the chemical behavior of radionuclides. Measuring the oxidation state distribution of plutonium and other redox sensitive radionuclides in trace concentrations below the detection limit of most spectroscopic methods ($\sim 10^{-6}$ M) requires the development of analytical techniques. These techniques must be very sensitive because of the low solubility limits of the actinides, especially the tri- and tetravalent ones and analysis should have a minimal impact on the redox equilibrium in the original sample. Besides the long-lived radionuclides plutonium and neptunium, iron is investigated as a main component in natural systems controlling redox related geochemical processes. Iron has also a very sensitive redox chemistry and the solubility of trivalent species is also very low.

Capillary electrophoresis (CE) is a suitable separation method for actinide ions [1-2]. Therefore, CE hyphenated to an inductively coupled plasma sector field mass spectrometer (CE-ICP-SF-MS) was used to measure redox speciation of Pu (III) to (VI), Np (IV) and (V) and Fe (II) and (III) at concentrations lower than 10^{-7} M. CE coupling and separation parameters such as sample gas pressure, make-up flow rate, capillary position, and auxiliary gas flow, as well as the electrolyte system were optimized to obtain the maximum sensitivity. With optimized parameters we achieve a speciation limit of 10^{-12} M for Np and Pu. The oxidation state species of Pu and Np in different samples were separated in an acetate based electrolyte system (BGE). Figure 1 (left) shows a combined electropherogram of four different runs where each solution contains a single Pu redox state, initially dissolved in 1 M $HClO_4$ before mixing with the BGE. The peaks result from a $2.5 \cdot 10^{-11}$ M Pu(III), a $5.0 \cdot 10^{-11}$ M Pu(VI) and a $5.0 \cdot 10^{-11}$ M Pu(V) standard solution, respectively. The last peak represents Pu(IV) and is characterized by a tailing at t > 600 s. The tailing is due to the formation of Pu(IV) polymeric species or partial sorption of Pu species to the capillary wall. The Pu(IV) concentration is $8.0 \cdot 10^{-11}$ M. Figure 1 (right) shows a combined electropherogram of two neptunium standard solutions. The first and the second peaks correspond to $1.0 \cdot 10^{-9}$ M Np(V) and Np(IV) solutions, respectively.
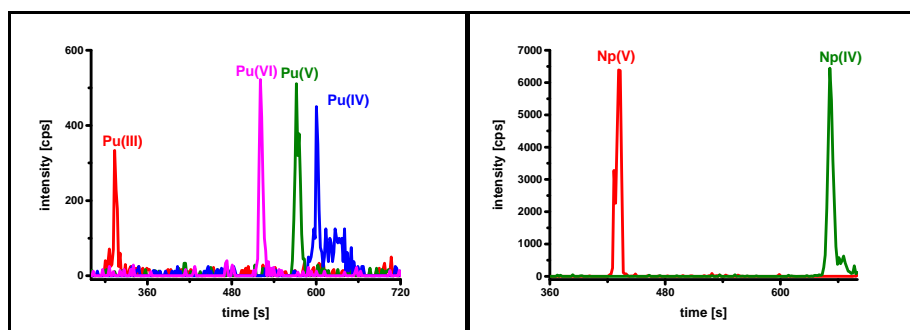
Figure 2: Electropherogram of plutonium (left) and neptunium (right) in BGE;

$[Pu]_{tot} = 10^{-10}$ M, $[Np]_{tot} = 10^{-9}$ M

The separation of Fe(II) and Fe(III) was investigated using different organic complexing ligands like EDTA and o-phenanthroline. For the Fe redox system a limit of detection of 10^{-9} M was calculated. The experimental electrophoretic mobilities of Pu (III) to (VI), Np (IV) and (V) and Fe (II) and (III) were calculated as a key parameter for sample characterization. Hence, unknown sample solutions could be characterized in concentration ranges where UV-Vis/NIR and liquid-liquid extraction techniques combined with radiometric methods were not applicable.

In two different experiments, we demonstrate the suitability of CE-ICP-SF-MS to measure the redox speciation in various solutions. In a first experiment the behavior of Pu(VI) in a Fe(II) containing solution was

monitored over 100 minutes. In another experiment, the redox speciation of neptunium in solution in contact with illite, an important clay mineral regarding safety analysis of a nuclear repository in claystone as host rock, was examined.

The presented work clearly shows that CE-ICP-SF-MS is a suitable separation method for the oxidation states of plutonium, neptunium and iron present in various solutions. The studies with CE-ICP-SF-MS will be extended to other redox sensitive elements with the aim of establishing a robust experimental approach to determine and quantify redox speciation at trace level concentrations.

[1] C. Ambard, A. Delorme, N. Baglan, J. Aupiais, F. Pointurier, C. Madic, Interfacing capillary electrophoresis with inductively coupled plasma mass spectrometry for redox speciation of plutonium. *Radiochim Acta* 2005, *93*. 665-673.

[2] B. Kuczewski, C. M. Marquardt, A. Seibert, H. Geckeis, J. V. Kratz, N. Trautmann, Separation of plutonium and neptunium species by capillary electrophoresis-inductively coupled plasma-mass spectrometry and application to natural groundwater samples. *Anal Chem* 2003, *75*. 6769-6774, DOI: 10.1021/Ac0347213.

DEVELOPMENT OF ANALYTICAL TECHNIQUES FOR THE IDENTIFICATION OF ORGANIC SPECIES OF CARBON-14 RELEASED DURING ANOXIC CORROSION OF ACTIVATED STEEL IN A CEMENTITIOUS REPOSITORY FOR RADIOACTIVE WASTE

B. Z. Cvetković[1)], E. Wieland[1)], D. Kunz[1)], G. Salazar[2)], S. Szidat[2)],

[1)] *Paul Scherrer Institut, Laboratory for Waste Management, 5232 Villigen PSI, Switzerland*
[2)] *University of Bern, Department of Chemistry and Biochemistry & Oeschger Centre for Climate Change Research, 3012 Bern, Switzerland*

Carbon-14 is one of the main contributors to the annual dose released from a cement-based repository for low- and intermediate-level radioactive waste (L/ILW) in Switzerland [1]. In current performance assessment it is assumed that ^{14}C mainly contributes to the dose in its organic form, e.g. as ^{14}C-bearing organic compounds, which are only weakly retarded in the cementitious near field [1]. Compilations of the activity inventories reveal that the ^{14}C-inventory in L/ILW in Switzerland is mainly associated with activated steel (~85 %). In nuclear power plants ^{14}C is produced by the activation of nitrogen impurities in stainless steel exposed to thermal neutron fluxes (e.g. in nuclear reactors) according to the reaction $^{14}N(n,p)^{14}C$ [2]. While the ^{14}C-inventory is well known, the chemical speciation of ^{14}C in the cementitious near field upon release from activated steel is only poorly understood.

Identification and quantification of the ^{14}C-bearing organic compounds formed during the anoxic corrosion of activated steel is a difficult task. The analytics is very challenging because of the low ^{14}C-inventory of activated steel and additionally because of the low corrosion rate of stainless steel in alkaline solution (few nm/year) [3]. Therefore, identification and quantification of the ^{14}C-bearing compounds released requires an extremely sensitive analytical method. One of the few potential analytical techniques to solve this problem is compound-specific ^{14}C-accelerator mass spectrometry (AMS).

As a first step towards the development of such an AMS-based analytical technique batch-type corrosion experiments with non-activated, carbon-containing iron powders were carried out under anoxic alkaline conditions relevant to a cement-based repository. The aim of these experiments was to identify potentially ^{14}C-bearing compounds. Dissolved and volatile organic compounds were detected in the supernatant solution using high-performance ion exclusion chromatography (HPIEC) coupled to conductivity detection (CD) and mass spectrometry (MS) as well as headspace gas chromatography (GC) coupled to MS. Dissolved organic carbon species were identified to be carboxylic acids, with a maximum of four carbon atoms. To be able to identify these compounds as ^{14}C-species produced during the corrosion of activated steel, the chromatographic separation has to be coupled to the ^{14}C-sensitive AMS. Tests with ^{14}C-labelled carboxylic acids were performed with the aim of demonstrating the feasibility of the analytical method and to establish the link between chromatographic separation and ^{14}C-detection by AMS. Results obtained in the course of the development of the method will be presented along with results from the corrosion experiments using non-activated iron powders. Additionally the conceptual approach for future corrosion studies with activated steel, including also the analysis of volatile corrosion products, will be outlined.

[1] NAGRA Technical Report NTB 08-05 (2008).

[2] J.F. Berg, J.E. Fonnesbeck, Anal. Chim. Acta 447 (2001).

[3] N. R. Smart, D. J. Blackwood, L. Werme, Corrosion 58, 8 (2002).

COMPLEX FORMATION OF TETRAVALENT ACTINIDES WITH SMALL CARBOXYLATE LIGANDS

C. Hennig[1], A. Iheda-Ohno[1], S. Takao[2], K. Takao[3], W. Kraus[4], A. C. Scheinost[1]

[1]*Helmholtz-Zentrum Dresden-Rossendorf, Institute of Resource Ecology, Bautzner Landstrasse 400, D- 01314 Dresden, Germany*
[2]*Innovation Research Center for Fuel Cells, The University of Electro-Communications Chofu, Tokyo 182-8585, Japan*
[3]*Research Laboratory for Nuclear Reactors, Tokyo Institute of Technology 2-12-1-N1-32, O-okayama, Meguro-ku,152-8550 Tokyo, Japan*
[4]*BAM Federal Institute for Materials Research and Testing, Richard-Willstätter-Strasse 11, D-12489 Berlin, Germany*

Tetravalent actinides form strong complexes with the carboxylic acids. Although there is a number of thermodynamic data reported [1-2] there is no information available on the complex structure in aqueous solution.

We used EXAFS spectroscopy to estimate the complex structure of Th^{4+}, U^{4+}, Np^{4+} and Ce^{4+} with different carboxylates ($RCOO^-$; R = H, CH_3, $C_2H_2NH_2$) in aqueous solution [3-6]. The structural information from EXAFS data is limited to radial pair distribution functions. To overcome this limitation we forced single crystals to precipitate in different stability ranges of the solution species. Whether or not a species is preserved in a crystal structure was subsequently investigated by EXAFS spectroscopy. The crystal structure, revealed by single-crystal diffraction, and combined with EXAFS spectroscopy on liquid and solid samples, provides precise information of coordination and structure of the related solution species. These studies show that in all of the investigated aqueous systems hexanuclear complexes $[M_6O_4(OH)_4(RCOO)_{12}]$ appear, which become predominant with increasing ligand concentration as well as increasing pH, and dominate finally the species distribution.

An example is shown in Figure 1. EXAFS spectra were recorded on samples in aqueous solution with 0.05 M Th(IV), 1 M glycine and pH values ranging from 0.5 to 3.2. The spectrum at pH 0.5 shows a single peak representing mononuclear complexes of $Th(OH)_n^{(4-n)+}$ with n ≤ 2. With increasing pH, the first peak in the Fourier transform becomes more asymmetric and finally splits. A second peak appears at R+Δ = 3.75 Å, and its intensity rises with increasing pH. This latter feature represents a Th-Th scattering interaction. The data fit indicate the appearance of a hexanuclear complex. This complex is stable until pH 3.2. At higher pH values precipitates a crystalline material. The EXAFS spectrum of this precipitate is identical with that of the solution at pH 3.2, indicating that the structure of the solution species remains preserved in the crystal structure. Crystals from the precipitate were used for structure analysis by X-ray diffraction. A drawing of the crystal structure is shown in Figure 2, which is in turn representative for the coordination of the predominating solution species at pH 3.2.

The appearance of hexanuclear complexes in aqueous solution corresponds with both, the onset of the metal hydrolysis at the one hand, and the deprotonation of the carboxylic function at the other hand. This results in a competing reaction between hydrolysis and ligation. The hydrolysis results in a polymerization via oxo and hydroxo bonds, whereas the carboxylic function of the ligand results in the formation of 12 terminating chelate rings providing charge neutrality of the hexanuclear core and preventing further polymerization. Most of the thermodynamic data of actinide(IV) carboxylates are estimated assuming mononuclear solution species. Our studies indicate that future work on tetravalent actinide carboxylates in aqueous solution need consideration of hexanuclear species.

[1] G.M. Sergeev, Radiokhimija 22, 536 (1980).
[2] A. Bismondo, L. Rizzo, G. Tomat, Inorg. Chim. Acta 74, 21 (1983).
[3] S. Takao, K. Takao, W. Kraus, F. Emmerling, A.C. Scheinost, G. Bernhard, C. Hennig, Eur. J. Inorg. Chem. 4771 (2009).
[4] K. Takao, S. Takao, A.C. Scheinost, G. Bernhard, C. Hennig, Inorg. Chem. 51, 1336 (2012).
[5] C. Hennig, S. Takao, K. Takao, S. Weiss, W. Kraus, F. Emmerling, A.C. Scheinost, Dalton Trans. 41, 12818 (2012).
[6] C. Hennig, A. Ikeda-Ohno, W. Kraus, S. Weiss, P. Pattison, H. Emerich, P.M. Abdala, A.C. Scheinost, Inorg. Chem. 52, 11734 (2013).
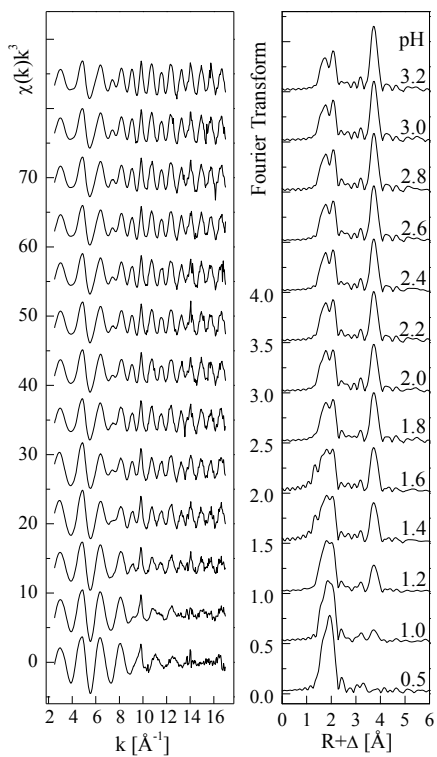
Figure 1: Th *L₃*-edge *k³*-weighted EXAFS data (left) and the corresponding Fourier Transforms (right) of a sample series with 0.05 M Th(IV), 1 M glycine, pH range of 0.5-3.2.
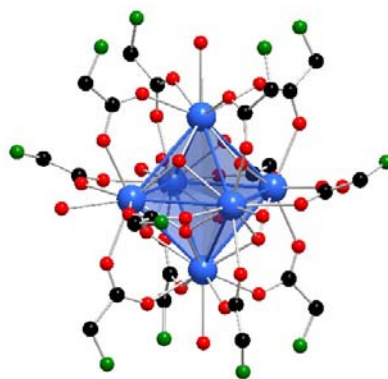

Figure 2: The $[Th_6(\mu_3\text{-}O)_4(\mu_3\text{-}OH)_4(H_2O)_6(Gly)_6(HGly)_6]^{6+}$ unit. Th – blue, O – red, C – black, N – green.

PROPERTIES OF SELECTED TC(I) CARBONYL SPECIES RELEVANT TO HANFORD TANK WASTE

T.G. Levitskaia, B. M. Rapko, S. Chatterjee, J.M. Peterson, J. Romero, A. Andresen, N. Washton, E. Walter

Pacific Northwest National Laboratory

The long half-life, complex chemical behavior in tank waste, limited incorporation in mid- to high temperature immobilization processes, and high mobility in subsurface environments make technetium-99 (Tc) one of the most difficult contaminants to dispose of and/or remediate. Technetium exists predominantly in the liquid tank waste phase as pertechnetate, TcO_4^- (oxidation state +7). However, based on experimentation to-date, a significant fraction of the soluble Tc in tank waste may be present as a non-TcO_4^- species that has not been identified and, based on experimentation to date, cannot be effectively separated from the wastes. It remains uncertain whether alkaline tank conditions even support the formation of proposed low-valent Tc species, i.e., Tc(I) carbonyl compounds [1]. There is no definitive information on the origin of the non-TcO_4^- species, nor is there a comprehensive description of their composition and behavior. The objective of this work is to investigate aspects of the nature and chemistry of the non-TcO_4^- species derived from the $Tc(CO)_3^+$ coordination center, specifically under the conditions typical for the alkaline liquid fraction of the tank waste and to gain better understanding and control over their redox behavior.

Oxidative stability and hydrolytic speciation of $[Tc(CO)_3(H_2O)_3]^+$ in a pseudo-Hanford tank supernatant simulant solution at variable nitrate and hydroxide concentrations was investigated. The method used for these studies was primarily ^{99}Tc NMR spectroscopy. The pH speciation of the $[Tc(CO)_3]^+$ aqua complexes was found to be similar in water and in 5 M $NaNO_3$. The triaqua $[Tc(CO)_3(H_2O)_3]^+$ ion exists only in acidic aqueous solutions and undergoes extensive hydrolysis starting at near-neutral pH. Consistent with literature reports [2,3] the mono-hydrolyzed $[Tc(CO)_3(OH)(H_2O)_2]$ species was observed to undergo oligomerization readily and form the neutral, tetrameric $[Tc(CO)_3(OH)]_4$ species. Theoretical COSMO calculations resulted in excellent agreement of the predicted and experimental ^{99}Tc NMR chemical shifts of these Tc(I) $[Tc(CO)_3]^+$ aqua complexes. The $[Tc(CO)_3]^+$/gluconate complex is formed in alkaline solutions containing no to high concentrations of nitrate. The theoretical calculations revealed that this complex is unlikely to have chemical composition of $[Tc(CO)_3(gluconate)]^{2-}$; formation of a mixed hydroxo/gluconate $[Tc(CO)_3(OH)_n(gluconate)]^{n-2}$ species is feasible but is by no means the only alternative. This conclusion is supported by the appearance of two resonances in the NMR spectrum suggesting the existence of two non-equivalent Tc(I) centers. The positions of these resonances are shifted up-field from the calculated position of the single resonance predicted by the theory due to the shielding effect of OH^- ligand. Additional studies to elucidate the structure of the $[Tc(CO)_3]^+$/gluconate complex are currently under way.

It was demonstrated that in the solutions with the high hydroxide concentrations, the $[Tc(CO)_3]^+$ species undergo fast oxidative decomposition most likely due to the hydrolytic destruction of the Tc-CO backbone via OH^- nucleophilic attack at the carbonyl carbon. Presence of the high salt and relatively low OH^- concentrations in LAW (typical for the majority of tanks) increases the stability of non-pertechnetate species. Increasing hydroxide concentration promotes decomposition of the $[Tc(CO)_3]^+$ species. Interestingly, the oxidative stability of the hydrolyzed $[Tc(CO)_3(OH)(H_2O)_2]$ species in the supernatant simulants containing 0.42, 0.83, or 1.47 M OH^- was greater than that in the 5 M $NaNO_3$ solutions containing corresponding NaOH concentrations. In this study, under optimum conditions (0 – 0.01 M NaOH and 5 M sodium nitrate), several months have gone by either without any detectable pertechnetate formation or only small conversion to pertechnetate, a half-life for reoxidation under conditions compatible with those found in actual Hanford tank sludge. This observation implies that if the conditions required for formation of the Tc(I)-tricarbonyl compounds exist in the tank, the organic complexants are not required for the product to be stable in conditions associated with Hanford tank supernatants. Alternatively, instead of Tc(I)-tricarbonyl/complexant species being required, the Tc(I)-tricarbonyl hydrolysis products of general composition $[Tc(CO)_3(OH)_n(H_2O)_m]^{1-n}$ that are anticipated to exist in the alkaline waste may be sufficient.

These results indicate that a carbonyl complex is a viable candidate for the source of non-pertechnetate in tank waste. As indicated, testing has identified a range of conditions under which a significant portion of the carbonyl complex is stable for extended periods of time. Preliminary studies have shown a viable route for the formation of this complex under tank waste conditions.

[1] W. W. Lukens, D. K. Shuh, N. C. Schroeder, K. R. Ashley. Env. Sci. Tech. 38, 229 (2004).

[2] N. I. Gorshkov, A. A. Lumpov, A. E. Miroslavov, D. N. Suglobov. Radiochemistry, 45, 116 (2000).

[3] R. Alberto, R. Schibli, A. Egli, U. Abram, S. Abram, T. A. Kaden, P. A. Schubiger. Polyhedron 17, 1133 (1998).

THERMODYNAMIC DESCRIPTION OF An(III/IV) INTERACTION WITH GLUCONATE IN NaCl AND CaCl₂ SYSTEMS

X. Gaona[1], H. Rojo[1,2], T. Rabung[1], M. García-Gutiérrez[3], T. Missana[3], M. Altmaier[1]

[1] *Karlsruhe Institute of Technology, Institute for Nuclear Waste Disposal, Germany*
[2] *Laboratory for Waste Management, Paul Scherrer Institut, Villigen PSI, Switzerland*
[3] *CIEMAT, Research Centre for Energy, Environment and Technology, Madrid, Spain*

Radionuclide solubility and sorption in cementitious and saline systems can be affected by the presence of organic ligands. Gluconic acid ($C_6H_{12}O_7$, HGH_5) is a poly–hydroxocarboxylic acid expected in repositories for low and intermediate–level radioactive waste (L/ILW) as component of cementitious materials. Gluconic acid is also considered as close analogue of iso-saccharinic acid (ISA), a poly–hydroxycarboxylic ligand resulting from the degradation of cellulose at alkaline conditions. The formation of very stable An(III)–gluconate and An(IV)–gluconate complexes has been reported in the literature. In the case of An(IV), the stability of these complexes can be further increased in the presence of Ca^{2+} due to the formation of ternary Ca–An(IV)–gluconate complexes. On the contrary, no such ternary species have been described so far for An(III). All previous studies available in the literature have focussed on low ionic strengths and low Ca^{2+} concentrations. In CaCl₂–rich brines, which can be generated by the corrosion of cementitious waste forms in certain saline systems, the stabilization of binary Ca–gluconate complexes may decrease the availability of free gluconate in solution and thus outcompete the formation of complexes with An. The development of complete and correct chemical, thermodynamic and activity models for the ternary systems Ca–An(III)–gluconate and Ca–An(IV)–gluconate is thus required to properly assess the impact of this ligand on the mobilization of An(III) and An(IV) under repository-relevant conditions.

Undersaturation solubility studies with $Nd(OH)_3(am)$ were conducted in dilute NaCl (0.1 M) and CaCl₂ (0.1 and 0.25 M) solutions. Parallel experimental series were prepared at constant pH_c 12 and $10^{-6} \leq [GH_5^-] \leq 10^{-2}$ M, and also at $[GH_5^-] =$ constant $= 10^{-3}$ M and $9 \leq pH_c \leq 13$. The concentration of Nd in the aqueous solution was quantified by ICP–MS after 10 kD ultrafiltration, whereas $[GH_5^-]_{tot}$ in solution was measured as total organic carbon (TOC). Solid phases before and after solubility experiments were characterized by XRD.

TRLFS measurements were performed with $1×10^{-7}$ M Cm(III) per sample in NaCl (0.1 M) and CaCl₂ (0.1 and 0.25 M) solutions. In the NaCl systems, three different concentration levels of Ca^{2+} were fixed at 0, $1×10^{-3}$ M and $1×10^{-2}$ M. The initial concentration of gluconate in all samples ($1×10^{-6}$ M) was increased to $3×10^{-3}$ M by step–wise additions of NaGH₅–NaCl or Ca(GH₅)₂–CaCl₂ solutions.

Np(IV) was obtained by chemical reduction of a Np(V) stock solution with $Na_2S_2O_4$ 0.05 M at pH = 8, and quantitatively precipitated at $pH_m = 12$ as $NpO_2(am,hyd)$. The resulting solid phase was divided in different samples (~2 mg ^{237}Np per batch experiment) with 0.1–3.5 M CaCl₂ as background electrolyte, with $10^{-6} \leq [GH_5^-]_{tot} \leq 10^{-2}$ M and $9 \leq pH_m \leq 12$. All samples were prepared and stored at 22±2°C in Ar gloveboxes under exclusion of oxygen and CO₂.

The solubility of $Nd(OH)_3(am)$ remains unaffected by gluconate in 0.1 M NaCl solutions. XRD and TOC analyses confirm that no secondary (crystalline) solid phases are forming and that all gluconate remains in solution under these conditions. On the other hand, the solubility of $Nd(OH)_3(am)$ in 0.1 and 0.25 M CaCl₂ solutions is clearly increased by gluconate under hyperalkaline conditions. The species forming are pH–dependent and in all cases involve the coordination of Ca^{2+}. Slope analysis of $Nd(OH)_3(am)$ solubility under increasing gluconate concentration (log [Nd] *vs.* log $[GH_5^-]_{tot}$) likely indicates the formation of a Nd–gluconate complex with stoichiometry 1:2. At $[GH_5^-]_{tot} \geq 10^{-3}$ M, no further increase of the Nd(III) concentration is observed, resulting in an upper solubility limit at [Nd] $10^{-6.5}$ M which suggests the formation of a new Ca–Nd(III)–gluconate solubility limiting solid phase. Consistently with Nd(III) solubility data, TRLFS confirms the key role of Ca^{2+} in the complexation of gluconate with Cm(III). Hence, at least three Ca–Cm(III)–gluconate species are identified by TRLFS in Ca-bearing solutions, pointing to a very

complex chemistry and speciation for this system. Weaker Cm(III)–gluconate complexes are observed by TRLFS in the absence of Ca.

The presence of gluconate induces a significant increase on NpO_2(am,hyd) solubility in $CaCl_2$ solutions. This increase is stronger at higher concentrations of Ca^{2+}, thus suggesting the formation of ternary complexes analogous to those described in the literature for Th(IV) ($CaAn^{IV}(OH)_4(GH_5)_2$(aq)). Independent of [$CaCl_2$], the system reaches a saturation level at [Np] $10^{-5.5}$ M. This observation can be explained by the formation of a new Ca–Np(IV)–gluconate solid phase, although this hypothesis remains to be further confirmed by appropriate solid phase characterization (XRD, SEM–EDS) currently under way.

These results indicate that gluconate has a clear but limited impact on the solubility of An(III) and An(IV) under repository-relevant conditions. In both cases, the possible formation of a ternary Ca–An–gluconate solid phase could be considered as a potential mechanism for the retention of actinides at elevated gluconate concentrations.

ACTINIDE BORATES: FROM THORIUM TO CALIFORNIUM AND EVERYTHING IN BETWEEN

Thomas E. Albrecht-Schmitt

Department of Chemistry and Biochemistry, Florida State University, Tallahassee, Florida USA

Borate has been shown to be the primary complexant for trivalent actinides in brines such as those found in WIPP.[1] It was initially proposed that these borate complexes remain in solution. However, subsequent studies have shown that precipitates can form, and that these solids are highly complex.[2,3] The aging of these amorphous solids may lead to crystalline materials for which my group has provided a variety of models via the synthesis of actinide borates in boric acid fluxes. The focus of this talk is on elucidating changes that occur between plutonium and americium, which are the trivalent actinides of primary concern in WIPP. The talk will also highlight the comparative chemistry of Pu^{3+}, Am^{3+}, Cm^{3+}, Bk^{3+}, and Cf^{3+}, and will be used to demonstrate that californium is the second transitional element in the actinide series. While much of the data presented on this talk was obtained by measurements of compounds in the solid state, efforts will be made to place this work in the context of aforementioned solution complexation and precipitation studies.

1. M. Borkowski, M. Richmann, D. T. Reed, Y. Xiong, *Radiochim. Acta* **2010**, *98*, 577-582.
2. J. Schott, J. Kretzschmar, S. Tsushima, B. Drobot, M. Acker, A. Barkleit, S. Taut, V. Brendler, T. Stumpf, *Dalton Trans.*, **2015**, *44*, 11095-11108.
3. J. Schott, J. Kretzschmar, M. Acker, S. Eidner, M. U. Kumke, B. Drobot, A. Barkleit, S. Taut, V. Brendler, T. Stumpf, *Dalton Trans.*, **2014**, *43*, 11516-11528.

AGGREGATION AND SOLUBILITY OF CLUSTERS OF ACTINIDES

P.C. BURNS[1,2]

[1] *Department of Civil and Environmental Engineering and Earth Sciences, University of Notre Dame, Notre Dame, Indiana, USA*
[2] *Department of Chemistry and Biochemistry, University of Notre Dame, Notre Dame, Indiana, USA*

Over the past decade we have developed an extensive family of nano-scale uranyl peroxide clusters, most of which are cages with inner and outer surfaces truncated by the oxygen atoms of uranyl ions. These clusters, which contain from 16 to 124 uranyl ions, all contain peroxide bridges between uranyl ions, as well as a wide variety of other bridges that include hydroxyl, nitrate, phosphate, oxalate, transition metal polyhedra, pyrophosphate, and phosphite. Each of these clusters have been crystallized and their structures were provided by X-ray diffraction, as well as neutron diffraction in selected cases. Combinations of light and X-ray scattering techniques, as well as electrospray ionization mass spectrometry, have been used to study their behaviour in solution. These studies have shown that many of these clusters are highly soluble in water, that they persist for many months in solution, and that they withstand large doses of gamma irradiation. As such, these clusters are a unique family of actinide-based nanomaterials that serve as models for behaviour in water.

We have extensively studied the behaviour of two clusters, U60 and U24P, in aqueous solution. U60 is a cage with a fullerene topology and sixty identical uranyl polyhedra arranged to form a fullerene topology identical to C60. U24P contains four-membered rings of uranyl polyhedra that are bridged into a cage cluster by 12 pyrophosphate groups. Both clusters can be produced in high purity and good yields, providing ample material for further study. The solubility of crystals of each have been measured in water, and are found to result in uranium concentrations in solution that are several orders of magnitude higher than would form where water contacts uranyl minerals of similar composition, but lacking the nanoscale structure. These results indicate that U60 and U24P behave as soluble species in water, but their size/charge ratios are dramatically different than simple species in solution. At their highest concentrations in solution, the clusters are separated by as little as three nanometers, and their spacings appear to be sufficient only to accommodate the electrical double layers about the clusters. However, the solubility limits are found to be strongly dependent on the nature of the associated counterions.

Whereas the uranyl peroxide cage clusters are essentially homogeneously distributed in solution upon dissolution, addition of various salts triggers their rapid aggregation into blackberry structures that have dimensions in the range of tens of nanometers. Once formed, these aggregates tend to be stable, and changing the counter cations present can modify their size. Direct imaging of these using cryogenic TEM has demonstrated that the blackberries are usually hollow and spherical, with some size polydispersity. Their assembly is rapid, as time-resolved TEM studies indicate the process requires only tens of minutes.

Molecular dynamics simulations were used to study the dissolution behaviour of U60 clusters in the presence of Li and K, the counterions that are used in their synthesis and that serve to balance the -60 charge of the cage. The simulations demonstrate that the distribution of counterions change dramatically as the concentration of U60 is increased, in large part because many cations move through the windows of the cage to assume positions within, thereby lowering the overall charge of the cluster.

In summary, using uranyl peroxide cage clusters as models, we are developing an understanding of the behavior of nanoscale actinide materials in aqueous solutions, including their dissolution and aggregation behavior, and the role of ionic strength and different counterions on impacting that behavior.

FORMATION OF PLUTONIUM HYDROXIDE COLLOIDS UNDER REDUCING CONDITIONS OBSERVED BY LASER-INDUCED BREAKDOWN DETECTION

H.-R. Cho[*], W. Cha, E. C. Jung

Nuclear Chemistry Research Division, Korea Atomic Energy Research Institute,
989-111 Daedeok-daero, Yuseong-gu, Daejeon 305-353, Republic of Korea

Under environmental conditions, plutonium can coexist in several different oxidation states: Pu(III), Pu(IV), Pu(V) or Pu(VI), which show drastically different chemical behaviors. The thermodynamic data of plutonium have been critically discussed in OECD/NEA-TDB reviews [1, 2], but it is still difficult to reliably predict chemical behaviors of plutonium under geochemical conditions when excluding oxygen or involving reducing agents. There have been several investigations on the solubility of Pu(IV) hydroxide in the presence of reducing agents such as 50 bar H_2 [3], $Na_2S_2O_4$ [4], hydroquinone, and $FeCl_2$ [5]. In these studies, higher concentrations of dissolved plutonium species than the concentration predicted from the solubility product of Pu(IV) hydroxide were reported owing to the dominant oxidation state of Pu(III) in a solution under reducing conditions. However, only one study [6] providing experimental solubility products for Pu(III) hydroxide as an equilibrium solid phase has been reported.

The aim of this work is the determination of a solubility product of Pu(III) hydroxide under electrolytic reducing conditions. A stock solution of Pu(III) in a high acidic solution (0.2 M $HClO_4$) was prepared through the electrolytic reduction of a chemically purified Pu(VI) solution [7]. The concentration of hydrogen ions (H^+) of diluted Pu(III) samples in 0.1 M $NaClO_4$ was reduced using an electric current from a Ag/AgCl electrode to a Pt working electrode, which called coulometric pH titration. Figure 1. shows the experimental setup for the coulometric titration. The reducing condition during coulometric titration maintains the dominant oxidation state of Pu(III). Soluble plutonium species were investigated using absorption spectroscopy adopting a liquid waveguide capillary cell, which has an optical path-length of 100 cm. The limit of detection for Pu^{3+} at 601 nm and Pu^{4+} ions at 470 nm in 0.1 M $HClO_4$ was 0.13 and 0.10 M, respectively. The concentrations of soluble Pu(IV) were below its limit of detection. The typical absorption spectra of Pu^{3+} ions in $HClO_4$ solutions in visible wavelength range of 500 to 700 nm [8] were not changed with an increase in the pH and the formation of the hydrolysis species of Pu(III). The formation of plutonium colloids was observed using laser-induced breakdown detection as a function of pH during coulometric titration. The solubility of the plutonium hydroxide investigated under electrolytic reducing conditions will be discussed in comparison with the previous results [3, 6].
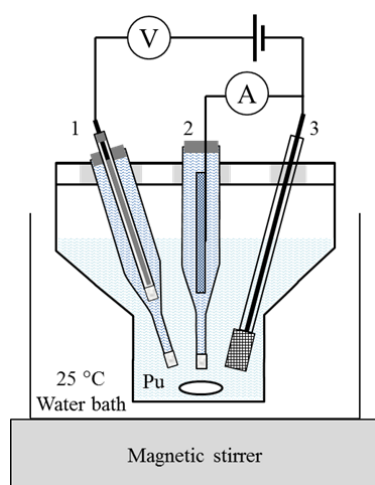

Figure 1. Experimental setup for electrolysis. 1. Reference electrode (Ag/AgCl filled with saturated KCl), 2. auxiliary electrode (Pt gauze), and 3. working electrode (Pt gauze covered with a borosilicate tube). Two quartz tubes with Vycor tips filled with 0.1 M $NaClO_4$ were used for electrodes 1 and 2.

[1] R. J. Lemire, J. Fuger, H. Mitsche, P, Potter, M. H. Rand, J. Rydberg, K. Spahiu, J. C. Sullivan, W. J. Ullman, P. Vitorge, H. Wanner, (OECD/NEA-TDB) Chemical Thermodynamics Vol. 4, Elsevier, North-Holland, Amsterdam (2001).

[2] R. Guillaumont, Th. Fanghänel, J. Fuger, I. Grenthe, V. Neck, D.A. Palmer, M. H. Rand, (OECD/NEA-TDB) Chemical Thermodynamics Vol. 5, Elsevier, North-Holland, Amsterdam (2003).

[3] H. Nilsson, Y. Albinsson, G. Skarnemark, Mat. Res. Soc. Symp Proc. 807, 615 (2004).

[4] K. Fujiwara, H. Yamana, T. Fujii, H. Moriyama, Radiochim. Acta 90, 857 (2002).

[5] D. Rai, Y.A. Gorby, J. K. Fredrickson, D. A. Moore, M. Yui, J. Sol. Chem. 31, 433 (2002).

[6] A. R. Felmy, D. Rai, J. A. Schramke, J. L. Ryan, Radiochim. Acta 48, 29 (1989).

[7] H.-R. Cho, E. C. Jung, K. K. Park, K. Song, J.-I. Yun, Radiochim. Acta 98, 555 (2010).

[8] D. Cohen, J. Inorg. Nucl. Chem. 18, 211 (1961).

INTERACTION OF Pu, U AND Tc WITH IRON CORROSION PRODUCTS UNDER HYPERALKALINE REDUCING CONDITIONS

M. R. González-Siso[1)], X. Gaona[2)], L. Duro[1)], D. Schild[2)], D. Fellhauer[2)], I. Pidchenko[2)], T. Vitova[2)], M. Altmaier[2)], J. Bruno[1)]

[1)]Amphos 21 Consulting S.L., Passeig Garcia i Faria, 49-51, 1-1a, 08019 Barcelona, Spain
[2)]Karlsruhe Institute of Technology, Institute for Nuclear Waste Disposal, Germany

Iron will be present in several of the currently considered repository concepts for disposal of radioactive waste as a structural component in reinforced concrete structures, as main component of the steel canisters and as part of the wastes materials. Anoxic corrosion of Fe is expected to generate very reducing conditions, which will impact the chemical behaviour of the redox sensitive radionuclides present in the waste. In the Swedish Final Repository (SFR) for low- and intermediate level radioactive waste, the presence of cementitious materials will impose highly alkaline pH conditions to the contacting water. Magnetite (Fe_3O_4) has been identified as one of the main products resulting from the anoxic corrosion of metallic iron and steel. Besides, the question of redox equilibrium and disequilibrium is particularly relevant for electron transfer processes in heterogeneous reactions that have, in principle, slow kinetics, but maybe catalysed by the presence of solid surfaces. The determination of the response of the redox sensitive radionuclides to the evolution of the system containing large amounts of iron and concrete is fundamental to the performance assessment of nuclear waste management systems. Redox transitions in the hyperalkaline pH range of the radionuclides chosen in this study (Pu(IV) $\rightarrow$ Pu(III) at pe+pH $\sim$ −1, U(VI) $\rightarrow$ U(IV) at pe+pH $\sim$ +2, Tc(VII) $\rightarrow$ Tc(IV) at pe+pH $\sim$ +6) strategically cover the field of stability of the system Fe(0)–Fe_3O_4–Fe(II)$_{aq}$, and thus are expected to provide a key understanding on the interaction of the waste with Fe corrosion products under repository conditions.

All experiments were performed at 22±2°C under inert gas (Ar) atmosphere (O_2 < 5 ppm). Batch experiments were performed with a hydrothermally prepared α-Fe_3O_4(cr) [1]. The same solid phase has been exhaustively characterized in a simultaneous study in the absence of radionuclides [2]. Independent samples were prepared at −log [H^+] = pH$_c$ ~9 and pH$_c$ = 12.8 in 0.1 M NaCl–NaOH solutions. Four different redox systems were defined: i. α-Fe_3O_4(cr) + RN, ii. α-Fe_3O_4(cr) + Fe(cr) + RN, iii. α-Fe_3O_4(cr) + 0.01 M $SnCl_2$ + RN and iv. α-Fe_3O_4(cr) + 0.01 M $Na_2S_2O_4$ + RN. The most soluble redox state of each radionuclide (Pu(V), U(VI) and Tc(VII)) were considered for the addition to a magnetite suspension with solid-to-liquid ratio (S:L) of 2 g·L^{-1}. The initial radionuclide concentration in the resulting suspension was in all cases 3·10^{-5} M. Total radionuclide concentration in solution was quantified after 10 kD ultrafiltration by LSC (^{99}Tc and ^{242}Pu) and ICP–MS (^{238}U). Samples were equilibrated for up to 290 days; pH$_c$, redox potential (as pe = 16.9·E_H) and [RN] were monitored at regular time intervals. Plutonium redox speciation in the aqueous phase was investigated by solvent extraction. The redox state of Pu, U, Tc and Fe at the surface of magnetite was characterized by XPS at t = 170 and 290 days. Redox state and molecular environment of Pu in the solid phase was characterized by XANES/EXAFS following the Pu L$_{III}$ edge (18.057 keV) at the INE beamline at ANKA synchrotron facility. Spectra were calibrated against the first inflection point in the XANES spectrum of a Zr foil (17.998 keV).

The concentration of Pu in solution decreases rapidly to values below or at the detection limit of LSC ($10^{-8.8}$ M) in most of the samples, indicating the reduction of Pu(V) to less mobile redox states. A significantly higher [Pu] ($\approx 10^{-6}$ M) is measured at pH$_c$ = 8 in the presence of $Na_2S_2O_4$ (pe+pH$_m$ = −1). The predominance of Pu(III) in the aqueous phase is thermodynamically predicted in these near-neutral pH and very reducing

conditions, and is also confirmed in this study by solvent extraction techniques. XPS confirms the predominance of Pu(IV) on the surface of magnetite, although the presence of Pu(III) is also observed in the most reducing systems ($Na_2S_2O_4$, $SnCl_2$) at $pH_c = 9$. Both XPS and XANES analyses confirm the co-existence of Pu(III) and Pu(IV) at pH=12.8 for the magnetite system in $SnCl_2$. Previous studies have reported the formation of very stable Pu(III) surface complexes with magnetite under near-neutral pH conditions [3], but this is the first time that the stabilization of Pu(III) on the surface of magnetite is also reported under hyperalkaline pH conditions. The concentration of uranium decreases below 10^{-8} M in all the samples except those with $pH_c = 12.8$ and less reducing conditions (Fe_3O_4 and Fe_3O_4+Fe), where [U] $\approx 10^{-5}$ M. These observations are in good agreement with the expected formation of U(VI) under the $pe+pH_m$ conditions defined by both systems. Note further that the predominance of $UO_2(OH)_4^{2-}$ at $pH_c = 12.8$ is expected to promote a higher solubility and weaker sorption of uranium. The concentration of technetium in solution decreased steadily from t = 1 day, indicating that Tc(VII) is reduced to Tc(IV) as predicted from thermodynamic calculations. The reduction proceeds slower for those samples with $pe+pH_m$ values closer to the Tc(VII)/Tc(IV) borderline. The predominance of Tc(IV) on the surface of magnetite is also confirmed by XPS.

[1]   Schwertmann, U., Cornell, R.M. (2000). Weinheim; New York: Wiley-VCH.
[2]   González-Siso, M. R., Gaona, X., Duro, L., Schild, D., Lagos, M., Darbha, G., Finck, N., Altmaier, M., Bruno, J. (2015). This conference.
[3]   Kirsch, R., Fellhauer, D., Altmaier, M., Neck, V., Rossberg, A., Fanghänel, T., Charlet, L., Scheinost, A. C. Environ. Sci. Technol. 45, 7267–7274 (2011).

LONG-TERM REDOX CYCLING OF TECHNETIUM UNDER CONDITIONS RELEVANT TO THE NUCLEAR LEGACY

N. Masters-Waage[1], K. Morris[2], J. R. Lloyd[2], F. R. Livens[1], J. F. M. Mosselmans[3], P. Bots[2], C Boothman[2], G. T. W. Law[1]

[1]*Centre for Radiochemistry Research, School of Chemistry, The University of Manchester, Oxford Road, Manchester, M13 9PL, United Kingdom*
[2] *Research Centre for Radwaste Disposal and Williamson Research Centre, School of Earth, Atmospheric and Environmental Sciences, The University of Manchester, Oxford Road, Manchester, M13 9PL, United Kingdom*
[3]*Diamond Light Source Ltd, Diamond House, Harwell Science and Innovation Campus, Didcot, OX11 0DE, United Kingdom*

The management of radioactive wastes generated as a result of nuclear power and nuclear weapons production is of global concern and long lived radionuclides such as uranium, neptunium and fission products such as technetium will be contributors to radiological risk over geological timescales. Technetium is a β-emitting fission product whose solubility is largely determined by its oxidation state. The highly soluble pertechtenate ion (TcO_4^-) predominates under oxic conditions, sorbing poorly to geomedia. Conversely, poorly soluble Tc(IV) (as TcO_2, TcS_2 or sorbed Tc(IV) [1]) is formed under reducing conditions promoted by microbial processes [2, 3]. Interestingly, our understanding of Tc behaviour is focused on one bioreduction cycle, but it is clear that in many natural and engineered environments, repeated redox cycles will occur as conditions fluctuate from anoxic / sub-oxic to oxic as a result of changes in groundwater flow, land mass movement, glaciation, flooding, and release of effluents from industry and agriculture [4]. The long half-life of Tc (2.1 x 10^5 years) means that multiple redox cycles are likely to occur over the 10^6 years that radioactive decay will be significant and this may impact its speciation, fate and long-term mobility. Reflecting this, we have investigated the influence of multiple redox cycles on Tc behaviour, extending current observations beyond single bioreduction / oxidation cycles [e.g. 5].

In experiments, air exposure and acetate addition were used periodically to promote oxidising and reducing conditions, respectively. During the course of the experiments three complete redox cycles were undertaken. In the first cycle, reduction resulted in removal of 96.2 ± 0.1 % of the added Tc from solution, with 42.7 ± 13.2 % subsequently remobilised after re-oxidation. The second reduction cycle showed a relative decrease in Tc removal compared to the first cycle and in the subsequent re-oxidation, less Tc was remobilised to solution compared to the first re-oxidation cycle. The final reduction cycle showed similar removal levels compared to the middle system, although, interestingly on reoxidation the extent of remobilisation was at its lowest. The results show a clear trend with increased numbers of redox cycles decreasing the total Tc remobilisation during oxidation events. Further, the results also suggest that some fraction of Tc is recalcitrant to reductive immobilisation in these systems. In this contribution, solution data are complemented by a range of speciation techniques including XAS, electron microscopy, wet chemical extractions and ultra filtration to track speciation and fate of Tc, and pyrosquencing to identify the microbial cycling in these complex systems. This study provides the first insight into the long-term biogeochemical fate of Tc in dynamic redox cycling environments relevant to its fate in natural and engineered environments.

[1] J. Lee, et al., Geochim. Cosmochim. Acta 136, 247 (2014).
[2] J. R. Lloyd, et al., Appl. Environ. Microbiol. 66, 3743 (2000).
[3] G. Lear, et al., Environ. Sci. Technol. 44, 156 (2010).
[4] I. T. Burke, et al., Environ. Sci. Technol. 40, 3529 (2006).
[5] G. T. W. Law, et al., Environ. Sci. Technol. 44, 150 (2010).

A BIG PROGRESS ON HIGH LEVEL RADIOACTIVE WASTES DISPOSAL IN CHINA: FROM FOLLOW SUIT TO SCIENCE DRIVEN

C.L. Liu

Beijing National Laboratory for Molecular Sciences，Fundamental Science Laboratory on Radiochemistry & Radiation Chemistry，College of Chemistry & Molecular Engineering，Peking University, Beijing 100871, PR China

With the development of nuclear energy in China, and the recognition of the importance of safe disposal of high-level radioactive wastes (HLW), China initiated the development of a formal High-level Radioactive Waste Disposal Program in 1985 with the establishment of the Coordination Group on High-level Radioactive Waste Disposal. Research on site selection, geological survey, and migration of radionuclides in different geologic media were initiated by the China Institute of Atomic Energy, China Institute for Radiation Protection, Peking University and Tsinghua University [1]. At the beginning of the 21st century, when China began planning for rapid growth in nuclear energy, the country entered a phase of rapid development and research into the safe disposal of HLW. In 2005, a 25 member Expert Group on High-level Radioactive Waste Disposal tasked by the Chinese Atomic Energy Agency (CAEA) for providing technical and consulting support to CAEA in the long term planning and design, setting up of the targets at different stages, providing guidance on basic research programs and reviewing the important research projects of **C**hina's **Hi**gh **L**evel **Ra**dioactive **W**astes **D**isposal (CHILRAWD) Program. In Feb. 2006, a planning and policy document for the R&D on Geologic Disposal of High-level Radioactive Wastes was jointly released by the Commission of Science Technology and Industry for National Defense, the Ministry of Science and Technology of the People's Republic of China, and the State Environmental Protection Administration of China. This document outlines the research framework of the CHILRAWD. On the first annual meeting of the expert group held on October 27, 2006, the first 17 projects proposed by the institutions from the China National Nuclear Corporation, the Chinese Academy of Sciences and Universities, covering radionuclide migration, safety assessment methodology, engineering design and site investigation were reviewed and approved. Currently, 12 geological sites are being investigated and ultimately 3 sites will be selected for the potential geological repository in China. In this paper, the CHILRAWD program will be presented and discussed.

[1] C.L.Liu, Recent Progress on High Level Radioactive Wastes Disposal in China. Presented at Berkeley Laboratory, Fe. 28, 2014. (Invited and Chaired by Professor Heino Nitsche)

ALL WE HAVE LEARNED ABOUT RADIONUCLIDE MIGRATION IN THE LAST 30 YEARS AND HOW THIS IS SHAPING OTHER ENVIRONMENTAL AREAS OF WORK

Jordi Bruno

Amphos 21, Barcelona Spain

In the last 30 years the radioactive waste management community has put enormous efforts in understanding and quantifying radionuclide migration in the geosphere and more recently in the biosphere.

Many efforts have been made by the "Migration" research community to qualify and quantify the processes that control the release and fate of key radionuclides disposed as waste in diverse geological environments.

At the onset of this work we had to do substantial efforts to integrate knowledge of from other areas of environmental geochemistry to break through some of the autism of the nuclear waste management community. The present situation is the opposite; many of the key processes and their quantification are now being extensively used in other environmental areas of work.

In particular in the field of CO_2 geological storage and more recently in the poly- metallic mining industry as well as in secondary mining and recycling industries.

In my presentation I will perform a historical analyses of the development of the scientific knowledge put forward by the radwaste community and how this has encompassed the scientific development in the general environmental scientific community.